UNIVERSIDADE DE LISBOA
FACULDADE DE CIÊNCIAS

Sedimentary Dynamics in the Estremadura Spur Continental Shelf

" Documento Definitivo"

Doutoramento em Geologia
Especialidade de Sedimentologia

Maria João Ferrão Balsinha

Tese orientada por:
Professor Doutor Rui Pires de Matos Taborda
Doutora Aurora da Conceição Coutinho Rodrigues Bizarro

Documento especialmente elaborado para a obtenção do grau de doutor

2020

UNIVERSIDADE DE LISBOA
FACULDADE DE CIÊNCIAS

Sedimentary Dynamics in the Estremadura Spur Continental Shelf

Doutoramento em Geologia

Especialidade de Sedimentologia

Maria João Ferrão Balsinha

Tese orientada por:

Professor Doutor Rui Pires de Matos Taborda

Doutora Aurora da Conceição Coutinho Rodrigues Bizarro

Júri:

Presidente:

- Doutora Maria da Conceição Pombo de Freitas, Professora Catedrática e Presidente do Departamento de Geologia, da Faculdade de Ciências da Universidade de Lisboa (FCUL).

Vogais:

- Doutor Fernando Joaquim Fernandes Tavares Rocha, Professor Catedrático do Departamento de Geociências da Universidade de Aveiro
- Doutora Aurora da Conceição Coutinho Rodrigues Bizarro, Investigadora Auxiliar do Instituto Hidrográfico, Orientadora;
- Doutora Cristina Carvalho Veiga Pires, Professora Auxiliar da Faculdade de Ciências e Tecnologia da Universidade do Algarve;
- Dr. Fernando Mendes de Queirós Magalhães, Técnico Superior da Agência Portuguesa do Ambiente, na qualidade de individualidade de reconhecida competência na área científica;
- Doutor César Augusto Canêlhas Freire de Andrade, Professor Catedrático da Faculdade de Ciências da Universidade de Lisboa.

Documento especialmente elaborado para a obtenção do grau de doutor

Fundação para a Ciência e Tecnologia, no âmbito da Bolsa de Doutoramento com a referência SFRH/BD/45878/2008

2020

AGRADECIMENTOS

O presente trabalho foi possível graças ao apoio da Fundação para a Ciência e Tecnologia através da concessão da bolsa de doutoramento SFRH/BD/45878/2008. O trabalho desenvolveu-se no Instituto Hidrográfico (IH), no Instituto Dom Luiz e no Departamento de Geologia da Faculdade de Ciências da Universidade de Lisboa. A estas instituições, nas pessoas dos seus Diretores e Presidentes, agradeço o acolhimento prestado, a cedência do espaço e das condições laboratoriais, imprescindíveis à elaboração desta dissertação.

Mais importante ainda, tive a sorte de contar com o apoio de meus orientadores, que foram meus mentores bem antes do esforço para a realização deste doutoramento e me encorajaram a avançar.

À Doutora Aurora Rodrigues Bizarro e ao Professor Doutor Rui Taborda, orientadores desta dissertação, cujo incentivo constante, disponibilidade e apoio permanente do primeiro ao último dia foram vitais na execução deste trabalho.

Para a realização desta dissertação contei com o auxílio e apoio de diversas pessoas a quem estou profundamente reconhecida e a quem quero expressar os meus sinceros agradecimentos.

À Doutora Anabela Oliveira, que me transmitiu o conhecimento e gosto pelo estudo das argilas. Pelo acompanhamento nas interpretações dos vários difractogramas e análise de distribuição espacial, e também pelo seu grande interesse e entusiasmo demonstrado na observação das amostras à lupa binocular e respetivos resultados.

Ao Doutor Mário Cachão pela disponibilidade e orientação relativamente à preparação das lâminas delgadas e análise do nanoplâncton calcário.

Ao Doutor Francisco Fatela e Cecília Luz pela orientação e disponibilidade no que respeita a análise de foraminíferos.

À Doutora Carla Palma pelo auxílio na análise geoquímica das amostras no laboratório de Química do IH. À Doutora Sandra Moreira e Doutora Anabela Oliveira pela disponibilidade na discussão dos dados de geoquímica.

Ao Doutor João Cascalho pelo acompanhamento e discussão no que respeita a análise de minerais pesados.

Ao Doutor Joaquim Pombo e João Duarte, pelo imprescindível acompanhamento nas várias sessões de identificação dos grãos à lupa binocular. Aos dois quero expressar o meu profundo agradecimento.

À Professora Doutora Conceição Freitas e Professor Doutor César Andrade pelas intensas discussões relativamente à evolução recente dos ambientes costeiros e cujas conclusões foram deveras fundamentais para esta dissertação.

À Dr.ª Alexandra Morgado pelo seu incentivo e apoio incondicional.

À Eng.ª Ana Santos, sempre disponível a ajudar, pelo seu apoio e incentivo.

À D. Fernanda Dias e D. Julieta Vieira pelo imprescindível apoio laboratorial, disponibilidade e amizade.

Queria também agradecer a todos os meus amigos, muitos dos quais permanecerão anónimos pela impossibilidade de todos referenciar. Ficam então os meus sinceros agradecimentos à Cati pelo apoio, amizade, incentivo e vários meses de companhia na observação à lupa binocular, que resultaram numa grande cumplicidade. À Joana e à Mo, também pelo incentivo, apoio e amizade nos vários meses de redação desta dissertação. Sem elas, tudo isto tornar-se-ia mais pesado e difícil.

Ao Tone um agradecimento especial pelo seu carinho e dedicação, pela sua confiança, paciência e por saber compreender as minhas ausências, que esteve sempre comigo nos bons e maus momentos para me incentivar e apoiar.

Por fim, aos meus filhos do coração (Catarina e Manuel), que contribuíram em muito para o meu crescimento como pessoa e ser humano, que me tornam mais resiliente e que poem à prova tudo o que tenho como certo na vida.

Aos meus Pais, como sempre, obrigada por tudo….

ABSTRACT

The marine environment is affected by multiple natural drivers and anthropogenic stressors that can have a strong impact on the sustainability of marine ecosystems and resources. Understanding the marine environment dynamics, in its various aspects, has therefore become a worldwide priority to the study of the sedimentary cover. Understanding of its spatial and temporal patterns, can be of critical importance for resource management, environmental protection initiatives and effective marine governance.

The present work aims at the study of the sedimentary processes affecting the Estremadura Spur in order to understand its evolution of marine systems in an environmental and climate change context. With this goal, a multidisciplinary approach will attain the different aspects of marine processes on the Estremadura Spur continental shelf. With a triangular shape, the Estremadura Spur is a prominent geomorphological unit that stands out from the general morphology of the West Iberian Peninsula. This sector is isolated from the nearby sectors by the northern Nazaré Submarine canyon and the Lisboa Canyon in the south. The Estremadura Spur continental shelf has variable width, ranging from 15 km (in front of Peniche) to 70 km (in Ponta da Lamparoeira parallel) and its external border (shelf break) is located at variable depth, ranging from ~50 m to more than ~300 m. The continental shelf is characterized by large areas of carbonated rocky outcrops and a thin layer of unconsolidated sediments and the coastal zone is predominantly composed by rocky cliffs with few embayed beaches, closer to the mouth of small rivers and creeks.

This sector of the Portuguese shelf is affected by a high energetic wave regime that dominates inner and middle shelf sediment dynamics. At the outer shelf and upper slope, oceanographic phenomena, like internal waves, have been recognized to occur, which impact particle resuspension and transport. In the Portuguese continental shelf, during the winter, the predominant current direction is northward; however, during the three months period of in situ observations (winter time), in the outer shelf of the Estremadura Spur, the dominant current direction was oriented southward, inducing a particle transport with the same direction; the observed residual current from current meter data ranged from 0 to 13 cm/s. Two main components were identified, namely cross-shelf and along shelf.

As a result of this morphology and wave regime exposition, sedimentary patterns indicate that the contribution of recent sand terrigenous particles is only significant in the inner shelf. In the northern sector, the middle shelf is covered by very coarse deposits in the vicinity of extensive rocky outcrops. Immediately south of those outcrops, sediments become finer, with muddy sand deposits covering the entire Mar da Ericeira. Muddy sands also cover the outer domains of the Estremadura Spur, with a large elongated sandy deposit located along the outer shelf. Sedimentary particles from adjacent beaches and rivers that drain directly into the Estremadura Spur are mainly sand-sized. River sediments also have a significant component of fine particles, while the beach sediments have no fine fraction and gravel is only important at Foz do Arelho beach.

There is no clear relationship between minerals present in the fine fraction of river sediments that drain to the Estremadura Spur and those found in the shelf. The high percentage of potassium feldspar and plagioclase near the coast can be explained by the proximity to the terrigenous particle sources (continental origin), while the other minerals seem to be related to the effect of distribution processes that control the distribution of the main mineral species. The riverine environment has clearly different assemblages of heavy minerals than the ones found on beaches and inner shelf. The heavy minerals highlight two distinct coastal sedimentary cells, characterized by distinct associations. The beach sediments present a similar heavy mineral content to inner shelf sediments, but the influence of the riverine/continental input is higher at the beaches, as demonstrated by high percentages of tourmaline and andaluzite in the north, and pyroxenes in the south.

The analysis of present-day sedimentary dynamics revealed characteristics of wave/storm dominated continental shelf. Threshold orbital velocity near the bottom computed with SWAN, using 22 years of wave data, for coarse (0.500 mm) and fine particles (0.063 mm), show that coarse particles are remobilized more that 40 % of the time for depths up to 30 m and fine particles can be remobilized 50 % of the time till 40 m depth and 10 % of the time till 100 m. The sediment transport pathways over the Estremadura Spur, deduced from the GSTA (Grain Size Trend Analysis), indicate four different sectors in relation to distinct oceanographic, sediment supply and geomorphologic constraints. Due to lower sediment sampling resolution, GSTA was not able to resolve the sedimentary transport in the inner shelf sector.

The study of a vertical sample collected offshore Ericeira (in the center of the largest muddy deposit of the Estremadura Spur) allowed the understanding of the environmental shelf changes during the Holocene, with impact on the sediment record. The oldest sedimentary sequence corresponds to a high energy environment, likely representing a coastal deposit in close connection to the terrigenous particle sources. The middle sedimentary sequence shows an increased presence of biogenic particles and a decrease in coarser particles indicating a deeper and lower energy environment, when compared with the older sequence. In the superficial sequence (which is only 20 cm thick), sediments are compatible with middle shelf dynamic processes very similar to present day characteristics. The sudden increase of heavy metals like mercury (Hg) and lead (Pb) can be explained by the increase of anthropogenic activity, either related to deforestation or mining. These activities increase soil erosion, leading to a characteristic inorganic detrital deposit in most aquatic systems (lakes, rivers and seas).

The reconstruction of the evolution of the Estremadura Spur during the recent Quaternary was performed by the integration of morphological and sedimentological characteristics. As an important input to this model and to explain the origin of the three sedimentary sequences, additional radiocarbon analyses of benthic organisms were used as reference, as well as published sea level curves for the Portuguese continental shelf and other several studies on paleoreconstruction of the Portuguese margin.

During the Last Glacial Maximum, the coastline was at ~ 130 m depth and the present day rivers were active valleys carrying sediment into the shelf break. During this period, the rocky

outcrops at Ponta da Lamparoeira parallel, formed a morphological barrier between the northern and southern areas of Estremadura Spur. The sedimentation over the shelf was very scarce at this time due to the cold and arid conditions. In the beginning of the deglaciation (warmer climate), the coastline started to migrate landward and coastal areas were invaded by the sea up to ~ 110/100 m depth and sediment export increased quite slowly. At the end of the deglaciation the sea level rose very rapidly settling at ~ 50/40 m depth. This sudden sea level rise induced such an imbalance that estuaries became sediment traps and few sediments were able to reach the continental shelf, which resulted in a scarcity of sediments and the coastline maintained its rocky characteristics. During the Younger Dryas, the sea surface temperature dropped below 10 ºC and the relative mean sea level (rmsl) lowered 20 m in 1000 years. By the end of this event the msl was ~ 60 m depth. This new cycle induces the remobilization of coastal and estuarine particles deposited in the previous phase. In the Holocene, the establishment of a warmer period contributed to the multi-phase rise of the msl. These multi-phase events are represented by Early, Middle and Late Holocene. In the Early Holocene, the sea level rose almost 40 m in 2000 years, leading to thick transgressive sequences, due to the high levels of precipitation. At this time, the conditions were similar to those of an inner shelf like environment with high energy conditions. During the Middle Holocene, the overall conditions of sea level rise and rapid environmental conditions were maintained (msl rise ~15 m above present sea level). This period is represented in the sediment core as a ~ 80 cm thick layer, indicating a drastic decrease in energy conditions, concurrent with an increase of the living conditions represented by species diversity. In the Late Holocene, the msl settled at the present level. With the increasing human activity, with impacts on deforestation and mining processes, the presence of heavy metals in the sedimentary record also increases. A high fluvial/continental input was expected, with higher species diversity due to higher availability of nutrients and fine particles. Although the sediment input might have increased, the accumulation rate is still very low when compared to other sectors of the Portuguese continental margin.

Keywords: Sedimentary dynamics, Estremadura Spur, Paleoenvironmental proxies, Holocene evolution, Grain size trend analysis

RESUMO

O ambiente marinho é afetado por vários fatores naturais e antropogénicos que podem ter um forte impacto na sustentabilidade dos ecossistemas e recursos marinhos. Compreender a dinâmica do meio marinho nos seus vários aspetos, tornou-se, portanto, uma prioridade mundial. Para o estudo da cobertura sedimentar, a compreensão de seus padrões espaciais e temporais pode ser de fundamental importância para a gestão de recursos, iniciativas de proteção ambiental e governação marinha eficaz.

O presente trabalho tem como objetivo o estudo dos processos sedimentares que afetam o Esporão da Estremadura, de forma a compreender a evolução dos sistemas marinhos num contexto ambiental e de alterações climáticas. Com este objetivo, uma abordagem multidisciplinar irá focar-se nos processos marinhos da plataforma continental do Esporão da Estremadura. Com uma forma triangular, o Esporão da Estremadura é uma unidade geomorfológica de destaque na morfologia geral do Oeste da Península Ibérica. Este setor está isolado dos setores vizinhos pelo canhão submarino da Nazaré a norte e pelo canhão de Lisboa a sul. A plataforma continental do Esporão da Estremadura tem largura variável, variando entre 15 km (frente a Peniche) a 70 km (no paralelo da Ponta da Lamparoeira) e o seu limite externo (bordo de plataforma) situando-se a uma profundidade variável entre ~ 50 m e mais de ~ 300 m. A plataforma continental é caracterizada por extensas áreas de afloramentos rochosos carbonatados e uma fina camada de sedimentos não consolidados. A zona costeira é predominantemente composta por falésias rochosas com poucas praias encaixadas, com fozes de pequenos rios e riachos.

Este setor da plataforma portuguesa é afetado por um regime de ondas de alta energia que domina a dinâmica dos sedimentos da plataforma interna e média. Na plataforma externa e no bordo superior, fenómenos oceanográficos, como ondas internas, foram reconhecidos com efeitos na ressuspensão e transporte das partículas.

Como resultado desta morfologia e exposição do regime de ondas, os padrões sedimentares indicam que a contribuição das partículas terrígenas de areia recente é significativa apenas na plataforma interna. No setor norte, a plataforma média é coberta por depósitos muito grosseiros nas proximidades de extensos afloramentos rochosos. Imediatamente a sul desses afloramentos, os sedimentos tornam-se mais finos, com depósitos de areia lodosa cobrindo todo o Mar da Ericeira. As areias lodosas também cobrem os domínios externos do Esporão da Estremadura, com um grande depósito arenoso alongado localizado ao longo da plataforma externa. As partículas sedimentares das praias e rios adjacentes que drenam diretamente para o Esporão da Estremadura são maioritariamente do tamanho das areias. Os sedimentos dos rios também têm uma componente significativa de finos, enquanto os sedimentos da praia não têm fração fina e o cascalho é importante apenas na praia da Foz do Arelho.

Não existe uma relação clara entre os minerais presentes na fração fina dos sedimentos fluviais que drenam para o Esporão da Estremadura e os que se encontram na plataforma. A elevada percentagem de feldspato potássico e plagioclase próximo do litoral pode ser explicado pela proximidade das fontes de partículas terrígenas (origem continental), enquanto os demais minerais parecem estar relacionados com processos de distribuição que controlam as principais espécies minerais. O ambiente ribeirinho apresenta associações de minerais pesados claramente diferentes daqueles encontrados nas praias e na plataforma interna. Os minerais pesados isolam duas células sedimentares, caracterizadas por associações distintas. Os sedimentos da praia têm um conteúdo mineral pesado semelhante aos sedimentos da plataforma interna, mas a influência da contribuição ribeirinha/continental é maior nas praias, conforme demonstrado por elevadas percentagens de turmalina e andaluzite a norte e piroxenas a sul.

A análise da dinâmica sedimentar atual revelou características da plataforma continental dominada por ondas / tempestades. A velocidade orbital limite junto ao fundo foi calculada com o SWAN, usando 22 anos de dados de ondas, para partículas grosseiras (0,500 mm) e finas (0,063 mm). Este mostra que as partículas grosseiras são remobilizadas mais de 40 % do tempo para profundidades até 30 m (plataforma interna) enquanto as partículas finas podem ser remobilizadas 50 % do tempo até profundidades de 40 m e 10 % do tempo até aos 100 m. O padrão de transporte de sedimentos no Esporão da Estremadura, deduzido do GSTA, indica quatro setores diferentes em relação a distintos condicionantes oceanográficos, geomorfológicos e de contribuição de sedimentos. O GSTA não foi capaz de resolver o transporte sedimentar no setor da plataforma interna devido à menor resolução de amostragem de sedimentos.

O estudo de um testemunho vertical recolhido ao largo da Ericeira (no centro do maior depósito lodoso do Esporão da Estremadura) permitiu compreender as alterações ambientais da plataforma durante o Holocénico, com impacto no registo de sedimentos. A sequência sedimentar mais antiga corresponde a um ambiente de alta energia, provavelmente representando um depósito costeiro em estreita conexão com as fontes de partículas terrígenas. A sequência sedimentar intermédia, mostra um aumento na presença de partículas biogénicas e uma diminuição nas partículas mais grosseiras, indicando um ambiente mais profundo e de menor energia, quando comparada com a sequência mais antiga. Na sequência sedimentar superficial (que tem apenas 20 cm de espessura), os sedimentos são compatíveis com processos dinâmicos de plataforma (média/externa) muito semelhantes às características atuais. O aumento repentino de metais pesados como mercúrio (Hg) e chumbo (Pb) pode ser explicado pelo aumento da atividade antropogénica, relacionada quer à desflorestação quer à mineração. Estas atividades aumentam a erosão do solo, levando a um depósito detrítico inorgânico característico na maioria dos sistemas aquáticos (lagos, rios e mares).

A reconstrução da evolução do Esporão da Estremadura durante o Quaternário recente foi realizada pela integração de características morfológicas e sedimentológicas. Como

importante contributo para este modelo e para explicar a origem das três sequências sedimentares, foram utilizadas como referência, análises isotópicas adicionais de organismos bentónicos, bem como curvas do nível do mar publicadas para a plataforma continental portuguesa e outros estudos sobre paleoreconstrução da margem portuguesa.

Durante o Último Máximo Glaciar, o litoral estava a ~130 m de profundidade e os rios atuais eram vales ativos transportando sedimentos para o bordo da plataforma. Durante este período, os afloramentos rochosos da Ponta da Lamparoeira formaram uma barreira morfológica costeira entre as zonas norte e sul do Esporão da Estremadura. A sedimentação sobre a plataforma era muito escassa nessa época devido às condições frias e áridas. No início do deglaciação (clima mais quente), o litoral começou a migrar para terra e as áreas costeiras foram invadidas pelo mar até a profundidade de ~110/100 m e a exportação de sedimentos aumentou muito lentamente. No final do deglaciação, o nível do mar subiu muito rapidamente, chegando a ~ 50/40 m de profundidade. Essa súbita elevação do nível do mar em tão curto período de tempo induziu um desequilíbrio tal que os estuários se transformaram em armadilhas de sedimentos e poucos conseguiram atingir a plataforma continental, o que resultou na escassez de sedimentos mantendo a linha de costa as suas características rochosas. Durante o *Dryas Recente*, a temperatura da superfície do mar caiu abaixo de 10 ºC e o nível médio do mar baixou cerca de 20 m em 1000 anos. No final deste evento, o nível médio do mar localiza-se aproximadamente a 60 m de profundidade. Este novo ciclo induz a remobilização de partículas costeiras e estuarinas depositadas na fase anterior. No Holocénico, o estabelecimento de um período mais quente contribuiu para uma elevação multifaseada do nível médio do mar. Estas fases são representadas pelo Holocénico Inferior, Médio e Superior. No Holocénico Inferior o nível do mar subiu quase 40 m em 2000 anos, permitindo a acumulação de sequências transgressivas espessas, devido aos elevados níveis de precipitação. Nessa época, as condições eram semelhantes às de um ambiente de plataforma interna com condições de alta energia. Durante o Holocénico Médio, as condições gerais de elevação do nível do mar e as condições ambientais rápidas foram mantidas (aumento médio do nível do mar ~ 15 m acima do nível do mar atual). Este período está representado na amostra vertical de sedimento como uma camada de ~ 80 cm de espessura, indicando uma diminuição drástica das condições energéticas, concomitante com um aumento da diversidade de espécies. No Holocénico Superior, o nível médio do mar estabilizou no nível atual. O aumento da atividade humana, com impactos na desflorestação e mineração, comprova o aumento de metais pesados no registro sedimentar. Nesta fase observou-se ainda um elevado aporte fluvial/continental, com maior diversidade de espécies devido à consequente disponibilidade de nutrientes e partículas finas. Embora a entrada de sedimentos possa ter aumentado, a taxa de acumulação ainda é muito baixa quando comparada com outros setores da margem continental portuguesa.

Palavras-chave: Dinâmica sedimentar; Esporão da Estremadura; *Proxies* paleoambientais; Evolução Holocénica; Análise de tendência textural

TABLE OF CONTENTS

TABLE OF FIGURES

TABLE OF TABLES

TABLE OF ANNEXES

LIST OF ABBREVIATIONS

APA	- Portuguese Environmental Agency
cal BP	- calibrated years before the present
CF/CS+SML	- Constant Flux Constant Sedimentation +surface mixed layer models
CLIMAP	- Climate: Long range Investigation, Mapping, and Prediction
CTD	- conductivity, temperature, and depth
ENACWst	- Eastern North Atlantic Central Waters of subtropical
EF	- Enrichment factor
GSTA	- Grain Size Trend Analysis
INAG	- Water Institute
IPC	- Iberian Poleward Current
LGM	- Last Glacial Maximum
MAR	- Mass accumulation rate
NEA	- North East Atlantic
NIOZ	- Royal Netherlands Institute for Sea Research
N.R.P.	- Ship of the Portuguese Republic
RSL	- Relative sea level
SAR	- Sediment accumulation rate
SEPLAT	- Sedimentary Deposits of the Portuguese Shelf and Upper slope Program
SNIRH	- National system of geographic information of water resources
SPM	- Suspended particulate matter
TC	- Total carbon
TIC	- Total inorganic carbon
TOC	- Total organic carbon
XRD	- x-ray diffractometry

Chapter I – Introduction and objectives

1.1. Introduction

Continental shelves are very sensitive marine ecosystem hotspots due to their diversity and biota, abundance of sunlight and proximity to nutrient and particle sources. The continental shelf is the part of the seafloor most used by society but, according to Chiocci & Chivas (2014) shelf areas account for little more than 8 % of marine areas of the world. The knowledge and understanding of the spatial and temporal natural seafloor patterns and variability can be of critical importance. Such knowledge can also support important and diverse economic activities (such as navigation, recreation, mineral exploration and production of renewable energy) and be crucial for the installation of seafloor engineering structures (cables, pipelines, platforms), and fishery economy (trawling, dredging, aquaculture), as well as for environment protection measures (e.g. oil-spill remediation).

Being a dynamic entity, the continental shelf characteristics are the result of the complex interplay between many processes and phenomena, as synthetized at Figure 1.1.

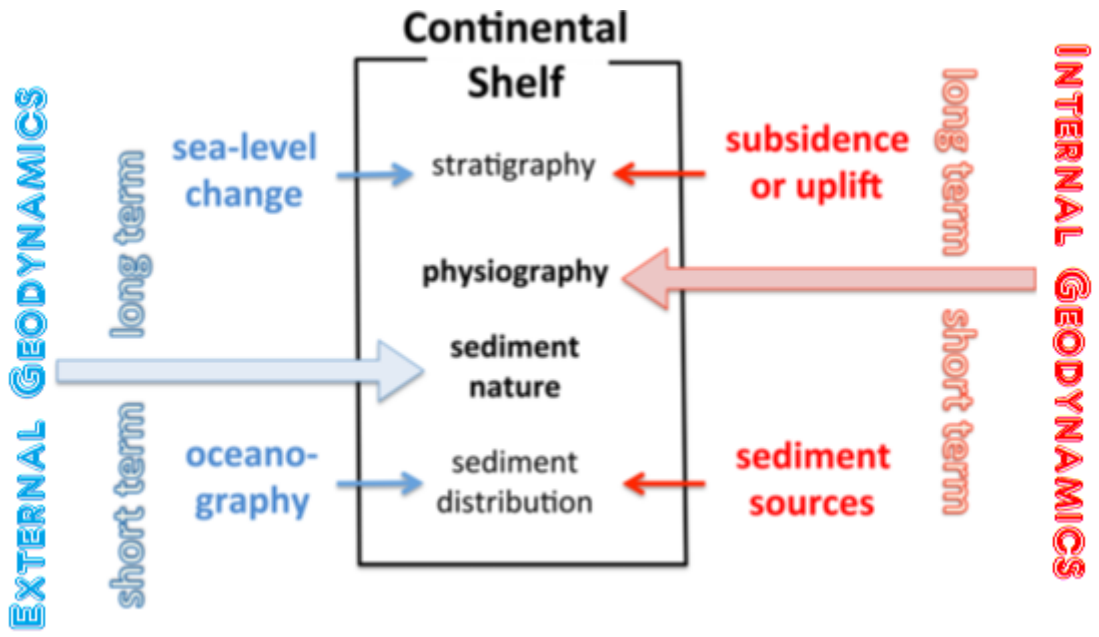

Figure 1.1 - Factors that control shelf character - Geological timescales (Chiocci & Chivas 2014).

Long-term endogenous processes, such as the subsidence or uplift of crustal masses, constrain the shape and morphology of the continental shelf. The origin and distribution of the geologic formations reflect the nature of the outcrops, coastal and shelf geomorphology. Earth surface processes, associated with the physical, biological and chemical processes acting across

the terrestrial landscape, are responsible for the sediment delivery to the shelf and constitute the primary sources for terrigenous particles. Sea level changes and oceanographic forcing (waves, currents and tides) constrain the sedimentary dynamics and the distribution processes across the continental shelf.

The scheme of Figure 1.1 -highlights a delicate equilibrium between internal and external geodynamic processes and also the fact that marine sediments are detailed archives of environmental changes, through the geologic time until the present day and provide a unique opportunity to understand past evolution of sediment supply and distribution processes, particularly those related to environmental changes. Therefore, the study of the continental shelf sedimentary dynamics, across a wide range of spatial and temporal scales, by the international research community has received a lot of attention.

In Portugal, many research projects and studies were performed in the last 40 years in the continental shelf by several generations of marine scientists (Figure 1.2).

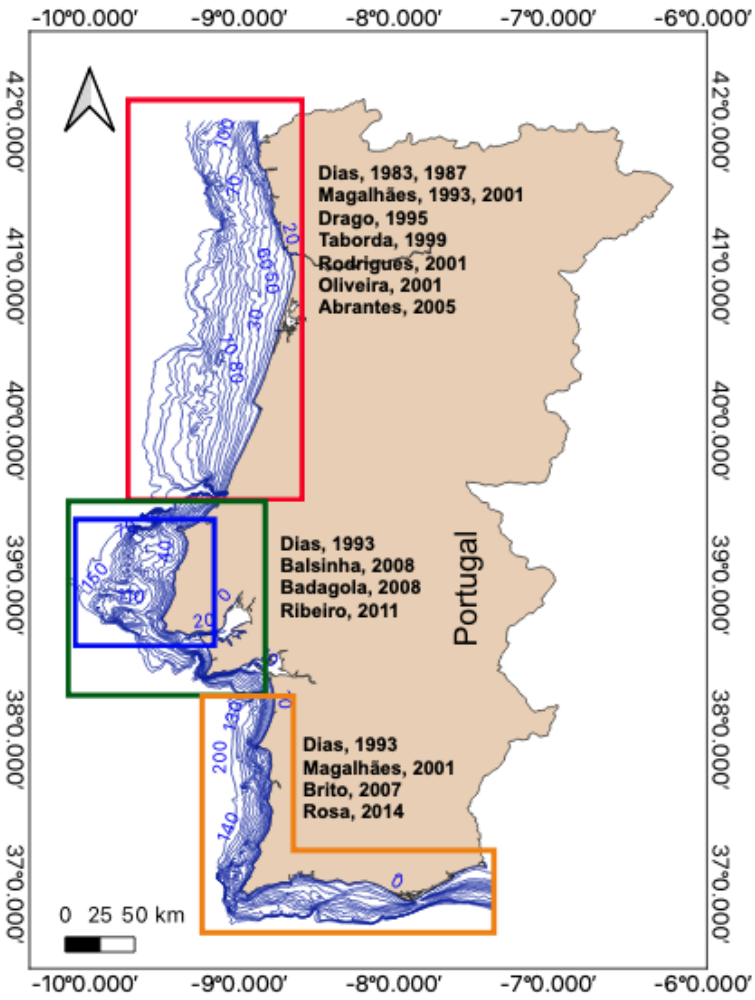

Figure 1.2 - Previous studies (MSc and PhD thesis) on the Portuguese continental shelf red – north sector; green – central sector; yellow – south sector; blue – study area.

Detailed descriptions of marine sediments of the continental shelf were presented by Dias (1987), Magalhães (1993, 2001), Abrantes (1994), Drago (1995), Roque (1998), Cascalho (2000), Pombo (2004) and Balsinha (2008). Studies concerning the sedimentary dynamics are also identified in Figure 1.2 (Taborda, 2000; Oliveira, 2001 and Abrantes, 2005), as well as the structural and tectonic characterization of the Portuguese margin (Musellec, 1974; Mougenot, 1976, 1989; Vanney & Mougenot, 1981; Rodrigues, 2001 and Badagola, 2008).

Despite those references, the knowledge on the sedimentary dynamics of the Portuguese continental shelf is still incomplete, thematically and geographically heterogeneous.

1.2. Research objectives and thesis organization

At the west border of Iberia, the Estremadura Spur represents a remarkable morphostructure feature which stands out in any geological and geomorphological map. Since its individualization, during the early stages of the origin of the Atlantic Ocean, Estremadura Spur has experienced a peculiar evolution different from the ones occurring at the nearby areas, with a deeper shelf break, and with minor influence from sedimentary processes occurring at adjacent continental shelf sectors. This distinctive regional setting is the reason why Estremadura Spur has revealed itself as a key sector in the study of recent evolution of sedimentary systems and the evaluation of the impact of environmental and climate changes in the marine environment. Benefiting from this distinctive setting, this work addresses the study of the sedimentary processes affecting the Estremadura Spur with the general aim of increasing the understanding on the evolution of marine systems in the context of environmental and climate changes. With this goal in mind, a multidisciplinary approach addressing the following topics was performed:

- Morphologic and sedimentary cover characterization of the Estremadura Spur, with description of sedimentary deposits, how they are distributed in the continental shelf and its characterization (textural and composition) (Chapter II);
- Description of present-day main sediment sources at the Estremadura Spur (Chapter III);
- Characterization of source-to-sink processes deduced from particle characterization and environmental context (Chapter IV);
- Characterization of the temporal evolution at Ericeira shelf during Late Quaternary (Chapter V);
- Definition of an evolution model for the Estremadura Spur since the Last Glacial Maximum (Chapter VI)
- Final considerations and future work to be developed in the studied area (Chapter VII).

The first chapter introduces the research theme, the motivation, the study area, the objectives to be attained and the document organization.

Chapter II – Estremadura Spur continental shelf

This chapter is dedicated to the description of the Estremadura Spur, highlighting its morphologic peculiarities and the sedimentary cover as well as a brief description on climate and oceanography.

2.1. Regional setting

With a triangular shape, the Estremadura Spur is a prominent geomorphological unit that stands out from the general morphology of the West Iberian Peninsula (Badagola, 2008). The littoral zone of the Estremadura region is characterized by a coastal plain, bounded on the east by Serra Montejunto and south by Serra de Sintra. The continuation of these reliefs into the oceanic domain explains the intense roughness of the seabed and the existence of several reliefs (Figure 2.1).

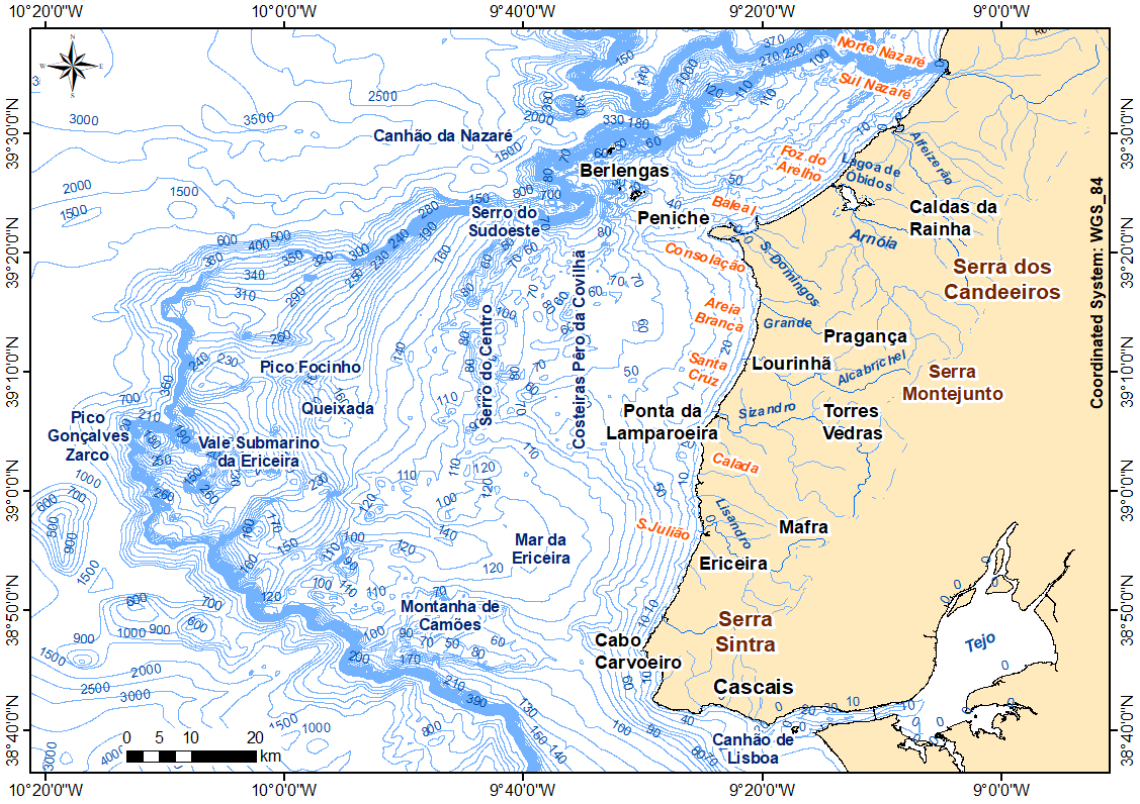

Figure 2.1 - Location of Estremadura Spur
Blue – rivers; orange – beaches; black – local cities; brown – principal reliefs; blues – submarine reliefs.

At north, Lagoa de Óbidos is a separate shallow sedimentary basin of the marine environment, formed by a string of coastal dunes, which isolate the lagoon from the coastal system (Freitas, 1989; Malhadas *et al.*, 2009). The main small watercourses, usually with dendritic

geometry and draining in natural regime are the Alfeizerão, Arnóia, S. Domingos, Grande, Alcabrichel, Sizandro and Lizandro rivers (Figure 2.2).

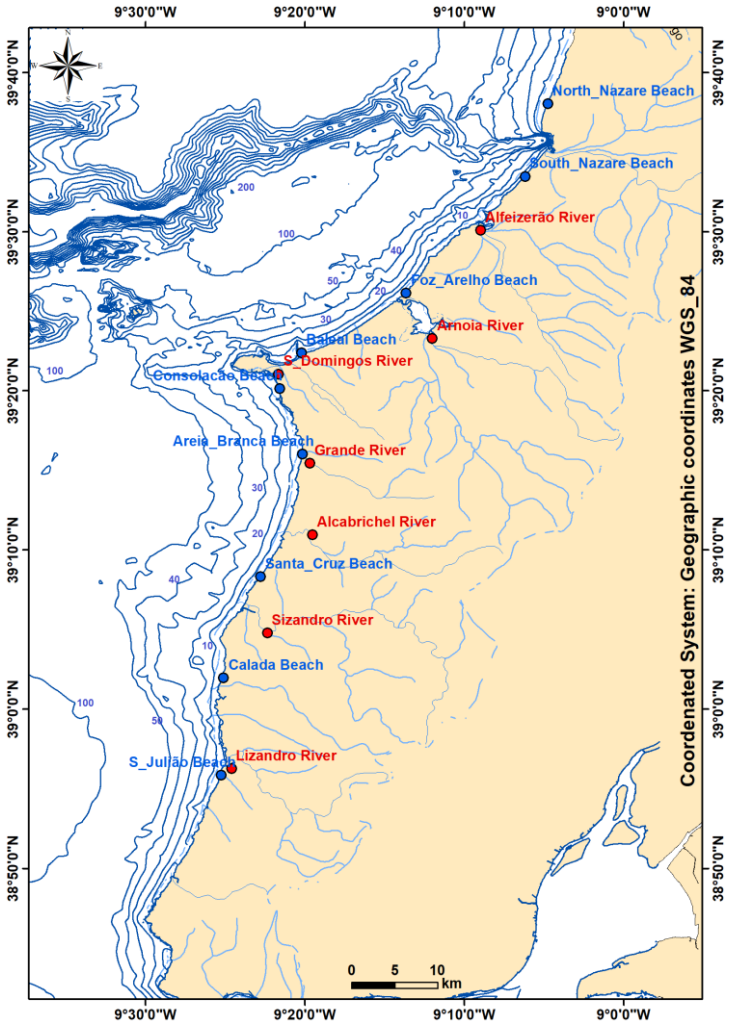

Figure 2.2 - Location of rivers and beaches of the study area
Bathymetry from Instituto Hidrográfico (line spacing of 10 m till 50 m; 100 m; 200 m; 500 m till 4000 m).
Drainage network from SNIRH (https://snirh.apambiente.pt/)
Rivers (red); Beaches (blue).

According to Manuppella *et al.* (1999) the Alcabrichel river and some of its watercourses have terrace deposits, represented by sand and gravel, particularly at 20 and 30 m of altitude. Along major rivers there are landslides, particularly developed in Alcabrichel river that can reach 21 m thick. These landslides are formed by silty mud with mollusks shells and in the base present gravelly deposits (Manuppella *et al.*, 1999).

2.1.1. River Runoff

The characterization of the precipitation is based on study carried out in Part 2 of the PGRH (Plano de Gestão da Região Hidrográfica do Tejo e Ribeiras do Oeste 2009-2015). The precipitation analysis in the hydrographic region began with the collection of the data compiled

in the National Water Resources Information System (SNIRH) (https://snirh.apambiente.pt/), of the hydrological years between 1940/1941 and 2007/2008. The udometric network susceptible to be used in the annual rainfall characterization was based on the existing records of 15 years. A total of 171 stations were used in the Tejo basin and 24 in the Ribeiras do Oeste, western streams basin (APA – Plano de Gestão de Região Hidrográfica, 2016).

In the river basins of the Ribeiras do Oeste, it was observed that the most frequent values of the annual precipitation are concentrated between 600 mm and 1100 mm, representing about 84 % of the occurrences.

Óbidos has lower average annual precipitation and the highest precipitation occurs in the Serra dos Candeeiros area (northeast border of the basin). As for the average monthly distribution of precipitation in the watersheds of the western streams, this does not differ significantly from that recorded for the generality of the country, with about 75 % of precipitation occurring in the wet semester and only 25 % remaining in the dry semester. Precipitation data from Pragança meteo station show that precipitation varied from 552 to 826 mm in the years 2008/09 and 2011/12 to 826 to 1223 mm during the years 2009/10 and 2010/11.

The average annual distribution of the flow, which is essentially the distribution of mean annual precipitation, is characterized by a great variability of the monthly flow, which is also present in the different river basins.

Table 2.1 shows the annual values of flow in natural regime.

Table 2.1 - Average annual flow (hm^3) from Ribeiras do Oeste rivers (https://snirh.apambiente.pt/).

Hydrographic Basin	Average annual Flow (hm^3)		
	80 % (humid year)	50 % (mean year)	20 % (dry year)
Arnóia	171	94	17
S. Domingos	23	12	1
Alcabrichel	52	28	4
Sizandro	101	52	4
Lizandro	51	28	5

2.2. Geomorphology

2.2.1. Coastal zone

The Estremadura coastline is almost exclusively formed by cliffs, cut in limestones, marls and sandstones, with localized dune systems occurring near river's mouths, except for the northern littoral stretch (Norte Nazaré beach – Baleal beach) where the sandy coast is backed by a dune field (Santos *et al.*, 2014; National System of Information Resources of the Littoral – INAG; Marques *et al.*, 2013).

Immediately south of Peniche, down to Ericeira, the littoral landscape is dominated by rocky steep cliffs (up to 80 m command) cut in Jurassic and Cretacic formations (Manuppella *et al.*, 1999) with frequent abrasion platforms. The small promontories give the coast a carved character with isolated recessed or semi-recessed sandy beaches, located near river mouths. These

sandy beaches, such as Santa Cruz and São Julião, are generally narrow but well defined associated with sedimentary retention promoted by headlands (Figure 2.3).

Figure 2.3 - Lizandro river mouth (http://portugalfotografiaaerea.blogspot.pt).

The coastal sector between Peniche and Ericeira (Figure 2.4) accommodates numerous embayed beaches (Figure 2.5) (Ponte Lira *et al.*, 2016).

Figure 2.4 - Ericeira village (http://portugalfotografiaaerea.blogspot.pt

Figure 2.5 - Calada beach (http://portugalfotografiaaerea.blogspot.pt)

South of the study area, the Tejo river is the main regional sediment source to the continental shelf, with an average annual water discharge ranging from 80 to 720 $m^3.s^{-1}$ (Loureiro & Macedo, 1986; Jouanneau *et al.*, 1998) and delivers an average suspended load to the shelf of approximately 4×10^5 $t.y^{-1}$ (Vale & Sundby, 1987) to 6×10^5 $t.y^{-1}$ (Portela, 2004).

2.2.2. Continental shelf

The continental shelf of Estremadura Spur has a variable width, ranging from 15 km (offshore Peniche) to 70 km (at Ponta da Lamparoeira parallel). The shelf break depth is also variable, ranging between ~ 50 m and more than 300 m (Figure 2.6) (Duarte *et al.*, 2017). The study area is limited in the north by Canhão da Nazaré and south by a steep slope highly carved by valleys (Figure 2.6). It has a peculiar morphological characteristic in the way that the shelf break is located at an unusual depth (> 300 m) with maximum depths of 418 m, much deeper than most of the Portuguese continental shelf break (~140 m) (Dias, 1987; Balsinha *et al.*, 2010). The layout of the bathymetry in the inner and middle shelf represents roughly the coastline geometry and its boundary is smooth, although sometimes has some sinuosity, resulting from the presence of rocky outcrops. In general, the irregularity observed in the bathymetric contour of the inner shelf coincides with the offshore extension of the two headlands that shape the coastline of the study area (Peniche and Ponta da Lamparoeira).

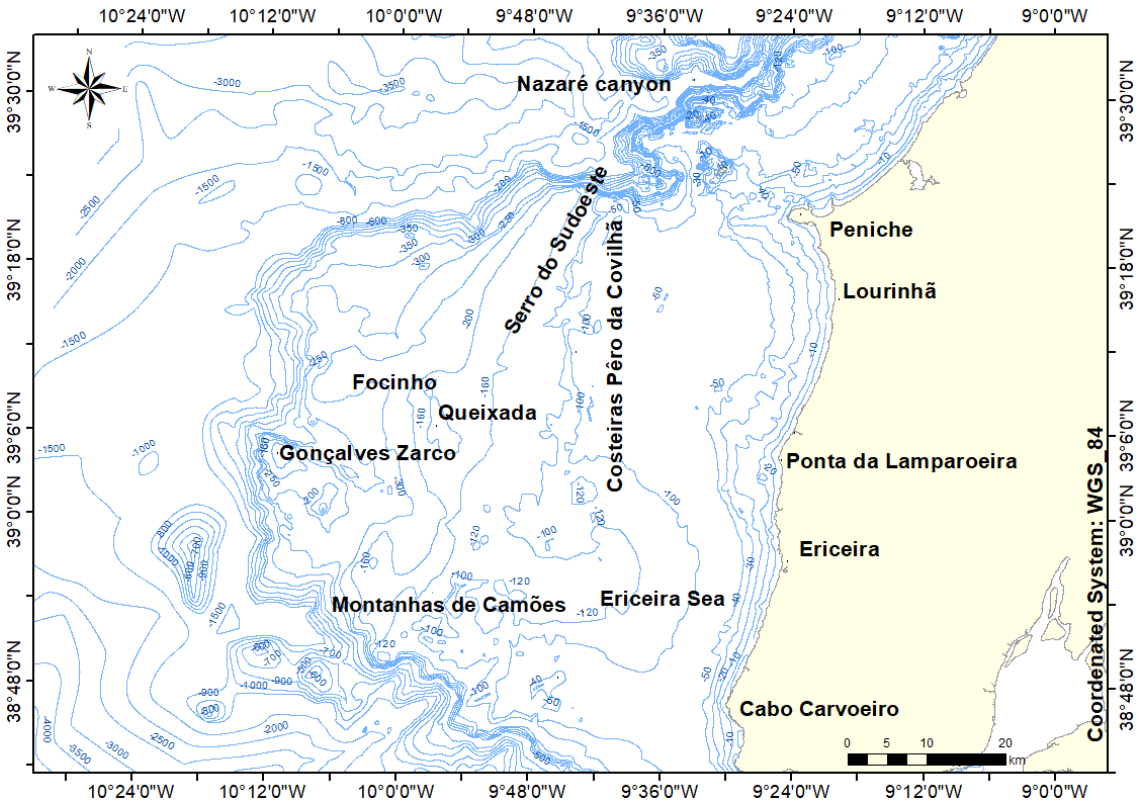

Figure 2.6 - Estremadura Spur bathymetric map with identification of main submarine reliefs Bathymetry from Instituto Hidrográfico (line spacing of 10 m till 50 m; 100 m; 120 m; 160 m; 200 m; line spacing of 50 m till 1000 m; line spacing of 500 m till 4000 m).

The morphology of the Estremadura Spur continental shelf is very peculiar and diversified with important reliefs (extensive outcrops of rocky formations) alternating with smooth monotone areas and irregular valleys, concentrated in deeper domains. As positives reliefs, the bathymetric chart allows the identification of the Berlengas archipelago (off Cabo

Carvoeiro), the Costeiras Pêro da Covilhã, an elongated NNE-SSW and ENE-WSW oriented relief (average length of 4 km), marking the central Estremadura Spur, immediately south of Berlengas islands and the Pico Focinho and Queixada structures, below 200 m deep. As negative reliefs, the more dominant feature is the Pico Gonçalves Zarco, located in the continental slope off Ericeira, near the wide and smooth Mar da Ericeira.

The slope of the morphological surface (Figure 2.7), presents clear latitudinal and longitudinal differences. The sectors where slope presents values higher than 0.31 % are associated with the reliefs over the continental shelf and along the continental slope, where values generally exceed 5 %.

Within such a wide area, the marine processes show a large spatial variability, therefore a subdivision is useful to study and describe the marine environment in the different continental shelf domains. Regarding this division, there were no particular criteria or limits analyzed to differentiate between inner, middle and outer shelf than oceanographic, sedimentological or geomorphological criteria. For the purpose of this study, the geomorphological criteria seem to be the more adequate and it will be applied to the Estremadura Spur description.

A total of 14 E-W profiles were plotted along the entire continental shelf (Figure 2.8) to define the morphological criteria that would allow the segmentation of the Estremadura Spur shelf. By the observation of those profiles, variations in slope can be used to individualize subsectors of the continental shelf and identify some heterogeneities on the Estremadura Spur.

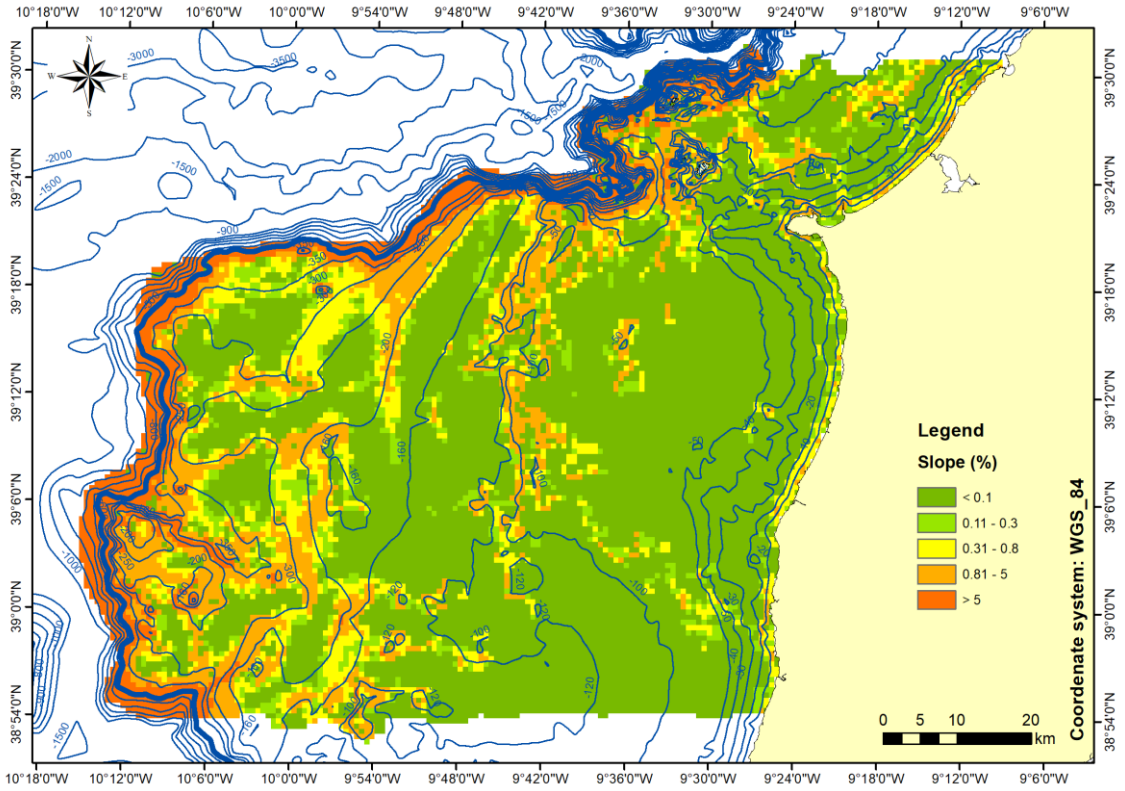

Figure 2.7 - Slope of the Estremadura Spur (Balsinha, 2008).

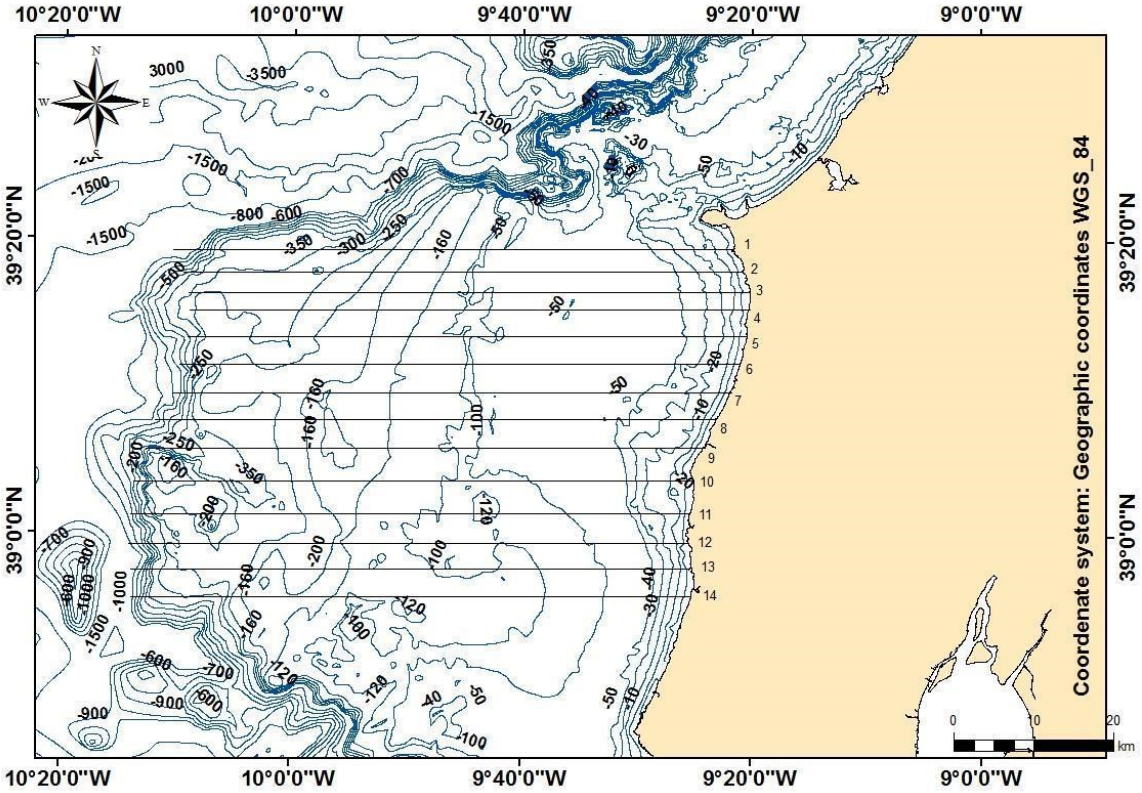

Figure 2.8 - Bathymetric map of Estremadura Spur, with the 14 E-W profiles

From the analysis of those profiles, represented in Figure 2.9, the location of subdivisions was established based on slope variations and discontinuities in the general geometry (Figure 2.10). Results indicate that the offshore inner shelf limit ranges from 20 m (at 1.9 km from the coastline) to 40 m depth (6 km from the coastline) with an average depth of about 30 m.

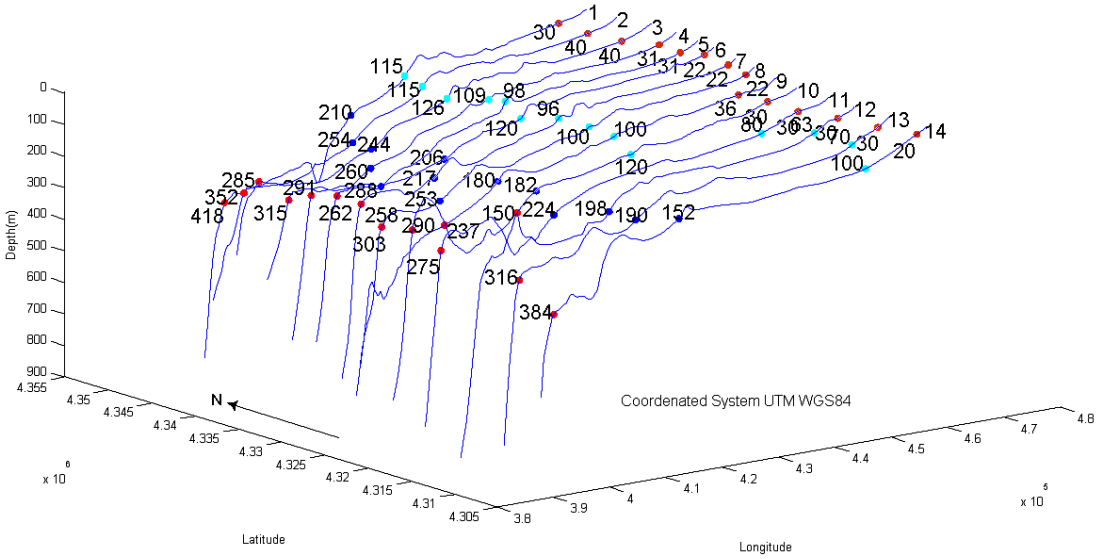

Figure 2.9 - The 14 bathymetric profiles with indication of the shelf domains orange: inner shelf; light blue: middle shelf; dark blue: proximal outer shelf; red: distal outer shelf and shelf break.

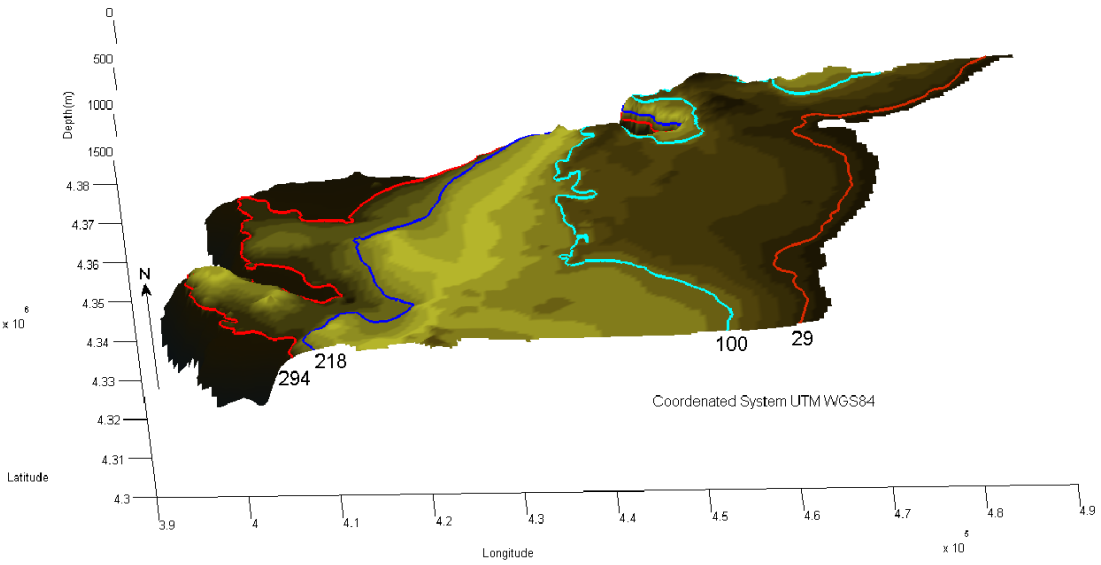

Figure 2.10 - Digital terrain model of Estremadura Spur with the boundaries of shelf domains orange line – limit between inner and middle shelf; blue line – limit between middle and proximal outer shelf; dark blue line – limit between proximal and distal outer shelf; red line – limit between distal outer shelf and shelf break.

The middle shelf is defined onshore by the limit of the inner continental shelf while the offshore boundary depth varies from 63 m (at 14 km from the coast in the southern sector) to 126

m depth (at 36 km from coast in the northern sector) with a mean depth of 100 m. This frontier marks the boundary from an internal irregular morphological domain, where contour lines display a sinuous and irregular pattern, with several elongated reliefs of varying morphological expression, to an external lower domain of smoothed bathymetry with regular contour lines. This morphologic contrast is quite evident in the northern sector, north of Ponta da Lamparoeira. At the southern sector, the shelf profile has a smooth gradient without any significant irregularities, except for the presence of several deep morphological features (Pico Focinho, Queixada e Pico Gonçalves Zarco).

As mentioned before, the southern middle shelf of the Estremadura Spur is dominated by the Mar da Ericeira, a wide depression slightly elongated in E-W direction, located offshore Ericeira. The basin is wider in its eastern sector (10 km) and narrower in its western sector (3.5 km) and is framed on the north and south by submarine reliefs. In the shallower region, Mar da Ericeira presents an arc convex geometry facing East. In the middle shelf, one can individualize two asymmetric submarine reliefs: the Serro do Sudoeste, with NE-SW orientation, with 14 km extension and the Serro do Centro, oriented N-S, located further south with 15 km extension.

In the outer-shelf domain, due to the sharp notches induced by valleys and gullies, the contour of the shelf break is quite irregular along its entire length. The bottom intense gullied morphology and the steep gradients suggest that the shelf break might be agradational to retrogradational, meaning that no accumulation occurs, and erosional processes can dominate, sometimes with active downslope mass movements. However, at the north side, between the meridians 9º 48' W and 9° 55' W, there is a smooth transition which leads us to characterize the morphology of the continental shelf break in this sector as progradational.

At the western edge centered on the parallel 39º 10’ N, there is a noticeable indentation of approximately 18 km and the shelf break retreats almost 6.5 km, assuming an arcuate configuration. Further south, the Pico Gonçalves Zarco is the most remarkable morphological feature, dominating the area off Mar da Ericeira. This valley is a rectilinear submarine deeply embedded depression, with low-sinuosity with SI values (sinuosity index) of 1.15, which provides substantially deep grooving from 260 m depth to deeper domains (Badagola, 2008). Sinuosity Index (SI) is defined as the ratio between the distance measured along the channel and the distance measured following the direction of the overall planimetric course (Leopold & Wolman, 1957).

The outer continental shelf is defined between the deeper limit of the middle continental shelf (around 100 m depth) and the shelf break. Considering that in this peculiar continental shelf, the outer shelf occupies almost half of the entire area of the Estremadura Spur, it was reasonable to divide the outer shelf into two domains named proximal outer shelf and distal outer shelf.

The shallower limit of the proximal domain of the outer shelf corresponds to the deeper limit of the middle shelf (around 100 m depth). From the profile analysis, one can say that the inferior limit for the proximal outer shelf domain, is very irregular, because values range from

minimums of 152 m depth (44 km from coast in the southern domain) to 288 m depth (58 km from coast in the northern domain) (Figure 2.9 and Figure 2.10). The distal outer shelf domain is comprehended between this depth and the shelf break (~ 300 m).

Considering the description of the shelf break, the minimum value was observed at 150 m depth (southern sector) and a maximum value of 418 m depth (northern sector) (Figure 2.9). The mean of all shelf break values for the 14 profiles allowed to establish an average value of ~ 300 m (Figure 2.10).

2.3. Geology

The oldest formations outcropping in the Estremadura inland are Jurassic in age (in the north region of Torres Vedras, Mafra and Sintra (Figure 2.11a)), corresponding to a thick carbonate series formed during the Mesozoic rifting phases. These carbonated formations extend to the entire continental shelf of the Estremadura Spur (Figure 2.11b) (Duarte *et al.*, 2017). Only south of Ericeira, younger Cenozoic formations can be found at the middle and outer shelf, probably in tectonically depressed basins (from Boillot *et al.*, 1978).

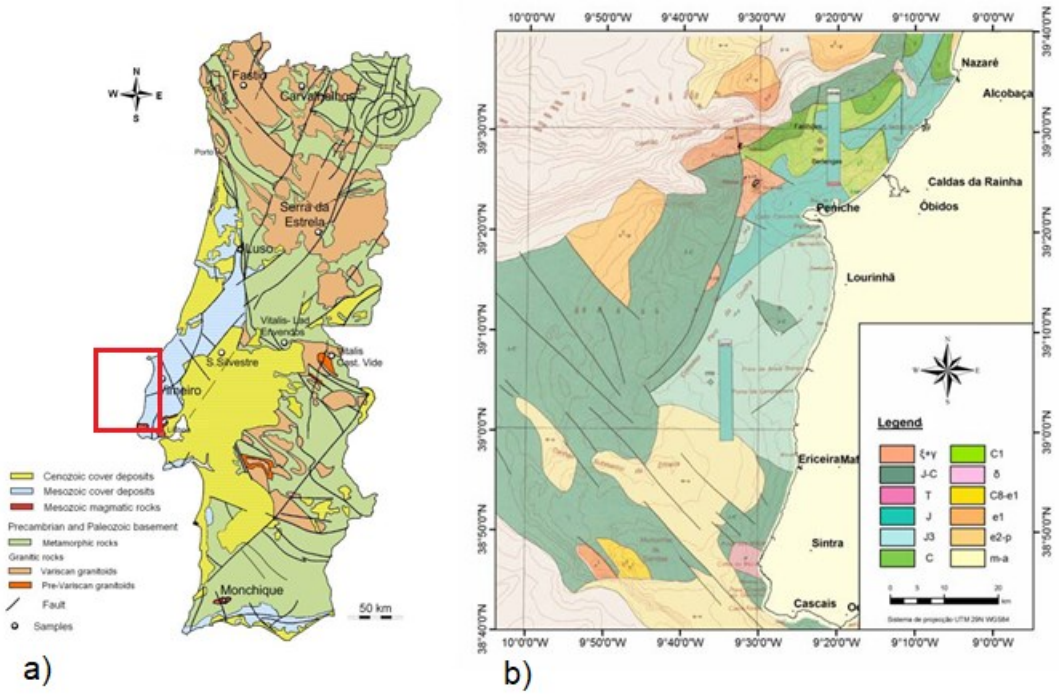

Figure 2.11 - Geological map of Estremadura Spur
a) Simplified Portuguese Geological map (Ribeiro *et al.*, 2014) with the location of the study area; b) Extract from Portuguese Geological map of Estremadura Spur. Scale 1:500 000 (from Boillot *et al.*, 1978). Legend: ξ+γ - Paleozoic undifferentiated; T - Infra-Lias and Triassic; J - Jurassic undifferentiated; J3 - Upper Jurassic (Malm); C - Cretaceous undifferentiated; C1 - lower Cretaceous (Cenomanian Berriasian); J-C - Jurassic-Cretaceous undifferentiated; δ – Sintra igneous Massif (Upper Cretaceous); C8- e1 - Maastrichiano Eocene-inf. e1 - Eocene inf.; e2-p - Upper Eocene and Neogene; m-a -Neogene and Pleistocene.

The upper Cretaceous was marked by an important epirogenic phase and signs of magma manifestation, with the installation of the Mafra complex (100 Ma, Ribeiro *et al.*, 1979).

According to Berthou (1973), the Cenomanian transgression imprinted on sediments of the Lusitanian Basin a marine signature well represented in the upper Cenomanian, which corresponds to a mega-transgressive sequence.

During the Paleocene-Eocene the mean sea level (msl) remained stable. Inland, formations of this age are only documented as continental sequences (Benfica complex), while in the continental shelf, Musellec (1974) and Mougenot (1976) concluded that marine Paleogene covers a massive area north of the Canhão da Nazaré (Musellec, 1974) and occasionally, the continental shelf to the south. Mougenot (1976) refers only to bioclastic limestones sampled in Montanha de Camões, whose age is attributed to the lower Eocene. In a sample taken west of Serro do Sudoeste, the author describes sedimentary facies with lamellibranches, gastropods (*Elphidium*), echinoderms and rare foraminifera in quartz sandstone, assigned to the Pliocene.

In terms of geological structures and deformation styles, the geological map of the continental shelf indicates that deformation is predominantly fragile, although some local ductile structures can be identified. At the continental shelf north of Nazaré, the structure is represented by a monoclinal slightly tilted to W-NW. The occurrence of three diapiric domes structurally breaks this monotony (Boillot *et al.*, 1972) and induces ductile deformation. At the Estremadura Spur, the presence of diapiric activity is eluded by Vanney & Mougenot (1981) to justify the presence of a depression in the inner shelf off Lourinhã.

In terms of fragile structures, two sets of faults stand out: NE-SW to NNE-SSW and NW-SE to NNE-SSW. The direction NE-SW to NNE-SSW (sub-parallel to the Nazare fault) is observed between Costeiras Pêro da Covilhã reliefs and Cerro do Sudoeste. These faults are responsible for the outcrop of several Paleozoic formations, as in Lourinhã marginal "horst", included in Costeiras Pêro da Covilhã and in Berlengas "horst". The NW-SE direction is observed mainly south of latitude 39º 05' N, affecting the Mesozoic sequence and controlling the boundaries of younger Neogenic basins.

South of Ponta da Lamparoeira, in the inner shelf domain, symmetrical folds NE-SW identified by Mougenot (1976) affect Neogenic and Mesozoic formations as result of the effect of reactivation of deep fractures.

At the top of the stratigraphic column, a thin layer of unconsolidated sediments represents the youngest geologic unit. Covering meso-cenozoic formations, this unit was deposited over an extensive erosional surface, and comprehends terrigenous sediments originated from erosional processes, which affect the exposed formations in the adjacent inland and littoral. Due to the succession of quaternary glacio-eustatic cycles, different marine sedimentary systems experienced spatial and facies variations, as the climate and oceanographic regimes changed. Since the work performed in the North Atlantic deep basin (summarized in Ruddiman &

McIntyre, 1981) that the evolution of the location of the polar front since the Last Glacial Maximum (20 000 – 18 000 years ago) until present time is well known. Due to the northward migration of the polar front, the position of the msl rises from -130 m to its present position. This important climate study allowed Dias (1987) to establish the first Portuguese msl curve for the post-glacial period and Dias *et al.* (2000) and Rodrigues (2001) applied this curve to determine the distribution of littoral and fluvial systems during the post glacial evolution. These authors attributed to the erosional surface under the sedimentary layer an origin related to the marine abrasion (during the sea level fall) and a pos-glacial age for the uppermost sedimentary layer.

2.3.1 Sedimentary cover

In the Estremadura Spur, the recent sedimentary cover is generally very thin with high spatial variability due not only to the sedimentary processes but also to the imprint of the recent climate changes and related oceanographic processes.

The superficial sedimentary deposits of the Portuguese continental shelf were extensively studied by several authors concerning the surface sedimentary deposits of Portuguese continental shelf (Dias, 1983/85; Abrantes, 2005; Magalhães, 2001; Pombo, 2004 and Balsinha, 2008). In the present study the sedimentary cover was described using 66 samples (Figure 2.12), collected under the scope of the SEPLAT Program (*Sedimentary Deposits of the Portuguese Shelf and Upper slope*).

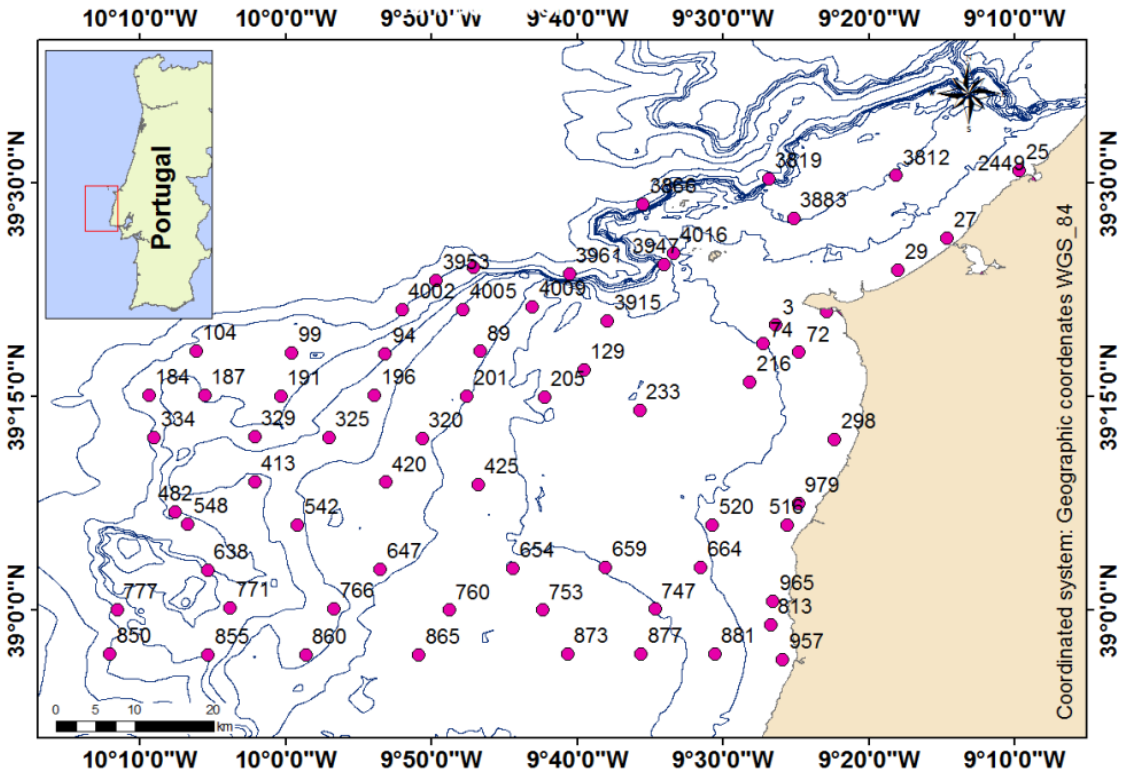

Figure 2.12 - Location of the sediment samples collected under the SEPLAT program.

The SEPLAT Program was undertaken by the Portuguese Instituto Hidrográfico, and is based on a regular sampling grid that considers the collection of a representative sample of the sea bottom in each nautical mile and respective laboratory classification (grain-size and calcium carbonate content). Final products are 8 sedimentological charts of the continental shelf between the coastline and the 500 m isobath. Additionally, the sandy fraction was analyzed under a microscope for a morphoscopic description and compositional analysis.

The first sedimentary deposit description of the Estremadura Spur was presented by Balsinha (2008), which considered the sediment grain size, composition and depth of the studied sedimentary samples (Figure 2.13). A brief description of the laboratory methods is presented in Annex 1.

In Figure 2.13 are highlighted the main aspects regarding the Estremadura Spur sedimentary cover.

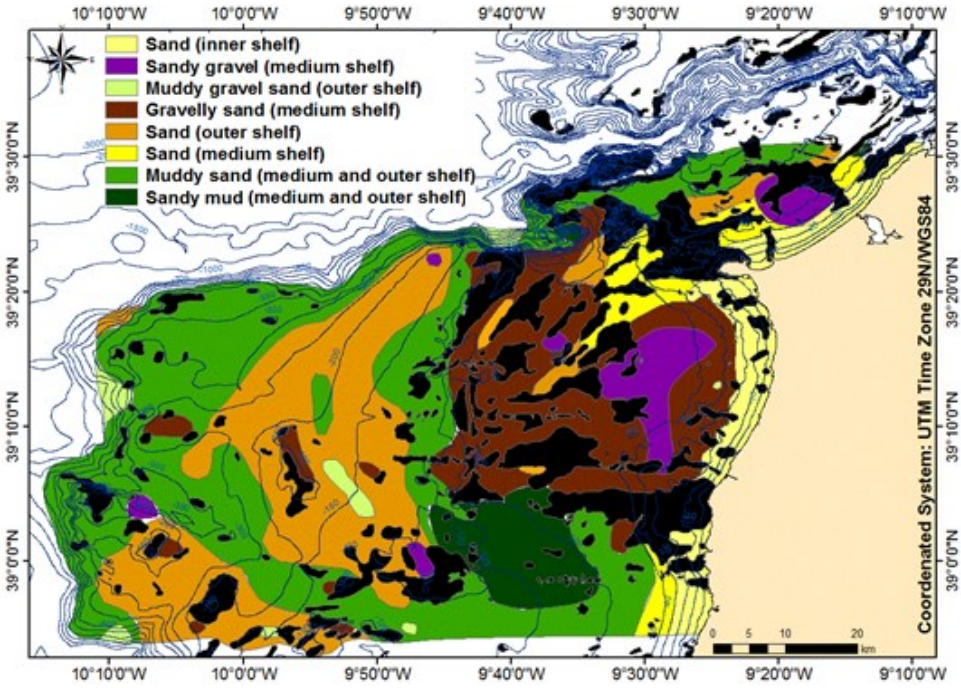

Figure 2.13 - Sedimentary deposits continental shelf; rocky outcrops are marked in black (Balsinha, 2008).

The density of outcrops indicate that the sedimentary layer is relatively thin and local contribution (both detritical and biogenic particles) must be significant. There is a large area of the continental shelf covered by very coarse sediments (sandy gravel to sand) and finer deposits (muddy sand) can be found only in the southern middle shelf, at Mar da Ericeira. This distribution is related to sediment transport processes and distance to particle sources. The composition analysis of the sandy fraction, expressed on Figure 2.14, also reflects the relation between these parameters and the presence of rocky outcrops.

Storm-dominated shelves, such as the Estremadura Spur, are typically characterized by an offshore progressive decrease in sediment grain-size as the amount of sand-size (primarily quartz) sediment deposited by storms decreases (Brooks *et al.*, 2003).

In the study area, the inner shelf is constituted by fine-grained sand-rich deposits, composed mainly by quartz grains, mollusks and other biogenic particles (remains of corals, fish vertebra, bryozoans, echinoderms and spicules of sponges). In general, considering the sediment composition, the ***inner shelf sands*** are mainly constituted by terrigenous particles (supplied by rivers and cliff erosion).

Middle shelf sediments are generally coarser than inner shelf ones. In the northern sector, the sedimentary cover is, in general, composed by very coarse-grained deposits. At 40 m depth, the inner shelf sands, transit abruptly to an extensive ***gravelly sand deposit*** with a nucleus of ***sandy gravel*** (approximately at 60 m depth). These deposits are mainly constituted by coarse particles (mean grain-size of 2 mm), like aggregates (mainly lithoclasts), mollusks and other biogenic particles (including remains of corals, fish vertebra and bryozoans). These deposits are characterized by a mixture of relict and modern particles, indicating that they are not currently being supplied to the sedimentary layers, but inherited from previous sedimentary cycles (Magalhães, 2001; Dias *et al.*, 2000).

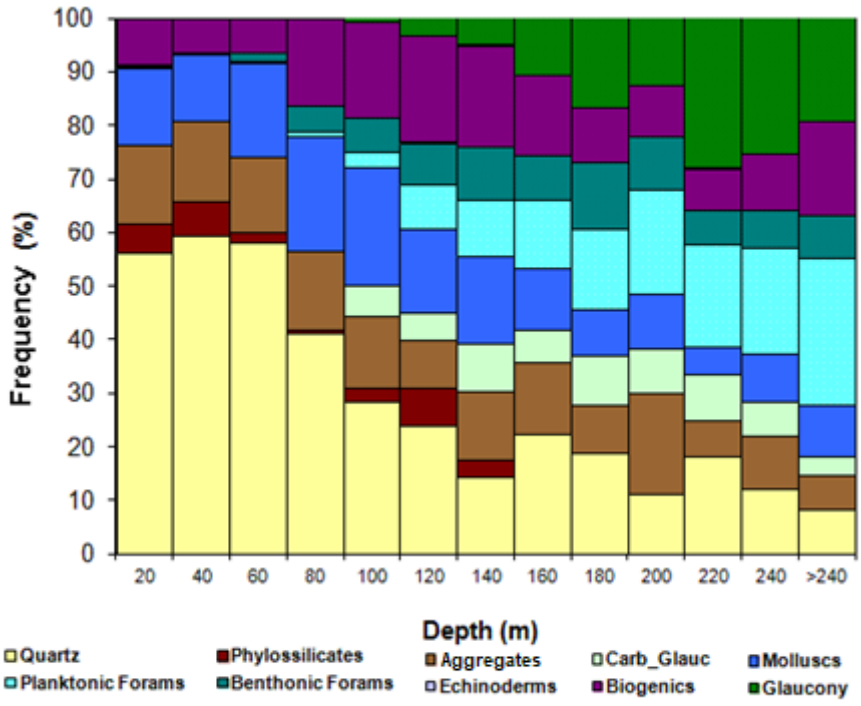

Figure 2.14 - Diagram of average percentage distribution along depth; sand compositional classes, for different depth classes (Balsinha, 2008).

In the southern sector, the middle shelf is mainly covered by fine and muddy sand deposits. The fine-grained sandy deposits have a similar composition to the littoral sands while the muddy sand deposits are composed essentially of planktonic organism, other biogenic particles and carbonates with glauconitic remains. The mean grain size of the ***muddy sand deposit*** is 0.125 mm (Balsinha, 2008). The ***sandy mud deposit*** located at Mar da Ericeira presents a mean grain-size of 0.028 mm. This sandy mud deposit is mainly composed of very fine particles of quartz, phyllosilicates, benthic and planktonic foraminifera (Balsinha, 2008).

Being the most extensive sector of the Estremadura Spur continental shelf, the outer shelf is covered by ***sand***, ***muddy sand*** and ***sandy mud***. The sandy deposits are present between 150-250 m depth, in a long elongate deposit, generally parallel to the coast line, only interrupted by Vale Submarino da Ericeira. In terms of composition, the more abundant particles of these deposits are biogenic particles (planktonic and benthic foraminifera), glaucony and aggregated particles formed by carbonates and glaucony, with minor contribution of quartz and aggregates, indicating a deficiency on present day terrigenous contribution.

The described sedimentary pattern agrees to the general processes expected to occur in this sector of the Portuguese margin. There is an active transport of sandy particles along the inner shelf promoted by the wave regime. Below this domain, sediments become muddy sands, as modern fine particles, transported in suspension, will settle and mix with relict coarser particles. Exceptions to this general model are: 1) the coarser deposits associated to rocky outcrops in the northern middle shelf, where the balance between energetic levels and low sediment input inhibits the deposition of fine grained particles; 2) the finer muddy sand covering the Mar da Ericeira, in a depressed smooth area, immediately south of the extensive rocky outcrops, and 3) the external sandy deposit on the outer shelf, probably reflecting an older deposit, not covered by recent particles due to the effect of oceanographic processes acting at the shelf break and upper slope and the reduce, or deficient, settling of recent terrigenous fine particles.

Considering the origin of particles, the dominance of the terrigenous contribution is restricted to inner and middle shelf areas (more than 70 % of the sandy particles are quartz, phyllosilicates and aggregates). Below that depth, the biogenic components increase in relation to a relative decrease in the terrestrial source. It is interesting to note that phyllosilicates disappear at 140 m, coinciding with a slight enrichment of quartz and decrease of mollusks (the second more important class of shelf sedimentary cover).

2.4. Oceanographic forcing

2.4.1. Waves

The western coast of Portugal is a high energetic environment which is fully exposed to NW swell from the North Atlantic. According to Andrade *et al.* (2013), the distribution of the significant wave height (Hs) is concentrated in class 1 to 2 m (more than half of the cases); values

between 2 and 3 m account for about 22 % of the observations while values greater than 5 m represent 2.5 % of cases (for values between 1956 – 2009). Offshore wave climate is characterized by an average significant wave height of about 2 m and a peak period of 11 s (Dodet *et al.*, 2010). During storm events significant wave height can exceed 10 m and attain a peak period of 15 s. Near-bed wave orbital velocities vary rapidly in the cross-shelf direction, being relatively high at the inner shelf and negligible at the outer shelf.

The average annual value of Hs is 2 m with a standard deviation of 1.1 m. The average and modal values of Hs agree with the observations made in Leixões (1996-2008) and Sines (1988-2008) reported in the study of Costa & Esteves (2009).

2.4.2. Tides and tidal currents

According to the Portuguese Instituto Hidrográfico tide table, the Portuguese tide is semi-diurnal with periods of 12 h 25 min and spreads northwards. The range varies from 1.5 m during neap tides to 4.0 m during spring tides. In general, the tide ellipses rotation is controlled by the shelf break geometry, although, for Estremadura Spur this pattern has high anomalies, either for diurnal or semidiurnal barotropic velocities. Estremadura Spur shelf-break is also a region where these velocities are higher.

Considering the propagation of tidal current, the bottom morphology of the Estremadura Spur induces a peculiar interference on the tidal effect (Figure 2.15), as observed by Quaresma & Pichon (2013). Quaresma & Pichon (2013) obtained values for barotropic forcing terms of approximately three to four times higher than the ones observed on the rest of the continental shelf. The same study estimates a value of M2+K1 (principal lunar tidal constituent + luni-solar declinational tidal constituent) that will give a limit of tidal stream based on a model validated with *in situ* data (Figure 2.15).

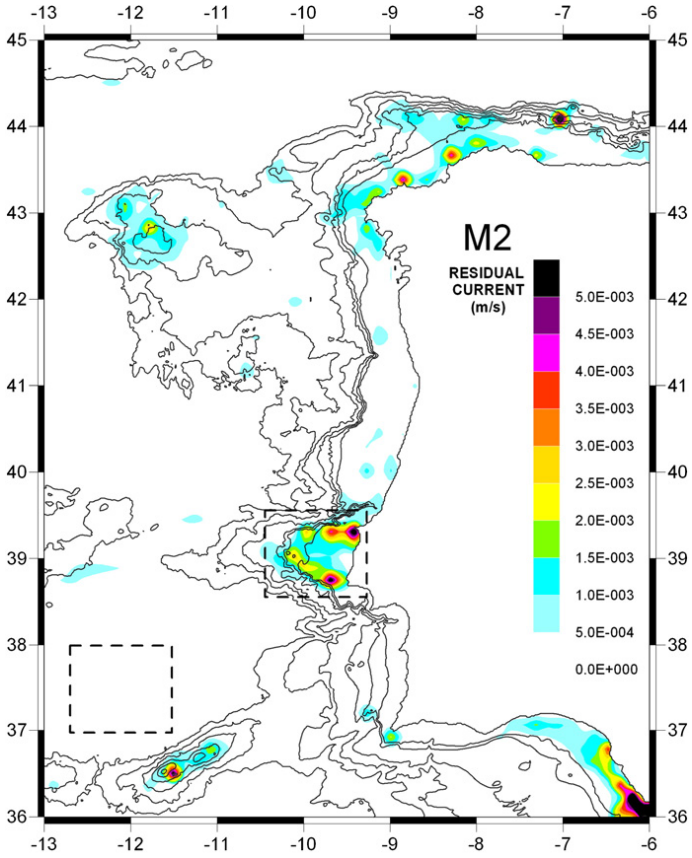

Figure 2.15 - Plot of the component M2 residual current along the Iberian margin (Quaresma and Pichon, 2013).

The region SW of Peniche has values of M2 for current maximum of 10-12 cm/s to which we can add (in a first approximation) the values of K1 (3-4 cm/s) to obtain an estimate value of 15 cm/s at least once a day due to tide diurnal inequality. To this value other velocity components can be added, like speed induced by internal tides and mesoscale processes.

These high values of residual currents induced by M2 in Estremadura Spur will increase the amplitude of local sedimentary processes such as vertical mixing, bottom nepheloid layer formation and dynamics (McCave & Hall, 2002; Quaresma *et al.*, 2007; Arzola *et al.*, 2008).

2.4.3. Currents

According to Teles-Machado *et al.* (2016), the IPC (Iberian Poleward Current) has an important role in driving the seasonal cycle of temperature and salinity in the upper 200 m of the water column. Regarding salinity, the advection terms dominate the salinity budgets seasonal cycle, showing that the seasonal cycle of salinity is mainly controlled by the IPC. Llope *et al.* (2006) analyzed monthly series of CTD samplings from 1993 to 2003 and observed intrusions of Eastern North Atlantic Central Waters of subtropical origin (ENACWst) in the Northern Iberia almost every winter, which suggested the important role of the IPC in driving the average temperature and salinity seasonal cycles on the northern coast. The authors verified that the

seasonal cycle of the temperature is forced by both the circulation (IPC and upwelling) and by local air-sea fluxes (Figure 2.16).

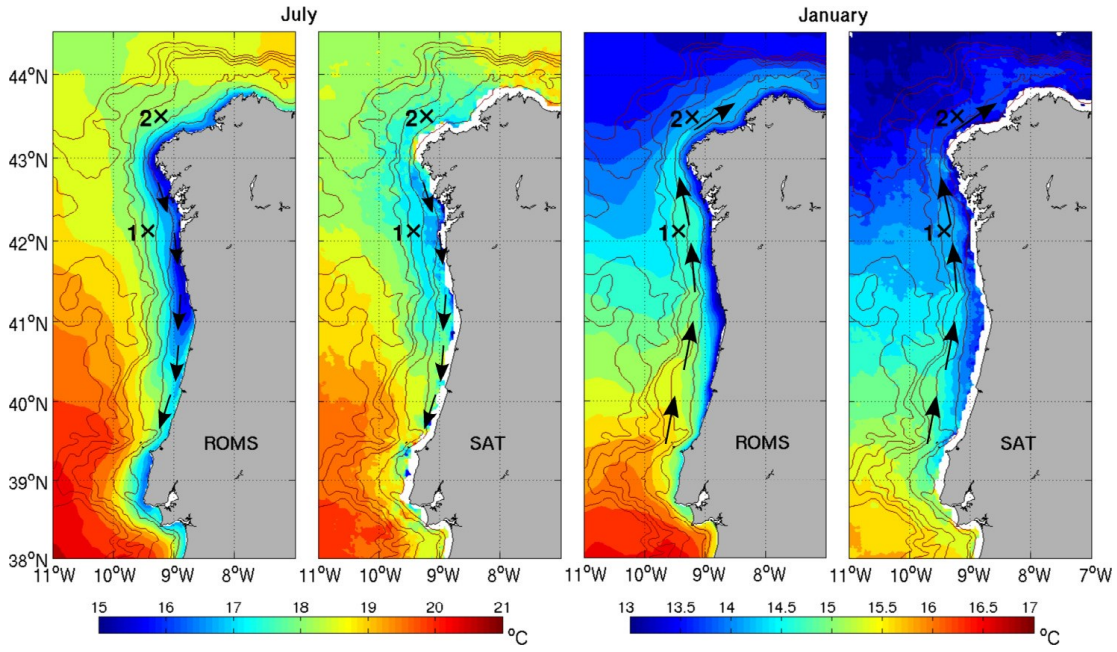

Figure 2.16 - Average SST fields
July (left) and January (right), obtained averaging the 20-year model output (ROMS – Regional Ocean Modelling System), and 20-year PATHFINDER satellite data (SAT). The arrows are a schematic representation of the average typical currents: southward flowing upwelling jet in July, and northward flowing IPC in January. The crosses 1 and 2 represent the position of 2 moored buoys (adapted from Teles-Machado *et al.*, 2016).

In the continental shelf, the circulation is highly conditioned by meteorological conditions. During summer, the regular Trade Winds induce upwelling phenomena, associated with the equatorward flow (present at the continental shelf and slope). When this phenomenon occurs, a poleward subsurface flow is common (Coelho, 2002). When upwelling is established, cold, less salty and nutrient-rich waters are brought to coastal areas, sometimes covering the entire shelf. Offshore coastal areas are characterized by the presence of capes, filaments of detached upwelled water can be formed, reaching more than 200 km offshore (Fiúza, 1983).

In wintertime, a northward surface flow arises despite being relatively narrow and weak (Haynes & Barton, 1990; Frouin *et al.*, 1990; Mazé *et al.*, 1997), with a width of around 100 km, and several hundred meters deep. When the wind stress acting on the sea surface is oriented poleward, a downwelling regime can be stablished on the continental shelf (Fiúza *et al.*, 1982; Vitorino *et al.*, 2002a).

Being Estremadura Spur continental shelf fully exposed to the high energetic wave regime generated in the North Atlantic, two current meters were deployed in the study area (middle and outer shelf) in order to obtain *insitu* data, but unfortunately only data from one equipment (outer shelf) was retrieved.

Data given by the current meter deployed at 250 m depth in Estremadura Spur (see Annex 1 - 1.19) (Annex 20) and from the MONICAN (Canhão da Nazaré Monitoring Project from the Portuguese Instituto Hidrográfico) wave buoy (significant wave height, direction and period) allowed to create the scenario during which the current meter was acquiring. During three winter months acquisition (November 2010 – January 2011) in the outer continental shelf of Estremadura Spur the dominant residual current directions measured by the current meter were from NE – SW (225) with a maximum speed of 13 cm/s (Figure 2.17). The current pattern directions were mainly to the south with a very weak component to north.

Data given by the MONICAN buoy indicate that, during the acquisition period, there were three predominant wave directions: NNW (350), W (270) and SW (225) and respective significant wave heights, 5 m, 4 m and 3.5 m and periods of 12 s, 16 s and 9 s, respectively (Figure 2.17, Figure 2.18 and Figure 2.19).

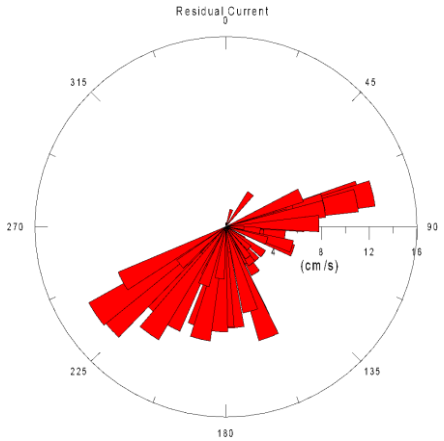

Figure 2.17 - Residual current measured (cm/s) by the current meter. November 2010 – January 2011.

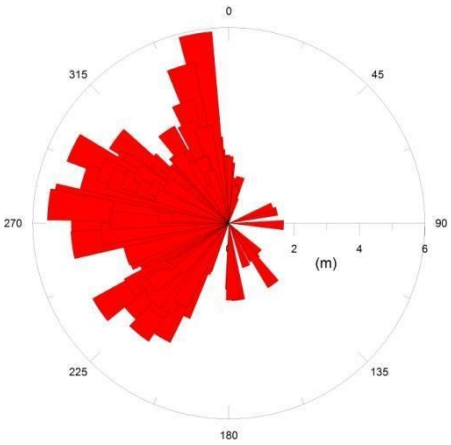

Figure 2.18 - Direction and significant wave height (m) of MONICAN buoy. November 2010 - January 2011.

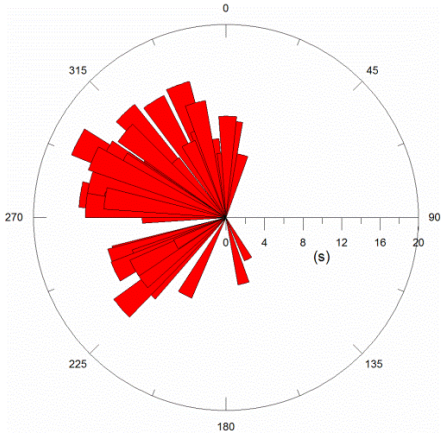

Figure 2.19 - Wave period (s) of MONICAN buoy November 2010 - January 2011.

2.4.4. Major sedimentary transport oceanographic drivers

Along the continental shelf, sedimentary processes are induced by the action of waves, tides and currents, depending on the distance to shoreline, the bottom morphology and depth. Usually, the continental shelf is divided into sectors (systems or zones) in accordance with dynamic, geomorphologic and sedimentological characteristics, being the morphological ones the most common. The morphology of the Estremadura Spur, is detailed in section 2.2, with the differentiation in three oceanographic subzones: inner shelf, middle shelf and outer shelf. The inner sector, with a wave and tide dominated sediment transport, the mid sector where both waves and currents interact to promote resuspension events and sediment transport, and the outer sector, where currents are dominant in the suspended particle transport (Figure 2.20).

Although the depth and width of the world's continental shelves vary widely, it was commonly agreed that the depth limit for the inner sector would be between 0 – 50 m (Wright, 1995). First statements argued that, on wind-driven cross-shelf, the inner shelf was defined as the region offshore of the surf zone, where the surface and bottom layers interact (Lentz, 1993). Later in 1995, Lentz defined this inner sector as "*the region characterized by cross-shelf divergence in the (surface) Ekman transport due to the interaction of the surface and bottom boundary layers*". In 2002, Austin & Lentz (2002) defined the inner sector, as the region inshore of the upwelling or downwelling front, which was a more practical definition to apply to field observations, as these fronts are considerably easier to observe than divergence in the surface Ekman transport (Lentz, 2001).

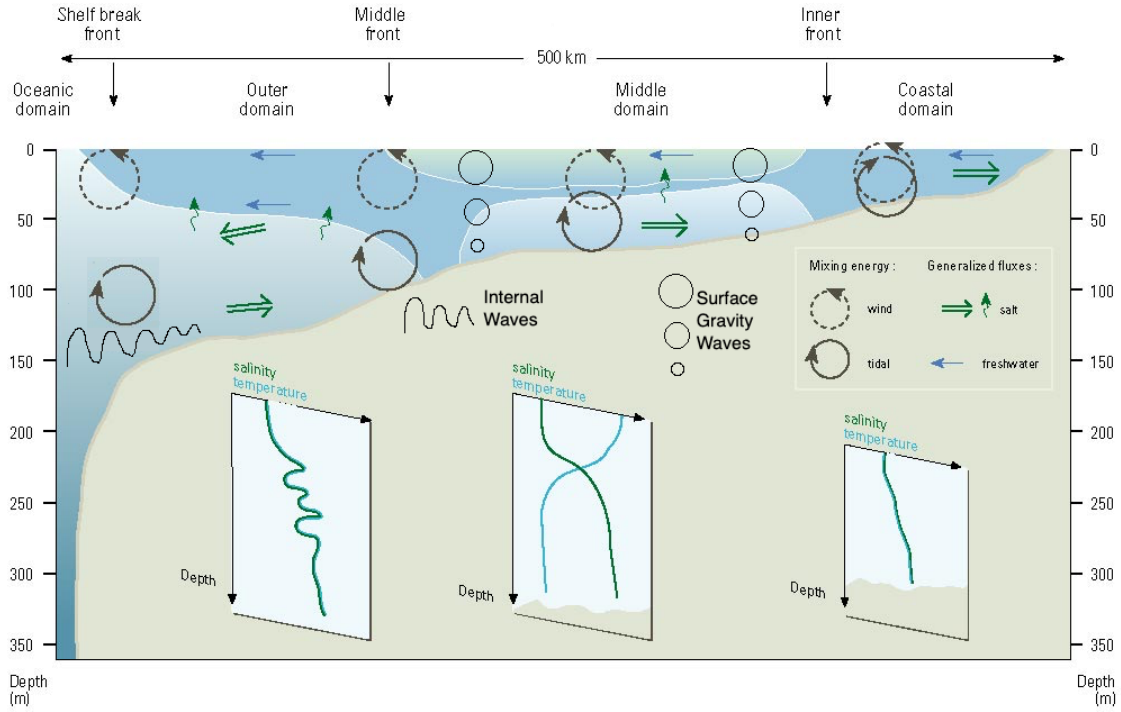

Figure 2.20 - Conceptual model of main forcing mechanisms occurring in the different continental shelf domains (Coachman & Walsh, 1981).

Despite the definition or the outer limits for the inner zone, there is a general agreement that intense processes act in this domain enhancing the sediment transport and distribution. The most effective transport processes are cross-shelf gradients in wave energy, nonlocal sediment availability, direction and magnitude of cross-shelf current (Austin & Lentz, 2002; Harris, 2002) and upwelling and downwelling events (Fiúza *et al.*, 1998).

For mid-sector environments, it was also agreed that the width and depth were between 50 – 100 m (Wright, 1995). On the mid-sector, circulation responds to the restricted depths controlled by interaction with ocean currents or near-shore circulation. Similar to the shallower dynamics, the mid-sector domain presents an influence of upwelling and downwelling events. The tides and waves regime also affect the bottom but with minor intensity.

Episodes of particles resuspension can occur in middle shelf during winter time, due to the effect of high bottom shear stress, induced by storm waves (Taborda, 2000; Vitorino *et al.*, 2002b; Jouanneau *et al.*, 2002; Oliveira *et al.*, 2002). Such events intensify the bottom nepheloid layer (BNL) that covers the entire continental shelf (Oliveira *et al.*, 2002). Also, low-frequency current observations show that even when they are too weak to promote resuspension, they are strong enough to transport the suspended particles (Taborda, 2000). As such, during upwelling events, this transport is oriented southwards and shoreward, in the bottom Ekman layer (Vitorino *et al.*, 2002b).

As for the outer section, although with different magnitudes and interactions with bottom morphologies, the same oceanographic agents (tides, internal waves and currents) are expected to interact with bottom sedimentary particles (Felix & McCaffrey, 2005), and promote resuspension and nepheloid layers formation. At the shelf break it is common to observe BNL detachment and the formation of intermediate nepheloid layers (Puig *et al.*, 2013).

2.5. Synthesis

Estremadura Spur is located in the Portuguese continental margin between parallels 39º 30' N and 38º 54´ N, and meridians 10º 20' W and 9º 24' W. This peculiar geomorphologic unit has a variable width, ranging from 15 km (offshore Peniche) to 70 km (at Ponta da Lamparoeira parallel), depending on the distance to shoreline of the shelf break (located at variable depth, ranging from ~ 50 m and ~ 400 m). It is very peculiar and diversified with important reliefs (extensive outcrops of rocky formations) alternating with smooth areas and irregular valleys in deeper domains.

From the geomorphological point of view, the coastal zone of the Estremadura Spur is predominantly composed of rocky cliffs with few embayed beaches from Jurassic and Cretacic, the majority in relation with the mouth of small rivers.

The continental shelf is characterized by large areas of rocky outcrops and a thin layer of unconsolidated sediments. These outcrops correspond mainly to meso-cenozoic carbonate formations while the unconsolidated sediments vary from sandy gravel to sandy mud deposits depending on the sediment transport processes and distance to particle sources.

The Estremadura Spur coastal area is affected by a high energetic wave regime that dominates inner shelf sediment dynamics and extends to the middle shelf. Unprecedent current data acquired at 250 m depth shows that despite in the Portuguese continental shelf the predominant current direction is northward during the winter (Oberle *et al.*, 2014), during the three months period observation, in the outer shelf of the Estremadura Spur, the dominant current direction was oriented southward, inducing a particle transport with the same direction.

The residual current meter data acquired in winter time in the outer shelf of Estremadura Spur ranged from 0 to 13 cm/s and can be decomposed in cross-shelf and along shelf components. The magnitude and frequency of the ENE along shelf component is slightly lower than the WSW component, which induces a weak residual net transport toward WSW. On the other hand, the cross-shelf component presents a clear SSE dominance inducing a strong net transport towards shallower areas.

At the outer shelf and upper slope oceanographic phenomena like internal waves have been recognized to occur with impact on the particle resuspension.

The sedimentary deposits pattern indicates that the contribution of recent sand terrigenous particles is only significant at the inner shelf. In the northern sector, the middle shelf is covered

by very coarse biogenic and aggregate deposits in the vicinity of extensive rocky outcrops. Immediately south of those outcrops, sediments become finer, with a muddy sandy deposit covering the entire Mar da Ericeira. The outer domains of the Estremadura Spur are covered by muddy sands, with a huge elongated sandy deposit located along the outer shelf.

Chapter III – Present day sedimentary sources of the Estremadura Spur

To understand present day continental shelf sedimentary dynamics, it is important to identify the main particle sources and quantify, at least in a qualitative way, their contribution to marine depocenters. As stated in the previous section, the main sources of terrigenous particles to the Estremadura Spur are the fluvial input and cliff erosion, which are nowadays strongly altered by human intervention in both fluvial and coastal systems.

In this chapter, sediments collected in different environments (rivers, inner shelf and beaches) will be described, in terms of grain-size and composition, as well as some characteristics that were used as indicators (natural tracers) for the sedimentary processes.

3.1. Introduction

The diversity of forms of the entire coastal region (promontories, bays, lagoons and rivers), has a strong influence on the coastal dynamics. The influence of this dynamics is imprinted not only in the volume and type of particles introduced in the marine systems, but also in their pathways and the location of sectors more susceptible to erosion, sediment bypass or to temporal accumulation.

Taking into account the climatic changes that affect the coastal area, it is essential to understand how past changes are imprinted in the sedimentary record and infer and predict how the system will evolve/change in the future.

For this, it is necessary to characterize and understand the processes that affect the sedimentary particles that are found in rivers and beaches, since they result from the balance between physical (currents, tides, waves, and river discharge) and geological processes (sedimentary basins, rocky outcrops, platform morphology and coastal physiography).

A starting point for this study is the sedimentological and geochemical characterization of sediments that are continuously being exported through river discharges to the Estremadura Spur. Previous studies performed in this margin (Oliveira, 1994; Garcia, 1997) showed a strong seasonal signal of SPM (suspended particulate matter) composition in the water column from Tejo river, with a terrigenous component (heavier) dominating during autumn and winter, showing a correlation of near 1, and a biological component (lighter) prevailing during spring and summer, with a correlation between 0.5 – 0.7. In general, the water column in the inner and middle shelf off the Tejo estuary is stratified with two distinct nepheloid layers: at the surface and close to the bottom. Under the influence of a more energetic wave regime, the stratified structure will disappear and the entire water column is turbid. The superficial nepheloid layer is very rich in biogenic particles and may reach 30 km in length, extending normally in a westward direction. The bottom nepheloid layer usually shows higher nephelometer values (~10 FTU (Formazine

Turbidity Units)), due to the content on detritical riverine particles, and it is usually diverted southward, in the direction of the Canhão de Lisboa. Under the SW wave regime and high river discharge, the concentration of suspended particles will increase and both nepheloid layers will develop in length and cover the inner and middle shelf. In these conditions, it is possible that terrigenous fine particles will be transported westward, from the rivermouth until the Ericeira region. The above authors estimate the amount of suspended matter being discharged annually from the Tejo estuary to be between 0.4 and 1×10^6 t.

3.2. Methods

In order to characterize local sedimentary sources for the Estremadura Spur, two sampling surveys were performed at the nearby rivers and beaches and 8 inner shelf samples were also used from the SEPLAT program. The first was carried out in September 2009, at the end of summer season under virtually no river flow, and the second one in March 2010, after the occurrence of several major storms and very high flow rates (several streams were overflowing). In these surveys sixteen surface sediment samples were collected in seven rivers (Figure 3.1A) and at nine beaches (Figure 3.1B).

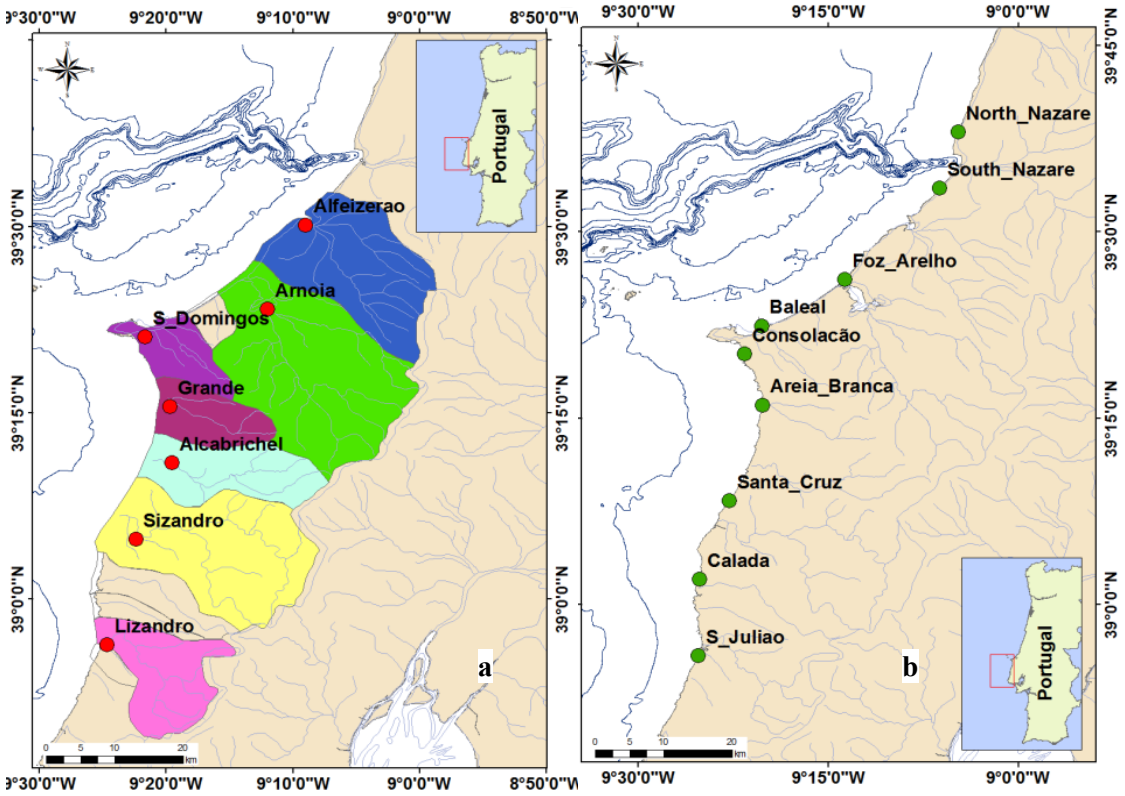

Figure 3.1 - River survey September 2009 (a); Beach survey in March2010 (b).

The river samples were collected along margin deposits, close to the running water (Figure 3.2a) and b); the beach samples, sediments were collected at the beach face (Figure 3.2c).

Figure 3.2 - Example of sampling collection
Sizandro river (a), Arnóia river (b) and at the North Nazaré beach face (c).

The sediment samples were analyzed using the protocols which are briefly presented in Annex 1. The sedimentological analysis was performed in the Instituto Hidrográfico laboratory and consists in grain size (Annex 1 – 1.9) (Annex 2) and mineralogical composition (Annex 1 – 1.12, 1.13 and 1.14) (Annex 3 and 4). The mineralogical analysis includes fine fraction mineralogy from river and shelf samples, heavy metals only from shelf and river samples and heavy mineral identification of the fine sandy fraction (only on beach, river and inner shelf samples, (Figure 3.2).

Results were integrated with the ones obtained in the 66 superficial samples of the continental shelf sedimentary cover collect under the SEPLAT program from Instituto Hidrográfico (Figure 2.12).

	Local	Long	Lat	Sample
Rivers	Sizandro	-9.3727	39.08	2444
	Alcabrichel	-9.3256	39.183	2445
	Grande	-9.3264	39.262	2446
	Arnoia	-9.2003	39.388	2447
	S.Domingos	-9.3611	39.351	2448
	Alfeizerão	-9.1496	39.501	2449
	Lizandro	-9.41	38.938	2450
Beaches	N_Nazaré	-9.0793	39.634	777
	S_Nazaré	-9.1033	39.558	778
	Foz Arelho	-9.2276	39.436	781
	Baleal	-9.3369	39.373	784
	Consolação	-9.3596	39.336	786
	Areia Branca	-9.3361	39.267	788
	Santa Cruz	-9.38	39.139	793
	Calada	-9.4186	39.033	796
	S_Julião	-9.4209	38.931	798
Shelf		-9.367	39.217	297
		-9.37	39.167	984
		-9.4529	38.917	953
		-9.4033	39.116	978
		-9.2882	39.409	10606
		-9.2223	39.46	10635
		-9.43	38.96	959
		-9.3804	39.267	145

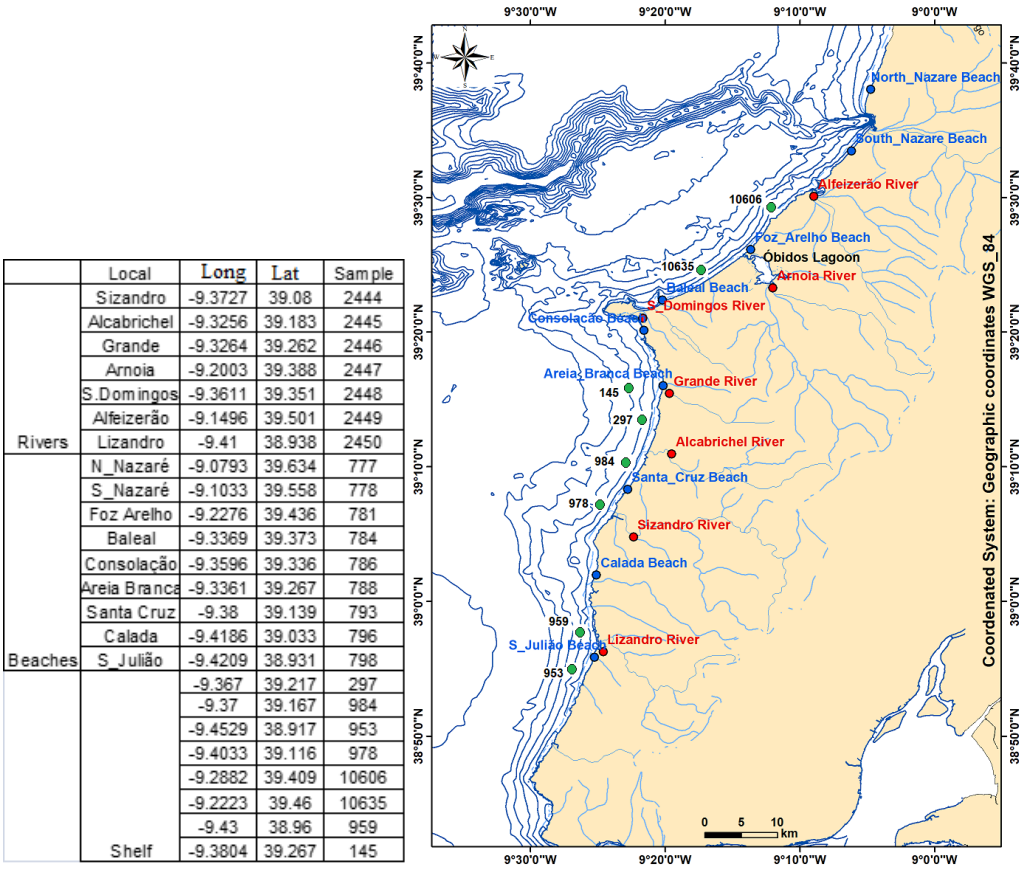

Figure 3.3 - Sample collection along the coast of the study area.
Rivers- red dots; Beaches- blue dots; Inner continental shelf- green dots.

3.3. Results and discussion

3.3.1. Grain size

As expected, sediments from rivers, coastal and shelf environments present different textural signatures (Figure 3.4) (Annex 2). River samples exhibit the wider grain size spectrum (Figure 3.5) with sedimentary particles ranging from -4 phi (16 mm) to 11 phi (0.000488 mm) (Figure 3.4). The first and third quartiles are approximately 1 phi (0.5 mm) and 3 phi (0.125 mm) and the median is located at 1.5 phi (0.353 mm). Most samples are also poorly sorted as seen in Figure 3.5, ranging from 1.52 phi (0.349 mm) to 2.66 phi (0.158 mm).

Considering beach samples, the granulometric curves extend from -3 phi (8 mm) to 2.75 phi (0.14 mm) (Figure 3.4) and the mean values vary between 0 phi (1 mm) and 1.75 phi (0.297 mm) centered in 0.5 phi (0.710 mm). Beach samples are usually better sorted presenting values that range from 0.38 phi to 0.74 phi (Annex 2).

Samples from the inner shelf present grain size values ranging from -3 (8 mm) phi to 11.25 phi (0.00041 mm). The mean values are concentrated between 1.46 phi (0.36 mm) and 2.86 phi (0.137 mm) and centered in 2.3 phi (0.203 mm). These sediments vary from moderately sorted to poorly sorted (Figure 3.5) (Annex 2).

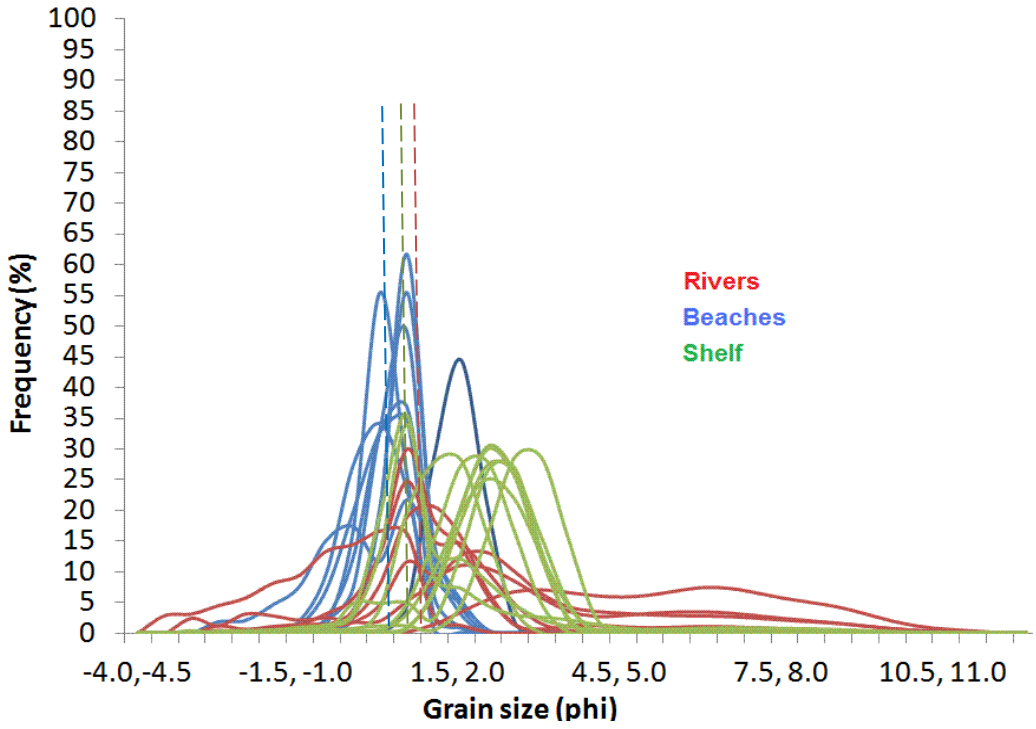

Figure 3.4 - Grain size distribution (phi): rivers in red; beaches in blue; inner continental shelf in green; dash lines indicate the principal mode for each environment.

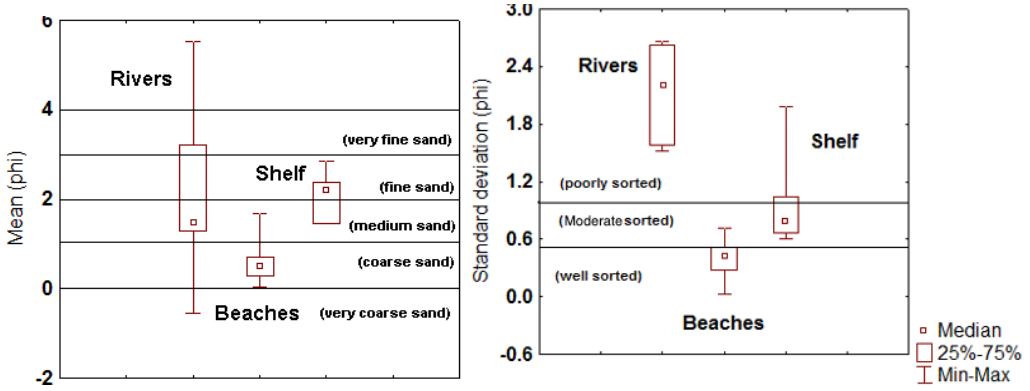

Figure 3.5 - Mean grain-size (phi) and standard deviation (phi) boxplot of river, beach and inner shelf samples.

Sediments collected in rivers and beaches are mainly constituted by sand (Table 3.1, Figure 3.6), with some distinct and important differences.

In general, beach sediments have no fine component (silt and clay) and gravel is only important at Nazaré and Foz do Arelho beaches, while river samples always have a fine component (that can reach a maximum of 33 %). Two exceptions were observed at the Lizandro (where fine fractions are replaced by the gravel component) and S. Domingos rivers, where sediments are mainly composed of silt with considerable percentages of sand and clay (31 % and 17 % respectively).

Table 3.1 – Percentage of textural parameters from river and beach samples.

	Local	Sample	Pebble (%)	Gravel (%)	Sand (%)	Silt (%)	Clay (%)
	Sizandro	2444	0,00	4,52	65,86	23,15	6,47
	Alcabrichel	2445	0,00	2,36	92,97	3,52	1,15
Rivers	Grande	2446	0,00	11,81	78,30	8,09	1,80
	Arnóia	2447	0,00	1,51	89,63	7,25	1,61
	S.Domingos	2448	0,00	0,00	31,10	51,94	16,96
	Alfeizerão	2449	0,00	1,15	68,08	24,37	6,40
	Lizandro	2450	0,00	33,77	65,06	0,95	0,22
	N_Nazaré	777	0,00	13,82	86,18	0,00	0,00
	S_Nazaré	778	0,00	0,53	99,47	0,00	0,00
	Foz Arelho	781	0,00	15,88	84,12	0,00	0,00
Beaches	Baleal	784	0,00	0,00	100,00	0,00	0,00
	Consolação	786	0,00	2,19	97,81	0,00	0,00
	Areia Branca	788	0,00	0,08	99,92	0,00	0,00
	Santa Cruz	793	0,00	0,98	99,02	0,00	0,00
	Calada	796	0,00	0,13	99,87	0,00	0,00
	S_Julião	798	0,00	0,29	99,71	0,00	0,00

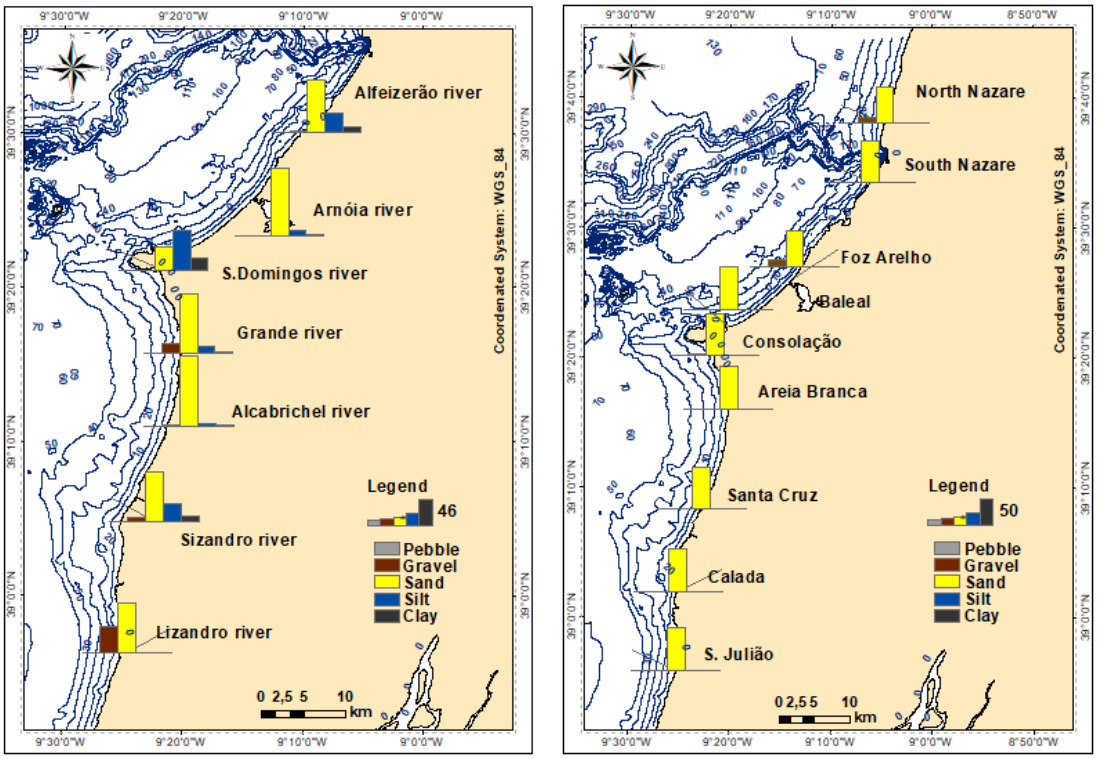

Figure 3.6 - Textural parameters of sediments collection.
Rivers on the left; beaches on the right.

3.3.2. Fine fraction mineralogy

Fine fraction mineralogy was analyzed in river sediments and compared to the fine fraction mineralogy of shelf sediments, taken from Balsinha (2008). Beach sediments were not included in this study because fine fractions are absent. The main minerals present in the analyzed riverine samples are illite, kaolinite, quartz, opal, K feldspar (FK), plagioclase, calcite, dolomite and siderite (Table 3.2). Statistical parameters are summarized in Table 3.3, for both river and shelf sediment samples (Annex 3).

Table 3.2 - Fine fraction mineralogy of river samples.

Samples	Illite	Kaolinite	Quartz	Opal	FK	Plagioclase	Calcite	Dolomite	Siderite
Sizandro	16.7	16.2	16.7	2	19.7	12.2	10.7	4.1	1.1
Alcabrichel	6.8	5.8	18.4	3.2	23.1	11.7	28.7	0	2.4
Grande	15.4	3.9	14.9	2.2	29.5	23.1	4.4	2.4	0.4
Arnóia	13.7	14.9	20.9	1.9	38.2	5.2	3.3	0	0.8
S. Domingos	22.6	3.7	21.7	4.9	18.9	13.3	13.7	0	1.3
Alfeizerão	23.5	14.5	17.4	2.8	20.4	5.7	13	0	1.4
Lizandro	4.6	1.7	8.6	0	8.7	15.3	61.2	0	0

Table 3.3 - Values of mean, max, min and standard deviation for river and shelf samples.

Samples	Parameter	Illite	Kaolinite	Quartz	Opal	FK	Plagioclase	Calcite	Dolomite	Siderite
rivers	mean	14.75	8.67	16.92	2.43	22.63	12.35	19.28	0.92	1.04
	max	23.53	16.19	21.66	4.92	38.17	23.09	61.24	4.07	2.36
	min	4.55	1.66	8.60	0.00	8.67	5.16	3.25	0.00	0.00
	sd	7.18	6.24	4.35	1.49	9.23	6.07	20.29	1.65	0.77
shelf	mean	10.25	2.39	7.64	1.90	7.71	6.90	55.41	0.53	0.98
	max	37.12	16.19	30.04	6.77	38.17	27.16	86.23	6.05	3.43
	min	2.60	0.00	2.73	0.00	0.00	0.00	3.25	0.00	0.00
	sd	6.49	3.24	4.53	1.37	7.44	5.21	21.93	1.21	0.79

Results indicate that the fine fraction of river sediments are, in general, dominated by illite, quartz, potassium feldspar, plagioclase and calcite, which agree with the geological formations present in the drainage basins. In river samples, illite is abundant in the Alfeizerão and S. Domingos sediments but, in the continental shelf, it is concentrated in three main areas: middle shelf north of Peniche (between 50 and 100 m depth), between Peniche and Ponta da Lamparoeira (around 50 m depth) and in the Mar da Ericeira, between 100 and 120 m depth. The lower values of illite are located in the outer shelf below 150 m depth (Figure 3.7).

Potassium feldspar content in the fine fraction of river sediments is high, always above 20 % (maximum of 38 % in Arnoia river), with the exception of Lizandro river, which represents only 9 % of this mineral. When compared to the distribution on the continental shelf (Figure 3.8), it is possible to observe that its distribution is restricted to the coastal areas (shallower than 60 m depth) and associated to the Pêro da Covilhã outcrops (100 to 140 m depth).

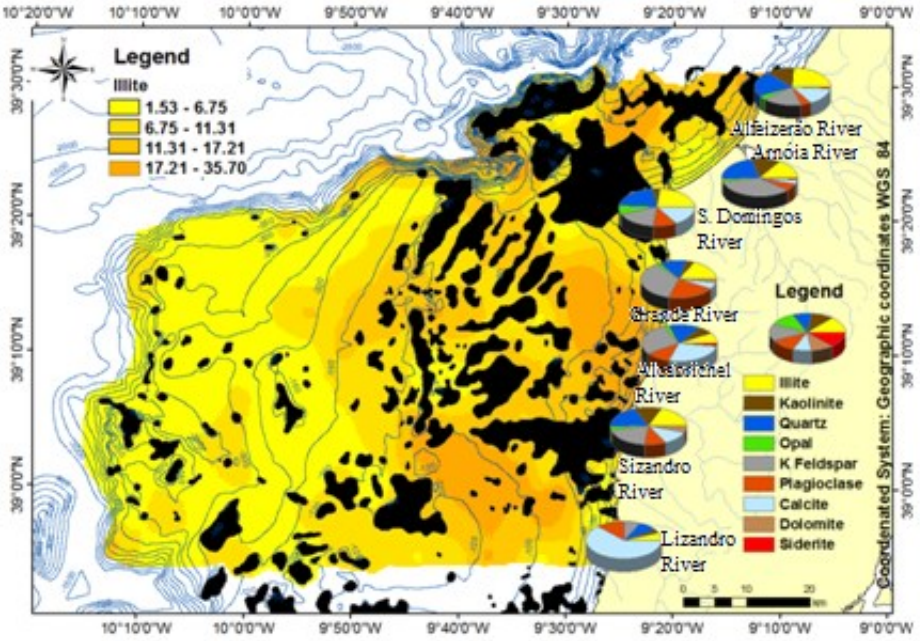

Figure 3.7 - Illite percentage on the fine fraction of sediments collected in rivers (pie charts) and at the continental shelf.

The distribution pattern shows that the higher values are closely related to inner shelf and rocky outcrops, and highlights the importance of the older geological formations, exposed in cliffs and drained by rivers and small streams as major particle sources to the shelf sedimentary cover.

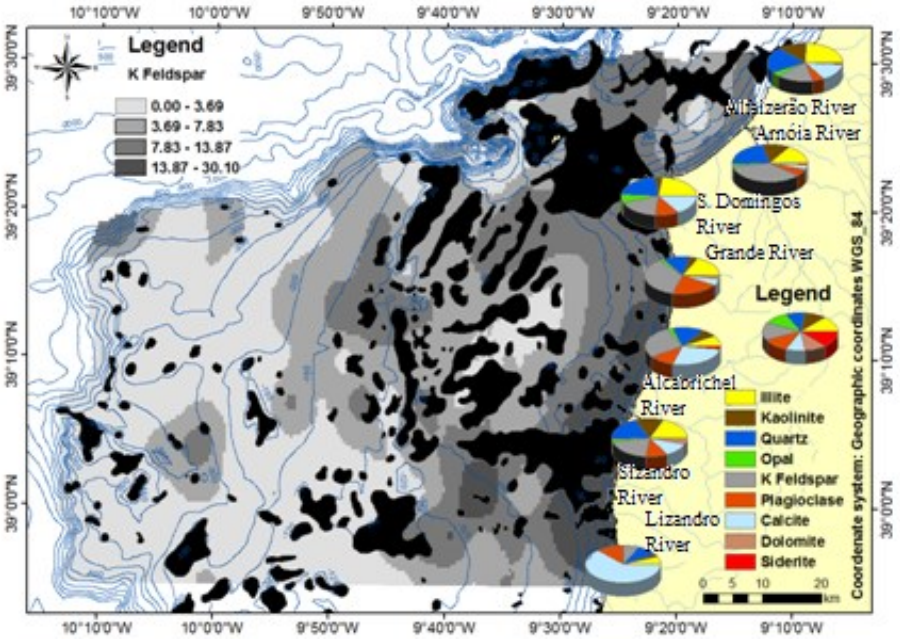

Figure 3.8 - Potassium feldspar percentage from rivers (pie charts) and continental shelf samples.

The same pattern was observed for the plagioclase distribution (Figure 3.9), which is a very abundant element in the inland geological formations (Kullberg *et al.*, 2013). In river sediments, the higher value was observed in Grande river (23 %) and only Arnóia and Alfeizerão showed values below 10 %. In the continental shelf, this mineral presents higher concentrations, with values ranging between 11 % and 25 %, near the continent and to Costeiras Pêro da Covilhã.

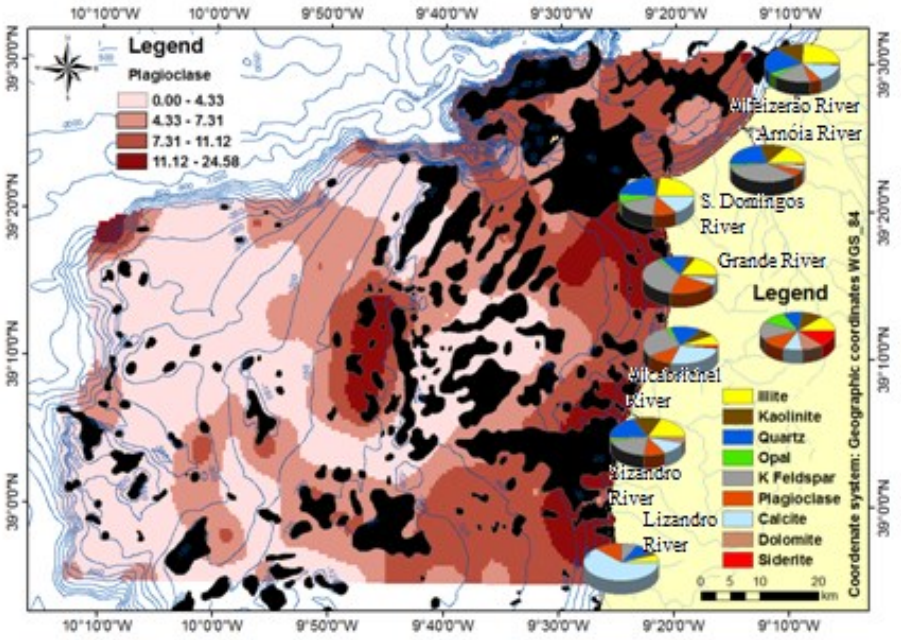

Figure 3.9 - Plagioclase percentage from rivers (pie charts) and continental shelf samples.

3.3.3. Heavy minerals

By definition, heavy minerals are high density minerals, with densities greater than 2.9 (Rothwell, 1989). In sedimentary dynamic process analysis, heavy minerals are subject to a very effective selective process, in accordance to their size, shape and density (Komar, 2007).

As a consequence, in a natural environment, their distribution reflects source and transport processes. For example, heavy mineral assemblages have been used to identify particle sources, evaluate weathering, diagenetic evolution and in a paleogeographic analysis, being a useful tool for stratigraphic correlations (Parfenoff *et al.*, 1970; Mange & Maurer, 1991; Dill, 1998).

In the study area, heavy minerals were weighted for sand fraction, identified on sediment samples collected in rivers, inner shelf and beaches (Table 3.4). It was observed that percentage of heavy minerals in the sandy fraction increases with decreasing grain size, except for inner shelf samples (Figure 3.10) and their distribution is significantly different in the three environments (rivers, shelf and beaches) (Annex 4).

Table 3.4 - Percentages of heavy minerals in the sand fraction of samples collected in rivers, inner shelf and beaches.

Location	Sample	Tur	And	Stau	Gar	Phyllo	Zir	Mon	Amp	Px	Gla
Sizandro	2446	21.59	9.00	7.46	3.86	56.56	1.54	0.00	0.00	0.00	0.00
Alcabrichel	2448	44.25	12.20	15.68	10.45	11.85	2.44	0.00	0.00	3.14	0.00
Grande	2445	37.28	33.50	9.82	6.30	1.26	8.56	0.50	0.00	2.77	0.00
Arnóia	2447	53.08	13.51	11.14	5.45	5.45	3.32	0.24	0.00	7.58	0.00
S. Domingos	2449	34.93	6.39	15.53	9.13	31.74	2.28	0.00	0.00	0.00	0.00
Alfeizerão	2444	19.07	1.71	6.85	14.91	1.96	2.69	0.98	5.87	45.72	0.00
Lizandro	2450	2.61	0.71	1.66	1.18	0.71	0.47	0.00	9.48	83.18	0.00
	Mean	30.40	11.00	9.73	7.33	15.64	3.04	0.25	2.19	20.34	0.00
	Max	53.08	33.50	15.68	14.91	56.56	8.56	0.98	9.48	83.18	0.00
	Min	2.61	0.71	1.66	1.18	0.71	0.47	0.00	0.00	0.00	0.00
Shelf	10606	35.07	15.36	24.64	8.12	0.87	7.83	0.00	0.00	8.12	0.00
	978	27.47	11.43	9.23	17.58	2.64	14.73	1.10	3.96	10.77	0.00
	984	30.08	14.76	11.14	21.45	0.00	14.76	3.06	4.74	0.00	0.00
	297	26.54	11.61	12.80	22.99	0.00	9.72	3.55	1.66	11.14	0.00
	959	27.94	14.88	2.87	22.72	0.00	12.79	6.27	2.87	9.14	0.00
	145	30.64	17.51	9.43	13.47	7.41	1.68	2.69	12.46	4.71	0.00
	953	23.61	14.22	13.73	18.55	0.00	10.36	1.93	4.58	12.29	0.00
	10635	28.28	19.28	10.28	22.37	0.77	13.11	1.80	1.80	2.31	0.00
	Mean	28.70	14.88	11.77	18.40	1.46	10.62	2.55	4.01	7.31	0.00
	Max	35.07	19.28	24.64	22.99	7.41	14.76	6.27	12.46	12.29	0.00
	Min	23.61	11.43	2.87	8.12	0.00	1.68	0.00	0.00	0.00	0.00
S Nazaré	778	37.07	32.53	8.00	5.87	0.53	6.40	0.53	8.80	0.27	0.00
N Nazaré	777	35.94	32.53	12.45	4.82	0.60	0.60	1.20	11.85	0.00	0.00
Consolação	788	56.67	11.90	12.38	12.86	0.00	4.76	0.00	1.43	0.00	0.00
Areia Branc	786	47.47	33.33	4.04	9.09	0.00	0.00	1.01	1.01	4.04	0.00
Foz Arelho	781	59.48	8.55	13.01	13.38	0.00	4.46	0.37	0.74	0.00	0.00
Calada	796	22.78	6.33	9.49	9.49	0.00	3.16	0.63	19.62	28.48	0.00
Baleal	784	44.89	21.36	17.96	9.60	0.00	4.64	0.00	1.55	0.00	0.00
Santa Cruz	793	9.90	3.30	18.06	33.85	0.00	22.40	9.20	1.91	1.39	0.00
S. Julião	798	11.41	3.33	10.30	23.45	0.00	17.27	10.94	6.02	17.27	0.00
	Mean	36.18	17.02	11.74	13.60	0.13	7.08	2.65	5.88	5.72	0.00
	Max	59.48	33.33	18.06	33.85	0.60	22.40	10.94	19.62	28.48	0.00
	Min	9.90	3.30	4.04	4.82	0.00	0.00	0.00	0.74	0.00	0.00

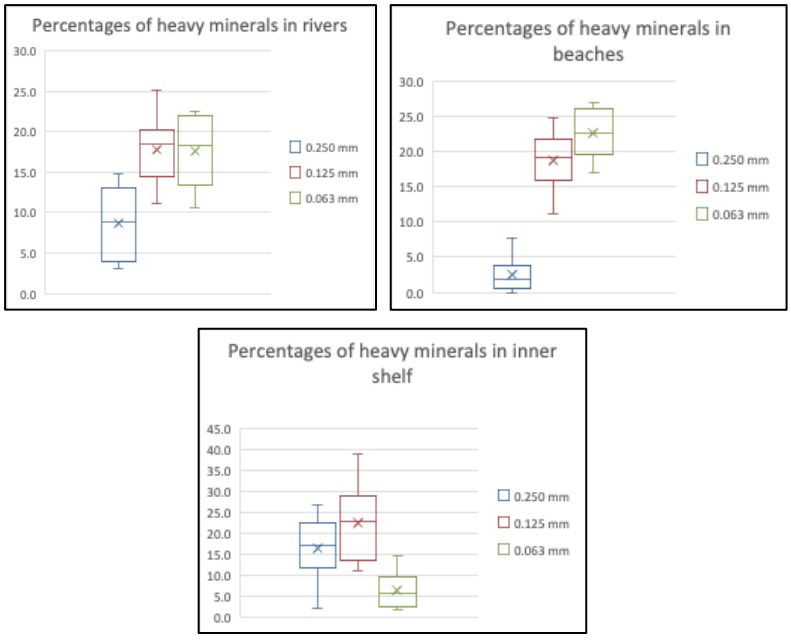

Figure 3.10 - Percentage of heavy minerals in the three sandy fractions 0.250 mm, 0.125 mm and 0.063 mm for rivers, beaches and inner shelf samples.

The highest percentages between 0.3 and 0.5 %, were found in river sediments located in São Domingos river and south of Peniche in Grande river, respectively (Figure 3.11). These values of heavy minerals percentages were calculated for the entire sediment sample and not only for the sand fraction as in Table 3.4.

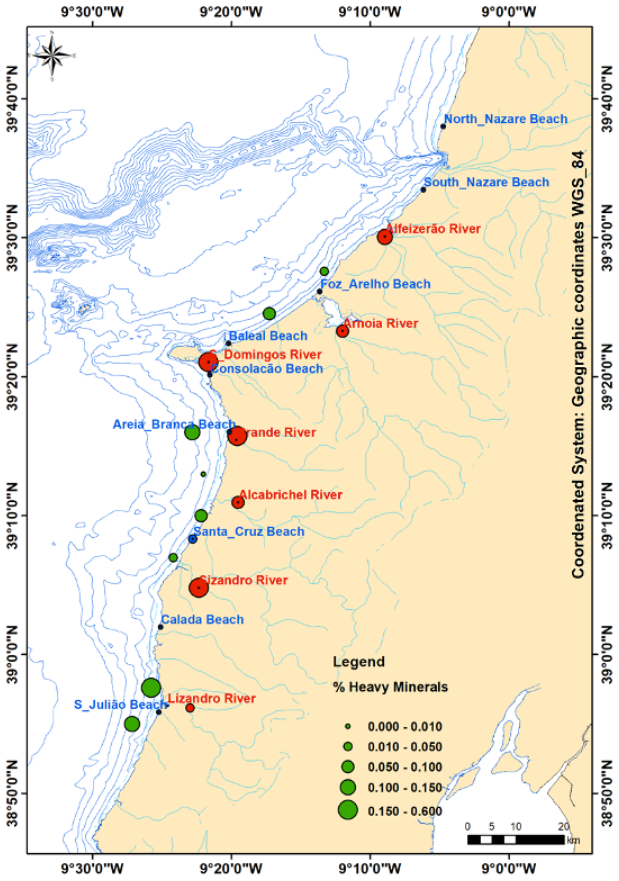

Figure 3.11 - Heavy minerals percentage of sediment samples collection. Rivers: red; beaches: blue; inner shelf: green.

Considering river samples, two domains can be individualized: one, located north, includes Alfeizerão, Arnoia, S. Domingos, Grande and Alcabrichel rivers, being characterized by the occurrence of tourmaline, andaluzite and staurolite; and another one that comprises Sizandro and Lizandro rivers and includes pyroxenes and amphiboles (Figure 3.12a).

In the adjacent inner shelf (shallower than 40 m depth), the heavy mineral assemblages present no evident variation, being quite homogeneous. This homogeneity is due, probably, to the effect of the incident wave action and the intense long littoral drift (Figure 3.12b). The more distinctive features are: 1) the almost absence of phyllosilicates in the shelf sediments and 2) the increase of garnet and zircon in the shelf sediments, when compared to river sediments. The values presented in Table 3.4 indicate that phyllosilicates decreased from a mean percentage of 15.64 % (river samples) to 1.46 % (shelf samples), garnet and zircon increased from 7.32 % to 18.40 % and from 3.04 % to 10.62 %, respectively. These variations can be justified by the

relatively high energy of the incident wave regime which prevents the settling of phyllosilicates and promotes the concentration of species with more resistant grains to the marine abrasion (minerals like the garnet and zircon).

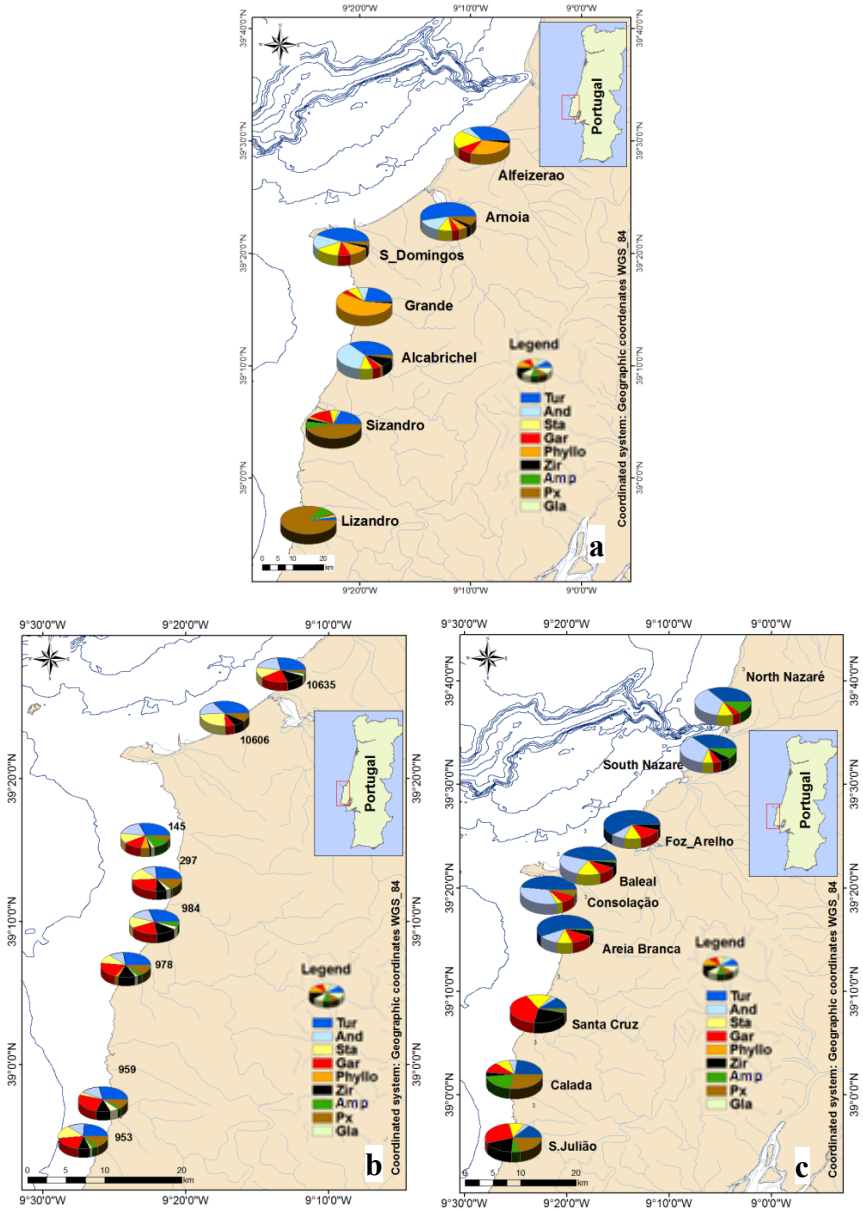

Figure 3.12 - Heavy mineral assemblages.
River samples (a), inner shelf (b) and beaches (c).

Analyzing the distribution of heavy minerals along the sampled beaches it is possible to conclude that littoral sediments are composed by particles with a fluvial and a beach origin, since the assemblages from the rivers are less reworked than the ones present in beach samples, which indicate that beach samples suffered several rework cycles. In fact, in the beach environment it is also possible to individualize two sectors (Figure 3.12c), considering the distribution on heavy

minerals and their possible origin: 1) the northern domain, include beaches between Norte Nazaré and Areia Branca, with mineral assemblages characterized by high percentages of tourmaline, andaluzite and staurolite (river signature) and also garnet (shelf signal); 2) the southern domain comprehends Santa Cruz, Calada and S. Julião beaches, where sediments present heavy minerals assemblages composed by a mixture of pyroxenes and amphiboles (river signature), garnet and zircon (beach signal).

In order to support some of the above findings, a cluster analysis was performed based on the heavy mineral percentage. This cluster analysis was made using the Group *Analysis* ArcGIS® tool. Given the number of groups to be created, the tool looks for a solution where all the features within each group are as similar as possible, and all the groups themselves are as different as possible. In this process, all samples (rivers, beaches and continental shelf) were considered. Based on cluster analysis, samples were grouped into four clusters (Figure 3.13).

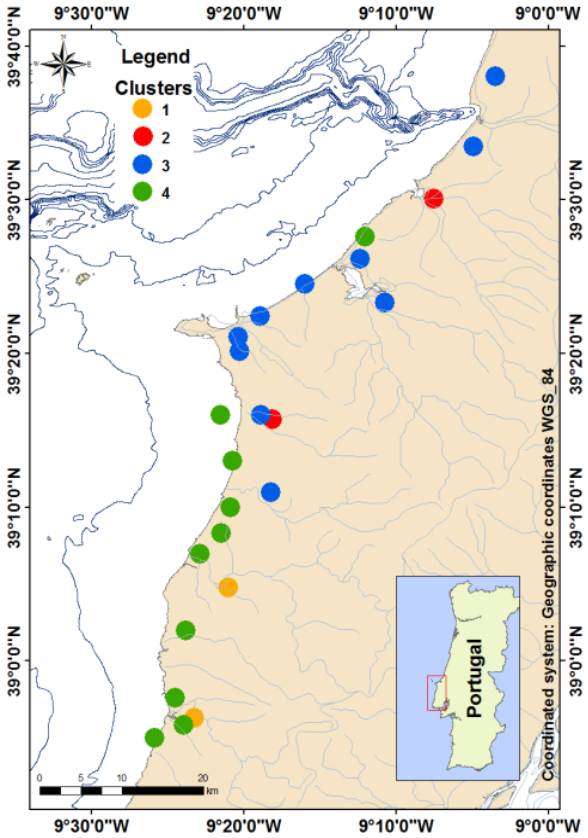

Figure 3.13 - Cluster distribution from heavy mineral association in the analyzed sediments.

The four clusters can be described as follows (Figure 3.13):

- The ***first cluster*** (orange) is formed by the river samples of Lizandro and Sizandro, dominated by pyroxene and amphibole.

- The ***second cluster*** (red) is formed by samples from the mouth of the Grande and Alfeizerão rivers, dominated by biotite.
- The ***third cluster*** (blue) has less mineralogical variety and the predominant heavy minerals are tourmaline and andaluzite.
- The ***fourth cluster*** (green) is represented by samples with a greater variety of heavy minerals, predominantly garnet and zircon with clear decrease of tourmaline and andaluzite.

These results put in evidence the importance of terrigenous sources to the coast and continental shelf (*cluster 1* and *cluster 2*) with the existence of two distinct populations, separated by the Cabo Carvoeiro, representing two sedimentary cells (*cluster 3*, from a more selective environment, and *cluster 4*, representing a stretch with multiple and variable sediment inputs). These conclusions are in agreement with previous works made by Ribeiro (2017), where relative percentages of major heavy mineral transparent species (tourmaline (24.5 %), clinopyroxene (21.3 %), garnet (18.4 %), staurolite (15.4 %), andaluzite (7.2 %), amphibole (5.0 %) and zircon (1.2 %) are in accordance with the ones encountered in this study. In the north, the high values of mafic minerals are related to eruptive outcrops between Caldas da Rainha and Serra dos Candeeiros. These outcrops have a significative dimension, with approximately 4-5 km in extension (Zbyszewski & Moitinho de Almeida, 1960), being compose mainly by basalts rich in plagioclase and pyroxene (augite) and phyllosilicates (biotite) that derive from pyroxenes. In the south, the abundance of mafic minerals is related to gabbro outcrops, located south of Calada beach, and basaltic veins, which disperse along the littoral. These basalts are leached and drained to the coast through river flow (Zbyszewski & Moitinho de Almeida, 1955). Other heavy minerals, like tourmaline, andaluzite and staurolite are the remains of weathering processes acting during several sedimentary cycles, which obliterate the less resistant minerals and concentrate the ultra-resistant ones in the sand fraction (Galopim de Carvalho, 1968).

3.3.4. Heavy metals

Heavy metals are natural elements that have a high atomic weight and a density at least 5 g cm^{-3} (Koller & Saleh, 2018). Their multiple industrial, domestic, agricultural, medical and technological applications have led to their wide distribution in the environment and abnormal concentration had raised multiple concerns over their potential effects on human health and on the environment quality (Tchounwou, 2012).

In coastal and estuarine areas, especially those close to industrial and urban areas, sediments are important sinks and potential sources of metallic contaminants derived from land (e.g. Loring, 1991). Heavy metals contents were determined in the chemistry laboratory of Instituto Hidrográfico, in the superficial continental shelf samples and in the river samples (2009

survey). The mean heavy metal Al- normalized values are described in Table 3.5. The heavy metal data content for rivers and inner shelf are in a table in annex 4.

Table 3.5 - Al-normalized heavy metal mean values for surface sediment samples.

Heavy metals	Hg /Al	Cu/Al	Zn/Al	Mn/Al	Pb/Al	Ni/Al	Cr/Al
Normalized values	7.61E-06	1.48E-03	9.45E-03	2.27E-02	5.16E-03	1.64E-03	1.02E-02

From the observation of Figure 3.14 one can conclude that the higher values of Al in rivers are located in Sizandro river (3.0 %) and Alfeizerão river (2.6 %). S. Domingos river has 2.4 %, and all the other rivers have less concentration of this element (values below 1.5 %). In the continental shelf the higher values of Al are distributed along the inner and middle shelf, with concentration areas in Mar da Ericeira and in the northern outer shelf near the slope around 250 m depth.

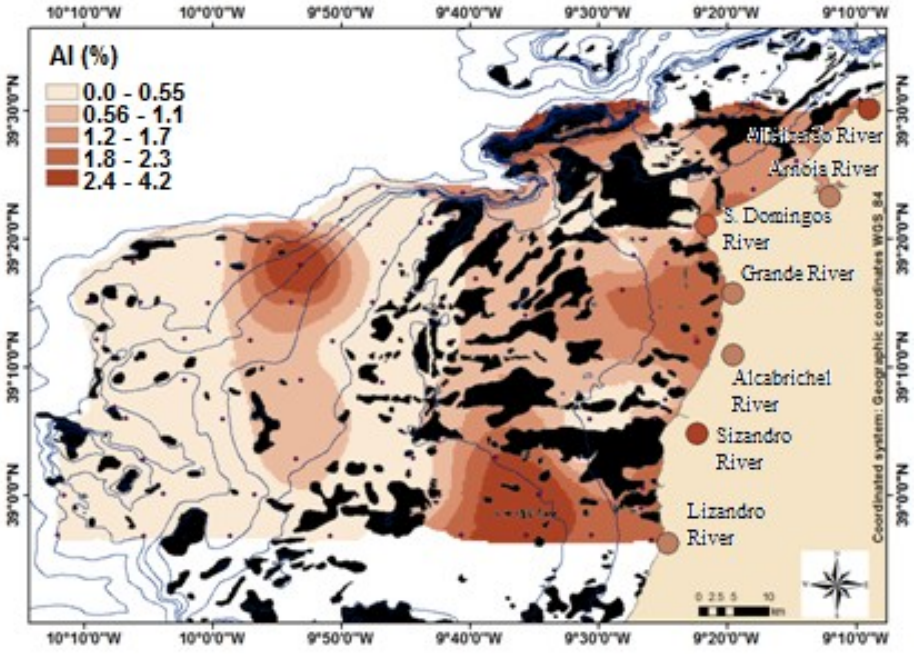

Figure 3.14 - Al percentage from rivers and continental shelf samples.

In riverine sediments Fe presents very low values, reaching its highest value in Lizandro river with a Fe/Al of 10.7 (Figure 3.15). The lower value of Fe/Al is 3.1 and is attained in the Sizandro river, for the remaining riverine samples, this ratio never exceeds 8. On the continental shelf sediments, the higher values (Fe/Al ratio between 10 and 27) are concentrated in the northern outer continental shelf, in the middle shelf off Peniche, in the Pico Gonçalves Zarco area and close to Pêro da Covilhã outcrops.

The lower values of the Fe/Al ratio are located in the inner and middle shelf (below approximately 100 m depth) and in the outer continental shelf defining an N-S oriented corridor parallel to the Pêro da Covilhã relief (Figure 3.15).

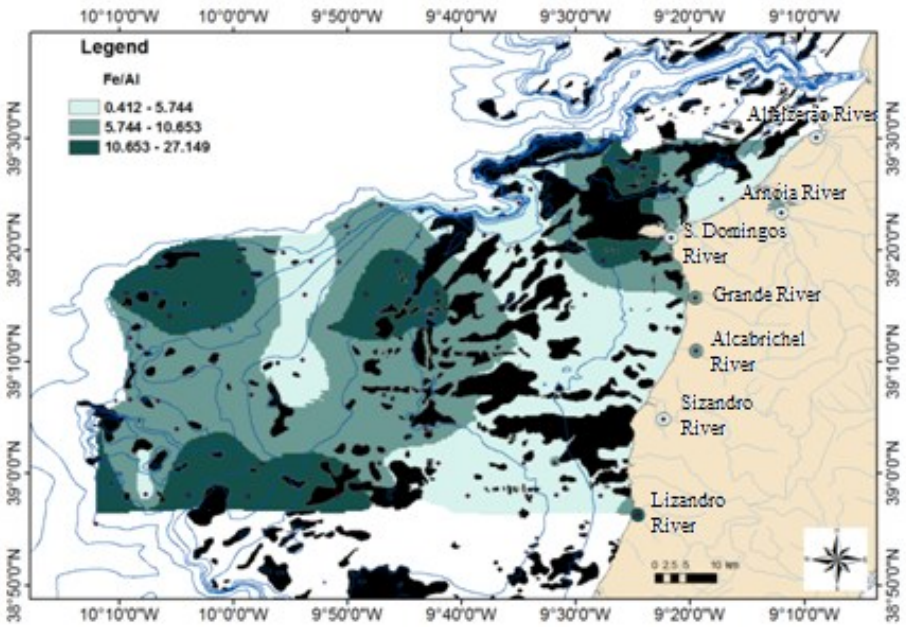

Figure 3.15 - Normalized values for Fe from rivers and continental shelf samples.

Values of Cu (Figure 3.16) in riverine sediments are low, never exceeding 0.001 Cu/Al except for Grande river (0.005 Cu/Al). In continental shelf sediments, the distribution pattern is similar to the one displayed by Fe, being the higher values located near Peniche outcrops and in the deeper domain. The lower values are distributed along the inner and middle shelves (till 100 m depth), and in the same N-S elongated area, around 200 m depth.

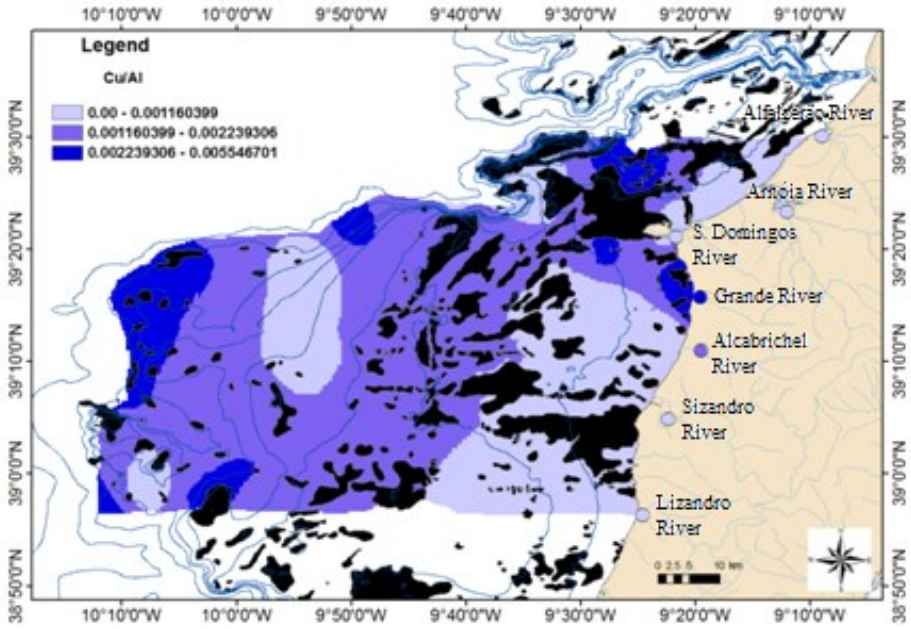

Figure 3.16 - Normalized values for Cu from rivers and continental shelf samples.

When comparing mean Al-normalized values of surface samples in this study with values obtained from other authors, the values have, in general, an order of magnitude higher. According to Mil-Homens *et al.* (2006) in a sediment core realized offshore Nazaré at 120 m depth, the surface samples have approximately Al-normalized values of Cr – $0.9x10^{-4}$, Cu – $2.2x10^{-4}$, Ni – $3.8x10^{-4}$, Pb – $3.7x10^{-4}$ and Zn – $13x10^{-4}$, while in this study the mean Al-normalized values area for Cr – $1.02x10^{-2}$, Cu – $1.48x10^{-3}$, Ni – $1.64x10^{-3}$, Pb – $5.16x10^{-3}$ and Zn – $9.45x10^{-3}$ (Table 3.6).

Table 3.6 - Al-normalized heavy metal mean values for Mil-Homens *et al.* (2006) and the present study.

Al-normalized values	Cr	Cu	Ni	Pb	Zn
Mil-Homens *et al.* (2006)	$0.9*10^{-4}$	$2.2*10^{-4}$	$3.8*10^{-4}$	$3.7*10^{-4}$	$10*10^{-4}$
Present Study	$1.02*10^{-2}$	$1.48*10^{-3}$	$1.64*10^{-3}$	$5.16*10^{-3}$	$9.45*10^{-3}$

According to Oliveira *et al.* (2011), for the same elements in the Canhão da Nazaré adjacent shelf the values are very similar to the ones presented in this study, where Cr varies from 5.40 – 118 mg/kg, Cu from 2.13 – 40 mg/kg, Ni from 2 – 44 mg/kg, Pb from 2 – 69 mg/kg, Zn from 25 – 206 mg/kg, Mn from 116 – 1323 mg/kg and Hg from 0.002 – 0.363 mg/kg. In this study the heavy metal concentrations vary in Cr form 0 – 144 mg/kg, Cu from 1.36 – 89.00 mg/kg, Ni from 0 – 52 mg/kg, Pb from 1 – 75 mg/kg, Zn from 4.52 – 90.00 mg/kg, Mn from 14.11 – 380 mg/kg and Hg from 0.005 – 0.20 mg/kg (Table 3.7).

Table 3.7 - Heavy metal concentration (mg/kg) from Oliveira *et al.* (2011) and this study.

Heavy metals concentration (mg /kg)	Cr	Cu	Ni	Pb	Zn	Mn	Hg
Oliveira *et al.* (2011)	5.40-118	2.13-40	2-44	2-69	25-260	116-1323	0.002-0.363
Present study	0-144	1.36-89	0-52	1-75	4.52-90	14.11-380	0.005-0.20

Comparing mean values of surface sediment samples (Cr – 40 mg/kg; Cu – 8.19 mg/kg; Ni – 6.8 mg/kg; Pb – 21.5 mg/kg and Zn – 38.6 mg/kg) with mean values of Portuguese submarine canyons (Cr – 57 ± 8 mg/kg); Cu – 12 ± 19 mg/kg; Ni – 37 ± 22 mg/kg; Pb – 23 ± 6 mg/kg and Zn – 78 ± 12 mg/kg) Jesus *et al.* (2010) the results are also similar (Table 3.8).

Table 3.8 - Comparison between mean values of heavy metal concentration (mg/kg) for Portuguese submarine canyons from Jesus *et al.* (2010) and the present study.

Mean values of heavy metals concentration (mg /kg)	Cr	Cu	Ni	Pb	Zn
Jesus *et al.* (2010)	57±8	12±19	37±22	23±6	78±12
Present study	40	8,19	6,8	21,5	38,6

3.3.5. Heavy metals enrichment factor

High element enrichment factors (EFs) are commonly used in the literature to support the hypothesis that a particular suite of elements is of anthropogenic origin (Barbieri, 2016). Due to the human activities most soils of industrial, rural and urban environments may accumulate one or more heavy metals. Many metals, such as Cu and Se, are essential elements for plant growth and for living organisms, but high concentrations of these elements become toxic. Industrialization, urbanization and agricultural practices are the three main sources for abnormal metals contents in soils. Heavy metals in the soil from anthropogenic sources tend to be more mobile, hence bio-available than pedogenic or lithogenic ones (Kuo *et al.*, 1983; Basta *et al.*, 2005). Metal-bearing soils in contaminated sites can originate from a wide variety of anthropogenic activities in the form of metal mine tailings, disposal of high metal wastes in improperly protected landfills, leaded gasoline and lead-based paints, land application of fertilizer, animal manures, biosolids (sewage sludge), compost, pesticides, coal combustion residues, petrochemicals, and atmospheric deposition (Wuana & Okieimen, 2011). It is estimated that the contribution of metals from anthropogenic sources in soils is higher than the contribution from natural ones (Nriagu & Pacyna, 1988). The baselines values used for the calculus of enrichment factor are the ones defined on the uppermost 20 cm of a vertical sediment sample (collected at Mar da Ericeira and described at Chapter V) and the values proposed in 1985 by Taylor-McLennan (Table 3.9). According to Reimann & Caritat (2017), in environmental geochemistry the main purpose of the term background is probably to distinguish between natural

concentrations of potentially toxic elements (e.g. As, Cd, Cr, Hg, Pb, Zn) and anthropogenic contamination. The main assumption is that contamination will lead to unusually high element concentrations in the samples, which can then be separated from the main body of data using statistical techniques (Matschullat *et al.*, 2000).

Table 3.9 - Reference values for the determinations of Enrichment Factor (EF) for the different metals (mg/kg).

Baselines	Hg	Cu	Zn	Mn	Fe	Pb	Ni	Cr	Al
Upper continental crust Taylor and McLennan, 1985	-	25	71	600	30500	20	20	98	80400
First 20 cm sediment core	0.0734	17	92	330	32751	17	18	61	78436

Comparing the obtained enrichment factors (EF) one can observe that the spatial pattern of Fe distribution is similar, although when it is applied to the local background, the EF values are lower. The areas near Peniche outcrops, northern and southern outer continental shelf and the area along the middle shelf outcrops, present higher EF (25<EF<50) for both cases. The coastal area in front of Lourinhã, Mar da Ericeira and the corridor at 200 m depth in the outer continental shelf present the lower EF (Figure 3.17a and b). Concerning the river samples, all samples are enriched in Fe. The Lizandro river sample presents the higher value (25 – 50) while the Sizandro river presents the lower values (5 – 10).

a)

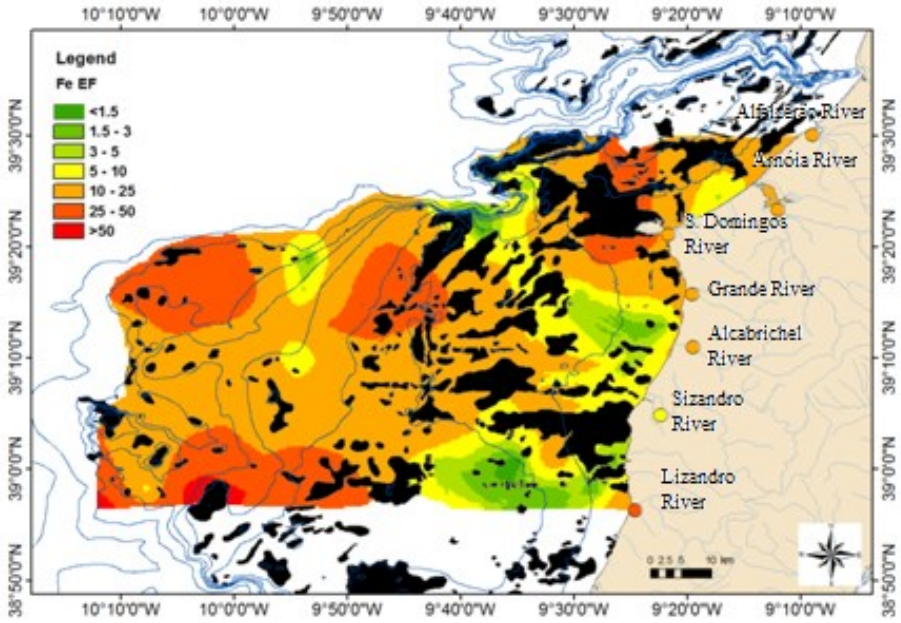

b)

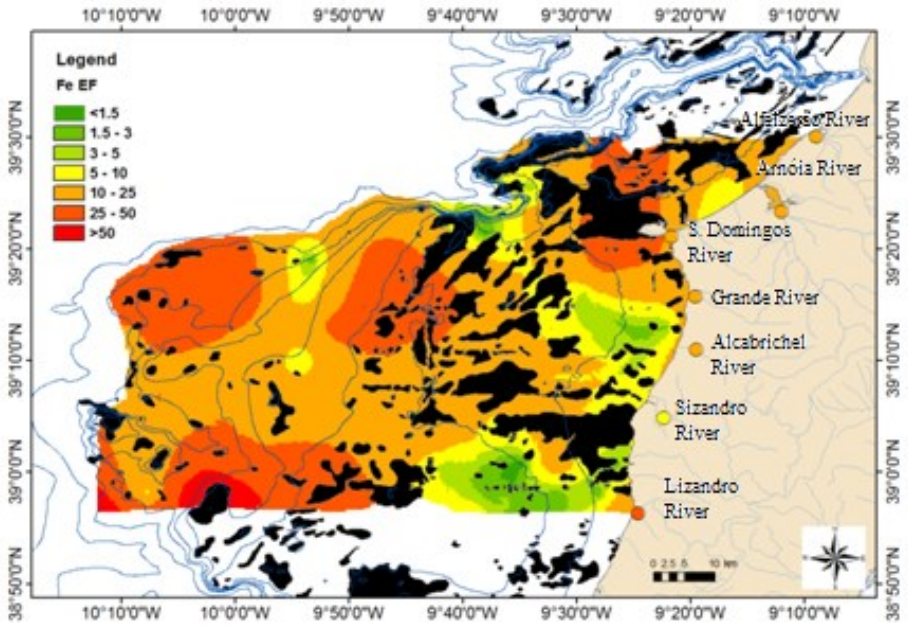

Figure 3.17 - Fe enrichment factor values; a) using baseline values of the uppermost 20 cm thick layer; b) using baselines values of Taylor-McLennan (1985).

Considering the Cu enrichment factor in the shelf domain (Figure 3.18a and b) the lower values (<5 EF), are concentrated in the northern outer shelf and in the middle and inner shelf, with exception of the coastal area closer to Grande river, where higher values (25-50 EF) occur. The higher values of EF are localized in the middle shelf, near Peniche outcrops and in the outer continental shelf in deeper areas.

a)

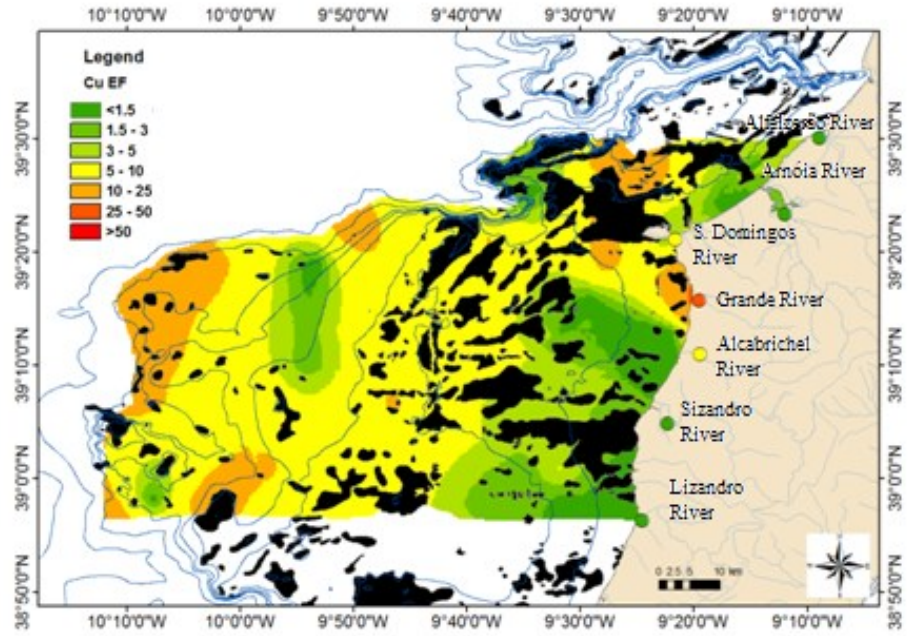

b)

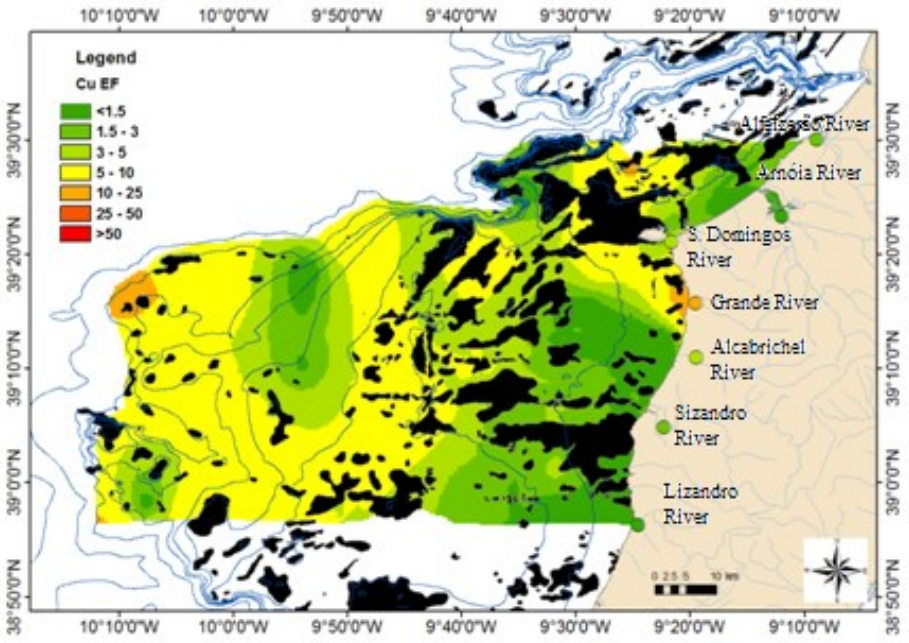

Figure 3.18 - Cu enrichment factor values.
a) using baseline values of the first 20 cm thick layer; b) using baselines values of Taylor-McLennan (1985).

When comparing the above distributions, it is clear that the enrichment values are generally higher in the middle and outer continental shelf and, in a large extent, related to the distribution of the fine-grained fraction in the sediments deposited where hydrodynamics is lower. Also, the N-S elongated area, located in the outer shelf is always characterized by low values of EF, very similar to coastal areas and inner shelf.

3.4. Synthesis

Collected sediments from the rivers that drains directly to the Estremadura Spur and from adjacent beaches are mainly constituted by sand-sized particles. Sediments from river systems have a relevant fine component (except the sample from Lizandro, where the gravelly component is more important). Beach sediments have no fine-grained component, and gravel is only important at Foz do Arelho beach. The comparison of the textural signature of river, inner-shelf and beach sediments suggests a very effective sorting processes: while rivers supply a wide range of grain sizes to the coast and shelf (from gravel to mud), the coarser fractions (medium sand or larger) are retained at the beach. Medium and fine sands are supplied and retained at the inner shelf, and the finer fractions are exported to the middle and outer shelf. The latter processes are responsible for the terrigenous mud deposits that accumulate in the middle continental shelf probably by cross-shelf transport in relation to dense suspensions, that were found to be an important mechanism for the emplacement of mud on the mid-shelf (Hill *et al.*, 2007).

Despite the sediment input from rivers, there is no clear relation between minerals present in the fine fraction that drain to the Estremadura Spur and those found in the shelf. The high percentage of potassium feldspar and plagioclase near the coast was justified due to the proximity to the terrigenous particle sources (continental origin), while the other minerals seem to be related to the effect of distribution processes which controls the distribution of the main mineral species. The riverine environment has clearly different assemblages of heavy minerals from the ones presented by beaches and inner shelf, but they indicate the signature of the geologic formations outcrops: 1) tourmaline, andaluzite, staurolite and phyllosilicates associated to the northern Jurassic and Cretacic limestones with pyroxenes and some amphiboles present in the local basaltic outcrops and dykes; 2) pyroxenes, garnet and zircon with clear decrease of tourmaline.

The heavy minerals put in evidence two distinct coastal sediment cells, characterized by distinct associations. The beach sediments have a similar heavy mineral content when compared to inner shelf sediments, but the signal of the riverine/continental input is higher at the beaches, demonstrated by high percentages of tourmaline and andaluzite in the north, and pyroxenes in the south.

Considering the normalized heavy metal values, excluding Cu in Grande river sample and the major elements (Al and Fe), all the other river samples have no Al-normalized significant values. The higher values of Al-normalized heavy metal values are localized in general in the middle and outer continental shelf.

Chapter IV - Distribution processes in the Estremadura Spur

This Chapter is based on a manuscript published in the Journal of Sea Research:

- Balsinha M, Fernandes C, Oliveira A, Rodrigues A, Taborda R. 2014. *Sediment transport patterns on the Estremadura Spur continental shelf: insights from grain-size trend analysis*. Journal of Sea Research 93, Pages 28–32. DOI: 10.1016/j.seares.2014.04.001

4.1. Introduction

Patterns of sediment movement and associated physical processes are complex in marine environments, causing difficulties in the calculation of sediment transport rates using empirical formulae (Gao & Collins, 2001).

Thus, any information on material movement is beneficial to the study of transport processes and to the test of the transport formulae. Understanding the magnitude and frequency of transport requires knowledge of the wave and current conditions on the shelf over sufficiently long time-series to develop statistical characterizations of the wave and current fields and to document the resulting particles resuspension and transport. This information also provides critical input, and tests off, shelf sediment-transport models that can be used to examine transport patterns over longer time scales and broader spatial scales.

While there are several oceanographic processes relevant to the sediment distribution such as internal waves and currents (geostrophic, density, wave-driven, wind-driven, tidal), the dominant oceanographic forcing responsible for the sediment remobilization on the coastal sector of the Estremadura Spur are the wind-driven surface waves. To understand spatial and temporal predictions of wave-driven sediment remobilization and transport on the Estremadura Spur continental shelf a complementary modelling approach was used: 1) evaluate wave related sediment threshold conditions using a physics-based numerical modeling approach using the **SWAN** model coupled with a formulation for sediment threshold (Booij *et al.*, 1997); and 2) **GSTA-** Grain Size Trend Analysis.

The **SWAN model** (SWAN Team, 2006), a third-generation wave model, developed at Delft University of Technology that computes random, short-crested wind-generated waves in coastal regions and inland waters from given wind, bottom and current conditions, was used to model sediment threshold conditions across the entire shelf.

GSTA (Grain Size Trend Analysis) analyzes transport patterns using Sediment Trend Analysis (STA®) based on sediment grain-size distributions, which can be an indicator of sediment transport. Grain size distribution curves of natural sediments have been used for a long time by sedimentologists to identify the characteristics of depositional environments. It has been found that, within the same sedimentary environment, the grain size distribution of seabed sediment tends to vary according to sampling locations. The spatial changes in size parameters

(i.e., grain size trends) result from a variety of transport processes such as abrasion, selective transport, and mixing of sedimentary material derived from different sources. An inverse problem arises from this observation: can we infer the transport processes on the basis of spatial variations from grain size data (Shu & Collins, 2001)? In other words, the grain-size distribution may change as sediment moves along a pathway, and every sedimentary deposit is the result of a constant and active transport process. The basic assumption inherent in Sediment Trend Analysis (STA®) (McLaren, 1981) is that in the natural environment, differences in grain-size distributions of a given sedimentary depository can be explained by selective transport (Annex 1 – 1.17).

4.2. SWAN: Wave threshold conditions

The methodology was based on the SWAN wave model coupled with a threshold condition in relation to near bottom orbital velocity (Annex 1 – 1.18). SWAN is a third-generation wave model, developed at Delft University of Technology that computes random, short-crested wind generated waves in coastal regions and inland waters (SWAN manual).

In this study, the wave climate in the NEA Ocean was hindcasted with the version 3.14 of the third-generation spectral wave model WAVEWATCH IIITM (henceforth denoted as WW3) (Tolman, 2009). For this study, a series of 22 years of oceanographic data was used (1953-1975) (Dodet *et al.*, 2010). Threshold orbital velocity (m/s) was based on the method of Hanson & Camenen (2007):

Proposed threshold relationship employing the classical definition of the wave friction factor, f_w, according to $\tau_{w,cr} = 0.5\, f_w U_{w,cr}^2$ together with the definition of the Shields parameter, $\theta_{w,cr} = \frac{f_i U_1^2}{2(s-1)g d_{50}}$, where the subscript i maybe replaced by c (current related terms) or w (wave related terms), s = ρs/ρ is the relative density of the sediment, and g the acceleration of gravity, we can derive:

$$f_w U_{w,cr}^2 = 2\theta_{w,cr}(s-1)g d_{50} = \varphi_{cr} \qquad (4.1)$$

In the rough turbulent case, the wave friction factor, f_w, is independent of the wave Reynold's number, $\Re$, and related to the relative roughness $\frac{k_s}{A_w}$ only (Jonsson, 1966) as

$$\left(\frac{1}{4\sqrt{f_w}}\right) + \left(\frac{1}{4\sqrt{f_w}}\right) = \left(\frac{A_w}{k_s}\right) - 0.08 \qquad (4.2)$$

where k_s is the Nikuradse roughness height. It is difficult to estimate k_s for a rippled and duned bottom, but for a plane horizontal bottom of non-cohesive material, it may be taken as $k_s = 2d_{50}$ (Yalin 1977). It should be noted however that Eq. (4.2) is not applicable for small values of $\frac{A_w}{K_s}$. In order to better fit the data (see below), the original formulation of (Jonsson, 1966) is slightly modified in this study according to:

$$\left(\frac{1}{4\sqrt{f_w}}\right)^{0.9} + \left(\frac{1}{4\sqrt{f_w}}\right)^{1.1} = \left(\frac{A_w}{k_s}\right)^{1.1} - 0.08 \quad (4.3)$$

with $A_w = U_w\, T/(2\pi)$

where T is the wave period. Equation (4.3) may be combined with Eq. (4.1) to yield a closed form solution of the critical threshold velocity as:

$$U_{w,cr} = 4\sqrt{\varphi_{cr}}[1.1\ log_{10}\left(\frac{\sqrt{\varphi_{cr}T}}{\pi d_{50}}\right) - 0.08]^{1/0.9} \quad (4.4)$$

$U_{w,cr}$ is the maximum near-bottom horizontal velocity

4.3. GSTA: Sediment transport

This approach is described in Gao & Collins (1992) were the authors re-examined the basic assumptions of the grain-size trend analysis (GSTA).

Gao & Collins (1991, 1992) and Gao (1996) proposed **GSTA**, as a two-dimensional method to estimate sediment trends. In a complex open marine environment, namely the continental shelf, the application of a two-dimensional approach is recommended (GSTA) in which no *a priori* transport directions are known (Poizot *et al.*, 2006), as demonstrated in the English Channel and in the upper slope of the continental shelf of south-central Black Sea where net transport vectors identified using residual grain-size trends are consistent with the local dominant oceanographic conditions. Cheng *et al.* (2004) supports the use of GSTA for large-scale areas on the continental shelf, namely over the Bohai Straight, where results were consistent with current circulation patterns. Additional studies carried out on other continental shelves also support the use of GSTA for open marine environments (Lanckneus *et al.*, 1993; Zhu & Chang, 2000; Shi *et al.*, 2002; Ravaioli *et al.*, 2003).

In an open sedimentary basin, delivery processes interact with physical forcing (the distribution processes) in a constant and delicate equilibrium which prevail until the occurrence of any local or regional alterations. Supply processes are responsible for the input of particles into a depositary while the resuspension and transport processes will promote circulation of particles until final and definitive settling. The formation of sedimentary deposits only occurs when transport ceases and particles accumulate. Considering these assumptions, the grain size of bottom sedimentary particles always reflects dominant physical processes.

Gao & Collins (1992, 1994) include filtering techniques and significance tests for all cases possible, that generates a two-dimension method with residual vector patterns of sediment transport. The significance test used by Gao & Collins (1992) was the *L* test. In this method are also defined the trend vectors, followed by summing, averaging and calculating the length of the characteristic vector.

The repetition of the experiment was sufficient to establish a frequency distribution. From this distribution was defined a critical value L_{99}, with a 99 % confidence.

Then if:

$L > L_{99}$, trends are significant (trends should represent the net sediment transport with high level of significance);

$L \leq L_{99}$, trends are not significant (trends do not represent the net sediment transport).

In 1996 Gao published the **GSTA** software where he uses eight types of sediment transport.

Type 1 - $\sigma_2 \leq \sigma_1$, $\mu_2 \geq \mu_1$ & $Sk_2 \leq Sk_1$

Type 2 - $\sigma_2 \leq \sigma_1$, $\mu_2 \leq \mu_1$ & $Sk_2 \leq Sk_1$

Type 3 - $\sigma_2 \leq \sigma_1$, $\mu_2 \geq \mu_1$ & $Sk_2 \geq Sk_1$

Type 4 - $\sigma_2 \leq \sigma_1$, $\mu_2 \leq \mu_1$ & $Sk_2 \leq Sk_1$

Type 5 - $\sigma_2 \geq \sigma_1$, $\mu_2 \geq \mu_1$ & $Sk_2 \leq Sk_1$

Type 6 - $\sigma_2 \geq \sigma_1$, $\mu_2 \leq \mu_1$ & $Sk_2 \geq Sk_1$

Type 7 - $\sigma_2 \geq \sigma_1$, $\mu_2 \geq \mu_1$ & $Sk_2 \geq Sk_1$

Type 8 - $\sigma_2 \geq \sigma_1$, $\mu_2 \leq \mu_1$ & $Sk_2 \leq Sk_1$

According to Gao (1996) the determination of sediment transport trends should consider the following assumptions:

- The parameters of each station must be compared with the neighboring stations. If type 1 or 2 tendency occurs between a central station and another neighbor station, as a result a non dimensional vector is defined for the central station. To identify a neighboring station a characteristic distance (Dcr) must be defined, which represents the maximum distance between samples. If the distance between two stations is shorter than Dcr, then they are considered neighbors and their parameters are compared.
- The Dcr has the same unit as Y data. Therefore, if Y data are in m, then Dcr is also in m. The same happens for geographical coordinates.
- The X and Y data may be expressed as longitude and latitude values, respectively. The scaling factor is defined by:

$$A = \frac{Dlat}{Dlong} = cos\varphi \qquad (4.5)$$

where *Dlat* is the distance corresponding to 1º along a parallel, *Dlong* is the distance corresponding to 1º along a meridian and φ is the mean latitude of the sampling sites.

The grain-size parameters at the original sampling stations (original data set) are randomly re-allocated to other stations to produce many empirical data sets in order to test whether the residual vectors are the preferred directions of sediment transport. These empirical

data sets are then used to re-calculate the residual vectors according to the method described in the previous section. This experiment is repeated many times in order to obtain a series of residual vectors for each station and data set.

It is arguable which confidence interval one should use and how many empirical data sets one should produce in the grain-size trend analysis. It is clear that in this example the number of residual vectors remains constant above 100 iterations at a range of confidence levels. However, Kemp & Manly (1997) suggested that 1000 iterations are likely to be the minimum requirement for the 95% confidence interval and 5000 repetitions for the 99 % confidence interval, therefore it is recommended that the number of repetitions is tested in the analysis.

The number of iterations needed to run the software for a confidence of 95 %, were tested with a sensitivity test and are represented in Figure 4.1.

Stations that have more than one tendency vector are then transformed resulting in just one tendency vector for each station. Filters are then applied to remove any noise (vectors that are not consistent, in terms of direction, in transport patterns).

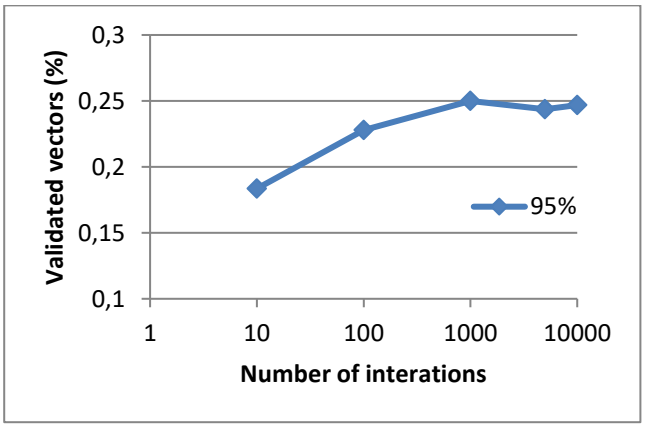

Figure 4.1 - Sensitivity test.

4.3.1. GSTA modelling uncertainties

When a model is used to represent the natural environment, uncertainties occur. These uncertainties can be due to input data, application, structure and finally due to incorrect interpretation of the results. In what concerns model inputs, the authors, cited above, have highlighted some problems such as different procedures of sampling and analysis. Other uncertainties, like the ones mentioned below are related to the sediment properties and diagenetic processes. All of these factors can lead to determining incorrect sediment trend paths.

4.3.1.1. Sediment properties

Assuming that grains of equal size have similar shape and specific gravity, sediment transport processes are more likely to move fine grains instead of coarser (McLaren, 1981); and

for a particular transport, both transported and deposited sediments are assumed to have the same density and porosity (Gao & Collins, 1992), all the sedimentary particles transported by a given process should exhibit the same hydraulic behavior (Poizot *et al.*, 2008). However, for McLaren (1981) "preferential transport due to shape or specific gravity will occur within the grain sizes encompassed by the probability function of particle movement based on size alone". It appears that particle shape has a major influence on the results of grain-size analysis, and this influence varies greatly according to the granulometric method used (Flemming & Thum, 1978; Flemming, 2004). In the same way, the grain density should be taken into account, being a function of water temperature (kinematic viscosity), since it not only affects the mean settling velocity but also the sorting and the skewness of the size distribution (Flemming, 2007).

4.3.1.2. Behavior of particles during transport

The most important fact concerning fine sediments is the occurrence of flocculation, which originates from bigger particles with different hydraulic behavior during the transport process. The difficulty of determining a sediment trend in a mud deposit arises from the fact that the finer particles have this complexity and they naturally constitute aggregates with unknown physical properties and reactions under the effect of hydrodynamic conditions.

4.3.1.3. Behavior of particles after transport

When certain sediment is subjected to high-energy transport that can induce the breaking of grains, the origin particle population is altered, and the deposit cannot be directly related to the original source. After it is deposited, all mechanisms, like bioturbation and diagenesis, alter the chemical composition of sediments. All these modifications are going to mask the sediment trend analysis. This mechanism involves the sequential oxidation of organic matter mediated by microbial activity. Organic matter decomposition drastically modifies the chemical composition of the pore waters and can induce authigenic mineral formation and dissolution of some minerals (Curtis, 1977; Gieskes, 1981). Such modifications can clearly affect the grain populations of the sediments and thus disturb the sediment trends analysis.

4.3.1.4. Depth and density sampling

In any interpretation of sediment trend analysis, one must consider the time-scale and the fact that sampling depth should not be too great (Gao & Collins, 1992), to avoid the combination of ancient and modern trends. These authors defined that sampling depth should be the depth of disturbance, which depends upon the intensity of local dynamic forces. In what concerns density sampling, the optimal distance between samples depends on the spatial scale that someone is working with, geographical configuration and on the sedimentary environments (Poizot *et al.*, 2008).

The sediment trend analysis was made in the Portuguese continental shelf using the program mentioned above in Balsinha *et al.* (2014), where the author concludes that the sediment transport pathways over the Estremadura Spur, deduced from the GSTA, indicate three different sectors in relation to distinct oceanographic, sediment supply and geomorphologic constraints. On the sector offshore Costeiras Pêro da Covilhã the radial upslope sediment transport can be related to a generation of internal waves ("hot-spot" at the shelf break) and upwelling conditions. The northern mid-shelf is clearly dominated by the rocky outcrop barrier effects which interfere with sedimentary distribution processes inducing a much-disorganized transport pattern.

The transport in the southern mid-shelf is affected by the outer shelf transport directed eastwards and by rocky outcrops functioning as natural sediment barriers. GSTA was not able to resolve the sedimentary transport in the inner shelf sector, which is characterized by littoral sands, due to lower sediment sampling resolution.

4.4. Results

To assist in the interpretation of sediment transport modelling results, the distribution maps of the bottom sediment statistical parameters (mean, sorting and skewness) are represented in Figure 4.2, Figure 4.3 and Figure 4.4 (Balsinha, 2008) (Annex 1 – 1.17) (Annex 19)

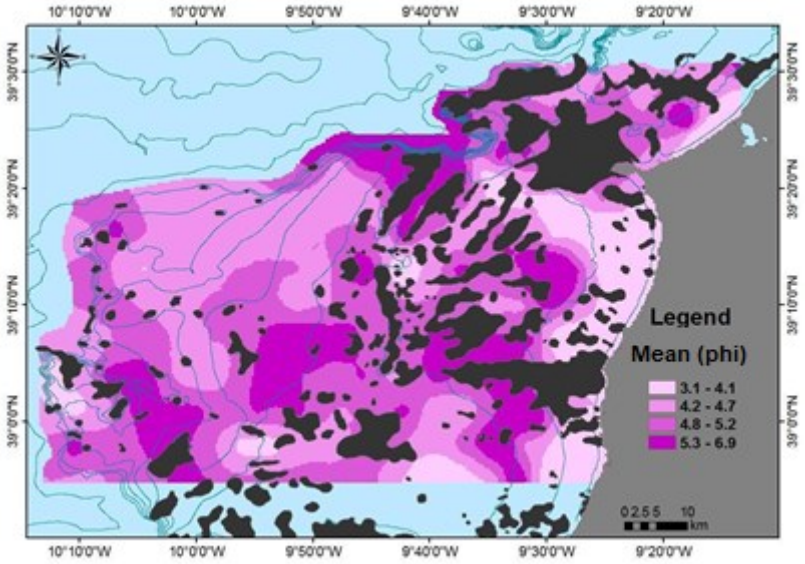

Figure 4.2 - Mean grain size distribution (phi) over the Estremadura Spur. Sample location in Figure 2.12.

The spatial distribution map of sediment mean shows that the coarser sediments are located along the littoral and dispersed along the rocky outcrops and the outer shelf. The very fine sediments are confined to several deposits located in specific areas like Ericeira mud deposit, northern slope and submarine valley near Pico Gonçalves Zarco. These deposits are poorly sorted with negative and positive skewness. Sorting and mean have a similar behavior concerning the littoral deposits, while skewness and mean behave in the same way in the rest of the area (Figure 4.3 and Figure 4.4).

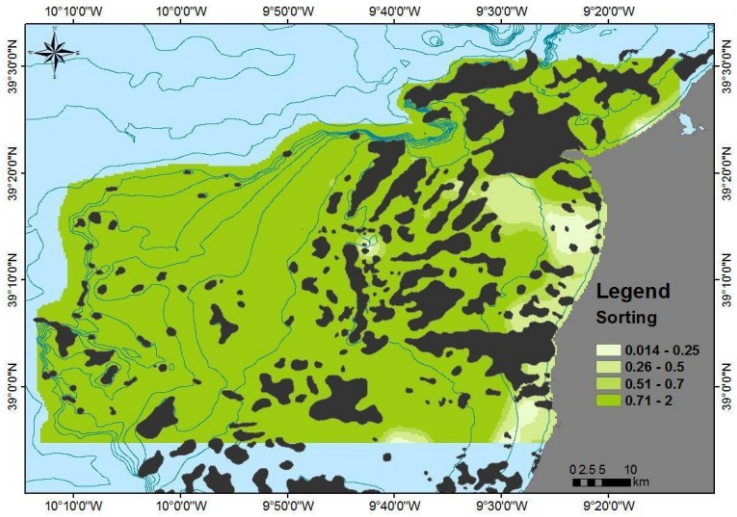

Figure 4.3 - Sediment sorting distribution over the Estremadura Spur.

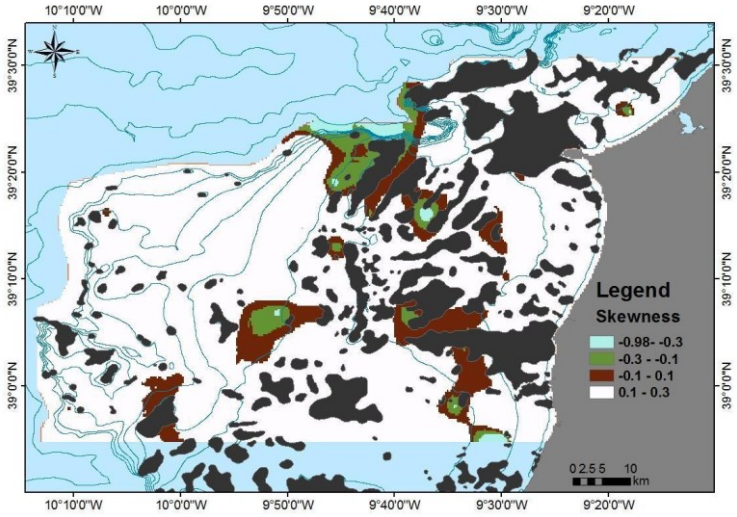

Figure 4.4 - Sediment skewness distribution over the Estremadura Spur.

Textural classification indicates that most samples are poorly sorted with deviations to moderately sorted (Figure 4.5).

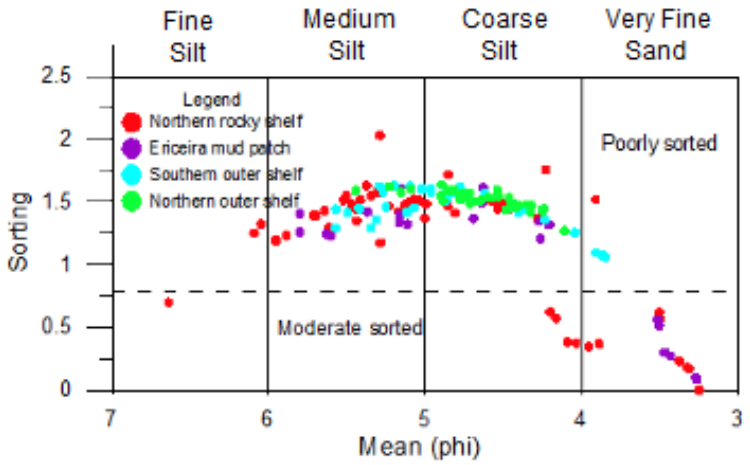

Figure 4.5 - Textural characterization: mean (phi) versus sorting.

The coarser and moderately sorted particles are located near the coast making part of littoral sand deposits. The northern rocky shelf area and the Ericeira mud deposit are the ones with higher variability in terms of grain size and calibration contrasting with deposits from northern and southern outer shelf sectors. Also, the sediments vary from symmetric to a very positive symmetry (Figure 4.6).

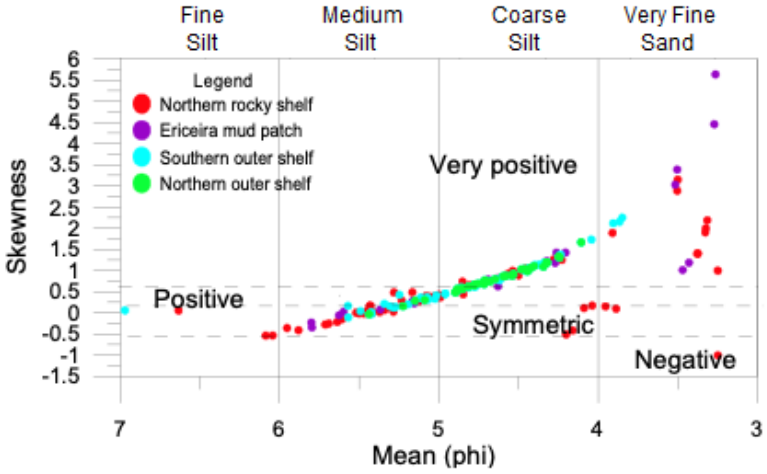

Figure 4.6 - Textural characterization: mean (phi) versus skewness.

4.4.1. Threshold conditions based on the Swan Model

The application of the SWAN and critical velocity models gave valuable insights on the remobilization frequency across the entire shelf (Annex 1 – 1.18).

. For coarse sand particles (0.500 mm) (Figure 4.7) results show that in the inner shelf (until ~ 30 m depth), in general, sedimentary particles are remobilized ~ 40 % of the time. Till 100 m depth the coarse particles results show that particles are remobilized at most, 10 % of the

time, which in the northern area has as expression of ~ 35 km wide, while in the southern it reaches only ~ 5 km.

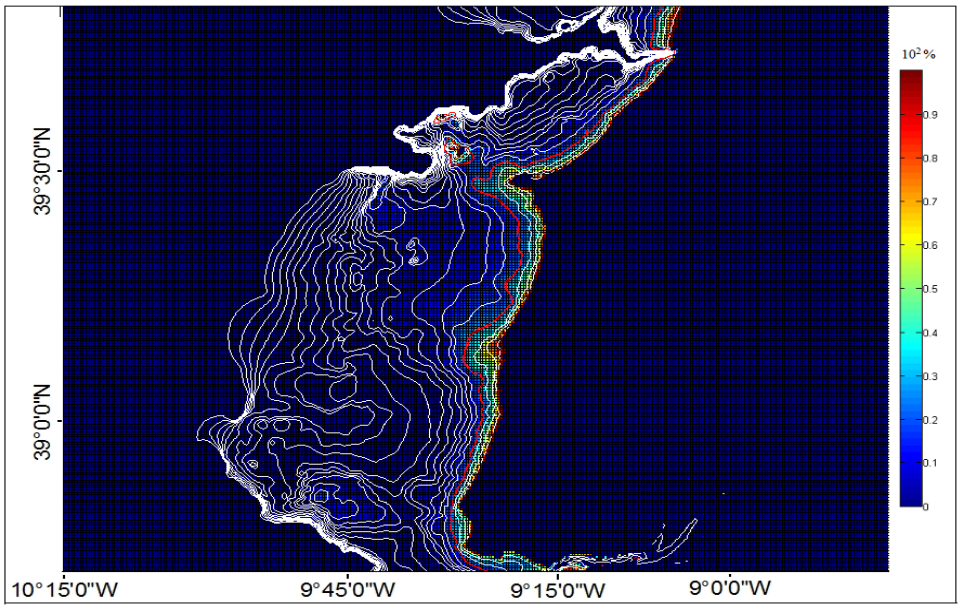

Figure 4.7 - Map of percentage of time of orbital velocity near the bottom in m/s for 0.500 mm particles. Red line marks the limit where particles are remobilized 40 % of the time.

Using threshold velocities for fine particles (0.063 mm) one can determine the percentage of time that these particles are remobilized (Figure 4.8). For depths greater than 100 m, the particles are remobilized less than 10 % of the time, while at 40 m depth fine particles are remobilized ~ 50 % of the time.

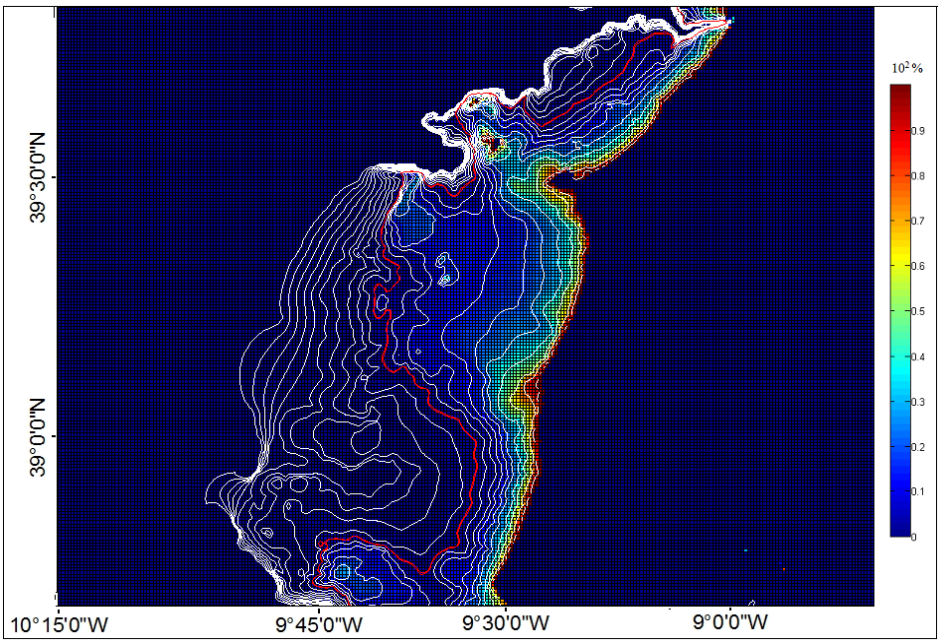

Figure 4.8 - Map of percentage of time of orbital velocity near the bottom in m/s for 0.630 mm particles. Red line marks the limit where fine particles remobilized 10 % of time.

4.4.2. GSTA

Grain-size trend analysis (GSTA) was used to infer sediment transport patterns on Estremadura Spur continental shelf. Sediment transport patterns were defined using the Gao & Collins (1992) method applied on an extensive collection of superficial sediment samples collected from 14 to 706 m water depths and using a characteristic distance based on geostatistical analysis that when observations, variogram, and prediction locations are specified, the default action is ordinary kriging.

Results are in relatively good agreement with known oceanographic drivers for the external shelf (internal waves, and upwelling) and measured near-bottom currents. At inner and middle shelf sectors, computed sediment transport vectors yielded less coherent patterns probably related with low sampling density in relation to surficial sedimentary deposit dimensions and the presence of rocky outcrops (Figure 4.9).

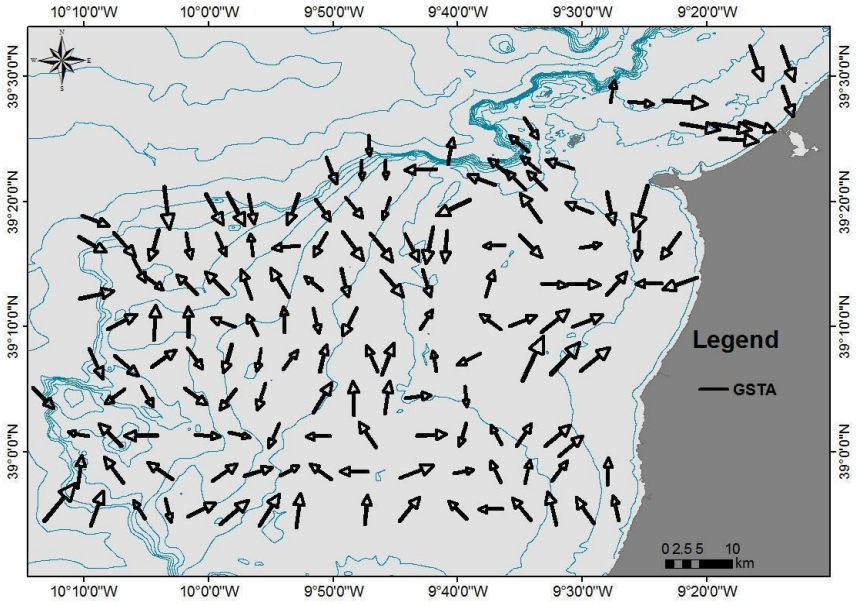

Figure 4.9 - Vector distribution pattern using GSTA program Balsinha *et al.* 2014.

In general, the sediment transport vectors are consistent with a dominant onshore direction, covering the entire western outer shelf. This transport trend also dominates in the northern sectors with a general south to south-eastward directions. In the middle and inner shelf vectors become less organized, probably reflecting the morphologic barrier of the existing rock outcrops. At the mid shelf north of Ponta da Lamparoeira it is not possible to define a clear transport trend due to erratic behavior in the transport vectors; sometimes contiguous vectors present opposite directions that may be related to a decrease in transport intensity. This pattern can be associated with the nature of the sedimentary cover where discontinuous coarse sediments patches are scattered over a hard rock bottom. The characteristics of these deposits suggests a

dominance of local supply processes over the distribution which goes against the assumptions of grain-size trend analysis (at least with the present sampling density) and therefore results over this area cannot be considered representative of the prevailing transport patterns.

At the inner shelf, transport vectors are either inexistent or directed onshore. This aspect is not in agreement with previous studies conducted at the inner shelf north of Peniche, which considers that in Almagreira beach (north of Peniche) the morphodynamics of the inner shelf is conditioned by seasonal wave regime that causes higher sediment mobilization during winter periods. During this regime, the waves come from a westward direction, inducing a northward longshore current with a general net sediment loss (Lapa *et al.*, 2012). This disagreement can be explained by the narrow nature of the inner shelf deposits where the present sampling density cannot be resolved by the model.

The outer shelf transport pattern, perpendicular to the general bathymetry and oriented to the central areas of the Estremadura continental shelf is consistent with the internal waves "hot-spots" location. This fact suggests that particles are resuspended in the upper slope and in the shelf break area and forced, by the propagation and dissipation of internal waves, to be transported to shallower regions of the outer and mid shelf. In some periods, due to persistent northerly winds, the occurrence of upwelling events can intensify this upshelf sediment transport pattern. This vector pattern is congruent with the measured current meter data. Considering vectors length and magnitude, they are higher in the shelf-break and outer continental shelf and weaker towards the middle and inner shelf. In the southern mid shelf off Ericeira, the transport vectors are oriented towards the coast and southeastern and do not reflect the presence of an important mud patch, recognized by Balsinha (2008) and mapped by Instituto Hidrográfico (2010). This is probably due to frontiers imposed to the model. Nevertheless, it is anticipated that their location can be related by the influence of internal waves originated in the southern shelf break, which migrate towards northeast and will interact with the described southward transport of the mid shelf particles. As a result, a deceleration area will be formed and particles will settle in the mid shelf.

4.5. Synthesis

Threshold orbital velocity near the bottom computed with SWAN, using 22 years of wave data, for coarse (0.500 mm) and fine particles (0.063 mm) show that coarse particles are remobilized about 40 % of the time just under 30 m depth (inner shelf) and fine particles are remobilized ~ 10 % of the time for depths up to 100 m. Such results are consistent with previous results already obtained by Magalhães (2001) and compatible with a high energy wave/storm dominated continental shelf. This result is also in-line with the relative high depth of the SMT (the sand–mud transition which marks the boundary on the sea floor where the dominant grain size changes from sand to silts and clays, which is around 60 m depth (Rey *et al.*, 2014).

The sediment transport pathways over the Estremadura Spur, deduced from GSTA, indicate four different sectors in relation to distinct oceanographic, sediment supply and geomorphologic constraints. On the sector offshore Costeiras Pêro da Covilhã the radial upslope sediment transport can be related to the presence of internal waves ("hot-spot" at the shelf break) and upwelling conditions. The northern mid-shelf exhibits a patchy sedimentary cover in relation to the rocky outcrop effects which interfere with sedimentary distribution processes, complicating the interpretation of deduced transport pattern. The transport in the southern mid-shelf is affected by the outer shelf transport directed eastwards and by rocky outcrops functioning as natural barriers to sediment transport. GSTA was not able to resolve the sedimentary transport in the inner shelf sector, which is characterized by littoral sands, due to low sediment sampling resolution.

Chapter V - Holocene evolution of Ericeira mud patch

5.1. Introduction and data

The superficial sedimentary characteristics of shelf deposits reflect the present and recent past dynamic processes (particle input, transport and deposition) and are very important to understand the sedimentary dynamics of the marine environment. This analysis was performed in the previous chapters, with a description of the shelf sedimentary cover (Chapter III) as well as the main physical processes involved in sediment transport (Chapter IV). In this chapter the former analysis is extended to the third dimension, through the inclusion of the vertical length (depth), enabling the understanding of the variation of meteo-oceanographic forcing and sediment availability through time.

The study of climate change for which there is no instrumental record ("paleoclimatology") is mostly inferred from geological proxies preserved in sedimentary record, which enable scientists to reconstruct the climatic conditions that prevailed during the Earth's history. Establishing the evolution of sedimentary, oceanographic and climatic processes, through geological time allows, not only the study of past environments and processes, but also the quantification of the impact of extreme events, being a useful tool to understand, predict and model future environment scenarios related to climate change.

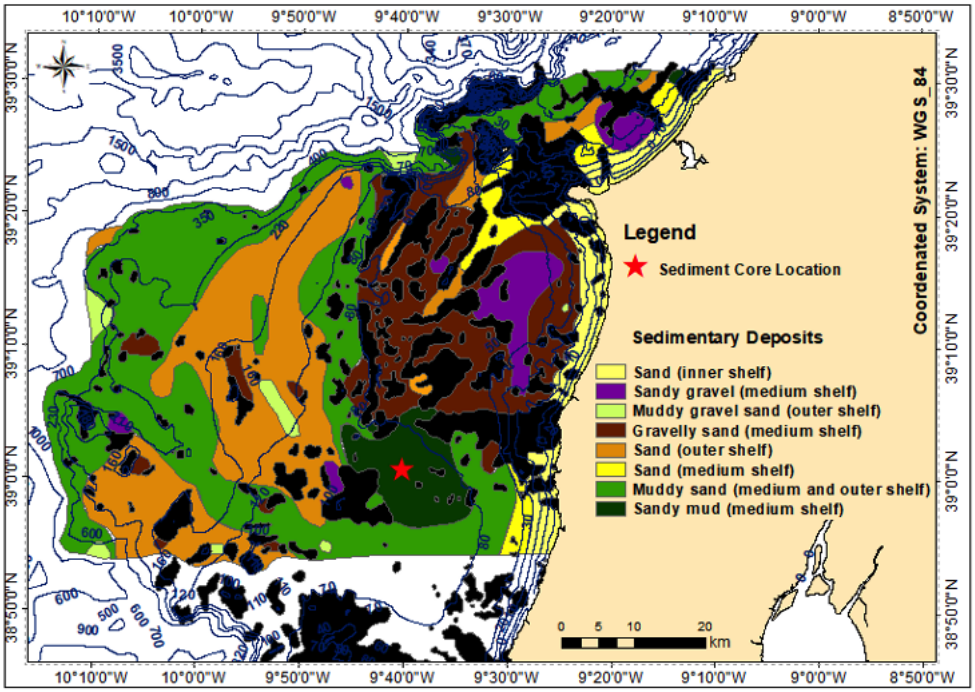

Figure 5.1 - Sediment core location over the sedimentary deposits map from Balsinha (2008).

To describe the vertical variation of sedimentary facies (related to the evolution of sedimentary processes) at the Estremadura Spur, a 162 cm long vertical sample was collected at 115 m depth, on the Ericeira mud deposit, the main fine-grained deposit of Estremadura Spur (Figure 5.1).

At the sampling site, the collected sample represents the entire unconsolidated sedimentary column, consisting generally of mud and sandy mud, deposited on top of very coarse material (gravelly sand), probably the base of the sedimentary layer. The sample was fully and extensively analyzed, and results are summarized in the following sections.

5.2. Internal description of the Ericeira sediment core

5.2.1. Internal structure

5.2.1.1. Visual description and X-Ray imagery

Five photographs and x-ray images of 30 cm were taken (with 5 cm of overlap), in order to distinguish different sedimentary sequences and features along the sedimentary column (Figure 5.2a, Figure 5.2b) (Annex1 - 1.3) (Annex 5).

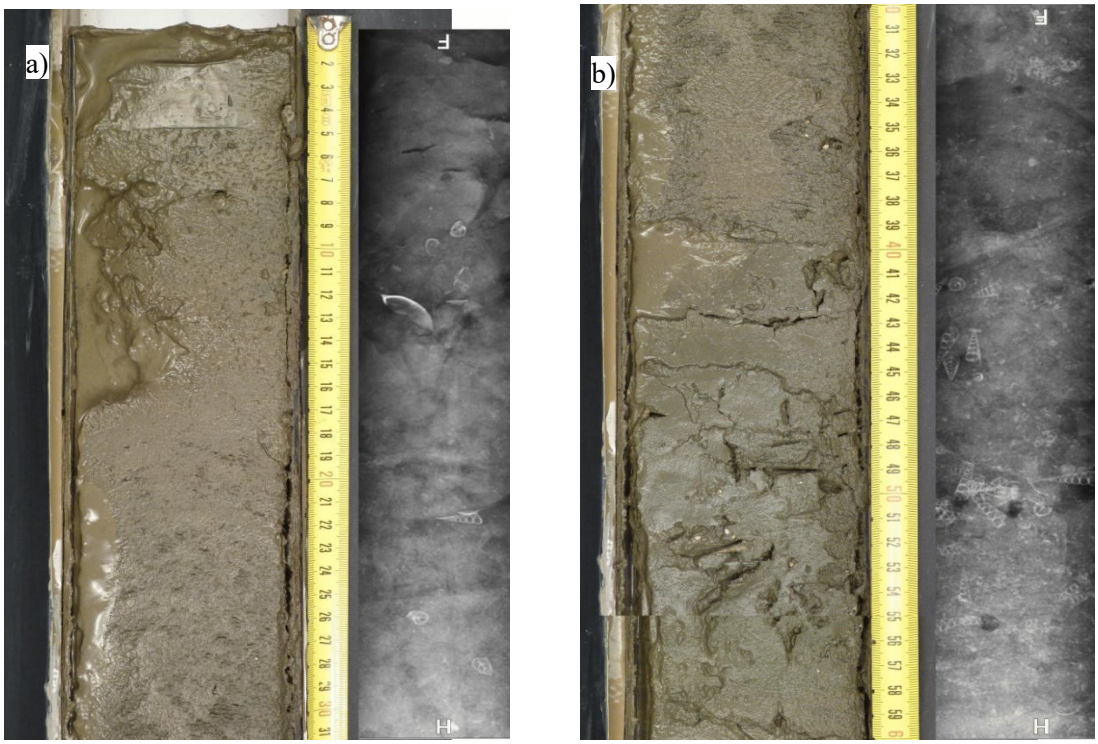

Figure 5.2 - Estremadura Spur sediment core photographs and x-ray imagery (0-60 cm). Image (a) represents the top section (0-30 cm) and (b) represents the second section (30-60 cm).

The first 33 cm are characterized by muddy sediments with fine grain texture with brownish color, presenting vertical and horizontal bioturbation and some scattered shells of

gastropods (Figure 5.2a). As expected, the first centimeters have a fluffier texture with higher water content, becoming drier and more compact with depth. The second section (34-60 cm; Figure 5.2b) presents some differences, regarding the color and grain texture: sediment is slightly more grayish (Munsell - N 5/) with the correspondent grain size coarseness. At the 50-55 cm level a dense accumulation of gastropods *Turritella communis* was detected, being present until 115 cm depth.

The following sections (60-90 cm and 90-120 cm) have a similar trend. Most particles have a biogenic nature, although there is no evidence of biogenic activity as there is an increase in coarser particles to the bottom (Figure 5.3b). At approximately 115 cm below the surface, an abrupt color change is visible related to the increase of terrigenous particles and carbonate content, as it is observed in the x-ray image.

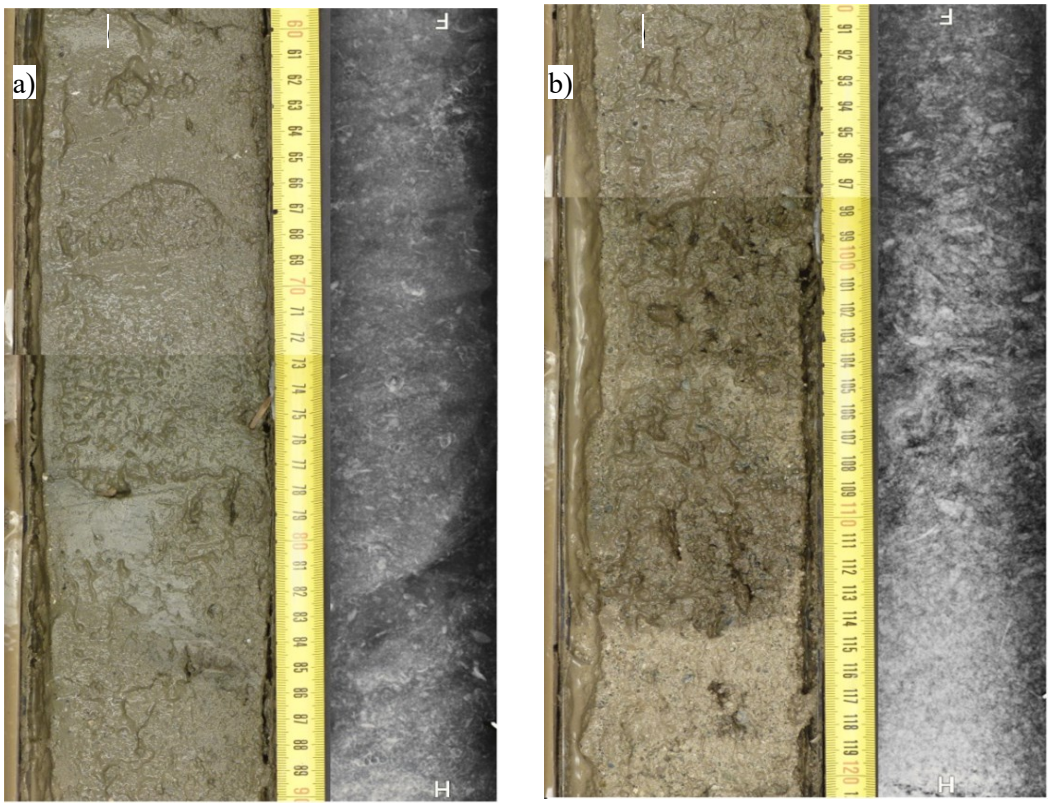

Figure 5.3 - Estremadura Spur sediment core photographs and x-ray imagery (60-120 cm). Image (a) represents the 60-90 cm section and (b) represents the 90-120 cm section.

In the deepest section of the vertical sample, it is perceptible, either from the core photography or from the x-ray imagery, the change in sedimentary texture, with high concentration of very coarse particles, constituted mainly by lithoclasts and shell fragments (Figure 5.4).

Considering the visual description of the above sections, it is possible to identify a clear change in the vertical sedimentary facies. The topmost muddy sediments are affected by bioturbation and present significant biogenic particles. Below 50-55 cm, the second sequence with ~50 cm thick is dominated by biogenic particles, which remain until 115 cm depth, when an abrupt change in the sedimentary texture and structure is observed. The third sequence seems to be dominated by sandy particles, very tightly packed and showing no bioturbation. The last sequence was observed at the bottom of the sedimentary column, where coarse material (gravelly sand with large pebbles) prevails.

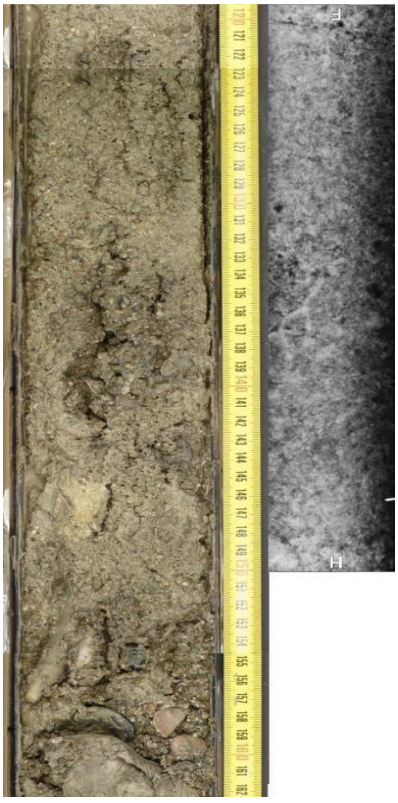

Figure 5.4 - Estremadura Spur sediment core photographs and x-ray image (120 - 160 cm).

5.2.1.2. Magnetic susceptibility

The results of the magnetic susceptibility measurements along the sediment core are projected in Figure 5.5, showing the presence of a high-level peak of magnetic susceptibility (475×10^{-6} SI) at 156 cm (Annex1 - 1.4) (Annex 6).

At this level there is an extremely high concentration of very coarse terrigenous particles (visually detected through morphoscopy) and high percentages of siderite (fine mineralogy analysis), glaucony, heavy minerals (pyroxenes) and volcanic lithoclasts with phenocrystals (Figure 5.6).

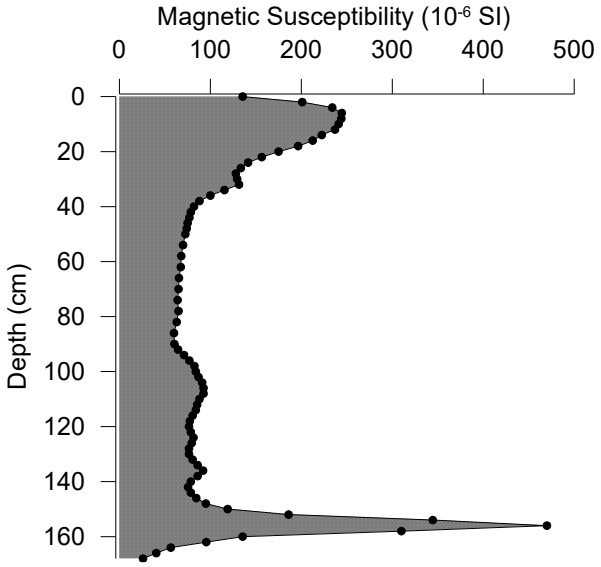

Figure 5.5 - Magnetic susceptibility values along the core (units: 10^{-6} SI).

Figure 5.6 - Volcanic lithoclasts with phenocrystals, collected at the core base that are related to the maximum value of magnetic susceptibility.

The presence of these iron rich particles in the sediments can explain the observed values on the magnetic susceptibility. Above the 156 cm level, the values of magnetic susceptibility rapidly decrease to values around 100 x10^{-6} SI, with two sectors with minor differences. The deeper one, presents values around 100 x10^{-6} SI until 90 cm depth and the second (from 90 cm to 40 cm) with consistent values around 50 - 70 x10^{-6} SI. Shallower than 40 cm, the magnetic susceptibility increases its intensity, with a small peak at 35 cm depth (130 x10^{-6} SI) and the second peak with a value of 240 x10^{-6} SI at 6 cm depth. After this value, the magnetic susceptibility decreases until 130 x10^{-6} SI, observed at the top of the sedimentary core.

5.2.2. Texture and composition

5.2.2.1. Dry bulk density

The values for dry bulk density are described in Table 5.1. Is visible that dry bulk density increases with depth, with a minimum value of 0.77 g/cm^3 at the bottom and a maximum at level 137 cm with 1.77 g/cm^3. It is also visible a significant increase in this parameter, between levels 75 cm and 109 cm, where values increase from 1.09 g/cm^3 to 1.72 g/cm^3. At around 32 cm the dry bulk density increases slightly till 1.20 g/cm^3 decreasing to the top to 0.89 g/cm^3 (Annex 1 - 1.5) (Annex 7).

Table 5.1 - Dry bulk density values (g/cm^3) for selected levels.

Depth (cm)	DBD (g/cm3)
1	0.89
10	1.00
20	1.03
32	1.21
52	1.19
75	1.09
109	1.72
124	1.58
137	1.78
157	0.77

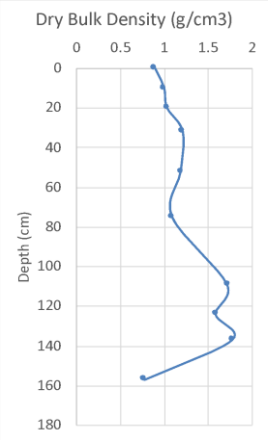

5.2.2.2. ^{210}Pb

For this study the first 20 cm were sampled and analyzed by the Marine Geology Department of the Royal Netherlands Institute of Sea Research (NIOZ).

The ^{210}Pb activity profile of Estremadura core, revealed to be adequate for calculating MAR (Mass Accumulation Rate) (Figure 5.7). The core provided well fitted-profiles with the CF/CS+SML model (Constant Flux Constant Sedimentation + surface mixed layer models) (Annex 1 - 1.6) (Annex 8). The core registers a sedimentation rate of 0.07 cm/y with a surface mixed layer of ~10 cm (Figure 5.7).

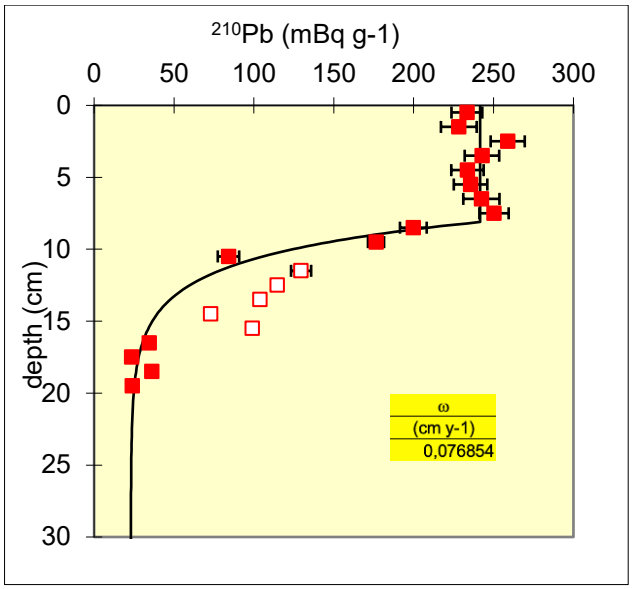

Figure 5.7 – Total ^{210}Pb activity values (supported and unsupported) (mBq g^{-1}) for Estremadura core for the first 20 cm. The white squares are outliers excluded from MAR.

5.2.2.3. Carbon content

The carbon content in sediments, analyzed as Total Organic Carbon (TOC) and Total Inorganic Carbon (TIC), indicate that TOC values are very low in the bottom core (0.4 %) while TIC values are higher (7 %) due to the presence of high concentrations of mollusk shells (Figure 5.8). Along the sediment core, TOC values increase gradually from the core base (0.4 %) till approximately 20 cm (1 %), and abruptly in the uppermost level, reaching values of 1.4 % at the top. On the other hand, TIC has an opposite behavior, despite the observed variation along the sediment column, from 7 % at the base to 3 % at the top (Annex 1 - 1.7) (Annex 9). This along core variation, can be explained by the biogenic particles that were referred to in the core photographs and x-ray imagery description.

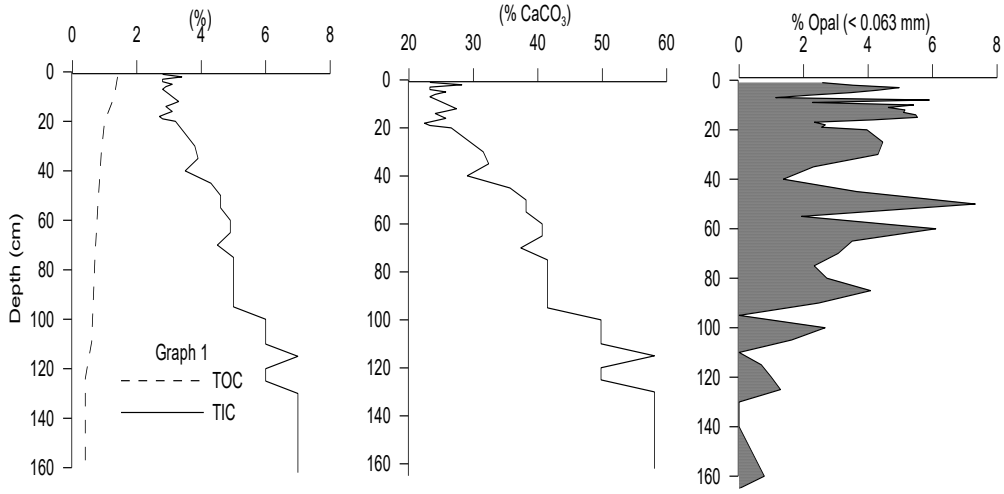

Figure 5.8 - Percentages of TOC, TIC, CaCO3 (estimated from the TIC content) and opal along the sediment core.

The calcium carbonate ($CaCO_3$) content variation along the sediment core was estimated by applying the 8.33 factor to TIC values, assuming that all the inorganic carbon is present in the form of calcium carbonate (Liu *et al.*, 2014). As expected, $CaCO_3$ values have the same behavior of TIC, increasing its values downwards, from 25 % until the maximum value of 60 %.

Biogenic silica, as well as TOC, are major components of the marine-derived biogenic sediments that constitute a small source of $CaCO_3$. Concentrations of biogenic silica (BSi – opal percentage) in the fraction < 0.063 mm reveal consistently low values at the bottom of the core compared with those obtained in the upper muddy sequence. Opal content falls in the range of 0.78 % (bottom), starting to increase at 85 cm (4.08 %) achieving peaks of 7.32 % at 50 cm depth. To the top, the values vary between 1 % and 5 % with a mean value of 4 %, being the top value of 2.58 %. This increase of TOC can be due to the appearance of diatoms, radiolarians, silicoflagellates, which are related to high levels of productivity in relation to sediment deposition.

5.2.2.4. Grain-size

To describe the vertical textural variation along the core, grain size analyses were executed in subsamples extracted from the core, using standard sieve and laser techniques (for details, see Annex 1 - 1.9). Grain size distribution allowed sediment textural classification (gravel, sand, silt and clay) and the computation of classical statistical parameters: mean, sorting, skewness and kurtosis (Annex 10).

The grain-size distributions, along the core are plotted in 2D view (Figure 5.9a) and 3D view (Figure 5.9b).

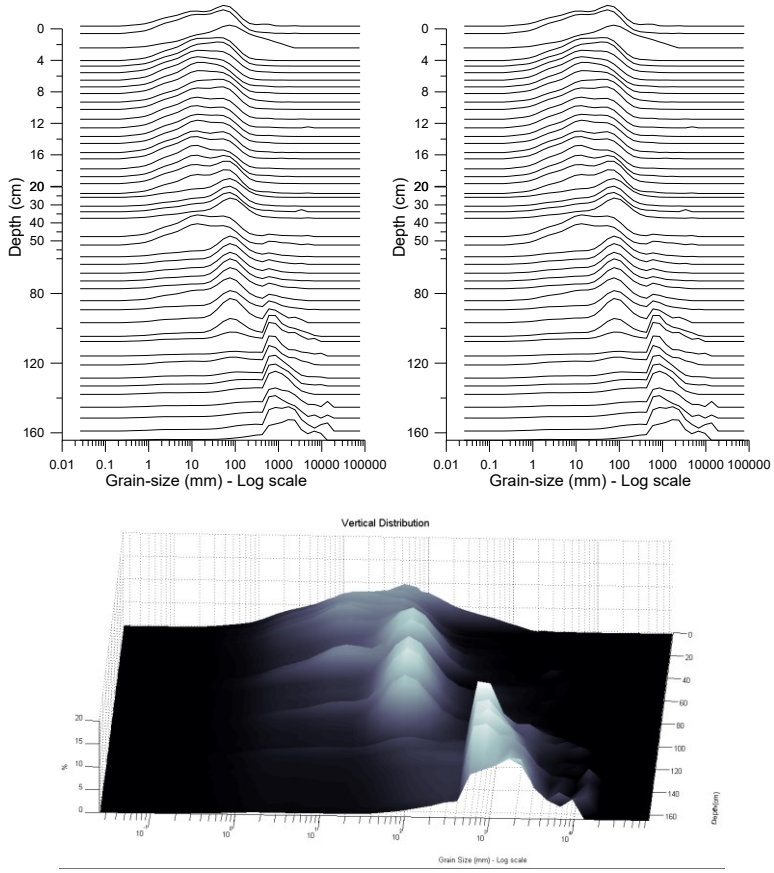

Figure 5.9 - Particle-size (mm) distribution along the sediment core. Representation in 2D (a) and 3 D (b).

Results of grain size analysis, summarized in Figure 5.10, indicate that in general silt and sand are the dominant classes.

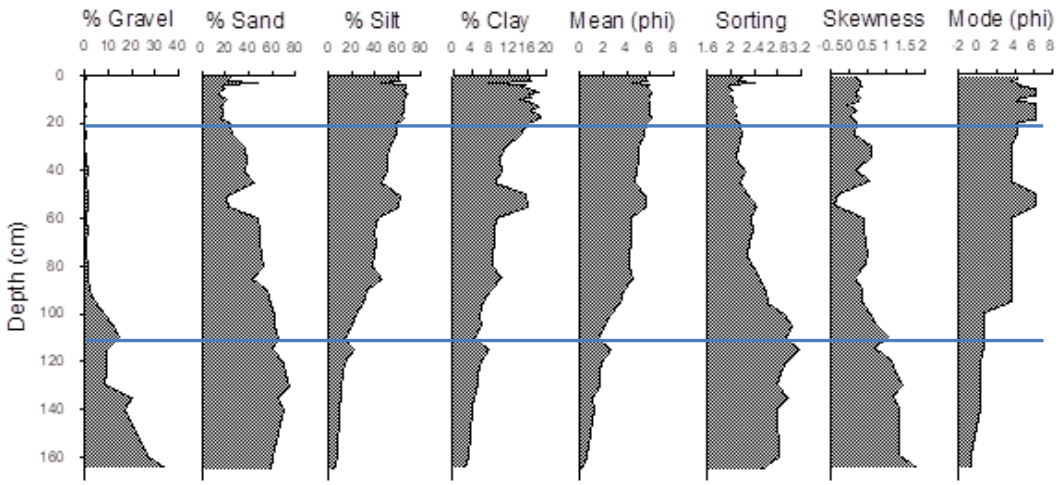

Figure 5.10 - Grain-size distribution and textural parameters percentage from Estremadura core.

Along the sediment core, sand presents higher percentages below 130 cm depth (values between 58 % at the core base, and the maximum value of 74 % at 130 cm), and then gradually decreases to 20 % at the top. A more detailed analysis on the sand content along the core, allowed to identify three discontinuities well marked at 115 cm, 90 cm and 55 cm, which coincide with enrichment of the fine fractions. The silt and clay fractions have an opposite behavior of sand. Silt presents values of 4 % in the bottom, increasing to 21 % at 115 cm, and then a rapid increase to 46 % at 85 cm. At 55 cm, silt presents values of 60 % that descend to 45 % at 45 cm, restarting to rise to the top, achieving values of 60 %. The clay fraction is similar to the silty one but with lower values (2 % at the bottom and the similar peaks at 115 cm, 85 cm and 55 cm with values of 7 %, 10 % and 15 % respectively, continuing to increase to the top reaching values of 16 %). Regarding the gravel content, values are higher at the core base (35 %) and decrease upwards, until reaching a value of around 2 % (at 90 cm). From this layer to the top, the gravel percentage is very low and almost null at the uppermost layers.

Concerning the grain-size statistical parameters, mean has a similar pattern to silt and clay. The bottom values are the lowest (larger grains, 0.08 phi, ~ 0.94 mm), increasing gradually upward until values of 6 phi (~ 0.016 mm), at the top, with a peak of 2.56 phi (~ 0.16 mm) at 115 cm, 4.5 phi (~ 0.04 mm) at 85 cm and 5.6 phi (~ 0.02 mm), at 55 cm with decreasing of particles diameter.

The lower layers of the sediment core are poorly sorted (~ 3) until the 85 cm level. Upwards, a decreasing trend in sorting is observed. Relatively to skewness, the bottom core is extremely positive, indicating an excess of fine particles (1.83), decreasing to the top (0.18) where the skewness is positive. The excess of finer particles at the bottom, where sediments are coarser, is consistent with the observed deviation of fine particles relatively to the mode, which is greater in the bottom (Figure 5.10).

Considering the grain-size distribution and the textural classification it is possible to define three domains:

- a lower domain (from 162 cm to 100 cm), dominated by coarse particles (gravel and sand) and minor occurrence of finer particles;

- an intermediate domain (100 cm to 20 cm) with no gravel and an upward increasing content of finer particles;

- an upper domain (the uppermost 20 cm) where sand, silt and clay frequencies are more or less constant, but showing small scale variations.

5.2.2.5. Mean sortable silt analysis

Fine grain-size parameters have been used for inference of paleoflow speeds of near-bottom currents in the deep-sea (McCave *et al.*, 2017) (Annex 1 - 1.11) (Annex 11).

When comparing the results given by carbonated mean sortable silt, one can verify that the values increase upwards, from a mean value less than 2 % (at the core base), ~ 6.5 % (between 115 cm and 40 cm) with a peak of 8 % at 55 cm and about 9 % at the top (Figure 5.11) (Annex 11).

When analyzing results of the mean sortable silt vertical variation, one can verify the existence of 4 vertical sequences along the sediment core. The basal 52 cm thick layer, the sortable silt has a mean size of 0.035 mm, being the silt/clay ratio of about 2 %. The decarbonated sortable silt has a mean value of 9.5 %, while the carbonated silt presents the lowest values (less than 2 %).

The following sequence (from the 110 cm until the 60 cm) is characterized by the increase in all the sortable silt studied parameters (mean grain size near the 0.04 mm, 4.5 % on the silt/clay ratio, 11.5 % and 6 % of decarbonated and carbonated sortable silt). On the top layer, abnormal high values were measured in the carbonated silt (8 %) and decarbonated silt (12 %), while the silt/clay ratio and the mean grain size indicate a negative variation (4 % and 0.03 mm, respectively). After this abnormal 10-15 cm thick level, the silt/clay ratio increased to the maximum value of 5 %, as well as the carbonated sortable silt (8 %); the decarbonated sortable silt decreased to 11 % and the mean size decreased to 0.035 mm. The uppermost 20 cm thick sequence presents high internal variability regarding the silt/clay ratio (mean value of 4 %), mean size (0.03 mm), decarbonated particles (10 %) and carbonated particles (9 %).

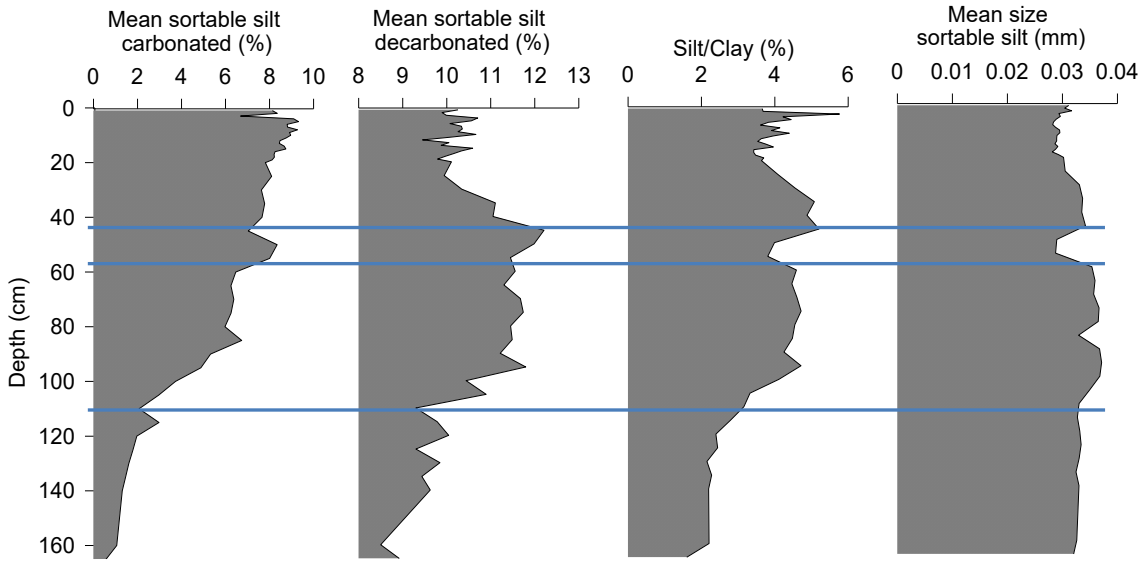

Figure 5.11 - Percentage of mean sortable silt (mm) and silt/clay ratio.

5.2.2.6. Sandy fraction morphoscopy

A detailed compositional analysis was made in the five following fractions of the sand class: very coarse sand (1 – 2 mm), coarse sand (0.5 – 1 mm), medium sand (0.250 – 0.5 mm), fine sand (0.125 – 0.250 mm), and very fine sand (0.063 – 0.125 mm). The main mineralogical components (quartz, phyllosilicates, aggregates, terrigenous, mollusks, benthic and planktonic foraminifera, other biogenic particles such as remains of corals and bryozoan and glaucony), were optically identified, counted and plotted in downcore graphics (for details on the method see Annex 1 – 1.10) (Annex 12).

In the very coarse sand fraction (Figure 5.12), terrigenous particles are more abundant than the biogenic ones, and quartz is the dominant component (reaching the maximum value of 20 % at 130 cm), followed by aggregates (with 20 % at 100 cm), other terrigenous (with 50 % at 115 cm) and biogenic particles (almost 15 % at 65 cm). The percentage of mollusks is high, reaching values of 37 %, while phyllosilicates and glaucony are absent. These components present some variations along the core sample below the 60 cm, because in the uppermost layer sediments are much finer.

Coarse sand fraction (0.5 – 1 mm) is only present below 35 cm depth (Figure 5.13). In this fraction, the values of quartz increase to levels of 40 % at 75 cm, being the mean around 22 %. Aggregates decrease to values of 16 % at 55 cm, being the mean values of aggregates around 10 %. The terrigenous particles maintain their abundance, with 41 % at 125 cm. The percentage of mollusks is higher, as in the coarser fraction, but with minor oscillations of lower percentages throughout the core.

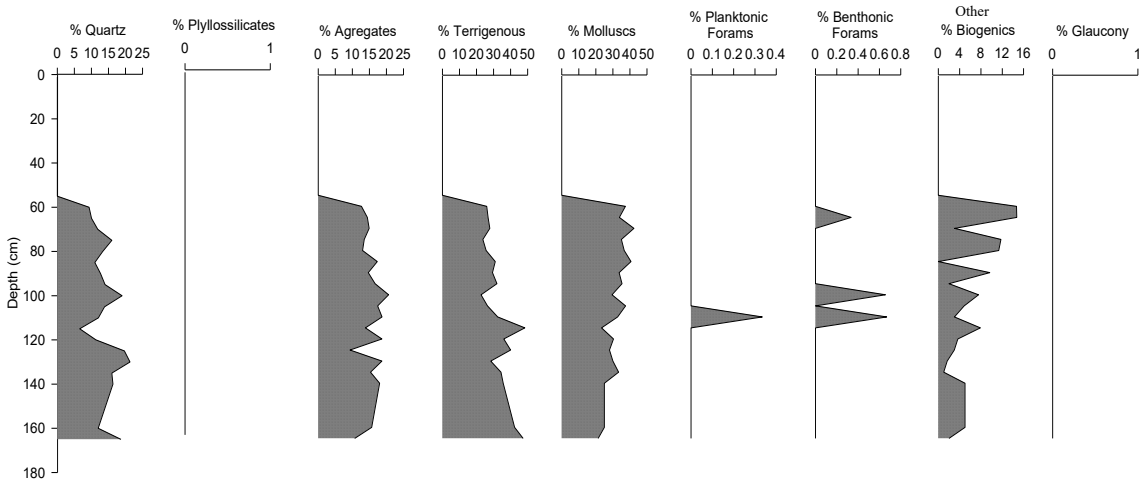

Figure 5.12 – Percentage of morphoscopic elements for the very coarse sand fraction (1 – 2 mm).

In the coarse sand fraction, biogenic particles and foraminifera start to be a representative fraction. Benthic foraminifera, present values of 12 % (at 115 cm), while planktonic foraminifera

reach a percentage of 20 % at 50 cm. Grains of glaucony start also to be common, although with very low abundance. Phyllosilicates are still absent in this grain-size class.

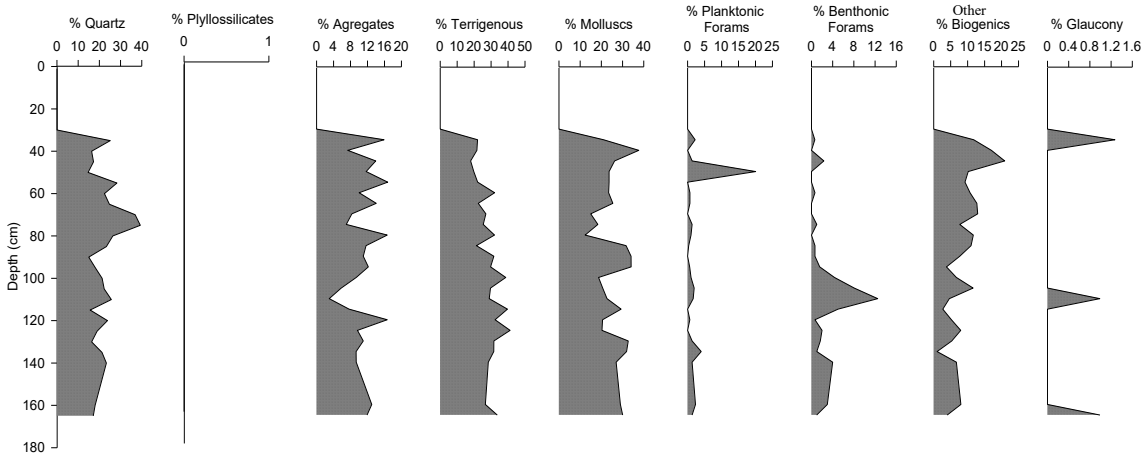

Figure 5.13 - Percentage of morphoscopic elements for the coarse sand fraction (0.5 – 1 mm).

In the medium sand fraction (0.250 – 0.5 mm) (Figure 5.14) composition is very different from the coarser sand fraction.

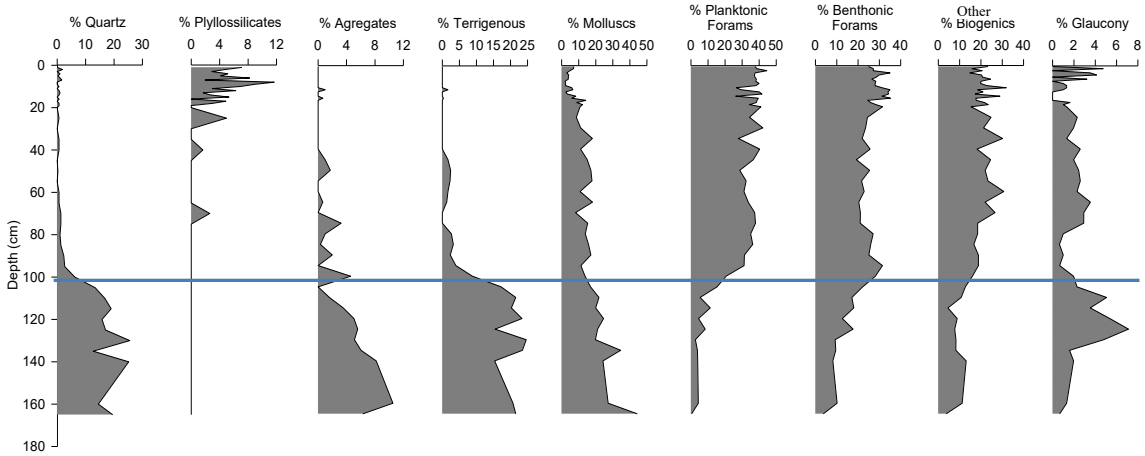

Figure 5.14 - Percentage of morphoscopic elements for the medium sand fraction (0.250 – 0.5 mm).

Quartz is no longer the dominant component, with frequencies lower than 25 %, in the core base, decreasing to 13 % (at 105 cm), and almost disappearing at the top layers. Also, aggregates are a less important component (8 %) and its occurrence is restricted to the bottom 105 cm thick layer. The terrigenous particles have a similar behavior when compared to aggregates. Their percentage is reduced at the top as registered in the previous fraction, starting to decrease also around 105 cm. The percentage of mollusks has a steady decrease throughout the core, with values of 44 % in the base and 7 % in the core top. With a contrasting behavior from

the aggregates and terrigenous particles, the planktonic and benthic foraminifera become relevant classes. The planktonic foraminifera have almost no significance in the bottom layers of the core and, around 105 cm depth, their percentages rise from values of 5 % to 30 % in just 15 cm, maintaining values of almost 40 % until the top. Benthic foraminifera and biogenic particles have the same pattern but with slightly lower values. Grains of glaucony start to occur, with high percentages (6 %) at 130 cm, decreasing to 0.9 % (a negative variation at 80 cm) and again increasing to 2 % from 80 cm to 20 cm. In the first 20 cm, glaucony has visible oscillations between 0 – 5 %. It is also relevant that phyllosilicates start to be an important component, being identified as an isolated 4 % peak (centered at 70 cm depth) and being a constant component in the top 40 cm thick layer with values of 7 %.

The fine sand fraction (0.125 – 0.250 mm) has a composition dominated by phyllosilicates (Figure 5.15), which appear at the base of the core until 105 cm depth (with values of 1.8 %) and will become present in the rest of the core, with percentages between 10 % and 20 %, with a pronounced decrease at 65 cm.

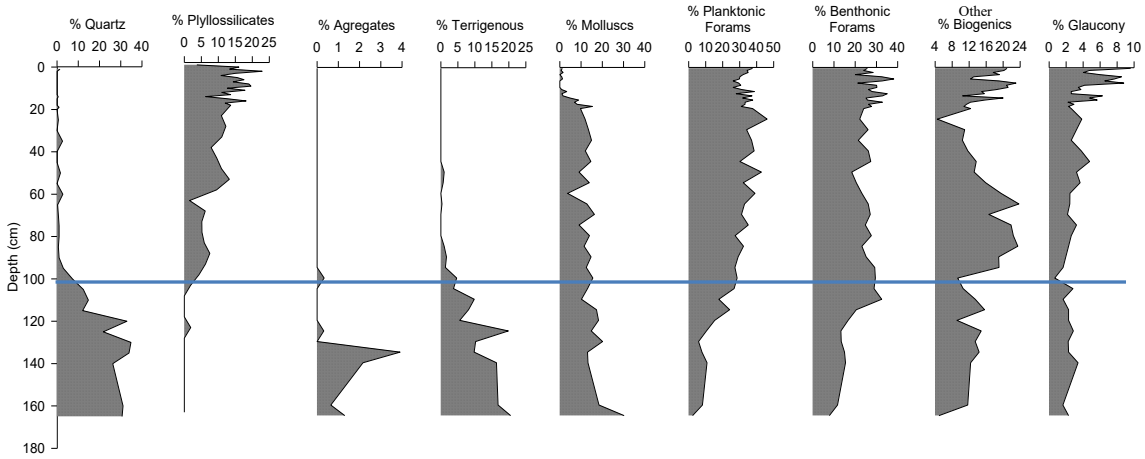

Figure 5.15 - Percentage of morphoscopic elements for the fine sand fraction (0.125 – 0.250 mm).

Quartz is restricted to the bottom levels, below 100 cm, with maximum values of 34 % observed at 130 cm. When compared to coarser fractions, the percentage of aggregates decreases drastically to values of less than 12 %. The terrigenous particles present a trend similar to aggregated particles. Regarding planktonic and benthic foraminifera, there is an increase from 130 cm upwards, together with other biogenic particles. Compared to the coarser fraction, glaucony presents a different pattern, with an even concentration throughout the entire core (values increasing from around 2 %, to approximately 9 % in the uppermost level).

In the very fine sand fraction (0.125 – 0.063 mm) (Figure 5.16) several components become quite abundant. In the case of quartz, the bottom presents values of 53 % decreasing to 10 % at 110 cm, rising again with mean values of 18 % till 20 cm and decreasing again to 10 %

in the top. Phyllosilicates start to appear at 105 cm, rising rapidly to 10 % at 80 cm and then increasing slowly to 20 % (in the 20 cm topmost layer).

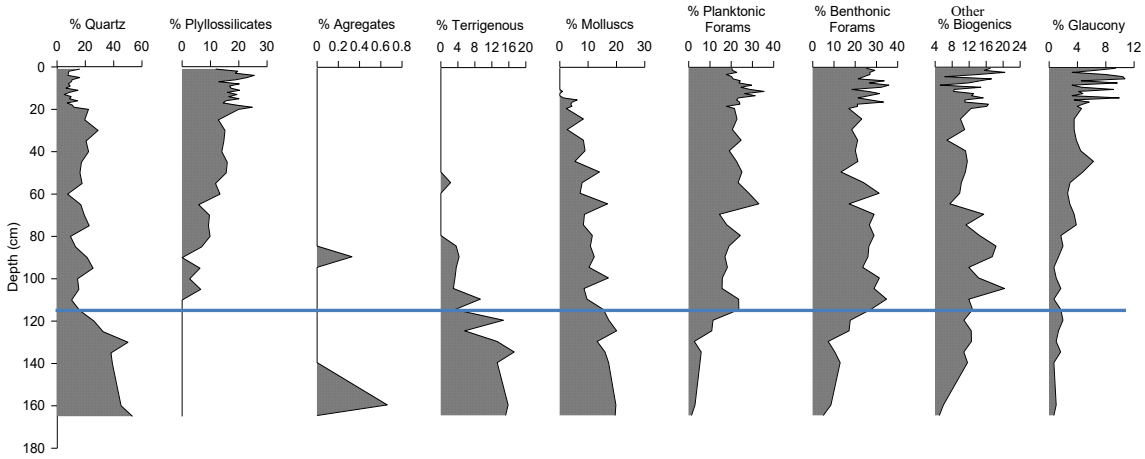

Figure 5.16 - Percentage of morphoscopic elements for the very fine sand fraction (0.125 – 0.063 mm).

The aggregate particles lose their significance, being almost absent, and the terrigenous decrease their percentage. In what concerns, planktonic and benthic foraminifera, biogenic particles and glaucony, their pattern remains the same as in the fine sand fraction.

Sand composition pattern along the core allowed to identify three main sequences, that roughly matches the three domains identified in the grain-size parameters:

1- the basal one, till 110 cm, dominated by quartz, aggregates and terrigenous particles;
2- an intermediate sequence between 110 cm and 20 cm, without the previous components and dominated by biogenic particles including foraminifera
3- the topmost 20 cm, with phyllosilicates and frequent variations on biogenic, glaucony and foraminifera contents.

5.2.2.7. Fine fraction mineralogy

The mineralogy of fine fraction allowed the identification of distinctive mineral assemblages (Figure 5.17) (Annex1 - 1.11) (Annex 13).

The first sequence comprehends the layer between the core base and the 95 cm level, and presents high percentages of aragonite, calcite, magnesite, rhodochrosite and pyrite. The maximum value of aragonite (12 %) was measured at the bottom, decreasing upwards to 3 % (from 95 cm until 20 cm) and almost disappearing in the upper 20 cm thick layer. With slightly internal variations, calcite percentages range from 53 % (at the bottom) to 30 % (in the uppermost 20 cm layer). Magnesite and rhodochrosite show very high values in the bottom (17 % and 1.3 % respectively), decreasing till 90 cm. Magnesite disappears completely to the top. Pyrite has the same behavior as aragonite, but with different percentages (maximum value of 8 % in the bottom decreasing to 2 % in the top).

The second mineral assemblage occurs between 95 cm depth until the top and is characterized by the increasing percentages values of chlorite, illite, kaolinite, quartz, opal, anhydrite, plagioclase, dolomite and siderite. Quartz is the mineral that presents the most significant variation, going from values of 4 % at the bottom, to 13 % at 100 cm and maintaining values of approximately 12 % to the top, with a peak of 16 % around 45 cm. Opal is another mineral with a similar behavior to quartz but with lower percentages. Chlorite presents sporadic values inferior to 2 % along the core. Illite shows values lower than 10 % at the base, and a peak of 24 % at 85 cm, decreasing to values between 10 and 20 %, rising at the top 20 cm to values above 20 %. Kaolinite has the same pattern of illite, starting with values below 2 %, with a peak of 4 % also at 85 cm and another one less pronounced at 45 cm, like quartz and opal. Anhydrite begins also with null values at the base (0 %), starting to increase along the core never exceeding 2 %. Plagioclase presents in the bottom of the core also low values (1 %) rising to a peak of 13 % at 75 cm, decreasing again to values around 5 % and rising gently to values of 8 % in the top. Dolomite only appears above 95 cm with very low values (0.31 %), presenting a peak of 6 % at 60 cm, decreasing to 0 % around 45 cm and rising again with oscillations to the top below 3 %. Like dolomite, siderite appears above 85 cm, never exceeding 2 % to the top. Fluorite presents a constant behavior in terms of concentration, with values of approximately 3 % from the bottom until 35 cm where it reaches almost 4 %, decreasing to values around 2 % to the top. Finally, potassium feldspar presents low values at the bottom (6 %) rising to 20 % at 100 cm and then has a very irregular pattern till the top varying from high values (approximately 17 %) to low values (approximately 5 %).

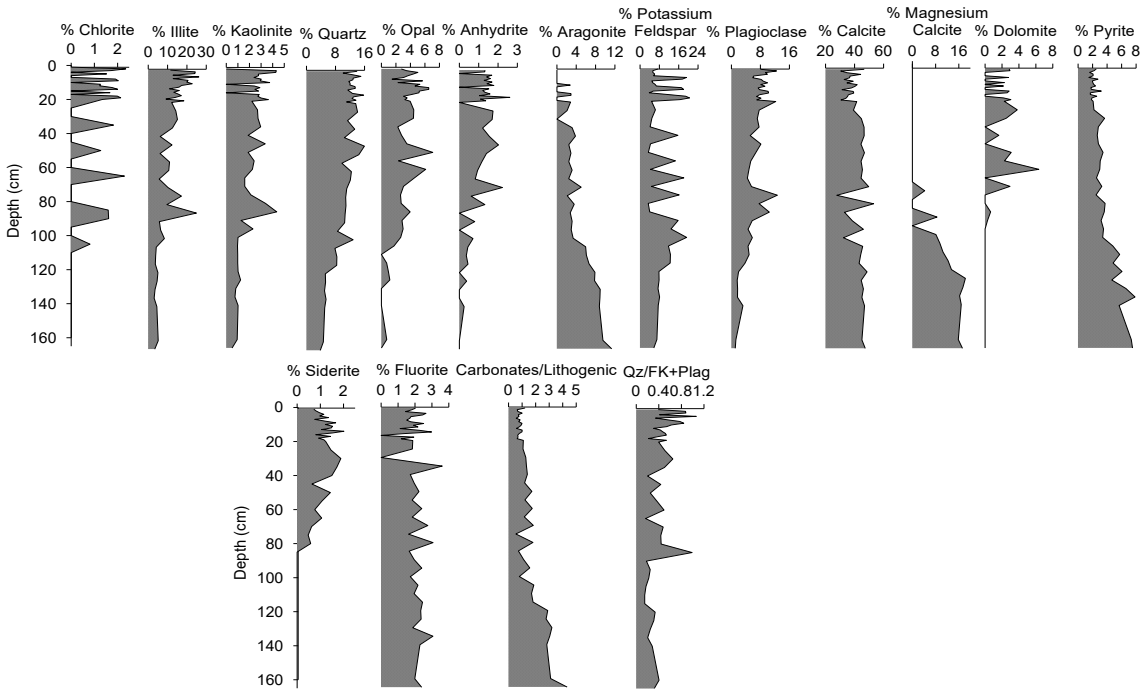

Figure 5.17 – Percentage of fine fraction mineralogy.

The ratio of carbonates against lithogenic minerals indicates that, along the core sediment, there is some variation on this relationship: at the core base values are higher than 4, decreasing to 2 at 100 cm and to values below 1 near the top, showing and inverse relationship.

The ratio Qz/FK+ Plag indicates that from the bottom till 85 cm there was no variation in the contributions of either minerals, but from this level upwards the input of quartz increased in some levels with a peak of 1.4 at 45 cm, while in others decreased.

5.2.2.8. Heavy minerals content

The heavy mineral fraction presented in the sediment core is described in Table 5.2, expressed in weight percentage considering the different sand fractions analyzed (from medium sand to very fine sand).

Table 5.2 - Heavy minerals percentages of each sandy fraction along the sediment core.

Depth (cm)	0.5-0.063 mm Total (%)	0.5-0.250 mm (%)	0.25-0.125 mm (%)	0.125-0.063 mm (%)
1	0.001	0	0	0.001
2	0.002	0	0	0.002
7	0.001	0	0	0.001
13	0.003	0	0	0.003
16	0.001	0	0	0.001
25	0.009	0	0	0.009
45	0.007	0	0.002	0.005
50	0.008	0.001	0.003	0.004
55	0.013	0.004	0.005	0.004
60	0.017	0.001	0.005	0.011
75	0.020	0.001	0.010	0.009
95	0.036	0.006	0.022	0.008
115	0.044	0.006	0.034	0.005
130	0.074	0.021	0.024	0.030
162	0.060	0.015	0.031	0.013

Total heavy mineral content in these samples reaches 0.05 % (at the core base), decreasing smoothly upwards until being almost vestigial (in the top 20 cm layer). This pattern is consistent in all fractions.

The coarser heavy mineral particles (grain size between medium and fine sand) are absent in the upper core layers and the 0.250 mm fraction is only present at the deepest 50 cm thick layer, with maximum values of 0.021 % at 130 cm and minimum values of 0.001 % at 50 cm. Between 130 cm and 95 cm levels there is an evident decrease of heavy mineral content (Figure 5.18).

Fraction 0.125 mm presents maximum heavy mineral content at the core base (0.031 %), decreasing to the top, disappearing at 45 cm with values of 0.002 %. The finer heavy minerals fraction (0.063 mm) has maximum values (approximately 0.030 %) at the core base, decreasing to the top (minimum values of 0.001 %).

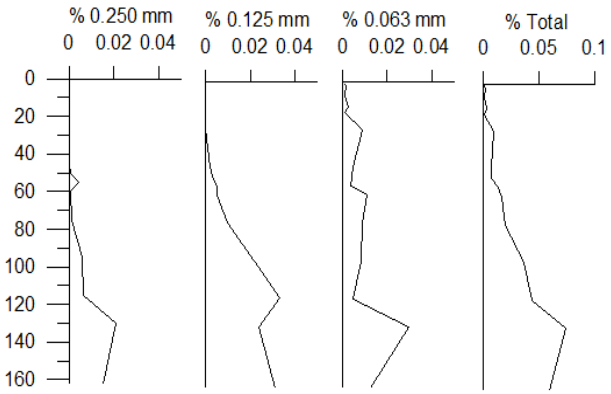

Figure 5.18 - Heavy minerals percentages present in the medium to very fine sandy fraction.

When analyzing the composition of heavy fraction, species such as tourmaline, andalusite, staurolite, garnet, phyllosilicates, zircon, sphene, amphibole and pyroxene were identified (Figure 5.19). Total sediment content reveals a consistent upward decrease upward for all minerals, with negligible values in the upper 55 cm. The only exception are phyllosilicates, which present a peak at 95 cm (max. value of 2.7 %) but also decrease to the top. The most abundant mineral is pyroxene (5 % at the core base) followed by tourmaline and garnet (1.33 % and 0.7 % respectively) (Annex 1 - 1.14) (Annex 14).

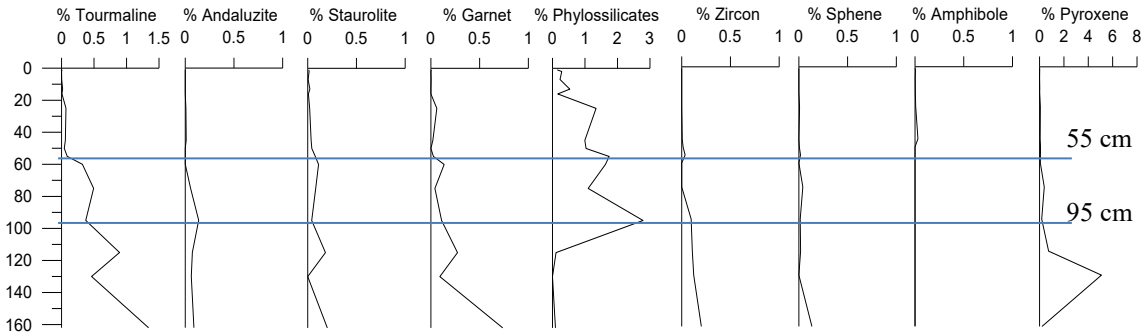

Figure 5.19 - Heavy minerals percentages of the sediment core for the total sediment.

5.2.2.9. Benthic and planktonic foraminifera assemblages

In total, 103 species of benthic foraminifera were identified, distributed by 36 genders, with a total of 5756 individuals. A total of 2686 planktonic individuals were also counted for statistical purposes only (Taxonomy is included in Annex 1 - 1.15) (Annex 15).

Four associations were recognized, based on species relative abundance, pattern of dominant and common species and respective ecological characteristics. For graphical representation, only species with relative abundance higher than 5 % were considered. They were considered as *dominant species*, if their relative abundance is always superior to 10 %, and

common species, if their abundance is sometimes more than 10 %. *Accessories Species* are those representing always less than 5 % (Murray, 2007). For paleoecological interpretation the benthic and planktonic standing crops (density), were calculated together with diversity index (Hs) and also the number of species identified was taken into account (Figure 5.20).

In the Figure 5.20 standing crop values for benthic foraminifera are higher than those of planktonic. Benthic values vary from a minimum value of 998 (individuals/cm^3) in the base and a maximum of 64 717 (individuals/cm^3) at 30 cm. These values are lower from the core base until 120 cm, increasing from 2108 (individuals/cm^3) to slightly over 50 000 (individuals/cm^3) at 110 cm. From 110 cm until 30 cm there are slight variations, being the mean value of 47 667 (individuals/cm^3). At 20 cm these values decrease to 12 356 (individuals/cm^3) with a mean value of 23 996 (individuals/cm^3) until the top of the core.

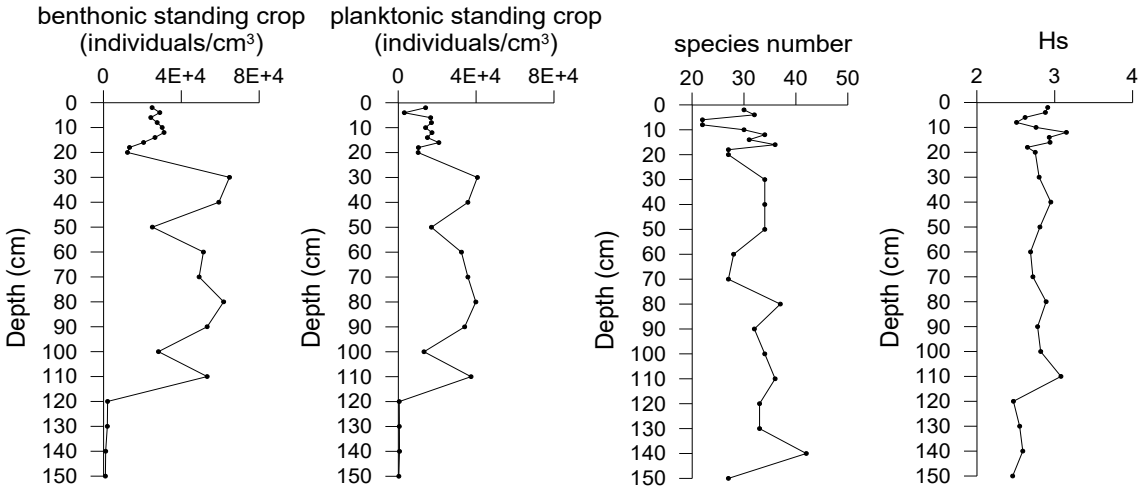

Figure 5.20 - Benthic and planktonic standing crop (individuals/cm^3), species number and diversity index (Hs) of benthic foraminifera along the sediment core.

The pattern for planktonic foraminifera is the same as for benthic, but with lower values. The minimum value encountered for planktonic foraminifera is also at the base (316 individuals/cm^3) and the maximum of 46 687 (individuals/cm^3) at 30 cm. The lower values were observed until 120 cm, increasing at 110 cm; small variations also occur between 110 cm and 30 cm, decreasing at 20 cm maintaining lower values in the top.

Concerning the number of species, the levels with lower number of species are between 4 and 8 cm (22 species), while the level with higher number of species is at 140 cm (42 species). There are several peaks with high values throughout the core, namely at 140 cm, 80 cm (37 species) and 16 cm (36 species).

The diversity index (Hs) shows that the core base has the lowest diversity compared to the levels above. The diversity also increases at 110 cm, where the base values rise from 2.46 to 3.08. Between 110 cm and 20 cm there are small oscillations in diversity, with a mean value of

2.80. From 20 cm to the top there are significant oscillations in diversity, varying from 3.15 at 12 cm to 2.51 at 8 cm, rising again to 2.91 at the top. The identified species, with relative abundances superior to 5 % of the faunistic association, are plotted in Figure 5.21 (Annex 15).

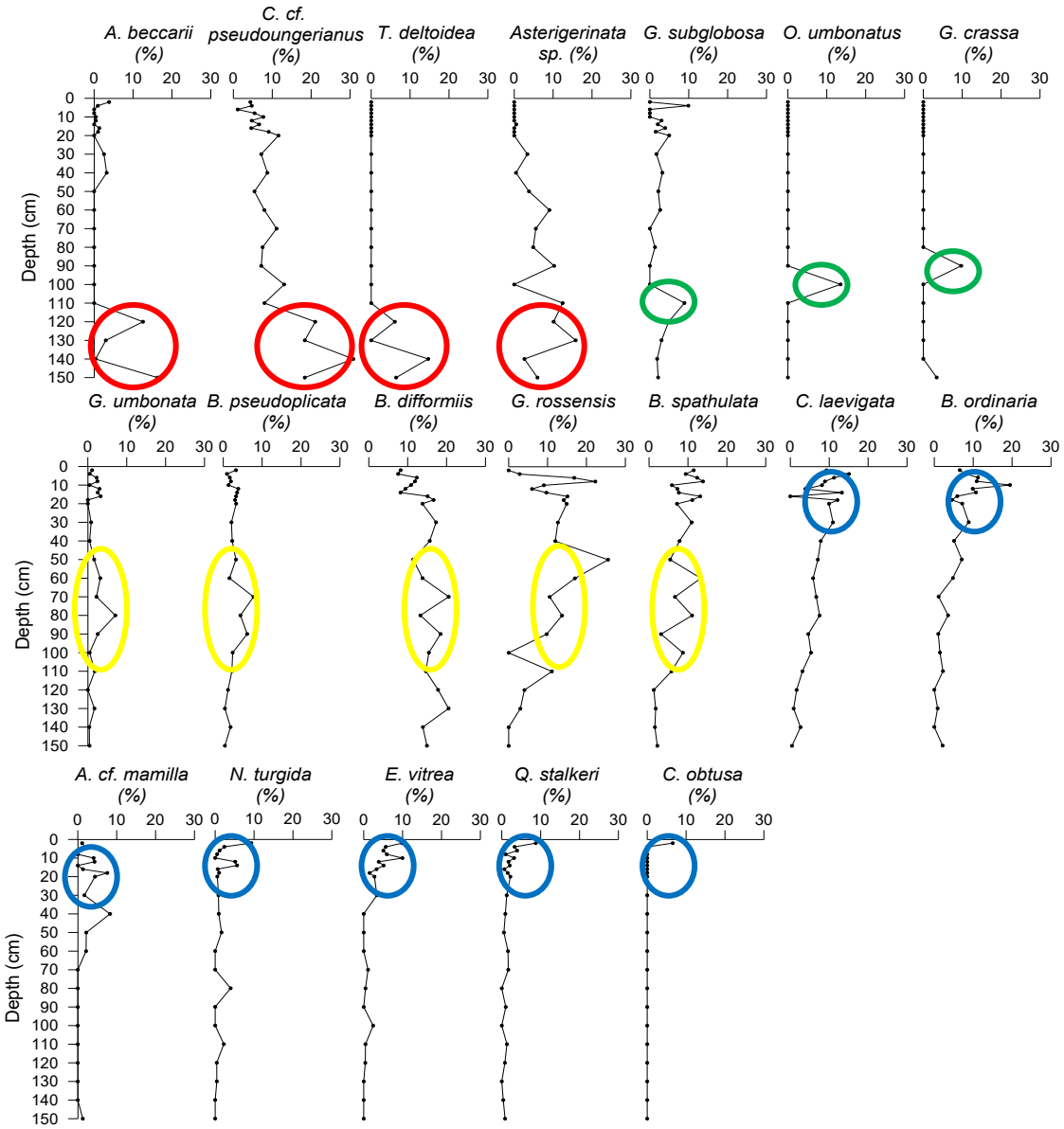

Figure 5.21 - Percentage of identified species of benthic foraminifera.
Red circle is first association; green circle is second association; yellow circle is third association; blue circle is fourth association.

Along the core sample, four associations were recognized based on abundance and depths:

- The first one is comprised by *A. beccarii*, *C. cf. pseudoungerianus*, *T. deltoidea* and *Asterigerinata sp*. and is present deeper than 110 cm.

- The second association is composed by *G. subglobosa*, *O. umbonatus* presents a 10 % peak at 100 cm, *G. crassa* with a 10 % peak at 90 cm.
- The third association consists of *B. difformiis*, G. *rossensis* and *B. spathulate*, *G. umbonata* and *B. pseudoplicata* presents also 10 % peak but at 110 cm. *Giroydina umbonata* and *B. pseudoplicata* do not present defined peaks but reach almost the 10 % at 80 cm at 70 cm respectively.
- The fourth association is dominated by *C. laevigata*, *B. ordinaria*, *A. cf. mamilla*, *N. turgida*, *E. vitrea*, *Q. stalkeri* and *C. obtuse* and is present in the uppermost 40 cm of the sediment column.

Factor analysis (Table 5.3) applied to relative abundance of benthic foraminifera species and texture of the sediment (gravel, sand, silt and clay percentage in total sediment) allowed to extract 5 dominant factors (which represent the total amount of variance that can be explained by a given principal component, they can be positive or negative in theory, but in practice they explain variance which is always positive). The extraction of principal components with rotation (varimax), is an orthogonal rotation method and it is intended that for each major component there are only a few significant weights and all others are close to zero, i.e. the goal is to maximize the variation between the weights of each major component, hence the name Varimax.

The first factor explains 36.7 % of total variance, the second 12.5 % and the third 8.5 %. Together, these factors explain 58 % of the total variance observed in the micro faunistic and grain-size characteristics of the sediments.

Table 5.3 - Variance percentage of each factor.

Value	Eigenvalues Extraction: Principal factors (comm.=multiple R-square)			
	Eigenvalue	% Total variance	Cumulative Eigenvalue	Cumulative %
1	8.462886	36.79516	8.46289	36.79516
2	2.895045	12.58715	11.35793	49.38231
3	1.972929	8.57795	13.33086	57.96027
4	1.231110	5.35265	14.56197	63.31292
5	1.080450	4.69761	15.64242	68.01053

When plotting the factor 1 versus factor 2 (Figure 5.22) is possible to identify the associations mentioned before represented in respective colors.

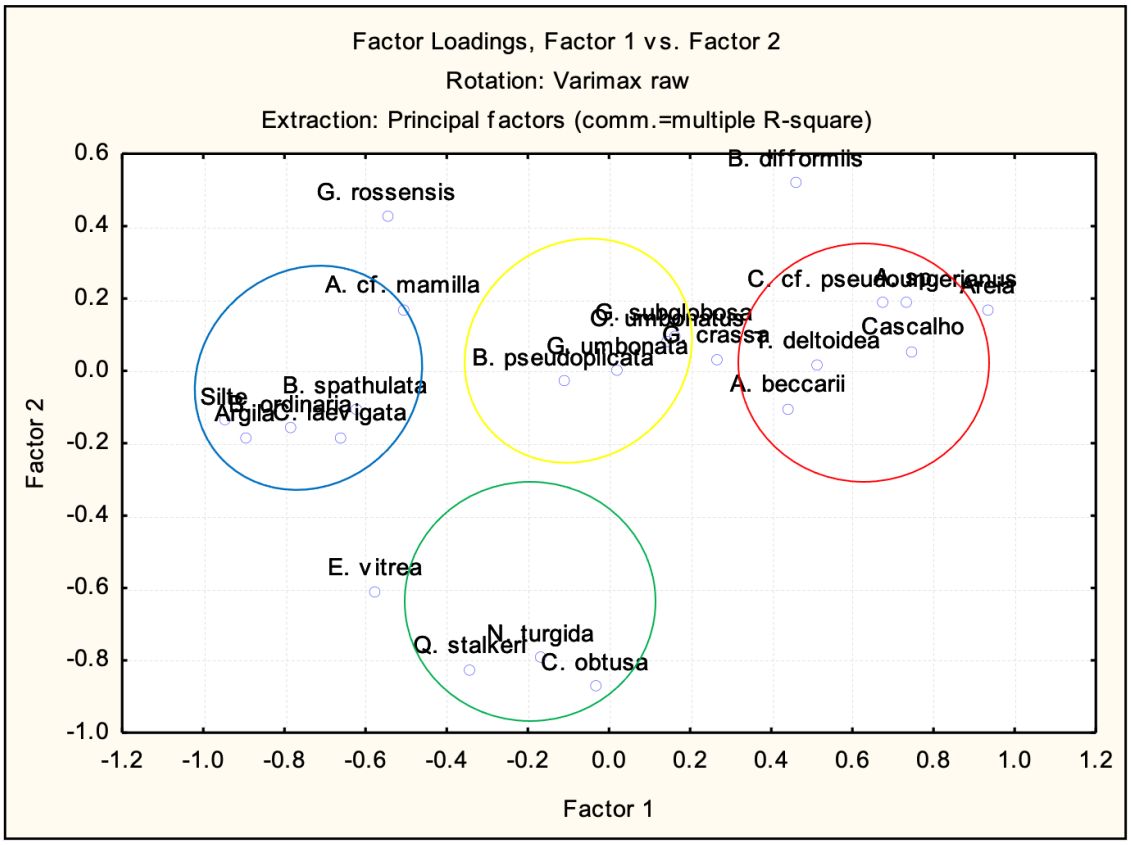

Figure 5.22 - Factor loadings of factor 1 versus factor 2.
Red circle is first association; green circle is second association; yellow circle is third association; blue circle is fourth association.

5.2.2.10. Calcareous nannoplankton assemblages

Analyzing the abundances of coccolith species in 10 different levels of the sediment core it is visible the predominance of *Emiliania huxleyi, Gephyrocapsa oceanica* throughout the core and the low abundance of coccoliths in the core base (Figure 5.23) (Annex 1 - 1.16) (Annex 16).

Besides the abundance of *G. oeanica, Braarudosphaera ericsonii* and *Helicosphaera carteri*, some species like *Pontosphaera discospora, Tubodiscus sp*. and *Reticulofenestra genus* completely disappears above the 120 cm. Considering other species, *E. huxleyi* presents values of $2.06x10^6$ coccoliths/g in the core base rising to 54 cm ($1.37x10^8$ coccoliths/g), maintaining these values until the last 20 cm when it decreases to values of $2.12x10^6$ coccoliths/g. *Syracosphaera histrica-pulchra* also presents low values at the core bottom (around $5.29x10^4$ coccoliths/g) increasing gradually till 54 cm ($20x10^6$ coccoliths/g), decreasing slowly until 22 cm ($99.57x10^4$ coccoliths/g) and then rising again to the top ($11.19x10^6$ coccoliths/g).

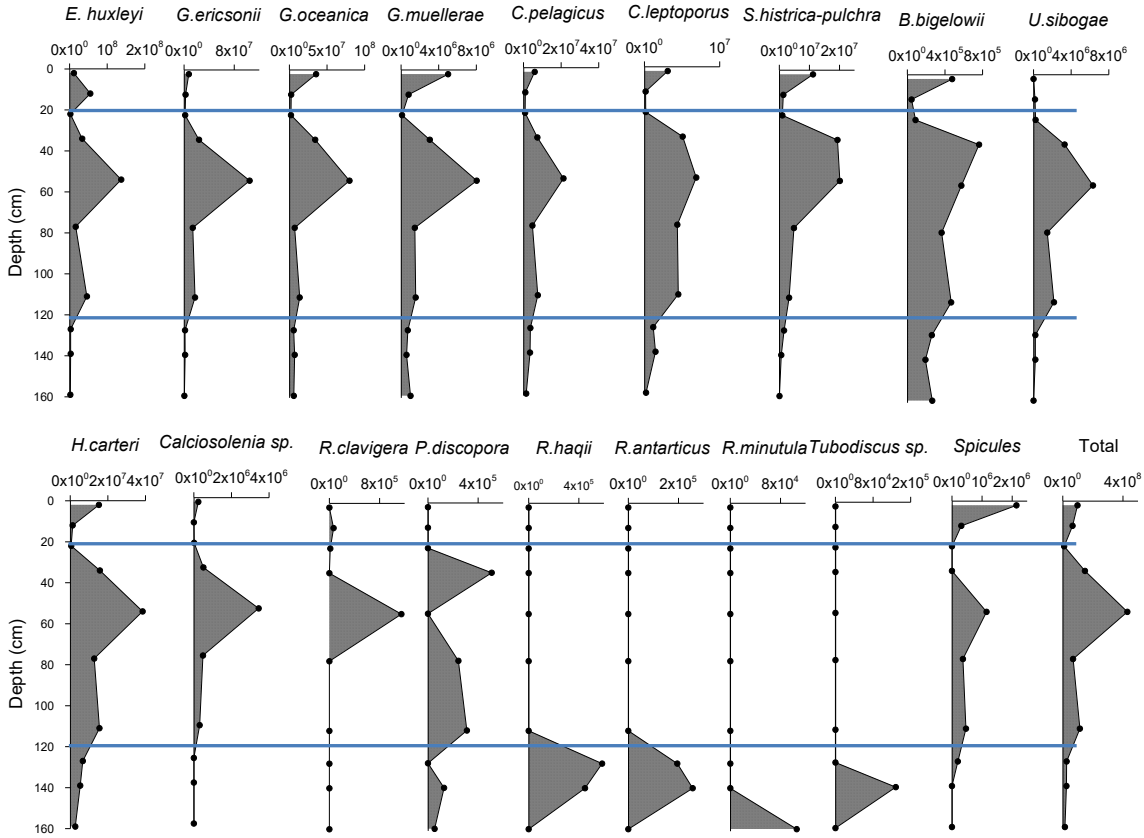

Figure 5.23 - Number of species, and distribution and relative abundance (coccoliths per gram) of the main coccolith species in Estremadura core.

From 111 cm till 22 cm there is a high, persistent and diversified record of nannoliths, namely oceanic species such as *E. huxleyi, Gephyrocapsa ericsonii, Helicosphaera carteri*, *Umbilicosphaera sibogae*, *Gephyrocapsa muellerae, Calsiosolenia sp.* and *Calcidiscus leptoporus*. Between 22 cm and 10 cm all species suffer a decrease in abundance, excepting *E. huxleyi* that rapidly recovers at 12 cm. The top 10 cm are characterized by an increase of abundance, of oceanic and neritic species like *G. muellerae*, *E. huxleyi, C. leptoporus*, *C. pelagicus*, *Calciosolenia sp.*, *H. carteri*, *S. histrica-pulchra* and *B. bigelowii*.

5.2.2.11. Geochemical content: heavy metals

Table 5.4 displays metal concentration (Hg, Cu, Zn, Mn, Pb, Ni, Cd, Cr, Li, As and major elements Al and Fe) obtained in Instituto Hidrográfico chemistry laboratory (Annex 1 - 1.13) (Annex 17).

Minimum values are presented in green while maximum values are presented in pink. One can observe that minimum values are always present in the core base except for Ni, Cr and As, where minimum values are present between 100 cm and 80 cm. For Pb the values on the core base are so low that they are under the detection limit. Therefore, the values are always 1 (mg/kg).

The same happens with Cd where the values are also under the detection limit, except for levels 19 cm, 25 cm and 85 cm, where a higher concentration of Cd was detected.

Concerning the maximum concentration values, there is a level where almost every metal presents its higher concentration, which is at 18 cm. Although some metals, like Ni and Li, present maximum values at different levels, the 18 cm seems to mark a frontier from the levels below. For major elements, the maximum values are in the top core, but as in Ni and Li, the values present at 18 cm also limit a frontier from the levels below.

Comparing these values from Table 5.4 with others identified in the Portuguese coast, Martins *et al.* (2012), studied superficial sediment samples collected at the Estremadura Spur collected in 2007 and 2008, where only the Pb values identified are higher than the values identified in this work.

Table 5.4 - Metal concentrations (mg/kg) and major elements Fe and Al and $CaCo_3$ quantifications along the core.
Higher values in pink, lower values in green.

Depth (cm)	Hg (mg/kg)	Cu (mg/kg)	Zn (mg/kg)	Mn (mg/kg)	Fe (%)	Pb (mg/kg)	Ni (mg/kg)	Cd (mg/kg)	Cr (mg/kg)	Al (%)	Li (mg/kg)	As (mg/kg)	CaCO3 (%)
1	0.06	13.00	68.00	240.00	2.50	12.30	13.40	0.20	46.00	6.20	68.00	14.90	23.32
2	0.04	12.00	64.00	250.00	2.50	11.30	13.00	0.20	45.00	6.00	66.00	14.00	28.32
3	0.02	12.00	62.00	250.00	2.70	7.77	13.20	0.20	49.00	6.50	74.00	14.00	23.32
4	0.03	13.00	63.00	250.00	2.70	9.33	13.80	0.20	45.00	5.80	71.00	15.70	23.32
5	0.05	12.00	66.00	240.00	2.40	12.50	13.00	0.20	42.00	5.70	65.00	12.90	25.82
6	0.04	12.00	64.00	250.00	2.30	10.30	14.30	0.20	44.00	6.20	68.00	13.10	24.16
7	0.02	13.00	61.00	260.00	2.60	6.72	13.80	0.20	48.00	6.20	70.00	13.50	23.32
8	0.02	12.00	59.00	260.00	2.50	4.12	13.40	0.20	46.00	6.00	67.00	10.70	24.16
9	0.02	11.00	56.00	250.00	2.30	3.63	12.60	0.20	45.00	5.80	64.00	14.80	24.99
10	0.01	11.00	62.00	230.00	2.30	8.52	17.30	0.20	47.00	5.70	61.00	16.20	25.82
11	0.07	11.00	67.00	230.00	2.20	13.70	11.10	0.20	44.00	6.10	53.00	10.20	26.66
12	0.07	12.00	70.00	240.00	2.20	14.50	11.50	0.20	44.00	5.30	58.00	9.63	27.49
13	0.08	13.00	74.00	240.00	2.40	16.40	12.10	0.20	45.00	5.50	60.00	10.80	25.82
14	0.09	13.00	77.00	250.00	2.50	17.80	13.20	0.20	46.00	5.60	63.00	13.80	24.16
15	0.08	14.00	77.00	250.00	2.50	17.70	13.50	0.20	46.00	5.80	63.00	11.10	24.99
16	0.09	14.00	77.00	250.00	2.50	17.70	13.00	0.20	48.00	5.80	64.00	10.90	25.82
17	0.09	14.00	78.00	250.00	2.50	19.20	14.20	0.20	47.00	5.80	64.00	12.30	24.16
18	0.09	14.00	82.00	260.00	2.60	21.00	14.00	0.20	51.00	6.20	72.00	12.60	22.49
19	0.08	13.00	76.00	250.00	2.50	17.90	12.00	0.30	46.00	5.70	63.00	12.00	23.32
20	0.07	13.00	75.00	250.00	2.50	17.10	12.80	0.20	47.00	5.90	64.00	12.20	26.66
25	0.01	10.60	55.00	250.00	2.50	4.66	11.60	0.31	42.00	5.40	67.00	12.80	29.16
30	0.01	9.30	48.00	220.00	2.20	3.90	9.94	0.20	37.00	4.90	56.00	14.70	31.65
35	0.03	9.50	53.00	220.00	2.10	8.21	9.26	0.20	37.00	4.50	52.00	10.20	32.49
40	0.02	10.40	51.00	230.00	2.30	2.59	9.36	0.20	39.00	5.30	59.00	10.20	29.16
45	0.01	6.60	33.00	190.00	1.80	1.00	3.56	0.20	29.00	3.60	38.00	9.61	35.82
50	0.01	6.30	33.00	180.00	1.80	1.00	3.58	0.20	28.00	3.40	38.00	10.10	38.32
55	0.01	6.30	31.00	180.00	1.70	1.00	3.46	0.20	26.00	3.20	36.00	9.08	38.32
60	0.01	5.80	28.00	170.00	1.50	1.00	3.21	0.20	24.00	3.00	33.00	7.66	40.82
65	0.01	5.70	27.00	160.00	1.40	1.00	2.46	0.20	24.00	2.70	29.00	7.98	40.82
70	0.01	5.10	26.00	160.00	1.40	1.00	2.11	0.20	23.00	2.70	28.00	7.16	37.49
75	0.01	4.00	25.00	170.00	1.30	1.00	2.22	0.20	22.00	2.60	27.00	7.41	41.65
80	0.01	4.00	24.00	160.00	1.30	1.00	0.10	0.20	22.00	2.60	26.00	5.60	41.65
85	0.01	6.10	29.00	180.00	1.50	1.00	4.21	0.30	27.00	3.10	34.00	8.19	41.65
90	0.00	4.00	21.00	150.00	1.20	1.00	0.10	0.20	19.90	2.30	22.00	6.10	41.65
95	0.00	4.00	20.00	140.00	1.20	1.00	0.10	0.20	19.70	2.10	22.00	8.32	41.65
100	0.00	4.00	20.00	150.00	1.20	1.00	0.10	0.20	19.90	2.10	22.00	8.00	49.98
105	0.00	4.00	16.00	120.00	1.00	1.00	2.69	0.20	23.00	1.45	18.00	10.40	49.98
110	0.00	4.00	14.00	110.00	0.90	1.00	5.11	0.20	29.00	1.36	17.20	11.80	49.98
115	0.00	4.00	17.00	110.00	1.20	1.00	3.68	0.20	24.00	1.54	22.00	15.50	58.31
120	0.00	4.00	14.00	120.00	0.82	1.00	5.28	0.20	29.00	1.35	17.40	11.20	49.98
125	0.00	4.00	10.90	110.00	0.74	1.00	2.55	0.20	22.00	1.12	15.10	10.70	49.98
130	0.00	4.00	12.00	110.00	0.74	1.00	5.54	0.20	29.00	1.19	15.60	13.60	58.31
135	0.00	4.00	12.00	110.00	0.75	1.00	4.80	0.20	28.00	1.27	14.80	10.50	58.31
140	0.00	4.00	11.50	110.00	0.73	1.00	5.94	0.20	30.00	1.08	14.70	9.35	58.31
160	0.00	4.00	9.70	110.00	0.67	1.00	3.43	0.20	24.00	1.05	12.20	12.40	58.31
162	0.00	4.00	12.00	100.00	0.63	1.00	10.50	0.20	40.00	1.08	13.40	7.98	58.31

For example, for Cu, Cr, As, Zn, Pb and Ni Martins *et al.* (2012) determined a concentration of 8.1 ppm, 40.8 ppm, 8.3 ppm, 37.4 ppm, 21.6 ppm and 8.8 ppm, while in this work the surface the values for respective elements are 13 mg/kg, 46 mg/kg, 14.9 mg/kg, 68 mg/kg, 12.3 mg/kg and 13.4 mg/kg.

When comparing the values obtained in this work with the ones obtained by Mil-Homens *et al.* (2009) in the Tejo mud-patch, the values of Mil-Homens *et al.* (2009) are much higher regarding to Zn, Pb, Hg, Cu and Ni values.

As it was observed in the fine fraction mineralogy, the geochemistry of the core base is controlled by the presence of gravel and sands, which causes a substantial dilution of major and minor elements.

Table 5.5 - Heavy metal data concentration (mg/kg) with carbonate-free basis.
Higher values in pink, lower values in green.

Depth (cm)	Hg (mg/kg)	Cu (mg/kg)	Zn (mg/kg)	Mn (mg/kg)	Fe (mg/kg)	Pb (mg/kg)	Ni (mg/kg)	Cd (mg/kg)	Cr (mg/kg)	Al (mg/g)	Li (mg/kg)	As (mg/kg)
1	0.07	16.95	88.68	313.01	3.26	16.04	17.48	0.26	59.99	8.09	88.68	19.43
2	0.06	16.74	89.29	348.78	3.49	15.76	18.14	0.28	62.78	8.37	92.08	19.53
3	0.03	15.65	80.86	326.05	3.52	10.13	17.22	0.26	63.91	8.48	96.51	18.26
4	0.04	16.95	82.16	326.05	3.52	12.17	18.00	0.26	58.69	7.56	92.60	20.48
5	0.07	16.18	88.98	323.55	3.24	16.85	17.53	0.27	56.62	7.68	87.63	17.39
6	0.05	15.82	84.38	329.63	3.03	13.58	18.85	0.26	58.01	8.17	89.66	17.27
7	0.02	16.95	79.56	339.09	3.39	8.76	18.00	0.26	62.60	8.09	91.29	17.61
8	0.02	15.82	77.79	342.81	3.30	5.43	17.67	0.26	60.65	7.91	88.34	14.11
9	0.02	14.66	74.66	333.29	3.07	4.84	16.80	0.27	59.99	7.73	85.32	19.73
10	0.02	14.83	83.58	310.07	3.10	11.49	23.32	0.27	63.36	7.68	82.24	21.84
11	0.09	15.00	91.35	313.59	3.00	18.68	15.13	0.27	59.99	8.32	72.26	13.91
12	0.10	16.55	96.54	330.98	3.03	20.00	15.86	0.28	60.68	7.31	79.99	13.28
13	0.11	17.53	99.76	323.55	3.24	22.11	16.31	0.27	60.67	7.41	80.89	14.56
14	0.12	17.14	101.53	329.63	3.30	23.47	17.40	0.26	60.65	7.38	83.07	18.20
15	0.11	18.66	102.65	333.29	3.33	23.60	18.00	0.27	61.33	7.73	83.99	14.80
16	0.12	18.87	103.81	337.03	3.37	23.86	17.53	0.27	64.71	7.82	86.28	14.69
17	0.12	18.46	102.84	329.63	3.30	25.32	18.72	0.26	61.97	7.65	84.38	16.22
18	0.12	18.06	105.79	335.44	3.35	27.09	18.06	0.26	65.80	8.00	92.89	16.26
19	0.10	16.95	99.12	326.05	3.26	23.34	15.65	0.39	59.99	7.43	82.16	15.65
20	0.09	17.72	102.26	340.86	3.41	23.31	17.45	0.27	64.08	8.04	87.26	16.63
25	0.02	14.96	77.63	352.88	3.53	6.58	16.37	0.44	59.28	7.62	94.57	18.07
30	0.02	13.61	70.23	321.89	3.22	5.71	14.54	0.29	54.14	7.17	81.94	21.51
35	0.05	14.07	78.50	325.86	3.11	12.16	13.72	0.30	54.80	6.67	77.02	15.11
40	0.03	14.68	71.99	324.65	3.25	3.66	13.21	0.28	55.05	7.48	83.28	14.40
45	0.01	10.28	51.42	296.04	2.80	1.56	5.55	0.31	45.18	5.61	59.21	14.97
50	0.01	10.21	53.50	291.82	2.92	1.62	5.80	0.32	45.39	5.51	61.61	16.37
55	0.01	10.21	50.26	291.82	2.76	1.62	5.61	0.32	42.15	5.19	58.36	14.72
60	0.01	9.80	47.31	287.24	2.53	1.69	5.42	0.34	40.55	5.07	55.76	12.94
65	0.01	9.63	45.62	270.35	2.37	1.69	4.16	0.34	40.55	4.56	49.00	13.48
70	0.01	8.16	41.59	255.94	2.24	1.60	3.38	0.32	36.79	4.32	44.79	11.45
75	0.01	6.86	42.84	291.35	2.23	1.71	3.80	0.34	37.70	4.46	46.27	12.70
80	0.01	6.86	41.13	274.21	2.23	1.71	0.17	0.34	37.70	4.46	44.56	9.60
85	0.01	10.45	49.70	308.48	2.57	1.71	7.22	0.51	46.27	5.31	58.27	14.04
90	0.01	6.86	35.99	257.07	2.06	1.71	0.17	0.34	34.10	3.94	37.70	10.45
95	0.01	6.86	34.28	239.93	2.06	1.71	0.17	0.34	33.76	3.60	37.70	14.26
100	0.01	8.00	39.98	299.88	2.40	2.00	0.20	0.40	39.78	4.20	43.98	15.99
105	0.01	8.00	31.99	239.90	2.00	2.00	5.38	0.40	45.98	2.90	35.99	20.79
110	0.00	8.00	27.99	219.91	1.80	2.00	10.22	0.40	57.98	2.72	34.39	23.59
115	0.01	9.59	40.78	263.85	2.88	2.40	8.83	0.48	57.57	3.69	52.77	37.18
120	0.00	8.00	27.99	239.90	1.64	2.00	10.56	0.40	57.98	2.70	34.79	22.39
125	0.00	8.00	21.79	219.91	1.48	2.00	5.10	0.40	43.98	2.24	30.19	21.39
130	0.01	9.59	28.78	263.85	1.78	2.40	13.29	0.48	69.56	2.85	37.42	32.62
135	0.01	9.59	28.78	263.85	1.80	2.40	11.51	0.48	67.16	3.05	35.50	25.19
140	0.01	9.59	27.58	263.85	1.75	2.40	14.25	0.48	71.96	2.59	35.26	22.43
160	0.00	9.59	23.27	263.85	1.61	2.40	8.23	0.48	57.57	2.52	29.26	29.74
162	0.01	9.59	28.78	239.87	1.51	2.40	25.19	0.48	95.95	2.59	32.14	19.14

Therefore, the core base is characterized by a relative decrease in minor and major elements (Fe and Mg), due to its incorporation in carbonates. The carbonate-free normalization of heavy metal data (Annex 1 - 1.13, Table 5.5) is made with the assumption that the carbonate fraction does not contain any of the inorganic constituents of interest.

As one can observe in Table 5.5, there are some major differences when comparing with Table 5.4, with some elements with significant variation. These results indicate that the influence of carbonates is high enough to make the correction suggested by Horowitz (1984). There is also an area around 18 cm where values are higher, namely in Hg, Cu, Zn, Mn, Fe and Pb. But elements like Cr, Ni and As changed its higher levels to the core bottom.

In the bottom of Table 5.6 are the baselines used for the calculation of EF. These baselines represent the mean value of different levels. The sedimentation sequence was divided in three sectors; from the base till 100 cm, from 100 cm till 40 cm and from 40 cm till the top. Mean values were calculated for the two first sectors (base to 100 cm; 100 cm to 40 cm) and used as baselines for calculating the EF for the sectors above. For example, for Hg, the baseline used to calculate the EF between 100 and 40 cm was 0.0018, and for the EF between 40 cm and the top was 0.0020. This procedure was made for all elements and the results are in Table 5.7. The results for EF indicate that only Hg, Pb and Ni have enriched values; in the bottom for Hg and Ni and in the top 40 cm for all three elements (Table 5.7). Only Hg and Pb present enrichment values over 3, mainly between 20 cm and 10 cm. The rest of the elements are all below the values of significant enrichment.

When normalizing the values, it is possible to observe that the higher values are all concentrated in the bottom of the core, except Al, Zn and Pb that are located in the top 20 cm (Figure 5.24). Although these values are relatively high, they are still low when compared to other authors already mentioned above.

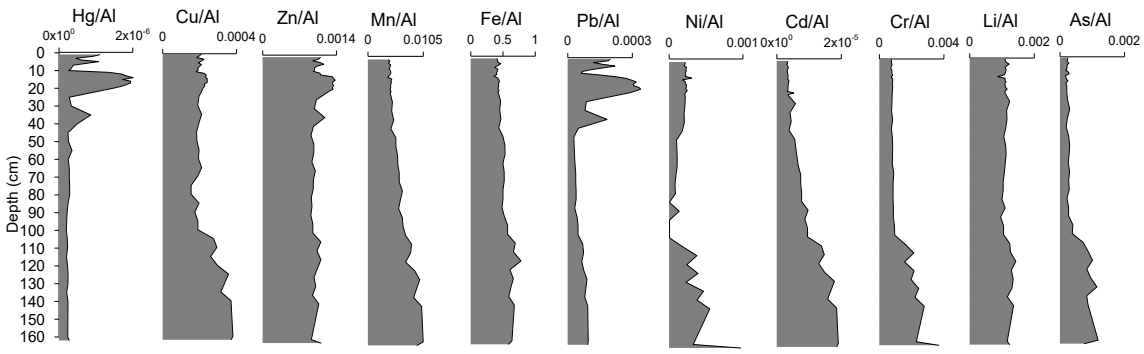

Figure 5.24 - Normalized values with Al.

Since the sedimentation is very heterogeneous along the entire core, different values (baselines) were taken into account when calculating the EF (Figure 5.25).

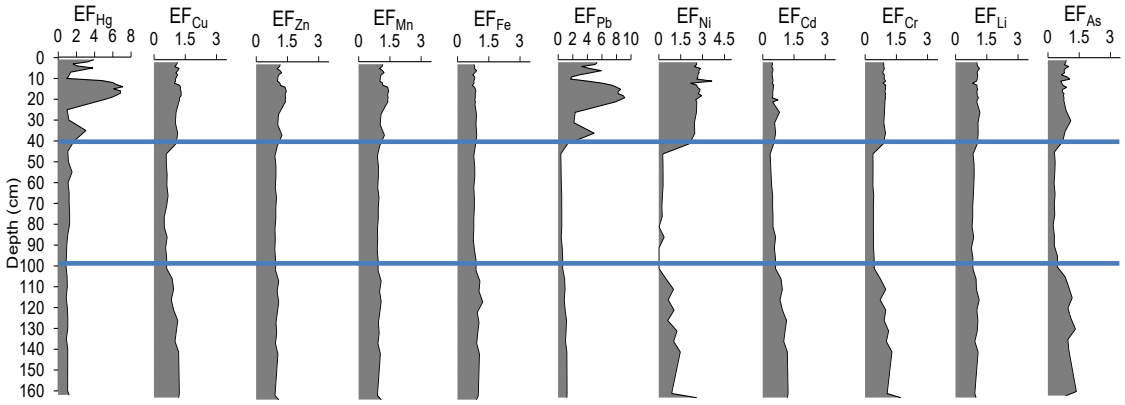

Figure 5.25 - Enrichment factor distribution. Lines in blue represent the separation in sectors for the calculation of baselines (base to 100 cm; 100 cm to 40 cm).

Table 5.6 - Normalized chemical data with Al.
Higher values in pink, lower values in green.
The baselines (mean value of different levels) used for the calculation of EF are indicated in lower rows.

Depth (cm)	Hg/Al	Cu/Al	Zn/Al	Mn/Al	Fe/Al	Pb/Al	Ni/Al	Cd/Al	Cr/Al	Li/Al	As/Al
1	0.0000009	0.00021	0.00110	0.00387	0.40323	0.00020	0.00022	0.00000	0.00074	0.00110	0.00024
2	0.0000007	0.00020	0.00107	0.00417	0.41667	0.00019	0.00022	0.00000	0.00075	0.00110	0.00023
3	0.0000004	0.00018	0.00095	0.00385	0.41538	0.00012	0.00020	0.00000	0.00075	0.00114	0.00022
4	0.0000005	0.00022	0.00109	0.00431	0.46552	0.00016	0.00024	0.00000	0.00078	0.00122	0.00027
5	0.0000009	0.00021	0.00116	0.00421	0.42105	0.00022	0.00023	0.00000	0.00074	0.00114	0.00023
6	0.0000006	0.00019	0.00103	0.00403	0.37097	0.00017	0.00023	0.00000	0.00071	0.00110	0.00021
7	0.0000003	0.00021	0.00098	0.00419	0.41935	0.00011	0.00022	0.00000	0.00077	0.00113	0.00022
8	0.0000003	0.00020	0.00098	0.00433	0.41667	0.00007	0.00022	0.00000	0.00077	0.00112	0.00018
9	0.0000003	0.00019	0.00097	0.00431	0.39655	0.00006	0.00022	0.00000	0.00078	0.00110	0.00026
10	0.0000002	0.00019	0.00109	0.00404	0.40351	0.00015	0.00030	0.00000	0.00082	0.00107	0.00028
11	0.0000011	0.00018	0.00110	0.00377	0.36066	0.00022	0.00018	0.00000	0.00072	0.00087	0.00017
12	0.0000014	0.00023	0.00132	0.00453	0.41509	0.00027	0.00022	0.00000	0.00083	0.00109	0.00018
13	0.0000015	0.00024	0.00135	0.00436	0.43636	0.00030	0.00022	0.00000	0.00082	0.00109	0.00020
14	0.0000016	0.00023	0.00138	0.00446	0.44643	0.00032	0.00024	0.00000	0.00082	0.00113	0.00025
15	0.0000014	0.00024	0.00133	0.00431	0.43103	0.00031	0.00023	0.00000	0.00079	0.00109	0.00019
16	0.0000016	0.00024	0.00133	0.00431	0.43103	0.00031	0.00022	0.00000	0.00083	0.00110	0.00019
17	0.0000016	0.00024	0.00134	0.00431	0.43103	0.00033	0.00024	0.00000	0.00081	0.00110	0.00021
18	0.0000015	0.00023	0.00132	0.00419	0.41935	0.00034	0.00023	0.00000	0.00082	0.00116	0.00020
19	0.0000013	0.00023	0.00133	0.00439	0.43860	0.00031	0.00021	0.00001	0.00081	0.00111	0.00021
20	0.0000012	0.00022	0.00127	0.00424	0.42373	0.00029	0.00022	0.00000	0.00080	0.00108	0.00021
25	0.0000002	0.00020	0.00102	0.00463	0.46296	0.00009	0.00021	0.00001	0.00078	0.00124	0.00024
30	0.0000003	0.00019	0.00098	0.00449	0.44898	0.00008	0.00020	0.00000	0.00076	0.00114	0.00030
35	0.0000007	0.00021	0.00118	0.00489	0.46667	0.00018	0.00021	0.00000	0.00082	0.00116	0.00023
40	0.0000004	0.00020	0.00096	0.00434	0.43396	0.00005	0.00018	0.00000	0.00074	0.00111	0.00019
45	0.0000002	0.00018	0.00092	0.00528	0.50000	0.00003	0.00010	0.00001	0.00081	0.00106	0.00027
50	0.0000002	0.00019	0.00097	0.00529	0.52941	0.00003	0.00011	0.00001	0.00082	0.00112	0.00030
55	0.0000003	0.00020	0.00097	0.00563	0.53125	0.00003	0.00011	0.00001	0.00081	0.00113	0.00028
60	0.0000002	0.00019	0.00093	0.00567	0.50000	0.00003	0.00011	0.00001	0.00080	0.00110	0.00026
65	0.0000002	0.00021	0.00100	0.00593	0.51852	0.00004	0.00009	0.00001	0.00089	0.00107	0.00030
70	0.0000002	0.00019	0.00096	0.00593	0.51852	0.00004	0.00008	0.00001	0.00085	0.00104	0.00027
75	0.0000002	0.00015	0.00096	0.00654	0.50000	0.00004	0.00009	0.00001	0.00085	0.00104	0.00029
80	0.0000002	0.00015	0.00092	0.00615	0.50000	0.00004	0.00000	0.00001	0.00085	0.00100	0.00022
85	0.0000002	0.00020	0.00094	0.00581	0.48387	0.00003	0.00014	0.00001	0.00087	0.00110	0.00026
90	0.0000002	0.00017	0.00091	0.00652	0.52174	0.00004	0.00000	0.00001	0.00087	0.00096	0.00027
95	0.0000002	0.00019	0.00095	0.00667	0.57143	0.00005	0.00000	0.00001	0.00094	0.00105	0.00040
100	0.0000002	0.00019	0.00095	0.00714	0.57143	0.00005	0.00000	0.00001	0.00095	0.00105	0.00038
105	0.0000002	0.00028	0.00110	0.00828	0.68966	0.00007	0.00019	0.00001	0.00159	0.00124	0.00072
110	0.0000002	0.00029	0.00103	0.00809	0.66176	0.00007	0.00038	0.00001	0.00213	0.00126	0.00087
115	0.0000002	0.00026	0.00110	0.00714	0.77922	0.00006	0.00024	0.00001	0.00156	0.00143	0.00101
120	0.0000002	0.00030	0.00104	0.00889	0.60741	0.00007	0.00039	0.00001	0.00215	0.00129	0.00083
125	0.0000002	0.00036	0.00097	0.00982	0.66071	0.00009	0.00023	0.00002	0.00196	0.00135	0.00096
130	0.0000002	0.00034	0.00101	0.00924	0.62185	0.00008	0.00047	0.00002	0.00244	0.00131	0.00114
135	0.0000002	0.00031	0.00094	0.00866	0.59055	0.00008	0.00038	0.00002	0.00220	0.00117	0.00083
140	0.0000002	0.00037	0.00106	0.01019	0.67593	0.00009	0.00055	0.00002	0.00278	0.00136	0.00087
160	0.0000002	0.00038	0.00092	0.01048	0.63810	0.00010	0.00033	0.00002	0.00229	0.00116	0.00118
162	0.0000002	0.00037	0.00111	0.00926	0.58333	0.00009	0.00097	0.00002	0.00370	0.00124	0.00074
baseline (100 - 40 cm)	0.0000002	0.00031	0.00102	0.00884	0.64363	0.00008	0.00037	0.00002	0.00216	0.00126	0.00086
baseline (base - 100 cm)	0.0000002	0.00019	0.00095	0.00581	0.50906	0.00004	0.00008	0.00001	0.00084	0.00106	0.00027

The results for EF, presented in (Table 5.7) indicate that, in the upper part of the core, only Hg, Pb and Ni have enriched values, while in the bottom, only Cr and Ni show moderate enrichment. Hg and Pb present enrichment values over 3, mainly between 20 cm and 10 cm. The rest of the elements are all below the values of significant enrichment.

Table 5.7 - Values of enrichment factor
(dark green – minor enrichment, light green - moderate enrichment, orange – moderately severe enrichment)
The degree of enrichment was classified as follows: 1.5>EF no enrichment, 1.5≤EF<3 minor enrichment, 3≤EF<5 moderate enrichment, 5≤EF<10 moderately severe enrichment, 10≤EF<25 severe enrichment, 25≤EF<50 very severe enrichment, EF>50 extremely severe enrichment (in Moreira *et al.*, 2009)

Depth (cm)	Hg	Cu	Zn	Mn	Fe	Pb	Ni	Cd	Cr	Li	As
1	3.92	1.13	1.15	0.67	0.79	5.35	2.60	0.45	0.88	1.03	0.88
2	3.24	1.08	1.12	0.72	0.82	5.08	2.60	0.46	0.89	1.03	0.85
3	1.63	1.00	1.00	0.66	0.82	3.22	2.44	0.43	0.90	1.07	0.79
4	2.06	1.21	1.14	0.74	0.91	4.34	2.86	0.48	0.92	1.15	0.99
5	3.80	1.14	1.22	0.72	0.83	5.91	2.74	0.49	0.88	1.07	0.83
6	2.56	1.04	1.09	0.69	0.73	4.48	2.77	0.45	0.84	1.03	0.77
7	1.35	1.13	1.04	0.72	0.82	2.92	2.67	0.45	0.92	1.06	0.80
8	1.25	1.08	1.04	0.75	0.82	1.85	2.68	0.46	0.91	1.05	0.65
9	1.14	1.02	1.02	0.74	0.78	1.69	2.61	0.48	0.92	1.04	0.93
10	0.93	1.04	1.14	0.69	0.79	4.03	3.64	0.49	0.98	1.01	1.04
11	4.78	0.97	1.16	0.65	0.71	6.06	2.19	0.46	0.86	0.82	0.61
12	6.00	1.22	1.39	0.78	0.82	7.38	2.61	0.53	0.99	1.03	0.66
13	6.42	1.28	1.42	0.75	0.86	8.04	2.64	0.51	0.97	1.03	0.72
14	7.10	1.25	1.45	0.77	0.88	8.57	2.83	0.50	0.98	1.06	0.90
15	6.09	1.30	1.40	0.74	0.85	8.23	2.80	0.48	0.94	1.02	0.70
16	6.85	1.30	1.40	0.74	0.85	8.23	2.69	0.48	0.98	1.04	0.69
17	6.85	1.30	1.42	0.74	0.85	8.93	2.94	0.48	0.96	1.04	0.78
18	6.41	1.22	1.39	0.72	0.82	9.13	2.71	0.45	0.98	1.09	0.74
19	5.89	1.23	1.40	0.75	0.86	8.47	2.53	0.73	0.96	1.04	0.77
20	5.16	1.19	1.34	0.73	0.83	7.82	2.61	0.47	0.95	1.02	0.76
25	0.98	1.06	1.07	0.80	0.91	2.33	2.58	0.81	0.93	1.17	0.87
30	1.17	1.02	1.03	0.77	0.88	2.15	2.44	0.57	0.90	1.07	1.10
35	3.04	1.14	1.24	0.84	0.92	4.92	2.47	0.62	0.98	1.09	0.83
40	1.75	1.06	1.01	0.75	0.85	1.32	2.12	0.53	0.88	1.05	0.70
45	1.05	0.59	0.90	0.60	0.78	0.35	0.26	0.35	0.37	0.84	0.31
50	1.12	0.59	0.95	0.60	0.82	0.38	0.28	0.38	0.38	0.89	0.34
55	1.52	0.63	0.95	0.64	0.83	0.40	0.29	0.40	0.38	0.89	0.33
60	1.08	0.62	0.91	0.64	0.78	0.43	0.29	0.43	0.37	0.87	0.30
65	1.20	0.67	0.98	0.67	0.81	0.47	0.24	0.47	0.41	0.85	0.34
70	1.20	0.60	0.94	0.67	0.81	0.47	0.21	0.47	0.39	0.82	0.31
75	1.25	0.49	0.94	0.74	0.78	0.49	0.23	0.49	0.39	0.82	0.33
80	1.25	0.49	0.90	0.70	0.78	0.49	0.01	0.49	0.39	0.79	0.25
85	1.05	0.63	0.91	0.66	0.75	0.41	0.36	0.62	0.40	0.87	0.31
90	0.94	0.56	0.89	0.74	0.81	0.56	0.01	0.56	0.40	0.76	0.31
95	0.90	0.61	0.93	0.75	0.89	0.61	0.01	0.61	0.43	0.83	0.46
100	0.85	0.61	0.93	0.81	0.89	0.61	0.01	0.61	0.44	0.83	0.44
105	0.97	0.88	1.08	0.94	1.07	0.88	0.50	0.88	0.73	0.99	0.83
110	1.00	0.94	1.01	0.92	1.03	0.94	1.00	0.94	0.99	1.00	1.00
115	0.88	0.83	1.08	0.81	1.21	0.83	0.64	0.83	0.72	1.13	1.16
120	1.00	0.95	1.01	1.01	0.94	0.95	1.05	0.95	1.00	1.02	0.96
125	1.06	1.14	0.95	1.11	1.03	1.14	0.61	1.14	0.91	1.07	1.10
130	1.05	1.07	0.99	1.05	0.97	1.07	1.24	1.07	1.13	1.04	1.32
135	0.90	1.01	0.92	0.98	0.92	1.01	1.01	1.01	1.02	0.92	0.96
140	1.05	1.18	1.04	1.15	1.05	1.18	1.47	1.18	1.29	1.08	1.00
160	1.03	1.22	0.90	1.19	0.99	1.22	0.87	1.22	1.06	0.92	1.37
162	1.20	1.18	1.09	1.05	0.91	1.18	2.60	1.18	1.72	0.98	0.85

5.2.2.12. Radiocarbon data (Carbon 14)

For the present study, three ^{14}C radiocarbon analyses were made, in elements from specific levels of the sediment core (where variations of grain-size and color were perceptible):

- A seashell identified as *Glycimeris* glycimeris (Linnaeus, 1767), collected at the core base (162 cm) (Figure 5.26);
- Two mixed benthic foraminifera samples (~10 mg to 20 mg), picked under magnifying lens with a fine brush (Figure 5.27), from the sedimentary size fraction >125 μm at 120 cm and 110 cm depth. When comparing both foraminifera samples, it is clear that individuals from 120 cm depth have larger dimensions than the ones from 110 cm depth.

Figure 5.26 - Glycimeris glycimeris, before (left) and after (right) treatment. Squares 1 mm x 1 mm.

Figure 5.27 - Picked foraminifera from 120 cm (left) and 110 cm (right). Square scale 1 mm x 1 mm.

The analysis was performed at "Beta Analytic Inc.", Miami, FL, USA, by AMS method. The analysis for this core, uses 2σ calibration intervals with a local marine reservoir correction (Delta–R) of approximately 222 +/- 60 yr, estimated for the Iberian Margin, using Marine13 database. Delta-R value was obtained from the website (http://calib.org/marine/) and considered the mapped sample number 129 (on the website from Queen's University in Belfast).

The seashell *Glycimeris glycimeris* (Linnaeus, 1767), collected at the core base, indicated an estimated radiocarbon age of 8840±40 BP or 10090 – 9540 cal BP (Table 5.8), while the foraminifera from level 120 cm indicated a measured radiocarbon age of 7750±50 BP or 8570 – 8280 BP and the those organisms from 110 cm indicated a measured radiocarbon age of 6710±40 BP or 7540 – 7280 cal BP (Table 5.8) (Annex 1 - 1.8) (Annex 18).

Table 5.8 - Results of radiocarbon dating determined in the Laboratory "Beta Analytic Inc.", Miami, FL, USA

Sample depth (cm)	Measured Radiocarbon Age	13C/12C Ratio	Conventional Radiocarbon Age *	2σ Calibration
110	6710+40 BP	0.0 ‰	7120+40 BP	7540 – 7280 cal BP
120	7750+50 BP	+0.5 ‰	8170+50 BP	8570 – 8280 cal BP
162 (Base)	8840+40 BP	+2.7 ‰	9290+40 BP	10090 – 9540 cal BP

* Conventional Radiocarbon Age calculated using an assumed delta ^{13}C.

5.2.2.13. Bayesian age-depth model (rbacon)

Bacon (Blaauw & Christen, 2011) is an approach to age-depth modelling that uses Bayesian statistics to reconstruct Bayesian accumulation histories for deposits, through combining radiocarbon and other dates with prior information.

Any age-depth model produces estimates of accumulation rates, implicitly or explicitly. For example, the popular method of connecting the mid-points of dated levels using linear sections (linear interpolation; Blaauw, 2010), assumes that a deposit accumulated constantly between each dated level, and that accumulation rates shifted abruptly and exactly at the dated depths.

The software used was the Bayesian age-depth modelling software (called rbacon in R) with the following parameters: ^{210}Pb age as 72 +- 50 cal BP (years before AD 1950, error 'guesstimated'), a local marine reservoir effect of 178 +- 63 14C years (based on the calib.org marine database) and Marine13 as the calibration curve (Reimer *et al.*, 2013) (Figure 5.28).

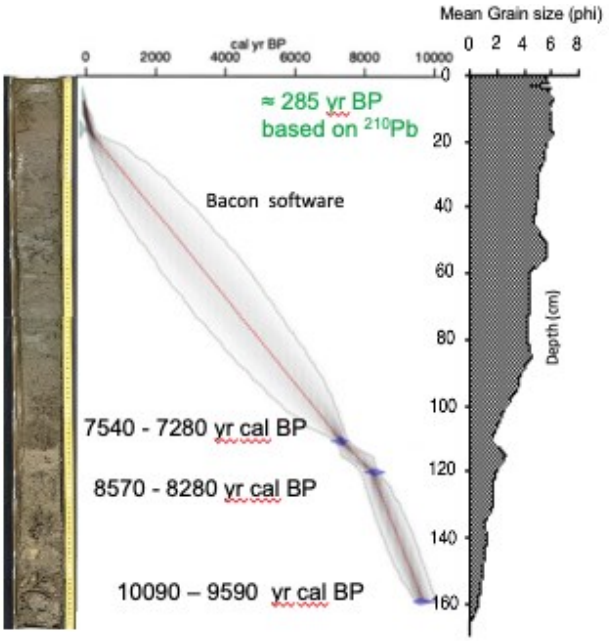

Figure 5.28 - Temporal evolution model according to Bacon software model.

5.3. Vertical variation of sedimentary facies

Collected at the center of the Ericeira mud deposit the 162 cm long sediment core was analyzed for several proxies, (x-ray analysis, magnetic susceptibility, TIC and TOC, grain-size, sortable silt, morphoscopy, fine fraction mineralogy, heavy minerals, heavy metals, benthic and planktonic foraminifera and calcareous nannoplankton) allowing a detailed vertical analysis of the sedimentary layer. The radiocarbon dating complemented this analysis in what concerns constraining the time frame for the evolution of the sedimentary processes.

Integrating the results described in previous sections, three main sedimentological units were identified, representing three depositional environments that characterized the Ericeira mud deposit since the beginning of the Holocene:

- a basal sequence (between 162 cm and 100/110 cm);
- a central sequence (between 100/110 cm and 20 cm);
- a superficial sequence (the upper 20 cm).

5.3.1. The basal sequence (base to 100/110 cm)

The basal sequence presents textural characteristics consistent with an energetic environment, due to the high percentages of gravel, sand and an absence of phyllosilicates. The magnetic susceptibility proxy indicates a very high level of susceptibility at approximately 157 cm related with an extremely high concentration of very coarse terrigenous particles and relatively high percentages of Fe/Mg rich minerals. The clay mineralogy is dominated by high percentages of aragonite and magnesite and the ratio of carbonates/lithogenic particles indicates a high proportion of carbonated particles. The concentration of heavy minerals is the highest in the entire sequence, dominated by tourmaline, garnet and pyroxene.

The higher values of pyrite and glaucony in the bottom may be associated with diagenetic processes. As stated by McCracken *et al. (*1996) the glaucony grains mottled dark to light brownish-green, fractured, variably rounded and can commonly be replaced by pyrite and also the iron-poor calcite that fills the shrinkage features overgrows pyrite rims developed on the glaucony grains (Figure 5.29).

Figure 5.29 - Fractures along glauconitic grains.

The percentage of inorganic carbon is extremely high in this basal sector, related with the carbonated shells high content. On the other hand, the percentage of organic carbon is low. The accumulation of carbonated elements, at this level of the core sediment can be seen in the x-ray image, where there is a greater accumulation of organisms like shells of gastropods and other mollusks.

When considering the microfaunal data collected (benthic and planktonic foraminifera and calcareous nannoplankton), one can observe that although the foraminifera data is more thorough, the results revealed from calcareous nannoplankton also indicate the same trend identified by foraminifera (Figure 5.21, Figure 5.23). Regarding to foraminifera species, this core section is characterized by the occurrence of *A. beccarii*, *C. cf. pseudoungerianus*, *T. deltoidea* and *Asterigerinata sp*., very common in high energy environments (Debenay *et al.,* 1998, Costa *et al.,* 2012), hence coarser grain-size, and well-oxygenated bottom waters can justify their high abundances (Martins *et al.,* 2007, 2012). Considering the calcareous nannoplankton, remobilized species like *P.discospora, R.antarticus, R.haqii, R.minutula* and *Tubodiscus sp*. dominate, probably indicating that this might be a eutrophic environment (Bartol *et al.,* 2008). All the other foraminifera and calcareous nannoplankton species identified, are nearly absent in this core section. *Reticulofenestra* genus, also considered a remobilized species, completely disappears above the 120 cm, being such a sensitive species to nutrients availability (Farida *et al.,* 2012).

Regarding the heavy metal concentrations along this first section, the values are low and related to natural processes, mainly metallic minerals from rocky outcrops, such as pyroxenes that incorporated Zn, Li, Fe and Cr in their structure.

The above results indicate that the first sequence of this vertical sample was deposited in a shallow and energetic marine environment, probably in a coastal system. The sample extracted at 162 and 110 cm (*Glycimeris* glycimeris and foraminifera) with an age of 10090 – 9540 cal BP and 8570 – 8280 cal BP, respectively are representative of this environment.

5.3.2. Intermediate sequence (100/110 cm – 20 cm)

The most remarkable feature of the intermediate sequence of the sedimentary layer is the abrupt decrease of coarse particles (mostly sand) and the relative increase of fine particles (silt and clay).

The decrease in the carbonated coarse particles content is visible in the x-ray images and it is gradual, although at 50 - 55 cm there is an accumulation of gastropods (*Turritella communis Risso*, *1826*) and diatoms, explaining also the high percentage of opal; along this sequence, the percentage of TIC decreases upwards as the TOC increases.

The coarser particles of sand (1 – 2 mm) are dominated by quartz, aggregates, terrigenous, mollusks and biogenic particles. Considering the finer fractions composition, there is an upward increase of phyllosilicates, planktonic and benthic foraminifera, biogenic particles and glaucony.

In the finer fractions, clay minerals become more important, namely chlorite, illite, kaolinite, opal, anhydrite, plagioclase, dolomite and siderite.

Benthic foraminifera are represented by two species assemblages. One group that is considered more opportunistic and the other group is characterized by species that are already adapted to the settling environment. Marine calcareous nannoplankton species start to develop and occupy the entire sediment record and increase their abundance to the top. In the level comprehended between 50 – 55 cm, the standing crop of benthic and planktonic foraminifera decreased while the abundance of calcareous nannoplankton and probably diatoms increased. The foraminifera association characteristic from this sequence is composed by *G. subglobosa*, *O. umbonatus*, *G. crassa, G. umbonata* and *B. pseudoplicata*. *Globocassidulina subglobosa*. *Oridorsalis umbonatus* presenting also a 10 % peak at 100 cm. The other association consisting in *B. difformiis*, G. *rossensis* and *B. spathulata* become more abundant as the percentage of fine sediment starts to increase. It is also characterized by a high, persistent and diversified record of oceanic species such as *E. huxleyi, G. ericsonii, H. carteri*, *U. sibogae*, *G. muellerae, Calsiosolenia* sp. and *C. leptoporus*.

Heavy metals have very low concentration in this intermediate sequence.

Compared to the first sequence, this intermediate unit was formed in an inner/middle shelf environment, with lower energy and increasing oceanic influence. This sedimentary sequence includes the foraminifera with an age of 7540 – 7280 cal BP.

5.3.3. The upper sequence (20 cm – top)

From the x-ray images of the uppermost and recent sequence of the sedimentary layer, one can observe the disappearance of the grainy texture. Visually, sediment's texture becomes fluffy and fine with evident bioturbation.

Sediments are dominated by fine grained particles (silt and clay totals about 80 % of the total sediment) and sandy fraction has a very minor role. In fact, the mean grain size of this sector varies between approximately 4 and 6 phi (0.063 and 0.015 mm).

The mean sortable silt decreases in the decarbonated form (due to the negligible importance of terrigenous particles), contrasting with increasing percentage of carbonated mean sortable silt, dominated by benthic and planktonic foraminifera, calcareous nannoplankton, phyllosilicates, glaucony, clay minerals and other biogenic particles. Siderite (FeCO3) is another carbonated mineral present in this core section.

Concerning the foraminifera content for this section, which comprises *C. laevigata*, *B. ordinaria*, *A. cf. mamilla*, *N. turgida*, *E. vitrea*, *Q. stalkeri* and *C. obtusa,* indicate a strong affinity with fine sediments, compatible with a low energetic environment.

Calcareous nannoplankton species experience a decrease in abundance, except for *E. huxleyi* that rapidly recovers at 12 cm. The top 10 cm are characterized by an increase of

abundance, of oceanic and neritic species like *G. muellerae*, *E. huxleyi, C. leptoporus*, *C. pelagicus*, *Calciosolenia sp*., *H. carteri*, *S. histrica-pulchra* and *B. bigelowii*. There is a high abundance of *G. oceanica.*

Considering the heavy metals, the relative high content of metals (such as Pb, Hg, Zn, Cu and Ni) is in agreement with the higher values of magnetic susceptibility in this core section contributing for the increase of magnetic susceptibility values.

In terms of sedimentary facies, the superficial sequence presents all the characteristics of a marine environment (middle/outer shelf) whose dynamics is similar to present day conditions.

5.4. Synthesis

The description of a vertical sample collected offshore Ericeira in the center of the largest muddy deposit of the Estremadura Spur allowed to understand shelf environmental changes during the Holocene.

Results allowed the segmentation of the core in three sedimentary sequences whose facies indicate a changing marine environment. The oldest one, corresponds to a high energy environment probably representing a coastal deposit in close connection to the terrigenous particle sources. In this core section, sediments are composed by coarse-grained particles, have a high carbonate content and a low content of organic matter. The presence of robust organisms like *A. beccarii*, *C. cf. pseudoungerianus*, *T. deltoidea* and *Asterigerinata sp* indicate the presence of high energy environments and also the higher percentage of heavy minerals at this section indicates that the energy was high enough to promote their transport.

The middle core section shows an increased presence of biogenic particles and a decrease in coarser particles indicating a deeper and lower energetic environment compared with the previous one (inner/middle shelf). In fact, the percentage of coarse particles present in the studied sediment sample decreases as fine particles (silt and clay) increase their concentration. The same decreasing trend was observed in the heavy minerals fraction although in the fine fraction mineralogy, the phyllosilicates family have a significant concentration in the whole sequence.

In the superficial sequence, only 20 cm thick, sediments are compatible with a middle/outer shelf dynamic process, very similar to present day characteristics. In the fine sand fraction, phyllosilicates, benthic and planktonic foraminifera dominate this sequence; the percentage of heavy minerals is negligent apart from phyllosilicates that dominate; the establishment of *C. laevigata*, *B. ordinaria*, *A. cf. mamilla*, *N. turgida*, *E. vitrea*, *Q. stalkeri* and *C. obtuse* are indicative of a marine environment characteristic of a mid-outer shelf as we know today (Martins *et al.,* 2019, Mendes *et al.,* 2004). The sudden arising of heavy elements like mercury (Hg) and lead (Pb) also evidence the presence of anthropogenic activity, probably either related with deforestation or mining (Dubois *et al.,* 2017). Deforestation and mining increase soil

erosion, leading to a characteristic inorganic detrital deposit in most aquatic systems (lakes, rivers and seas).

Chapter VI - Evolution of the Estremadura Spur during late Quaternary

6.1. Introduction

Continental shelves are highly complex depositional systems where deposits are formed under diverse hydrodynamic conditions. The stratigraphic study of the sedimentary sequences will enable the distinction of different sedimentary cycles, each one reflecting the equilibrium between external and internal geodynamic factors.

In previous chapters, the present-day characteristics of the Estremadura Spur was described, regarding morphology, sedimentary deposits distribution, particles transport processes and main particle sources. In chapter V, a vertical sample collected in the middle of the Mar da Ericeira, the most important depocenter of the Estremadura Spur, indicates that important changes in marine environment occurred in the last 10 000 years. Major changes are reflected in three sedimentary sequences, each one corresponding to a major phase of the evolution of the Ericeira mud deposit. Considering that paleo-environmental reconstructions based on shallow marine sedimentary sequences are essential for a better understanding of past climatic and oceanographic changes, in particular those that took place during the Holocene (last ~ 10,000 years; Rosa *et al.*, 2010), in the present chapter, a conceptual model for the evolution of the entire Estremadura Spur is presented. This model will cover the period since the Last Glacial Maximum (LGM ~ 20 000 years BP; Dias *et al.* (2000)).

6.2. Methodology

The reconstruction of the evolution of the Estremadura Spur, during the late Quaternary, will use, as a reference, the present-day characteristics (oceanographic, morphological and sedimentological) and the relationship between different sedimentary environments (fluvial, coastal and continental shelf), described in previous chapters, complemented with published studies. It will also take into consideration the accumulation rate of 0.07 cm/y for the first 20 cm and 0.12 cm/y, 0.009 cm/y and 0.2 cm/y from the other sectors (Figure 6.11). When compared with different locations of the Portuguese continental shelf, this value is quite low. This is true in Estremadura Spur because there is no significant local river input. Other locations, namely Douro, Tagus and Guadiana mud-patches present higher accumulation rates since the river input is highly significant. The accumulation rates vary in the three mud-patches presenting 0.12 ± 0.01 cm/y in Guadiana, 0.22 ± 0.03 cm/y in Tagus and 0.49 ± 0.11 cm/y in Douro (Burdloff *et al.*, 2008).

As such, the conceptual model of the Estremadura Spur evolution will highlight features generated by coastal or fluvial processes and others associated with older sedimentary cycles present in the bottom sedimentary cover. Paleo river drainage was deduced from present day bathymetry and rocky outcrops (Dias *et al.*, 2000; Rodrigues, 2001). Present day bathymetry

reflects the actual sedimentation, but in this specific case does not have a significant impact since the sediment accumulation rate nowadays is almost inexistent.

6.3. The sea level variation in the Portuguese margin

In the west Iberian margin, past environments have been studied in the last decades using a multiplicity of methods and different approaches, resulting in diverse and sometimes with not converging results. Lantzsch *et al.* (2009, 2010), applied different proxies like grain-size, foraminifera, x-ray diffraction and ^{14}C in the study of several sediment cores collected along the NW Iberia. The results were complemented with geophysical profiles and the recent evolution of a mud depocentre in NW Iberia was proposed and Martins *et al.* (2007/2012), detailed the study of the same mud depocentre with additional textural, mineralogical, geochemical and benthic foraminifera data.

Regarding the first local sea level curve variation since the LGM, established from the application of sedimentological and morphological criteria, and taking into account the post glacial evolution of the North Atlantic, was presented by Dias (1987). This curve (Figure 6.1) represents the evolution of the sea level on the Portuguese continental shelf, from its lower position (during the LGM, 20 000 - 18 000 years BP) until its present location (reached at ~3 500 years BP) and is concordant with the CLIMAP model for the evolution of the polar front (CLIMAP Project Members, 1976, 1981). More recently, others have also detailed sea level curves for the Holocene in different Atlantic systems. For example, Leorri *et al.* (2012) combined the indicative depositional meaning (derived from the micropalaeontological composition and sand content) with radiocarbon ages of 55 borehole samples, collected in three estuaries of the southern Bay of Biscay, and reviewed all available sea-level data from SW Europe (France, Spain and Portugal) to provide the regional trend and calibrate an isostatic model. Garcia-Artola *et al.* (2018) published sea level curves for the Holocene based on ACE (Atlantic Coast of Europe) database that covers most of the French, northern Spain's, and the Portuguese coast.

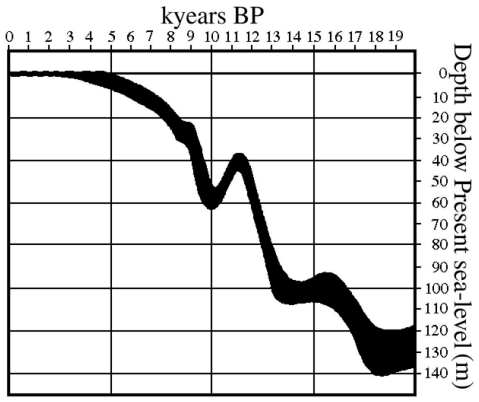

Figure 6.1 - Interval of sea level variation (m) at the Portuguese continental shelf Vertical accuracy is about 10m (from Dias, 1987).

The integrated analysis of the msl variation and the Polar Front position, defined by Ruddiman & McIntyre (1981), state that between 20 000 and 18 000 years ago, during the LGM peak (Phase I), the msl was 130/140 m below its current level, very close to the shelf break. During its subsequent relative rise, the msl stayed at -110/-100 m (Phase II) for 2 000 years (from 16 000 years to 14 000 years BP), after which it rapidly reached the - 40 m (11 000 years ago, corresponding to Phase IIIa). The generalized cold climate, which occurred during Phase IIIb and lasted for 1 000 years, resulted in the rapid fall of the msl to - 60 m by the end of this phase. Phase IIIc, between 10 000 and 9 000 years BP, corresponds to a rapid rise after this climate cold period. During Phase IV, the average level of the sea maintained a relatively steady behavior, rising gradually until reaching its current position between 5 000 and 3 500 years BP. The last phase, Phase V, corresponds to the period of small adjustments, extending to the present. Beginning at 10 000 years ago, the Holocene period corresponds to Phase IIIc, Phase IV and Phase V.

Despite recent publications on the evolution of transitional environments of the European and Portuguese margins (Freitas *et al.*, 2003; Dinis *et al.*, 2006; Drago *et al.*, 2006; Garcia-Artola *et al.*, 2018), the work of Ruddiman & McIntyre (1981), performed under the scope of the CLIMAP project, still is an important reference in the study of the North Atlantic. The postglacial Atlantic evolution stated by these scientists was applied to the west- Iberian margin (Dias, 1987; Rodrigues *et al.*,1991; Dias *et al.*, 2000; Rodrigues, 2001) and will be considered in the Estremadura Spur sector.

6.4. The sea level variation in Estremadura Spur

6.4.1. The environmental evolution of the Estremadura Spur since LGM

6.4.1.1. Last Glacial Maximum (20 000 – 18 000 years BP)

The Last Glacial Maximum occurred between 20 000 and 18 000 years before present (BP), with the onset of glacial atmospheric conditions at 25 000 years BP (Ruddiman & McIntyre, 1981). Reflecting this glacial period, sea level was much lower than the present due to the retention of water in the ice glaciers. Atmospheric and oceanographic circulation systems were also very different from the current ones and the polar front (present isothermal temperature of 0 °C/6 °C) was located lower than 40º N. The boundary between polar and subpolar waters was recognized by the transition of microfauna's species with glacial affinity to a much more diverse association of planktonic organisms.

The first interdisciplinary project to reconstruct climate began in the 1970s and led by the marine geologists John Imbrie and Jim Hayes and the geochemist Nick Shackleton. "*The Climate: Long-range Investigation, Mapping, and Prediction*" project (CLIMAP) reconstructed the surface of the Earth at the Last Glacial Maximum at 21 000 yr BP (CLIMAP Project Members, 1976, 1981), (Giraudeau & Beaufort, 2007). Based on a very accurate multi proxy study, the CLIMAP

project, summarized by Ruddiman & McIntyre (1981), described the Atlantic polar front location during LGM, 20 000 years before present, and the subsequent Atlantic evolution (Figure 6.2). The deglaciation evolution corresponds to the progressive improvement of climatic conditions and rearrangement of oceanic circulation systems with impacts on the regional location of the sea level.

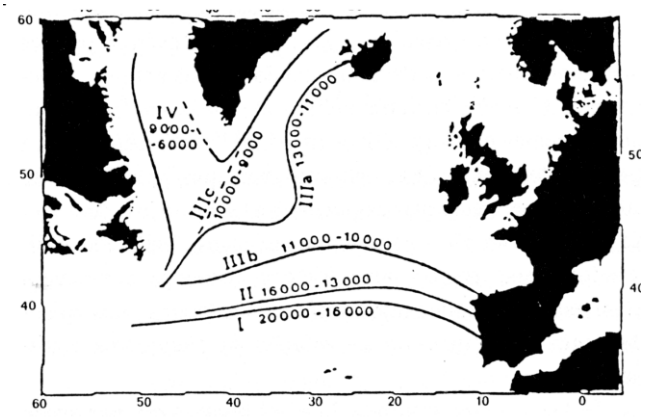

Figure 6.2 - Polar Front localization during the Last Glacial Maximum.
(Phase I) and the following deglaciation phases, Phase II to Phase IV (Ruddiman & McIntyre, 1981).

During the LGM, because of the cold and arid climate and the huge volume of ice retained at polar and mountain glaciers, the polar front was in its most southern position, being located at Iberian latitudes during the glaciation peak and beginning of the ice melting period (until 16 000 years BP). After that cold phase, the polar front occupied different positions in the North Atlantic due to the onset of favorable atmospheric conditions (rising temperatures) and the glaciers melting processes, which introduced large volumes of melted fresh water into the oceans (Rasmussen *et al.*, 2014).

This global climate evolution induced major modification on the oceanic environment and ecosystems distributions, as it controls the sea level location and oceanographic processes, with impacts on sedimentary processes (erosion and sediment delivery to the shelf, transport and deposition). Nevertheless, local specific features become dominant in a more restricted scale, when the global change signal decreases and the sea level remains stationary in a certain position. This observation is of extreme importance, because it implies that general evolution and changes affect the entire Atlantic margins but, each sector has its own identity and reacts individually.

During the LGM, between 20 000 and 18 000 years BP, the msl was 130 m below present one (Dias, 1987) and the sedimentary porcesses were significantly different from the present ones, due to the cold arid climate, the extension of mountain glaciers and coastal dynamics (Allen *et al.*, 2008). The proposed reconstruction of the coastline location and the

continental shelf morphology (Figure 6.3), indicates that at Esporão da Estremadura the river drainage extended westward, as far as 30 km, and the drainage basin areas were larger.

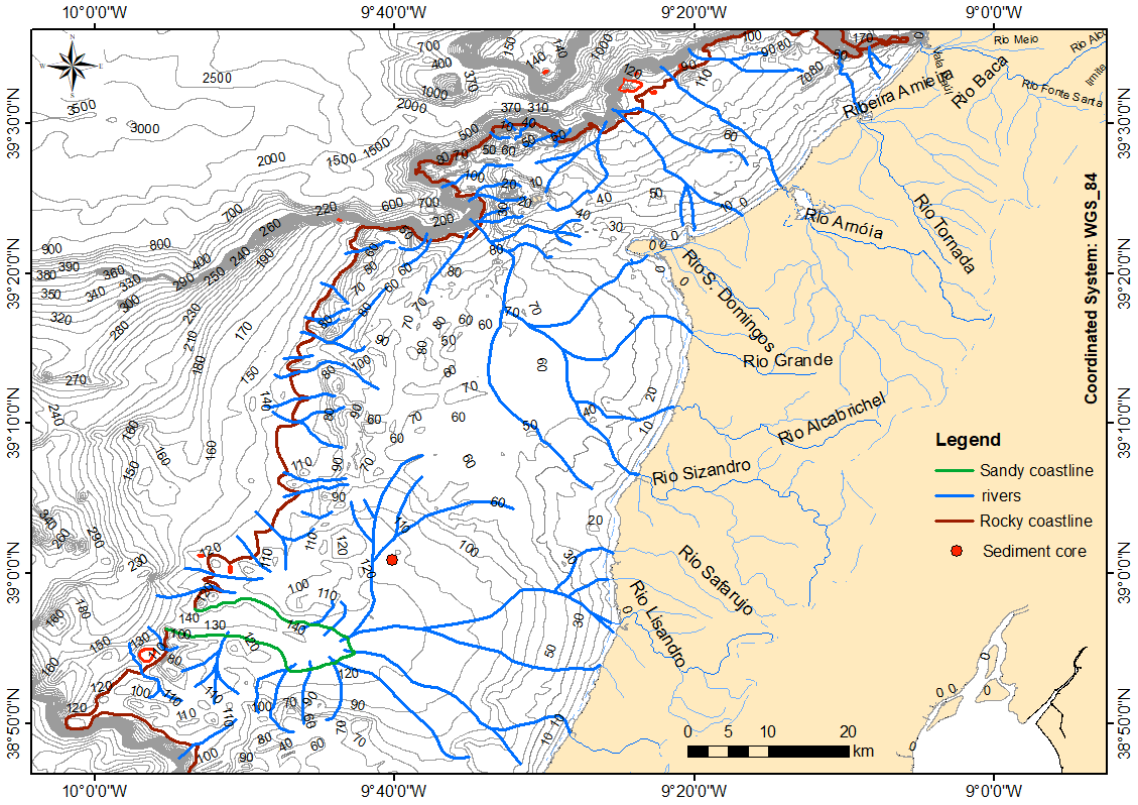

Figure 6.3 - Coastline position during LGM.
Characterization of coastline physiography (red – rocky; green – sandy) and main river drainage.

Limited by the Canhão da Nazaré, the northern sector of the Estremadura Spur coastline, north of Peniche, was very irregular, with cliffs carved in the rocky basement. Crossing the continental shelf, the three main rivers (S. Domingos river, Arnóia river and Tomada river) delivered sedimentary particles directly into the Nazaré canyon. At that time, probably there were no sandy coastal stretches in this coastal sector.

South of Cabo Carvoeiro, the thick carbonate formations from the Mesozoic rifting phases (Jurassic to Cretaceous undifferentiated) outcrops in the mainland, gave rise to the irregular morphology of Costeiras Pêro da Covilhã, exposed to subaerial erosional agents during this glacial period. These hard outcrops formed a morphological barrier along the littoral and because of this structural control, the drainage networks of the mainland were organized into two main systems, separated by Ponta da Lamparoeira outcrops, which extended more than 30 km further west. The northern hydrographic basin, with a SE-NW orientation, includes the prolongation of Alcabrichel River, Sizandro River and Grande River and drain directly into the Vale da Berlenga. South of Ponta da Lamparoeira. The hydrographic basin comprehends the extension of Colares River, Sarafujo River and Lizandro River and was organized with a general E-W direction, ending into a long-embedded cove, west of the Mar da Ericeira. This bay was

protected from the influence of the prevailing wave regime, by high barriers of hard carbonate formations, presenting a very smooth morphology, being the only sector where sedimentation could take place, during this glacial period.

Between these two larger river mouths (the Berlenga valley head and the Ericeira cove), a large number of small streams and rivulets were expected to exist, descending from the highest points of the reliefs to the coastline. Due to cold and arid meteorological conditions, their regime was, most likely, ephemeral.

During the LGM, the continental shelf presented a very reduced width in the northern section, close to the Canhão da Nazaré and in the southern area. Between 38º50' N (Colares) and 39º20' N (Peniche), the continental shelf extended for more than 30 km westward, being the shelf break located 130 m below the sea level (Figure 6.4).

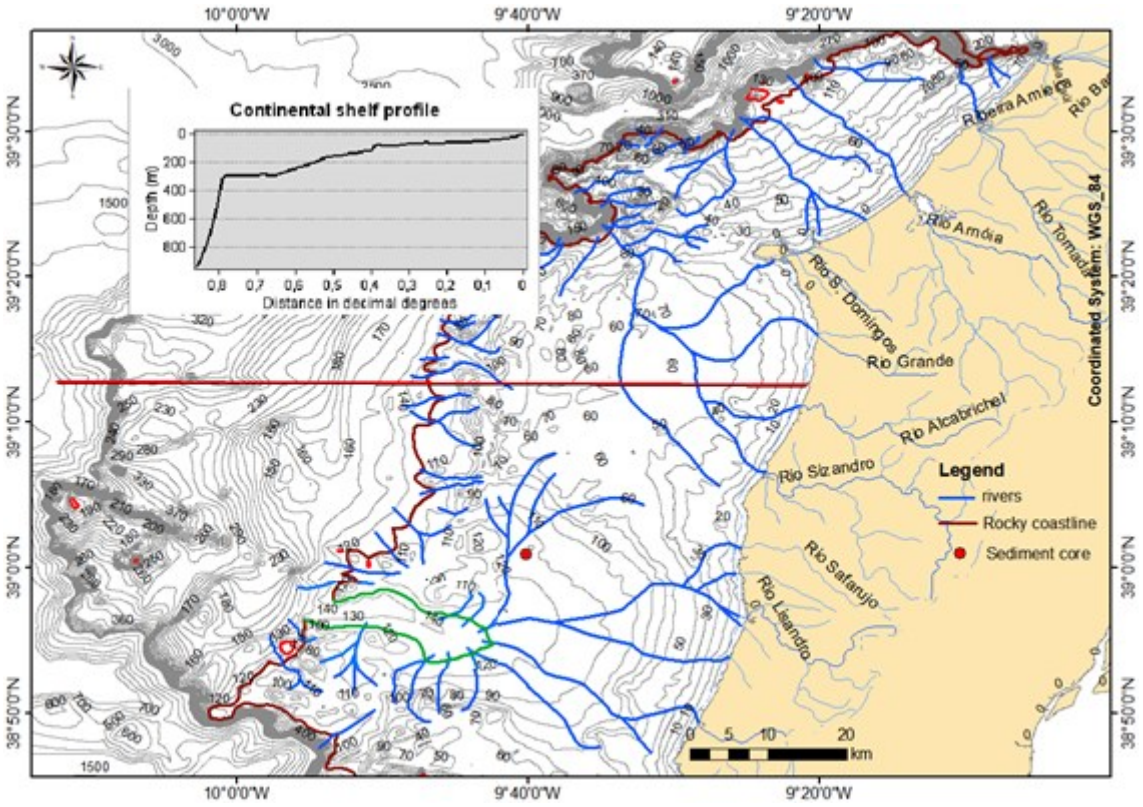

Figure 6.4 – Continental shelf transversal profile.
The red dot indicates the sample collected at Ericeira mud deposit.

The present sedimentary cover of the proximal and distal outer shelf still incorporates (as relict particles) sediments originated during the LGM. These particles have morphoscopic characteristics typical of a high level of remobilization, which is compatible with a shallow water environment and the effect of successive cycles of remobilization and sedimentation, as shown by the magnifying glass analysis performed on sediment coarse fraction (Figure 6.5).

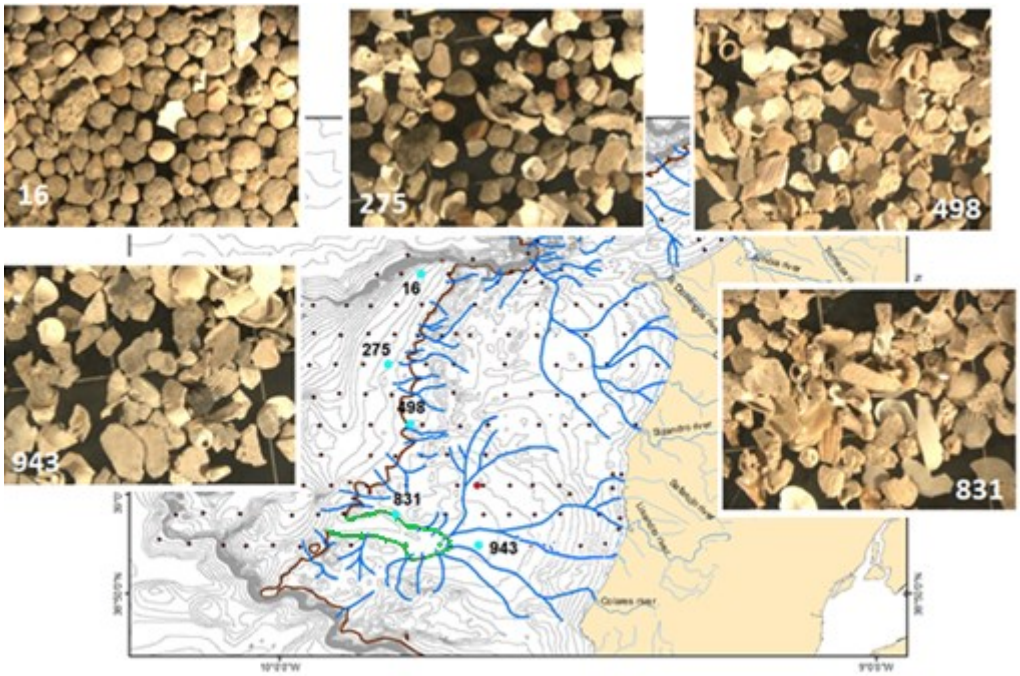

Figure 6.5 - Examples of paleolitoral samples reflecting a shallow water environment.

6.4.1.2. The beginning of the deglaciation (16 000 to 13 000 years ago)

After the initiation of the ice melting (deglaciation), when global warming occurred, the coastline migrated eastward and the coastal areas were progressively invaded by the sea; the former sedimentary deposits were affected by this sea level rise and dynamic processes had to adjust to the different oceanographic conditions. It is generally accepted that the melting of the large part of the ice caps occurred in the initial 3 000 years of the deglaciation period (Ruddiman & McIntyre, 1981). In the Portuguese continental shelf, the msl rose rapidly 20 to 30 m, standing at -100 / -110 m (Dias, 1987), when it remained stationary for about 1 000 years (Figure 6.6). Higher pluviosity combined with the effect of spring ice melting maintained high river discharge and consequently caused more sediment supply to the coastal zone.

Most of the Estremadura Spur coast presented cliffs and sediment deficit based on the geomorphologic features and the existing outcrops. This physiography is particularly visible at the proximity of Costeiras Pêro da Covilhã (south of Peniche) and Montanhas de Camões (at the southern area). Also, to the rocky character of the coastline, contribute the fact that fluvial input was insufficient to sustain a longshore sediment drift. In fact, the northern hydrographic system continues to introduce the terrigenous particles directly into the Berlenga valley and the southern rivers (Lizandro and Colares) and streams discharge fluvial sediments into the Ericeira bay that, at this stage, is much wider, despite the presence of several small rocky islands. These islands sheltered the coast from wave energy, promoting the development of a sandy coastline along the bay.

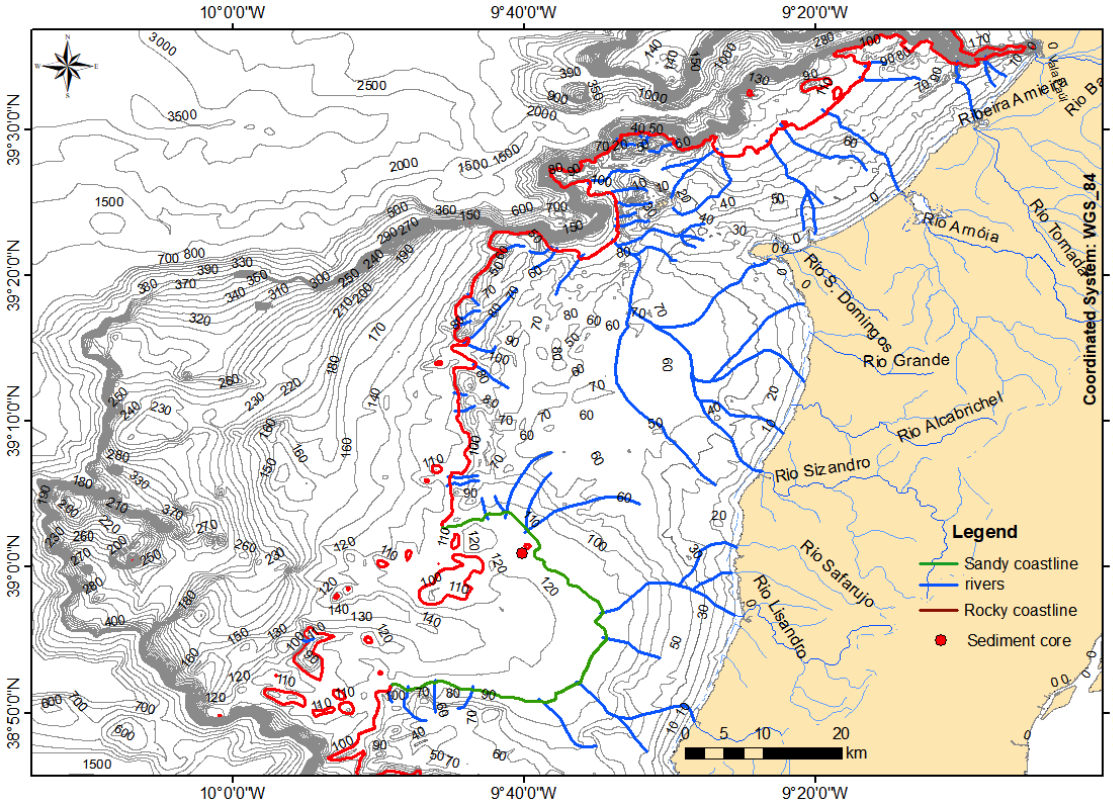

Figure 6.6 - Coastline position when the msl was 110 m depth (13 000 years BP). Characterization of coastline (red – rocky; green – sandy) and river drainage.

In the northern sector of Estremadura Spur, between Peniche and Nazaré, since the continental shelf is still narrow, the sediment accumulation is most likely inexistent due to the prevailing oceanographic conditions.

As deducted from the red dot plotted on Figure 6.6, the site where the vertical sample studied in chapter V was collected, was very close to the shoreline.

6.4.1.3. The end of the deglaciation (13 000 to 11 000 years ago)

According to Dias *et al.* (2000), the period between 13 000 and 11 000 years ago corresponds to the end of the deglaciation phase, bringing substantial changes to climate and oceanic circulation in the North Atlantic. The reappearance of the Gulf Stream provoked the rapid vanishing of ice in Western Europe (Ruddiman & McIntyre, 1973) and a consequently northward shift of the climatic belts (Rognon, 1976, 1980; Ruddiman & McIntyre, 1981). During two millennia, the ocean temperature was similar or slightly warmer than the present temperatures (Duplessy *et al.*, 1981) and the sea level rise velocity was close to its maximum.

In the Portuguese continental shelf, msl rose about 70 m in 2000 years till - 50/- 40 m depth (Dias *et al.*, 2000) and the Estremadura Spur had the configuration proposed in Figure 6.7.

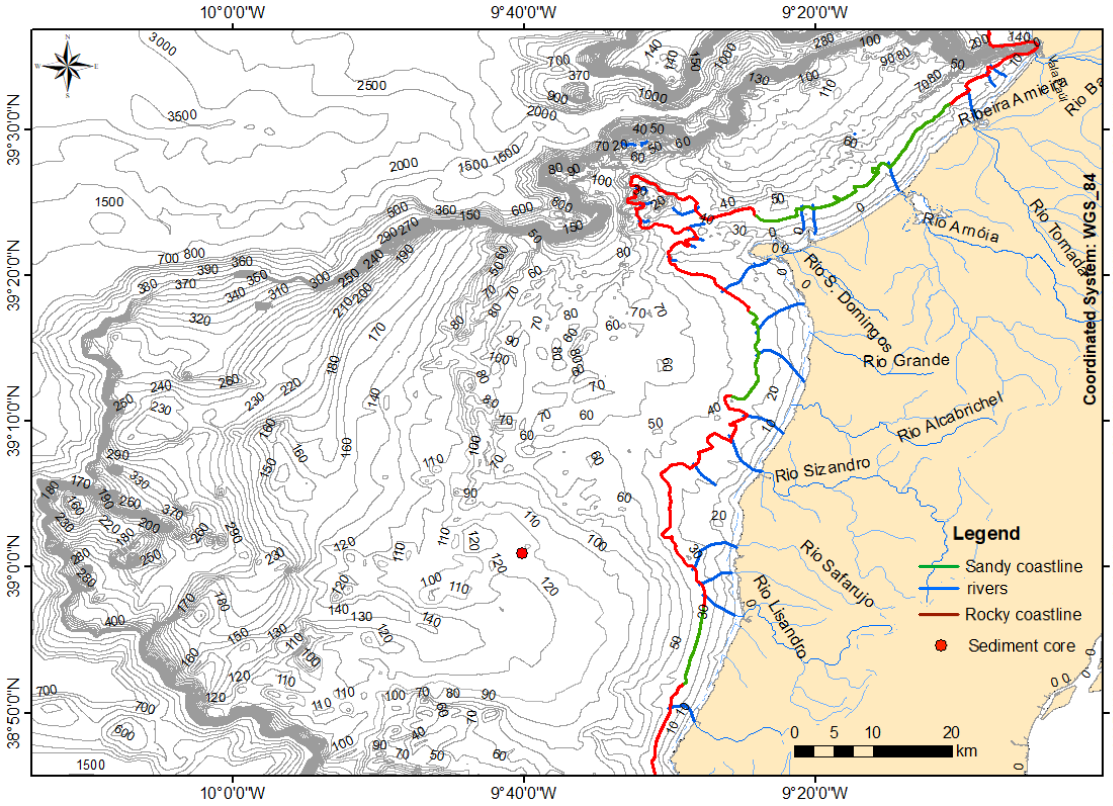

Figure 6.7 - Coastline position when the msl was 40 m depth (11 000 years BP). Characterization of coastline (red – rocky; green – sandy) and river drainage.

According to Dias *et al.* (2000), unable to equilibrate with such a rapid rise of sea level, the major Portuguese estuaries effectively became sediment traps, exporting to the shelf only a minor volume of fine-grained sediments. In the study area, the few estuaries hardly accommodate the scarce volume of fluvial sediments and the estuarine particles were rapidly integrated into the coastal dynamics. As a consequence, the coastline continued to be essentially rocky with very few sandy accumulations, essentially at the Ericeira sector. Such conditions also explain the striking lack of any remnant of preserved coastal morphology in the present-day middle to inner shelf fringe.

The studied vertical sample, marked with a red dot in Figure 6.7, was located 70 m below sea level, representing the (paleo) middle shelf domain. Despite being in the middle of the continental shelf, the vertical sample was located in a dynamically protected area. This means that sediments circulation pattern on Ericeira area was confined to the southern cell and sediment main sources were meagre and mostly related the local outcrops and also minor contributions from rivers or coastal erosion.

6.4.1.4. The Younger Dryas (11 000 to 10 000 years ago)

During Younger Dryas event, the polar front migrated southwards and reached the latitude of Galiza (Ruddiman & McIntyre, 1973; 1981) driving the sea surface temperature below 10 ºC and the lowering of the msl from - 40 m to - 60 m. By the end of this Younger Dryas event, between 9 500 – 10 500 ky BP, Dias *et al.* (2000) stated that the msl was found to be 60 m below the present msl, remaining stationary for almost 1000 years (Figure 6.8).

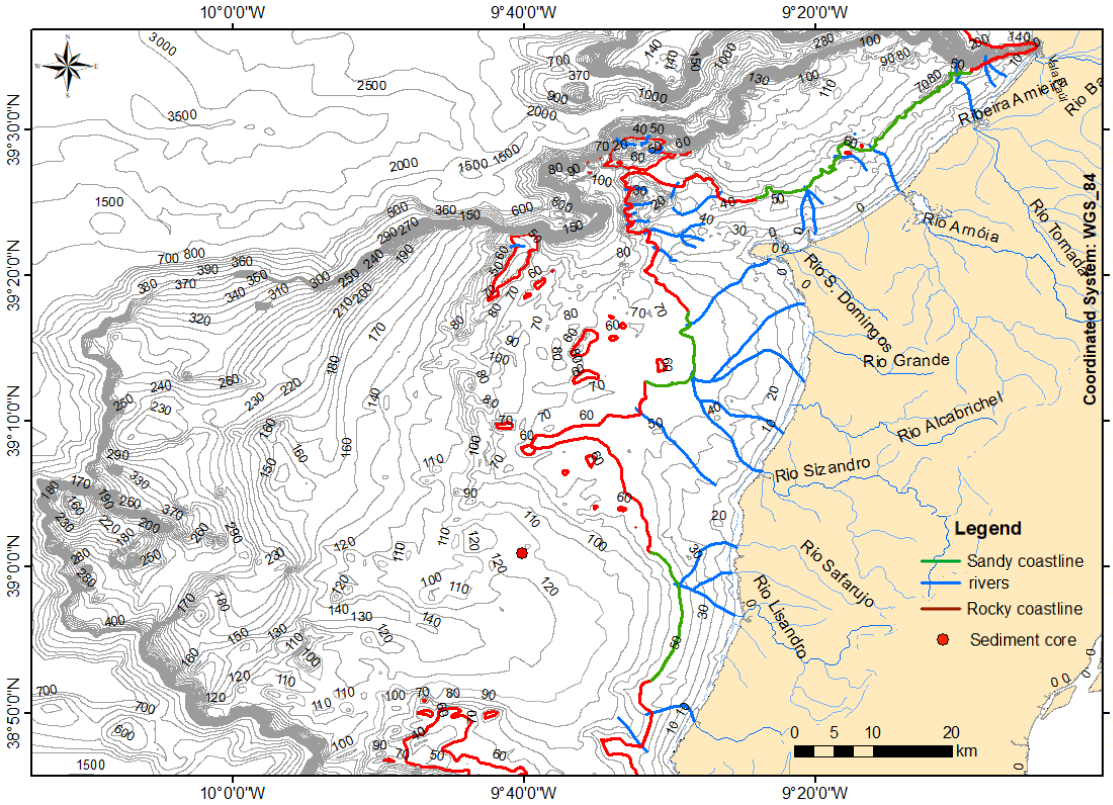

Figure 6.8 - Coastline position when the msl was 60 m depth (10 000 years BP). Characterization of coastline (red – rocky; green – sandy) and paleo river drainage.

Due to the rapid msl fall, a more significant exportation of terrigenous material into the continental shelf through the fluvial channels was expected. Although this supply was observed in some sectors of the continental shelf north of the Canhão da Nazaré (Dias *et al.*, 2000), in the Estremadura Spur there were no traces of this type of processes. According to Dias *et al.* (2000), the littoral zone had the characteristics of a desert as judged from the abundance of mass wasting deposits (Daveau, 1980) and consolidated (presently) aeolian deposits in Alentejo and Western Algarve (Pereira, 1985, 1992).

In terms of sedimentary dynamics, the new cycle remobilizes coastal and estuarine deposits and particles were dispersed and transported cross shore. As a consequence, coastal sediments (from the previous sedimentary cycle) will be integrated, as remobilized particles, in shelf deposits formed during this climatic event. Most of these particles are very well rounded

and present a distinct ferruginous coating, formed by precipitation, during the subaerial exposure (Dias *et al.*, 1980/1981; Dias & Nittrouer, 1984). The area between the coastline and Costeiras Pêro da Covilhã reveals itself keen to the development of very diverse marine life with predominance of mollusks shells, sea urchins and sponges' spicules (Figure 6.9), because the depth is quite shallow (10 - 20 m depth) and the sea bottom dominated by extensive outcrops and very coarse sand.

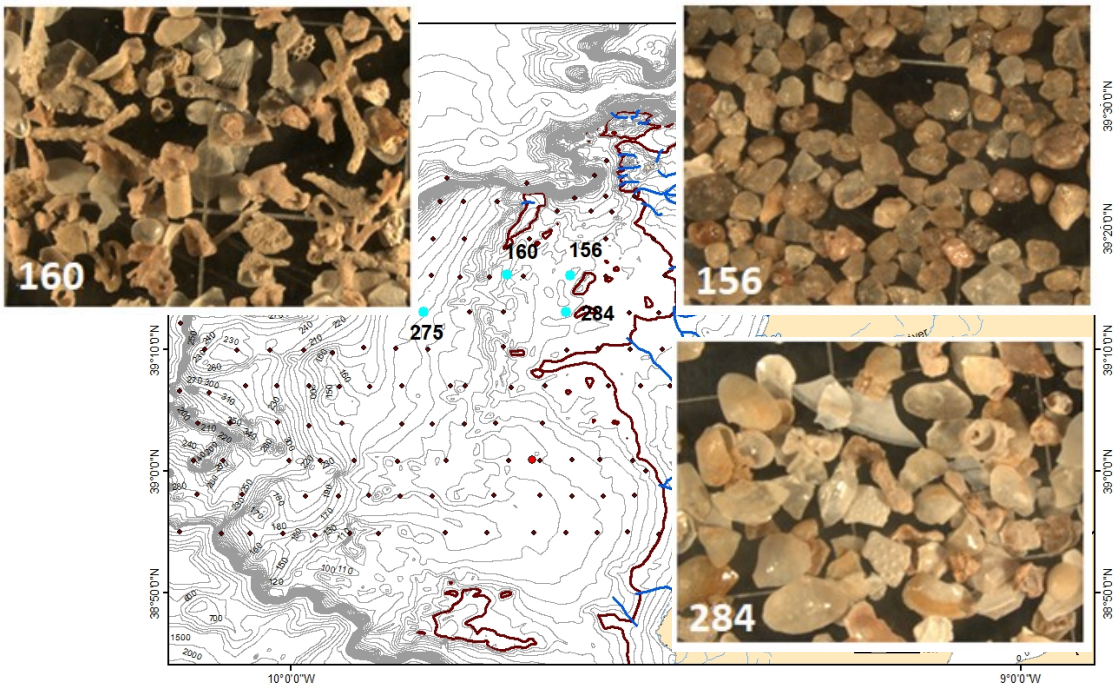

Figure 6.9 - Representation of coarse fraction from samples of the sedimentary cover: samples 160 and 284, with remains of shells (mollusks, gastropods, bryozoa, echinoderms); sample 156 with remobilized grains from a paleo littoral.

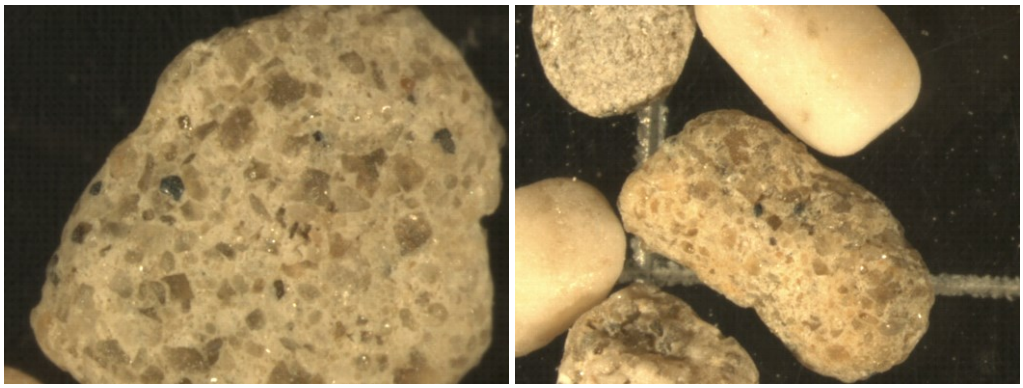

Figure 6.10 - Fragments of carbonated beach sands from sediment sample 275. See location on Figure 6.5.

Carbonate cemented fragments of sands from sample 275, are also abundant on the shelf and probably represent a Late Glacial Maximum paleo littoral (Figure 6.10). These kinds of grains are present along the same bathymetry, reinforcing the idea of the presence of a paleo littoral.

6.4.1.5 The Early Holocene (10 000 years to 9 000 years)

The beginning of the Holocene period is characterized by a rapid msl variation, almost 40 m in 2 000 years (10 000 years – 8 000 years) on the Portuguese shelf (Dias *et al.*, 2000, Moura *et al.*, 2007, Otto-Bliesner *et al.*, 2017). In transitional environments, boreholes and seismic profiling performed in terminal parts of the river estuaries (close to the present shoreline), revealed thick transgressive sequences accumulated in estuarine environments (Carvalho & Rosa, 1988; Boski *et al.*, 1998) and an accumulation of 20 m series of intertidal clayed sediments between 10 000 years and 7 000 years BP, documented at the Guadiana River estuary. However, in the west Portuguese coast, sporadic oscillations in marine advance were documented by Carvalho & Galopim de Ribeiro (1962) in the Leça river inlet (Northern Portugal).

Previous studies have shown that annual precipitation reached a maximum during this period in the eastern Mediterranean region (Bar-Matthews *et al.*, 1999; Rossignol-Strick, 1999; Kotthoff *et al.*, 2008a, Kotthoff *et al.*, 2008b). According to Dormoy *et al.* (2009) precipitation seasonality increased strongly, with winter precipitation attaining a maximum of 200 to 300 mm, and summer precipitation simultaneously reaching a minimum of 50 to 100 mm.

After a careful analysis of data obtained from the sediment core in Estremadura Spur, it was possible to present the data acquired in the scope of the present work on the Holocene RSL (relative sea level) for the mentioned area (Figure 6.11). The lines drawn on the curve are based on the radiocarbon dating (Table 5.8) and the relative depths deduced from the paleoenvironmental proxies. This Holocene RSL is based on the outer limit of inner, middle and shelves (30 m, 100 m and > 100 m, respectively) according to chapter II (2.2.2.), together with proxies analyzed in chapter V (5.2.2.). The graphic also presents in red dots the model from García-Artola .).

The first stage is characterized by the sediment column between 10090 – 9590 yr cal BP (9290 +/- 40 BP) and 8570 – 8280 yr cal BP (8170 +/- 50 BP).

For this interval, Dias *et al.* (2000) msl was defined between - 30 m and - 50 m, by Leorri *et al.* (2012) at -35 m below present sea level (bpsl), according to García-Artola .) relative sea level (rsl) was above ~22.7 ± 1.3 m at ~10.4 ka in northern Portugal and at ~36.7 ± 1.2 m at ~11.5 ka in Lisbon and Tagus valley.

In Mar da Ericeira the sediments present in the interval described above, can represent a depth range of 30 m, between -115 m and -85 m depth. The shell of *Glycymeris glycimeris,* dated for this purpose, is compatible with the ecological characteristics of this species, that has a broad biogeographic distribution, inhabiting the northeastern Atlantic continental shelf from Cape Verde to Norway in water depths of up to 100 m, even in areas with strong bottom currents (Savina & Pouvreau, 2004). Despite its broad depth distribution, one must consider also, the possibility of this shell being transported from another location.

The sediments in this interval are characteristic of a high energy environment where there are no anoxic conditions (no preservation of organic matter). There is no evidence of sediment exportation during this period and the sediment is characterized by high percentages of $CaCO_3$ which might derive from previous cycle (Younger Dryas) where according to Dias *et al.* (2000) carbonate cemented fragments of sands are also abundant on the shelf and probably represent the remnants of calcretes and beach rocks formed during this dry climatic phase.

According to Rodrigues *et al.* (2009) the most extreme cold episode of this present interglacial was the 8.2 cal ka BP ''event'' detected in North Atlantic marine deep sea sediments by several climate proxy data, which reinforces the absence of sediment in this sector. In this sector there is an accumulation rate of 0.02 cm/y.

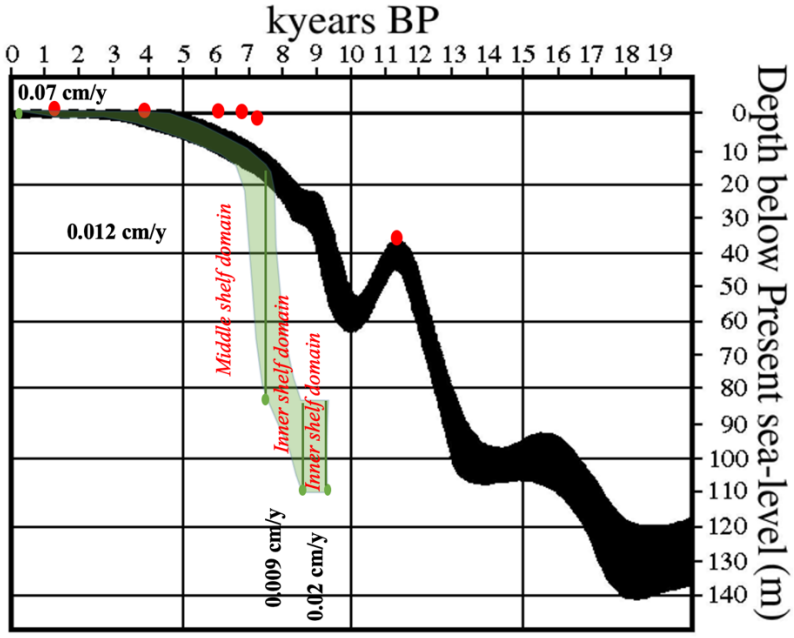

Figure 6.11 – Depth interval (m) for the Holocene RSL (relative sea level), deducted from the studied core (green). Data from García-Artola *et al.* (2018) (red); Sea level rise curve for the N part of Portuguese shelf since the LGM (black). The curve width expresses the quantitative incertitude with respect to sea level and age (Dias, 1987).

In fact, the benthic foraminifera present on the same level of Glycymeris glycimeris showed significant abrasion and signs of re-working, as they may be transported as sand-sized particles (Boltovskoy & Wright, 1976). Another reason to explain the observed differences, were already pointed by Garcia-Artola *et al.* (2018), and are related to the neotectonic activity of this sector of the Portuguese margin, well documented historical seismicity. Despite being very improbable, it cannot be discharged the hypotheses of tectonic movement of this sector which might have had controlled the sediment deposition relocating the *Glycymeris glycimeris* shell.

6.4.1.6. The Middle Holocene (9 000 to 4 000 years)

Between 8570 – 8280 yr cal BP and 7540 – 7280 yr cal BP (7120 +/- 40 BP) there is evidence of environmental changes present in the change of sediment color, sediment grain size, foraminifera species, etc. For this interface, Dias *et al.* (2000) defined the msl between - 20 m and - 10 m, Leorri *et al*. (2012) at -5 m below present sea level (bpsl), according to García-Artola .) relative sea level (rsl) was above ~6.7 ± 0.4 m at ~7.6 ka in northern Portugal and at ~2.4 ± 1.7 m at ~7.5 ka in Lisbon and Tagus valley.

After the rapid environmental changes occurred during the Early Holocene, the msl continued to rise until approximately 4 000 years BP (García-Artola *et al.*, 2018). With a fast sea level rise between 1.8 ± 0.5 to 0.5 ± 0.4 mm/y (García-Artola *et al.*, 2018) the sedimentary system was in constant mutation, readapting to new hydrodynamic conditions; new coastal features like barriers, spits and lagoons developed at the time when the rates of sea level rise were strongly attenuated and subsequently became more dependent on local factors than on the eustatic one (Bao *et al.*, 1999; Dias *et al.*, 2000). In the continental shelf, marine sediments become finer because coarser particle were retained at the coast. The finer particles were transported to the inner and middle shelf, settling when the environmental energy decreased, fossilizing older sequences. Facies change to finer-grained material resulting in a higher food availability as reflected by a change in the benthic foraminiferal distribution and the dominance of the shallow infaunal species (Abu-Zied *et al.*, 2008). The progradation of shelf environments is overprinted by more humid conditions with enhanced late summer/early fall rainfalls during the early of this period (Morellón *et al.*, 2018), with impacts on the increasing fluxes of freshwater, dissolved organic and inorganic matter and nutrients to the coastal marine system. On the seafloor, high organic matter fluxes and the appearance of the suspension feeding gastropod *T. communis* and the infaunal benthic foraminifera are synchronous.

This progradation likely causes apparent changes in productivity and related organic matter fluxes in the foraminiferal faunal record. Potentially independent from this general trend, the 10 300 – 5 500 years BP time interval is characterized by facies with higher contents of the benthic gastropod *T. communis*. This level was observed in other coastal regions from the North Atlantic and also in south Portugal, with ages around 7 400 to 4 100 years BP (Fletcher, 2005; Naughton *et al*., 2007; Milker *et al*., 2012)). According to Baltzer *et al.*, (2015) this layer materializes a global and rapid change in environmental parameters like sediment fluxes and/or sea level variations, depending on climate fluctuations.

6.4.1.7. The Late Holocene (4 000 years to present)

According to Dias *et al.* (2000), Hoffman, 1989, Ramos-Pereira *et al*. 2012 the approach of the present-day sea level by the global postglacial transgression is reflected by a more

diversified pattern of infilling of the estuaries and the sharp rising of planktonic/benthic foraminifera ratio in the estuarine record (Boski *et al.*, 1999). This period was characterized by the beginning of the industrial revolution, thus initiating the deforestation process, mining activity, and increasing human activity, being reflected in sedimentary record with a noticeable increase in heavy metals content, namely mercury, lead and nickel. Also, during this period, the fluvial/continental input gained strength, supported by increased river runoff. According to Dias *et al.* (2000) the sea level changed from ~ 10 below the present msl to approximately the actual msl. According to Leira *et al.* (2018) this slowdown in sediment deposition is ubiquitous along the Iberian south coast and has been attributed to a regional change in climate (drier) around 4000–3000 yr BP. According to Bernárdez *et al.* (2008) between 4700 and 3300 cal yr BP., a warm and dry period characterized by low nutrient levels and productivity at the inner Galician shelf occurred, as also revealed by planktonic foraminifera. As stated, this period might have led to the death of the *Turritella communis Risso*, *1826* as the changes in the surrounding environment might have induced significant alterations in the marine environment. According to Bernárdez *et al.* (2008) the most remarkable event during this period occurs ca. 2000–1700 cal. yr BP. This event is characterized by an increase in Fe, Al, phytoliths abundance and terrigenous percentage. The C/N ratio, however, falls in the range of marine organic matter which could indicate a reduced supply of organic matter of continental provenance. NE winds from land could have transported the ferro alumino-particles and phytoliths to the marine domain, but this climatic scenario would point to relatively dry and arid conditions, an explanation that the paleoenvironmental markers do not support. In fact, Desprat *et al*. (2003) identified a warm period and the development of temperate vegetation during the Roman colonization in Galicia (Roman Warm Period, peaking at 1800 cal. yr BP), suggesting relatively humid conditions.

6.5. Synthesis

The Estremadura Spur continental shelf has revealed itself as a very complex and diverse system, either in terms of textural, compositional and geochemical characteristics, or in sedimentary dynamic processes, mainly controlled by sea-level changes. The reconstruction of the evolution of the Estremadura Spur, during the recent Quaternary, was performed by the integration of morphological and sedimentological characteristics. As an important input to this model and to explain the origin of the three sedimentary sequences, additional radiocarbon analyses of benthic organisms were used as reference, as well as the sea level curve from Dias (1987) and several available papers on paleo reconstructions on the Portuguese margin.

During the Last Glacial Maximum, the coastline was at ~ 130 m depth and the actual rivers were active valleys exporting sediment into the shelf break. During this period, the rocky outcrops at Ponta da Lamparoeira parallel formed a coastal morphological barrier between the northern and southern area of Estremadura Spur. The sedimentation over the shelf was very scarce

at this time due to the cold and arid conditions. In the beginning of the deglaciation (warm climate), the coastline started to migrate landward and coastal areas were invaded by the sea till 110/100 m depth and sediment export increased but quite slowly. At the end of the deglaciation the sea level rose very rapidly settling at ~ 50/40 m depth. This sudden sea level rise in such a short time period induced such an imbalance that estuaries became sediment traps and few sediments were able to reach the continental shelf which led to a scarcity of sediments and the coastline maintained its rocky characteristics. During the Younger Dryas the sea surface temperature dropped below 10 ºC lowering the msl to ~ 60 m depth. This new cycle induces the remobilization of coastal and estuarine particles deposited in the previous phase. In the Holocene, the settlement of a warmer period rose the msl in distinct pulses being represented by Early, Middle and Late Holocene. In the Early Holocene the sea level rose almost 40 m in 2000 years, which revealed thick transgressive sequences, due to the high levels of precipitation. At this time, the conditions were similar to those of an inner shelf like environment with high energy conditions. In the Middle Holocene the rapid environmental conditions continued as well as msl continued its way up till ~ 10 m below present sea level. This period was registered in the sediment core as an 80 cm thick layer, which indicates a drastic decrease in the environmental conditions with an increase of the living conditions represented by the species diversity. In the Late Holocene the msl settled at the present level. With the increasing human activity, represented by the heavy metal content, deforestation and mining processes increased, a high fluvial/continental input was expected with higher species diversity due to increased availability of nutrients and fine particles. Although the sediment input might have increased, the accumulation rate is still very low when compared to other sectors of the Portuguese continental margin.

Chapter VII – Final considerations and future work

Bordering the mainland, the continental shelf is a peculiar environment where climatic and environmental changes, at a wide range of time scales from years to millennia, are imprinted in the sedimentary record.

The Estremadura Spur continental shelf was selected because it is the sector where the usual depth of the shelf break (~ 300 m) enables marine sedimentation to persist even during the Last Glacial Maximum when sea level was about 120 m below present level. Moreover, its peculiar morphological setting, bordered by two natural barriers (the Canhão da Nazaré and the steep slope carved by valleys), allowed it to remain isolated from processes acting in the northern and southern systems.

The Estremadura Spur continental shelf is quite wide (~ 70 km), when compared to the width of other continental shelf sectors in Iberia, ranging less than 5 km (in front of the Espichel Cape) to over 70 km (at the 39º N parallel, more or less offshore Ponta da Lamparoeira). The depth of the shelf break is also highly variable, located between 120 m depth (e.g. near the Raso cape) and over 300 m (at parallel 39º N). Comparing these values with those determined for the whole continental shelves of the world (Shepard, 1973), it is clear that this sector of the Portuguese continental shelf is relatively narrow (the world average width is 75 km), although its edge being located at higher depths (the world average shelf break depth is about 130 m).

Due to the well-defined morphological boundaries of the Estremadura Spur, the source of coarser sedimentary particles (transported as bedload) is constrained to local sources or rivers that drain directly to this shelf sector whereas the source of fine-grained particles (transported as suspended load) can be related to more distal sources, including the Tagus river or the northern continental shelf. The sedimentary cover of the Estremadura Spur is composed either by particles that have undergone through several sediment cycles (relict particles) or by modern particles that are being added to the existing deposits. Estremadura Spur is fully exposed to the Atlantic influence, responsible for the distribution processes (transport pathways and deposition) that characterize the sedimentary cover.

The inner shelf domain (from the coast to a depth of ~ 30 m) is dominated by waves which control the present-day sedimentary processes. Due to the higher energy levels in this domain, the bottom sedimentary cover is mostly sandy with very low content in mud. In the middle shelf domain (extending to a depth of ~ 100 m) wave energy is strongly reduced and the effect of currents increase. In this domain, the importance of surface waves is particularly important during storms, where they can resuspend a wide range of particles. Concerning the sedimentary characteristics, the middle shelf of the Estremadura Spur can be divided in two sectors: a northern one, dominated by very coarse biogenic deposits in the vicinity of extensive rocky outcrops and the southern one, dominated by finer deposits (sandy mud to muddy sand).

The outer shelf domain is very wide, extending to depths deeper than 300 m depth and is covered by sandy and muddy sandy deposits, reflecting the effect of currents (including tide related) and internal waves. In the northern section of the Estremadura Spur, a huge elongated sandy deposit characterizes the outer shelf.

The sedimentary cover composition of the Estremadura Spur continental shelf deposits reflects the interplay of two major particles sources: a marine local source (contributing with biogenic remains and terrigenous particles eroded from the extensive outcrops) and the continental sources (detritical particles discharged from nearby rivers or originated by cliff erosional processes).

The present-day river input to the continental shelf is almost nonexistent and it is restricted to the inner shelf, close to the river mouths. In fact, the sediment composition indicates that there is no relation between minerals present in the fine fraction of riverine sediments and those from the shelf sediments. Rivers supply a wide range of grain sizes to the coast and shelf (from gravel to mud), the coarser fractions (medium sand or larger) are retained at the beach. Medium and fine sands are supplied and retained at the inner shelf and the finer fractions are exported to the middle and outer shelf. This process revealed to be responsible for the terrigenous mud deposits that accumulate in the middle continental shelf probably by cross-shelf transport in relation to dense suspensions.

Nearshore longshore drift was confirmed from the distribution pattern of some minerals such as the potassium feldspar and plagioclase, which are also controlled by the proximity to the source. Heavy mineral assemblage put in evidence two distinct coastal sedimentary cells. The beach sediments have a similar heavy mineral content when compared to inner shelf sediments, but the influence of the river/continental input is higher at the beaches, demonstrated by high percentages of tourmaline and andaluzite in the north, and pyroxenes in the south.

The superficial sedimentary characteristics of shelf deposits reflect the present-day sedimentary dynamic processes (particle input, transport and settling) and allow us to understand the marine environment. However, as these characteristics only apply to the uppermost layer of the sedimentary cover, they are not representative of former conditions, especially those related with different past climate periods, reflected by distinct meteo-oceanographic forcing and msl position. In order to understand the past marine environment, a 162 cm long vertical sample, collected at the Mar da Ericeira has revealed itself a very complete sedimentary record of the continental shelf evolution since the beginning of the Holocene.

Through the analysis of 14 proxies, it was possible to differentiate three sedimentary sequences, correspondent to three different environmental conditions:

a) the *base sequence* was interpreted to be representative of a high energy coastal deposit, probably near to a terrigenous particle source. It is formed by coarse-grained

particles (rich in heavy minerals) with high carbonate content (with robust foraminifera) and low content of organic matter;

b) the *intermediate sequence* presents a decrease in coarse particles and an increase in fine particles and biogenic contribution, indicating a marine environment (middle/outer shelf);

c) the *superficial sequence* (20 cm thick) where the texture and composition of sediments are compatible with a (middle) shelf environment. Also, the sudden arising of heavy metals like mercury (Hg) and lead (Pb) evidence the impact of anthropogenic activity in the marine system.

Considering the vertical variation on the main sediment depocentre of Estremadura Spur, a conceptual model for the evolution of Estremadura Spur is proposed as follows:

1) during the Last Glacial Maximum (20 000 to 18 000 years BP), the msl was at ~ 120 m depth and most of Estremadura Spur was an extension of the continent, with two main drainage systems, separated by the morphological barrier of rocky outcrops at the Ponta da Lamparoeira parallel; the climatic conditions were not favorable to chemical weathering process.

2) the establishment of warmer conditions allows the beginning of the deglaciation (between 16 000 and 11 000 years BP), the coastline started to migrate eastward and coastal areas were invaded by the sea till ~ 50 m depth.

3) At the end of this phase, the sea level settled at ~ 50/40 m depth. This sudden sea level rise in such a short time period induced such an imbalance that estuaries became sediment traps and few sediments were able to reach the continental shelf leading to a scarcity of littoral sediments; the coastline maintained its rocky characteristics.

4) A new cold period affected the Estremadura Spur, between 11 000 and 10 000 years ago (the Younger Dryas), during which the sea surface temperature dropped below 10ºC and the msl fell to ~ 60 m depth. Consequently, the estuarine and coastal deposits were remobilized and dispersed into the continental shelf.

5) The last phase, which occurred until de stabilization of the msl, can be described by the Early, Middle and Late Holocene. In the Early Holocene the sea level rose almost 40 m in 2 000 years, which is consistent with the thick transgressive sequences, formed by the input of the terrigenous coarse particles. In the Ericeira shelf, the oldest sequence of the vertical sample, was probably deposited during this period, in a coastal and inner shelf environment. The intermediate sequence (Middle Holocene unit, between 9 000 and 4 000 years BP) shows a drastic decrease in bottom energy with an increase in conditions for preservation of the sedimentary record represented by the species diversity. In the Late Holocene (4 000 years to present), a high fluvial/continental input was estimated, dominated by fine particles (silt and clay totals about 80 % of the total sediment) and with higher species diversity. These characteristics indicate a middle/outer shelf environment, where there is a relatively high availability of silt and clay and

absence of coarser particles. The impact of human activity was also recognized in this superficial sequence. It is assumed that as Romans established in the Iberian Peninsula, they induced increasing deforestation and mining activity. The observed variation of sedimentological characteristics in the utmost 20 cm are attributed to common oceanographic oscillations after the stabilization of the msl.

7.1. Future Work

Like all theses this is an incomplete work, with several unanswered questions.

Examples are the understanding of present-day sedimentary dynamics, where a quantitative approach has yet to be made. This must be supported in systematic oceanographic monitoring (waves and currents) and the in-situ measurement of sediment transport. These observations should support a numerical modelling approach capable not only to explain the present sedimentary dynamics across the continental shelf but also give valuable insights on the past and be able to understand future patterns of change. But the challenges to accomplish this target are huge, as for example, the "apparent" simple effort to put a current meter in the outer shelf was unsuccessful, as the current meter was dragged probably by fishermen and was never recovered, and all data was lost. Further work needs to be done concerning the sedimentary dynamics. More current meter data is needed to validate model simulations not only in the northern outer continental shelf but also in areas like Mar da Ericeira, to understand if the mud deposit is either accumulating or eroding.

Another challenging topic is the study of the outer shelf deposits. This continental shelf sector is abnormally deep, so it probably preserves the sediment deposited at the Last Glacial Maximum and earlier times. The possibility to make a sedimentary core in this region can be the key to understanding the continent's climatic conditions during and before the LGM.

Although there is a very good area covered by seismic profiles, acquired in this area, these profiles are of high intensity and low frequency, providing a very good penetration in the sediment of several hundreds of meters. For future acquisitions high-resolution seismic profiles of the first 100 m is essential for the understanding of the sedimentary and hydrodynamic processes.

Also, more investigation and dating are needed to detail some variations along the vertical sample, such as the observed concentration of the *T. communis*, in order to better establish the temporal interval of the 8.2 ky event.

List of References

Abrantes, F., Winn, K., & Sarnthein, M. (1994). Late Quaternary Paleoproductivity Variations in the NE and Equatorial Atlantic: Diatom and Corg Evidence. Carbon Cycling in the Glacial Ocean: Constraints on the Ocean's Role in Global Change, 425–441. https://doi.org/10.1007/978-3-642-78737-9_19

Abrantes, I. (2005). Os sedimentos superficiais da margem continental, sector Espinho-Cabo Mondego: a utilização das fracções finas como traçadores de dinâmica sedimentar actual (PhD Thesis unpublished). Universidade de Aveiro, 239p.

Abu-Zied, R. H., Rohling, E. J., Jorissen, F. J., Fontanier, C., Casford, J. S. L., & Cooke, S. (2008). Benthic foraminiferal response to changes in bottom-water oxygenation and organic carbon flux in the eastern Mediterranean during LGM to Recent times. Marine Micropaleontology, 67, 46–68. https://doi.org/10.1016/j.marmicro.2007.08.006

Allen, R., Siegert, M. J., & Payne, A. J. (2008). Reconstructing glacier-based climates of LGM Europe and Russia – Part 2: A dataset of LGM precipitation/temperature relations derived from degree-day modelling of palaeo glaciers. Climate of the Past, 4, 249–263. https://doi.org/10.5194/cp-4-249-2008

Andrade, C., Taborda, R., Oliveira, M. A., Alves, M., Carapuço, A. M. (2013). Caracterização do clima de agitação ao largo. Estudo do litoral na área de intervenção da APA I.P./ARH do Tejo, 14p.

Arzola, R. G., Wynn, R. B., Lastras, G., Masson, D. G., & Weaver, P. P. E. (2008). Sedimentary features and processes in the Nazaré and Setúbal submarine canyons, West Iberian margin. Marine Geology, 250, 64–88. https://doi.org/10.1016/j.margeo.2007.12.006

Austin, J. A., & Lentz, S. J. (2002). The inner Shelf response to wind-driven upwelling and downwelling. Journal of Physical Oceanography, 32, 2171–2193. https://doi.org/10.1175/1520-0485(2002)032<2171:tisrtw>2.0.co;2

Badagola, A. (2008). Evolução morfo-tectónica da plataforma continental do Esporão da Estremadura (MSc Thesis unpublished). Universidade de Lisboa.

Balsinha, M. (2008). Estudo da dinâmica sedimentar da plataforma continental portuguesa entre o Canhão Submarino da Nazaré e a Ericeira (MSc Thesis unpublished). Universidade de Lisboa.

Balsinha, M., Rodrigues, A., Oliveira, A., Fernandes, C., Taborda, R. (2010). Nova descrição do bordo da plataforma continental portuguesa, 1as Jornadas de Engenharia Hidrográfica, Lisboa, 21-22 de junho.

Balsinha, M., Fernandes, C., Oliveira, A., Rodrigues, A., & Taborda, R. (2014). Sediment transport patterns on the ESTREMADURA spur continental Shelf: Insights FROM grain-size trend analysis. Journal of Sea Research, 93, 28–32. https://doi.org/10.1016/j.seares.2014.04.001

Baltzer, A., Mokeddem, Z., Goubert, E., Lartaud, F., Labourdette, N., Fournier, J., & Bourillet, J.-F. (2014). The "TURRITELLA Layer": A POTENTIAL proxy of a DRASTIC Holocene environmental change on the NORTH–EAST Atlantic Coast. Coastal Research Library, 3–21. https://doi.org/10.1007/978-94-017-9260-8_1

Bao, R., da Conceição Freitas, M., & Andrade, C. (1999). Separating eustatic from local environmental effects: A late-Holocene record of coastal change in Albufeira Lagoon, Portugal. The Holocene, 9, 341–352. https://doi.org/10.1191/095968399675815073

Bar-Matthews, M., Ayalon, A., Kaufman, A., & Wasserburg, G. J. (1999). The eastern Mediterranean paleoclimate as a reflection of REGIONAL Events: Soreq CAVE, ISRAEL. Earth and Planetary Science Letters, 166, 85–95. https://doi.org/10.1016/s0012-821x(98)00275-1

Barbieri, M. (2016). The importance of enrichment FACTOR (EF) and Geoaccumulation INDEX (Igeo) to evaluate the soil contamination. Journal of Geology & Geophysics, 5. https://doi.org/10.4172/2381-8719.1000237

Bartol, M., Pavšič, J., Dobnikar, M., & Bernasconi, S. M. (2008). Unusual braarudosphaera bigelowii and micrantholithus vesper enrichment in the Early miocene sediments from the Slovenian Corridor, a Seaway linking the CENTRAL PARATETHYS and the Mediterranean. Palaeogeography, Palaeoclimatology, Palaeoecology, 267, 77–88. https://doi.org/10.1016/j.palaeo.2008.06.005

Basta, N. T., Ryan, J. A., & Chaney, R. L. (2005). Trace element chemistry in residual-treated Soil: Key concepts and METAL BIOAVAILABILITY. Journal of Environmental Quality, 34, 49–63. https://doi.org/10.2134/jeq2005.0049dup

Bernárdez, P., González-Álvarez, R., Francés, G., Prego, R., Bárcena, M. A., & Romero, O. E. (2008). Late Holocene history of the rainfall in the Nw Iberian PENINSULA—EVIDENCE from a marine record. Journal of Marine Systems, 72, 366–382. https://doi.org/10.1016/j.jmarsys.2007.03.009

Berthou, P.Y. (1973). Le Cénomanien de l'Estrémadure portugaise. Memórias dos Serviços Geológicos, Portugal, 23, 1-168.

Blaauw, M. (2010). Methods and code for 'classical' age-modelling of radiocarbon sequences. Quaternary Geochronology, 5, 512–518. https://doi.org/10.1016/j.quageo.2010.01.002

Blaauw, M., & Christen, J. A. (2011). Flexible paleoclimate age-depth models using an autoregressive gamma process. Bayesian Analysis, 6, 457–474. https://doi.org/10.1214/ba/1339616472

Boillot, G., Dupeuble, P.-A., Hennequin-Marchand, I., Lamboy, M., & Lepretre, J.-P. (1973). Carte geologique de plateau continental nord-espagnol entre le canyon de capbreton et le canyon d'aviles. Bulletin De La Société Géologique De France, S7, 367–391. https://doi.org/10.2113/gssgfbull.s7-xv.3-4.367

Boillot, G., Mougenot, D., Enard, G., Baldy, P., Moita, I., Monteiro, J.H. & Musellec, P. (1978). Carta Geológica da plataforma continental. Escala 1:1 000 000. Instituto Hidrográfico, Serviço de Fomento Mineiro, Serviços Geológicos de Portugal, Centre National pour l'Exploration des Oceans, Université Rennes e Université Pierre et Marie Curie, Paris.

Boltovskoy, E., & Wright, R. (1976). Planktonic foraminifera. Recent Foraminifera, 159–195. https://doi.org/10.1007/978-94-017-2860-7_7

Booij, N., Holthuijsen, L. H., & Ris, R. C. (1997). The "swan" wave model for shallow water. Coastal Engineering 1996. https://doi.org/10.1061/9780784402429.053

Boski, T., Moura, D., Duarte, R. D. N., Dias, J. M. A. (1998). Changes in the pattern of sedimentary infill of Guadiana river estuary since the Last glacial Maximum. Proc. of

UNESCO-IUGS IGCP-367, INQUA Shorlines Com. & INQUA Neot. Com., Corinth, Greece, 7p.

Boski, T., Moura, D. M, Machado, L. M, Bebianno, J. M. (1999). Trace metals on the Algarve coast, I: Associations, origins and remobilization of natural components. Boletim Instituto Espanhol Oceanografia. 15, 457-463.

Brito, A. (2007). Caracterização sedimentar da plataforma interna do sotavento algarvio (MCs Thesis unpublished). Universidade do Algarve.

Brooks, G. R., Doyle, L. J., Davis, R. A., DeWitt, N. T., & Suthard, B. C. (2003). Patterns and controls of Surface sediment distribution: West-central Florida INNER SHELF. Marine Geology, 200, 307–324. https://doi.org/10.1016/s0025-3227(03)00189-0

Burdloff, D., Araújo, M. F., Jouanneau, J.-M., Mendes, I., Monge Soares, A. M., & Dias, J. M. A. (2008). Sources of organic carbon in the Portuguese continental shelf sediments during the Holocene period. Applied Geochemistry, 23, 2857–2870. https://doi.org/10.1016/j.apgeochem.2008.04.018

Carvalho, A. M. & Galopim de Ribeiro, A. (1962). Geologia dos depósitos pós-wurmianos da Foz do Leça. Lisboa. Boletim do Museu e Laboratório Mineralógico e Geológico da Faculdade de Ciências da Universidade de Lisboa, 9, 53-74.

Carvalho, A. F. & Rosa, M. M. P. (1988). Localizacão do Paleovale do Rio Douro. Anais Instituto Hidrográfico, 9, 77-82.

Cascalho, J. (2000). Mineralogia dos sedimentos arenosos da margem continental setentrional portuguesa (PhD Thesis unpublished). Universidade de Lisboa, Portugal.

Cheng, P., Gao, S., & Bokuniewicz, H. (2004). Net sediment TRANSPORT patterns over the Bohai Strait based on grain size trend analysis. Estuarine, Coastal and Shelf Science, 60, 203–212. https://doi.org/10.1016/j.ecss.2003.12.009

Chiocci, F. L., & Chivas, A. R. (2014). Chapter 1 an overview of the continental shelves of the world. Geological Society, London, Memoirs, 41, 1–5. https://doi.org/10.1144/m41.

Coachman, L. K., & Walsh, J. J. (1981). A diffusion model of cross-shelf exchange of nutrients in the SOUTHEASTERN Bering Sea. Deep Sea Research Part A. Oceanographic Research Papers, 28, 819–846. https://doi.org/10.1016/s0198-0149(81)80003-9

Coelho, H. S., Neves, R. J. J., White, M., Leitão, P. C., & Santos, A. J. (2002). A model for ocean circulation on the Iberian coast. Journal of Marine Systems, 32, 153–179. https://doi.org/10.1016/s0924-7963(02)00032-5

Costa, P. J. M., Andrade, C., Freitas, M. C., Oliveira, M. A., Lopes, V., Dawson, A. G., … Jouanneau, J.-M. (2012). A tsunami record in the sedimentary archive of the CENTRAL Algarve Coast, Portugal: Characterizing SEDIMENT, Reconstructing sources and INUNDATION PATHS. The Holocene, 22, 899–914. https://doi.org/10.1177/0959683611434227

Costa, M. & Esteves, R. 2009. Clima de Agitação Marítima na Costa Oeste de Portugal Continental. Instituto Hidrográfico, Marinha Portuguesa, Lisboa.

Curtis, C. (1977). Geochemistry: Sedimentary geochemistry: environments and processes dominated by involvement of an aqueous phase. Philosophical Transactions of the Royal Society of London. Series A, Mathematical and Physical Sciences, 286, 353–372. https://doi.org/10.1098/rsta.1977.0123

Daveau, M. J. (1980). Cypéracées du Portugal. Boletim Sociedade Broteriana. 9, 58-128.

Debenay, J.-P., Bénéteau, E., Zhang, J., Stouff, V., Geslin, E., Redois, F., & Fernandez-Gonzalez, M. (1998). Ammonia BECCARII and Ammonia tepida (foraminifera): Morphofunctional arguments for their distinction. Marine Micropaleontology, 34, 235–244. https://doi.org/10.1016/s0377-8398(98)00010-3

Desprat, S., Sánchez-Goñi, M.F., Loutre, MF. (2003). Revealing climatic variability of the last three millennia in northwestern Iberia using pollen influx data. Earth Planetary Science Letters, 213, 63–78. doi:10.1016/S0012-821X(03)00292-9.

Dias, J. A., Gaspar, L. C. & Monteiro, J. H. (1981). Sedimentos recentes da plataforma continental portuguesa a Norte do Canhão Submarino da Nazaré. Boletim da Sociedade Geológica de Portugal, 22, 181-195, Lisboa, Portugal.

Dias, JMA. (1983/85). Erosão versus Deposição na Plataforma Continental Portuguesa a Norte do Canhão da Nazaré. Boletim da Sociedade Geológica de Portugal, XXIV, 31-36, Lisboa, Portugal. ISSN: 0366-2101.

Dias, J. M. A. & Nittrouer, C. A. (1984). Continental shelf sediments of northern Portugal. Continental Shelf Research, 3, 147 – 165.

Dias, JMA. (1987). Dinâmica sedimentar e evolução recente da plataforma continental portuguesa setentrional (PhD Thesis unpublished), Universidade de Lisboa, 500p.

Dias, J. M. A., Boski, T., Rodrigues, A., & Magalhães, F. (2000). Coast line evolution in Portugal since the last Glacial maximum until present — a synthesis. Marine Geology, 170, 177–186. https://doi.org/10.1016/s0025-3227(00)00073-6

Dill, H. (1998). A review of heavy minerals in clastic sediments with case studies from the alluvial-fan through the nearshore-marine environments. Earth-Science Reviews, 45, 103–132. https://doi.org/10.1016/s0012-8252(98)00030-0

Dinis, J. L., Henriques, V., Freitas, M. C., Andrade, C., & Costa, P. (2006). Natural to anthropogenic forcing in the Holocene evolution of three coastal Lagoons (Caldas da Rainha Valley, western Portugal). Quaternary International, 150, 41–51. https://doi.org/10.1016/j.quaint.2006.01.025

Dodet, G., Bertin, X., & Taborda, R. (2010). Wave climate variability in the north-east Atlantic Ocean over the last six decades. Ocean Modelling, 31, 120–131. https://doi.org/10.1016/j.ocemod.2009.10.010

Dormoy, I., Peyron, O., Combourieu Nebout, N., Goring, S., Kotthoff, U., Magny, M., & Pross, J. (2009). Terrestrial climate variability and Seasonality changes in the Mediterranean region between 15 000 and 4 000 years BP deduced from marine pollen records. Climate of the Past, 5, 615–632. https://doi.org/10.5194/cp-5-615-2009

Drago, T. 1995. La vasière Ouest-Douro sur la plate-forme continentale nord-portugaise. Rôle, fonctionnement, évolution (Ph.D. Thesis unpublished). Université Bordeaux I, France, 295 pp.

Drago, T., Freitas, M.C., Rocha, F., Cachão, M., Moreno, J., Naughton, F., Fradique, C., Silveira, T., Oliveira, A., Cascalho, J., Fatela, F. (2006). Paleoenvironmental evolution of estuarine systems during the last 14 000 years - the case of Douro estuary (NW Portugal). Journal of Coastal Research, SI, 186-192. ISSN 0749-0208. eISSN. https://www.jstor.org/stable/25741559?seq=1#page_scan_tab_contents

Duarte, D., Magalhães, V. H., Terrinha, P., Ribeiro, C., Madureira, P., Pinheiro, L. M., … Duarte, H. (2017). Identification and characterization of Fluid escape Structures (POCKMARKS) in the Estremadura Spur, WEST IBERIAN MARGIN. Marine and Petroleum Geology, 82, 414–423. https://doi.org/10.1016/j.marpetgeo.2017.02.026

Dubois, N., Saulnier-Talbot, É., Mills, K., Gell, P., Battarbee, R., Bennion, H., Valero-Garcés, B. (2017). First human impacts and responses of Aquatic systems: A review of palaeolimnological records from around the world. The Anthropocene Review, 5, 28–68. https://doi.org/10.1177/2053019617740365

Duplessy, J.-C. (1982). North Atlantic Deep Water circulation during the last-climatic cycle, Bull. Inst. Geol. Bassin d'Aquitaine, Bordeaux, 31, 379–391.

Farida, M., Imai, R., & Sato, T. (2012). Miocene to PLIOCENE Paleoceanography of the Western Equatorial Pacific Ocean based on Calcareous Nannofossils, ODP Hole 805B. Open Journal of Geology, 02, 72–79. https://doi.org/10.4236/ojg.2012.22008

Felix, M., & McCaffrey, W. (2005). Sedimentary processes | Particle-Driven Subaqueous Gravity Processes. Encyclopedia of Geology, 1–7. https://doi.org/10.1016/b0-12-369396-9/00484-6

Fiúza, A. F. G., Macedo, M. E. and Guerreiro, M. R. (1982). Climatological space and time variation of the Portuguese coastal upwelling, Oceanologica Acta 5, 31–40.

Fiúza, A. F. (1983). Upwelling patterns off Portugal. Coastal Upwelling Its Sediment Record, 85–98. https://doi.org/10.1007/978-1-4615-6651-9_5

Fiúza, A. F. G., Hamann, M., Ambar, I., Díaz del Río Guillermo, González, N., & Cabanas, J. M. (1998). Water masses and their circulation off western Iberia during May 1993. Deep Sea Research Part I: Oceanographic Research Papers, 45, 1127–1160. https://doi.org/10.1016/s0967-0637(98)00008-9

Flemming, BW & Thum, AB. (1978). The settling tube - a hydraulic method for grain size analysis of sand. Kiel. Meeresforsch, Sonderh., 4, 82–95.

Flemming, B.W. (2004). Factors affecting the shape of particle frequency distributions and associated textural parameters. In: Flemming, B.W., Hartmann, D., Delafontaine, M.T. (Eds.), From E. Poizot et al. / Earth-Science Reviews 86 (2008) 15–41 37 Particle Size to Sediment Dynamics. International HWK-Senckenberg Workshop, 15–18 April 2004, Delmenhorst, Germany. Extended Abstracts, pp. 53–58.

Flemming, B. W. (2007). The influence of grain-size analysis methods and sediment mixing on curve shapes and textural parameters: Implications for sediment trend analysis. Sedimentary Geology, 202, 425–435. https://doi.org/10.1016/j.sedgeo.2007.03.018

Freitas, M. C. (1989). Lagoa de Óbidos: Morfo-sedimentogénese aplicada (MSc unpublished). Universidade de Lisboa, 239p.

Freitas, M. C., Andrade, C., Rocha, F., Tassinari, C., Munhá, J. M., Cruces, A., … Carlos Marques da Silva. (2003). Lateglacial and Holocene environmental changes in Portuguese coastal lagoons 1: THE sedimentological and Geochemical records of the Santo André coastal area. The Holocene, 13, 433–446. https://doi.org/10.1191/0959683603hl636rp

Frouin, R., Fiúza, A. F., Ambar, I., & Boyd, T. J. (1990). Observations of a POLEWARD Surface current off the coasts of Portugal and Spain during winter. Journal of Geophysical Research, 95, 679. https://doi.org/10.1029/jc095ic01p00679

Galopim de Carvalho, A. M. (1968). Depósitos Terciários situados na margem direita da bacia do Tejo. Contribuição para o conhecimento Geológico da Bacia Terciária do Tejo, Boletim da Sociedade Geológica de Portugal, 15, 190-211.

Gao, S., Collins, M., McLaren, P., & Bowles, D. (1991). A critique of the "McLaren Method" for defining sediment transport paths; discussion and reply. Journal of Sedimentary Research, 61, 143–147. https://doi.org/10.1306/d42676a9-2b26-11d7-8648000102c1865d

Gao, S., & Collins, M. (1992). Net sediment transport patterns inferred from grain-size trends, based upon definition of “transport vectors.” Sedimentary Geology, 81, 47–60. https://doi.org/10.1016/0037-0738(92)90055-v

Gao, S., & Collins, M. (1994). Analysis of grain-size trend for defining sediment transport pathways in marine environments. Journal of Coastal Research, 10, 70-78.

Gao, S. (1996). A FORTRAN program for grain-size trend analysis to define net sediment transport pathways. Computers & Geosciences, 22, 449–452. https://doi.org/10.1016/0098-3004(95)00100-x

Garcia, C. (1997). Dispersão e deposição da matéria particulada transportada em suspensão para a plataforma continental adjacente aos rios Tejo e Sado (MSc Thesis unpublished). Universidade de Lisboa, 186p.

Garcia-Artola, A., Stéphan, P., Cearreta, A., Kopp, R. E., Khan, N. S., & Horton, B. P. (2018). Holocene sea-level database from the Atlantic coast of Europe. Quaternary Science Reviews, 196, 177–192. https://doi.org/10.1016/j.quascirev.2018.07.031

Gieskes, J. (1981). Deep-Sea Drilling Interstitial Water Studies: Implications For Chemical Alteration Of The Oceanic Crust, Layers I And II. The Deep Sea Drilling Project: A Decade of Progress, 149–167. https://doi.org/10.2110/pec.81.32.0149

Giraudeau, J., & Beaufort, L. (2007). Coccolithophores: from extant populations to fossil assemblages, Proxies in Late Cenozoic paleoceanography–Developments in Marine Geology, edited by: Hillaire-Marcel, C. and De Vernal, A., Elsevier, 409-439, 2007.

Harris, C. K. (2002). Across-shelf sediment transport: Interactions between suspended sediment and bed sediment. Journal of Geophysical Research, 107(C1). https://doi.org/10.1029/2000jc000634

Hanson, H., & Camenen, B. (2007). Closed Form Solution for Threshold Velocity for Initiation of Sediment Motion under Waves. Coastal Sediments '07. https://doi.org/10.1061/40926(239)2

Haynes, R., & Barton, E. D. (1990). A poleward flow along the Atlantic coast of the Iberian Peninsula. Journal of Geophysical Research, 95, 11425. https://doi.org/10.1029/jc095ic07p11425

Hill, P. S., Fox, J. M., Crockett, J. S., Curran, K. J., Friedrichs, C. T., Geyer, W. R., Wheatcroft, R. A. (2007). Sediment Delivery to the Seabed on Continental Margins. Continental Margin Sedimentation, 49–99. https://doi.org/10.1002/9781444304398.ch2

Hoffman, G. 1989. Estratigrafia holocénica da linha de costa nos vales dos rios Sizandro (Portugal) e Guadiana (Portugal e Espanha). Geolis, 3, 137-143.

Horowitz, A. J. (1984). A primer on trace metal-sediment chemistry. Open-File Report. https://doi.org/10.3133/ofr84709

Jesus, C. C., de Stigter, H. C., Richter, T. O., Boer, W., Mil-Homens, M., Oliveira, A., & Rocha, F. (2010). Trace metal enrichments in Portuguese submarine canyons and open slope: Anthropogenic impact and links to sedimentary dynamics. Marine Geology, 271, 72–83. https://doi.org/10.1016/j.margeo.2010.01.011

Jonsson, I. G. (1967). Wave Boundary Layers and Friction Factors. Coastal Engineering 1966. https://doi.org/10.1061/9780872620087.010

Jouanneau, J. M., Garcia, C., Oliveira, A., Rodrigues, A., Dias, J. A., & Weber, O. (1998). Dispersal and deposition of suspended sediment on the shelf off the Tagus and Sado estuaries, S.W. Portugal. Progress in Oceanography, 42, 233–257. https://doi.org/10.1016/s0079-6611(98)00036-6

Jouanneau, J. M., Weber, O., Drago, T., Rodrigues, A., Oliveira, A., Dias, J. M. A., Reyss, J. L. (2002). Recent sedimentation and sedimentary budgets on the western Iberian shelf. Progress in Oceanography, 52, 261–275. https://doi.org/10.1016/s0079-6611(02)00010-1

Kemp, A. W., & Manly, B. F. (1997). Randomization, Bootstrap and Monte Carlo Methods in Biology. Biometrics, 53, 1560. https://doi.org/10.2307/2533527

Koller, M., & Saleh, H. M. (2018). Introductory Chapter: An Introduction to Trace Elements. Trace Elements - Human Health and Environment. https://doi.org/10.5772/intechopen.75010

Komar, P. D. (2007). Chapter 1 The Entrainment, Transport and Sorting of Heavy Minerals by Waves and Currents. Developments in Sedimentology, 3–48. https://doi.org/10.1016/s0070-4571(07)58001-5

Kotthoff, U., Müller, U. C., Pross, J., Schmiedl, G., Lawson, I. T., van de Schootbrugge, B., & Schulz, H. (2008). Lateglacial and Holocene vegetation dynamics in the Aegean region: an integrated view based on pollen data from marine and terrestrial archives. The Holocene, 18, 1019–1032. https://doi.org/10.1177/0959683608095573

Kotthoff, U., Pross, J., Müller, U. C., Peyron, O., Schmiedl, G., Schulz, H., & Bordon, A. (2008). Climate dynamics in the borderlands of the Aegean Sea during formation of sapropel S1 deduced from a marine pollen record. Quaternary Science Reviews, 27, 832–845. https://doi.org/10.1016/j.quascirev.2007.12.001

Kullberg, J. C., Rocha, R. B., Soares, A. F., Rey, J., Terrinha, P., Azerêdo, A. C., Callapez, P., Duarte, L. V., Kullberg, M. C., Martins, L., Miranda, J. R., Alves, C., Mata, J., Madeira, J., Mateus, O., Moreira, M. & Nogueira C. R. (2013). A Bacia Lusitaniana: Estratigrafia, Paleogeografia e Tectónica. (Dias, R., Araújo, A., Terrinha, P. & Kullberg, J. C., Ed.). Geologia de Portugal no contexto da Ibéria, Volume II, 195-350, Lisboa, Escolar Editora

Kuo, S., Heilman, P. E., & Baker, A. S. (1983). Distribution and forms of copper, zinc, cadmium, iron, and manganese in soils near a copper smelter1. Soil science, 135, 101–109. https://doi.org/10.1097/00010694-198302000-00004

Lanckneus, J., De Moor, G., Van Lancker, V., De Schaepmeester, G. (1993). The use of the McLaren model for the determination of residual transport directions on the Gootebank, southern North Sea: Progress in Belgian Oceanographic Research. Institute of Marine Research and Air Sea Interaction (IRMA), 1, 75-94.

Lantzsch, H., Hanebuth, T. J. J., & Bender, V. B. (2009). Holocene evolution of mud depocentres on a high-energy, low-accumulation shelf (NW Iberia). Quaternary Research, 72, 325–336. https://doi.org/10.1016/j.yqres.2009.07.009

Lantzsch, H., Hanebuth, T. J. J., & Henrich, R. (2010). Sediment recycling and adjustment of deposition during deglacial drowning of a low-accumulation shelf (NW Iberia). Continental Shelf Research, 30, 1665–1679. https://doi.org/10.1016/j.csr.2010.06.013

Lapa, N., Rodrigues, A., Taborda, R., Duarte, J., Pinto, JP. (2012.) The sedimentary processes of the Portuguese inner shelf off Almagreiro beach (Peniche), 2as Jornadas de Engenharia Hidrográfica, Lisboa.

Leira, M., Freitas, M. C., Ferreira, T., Cruces, A., Connor, S., Andrade, C., … Bao, R. (2018). Holocene sea level and climate interactions on wet dune slack evolution in SW Portugal: A model for future scenarios? The Holocene, 29, 26–44. https://doi.org/10.1177/0959683618804633

Lentz, S. J. (1993). The Accuracy of Tide-Gauge Measurements at Subtidal Frequencies. Journal of Atmospheric and Oceanic Technology, 10, 238–245. https://doi.org/10.1175/1520-0426(1993)010<0238:taotgm>2.0.co;2

Lentz, S. J. (2001). The Influence of Stratification on the Wind-Driven Cross-Shelf Circulation over the North Carolina Shelf. Journal of Physical Oceanography, 31, 2749–2760. https://doi.org/10.1175/1520-0485(2001)031<2749:tiosot>2.0.co;2

Leopold, L. B., & Wolman, M. G. (1957). River channel patterns: Braided, meandering, and straight. Professional Paper. https://doi.org/10.3133/pp282b

Leorri, E., Cearreta, A., & Milne, G. (2012). Field observations and modelling of Holocene sea-level changes in the southern Bay of Biscay: implication for understanding current rates of relative sea-level change and vertical land motion along the Atlantic coast of SW Europe. Quaternary Science Reviews, 42, 59–73. https://doi.org/10.1016/j.quascirev.2012.03.014

Liu, W., Baudin, F., Moreno, E., Dewilde, F., Caillon, N., Fang, N., & Bassinot, F. (2014). Comparison of 240 ka long organic carbon and carbonate records along a depth transect in the Timor Sea: Primary signals versus preservation changes. Paleoceanography, 29, 389–402. https://doi.org/10.1002/2013pa002539

Llope, M., Anadón, R., Viesca, L., Quevedo, M., González-Quirós, R., & Stenseth, N. C. (2006). Hydrography of the southern Bay of Biscay shelf-break region: Integrating the multiscale physical variability over the period 1993–2003. Journal of Geophysical Research, 111. https://doi.org/10.1029/2005jc002963

Loring, D. H. (1991). Normalization of heavy-metal data from estuarine and coastal sediments. ICES Journal of Marine Science, 48, 101–115. https://doi.org/10.1093/icesjms/48.1.101

Loureiro, J. M. & Macedo, M. E. (1986). Bacia hidrográfica do Rio Tejo. Monografias hidrológicas dos principais cursos de água de Portugal continental. Direção Geral dos Recursos e Aproveitamentos Hidráulicos, 281-337.

Magalhães, F. M. Q. (1993). A cobertura sedimentar da plataforma e vertente continental superior a norte de Espinho (MSc unpublished). Universidade de Lisboa, 191p.

Magalhães, F. M. Q. (2001). Os sedimentos da plataforma continental portuguesa: contrastes espaciais, perspetiva temporal, potencialidades económicas. Doctorate Thesis. Docs. Technicians of the Instituto Hidrográfico, 34, 287p.

Malhadas, M., Silva, A., Leitão, PC., Neves, R. (2009b). Effect of the bathymetric changes on the hydrodynamics and residence time of the Óbidos Lagoon (Portugal). Journal of Coastal Research, SI 56, 549–553.

Mange, M. A., & W., M. H. F. (1991). Heavy minerals in color. Chapman and Hall.

Manuppella, G., Antunes, M. T., Pais, J., Ramalho, M. M., Rey, J. (1999). Carta Geológica de Portugal, escala 1:50000, Folha 30A (Lourinhã) e respetiva notícia explicativa. Serviços Geológicos de Portugal, Lisboa, 83p.

Marques, F., Penacho, N., Queiroz, S., Sousa, H., Silveira, T. M., Gouveia, L., Matildes, R., Redweik, P., Garzón, V., Bastos, A. P. (2103). Estudo do litoral na área de intervenção da APA, I.P. /ARH do Tejo, Caracterização das principais unidades geológicas e da organização geomorfológica da faixa costeira. Entregável 1.2.1.a, 36p.

Martins, M. V. A., Hohenegger, J., Frontalini, F., Dias, J. M. A., Geraldes, M. C., Rocha, F. (2019). Dissimilarity between living and dead benthic foraminiferal assemblages in the Aveiro Continental Shelf (Portugal), PLoS ONE, 14, doi.org/10.1371/journal.pone.0209066

Martins, V., Dubert, J., Jouanneau, J.-M., Weber, O., da Silva, E. F., Patinha, C., … Rocha, F. (2007). A multiproxy approach of the Holocene evolution of shelf–slope circulation on

the NW Iberian Continental Shelf. Marine Geology, 239, 1–18. https://doi.org/10.1016/j.margeo.2006.11.001

Martins, V., Abrantes, I., Grangeia, C., Martins, P., Nagai, R., Sousa, S. H. M., … Rocha, F. (2012). Records of sedimentary dynamics in the continental shelf and upper slope between Aveiro–Espinho (N Portugal). Journal of Marine Systems, 96-97, 48–60. https://doi.org/10.1016/j.jmarsys.2012.02.001

Matschullat, J., Ottenstein, R., & Reimann, C. (2000). Geochemical background - can we calculate it? Environmental Geology, 39, 990–1000. https://doi.org/10.1007/s002549900084

Mazé, J. P., Arhan, M., & Mercier, H. (1997). Volume budget of the eastern boundary layer off the Iberian Peninsula. Deep Sea Research Part I: Oceanographic Research Papers, 44, 1543–1574. https://doi.org/10.1016/s0967-0637(97)00038-1

McCave, I. N., & Hall, I. R. (2002). Turbidity of waters over the Northwest Iberian continental margin. Progress in Oceanography, 52, 299–313. https://doi.org/10.1016/s0079-6611(02)00012-5

McCave, I. N., Thornalley, D. J. R., & Hall, I. R. (2017). Relation of sortable silt grain-size to deep-sea current speeds: Calibration of the 'Mud Current Meter.' Deep Sea Research Part I: Oceanographic Research Papers, 127, 1–12. https://doi.org/10.1016/j.dsr.2017.07.003

McCracken, S. R., Compton, J., Hicks, K. (1996). Sequence-stratigraphic significance of glaucony-rich lithofacies. In: Proceedings of the Ocean Drilling Program: Scientific Results, Vol. 150 (Ed. By K. G. Miller, G. S. Mountain, P. Blum, C.W. Poag and D. C. Twitchell), College Station, TX, 171-184.

Mendes, I., Gonzalez, R., Dias, J. M. A., Lobo, F., Martins, V. (2004). Factors influencing recent benthic foraminifera distribution on the Guadiana shelf (Southwestern Iberia). Marine Micropaleontology, 51, 171-192.

Mil-Homens, M., Stevens, R. L., Abrantes, F., & Cato, I. (2006). Heavy metal assessment for surface sediments from three areas of the Portuguese continental shelf. Continental Shelf Research, 26, 1184–1205. https://doi.org/10.1016/j.csr.2006.04.002

Mil-Homens, M., Branco, V., Vale, C., Boer, W., Alt-Epping, U., Abrantes, F., & Vicente, M. (2009). Sedimentary record of anthropogenic metal inputs in the Tagus prodelta (Portugal). Continental Shelf Research, 29, 381–392. https://doi.org/10.1016/j.csr.2008.10.002

Moreira, S., Freitas, M. C., Araújo, M. F., Andrade, C., Munhá, J., Fatela, F., Cruces, A. (2009). Contamination of Intertidal Sediments – The Case of Sado Estuary (Portugal). Journal of Coastal Research, SI 56, 1380 – 1384.

Morellón, M., Aranbarri, J., Moreno, A., González-Sampériz, P., Valero-Garcés, B. L. (2018). Early Holocene humidity patterns in the Iberian Peninsula reconstructed from lake, pollen and speleothem records, Quaternary Sci. Rev., 181, 1–18.

Mougenot, D. (1976). Géologie du plateau continental portugais (entre le Cap Carvoeiro et le Cap de Sines) (unpublished). These 3eme. cycle, Univ. Rennes, 140p.

Mougenot, D. (1989). Geologie de la Marge Portugaise. Documentos técnicos do Instituto Hidrográfico, vol. 32. 259p.

Moura, D., Veiga-Pires, C., Boski, T., Albardeiro, L., Rodrigues, AL., Tareco, H. (2007). Holocene sea level fluctuations and coastal evolution in the Central Algarve (southern Portugal). Marine Geology, 237, 127-142.

Murray, JW. (2007). Biodiversity of living benthic foraminifera: how many species are there? Marine Micropaleontology, 64, 163-176.

Musellec, P. (1974). Géologie du plateau continental portugais au Nord du Cap Carvoeiro. Université de Rennes, 170p.

Nriagu, J. O. & Pacyna, J. M. (1988). Quantitative assessment of worldwide contamination of air, water and soils by trace metals. Nature, 333, 134-139.

Oberle, F. K. J., Hanebuth, T. J. J., Baasch, B., Schwenk, T. (2014). Volumetric budget calculation of sediment and carbon storage and export for a late Holocene mid-shelf mudbelt system (NW Iberia), Continental Shelf Research, 76, 12– 24.

Oliveira, A. (1994). Plumas túrbidas associadas com os rios a norte de Espinho (MSc Thesis unpublished). Universidade de Aveiro, 182p.

Oliveira, A. T. C. (2001). Dinâmica da matéria particulada em suspensão na plataforma continental minhota e a sua relação com a cobertura sedimentar (PhD Thesis unpublished). Universidade do Algarve, 278 pp.

Oliveira, A., Rocha, F., Rodrigues, A., Jouanneau, J., Dias, A., Weber, O., & Gomes, C. (2002). Clay minerals from the sedimentary cover from the Northwest Iberian shelf. Progress in Oceanography, 52(2-4), 233–247. https://doi.org/10.1016/s0079-6611(02)00008-3

Oliveira, A., Palma, C., & Valença, M. (2011). Heavy metal distribution in surface sediments from the continental shelf adjacent to Nazaré canyon. Deep Sea Research Part II: Topical Studies in Oceanography, 58, 2420–2432. https://doi.org/10.1016/j.dsr2.2011.04.006

Otto-Bliesner, B. L., Braconnot, P., Harrison, S. P., Lunt, D. J., Abe-Ouchi, A., Albani, S., … Zhang, Q. (2017). The PMIP4 contribution to CMIP6 – Part 2: Two interglacials, scientific objective and experimental design for Holocene and Last Interglacial simulations. Geoscientific Model Development, 10, 3979–4003. https://doi.org/10.5194/gmd-10-3979-2017

Parfenoff, A., Pomerol, C., Toureng, J. (1970). Les minéreux en grains, méthodes d'étude et détermination. Masson and Cie, Paris, France.

Patrick McLaren. (1981). An Interpretation of Trends in Grain Size Measures. SEPM Journal of Sedimentary Research, Vol. 51. https://doi.org/10.1306/212f7cf2-2b24-11d7-8648000102c1865d

Pereira, A. R. (1985). Algumas notas sobre as dunas consolidadas do litoral alentejano. Congresso sobre o Alentejo, 2, 493-501.

Pereira, A. R. (1992). A geomorfologia da Margem Continental Portuguesa e a Interdependência das Plataformas Continental e Litoral. Linha de Acção de Geografia Física, Relatório Interno 30, 95p., Lisboa.

Poizot, E., Mear, Y., Thomas, M., & Garnaud, S. (2006). The application of geostatistics in defining the characteristic distance for grain size trend analysis. Computers & Geosciences, 32, 360–370. https://doi.org/10.1016/j.cageo.2005.06.023

Poizot, E., Méar, Y., & Biscara, L. (2008). Sediment Trend Analysis through the variation of granulometric parameters: A review of theories and applications. Earth-Science Reviews, 86, 15–41. https://doi.org/10.1016/j.earscirev.2007.07.004

Pombo, J. (2004). Surface Sediments of Portuguese continental shelf between the Mondego Cape S. Martin of Porto (MSc thesis unpublished). University of Coimbra, 185p.

Ponte Lira, C., Nobre Silva, A., Taborda, R., & Freire de Andrade, C. (2016). Coastline evolution of Portuguese low-lying sandy coast in the last 50 years: an integrated approach. Journal of Earth System Science, 8, 265–278. https://doi.org/10.5194/essd-2016-5-rc5

Portela, L. (2004). An approximate sediment budget for the Tagus Estuary. In 3rd International SedNet Conference: the future of sediment management in Europe, Conference Documents, European Sediment Research Network.

Poulos, S., Ballay A. (2010). Grain-size trend analysis for the determination of non-biogenic sediment transport pathways on the Kwinte Bank (southern North Sea), in relation to sand dredging. Journal of Coastal Research, 51, 87–92.

Puig, P., Madron, X. D., Salat, J., Schroeder, K., Martín, J., Karageorgis, A. P., … Houpert, L. (2013). Thick bottom nepheloid layers in the western Mediterranean generated by deep dense shelf water cascading. Progress in Oceanography, 111, 1–23. https://doi.org/10.1016/j.pocean.2012.10.003

Quaresma, L. S., & Pichon, A. (2013). Modelling the barotropic tide along the West-Iberian margin. Journal of Marine Systems, 109-110. https://doi.org/10.1016/j.jmarsys.2011.09.016

Quaresma, L. S., Vitorino, J., Oliveira, A., & da Silva, J. (2007). Evidence of sediment resuspension by nonlinear internal waves on the western Portuguese mid-shelf. Marine Geology, 246(2-4), 123–143. https://doi.org/10.1016/j.margeo.2007.04.019

Ramos-Pereira, A., Trindade, J., Ramos, C., Soares, A., Danielson, R., Granja, H., Torres, A., Ribeiro, A., Martins, J., Portela, P. (2012). A multi-proxy analysis in the assessment of fluvio-marine interactions over the last 5000 years. EGUGA, 12723.

Rasmussen, S. O., Bigler, M., Blockley, S. P., Blunier, T., Buchardt, S. L., Clausen, H. B., … Winstrup, M. (2014). A stratigraphic framework for abrupt climatic changes during the Last Glacial period based on three synchronized Greenland ice-core records: refining and extending the INTIMATE event stratigraphy. Quaternary Science Reviews, 106, 14–28. https://doi.org/10.1016/j.quascirev.2014.09.007

Ravaioli, M., Alvisi, F., & Vitturi, L. M. (2003). Dolomite as a tracer for sediment transport and deposition on the northwestern Adriatic continental shelf (Adriatic Sea, Italy). Continental Shelf Research, 23, 1359–1377. https://doi.org/10.1016/s0278-4343(03)00121-3

Reimann, C., & de Caritat, P. (2017). Establishing geochemical background variation and threshold values for 59 elements in Australian surface soil. Science of The Total Environment, 578, 633–648. https://doi.org/10.1016/j.scitotenv.2016.11.010

Reimer, P. J., Bard, E., Bayliss, A., Beck, J. W., Blackwell, P. G., Ramsey, C. B., … van der Plicht, J. (2013). IntCal13 and Marine13 Radiocarbon Age Calibration Curves 0–50,000 Years cal BP. Radiocarbon, 55, 1869–1887. https://doi.org/10.2458/azu_js_rc.55.16947

Rey, D., Álvarez-Iglesias, P., Araújo, M. F., Bernabeu, A. M., Comas, M., DeCastro, M., … Vilas, F. (2014). Chapter 8 The NW Iberian continental shelf. Geological Society, London, Memoirs, 41, 91–108. https://doi.org/10.1144/m41.8

Ribeiro, S., Azevedo, MR., Santos, JF., Medina, J., Costa, A. (2014). Sr isotopic signatures of Portuguese bottled mineral waters and their relationships with the geological setting. Comunicações Geológicas, 100, 89-98.

Ribeiro, A., Antunes, M. T., Ferreira, M. P., Rocha, R. B., Soares, A. F., Zbyszewszki, M. G., Almeida, F. M., Carvalho, D., Monteiro, JH. (1979). Introduction a la Géologie Generale du Portugal. Geologic Survey, Portugal, Lisboa.

Ribeiro, M. (2017). Headland sediment bypassing processes (PhD thesis unpublished). University of Lisbon, 229p.

Rodrigues, A., Magalhães, F., & Dias, J. A. (1991). Evolution of the North Portuguese coast in the last 18,000 years. Quaternary International, 9, 67–74. https://doi.org/10.1016/1040-6182(91)90065-v

Rodrigues, A. (2001). Tectono-Estratigrafia da Plataforma Continental Setentrional Portuguesa (PhD Thesis unpublished). Universidade de Lisboa, 227p.

Rodrigues, T., Grimalt, J. O., Abrantes, F. G., Flores, J. A., & Lebreiro, S. M. (2009). Holocene interdependences of changes in sea surface temperature, productivity, and fluvial inputs in the Iberian continental shelf (Tagus mud patch). Geochemistry, Geophysics, Geosystems, 10. https://doi.org/10.1029/2008gc002367

Rognon, P. (1976). Essai d'interprétation climatique au sahara depuis 40 000 ans. Revue de Géographie Physique & de Géologie Dynamique, 18, 251–282.

Rognon, P. (1980). Une extension des deserts au cours du Tardiglaciaere (18000 – 10000 ans B.P.). Revue de Géologie Dynamique et de Géographie, 22, 313-328.

Roque, A. C. (1998). Análise morfosedimentar da sequência deposicional do Quaternário Superior da plataforma continental Algarvia entre Faro e a foz do Rio Guadiana. Dissertação, Universidade de Lisboa. 221p.

Rosa, F. (2014). Climatic variability and recent sedimentation in the Continental Shelf off the Guadiana River (Phd Thesis unpublished). Universidade do Algarve, 246p.

Rosa, F., Dias, J. A., Mendes, I., & Ferreira, Ó. (2010). Mid to late Holocene constraints for continental shelf mud deposition in association with river input: the Guadiana Mud Patch (SW Iberia). Geo-Marine Letters, 31, 109–121. https://doi.org/10.1007/s00367-010-0219-6

Rossignol-Strick, M. (1999). The Holocene climatic optimum and pollen records of sapropel 1 in the eastern Mediterranean, 9000–6000BP. Quaternary Science Reviews, 18, 515–530. https://doi.org/10.1016/s0277-3791(98)00093-6

Rothwell, R. G. (1989). Minerals and Mineraloids Occurring in Marine Sediments. Minerals and Mineraloids in Marine Sediments, 27–35. https://doi.org/10.1007/978-94-009-1133-8_3

Ruddiman, W. F., & McIntyre, A. (1973). Time-Transgressive Deglacial Retreat of Polar Waters from the North Atlantic. Quaternary Research, 3, 117–130. https://doi.org/10.1016/0033-5894(73)90058-6

Ruddiman, W., & McIntyre, A. (1981). The North Atlantic Ocean during the last deglaciation. Palaeogeography, Palaeoclimatology, Palaeoecology, 35, 145–214. https://doi.org/10.1016/0031-0182(81)90097-3

Santos, F. D., Lopes, A. M., Moniz, G., Ramos, L., Taborda, R. (2014). Gestão da Zona Costeira. O desafio da mudança. Unpublished report, 237p.

Savina, M., & Pouvreau, S. (2004). A comparative ecophysiological study of two infaunal filter-feeding bivalves: Paphia rhomboïdes and Glycymeris glycymeris. Aquaculture, 239, 289–306. https://doi.org/10.1016/j.aquaculture.2004.05.029

Shepard, F. P. (1973). Submarine Geology, 3rd. edition, Harper & Row Publishers, New York, 517p.

Shi, X., Chen, C., Liu, Y., Ren, H., & Wang, H. (2002). Trend analysis of sediment grain size and sedimentary process in the central South Yellow Sea. Chinese Science Bulletin, 47, 1202–1207. https://doi.org/10.1007/bf02907610

Shu, G., & Collins, M. (2001). The use of grain size trends in marine sediment dynamics: A review. Chinese Journal of Oceanology and Limnology, 19, 265–271. https://doi.org/10.1007/bf02850664

SNIRH – Sistemas Nacional de Informação de Recursos Hídricos, 2010. Mapa de Pluviosidade Anual de Portugal 1959/60- 1990/91. Instituto da Água, Lisboa, Portugal. http://snirh.apambiente.pt/snirh/_atlasagua/galeria/mapasweb/pt/aa1008.pdf ou https://sniamb.apambiente.pt/content/geo-visualizador?language=pt-ptb.

SWAN Team (2006). SWAN: Technical Documentation. SWAN Cycle III version 40.51, Delft University of Technology, electronic version: in http://falk.ucsd.edu/modeling/swantech.pdf.

Taborda, R. (2000). Modelação da dinâmica sedimentar na plataforma continental portuguesa (MSc unpublished). Universidade de Lisboa, 366p.

Taylor, S. R., & McLennan, S. (1985). Composition and evolution of the continental crust. Planetary Crusts, 301–324. https://doi.org/10.1017/cbo9780511575358.014

Tchounwou, P. B., Yedjou, C. G., Patlolla, A. K., & Sutton, D. J. (2012). Heavy Metal Toxicity and the Environment. Experientia Supplementum, 133–164. https://doi.org/10.1007/978-3-7643-8340-4_6

Teles-Machado, A., Peliz, Á., McWilliams, J. C., Couvelard, X., & Ambar, I. (2016). Circulation on the Northwestern Iberian Margin: Vertical structure and seasonality of the alongshore flows. Progress in Oceanography, 140, 134–153. https://doi.org/10.1016/j.pocean.2015.05.021

Tolman, H.L. (2009). User Manual and System Documentation of WAVEWATCH-III Version 1.18, NOAA / NWS / NCEP / OMB Technical Note 166, 110 pp.

Vale, C., & Sundby, B. (1987). Suspended sediment fluctuations in the Tagus estuary on semi-diurnal and fortnightly time scales. Estuarine, Coastal and Shelf Science, 25, 495–508. https://doi.org/10.1016/0272-7714(87)90110-7

Vanney, JR. & Mougenot, D. (1981). La plate-forme continentale du Portugal et les provinces adjacentes: Analyse Geomorphologique. Memórias dos Serviços Geológicos de Portugal, 28, 86.

Vitorino, J., Oliveira, A., Jouanneau, J. M., & Drago, T. (2002). Winter dynamics on the northern Portuguese shelf. Part 1: physical processes. Progress in Oceanography, 52, 129–153. https://doi.org/10.1016/s0079-6611(02)00003-4

Vitorino, J., Oliveira, A., Jouanneau, J. M., & Drago, T. (2002). Winter dynamics on the northern Portuguese shelf. Part 2: bottom boundary layers and sediment dispersal. Progress in Oceanography, 52, 155–170. https://doi.org/10.1016/s0079-6611(02)00004-6

Wright, LD. (1995). Morphodynamics of Inner Continental Shelves. CRC Press, Inc., Boca Raton,FL, ISBN 0-8493-8043-X, 241p.

Wuana, R. A., & Okieimen, F. E. (2011). Heavy Metals in Contaminated Soils: A Review of Sources, Chemistry, Risks and Best Available Strategies for Remediation. ISRN Ecology, 2011, 1–20. https://doi.org/10.5402/2011/402647

Yalin, M. M. (1977). Mechanics of Sediment Transport, Pergamon, Oxford, N. Y.

Zbyszewski, G., & Moitinho de Almeida, F. (1955). Carta Geológica de Portugal, escala 1:50000, Folha 30C (Torres Vedras) e respetiva notícia explicativa. Serviços Geológicos de Portugal, Lisboa, 33p.

Zbyszewski, G., & Moitinho de Almeida F. (1960). Carta Geológica de Portugal, escala 1:50000, Folha 26D (Caldas da Rainha) e respetiva notícia explicativa. Serviços Geológicos de Portugal, Lisboa, 56p.

Zhu, Y., & Chang, R. (2000). Preliminary Study of the Dynamic Origin of the Distribution Pattern of Bottom Sediments on the Continental Shelves of the Bohai Sea, Yellow Sea and East China Sea. Estuarine, Coastal and Shelf Science, 51, 663–680. https://doi.org/10.1006/ecss.2000.0696

Websites

SWAN Manual - http://swanmodel.sourceforge.net/online_doc/swanuse/swanuse.html

Annex 1. Methods

TABLE OF CONTENTS

TABLE OF FIGURES

TABLE OF TABLES

1. Methods

1.1. Introduction

Two field campaigns promoted by Instituto Hidrográfico aim to collect surface sediment samples from rivers and beaches between Nazaré and Ericeira. The first campaign was made in September 2009 where river samples were collected and the second campaign in March 2010 where both river and beach samples were collected (Figure 1). The river samples were collected in its margins and in beached the samples were collected on the shoreface. These samples of surface sediments from rivers and beaches aim to characterize the type of sediment being exported to the continental shelf, in terms of texture, mineralogical composition and geochemistry for later comparison with surface sediment data of the continental shelf and to verify if the rivers sediments contribution is important as sedimentary sources for the continental shelf.

Figure 1 - Arnóia and Sizandro rivers

On September 2010, during a survey promoted by the Instituto Hidrográfico in the framework of another project, a sediment core with 162 cm length was collected in the middle of the Ericeira muddy deposit (39º00'58.711"N; 9º40'13.06"W; 120 m depth).

This gravity core was collected using a Portuguese Hydrographic vessel (N.R.P "Auriga") (Figure 2). The core was mainly constituted by mud and sandy mud on the top part and gravelly sand on the bottom. It was sealed and kept refrigerated for slicing.

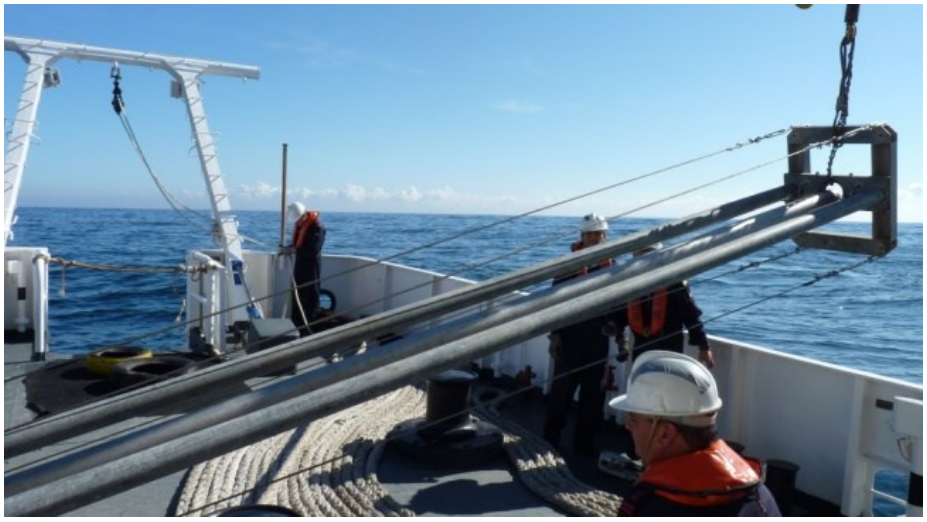

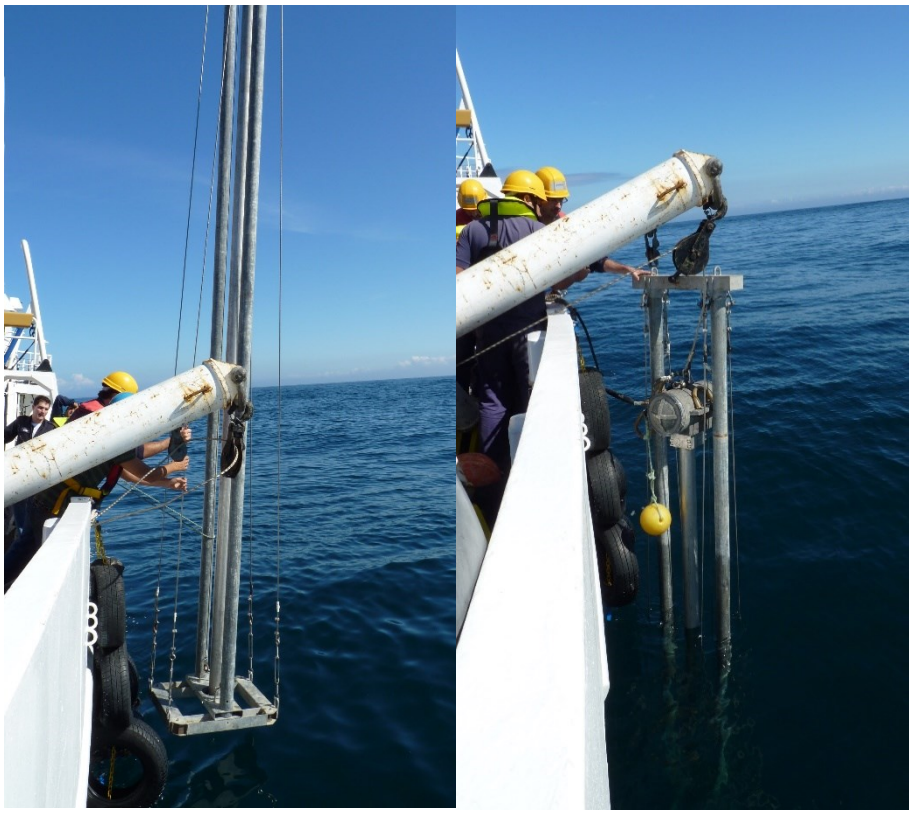

Figure 2 - Sediment core collect at Ericeira mud patch in N.R.P. "Auriga".

Each sample was subjected to different analyses. River and beach samples had total organic and inorganic analyses, grain-size, fine fraction mineralogy, and heavy minerals and metals. The sediment core was subjected to an x-ray and magnetic susceptibility analysis before slicing. The core was then sliced every centimeter in the first 20 cm, then every 5 cm till 140 cm and finally the last 22 cm were analyzed as a whole since it was the sediment inside the nose core (Figure 3).

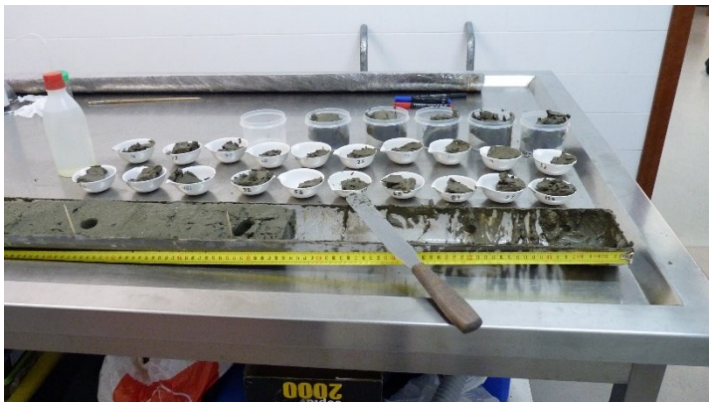

Figure 3 - Sediment core collected at Ericeira mud-patch.

A total of 46 subsamples from sediment core were analyzed, for total organic and inorganic carbon, ^{14}C. After total removal of organic matter were analyzed several proxies such as grain-size morphoscopy of sandy fraction, fine faction mineralogy, sortable silt, heavy minerals and metals, benthic and planktonic foraminifera and calcareous nannoplankton content.

Two mechanical Aanderaa RCM7 current meter were deployed during an opportunity winter cruise in 2010/2011. One current meter was deployed at a depth of 250 m, in the outer continental shelf and the other one at approximately 100 m depth in the Ericeira mud patch. Unfortunately, the one deployed in the Ericeira mud patch was not recovered since it was no longer in its position at the time of recovery, possibly dragged by fisherman or trawled, as it is very common in the area (Figure 4).

Figure 4 – Aanderaa RCM7 current meter
The Aanderaa RCM7 current meter consists of three fundamental components: the pressure box (1), the rudder body (2) and the rudder plate (3)

1.2. River and beach samples

In order to characterize the sedimentary sources for the Estremadura Spur, two field surveys on rivers that drain to the study area and beaches were made. The first was conducted in September 2009, where seven surface sediments were collected in the major rivers that drain the study area (Sizandro river, Alcabrichel river, Grande river, Arnóia river, Ribeira São Domingos, Ribeira de Alfeizerão and Lizandro river (Figure 5). The samples were collected at the river mouth along the banks of streams. The campaign was carried out in the end of drought season, with virtually no river flow.

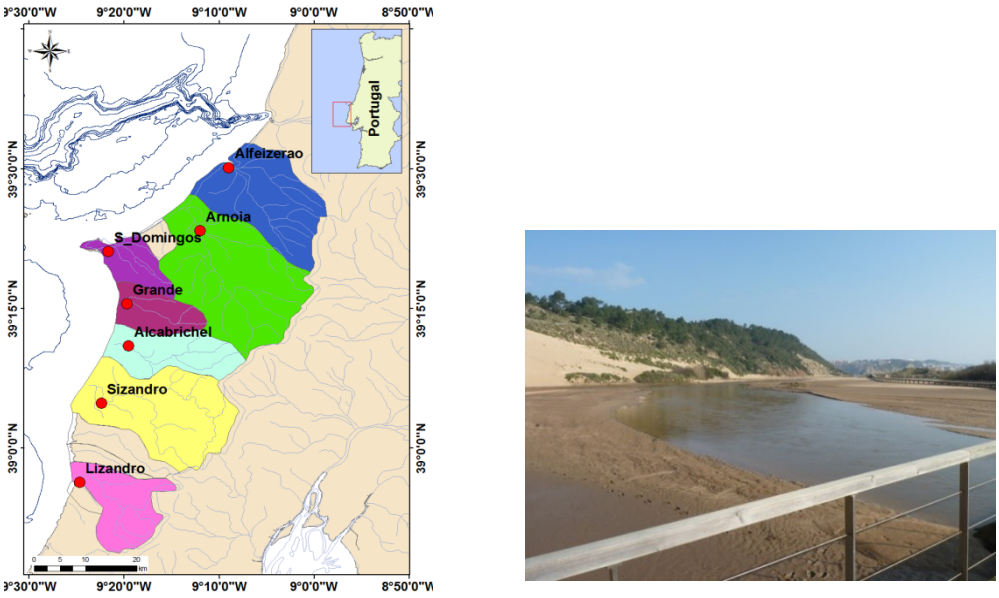

Figure 5 – River survey in September 2009. Photo of Sizandro river mouth

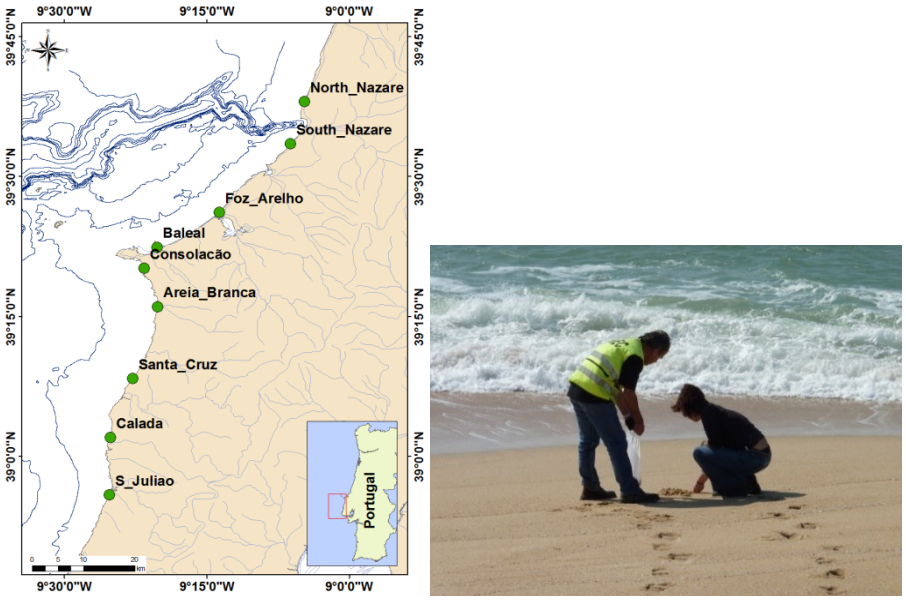

Figure 6 – Beach survey in 2010

The second survey was held in March 2010. The winter of 2009/2010 had major winter storms, where there were very high flow rates overflowing several streams. In this survey 9 beaches were sampled, and samples were collected in the shoreface (Norte beach, Sul Nazaré, Foz do Arelho, Baleal, Consolação (Figure 6), Areia Branca, Santa Cruz, Calada and S. Julião).

For grain size and fine fraction mineralogy analysis were used a total of 16 samples from river and beaches and 66 samples from SEPLAT program (Figure 7).

For heavy metals analyses were used only the 66 samples from SEPLAT program and river samples. For heavy minerals analyses, only the samples from the inner shelf from SEPLAT program, river and beach samples were analyzed in a total of 26 samples (Table 1).

Table 1 – River, beach and coastal continental shelf samples position and number

	Local	x	y	Sample
	Sizandro	-9.3727	39.08	2444
	Alcabrichel	-9.3256	39.183	2445
	Grande	-9.3264	39.262	2446
	Arnoia	-9.2003	39.388	2447
	S.Domingos	-9.3611	39.351	2448
	Alfeizerão	-9.1496	39.501	2449
Rivers	Lizandro	-9.41	38.938	2450
	N_Nazaré	-9.0793	39.634	777
	S_Nazaré	-9.1033	39.558	778
	Foz Arelho	-9.2276	39.436	781
	Baleal	-9.3369	39.373	784
	Consolação	-9.3596	39.336	786
	Areia Branca	-9.3361	39.267	788
	Santa Cruz	-9.38	39.139	793
	Calada	-9.4186	39.033	796
Beaches	S_Julião	-9.4209	38.931	798
		-9.8597	39.217	273
		-9.367	39.217	297
		-9.9812	39.165	400
		-9.37	39.167	984
		-9.4529	38.917	953
		-9.4033	39.116	978
		-9.2882	39.409	10606
		-9.2223	39.46	10635
		-9.43	38.96	959
	Shelf	-9.3804	39.267	145

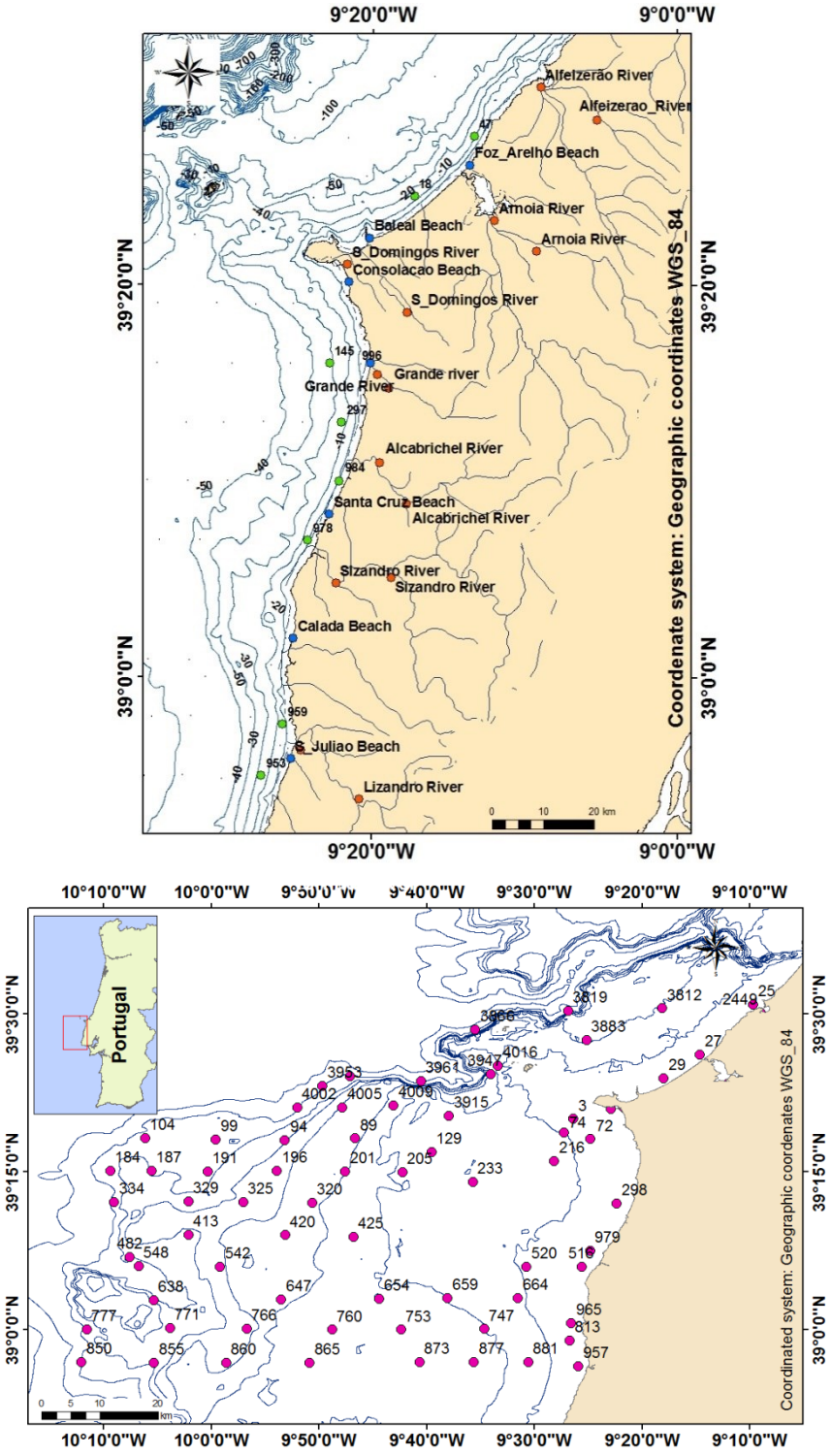

Figure 7 – Top figure presents samples from rivers (red), beaches (blue) and inner shelf (green); bottom figure presents continental shelf samples from SEPLAT.

1.3. X-ray analysis

X-ray radiography is a technique based on differential travel of X-rays through sediment (Bouma, 1969). During this travel, the incident X-ray beam is attenuated by various phenomena including absorption and scattering. The dominant control on beam attenuation is bulk sediment

density (Holyer *et al*., 1996; Jackson *et al*., 1996), which is in turn affected by parameters such as grain-size and lithology, including carbonate and silica contents. Beam attenuation can also be affected by physical parameters such as changes in water content, compaction and porosity. The gray scale intensity of X-ray images is proportional to X-ray attenuation. Consequently, these images reflect primarily sediment density and, in theory, provide a first order picture of downcore grain-size variations (Giraudeau & Beaufort, 2007).

X-ray analysis has been gaining acceptance as a routine core analysis tool, over the past several decades. In this case, a medical x-ray has been employed because of their availability and relative ease of use.

X-ray radiography of sediment cores is a fast, non-destructive scanning and recording technique which may reveal structures that are not revealed by other methods of analysis (Axelsson, 1983). The features that are possible to individualize in x-ray radiographies are bedding features and sedimentary structures, natural and coring-induced fractures, cement distribution, small-scale grain-size variation, and density (mineralogical and chemical composition) variation (Coles *et al.*, 1998).

At *Gravidus* Clinic, a set of five images were taken using digital X-ray equipment that consists in an *ODEL generator* (*Endeavour 65 kw – 150 kv*), an *Italray X-ray table* (*Statix model*), a Kodak-carestream Elite scanner and a *laser Kodak-carestream 8900* print (650 DPI resolution). The five images were then processed using *CorelDRAW Graphic Suites X6.*

1.4. Magnetic susceptibility

The use of magnetism in the study of Quaternary sediments began in the summer of 1926 when Gustav Ising made measurements of magnetic susceptibility and natural remanence on varved lake sediments from Sweden (Ising, 1943). Environmental magnetism investigates the magnetic properties of materials which have been formed under the influence of environmental processes. Magnetic measurements of soils, dusts and other sediments provide powerful and effective tools for analyzing problems and solve questions related to environmental and climate change, including anthropogenic pollution. The methods of environmental magnetism have been applied on all scales: global paleoclimatic variability has been reconstructed from the magnetism of well-dated and widely separated marine sediments of variable age; submicroscopically fine magnetic iron oxide particles have provided insight into iron mobilization, migration and precipitation during soil formation; and regional pollution by strongly magnetic spherical particles produced during fossil fuel combustion has been surveyed in industrialized areas (Maher & Thompson, 1999).

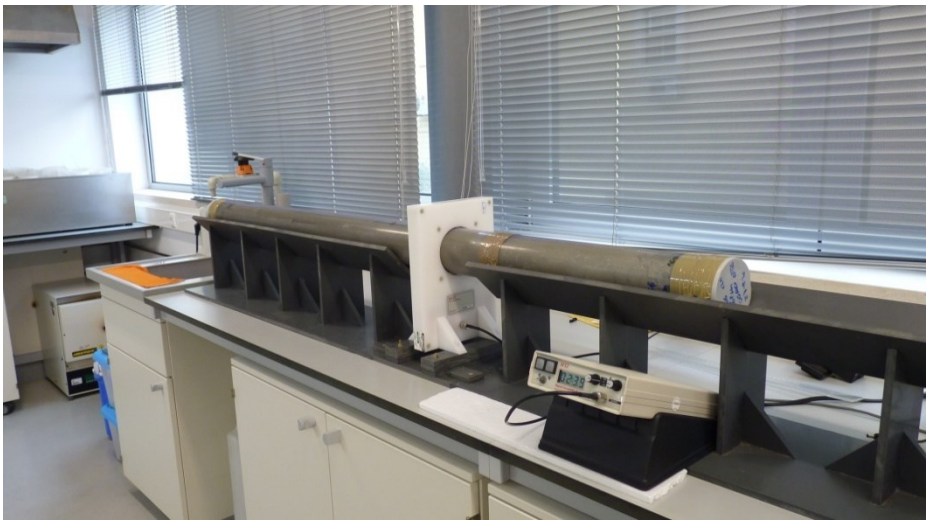

Figure 8 - Magnetic susceptibility measurement of the sediment core.

Magnetic susceptibility (MS) does not depend on changes in the earth's magnetic field, but reflect variations in the nature and origins of magnetic minerals in sediments (Dearing, 1999). Mineral magnetic susceptibility measures the degree to which a material can be magnetized; in other words, it is an index of its 'magnetization'. MS has a range of applications in the archaeological and environmental sciences (as an indicator of sediment flux and erosion in lake catchments, for example), but it has also been used as a basis for correlation between cores from Holocene lake sediment sequences and other paleoenvironmental records (Snowball *et al.*, 1999).

At the Instituto Hidrográfico laboratory, magnetic susceptibility was measured every centimeter with Magnetic Susceptibility Meter – MS2 (Bartington Instruments) (Figure 8).

1.5. Dry bulk density

According to Dadey *et al*. (1992), the dry bulk of a sediment deposit is a necessary component of any accumulation rate calculation. Mass accumulation rates incorporate the effects of depositional and postdepositional processes and sediment composition. Gravitational compaction is the primary postdepositional process affecting sediment porosity (and consequently dry-bulk density), by other processes such as early diagenetic changes (e.g. cementation and authigenic mineral formation) may also result in significant changes in the porosity of the deposit.

Dry-bulk density is defined as mass (weight) of dry solids divided by the total volume of wet sample; that is, dry-bulk density is the ratio of the mass of the mineral grains to the total volume.

For this analysis were chosen the following levels (1, 10, 20, 32, 52, 75, 109, 124, 137 and 157 cm). The volume of sample collect was 1 cm^3 with a syringe for each level and left to dry.

1.6. ^{210}Pb

The lead-210 (^{210}Pb), which is part of the uranium-238 (238U) decay series, is absorbed onto the sediment particles deposited in the sea bottom, and consist in two components: supported and unsupported ^{210}Pb. The supported ^{210}Pb (background) is derived from the in situ decay of radium-226 (226Ra) that has been directly washed into the system within the eroded material, and is in equilibrium with all the members of the decay chain which precede it. The unsupported ^{210}Pb (excess) is the one that was deposited afterwards, or that is currently being deposited, derived from radon-222 (222Rn) which diffuses as gas through the soil interstitial pore space into the atmosphere, where it rapidly decays to ^{210}Pb. The produced ^{210}Pb then attaches to aerosol particles2 and settles out of the atmosphere as dry fallout, or is washed out in rainfall events (Geyh & Schleicher, 1990).

Although the ^{210}Pb flux is normally assumed to be constant at any given site, its value may vary spatially by up to an order of magnitude, depending on factors such as rainfall and geographical location (APPLEBY, 2002).

As the superficial unsupported ^{210}Pb decays, the ^{210}Pb activity profile (downcore) will gradually reach ^{210}Pb background values, which are constant since it is continuously being produced in the sediment. By calculating the amount of ^{210}Pb that is in excess in relation to the background, and considering that ^{210}Pb has a certain decay constant (half-life of 22.2 yrs), it becomes possible to calculate the Mass Accumulation Rate (MAR) for a maximum of 100 years. The curve obtained from the ^{210}Pb activity profile will give us the SAR approximated value. Depending on the curve's degree of sloping, so it will be higher or lower the calculated SAR: a rapid downcore decrease in unsupported ^{210}Pb indicates low SAR; a more gradual downcore decrease indicates higher SAR.

The model used to calculate MAR (Mass Accumulation Rate) was The Constant Flux and Constant Sedimentation rate model (CF/CS model) for one-layer profiles = used for profiles that consist of an exponential downward decline in unsupported ^{210}Pb on top of the supported ^{210}Pb produced by the decay of ^{222}Rn in the sediment. The MAR is assumed to be constant and the reworking of sediment negligible.

$$A_{z(tot)} = A_{0(xs)}\exp^{\alpha/z} + A_{(sup)}$$

Where: where $A_{z(tot)}$ is the activity of total ^{210}Pb (mBq g^{-1}) at depth z, A_0(xs) is the activity of excess ^{210}Pb (mBq g^{-1}) delivered by sediment deposition at the sediment-water interface, and $A_{(sup)}$ is the constant background activity of supported ^{210}Pb (mBq g^{-1}) produced by radioactive decay of ^{234}U series isotopes in the sediment.

For this study the first 20 cm were sampled and analyzed by the Marine Geology Department of the Royal Netherlands Institute of Sea Research (NIOZ). This methodology was previously used in other studies such as Stigter et al., 2007 and Costa, 2008.

1.7. Total organic and inorganic carbon

The mass of carbon stored over the geologic history of the Earth in sedimentary limestones, dolomites, and undecomposed organic matter exceeds by a very large factor, about 100,000 the mass of carbon in atmospheric CO_2 at the present time (Mackenzie & Lerman 2006). Next in size is the carbon reservoir of the oceans or, more generally, of the oceanic and continental surface and ground waters that comprise most of the hydrosphere.

The main form of carbon in the global water reservoir is dissolved carbon dioxide and its ionic species, and the generally less abundant dissolved organic carbon from incomplete decomposition of living and dead organic matter. On the other hand, dissolved organic carbon includes a great variety of organic compounds ranging in molecular weight from light, simple organic acids to much heavier and structurally more complex species. Besides the dissolved forms of carbon, there are particles containing both inorganic and organic carbon in continental and ocean waters.

Total inorganic carbon or TIC in sediment is mostly grains of eroded carbonate rocks and skeletons of calcareous organisms formed in sediments that sink to the ocean floor.

Its organic counterpart, total organic carbon or TOC, consists of undecomposed cells, products of metabolic excretion by zooplankton (fecal pellets), soft parts of dead organisms and organic matter adsorbed on mineral-particle surfaces such as clays. The total mass of carbon in the global oceans, consisting mostly of TIC, is about 60 times greater than its atmospheric mass (Lerman, 2009). The greater mass of TIC in the ocean becomes either a source or sink of atmospheric carbon dioxide, depending on environmental conditions, namely pH, since it can contribute to the absorption or release of TIC (Giraudeau & Beaufort, 2007).

TIC and TOC were analyzed using Strohlëin TOC Analyzer C-mat 5500, according to internal procedures of the Instituto Hidrográfico laboratory. TIC analysis consists on measuring the carbon dioxide produced in the reaction in the fraction of the carbonate present in $CaCO_3$ form, with phosphoric acid. TOC analysis consists on measuring the carbon dioxide produced in the combustion and catalyzing of the total carbon present in the sample, thereby obtaining the total carbon content, to which is subtracted the total inorganic carbon.

The weight percentages (wt.%) of total carbon (TC), total organic carbon (TOC) and calcium carbonate ($CaCO_3$) were determined for every river sample and at defined sample intervals (2 cm, 10 cm, 20 cm, 32 cm, 52 cm, 75 cm, 109 cm, 124 cm, 137 cm and 157 cm) for the sediment core.

1.8. Carbon 14

Radiocarbon (^{14}C) is one several isotopes of carbon. By far the most abundant of these is ^{12}C which comprises around 98.9 % of all naturally occurring carbon. While only approximately

1 % of all carbon on Earth is of the ^{13}C isotopic form, ^{14}C is still much rarer. Only one out of every trillion carbon atoms is ^{14}C.

Which is an instable isotope 'decays' to a stable form of nitrogen, ^{14}N, through the emission of beta (β) particles. One β particle is released from the nucleus for every atom of ^{14}C that decays. It is this instability, or *radioactivity*, which gives the name 'radiocarbon'. Atoms of ^{14}C are formed in the upper atmosphere through the interaction between cosmic ray neutrons, which reach the earth's atmosphere from deep space, and nitrogen. This involves neutron capture by the nitrogen (^{14}N) atom, and the loss of a proton, to create ^{14}C. The ^{14}C atoms produced by this process combine with oxygen to form a particular form of carbon dioxide ($^{14}CO_2$) which mixes with the non-radiocarbon containing molecules of CO_2. In this way, ^{14}C becomes part of the global carbon cycle and is assimilated by plants through the photosynthetic process, and by animals through the ingestion of plant tissue. The majority of ^{14}C (more than 95 %) is absorbed into the oceans as dissolved carbonate, which means that organisms that live in sea water (corals, molluscs, etc.) will also take up ^{14}C during the course of their life cycle. Although the ^{14}C in the terrestrial biosphere and in the oceans is constantly decaying, it is continually being replenished from the atmosphere. So, the amount of ^{14}C that is stored in plant and animal tissue and in the world's oceans, mainly through photosynthesis and respiration, the *global carbon reservoir*, remains approximately constant through time. In effect, a position has been reached where the carbon that is used to build plant and animal tissue is in *isotopic equilibrium* with the atmosphere; in other words, the levels of ^{14}C activity in plants and animals are the same as that in the atmosphere (Walker, 2005).

Once an organism dies, however, it becomes isolated from the ^{14}C source, no further replenishment of ^{14}C can take place, and the 'radiocarbon clock' runs down by radioactive decay, which occurs at a constant rate. Hence, by measuring the amount of ^{14}C that remains in a sample of fossil material (the residual ^{14}C content) and comparing this to modern ^{14}C in standard material, an age can be inferred for the death of the organism (Giraudeau & Beaufort, 2007).

Accelerator mass spectrometry (AMS) employs particle accelerators as mass spectrometers to count the relative number of ^{14}C atoms in a sample, as opposed to the decay products.

However, by accelerating particles to very high speeds, the small ^{14}C signal can be separated from that of other isotopes, hence the term accelerator mass spectrometry (often abbreviated to AMS). It is important to emphasize, however, that it is not the *absolute* number of ^{14}C atoms that is being measured; the abundance of ^{14}C atoms is so small that it would be extremely difficult to measure total amounts. Rather, AMS determines the isotope ratio of ^{14}C relative to that of the stable isotopes of carbon (^{13}C or ^{12}C), and the age is determined by comparing this ratio with that of a standard of known ^{14}C content. The error term that accompanies all AMS dates reflects, as in conventional dating, statistical uncertainties relating to the ^{14}C decay

curve, random and systematic errors that occur during the measurement process, as well as uncertainties that arise in measuring the oxalic acid standards and in quantifying the natural background 14C.

Accelerator Mass Spectrometry (AMS) has reduced sample size requirements and increased measurement precision, in turn increasing the number of studies seeking to measure marine samples. These studies rely on overcoming the influence of the MRE on marine radiocarbon dates through the worldwide quantification of the local parameter ΔR, that is, the local variation from the global average MRE (Alves *et al.*, 2014).

Ages are reported as cal BP (radiocarbon years before present, "present" = AD 1950). By international convention, the modern reference standard was 95 % the 14C activity of National Institute of Standards and Technology (NIST) Oxalic Acid (SRM 4990C) and calculated using the Libby 14C half-life (5568 years). Quoted errors represent 1 relative standard deviation statistics (68 % probability) counting errors based on the combined measurements of the sample, background, and modern reference standards. Measured $^{13}C/^{12}C$ ratios (delta ^{13}C) were calculated relative to the PDB-1 standard. The Conventional Radiocarbon Age represents the Measured Carbon Age corrected for isotopic fractionation, calculated using the delta ^{13}C. On rare occasion where the Conventional Radiocarbon Age was calculated using an assumed delta ^{13}C, the ratio and the Conventional Radiocarbon Age will be followed by "**". When available, the Calendar Calibrated result in calculated from the Conventional Radiocarbon Age and is listed as "2σ Calibrated Result" with reservoir correction for each sample.

Radiocarbon dating was performed by Beta Analytic Laboratories (Miami, FL). For this purpose, benthic foraminifera tests (all species combined, 30–40 mg) were collected under the binocular microscope in the sand fraction of each selected depth interval (110 cm and 12 cm). For the bottom core (162 cm) the analysis was made in a sea shell named *Glycimeris glycimeris* (Linné Carl von. (1767).

1.9. Grain-size

The grain-size methodology applied was the one used by Instituto Hidrográfico according to the internal technical norm NT_LB_22 (sieving method – Annex B) for particles superior to 0.500 mm and NT_LB_23 (Laser Diffraction method – Annex H) for particles inferior to 0.500 mm (Figure 9). The sieving method consists in separation of a particulate material, through a set of sieves with meshes well established and calibrated (Figure 10).

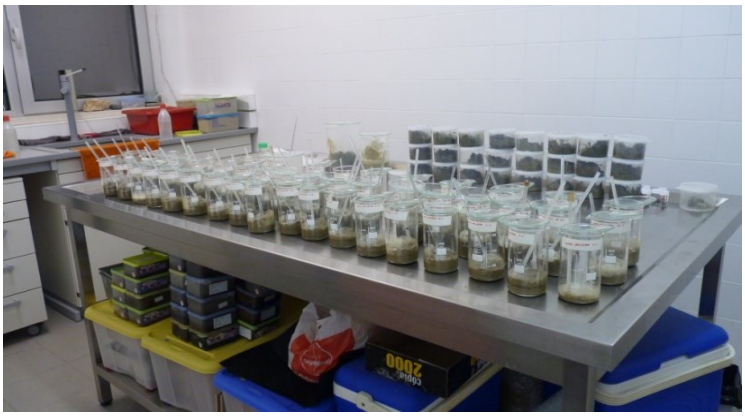

Figure 9 - Aliquots from Estremadura core.

The diffraction laser method consists in measuring the particle size distribution of sediment dispersed in a liquid, using the phenomenon of laser light beam dispersion.

The interaction between the incident light and the particles results in a dispersion pattern that is characterized by variations in intensity, resultant from the angle of deviation. From grain-size analysis the principal statistic parameters (mean, mode, standard deviation and asymmetry) were calculated.

Figure 10 - Sieving equipment with 0.5 phi interval.

1.10. Morphoscopy of sandy fraction

For morphoscopy, five sediment fractions were used for binocular microscope ((1 – 2 mm (very coarse sand), 0.5 – 1 mm (coarse sand), 0.250 – 0.5 mm (medium sand), 0.125 – 0.250 mm (fine sand), 0.063 – 0.125 mm (very fine sand)). For each fraction more than 300 particles (Dias, 2004) were classified and counted in the following categories: quartz, phyllossilicates (muscovite and biotite), aggregates (carbonate aggregates, silt-clay aggregates) terrigenous particles (lithoclasts), mollusks, planktonic foraminifera, benthic foraminifera, biogenic particles (coral,

echinoderms, spicules of sponges and ostracods) and glaucony. These data were then graphed using *Golden* software *Grapher 5.01*.

1.11. Sortable Silt

The fine grain size distribution was divided according to McCave *et al.*, 1995, into three terrigenous fractions; < 2 µm dominated by clay minerals, 2 - 10 µm called fine silt or cohesive silt with the same properties of a cohesive material, and 10 - 63 µm called coarse silt or sortable silt (SS) with non-cohesive behavior. The percentage of sortable silt (SS) in the total <63 mm terrigenous fraction has been suggested as an index of current-controlled grain size selection. The silt/clay ratio (S/C) also provides information about changes in paleocurrent intensity (Hall & McCave, 2000).

1.12. Fine fraction mineralogy

Mineralogy of fine fraction was determined in Instituto Hidrográfico laboratory using the internal technical norm NT.LB.78 for samples preparation and analysis. Sediment fraction inferior to 0.063 mm were powdered and carefully introduced in a XRD samples avoiding compression and crystal reorientation. The Philips PANalytical diffractometer uses Kα Cu radiation (45 Kv, 40 mA). To obtain quantitative and semi-quantitative results the scans were made between 2º and 60º (2Θ). The main groups of minerals identified are listed below (Table 2).

Table 2 – Main groups of minerals
(Oliveira, 2001)

Minerals	Peak for semi-quantification in natural specimen (Å)	Estimated factors
Chlorite	14.00	0.75
Illite	10.00	0.5
Kaolinite	7.00	1.0
Quartz	4.26	1.5
Opal	4.0	0.5
Anhydrite	3.49	1.5
Dolomite	2.88	1.0
Aragonite	3.40	1.0
K Feldspar	3.24	1.0
Plagioclase	3.18	1.0
Calcite	3.03	1.0
Mg calcite	3.00	1.0
Siderite	2.79	1.0
Pyrite	2.70	1.0
Fluorite	1.93	1.0

Statistical analysis of the magnetic and fine fraction mineralogy results were carried out using *Statistica 8* software. Correlation coefficients and the associated level of significance were employed to establish the relationship between heavy minerals levels and magnetic parameters. The Spearman correlation was used in order to minimize the influence of outliers.

1.13. Geochemical analysis: Heavy metals

In this study, heavy metals analysis were performed in Instituto Hidrográfico laboratory in sediment fraction inferior to 2 mm (Figure 11) and the following elements were determined: Arsenic (As), Aluminum (Al) Cadmium (Cd), Chromium (Cr), Copper (Cu), Iron (Fe), Lithium (Li), Mercury (Hg), Nickel (Ni), Lead (Pb) and Zinc (Zn) according to internal technical norms presented in Table 3.

This method was applied on sediments after complete dissolution through microwave using reagents as hydrofluoric acid and *aqua regia*. The quantitative analysis of metals was calculated using the atomic absorption spectrometry.

Table 3 - Technical norms for elements quantification in sediments in Annex 14.

Element	Technical norm
Arsenic	NT.LB.57
Aluminum	NT.LB.17
Cadmium	NT.LB.14
Chromium	NT.LB.15
Copper	NT.LB.07
Iron	NT.LB.16
Lithium	NT.LB.56
Mercury	NT.LB.09
Nickel	NT.LB.13
Lead	NT.LB.12
Zinc	NT.LB.10

Excepting mercury, quantification a certain element is based in sediment extracts by atomic absorption spectrometry with flame air / acetylene, and background correction with deuterium lamps and wavelengths that will vary with the element to be analyzed (ex: lead – 217 nm, zinc – 213.9 nm). For mercury, is used a different method that consists in volatilization of mercury existing in solid samples, resulting in a series of steps of controlled heating, in three decomposition furnaces in an atmosphere of oxygen.

Afterwards, a carbonate correction was made using a dilution factor in order to minimize the natural textural effect. The mathematics for normalizing chemical data is simple and straightforward (Horowitz, 1985).

The dilution factor is given by:

$$\text{Dilution factor} = \frac{100}{100 - carbonate\ percentage}$$

which will be applied to the chemical concentration.

A technique largely applied is 'normalization' where metal concentrations is normalized to a textural or compositional factor of sediments. Normalizing elements relative to Al is widely used to compensate for variations in both grain size and composition, since it represents the quantity of aluminosilicates, which is the predominant carrier phase for adsorbed elements in coastal sediments. Aluminum content was chosen as geochemical normalizer, since it is a conservative element, not significantly affected by early diagenetic processes and/or strong redox effects that are frequently observed in sediments, and it is a major constituent of fine-grained aluminosilicates, which are one of the main transport phases of trace metals (Corredeira *et al.*, 2008).

According to Nolting *et al. (*1999), this method is also a powerful tool for the regional comparison of trace metal content in sediments and can also be applied to determine enrichment factors (EFs) where the formula is as shown below:

$$EF(trace\ element) = \frac{\left(\frac{[trace\ element]}{[Al]}\right) sample}{\frac{\sum_1^n \left(\frac{[trace\ element]}{[Al]}\right)}{n} baseline}$$

The degree of enrichment was classified as follows: 1.5>EF no enrichment, 1.5≤EF<3 minor enrichment, 3≤EF<5 moderate enrichment, 5≤EF<10 moderately severe enrichment, 10≤EF<25 severe enrichment, 25≤EF<50 very severe enrichment, EF>50 extremely severe enrichment (Moreira *et al.*, 2009). For top core sediment samples, the enrichment factor was calculated using two different approaches. The first approach uses the values of the first 20 cm of the sediment core as baselines, since they were the values present in the area, although it was just in one point. The second approach was to use the values of Taylor-McLennan (1985) in order to compare them with published values (Table 4).

Table 4 – Reference values for the determinations of Enrichment Factor (EF)

Baselines	Hg (mg/kg)	Cu (mg/kg)	Zn (mg/kg)	Mn (mg/kg)	Fe (mg/kg)	Pb (mg/kg)	Ni (mg/kg)	Cr (mg/kg)	Al (mg/kg)
Upper continental crust									
Taylor and McLennan, 1985	-	25	71	600	30500	20	20	98	80400
First 20 cm sediment core	0.0734	17	92	330	32751	17	18	61	78436

Statistical analysis of heavy metal data was carried out using *Statistica 8* software. Correlation coefficients and the associated level of significance were employed to establish the relationship between heavy metal levels and magnetic parameters. The Pearson correlation was used in order to minimize the influence of extreme values.

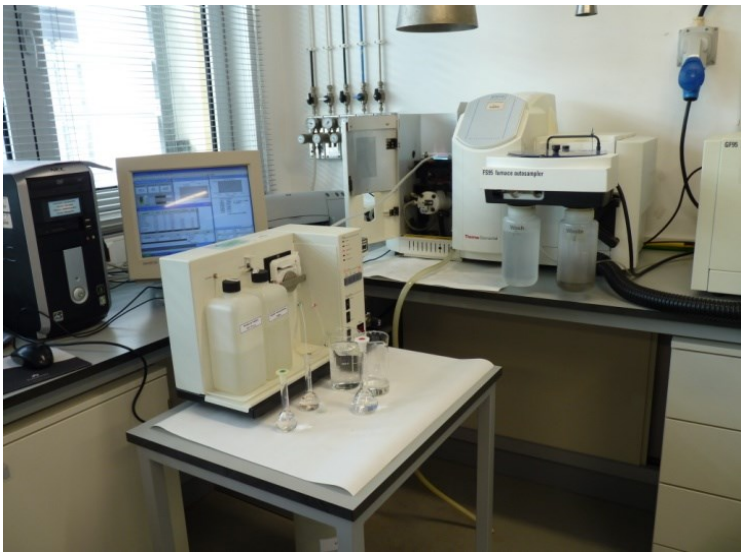

Figure 11 - Chemical laboratory

1.14. Heavy minerals

The general classification of heavy minerals is based on the degree of transparency and, therefore, heavy minerals can be divided in two categories: opaque and non-opaque. Differences in resistance to mechanical erosion and chemical weathering have divided the non-opaque minerals in two groups: ultrastable minerals (zircon, rutile and tourmaline) and metastable minerals (e.g. garnet, olivine, amphiboles, pyroxenes) Rothwell, 1989.

The bulk samples collected were treated with 10 % HCl to remove carbonate materials and then standard wet sieving was performed in three fractions: 0.063, 0125 and 0.250 mm. The sand grains, were then subdivided in light and heavy grains when immersed in a high-density liquid (sodium polytungstate ≈ 2.85 g/cm^3). The heavy sand grains were then mounted on glass slides with Canada balsam (RI = 1.52), and at least 300 grains were counted and identified through a transmitted light microscope to determine the abundance of each mineral type. The minerals identified are the following: tourmaline, andaluzite, staurolite, garnet, phyllossilicates, amphibole, pyroxene, glaucony, zircon, rutile, sphene, alterites and opac minerals.

Also, to have a better perspective of the sediment maturity, a ZTR index was determined. This index represents the proportions of Zircon, Tourmaline and Rutile. These three minerals are considered ultra-stable (Hubert, 1962) and reflect the mineral maturity of the sediment.

1.15. Benthic and Planktonic Foraminifera

For this study it was required the fraction superior to 0.063 mm. The samples were collected from the sediment core every 2 cm till 20 cm, and then every 10 cm till the bottom. The samples were then splitted with a mechanical splitter to ensure sample homogeneity and reliable results (Table 5).

At least 300 specimens were then picked out, and benthic foraminifera was counted and identified with a binocular microscope. Classification up to genera followed the systematic reviewed by Loeblich & Tappan (1988). Planktonic foraminifera were just counted for abundance.

Table 5 – Foraminifera sampling scheme
Number of times the samples were splitted and respective ratio (proportion of sample) for foraminifera identification.

Depth (cm)	Number of times	Ratio
0-2	11	1/2048
2- 4	11	1/2048
4-6	11	1/2048
6-8	11	1/2048
8-10	11	1/2048
10-12	11	1/2048
12-14	11	1/2048
14-16	11	1/2048
16-18	10	1/1024
18-20	10	1/1024
30	12	1/4096
40	12	1/4096
50	11	1/2048
60	12	1/4096
70	12	1/4096
80	12	1/4096
90	12	1/4096
100	11	1/2048
110	12	1/4096
120	7	1/128
130	7	1/128
140	6	1/64
150	6	1/64

The diversity of species in each sample was obtained by the Shannon-Wiener Index (Hs): $Hs = -\sum pi.\ln(pi)$, where pi represents the relative abundance of the species (i) in the sample. Higher values of Hs translate a higher diversity of foraminifera species. Density (or standing crop) is evaluated as the number of benthic foraminifera by cubic centimeter of sediment (individuals/cm^3). A multivariate statistical analysis (*Statistica 8*) was performed on combined

benthic foraminifera species distribution and granulometric parameters, to investigate correlations between the microfauna's and abiotic factors.

Below is the systematic list of the identified benthic foraminifera:

Kingdom **Protista**

Filo **Granuloreticulosa**

Order **Foraminiferida Eichwald, 1830**

Sub-Order Textulariina Delage & Hérouard, 1896

Super-family Textulariacea Ehrenberg, 1838

Family Textulariidae Ehrenberg, 1838

Sub-family Textulariinae Ehrenberg, 1824

Gender **Textularia deFrance**, 1824

***Textularia deltoidea* Reuss, 1850**

Sub-Order Miliolina Delage & Hérouard, 1896

Super-family Miliolacea Ehrenberg, 1839

Family Haverinidae Schwager, 1876

Sub-family Haverininae Schwager, 1876

Gender ***Quinqueloculina*** d'Orbigny, 1826

***Quinqueloculina akneriana* d'Orbigny, 1846**

***Quinqueloculina lamarckiana* d'Orbigny, 1826**

***Quinqueloculina stalkeri* Loeblich & Tappan, 1953**

***Quinqueloculina venusta* Karrer, 1968**

Quinqueloculina sp.1

***Quinqueloculina* sp.2**

Sub-family Miliolinellinae Vella, 1957

Gender ***Pyrgo*** Defrande, 1824

***Pyrgo murrhina* (Schwager, 1866)**

Pyrgo depressa (Schimdt, 1862)

Super-family Spiroloculinidae Wiesner, 1920

Family Spiroplectamminidae Cushman, 1927

Gender ***Spiroloculina*** d'Orbigny, 1826

***Spiroloculina caniculata* d'Orbigny, 1846**

Sub-Order Lagenina Delage & Hérouard, 1896

Super-family Nodosariacea Ehrenberg, 1839

Family Vaginulinidae Reuss, 1860

Sub-family Marginulininae Wedeking, 1937

Gender ***Amphycorina*** Schlumberger, 1881

Amphycorina scalaris **(Batch, 1791)**

Family Lagenidae Reuss, 1862

Gender ***Lagena*** Walker & Jacob, 1798

Lagena **cf.** ***interrupta*** **Williamson, 1868**

Lagena gracilima **(Costa, 1856)**

Lagena laevis **(Montagu, 1803)**

Lagena **sp.1**

Lagena **sp.2**

Family Ellipsolagenidae Silvestre, 1923

Sub-family Elipsolageninae Silvestre, 1923

Gender ***Fissurina*** Reuss, 1850

Fissurina fasciata **(Egger, 1857)**

Fissurina fasciata **(Egger) var.** ***carinata*** **(Sidebottom, 1906)**

Fissurina globosocaudata **Albani & Yassini, 1995**

Fissurina incomposita

Fissurina laevigata **Reuss, 1850**

Fissurina lucida **(Williamson, 1848)**

Fissurina semimarginata

Fissurina submarginata

Fissurina marginata **(Montagu, 1803)**

Fissurina orbignyana **Seguenza, 1862**

Fissurina **sp. 1**

Fissurina **sp. 2**

Sub-family Oolininae Loeblich & Tappan, 1961

Gender ***Oolina*** d'Orbigny, 1839

Oolina alcocki (White, 1956)

Oolina Melo

Oolina hexagona (Williamson, 1948)

Oolina sp.

Sub-Order Rotaliina Delage & Hèrouard, 1896

Super-family Bolivinacea Glaessner, 1937

Family Bolivinidae Glassner, 1937

Gender ***Bolivina*** d'Orbigny, 1839

Bolivina albatrosi

Bolivina ordinaria **Phleger & Parker, 1952**

Bolivina pseudoplicata **Heron-Allen & Earland, 1930**

***Bolivina seminuda* Cushman, 1911**

Bolivina *semipunctata* Höglund, 1947

Bolivina striatula

Bolivina translucens

***Bolivina pseudopunctata* Höglund, 1947**

***Bolivina* sp.**

Gender ***Brizalina*** Costa, 1856

***Brizalina alata* (Seguenza, 1862)**

***Brizalina difformis* (Williamson, 1848)**

***Brizalina spathulata* (Williamson, 1858)**

***Brizalina subaenaeriensis* (Cushman, 1922)**

***Brizalina variabilis* (Williamson, 1858)**

Super-family Cassidulininacea d'Orbigny, 1839

Family Cassidulinidae d'Orbigny, 1839

Gender ***Cassidulina*** d'Orbigny, 1826

***Cassidulina crassa* d'Orbigny, 1839**

***Cassidulina laevigata* d'Orbigny, 1826**

***Cassidulina obtusa* Williamson, 1858**

***Cassidulina teretis* Tappan, 1951**

***Cassidulina bradyi* Norman, 1880**

Cassidulina minuta

Cassidulina sp.

Gender ***Cassidulinoides*** Cushman, 1927

Cassidulinoide bradyi (Norman, 1881)

Gender ***Globocassidulina*** Voloshinova, 1960

***Globocassidulina rossensis* (Kennet, 1967)**

***Globocassidulina subglobosa* (Brady, 1881)**

Super-family Turrilinacea Cushman, 1927

Family Stainforthiidae Reiss, 1963

Gender ***Stainforthia*** Hofker, 1965

Stainforthia elongata

***Stainforthia* cf. *feylingi* (Knudsen & Seiden- krantz, 1994)**

***Stainforthia complanata* (Egger, 1893)**

Super-family Buliminacea Jones, 1875

Family Siphogenererinoididae Saidova, 1981

Sub-family Tubulogenerininae Saidova, 1981

Gender ***Rectuvigerina*** Mathews, 1945

***Rectuvigerina phlegeri* Le Calvez, 1959**

Family Buliminidae Jones, 1875

Gender ***Bulimina*** d'Orbigny, 1826

***Bulimina alazanensis* Cushman, 1927**

***Bulimina elongata* d'Orbigny, 1846**

***Bulimina marginata* d'Orbigny, 1826**

***Bulimina gibba* Fornasini, 1901**

***Bulimina striata* d'Orbigny, 1826 *in* Guérin-Méneville, 1843**

Bulimina aculeata

Bulimina mexicana

Family Uvigerinidae Haeckel, 1894

Sub-family Uvigerininae Haeckel, 1894

Gender ***Uvigerina*** d'Orbigny, 1826

***Uvigerina peregrina* Cushman, 1923**

***Uvigerina* sp.**

Sub-family Angulogerininae Galloway, 1933

Gender ***Trifarina*** Cushman, 1923

***Trifarina angulosa* (Williamson, 1858)**

***Trifarina carinata* (Cushman,** 1923)

Trifarina bradyana

Super-family Discorbacea Ehrenberg, 1838

Family Bagginidae Cushman, 1927

Sub-family Baggininae Cushman, 1927

Gender ***Cancris*** *d*e Montfort, 1808

***Cancris auriculus* (Fichtel, & Moll, 1798)**

Gender ***Valvulineria*** Cushman, 1926

***Valvulineria bradyana* (Fornasini, 1900)**

Valvulineria minuta

Family Rosalinidae Reiss, 1963

Gender ***Gavelinopsis*** Hofker, 1951

***Gavelinopsis praegeri* (Heron-Allen & Earland, 1913)**

Gender ***Rosalina*** d'Orbigny, 1826

Rosalina globularis var anglica d' Orbigny, 1826

***Rosalina* sp.**

Super-family Discorbinellacea Sigal, 1952

Family Pseudoparrellidae Voloshinova, 1952

Sub-family Pseudoparrellinae Voloshinova, 1952

Gender ***Epistominella*** Husezima & Maruhasi, 1944

Epistominella vitrea **Parker, 1953**

Super-family Planorbulinacea Schwager, 1877

Family Cibicididae Cushman, 1927

Gender ***Cibicides*** de Montfort, 1808

Cibicides **cf.** ***pseudoungerianus*** **(Cushman, 1922)**

Cibicides ungerianus **(d'Orbigny, 1846)**

Cibicides **sp. 1**

Cibicides **sp. 2**

Family Planulinidae Bermúdez, 1952

Gender ***Hyalinea*** Hofker, 1951

Hyalinea balthica **(Schröter, 1783)**

Gender ***Lobatula*** Fleming, 1828

Lobatula lobatula **(Walker & Jacob, 1798)**

Family Planorbulininae Schwager, 1877

Sub-family Planorbulininae Schwager, 1877

Gender ***Panorbulina*** d'Orbigny, 1826

Planorbulina **d'Orbigny, 1826**

Super-family Asterigerinacea d'Orbigny, 1839

Family Asterigerinatidae Reiss, 1963

Gender ***Asterigerinata*** Bermúdez, 1949

Asterigerinata **cf.** ***mamilla*** **(Williamson, 1848)**

Asterigerinata **sp.1**

Asterigerinata **sp.2**

Super-family Nonionacea Schultze, 1854

Family Nonionidae Schultze, 1854

Sub-family Nonioninae Schultze, 1854

Gender ***Nonion*** de Montfort, 1808

Nonion fabum **(Fichtel & Moll, 1798)**

Gender ***Nonionella*** Cushman, 1926

Nonionella iridea Heron-Allen & Earland, 1932

Nonionella turgida (Williamson, 1858)

Sub-family Pullenininae Schwager, 1877

Gender ***Melonis*** de Montfort, 1808

Melonis barleanum (Williamson, 1858)

Super-family Chilostomellacea Brady, 1881

Family Oridorsalidae Loeblich &Tappan, 1984

Sub-family Gavelinellidae Hofker, 1956

Gender ***Gyroidina*** d'Orbigny, 1826

Gyroidina umbonata **(Silvestri, 1898)**

Family Chilostomellidae Brady, 1881

Sub-family Chilostomellinae Brady, 1881

Gender ***Chilostomella*** Reuss, 1849

Chilostomella oolina **Schwager, 1878**

Super-family Rotaliacea Ehrenberg, 1839 Brady, 1881

Family Rotaliidae Ehrenberg, 1839

Sub-family Ammoniinae Saidova, 1981

Gender ***Ammonia*** Brünnich, 1772

Ammonia beccarii **(Linnaeus, 1758)**

Family Elphidiidae Galloway, 1933

Gender ***Cribroelphidium*** Cushman & Brönnimann, 1948

Elphidium gerthi **Van Voorthuysen, 1958**

Gender ***Elphidium*** de Montfort, 1808

Elphidium articulatum **(d'Orbigny, 1839)**

Elphidium complanatum **(d'Orbigny, 1839)**

Elphidium **cf.** ***complanatum*** **(d'Orbigny, 1839)**

Elphidium crispum **(Linnaeus, 1758)**

Elphidium discoidale **(d'Orbigny, 1839)**

1.16. Calcareous Nannoplankton

Coccolithophores are a major group of unicellular marine phytoplankton, representing the main component of extant calcareous nannoplankton. Their ability to produce delicate calcite platelets, the coccoliths, combined with their ocean-wide distribution, makes them the most productive calcifying organisms on Earth, with remarkable potential as paleoenvironmental markers (e.g. Winter, 1994; Ziveri *et al*., 2004; Silva *et al*., 2008).

Most of the late Quaternary species are also currently thriving in the world's oceans. Up to 200 extant coccolithophore species have been described so far (e.g., Winter, 1994), of which 30–40 are common in the sedimentary record. Of the 13–15 classified extant coccolithophore families, 6, whose representative species are both ecologically significant and abundant in the fossil record, are commonly used in late Quaternary palaeoceanographic studies. The Class Prymnesiophyceae includes both calcifying (e.g., *Emiliania, Gephyrocapsa, Coccolithus*) and non-calcifying taxa (e.g., *Phaeocystis, Prymnesium*). Coccoliths (calcareous plates with average

length = 7– 8 µm) link to form a spherical external skeleton, the coccosphere (average diameter 20 µm), which surrounds the living cell.

These plates have great value for palaeoceanographic studies, considering the importance of such information for refining the ecological niches of key taxa used in palaeoceanographic studies, to better understand sedimentation processes in the water column and at the water-sediment interface, and assessing the coccolith contribution to the global budget of biogenic carbonate (Giraudeau & Beaufort, 2007). The taxonomy of coccolithophore species relies historically on the morphological characteristics of coccoliths preserved in the sedimentary record (e.g., Tappan, 1980; Perch-Nielsen, 1985).

For the study of calcareous nannoplankton, samples from 10 levels were analyzed (0 – 2 cm, 10 – 12 cm, 20 – 22 cm, 32 – 34 cm, 52 – 54 cm, 75 – 77 cm, 109 – 111 cm, 125 – 127 cm, 137 – 139 cm and 157 – 159 cm). The technique of Random Settling, was developed by Flores & Sierro (1997) for samples of oceanic facies and later adapted to neritic facies (medium Portuguese continental shelf) and paralic (lagoons and estuaries) (Ferreira & Cachão, 2003). This methodology allows the quantification of absolute abundances of calcareous nannoplankton, by calculating the number of individuals per gram of sediment. The Random Settling also has the advantage of producing slides with evenly distributed; allowing the analysis of the total association or just of specific *taxa*.

Slides were observed under optical polarizing microscope (Olympus BX-40), at 1250× magnification. Quantification of the calcareous nannoplankton content (nannoliths/g) of each sample was determined according to the equation:

$$N = n \times \frac{V}{Vp} \times \frac{Pa}{Oa} \times \frac{1}{p}$$

Where,

N = nannoliths/g,

n = counted number of nannoliths,

V = volume of the bottle (10 000 ml),

Vp = volume pipette,

Pa = Petri dish area,

Oa = observed area,

p = sediment weight.

Below is the taxonomy of coccolithophores:

For taxonomic references, see Jordan *et al*. (2004)

Kingdom CHROMISTA Cavalier-Smith, 1986

Division HAPTOPHYTA Hibberd, 1972

Class PRYMNESIOPHYCEAE Hibbert, 1976 emend. Cavalier-Smith *et al*., 1996

Order COCCOLITHALES Schwartz, 1932 emend. Edvardsen *et al*., 2000

Family CALCIDISCACEAE Young and Bown, 1997

Genus *Calcidiscus* Kampter, 1950

*Calcidiscus leptoporus** (Murray and Blackman, 1898) Loeblich and Tappan, 1978

Genus *Umbilicosphaera* Lohmann, 1902

*Umbilicosphaera sibogae** (Weber-van Bosse, 1901) Gaarder, 1970

Family COCCOLITHACEAE Poche, 1913 emend. Young and Bown, 1997

Genus *Coccolithus* Schwartz, 1894

*Coccolithus pelagicus subsp. braarudii** (Gaarder, 1962) Geisen *et al*., 2002

Order ISOCHRYSIDALES Pascher, 1910 emend. Edvardsen and Eikrem in Edvardsen *et al*., 2000

Family NOELAERHABDACEAE Jerkovic, 1970 emend. Young and Bown, 1997

Genus *Emiliania* Hay and Mohler in Hay *et al*., 1967

Emiliania huxleyi *(Lohmann, 1902) Hay and Mohler, 1967

Genus *Gephyrocapsa* Kamptner, 1943

*Gephyrocapsa ericsonii** McIntyre and Bé, 1967

*Gephyrocapsa muellerae** Bréhéret, 1978

*Gephyrocapsa oceanica** Kamptner, 1943

Genus *Reticulofenestra* Hay, Mohler and Wade, 1966

Reticulofenestra haqii Backmann, 1978

Reticulofenestra minutula (Gartner, 1967) Haq and Berggren, 1978

Genus *Dictyococcites* M. Balck, 1967

Dictyococcites antarticus Haq, 1976

Order SYRACOSPHAERALES Hay, 1977 emend. Young *et al*., 2003

Family CALCIOSOLENIACEAE Kamptner 1937

Genus *Calciosolenia* Gran 1912; emend. Young *et al*. 2003

Family RHABDOSPHAERACEAE Haeckel 1894

Genus *Rhabdosphaera** Haeckel 1894

Rhabdosphaera clavigera Murray and Blackman 1898

Family SYRACOSPHAERACEAE (Lohmann, 1902) Lemmermann, 1903

Genus *Syracosphaera* Lohmann, 1902

Syracosphaera pulchara Lohmann, 1902

Order PODORHABDALES

Family *Tubodiscaceae* Bown & Rutledge, 1997

Genus *Tubodiscus* Thierstein

Tubodiscus sp.

GENERA INCERTAE SEDIS

Order ZYGODISCALES Young and Bown, 1997

Family HELICOSPHAERACEAE Black, 1971 emend. Jafar and Martini, 1975

Genus *Helicosphaera* Kamptner, 1954

*Helicosphaera carteri var. carteri** (Wallich, 1877) Kamptner, 1954

Family PONTOSPHAERACEAE Lemmermann 1908

Genus *Pontosphaera** Lohmann 1902

Genus *Scyphosphaera* Lohmann 1902

Pontosphaera discopora Schiller, 1925

NANNOLITH-BEARING FAMILIES

Family *Braarudosphaeraceae* Deflandre, 1947

Genus *Braarudosphaera* Deflandre, 1947

Braarudosphaera bigelowi (Gran & Braarud, 1935) Deflandre, 1947

1.17. GSTA (Geostatistical trend analysis)

On the continental shelf 164 samples of non-consolidated surface sediments, distributed along several E-W profiles were selected (Figure 12). These considered samples were collected in two different time frames. The area north of Peniche was sampled between November 1995 and October 1996, while the southern area was covered between January and May 1999, using a grab-type Smith-McIntyre sampler, during the cruise sponsored by the Portuguese Instituto Hidrográfico, in the framework of the SEPLAT program (which aimed to mapping of surface

sediment on the Portuguese Continental Shelf and upper slope). The laboratory sample processing was done in the laboratory of sedimentology of the Portuguese Instituto Hidrográfico.

Sedimentary analysis included grain-size (sieving method) and the fine fraction was treated using the laser diffraction method.

For each sampling position three parameters were extracted by the method of moments: mean (μ), sorting (σ) and skewness (Sk). Grain-size parameters distribution maps were constructed using ArcGIS® 9.3 (ESRI). Vector characteristics (magnitude and length) were obtained through GSTA software. The Gao & Collins (1992) state GSTA is a two-dimensional method that determines trend vectors through regular or irregular grids of sampling sites. Vectors were graphed using the application Surfer® 8.01 (Golden Software). The distance at which neighboring stations have a correlation (characteristic distance - Dcr) was computed through a geostatistical approach as recommended by Poizot *et al*, (2006).

1.18. Wave modeling

In this study, the wave climate in the NEA Ocean was hindcasted with the version 3.14 of the third-generation spectral wave model WAVEWATCH IIITM (henceforth denoted as WW3) (Tolman, 2009). For this study only a series of 22 years of oceanographic data was used (1953-1975). These data where then used in SWAN (SWAN Team, 2006), a third-generation wave model for obtaining realistic estimates of wave parameters in coastal areas, lakes and estuaries from given wind, bottom and current conditions.

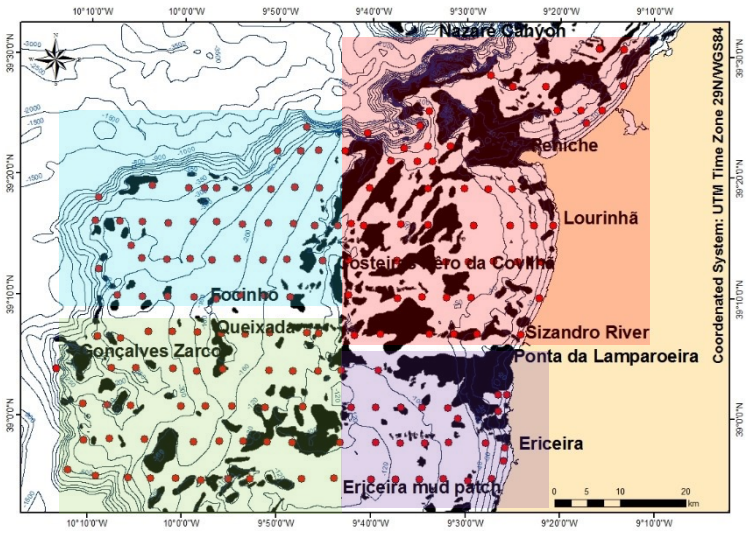

Figure 12 – Sediment samples location (red). Rocky outcrops (black) from IH (2005) Red square – northern rocky shelf; Violet square – Ericeira mud patch; Green square – southern outer shelf; Blue square – northern outer shelf.

1.19. Currents

From the current meter deployed at 250 m depth (Figure 13), the data acquired during a three-month period (November 2010, December 2010 and January 2011) was filtered with a 33 hours butterworth filter in order to remove mesoscale tidal effects. The current meter deployed at 100 m depth was declared missing, since it was lost and no data was retrieved, probably due to fishnets.

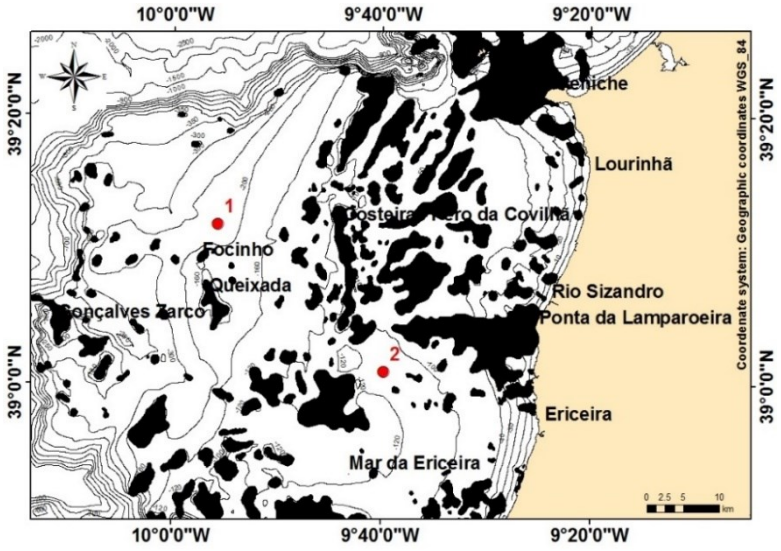

Figure 13 – Current meter deployment location
Number 1 – outer continental shelf at 250 m depth; number 2 – Ericeira mud patch at 100 m depth

List of References

Alves, E. Q., Macario, K., Ascough, P., & Bronk Ramsey, C. (2018). The Worldwide Marine Radiocarbon Reservoir Effect: Definitions, Mechanisms, and Prospects. Reviews of Geophysics, 56, 278–305. https://doi.org/10.1002/2017rg000588

Axelsson, V. (1983). The use of X-ray radiographic methods in studying sedimentary properties and rates of sediment accumulation. Paleolimnology, 65–69. https://doi.org/10.1007/978-94-009-7290-2_10

Bouma, A. H. (1969). Methods for the study of sedimentary structures. John Wiley and Sons, New York. xvi + 458. Limnology and Oceanography, 14, 966–966. https://doi.org/10.4319/lo.1969.14.6.0966a

Linné Carl von. (1767). Systema naturae per regna tria naturae. secundum classes, ordines, genera, species cum characteribus, differentiis, synonymis, locis ; tomus I-tomus Iii. Typis Ioannis Thomae nob. de Trattnern, caes. reg. aulae typogr. et bibliopolae.

Coles, M. E., Hazlett, R. D., Spanne, P., Soll, W. E., Muegge, E. L., & Jones, K. W. (1998). Pore level imaging of fluid transport using synchrotron X-ray microtomography. Journal of Petroleum Science and Engineering, 19, 55–63. https://doi.org/10.1016/s0920-4105(97)00035-1

Corredeira, C., Araújo, M., & Jouanneau, J. (2008). Copper, zinc and lead impact in SW Iberian shelf sediments: An assessment of recent historical changes in Guadiana river basin. Geochemical Journal, 42, 319–329. https://doi.org/10.2343/geochemj.42.319

Dadey, A., Janecek, R., & Klaus, A. (1992). (Table 1) Density values of ODP Leg 126 samples. PANGAEA, https://doi.org/10.1594/PANGAEA.775336.

Dearing, J. (1999). Magnetic susceptibility, in J. Walden, F. Oldfield, J. Smith (eds), Environmental Magnetism: A Practical Guide. Technical Guide 6, Quaternary Research Association, London, 35-62.

Dias, A. (2004). A análise sedimentar e o conhecimento dos sistemas marinhos (Uma Introdução à Oceanografia Geológica). Faro. Universidade do Algarve. 84p.

Ferreira J., Cachão, M. (2003). Nanofósseis calcários em fácies costeiras: revisão de técnicas de estudo. Ciências Da Terra (UNL), V, 76–78.

Flores, J. A., Sierro, F. J. (1997). Revised Technique for Calculation of Calcareous Nannofossil Accumulation Rates. Micropaleontology, 43, 321. https://doi.org/10.2307/1485832

Gao S., & Collins, M. (1992). Net sediment transport patterns inferred from grain-size trends, based upon definition of "transport vectors." Sedimentary Geology, 81, 47–60. https://doi.org/10.1016/0037-0738(92)90055-v

Giraudeau, J., & Beaufort, L. (2007). Coccolithophores: from extant populations to fossil assemblages, Proxies in Late Cenozoic paleoceanography–Developments in Marine Geology, edited by: Hillaire-Marcel, C. and De Vernal, A., Elsevier, 409-439, 2007.

Giraudeau, J., & Beaufort, L. (2007). Radiocarbon Dating of Deep-Sea Sediments. In: Konrad A. Hughen (eds.). Proxies in late cenozoic paleoceanography. Elsevier, The Netherlands, 409-439.

Hall I.R., & McCave, I. N. (2000). Palaeocurrent reconstruction, sediment and thorium focusing on the Iberian margin over the last 140 ka. Earth and Planetary Science Letters, 178, 151–164. https://doi.org/10.1016/s0012-821x(00)00068-6

Holyer, R.J., Young, D. K., Sandidge, J. C., & Briggs, K. B. (1996). Sediment density structure derived from textural analysis of cross-sectional X-radiographs. Geo-Marine Letters, 16, 204–211. https://doi.org/10.1007/bf01204510

Horowitz, A. J. (1985). A primer on trace metal-sediment chemistry, U.S. Geological Survey Water Supply Paper 2277, 67p. https://doi.org/10.3133/wsp2277

Hubert, F. J. (1962). A Zircon-Tourmaline-Rutile Maturity Index and the Interdependence of the Composition of Heavy Mineral Assemblages with the Gross Composition and Texture of Sandstones. SEPM Journal of Sedimentary Research, 32, 440–450. https://doi.org/10.1306/74d70ce5-2b21-11d7-8648000102c1865d

Ising, G. (1943). On the magnetic properties of varved clay. Ark. Mat. Astron, 29, 1-37.

Jackson, P.D., Briggs, K. B., & Flint, R. C. (1996). Evaluation of sediment heterogeneity using microresistivity imaging and X-radiography. Geo-Marine Letters, 16, 219–225. https://doi.org/10.1007/bf01204512

Lerman, A. (2009) Carbon Cycle. In: Gornitz V. (eds) Encyclopedia of Paleoclimatology and Ancient Environments. Encyclopedia of Earth Sciences Series. Springer, Dordrecht. https://doi.org/10.1007/978-1-4020-4411-3_28

Loeblich, A. R., & Tappan, H. (1988). Foraminiferal Genera and Their Classification. https://doi.org/10.1007/978-1-4899-5760-3

Mackenzie, F. T., & Lerman, A. (2006). Carbon in the Geobiosphere — Earth's Outer Shell. Topics in Geobiology, 402p. https://doi.org/10.1007/1-4020-4238-8

Maher, B. A., & Thompson, R. (1999). Quaternary Climates, Environments and Magnetism. Cambridge, New York. Geological Magazine, 137, 705-712. doi:10.1017/S0016756800254733.

McCave, I. N., Manighetti, B., & Robinson, S. G. (1995). Sortable silt and fine sediment size/composition slicing: Parameters for palaeocurrent speed and palaeoceanography. Paleoceanography, 10, 593–610. https://doi.org/10.1029/94pa03039

Moreira, C. S., Brunet, D., Verneyre, L., Sá, S. M., Galdos, M. V., Cerri, C. C., & Bernoux, M. (2009). Near infrared spectroscopy for soil bulk density assessment. European Journal of Soil Science, 60, 785–791. https://doi.org/10.1111/j.1365-2389.2009.01170.x

Nolting, R.F., Ramkema, A., & Everaarts, J. M. (1999). The geochemistry of Cu, Cd, Zn, Ni and Pb in sediment cores from the continental slope of the Banc d'Arguin (Mauritania). Continental Shelf Research, 19, 665–691. https://doi.org/10.1016/s0278-4343(98)00109-5

Oliveira, A. T. C. (2001). Dinâmica da matéria particulada em suspensão na plataforma continental minhota e a sua relação com a cobertura sedimentar (PhD Thesis unpublished). Universidade do Algarve, 278 pp.

Perch-Nielsen K. (1985). Cenozoic calcareous nannofossils. In: H. M. Bolli, J. B. Saunders & K. Poizot, E., Mear, Y., Thomas, M., Garnaud, S. (2006). The application of geostatistics

in defining the characteristic distance for grain size trend analysis. Computers & Geosciences 32, 360–370.

Rothwell, R. G. (1989). Minerals and Mineraloids Occurring in Marine Sediments. Minerals and Mineraloids in Marine Sediments, 27–35. https://doi.org/10.1007/978-94-009-1133-8_3

Silva, A., Palma, S., & Moita, M. T. (2008). Coccolithophores in the upwelling waters of Portugal: Four years of weekly distribution in Lisbon bay. Continental Shelf Research, 28, 2601–2613. https://doi.org/10.1016/j.csr.2008.07.009

Snowball, I., Sandgren, P., & Petterson, G. (1999). The mineral magnetic properties of an annually laminated Holocene lake-sediment sequence in northern Sweden. The Holocene, 9, 353–362. https://doi.org/10.1191/095968399670520633

SWAN Team (2006). SWAN: Technical Documentation. SWAN Cycle III version 40.51, Delft University of Technology, electronic version: in http://falk.ucsd.edu/modeling/swantech.pdf

Taylor, S. R., & McLennan, S. (1985). Composition and evolution of the continental crust. Planetary Crusts, 301–324. https://doi.org/10.1017/cbo9780511575358.014

Tolman, H.L. (2009). User Manual and System Documentation of WAVEWATCH-III Version 1.18, NOAA / NWS / NCEP / OMB Technical Note 166, 110 pp.

Winter, A., & Siesser, W. G. (1994). Coccolithophores. Cambridge University Press.

Ziveri, P., Baumann, K.-H., Böckel, B., Bollmann, J., & Young, J. R. (2004). Biogeography of selected Holocene coccoliths in the Atlantic Ocean. Coccolithophores, 403–428. https://doi.org/10.1007/978-3-662-06278-4_15

Annex 2. Grain-size from river, beach and shelf samples

(class)	phi	777	778	781	784	786	788	793	796	798	2444	2445	2446	2447	2448	2449	2450	10606	10635	145	297	953	959	978	984
>64.00mm	**<6.0 phi**	0.00	0.00	0.00	0.00	0.00	0.00	0.00	0.00	0.00	0.00	0.00	0.00	0.00	0.00	0.00	0.00	0.00	0.00	0.00	0.00	0.00	0.00	0.00	0.00
45.25-64.00mm	**-5.5,6.0 phi**	0.00	0.00	0.00	0.00	0.00	0.00	0.00	0.00	0.00	0.00	0.00	0.00	0.00	0.00	0.00	0.00	0.00	0.00	0.00	0.00	0.00	0.00	0.00	0.00
32.00-45.25mm	**-5.0,-5.5 phi**	0.00	0.00	0.00	0.00	0.00	0.00	0.00	0.00	0.00	0.00	0.00	0.00	0.00	0.00	0.00	0.00	0.00	0.00	0.00	0.00	0.00	0.00	0.00	0.00
22.63-32.00mm	**-4.5,-5.0 phi**	0.00	0.00	0.00	0.00	0.00	0.00	0.00	0.00	0.00	0.00	0.00	0.00	0.00	0.00	0.00	0.00	0.00	0.00	0.00	0.00	0.00	0.00	0.00	0.00
16.00-22.63mm	**-4.0,-4.5**	0.00	0.00	0.00	0.00	0.00	0.00	0.00	0.00	0.00	0.00	0.00	0.00	0.00	0.00	0.00	0.00	0.00	0.00	0.00	0.00	0.00	0.00	0.00	0.00
11.31-16.00mm	**-3.5,-4.0**	0.00	0.00	0.00	0.00	0.00	0.00	0.00	0.00	0.00	0.00	0.00	0.00	0.00	0.00	0.00	2.88	0.00	0.00	0.00	0.00	0.00	0.00	0.00	0.00
8.00-11.31mm	**-3.0,-3.5**	0.00	0.00	0.00	0.00	0.00	0.00	0.00	0.00	0.00	0.00	0.00	2.44	0.00	0.00	0.00	3.15	0.00	0.00	0.00	0.00	0.51	0.00	0.00	0.00
5.66-8.00mm	**-2.5,-3.0**	0.00	0.00	1.81	0.00	0.00	0.00	0.00	0.00	0.00	1.25	0.00	1.23	0.44	0.00	0.00	4.50	0.00	0.00	0.00	0.00	0.02	0.00	0.00	0.00
4.00-5.66mm	**-2.5,-2.0**	0.06	0.05	2.03	0.00	0.00	0.00	0.06	0.00	0.06	0.66	0.36	3.14	0.10	0.00	0.03	5.73	0.00	0.01	0.00	0.00	0.02	0.00	0.14	0.12
4.00 - 2.83mm	**-2.0, -1.5**	0.20	0.07	4.52	0.00	0.25	0.00	0.19	0.04	0.10	1.13	0.68	2.86	0.41	0.00	0.59	8.10	0.04	0.00	0.00	0.00	0.11	0.00	0.10	0.34
2.83 - 2.00mm	**-1.5, -1.0**	1.21	0.41	7.52	0.00	1.94	0.08	0.73	0.09	0.12	1.47	1.31	2.14	0.56	0.00	0.52	9.41	0.03	0.06	0.02	0.01	0.11	0.01	0.15	0.98
2.00 - 1.41mm	**-1.0, -0.5**	6.97	2.44	15.08	0.00	9.64	0.26	2.19	1.26	0.60	1.47	3.18	2.53	1.33	0.01	1.04	13.34	0.09	0.08	0.33	0.03	0.09	0.04	0.24	0.99
1.41 - 1.00mm	**-0.5, 0.0**	19.75	12.22	17.35	0.00	27.30	2.50	7.37	16.56	3.56	1.79	5.63	2.52	3.73	0.02	1.77	14.42	0.13	0.09	0.78	0.15	4.93	0.09	0.42	0.20
1.00 - 0.71mm	**0.0, 0.5**	32.86	32.67	11.70	0.02	34.12	19.52	33.17	55.49	20.63	2.04	13.04	8.00	12.93	0.05	4.67	16.62	0.33	0.18	1.20	4.12	4.95	0.16	0.57	0.39
0.71 - 0.50mm	**0.5, 1.0**	34.97	36.80	21.68	4.58	23.36	61.75	49.05	25.85	55.49	5.30	24.76	18.83	30.05	0.27	11.68	16.23	1.02	0.76	1.21	19.81	5.04	0.78	3.09	4.87
500.00 - 354.00 µm	**1.0, 1.5**	3.00	9.98	12.57	28.59	2.51	12.70	6.22	0.63	14.85	8.36	15.10	20.58	18.44	1.46	9.40	2.67	6.83	7.12	0.53	27.83	2.44	6.60	9.99	15.31
354.00 - 250.00 µm	**1.5, 2.0**	0.95	4.80	5.34	44.49	0.83	3.13	1.02	0.08	4.42	12.76	14.58	15.68	14.04	3.45	11.10	1.30	20.55	20.49	4.53	28.22	13.09	18.22	19.82	27.36
250.00 - 177.00 µm	**2.0, 2.5**	0.04	0.57	0.41	20.48	0.05	0.07	0.00	0.00	0.16	13.21	9.95	6.80	6.09	5.45	10.57	0.23	30.45	29.94	16.18	15.88	26.46	27.47	25.21	27.94
177.00 - 125.00 µm	**2.5, 3.0**	0.00	0.00	0.00	1.82	0.00	0.00	0.00	0.00	0.00	10.11	4.75	1.46	1.31	6.74	8.50	0.00	25.96	25.40	28.73	3.84	26.87	26.10	21.86	16.48
125.00 - 88.40 µm	**3.0, 3.5**	0.00	0.00	0.00	0.00	0.00	0.00	0.00	0.00	0.00	6.47	1.52	0.64	0.57	7.03	5.76	0.08	12.28	12.14	28.62	0.10	13.33	15.54	12.69	4.79
88.40 - 62.50 µm	**3.5, 4.0**	0.00	0.00	0.00	0.00	0.00	0.00	0.00	0.00	0.00	4.35	0.46	1.26	1.13	6.61	3.59	0.17	2.28	2.48	15.25	0.00	2.02	4.82	4.30	0.22
62.50 - 44.20 µm	**4.0, 4.,5**	0.00	0.00	0.00	0.00	0.00	0.00	0.00	0.00	0.00	3.60	0.41	1.37	1.23	6.10	2.76	0.15	0.00	0.01	2.63	0.00	0.00	0.17	0.41	0.00
44.20 - 31.25 µm	**4.5, 5.0**	0.00	0.00	0.00	0.00	0.00	0.00	0.00	0.00	0.00	3.31	0.44	1.06	0.95	5.89	2.88	0.11	0.00	0.05	0.00	0.00	0.00	0.00	0.03	0.00
31.25 - 22.10 µm	**5.0, 5.5**	0.00	0.00	0.00	0.00	0.00	0.00	0.00	0.00	0.00	3.05	0.39	0.91	0.81	6.19	3.24	0.11	0.00	0.55	0.00	0.00	0.00	0.00	0.40	0.00
22.10 - 15.63 µm	**5.5, 6.0**	0.00	0.00	0.00	0.00	0.00	0.00	0.00	0.00	0.00	2.90	0.38	0.99	0.89	6.87	3.47	0.13	0.00	0.51	0.00	0.00	0.00	0.00	0.40	0.00
15.63 - 11.00 µm	**6.0, 6.5**	0.00	0.00	0.00	0.00	0.00	0.00	0.00	0.00	0.00	2.86	0.45	1.09	0.97	7.41	3.49	0.13	0.00	0.11	0.00	0.00	0.00	0.00	0.17	0.00
11.00 - 7.81 µm	**6.5, 7.0**	0.00	0.00	0.00	0.00	0.00	0.00	0.00	0.00	0.00	2.76	0.51	1.04	0.94	7.28	3.27	0.12	0.00	0.00	0.00	0.00	0.00	0.00	0.00	0.00
7.81 - 5.52 µm	**7.0, 7.5**	0.00	0.00	0.00	0.00	0.00	0.00	0.00	0.00	0.00	2.50	0.50	0.89	0.80	6.53	2.85	0.10	0.00	0.00	0.00	0.00	0.00	0.00	0.00	0.00
5.52 - 3.91 µm	**7.5, 8.0**	0.00	0.00	0.00	0.00	0.00	0.00	0.00	0.00	0.00	2.19	0.44	0.73	0.66	5.68	2.40	0.08	0.00	0.00	0.00	0.00	0.00	0.00	0.00	0.00
3.91 - 2.76 µm	**8.0, 8.5**	0.00	0.00	0.00	0.00	0.00	0.00	0.00	0.00	0.00	1.92	0.37	0.61	0.55	5.01	2.02	0.07	0.00	0.00	0.00	0.00	0.00	0.00	0.00	0.00
2.76 - 1.95 µm	**8.5, 9.0**	0.00	0.00	0.00	0.00	0.00	0.00	0.00	0.00	0.00	1.63	0.31	0.50	0.44	4.27	1.64	0.06	0.00	0.00	0.00	0.00	0.00	0.00	0.00	0.00
1.95 - 1.38 µm	**9.0, 9.5**	0.00	0.00	0.00	0.00	0.00	0.00	0.00	0.00	0.00	1.22	0.23	0.36	0.32	3.20	1.18	0.04	0.00	0.00	0.00	0.00	0.00	0.00	0.00	0.00
1.38 - 0.98 µm	**9.5, 10.0**	0.00	0.00	0.00	0.00	0.00	0.00	0.00	0.00	0.00	0.78	0.16	0.23	0.21	2.03	0.73	0.03	0.00	0.00	0.00	0.00	0.00	0.00	0.00	0.00
0.98 - 0.69 µm	**10.0, 10.5**	0.00	0.00	0.00	0.00	0.00	0.00	0.00	0.00	0.00	0.46	0.08	0.10	0.09	1.17	0.42	0.02	0.00	0.00	0.00	0.00	0.00	0.00	0.00	0.00
0.69 - 0.49 µm	**10.5, 11.0**	0.00	0.00	0.00	0.00	0.00	0.00	0.00	0.00	0.00	0.29	0.00	0.00	0.00	0.71	0.26	0.01	0.00	0.00	0.00	0.00	0.00	0.00	0.00	0.00
0.49 - 0.35 µm	**11.0 , 11.5**	0.00	0.00	0.00	0.00	0.00	0.00	0.00	0.00	0.00	0.17	0.00	0.00	0.00	0.43	0.16	0.00	0.00	0.00	0.00	0.00	0.00	0.00	0.00	0.00
0.35 - 0.24 µm	**11.5, 12.0**	0.00	0.00	0.00	0.00	0.00	0.00	0.00	0.00	0.00	0.00	0.00	0.00	0.00	0.15	0.00	0.00	0.00	0.00	0.00	0.00	0.00	0.00	0.00	0.00
0.24 - 0.17 µm	**12.0, 12.5**	0.00	0.00	0.00	0.00	0.00	0.00	0.00	0.00	0.00	0.00	0.00	0.00	0.00	0.00	0.00	0.00	0.00	0.00	0.00	0.00	0.00	0.00	0.00	0.00
0.17 - 0.12 µm	**12.5, 13.0 phi**	0.00	0.00	0.00	0.00	0.00	0.00	0.00	0.00	0.00	0.00	0.00	0.00	0.00	0.00	0.00	0.00	0.00	0.00	0.00	0.00	0.00	0.00	0.00	0.00
0.12 - 0.09 µm	**13.0, 13.5 phi**	0.00	0.00	0.00	0.00	0.00	0.00	0.00	0.00	0.00	0.00	0.00	0.00	0.00	0.00	0.00	0.00	0.00	0.00	0.00	0.00	0.00	0.00	0.00	0.00
0.09 - 0.06 µm	**13.5, 14.0phi**	0.00	0.00	0.00	0.00	0.00	0.00	0.00	0.00	0.00	0.00	0.00	0.00	0.00	0.00	0.00	0.00	0.00	0.00	0.00	0.00	0.00	0.00	0.00	0.00
0.06 - 0.04 µm	**14.0, 14.5 phi**	0.00	0.00	0.00	0.00	0.00	0.00	0.00	0.00	0.00	0.00	0.00	0.00	0.00	0.00	0.00	0.00	0.00	0.00	0.00	0.00	0.00	0.00	0.00	0.00
0.04 - 0.03 µm	**14.5, 15.0 phi**	0.00	0.00	0.00	0.00	0.00	0.00	0.00	0.00	0.00	0.00	0.00	0.00	0.00	0.00	0.00	0.00	0.00	0.00	0.00	0.00	0.00	0.00	0.00	0.00
0.03 - 0.02 µm	**15.0, 15.5 phi**	0.00	0.00	0.00	0.00	0.00	0.00	0.00	0.00	0.00	0.00	0.00	0.00	0.00	0.00	0.00	0.00	0.00	0.00	0.00	0.00	0.00	0.00	0.00	0.00

Annex 3. Fine mineralogy from river and shelf samples

Fine Mineralogy Shelf - River											

x	y	Samples	Illite	Kaolinite	Quartz	Opal	FK	Plagioclase	Calcite	Dolomite	Siderite
-9,373	**39,080**	2444	17	16	17	2	20	12	11	4	1
-9,326	**39,183**	2445	7	6	18	3	23	12	29	0	2
-9,326	**39,262**	2446	15	4	15	2	29	23	4	2	0
-9,200	**39,388**	2447	14	15	21	2	38	5	3	0	1
-9,361	**39,351**	2448	23	4	22	5	19	13	14	0	1
-9,150	**39,501**	2449	24	15	17	3	20	6	13	0	1
-9,410	**38,938**	2450	5	2	9	0	9	15	61	0	0
-9,403	**39,116**	978	20	0	13	3	16	16	13	0	0
-9,453	**38,917**	953	13	0	19	4	11	11	24	0	2
-9,430	**38,960**	959	5	0	17	3	21	21	12	0	0
-9,222	**39,460**	10635	17	2	12	2	18	18	11	0	0
-9,288	**39,409**	10606	6	1	15	3	22	22	6	0	1
-9,367	**39,217**	297	14	0	15	7	17	17	28	0	3
-9,380	**39,267**	145	9	0	21	4	8	26	28	0	0

Annex 4. Heavy metals and minerals from river, beach and shelf samples

	heavy_minerals 1_2										
	Tourmaline	Andaluzite	Staurolite	Garnet	Phyllossilicates	Zircon	Rutile	Monazite	Amphibole	Pyroxene	Glaucony
2446	20	3	4	1	5						
2448		18									
2445	34	5	10	4	2					4	
2447	67	7	2							13	
2449	38	9	14	9	61						
2444	15	2	4					2	8	65	
2450	9	2	5						17	120	

	Tourmaline	Andaluzite	Staurolite	Garnet	Phyllossilicates	Zircon	Rutile	Monazite	Amphibole	Pyroxene	Glaucony
10606	2	3								1	
978	9	1		2	2					7	
984	8	2	1								
297	44	12	7	5				2		4	
959	1	1								1	
145											
953		5									
10635	8	7	4								

	Tourmaline	Andaluzite	Staurolite	Garnet	Phyllossilicates	Zircon	Rutile	Monazite	Amphibole	Pyroxene	Glaucony
778	59	59	4	1	2				1		
777	119	65	25	6	2				8		
788	50	10		5							
786	20	13	3	1					1	4	
781	79	14	16	7					2		
796	22	8	5	6					29	36	
784	12	2									
793	43	15	62	53					11	8	
798	54	13	27	41		4		1	36	89	

	heavy minerals 2_3											
	Tourmaline	Andaluzite	Staurolite	Garnet	Phyllos	Zircon	Rutile	Monazite	Amphibole	Pyroxene	Glaucony	
2446	33	29	16	4	115							
2448	76	13	30	15						7		
2445	58	57	20	8		3				2		
2447	88	37	27	2						11		
2449	61	15	22	11	50	3						
2444	26	3	13	22	2	2		1	12	81		
2450	1		1	2	2				11	121		

	Tourmaline	Andaluzite	Staurolite	Garnet	Phyllos	Zircon	Rutile	Monazite	Amphibole	Pyroxene	Glaucony	
10606	88	33	36	2	3	3				19		
978	72	42	17	31	1	17			9	30		
984	59	35	17	22		1			8			
297	46	30	29	34		10		2	3	33		
959	77	48	8	27		1	1	5	7	27		
145	37	32	9	4	18	2			20	7		
953	61	39	32	29				1	7	25		
10635	52	47	11	28	3			2	2	4		

	Tourmaline	Andaluzite	Staurolite	Garnet	Phyllos	Zircon	Rutile	Monazite	Amphibole	Pyroxene	Glaucony	
778	78	58	23	5					24	1		
777	60	84	35	12				3	24			
788	67	15	26	18		3			2			
786	23	20	1	8								
781	81	9	19	29				1				
796	14	2	10	7		2		1	2	8		
784	128	56	50	12		7			5			
793	13	4	41	111		17		4				
798	18	8	38	76		11		3	2	20		

	heavy minerals 3_4													
	Tourmaline	Andaluzite	Staurolite	Garnet	Phyllos	Zircon	Rutile	Monazite	Amphibole	Pyroxene	Glaucony			
2446	31	3	9	10	100	6								
2448	51	4	15	15	34	7				2				
2445	56	71	9	13	3	31		2		5				
2447	69	13	18	21	23	14	1	1		8				
2449	54	4	32	20	28	7								
2444	37	2	11	39	6	9	1	1	4	41				
2450	1	1	1	3	1	2			12	110				

	Tourmaline	Andaluzite	Staurolite	Garnet	Phyllos	Zircon	Rutile	Monazite	Amphibole	Pyroxene	Glaucony			
10606	31	17	49	26		24				8				
978	44	9	25	47	9	50	5	5	9	12				
984	41	16	22	55		52		11	9					
297	22	7	18	58		31		11	4	10				
959	29	8	3	60		48	1	19	4	7				
145	54	20	19	36	4	3		8	17	7				
953	37	15	25	48		43	3	7	12	26				
10635	50	21	25	59		51		5	5	5				

	Tourmaline	Andaluzite	Staurolite	Garnet	Phyllos	Zircon	Rutile	Monazite	Amphibole	Pyroxene	Glaucony			
778	2	5	3	16		24		2	8					
777		13	2	6	1	3		3	27					
788	2			4		7			1					
786	4							1						
781						12								
796				2		3				1				
784	5	11	8	19		8								
793	1		1	31		112		49						
798				31		94		65						

	Sum													
	Tourmaline	Andaluzite	Staurolite	Garnet	Phyllos	Zircon	Rutile	Monazite	Amphibole	Pyroxene	Glaucony	Soma		
2446	84	35	29	15	220	6	0	0	0	0	0	389		
2448	127	35	45	30	34	7	0	0	0	9	0	287		
2445	148	133	39	25	5	34	0	2	0	11	0	397		
2447	224	57	47	23	23	14	1	1	0	32	0	422		
2449	153	28	68	40	139	10	0	0	0	0	0	438		
2444	78	7	28	61	8	11	1	4	24	187	0	409		
2450	11	3	7	5	3	2	0	0	40	351	0	422		

	Tourmaline	Andaluzite	Staurolite	Garnet	Phyllos	Zircon	Rutile	Monazite	Amphibole	Pyroxene	Glaucony			
10606	121	53	85	28	3	27	0	0	0	28	0	345		
978	125	52	42	80	12	67	5	5	18	49	0	455		
984	108	53	40	77	0	53	0	11	17	0	0	359		
297	112	49	54	97	0	41	0	15	7	47	0	422		
959	107	57	11	87	0	49	2	24	11	35	0	383		
145	91	52	28	40	22	5	0	8	37	14	0	297		
953	98	59	57	77	0	43	3	8	19	51	0	415		
10635	110	75	40	87	3	51	0	7	7	9	0	389		

	Tourmaline	Andaluzite	Staurolite	Garnet	Phyllos	Zircon	Rutile	Monazite	Amphibole	Pyroxene	Glaucony			
778	139	122	30	22	2	24	0	2	33	1	0	375		
777	179	162	62	24	3	3	0	6	59	0	0	498		
788	119	25	26	27	0	10	0	0	3	0	0	210		
786	47	33	4	9	0	0	0	1	1	4	0	99		
781	160	23	35	36	0	12	0	1	2	0	0	269		
796	36	10	15	15	0	5	0	1	31	45	0	158		
784	145	69	58	31	0	15	0	0	5	0	0	323		
793	57	19	104	195	0	129	0	53	11	8	0	576		
798	72	21	65	148	0	109	0	69	38	109	0	631		

	%											
	Tourmaline	Andaluzite	Staurolite	Garnet	Phyllossilicates	Zircon	Rutile	Monazite	Amphibole	Pyroxene	Glaucony	
2446	21.594	8.997	7.455	3.856	56.555	1.542	0.000	0.000	0.000	0.000	0.000	100
2448	44.251	12.195	15.679	10.453	11.847	2.439	0.000	0.000	0.000	3.136	0.000	100
2445	37.280	33.501	9.824	6.297	1.259	8.564	0.000	0.504	0.000	2.771	0.000	100
2447	53.081	13.507	11.137	5.450	5.450	3.318	0.237	0.237	0.000	7.583	0.000	100
2449	34.932	6.393	15.525	9.132	31.735	2.283	0.000	0.000	0.000	0.000	0.000	100
2444	19.071	1.711	6.846	14.914	1.956	2.689	0.244	0.978	5.868	45.721	0.000	100
2450	2.607	0.711	1.659	1.185	0.711	0.474	0.000	0.000	9.479	83.175	0.000	100

	Tourmaline	Andaluzite	Staurolite	Garnet	Phyllossilicates	Zircon	Rutile	Monazite	Amphibole	Pyroxene	Glaucony	
10606	35.072	15.362	24.638	8.116	0.870	7.826	0.000	0.000	0.000	8.116	0.000	100
978	27.473	11.429	9.231	17.582	2.637	14.725	1.099	1.099	3.956	10.769	0.000	100
984	30.084	14.763	11.142	21.448	0.000	14.763	0.000	3.064	4.735	0.000	0.000	100
297	26.540	11.611	12.796	22.986	0.000	9.716	0.000	3.555	1.659	11.137	0.000	100
959	27.937	14.883	2.872	22.715	0.000	12.794	0.522	6.266	2.872	9.138	0.000	100
145	30.640	17.508	9.428	13.468	7.407	1.684	0.000	2.694	12.458	4.714	0.000	100
953	23.614	14.217	13.735	18.554	0.000	10.361	0.723	1.928	4.578	12.289	0.000	100
10635	28.278	19.280	10.283	22.365	0.771	13.111	0.000	1.799	1.799	2.314	0.000	100

	Tourmaline	Andaluzite	Staurolite	Garnet	Phyllossilicates	Zircon	Rutile	Monazite	Amphibole	Pyroxene	Glaucony	
778	37.067	32.533	8.000	5.867	0.533	6.400	0.000	0.533	8.800	0.267	0.000	100
777	35.944	32.530	12.450	4.819	0.602	0.602	0.000	1.205	11.847	0.000	0.000	100
788	56.667	11.905	12.381	12.857	0.000	4.762	0.000	0.000	1.429	0.000	0.000	100
786	47.475	33.333	4.040	9.091	0.000	0.000	0.000	1.010	1.010	4.040	0.000	100
781	59.480	8.550	13.011	13.383	0.000	4.461	0.000	0.372	0.743	0.000	0.000	100
796	22.785	6.329	9.494	9.494	0.000	3.165	0.000	0.633	19.620	28.481	0.000	100
784	44.892	21.362	17.957	9.598	0.000	4.644	0.000	0.000	1.548	0.000	0.000	100
793	9.896	3.299	18.056	33.854	0.000	22.396	0.000	9.201	1.910	1.389	0.000	100
798	11.410	3.328	10.301	23.455	0.000	17.274	0.000	10.935	6.022	17.274	0.000	100

Annex 5. X-ray imagery

Annex 6. Magnetic Susceptibility

Magnetic Susceptibility							
Depth	Value (10^6SI)	Depth	Value (10^6SI)	Depth	Value (10^6SI)	Depth	Value (10^6SI)
0	11,5	42	7,9	84	6,2	126	8,1
1	15,6	43	7,8	85	6,1	127	7,8
2	18,9	44	7,8	86	6,0	128	7,7
3	21,3	45	7,6	87	6,0	129	7,6
4	22,8	46	7,5	88	5,9	130	7,6
5	24,0	47	7,5	89	5,9	131	7,7
6	24,4	48	7,4	90	6,0	132	7,8
7	24,5	49	7,4	91	6,1	133	8,3
8	24,5	50	7,3	92	6,3	134	8,4
9	24,3	51	7,2	93	6,6	135	8,8
10	24,1	52	7,2	94	6,8	136	9,1
11	24,1	53	7,1	95	7,4	137	9,3
12	24,1	54	7,1	96	7,5	138	8,9
13	23,3	55	6,9	97	7,9	139	8,3
14	22,6	56	6,9	98	8,2	140	8,0
15	21,9	57	6,8	99	8,3	141	7,7
16	21,5	58	6,8	100	8,4	142	7,6
17	21,0	59	6,8	101	8,4	143	7,5
18	20,1	60	6,9	102	8,6	144	7,7
19	19,2	61	6,9	103	8,8	145	8,0
20	18,0	62	6,8	104	9,0	146	8,3
21	17,0	63	6,7	105	9,2	147	8,6
22	16,1	64	6,6	106	9,3	148	9,2
23	15,2	65	6,6	107	9,2	149	9,8
24	14,4	66	6,6	108	9,3	150	11,0
25	13,9	67	6,5	109	9,2	151	12,8
26	13,6	68	6,5	110	8,9	152	15,5
27	13,1	69	6,6	111	8,7	153	21,7
28	12,9	70	6,5	112	8,6	154	29,4
29	12,7	71	6,5	113	8,5	155	39,5
30	12,8	72	6,5	114	8,5	156	47,5
31	13,1	73	6,5	115	8,3	157	46,5
32	13,3	74	6,4	116	8,1	158	37,3
33	13,0	75	6,4	117	8,0	159	24,7
34	12,0	76	6,5	118	7,8	160	16,2
35	11,1	77	6,5	119	7,7	161	10,9
36	10,3	78	6,5	120	7,6	162	10,9
37	9,7	79	6,5	121	7,7	163	8,2
38	9,0	80	6,5	122	7,9	164	6,3
39	8,6	81	6,4	123	7,8	165	5,0
40	8,3	82	6,3	124	8,1	166	4,5
41	8,1	83	6,3	125	8,2	167	3,6
						168	2,6

Annex 7. Dry-bulk density

Dry Bulk Density

Depth (cm)	DBD (g/cm3)
0-2	0,89
10	1,00
20	1,03
32	1,21
52	1,19
75	1,09
109	1,72
124	1,58
137	1,78
157	0,77

Annex 8. ^{210}Pb

λ	excluded	Zmix	ω	Db	C(0)	Cback
	(cm)	(cm)	(cm y-1)	(?)	(mBq g-1)	(mBq g-1)
0,031083		8,106262	0,076854	3,2E+08	241,5324	23

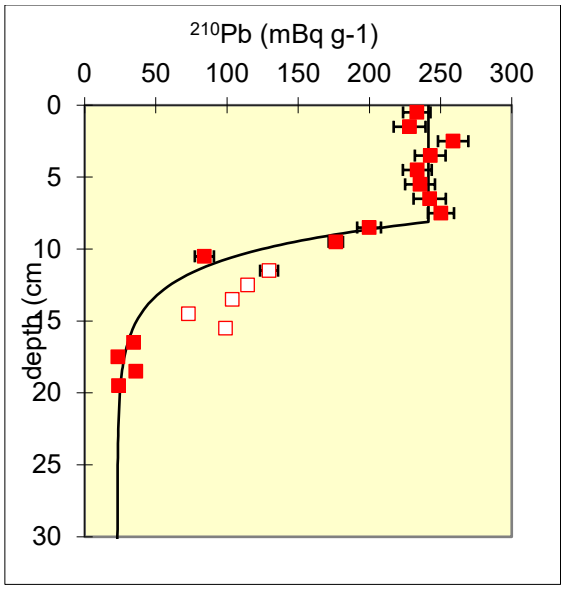

Annex 9. Carbon content

Depth (cm)	toc	tic
0-2	1.40	3.20
10	1.30	2.80
20	1.00	3.10
32	0.90	3.80
52	0.80	4.60
75	0.70	5.00
109	0.60	7.00
124	0.40	8.00
137	0.40	7.00
157	0.40	8.00

Annex 10. Grain Size

INSTITUTO HIDROGRÁFICO
DIVISÃO DE GEOLOGIA MARINHA

Station: **2104**

Diameter (class)	Diameter phi	Class midpoint (ci)	Class midpoint (mm)	Individual Frequency (Fi)	Cumulative Frequency	Fi x ci	Fi x (ci-X)^2	Fi x (ci-X)^3
>64.00mm	<6.0 phi	-6,25	76109,26	0,00	0,00	0,00	0,00	0,00
45.25-64.00mm	-5.5,6.0 phi	-5,75	53817,37	0,00	0,00	0,00	0,00	0,00
32.00-45.25mm	-5.0,-5.5 phi	-5,25	38054,63	0,00	0,00	0,00	0,00	0,00
22.63-32.00mm	-4.5,-5.0 phi	-4,75	26908,69	0,00	0,00	0,00	0,00	0,00
16.00-22.63mm	-4.0,-4.5 phi	-4,25	19027,31	0,00	0,00	0,00	0,00	0,00
11.31-16.00mm	-3.5,-4.0 phi	-3,75	13454,34	0,00	0,00	0,00	0,00	0,00
8.00-11.31mm	-3.0,-3.5 phi	-3,25	9513,66	0,00	0,00	0,00	0,00	0,00
5.66-8.00mm	-2.5,-3.0 phi	-2,75	6727,17	0,00	0,00	0,00	0,00	0,00
4.00-5.66mm	-2.5,-2.0 phi	-2,25	4756,83	0,00	0,00	0,00	0,00	0,00
4.00 - 2.83mm	-2.0, -1.5 phi	-1,75	3363,59	0,00	0,00	0,00	0,00	0,00
2.83 - 2.00mm	-1.5, -1.0 phi	-1,25	2378,41	0,19	0,19	-0,23	9,02	-62,52
2.00 - 1.41mm	-1.0, -0.5 phi	-0,75	1681,79	0,07	0,26	-0,05	2,90	-18,68
1.41 - 1.00mm	-0.5, 0.0 phi	-0,25	1189,21	0,05	0,31	-0,01	1,84	-10,90
1.00 - 0.71mm	0.0, 0.5 phi	0,25	840,90	0,15	0,46	0,04	4,56	-24,78
0.71 - 0.50mm	0.5, 1.0 phi	0,75	594,60	0,91	1,38	0,68	22,23	-109,68
500.00 - 354.00µm	1.0, 1.5 phi	1,25	420,45	0,95	2,32	1,18	18,58	-82,40
354.00 - 250.00µm	1.5, 2.0 phi	1,75	297,30	0,73	3,05	1,28	11,31	-44,50
250.00 - 177.00µm	2.0, 2.5 phi	2,25	210,22	1,32	4,38	2,98	15,61	-53,60
177.00 - 125.00µm	2.5, 3.0 phi	2,75	148,65	3,49	7,87	9,60	30,04	-88,16
125.00 - 88.40µm	3.0, 3.5 phi	3,25	105,11	6,73	14,60	21,88	39,90	-97,13
88.40 - 62.50µm	3.5, 4.0 phi	3,75	74,33	9,39	23,99	35,23	35,14	-67,98
62.50 - 44.20µm	4.0, 4.,5 phi	4,25	52,56	10,07	34,06	42,79	20,71	-29,71
44.20 - 31.25µm	4.5, 5.0 phi	4,75	37,16	8,88	42,94	42,18	7,75	-7,24
31.25 - 22.10µm	5.0, 5.5 phi	5,25	26,28	7,43	50,37	38,99	1,40	-0,61
22.10 - 15.63µm	5.5, 6.0 phi	5,75	18,58	6,98	57,35	40,15	0,03	0,00
15.63 - 11.00µm	6.0, 6.5 phi	6,25	13,14	7,28	64,63	45,49	2,33	1,32
11.00 - 7.81µm	6.5, 7.0 phi	6,75	9,29	7,23	71,86	48,83	8,22	8,76
7.81 - 5.52µm	7.0, 7.5 phi	7,25	6,57	6,43	78,29	46,59	15,76	24,67
5.52 - 3.91µm	7.5, 8.0 phi	7,75	4,65	5,39	83,68	41,74	22,98	47,48
3.91 - 2.76µm	8.0, 8.5 phi	8,25	3,28	4,66	88,33	38,42	30,65	78,65
2.76 - 1.95µm	8.5, 9.0 phi	8,75	2,32	4,01	92,34	35,09	37,69	115,56
1.95 - 1.38µm	9.0, 9.5 phi	9,25	1,64	3,07	95,41	28,36	38,98	139,00
1.38 - 0.98µm	9.5, 10.0 phi	9,75	1,16	1,98	97,39	19,28	32,69	132,91
0.98 - 0.69µm	10.0, 10.5 phi	10,25	0,82	1,17	98,56	12,03	24,47	111,74
0.69 - 0.49µm	10.5, 11.0 phi	10,75	0,58	0,75	99,31	8,10	19,33	97,91
0.49 - 0.35µm	11.0 , 11.5 phi	11,25	0,41	0,50	99,81	5,59	15,40	85,71
0.35 - 0.24µm	11.5, 12.0 phi	11,75	0,29	0,19	100,00	2,22	6,95	42,15
0.24 - 0.17µm	12.0, 12.5 phi	12,25	0,21	0,00	100,00	0,00	0,00	0,00
0.17 - 0.12µm	12.5, 13.0 phi	12,75	0,15	0,00	100,00	0,00	0,00	0,00
0.12 - 0.09µm	13.0, 13.5 phi	13,25	0,10	0,00	100,00	0,00	0,00	0,00
0.09 - 0.06µm	13.5, 14.0phi	13,75	0,07	0,00	100,00	0,00	0,00	0,00
0.06 - 0.04µm	14.0, 14.5 phi	14,25	0,05	0,00	100,00	0,00	0,00	0,00
0.04 - 0.03µm	14.5, 15.0 phi	14,75	0,04	0,00	100,00	0,00	0,00	0,00
0.03 - 0.02µm	15.0, 15.5 phi	15,25	0,03	0,00	100,00	0,00	0,00	0,00
METHOD: MALVERN laser sedimentograph (particles <2mm)				100,00		568,42	476,48	187,98
Sieving (particles> 0.5mm)								

Main Classes individual percentages:

Pebble	0,00
Gravel	0,19
Sand	23,81
Silt	59,68
Clay	16,32

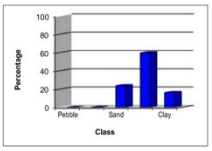

Statistical Parameters:

Mean	5,68
Standard Deviation	2,18
Asymmetry	0,18
P90	8,69
P50	5,48
P5	2,61
Mode	4,25

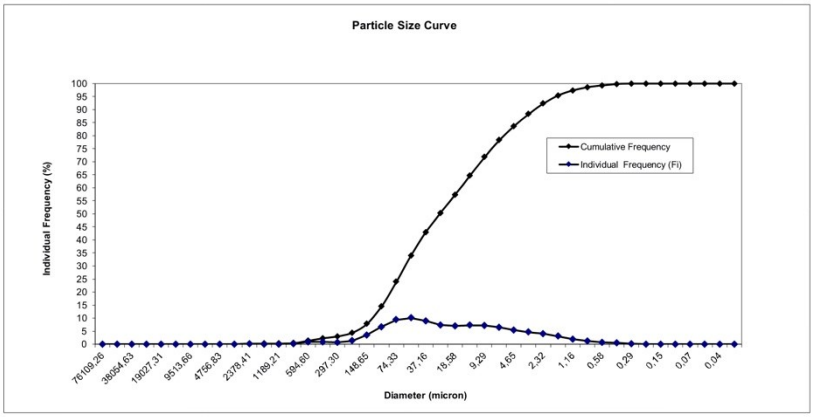

Technician: *Fernanda Dias*

Date:

INSTITUTO HIDROGRÁFICO
DIVISÃO DE GEOLOGIA MARINHA

Station: 2105

Diameter (class)	Diameter phi	Class midpoint (ci)	Class midpoint (mm)	Individual Frequency (Fi)	Cumulative Frequency	Fi x ci	Fi x (ci-X)^2	Fi x (ci-X)^3
>64.00mm	<6.0 phi	-6,25	76109,26	0,00	0,00	0,00	0,00	0,00
45.25-64.00mm	-5.5,6.0 phi	-5,75	53817,37	0,00	0,00	0,00	0,00	0,00
32.00-45.25mm	-5.0,-5.5 phi	-5,25	38054,63	0,00	0,00	0,00	0,00	0,00
22.63-32.00mm	-4.5,-5.0 phi	-4,75	26908,69	0,00	0,00	0,00	0,00	0,00
16.00-22.63mm	-4.0,-4.5 phi	-4,25	19027,31	0,00	0,00	0,00	0,00	0,00
11.31-16.00mm	-3.5,-4.0 phi	-3,75	13454,34	0,00	0,00	0,00	0,00	0,00
8.00-11.31mm	-3.0,-3.5 phi	-3,25	9513,66	0,00	0,00	0,00	0,00	0,00
5.66-8.00mm	-2.5,-3.0 phi	-2,75	6727,17	0,00	0,00	0,00	0,00	0,00
4.00-5.66mm	-2.5,-2.0 phi	-2,25	4756,83	0,00	0,00	0,00	0,00	0,00
4.00 - 2.83mm	-2.0, -1.5 phi	-1,75	3363,59	0,00	0,00	0,00	0,00	0,00
2.83 - 2.00mm	-1.5, -1.0 phi	-1,25	2378,41	0,14	0,14	-0,17	6,80	-47,83
2.00 - 1.41mm	-1.0, -0.5 phi	-0,75	1681,79	0,01	0,15	-0,01	0,39	-2,52
1.41 - 1.00mm	-0.5, 0.0 phi	-0,25	1189,21	0,12	0,27	-0,03	4,48	-26,99
1.00 - 0.71mm	0.0, 0.5 phi	0,25	840,90	0,09	0,36	0,02	2,90	-16,06
0.71 - 0.50mm	0.5, 1.0 phi	0,75	594,60	0,32	0,69	0,24	8,21	-41,32
500.00 - 354.00µm	1.0, 1.5 phi	1,25	420,45	0,49	1,18	0,61	10,02	-45,39
354.00 - 250.00µm	1.5, 2.0 phi	1,75	297,30	0,75	1,93	1,31	12,16	-49,02
250.00 - 177.00µm	2.0, 2.5 phi	2,25	210,22	1,54	3,46	3,46	19,15	-67,59
177.00 - 125.00µm	2.5, 3.0 phi	2,75	148,65	3,48	6,94	9,57	31,95	-96,82
125.00 - 88.40µm	3.0, 3.5 phi	3,25	105,11	6,33	13,27	20,56	40,49	-102,45
88.40 - 62.50µm	3.5, 4.0 phi	3,75	74,33	8,75	22,02	32,81	36,06	-73,20
62.50 - 44.20µm	4.0, 4.,5 phi	4,25	52,56	9,57	31,59	40,68	22,41	-34,28
44.20 - 31.25µm	4.5, 5.0 phi	4,75	37,16	8,87	40,46	42,14	9,41	-9,70
31.25 - 22.10µm	5.0, 5.5 phi	5,25	26,28	7,92	48,38	41,56	2,22	-1,18
22.10 - 15.63µm	5.5, 6.0 phi	5,75	18,58	7,63	56,01	43,90	0,01	0,00
15.63 - 11.00µm	6.0, 6.5 phi	6,25	13,14	7,76	63,77	48,50	1,71	0,81
11.00 - 7.81µm	6.5, 7.0 phi	6,75	9,29	7,48	71,25	50,46	7,03	6,82
7.81 - 5.52µm	7.0, 7.5 phi	7,25	6,57	6,56	77,80	47,55	14,17	20,83
5.52 - 3.91µm	7.5, 8.0 phi	7,75	4,65	5,53	83,33	42,84	21,45	42,26
3.91 - 2.76µm	8.0, 8.5 phi	8,25	3,28	4,82	88,16	39,80	29,43	72,70
2.76 - 1.95µm	8.5, 9.0 phi	8,75	2,32	4,15	92,30	36,29	36,58	108,65
1.95 - 1.38µm	9.0, 9.5 phi	9,25	1,64	3,13	95,43	28,96	37,69	130,79
1.38 - 0.98µm	9.5, 10.0 phi	9,75	1,16	1,98	97,42	19,32	31,23	123,97
0.98 - 0.69µm	10.0, 10.5 phi	10,25	0,82	1,15	98,57	11,83	23,07	103,10
0.69 - 0.49µm	10.5, 11.0 phi	10,75	0,58	0,74	99,31	7,94	18,25	90,70
0.49 - 0.35µm	11.0 , 11.5 phi	11,25	0,41	0,50	99,81	5,59	14,86	81,30
0.35 - 0.24µm	11.5, 12.0 phi	11,75	0,29	0,19	100,00	2,28	6,92	41,34
0.24 - 0.17µm	12.0, 12.5 phi	12,25	0,21	0,00	100,00	0,00	0,00	0,00
0.17 - 0.12µm	12.5, 13.0 phi	12,75	0,15	0,00	100,00	0,00	0,00	0,00
0.12 - 0.09µm	13.0, 13.5 phi	13,25	0,10	0,00	100,00	0,00	0,00	0,00
0.09 - 0.06µm	13.5, 14.0phi	13,75	0,07	0,00	100,00	0,00	0,00	0,00
0.06 - 0.04µm	14.0, 14.5 phi	14,25	0,05	0,00	100,00	0,00	0,00	0,00
0.04 - 0.03µm	14.5, 15.0 phi	14,75	0,04	0,00	100,00	0,00	0,00	0,00
0.03 - 0.02µm	15.0, 15.5 phi	15,25	0,03	0,00	100,00	0,00	0,00	0,00
METHOD: MALVERN laser sedimentograph (particles <2mm)				100,00		578,01	449,07	208,93
Sieving (particles> 0.5mm)								

Main Classes individual percentages:

Pebble	0,00
Gravel	0,14
Sand	21,88
Silt	61,31
Clay	16,67

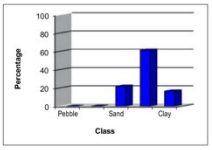

Statistical Parameters:

Mean	5,78
Standard Deviation	2,12
Asymmetry	0,22
P90	8,70
P50	5,61
P5	2,76
Mode	4,25

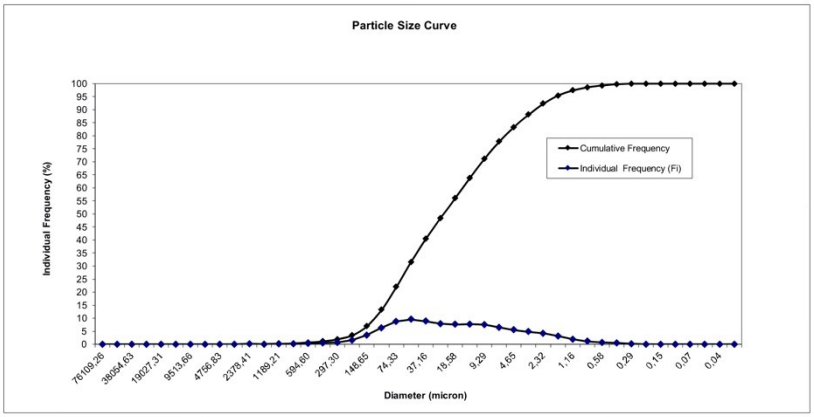

Technician: *Fernanda Dias*

Date:

INSTITUTO HIDROGRÁFICO
DIVISÃO DE GEOLOGIA MARINHA

Station: **2106**

Diameter (class)	Diameter phi	Class midpoint (ci)	Class midpoint (mm)	Individual Frequency (Fi)	Cumulative Frequency	Fi x ci	Fi x (ci-X)^2	Fi x (ci-X)^3
>64.00mm	<6.0 phi	-6,25	76109,26	0,00	0,00	0,00	0,00	0,00
45.25-64.00mm	-5.5,6.0 phi	-5,75	53817,37	0,00	0,00	0,00	0,00	0,00
32.00-45.25mm	-5.0,-5.5 phi	-5,25	38054,63	0,00	0,00	0,00	0,00	0,00
22.63-32.00mm	-4.5,-5.0 phi	-4,75	26908,69	0,00	0,00	0,00	0,00	0,00
16.00-22.63mm	-4.0,-4.5 phi	-4,25	19027,31	0,00	0,00	0,00	0,00	0,00
11.31-16.00mm	-3.5,-4.0 phi	-3,75	13454,34	0,00	0,00	0,00	0,00	0,00
8.00-11.31mm	-3.0,-3.5 phi	-3,25	9513,66	0,00	0,00	0,00	0,00	0,00
5.66-8.00mm	-2.5,-3.0 phi	-2,75	6727,17	0,00	0,00	0,00	0,00	0,00
4.00-5.66mm	-2.5,-2.0 phi	-2,25	4756,83	0,00	0,00	0,00	0,00	0,00
4.00 - 2.83mm	-2.0, -1.5 phi	-1,75	3363,59	0,00	0,00	0,00	0,00	0,00
2.83 - 2.00mm	-1.5, -1.0 phi	-1,25	2378,41	0,00	0,00	0,00	0,00	0,00
2.00 - 1.41mm	-1.0, -0.5 phi	-0,75	1681,79	0,79	0,79	-0,59	20,26	-102,44
1.41 - 1.00mm	-0.5, 0.0 phi	-0,25	1189,21	1,71	2,51	-0,43	35,53	-161,84
1.00 - 0.71mm	0.0, 0.5 phi	0,25	840,90	2,48	4,99	0,62	40,82	-165,50
0.71 - 0.50mm	0.5, 1.0 phi	0,75	594,60	3,36	8,34	2,52	42,40	-150,72
500.00 - 354.00µm	1.0, 1.5 phi	1,25	420,45	4,09	12,43	5,11	38,17	-116,59
354.00 - 250.00µm	1.5, 2.0 phi	1,75	297,30	4,79	17,22	8,38	31,27	-79,89
250.00 - 177.00µm	2.0, 2.5 phi	2,25	210,22	5,73	22,95	12,89	24,19	-49,71
177.00 - 125.00µm	2.5, 3.0 phi	2,75	148,65	7,20	30,15	19,80	17,41	-27,07
125.00 - 88.40µm	3.0, 3.5 phi	3,25	105,11	8,65	38,80	28,11	9,62	-10,15
88.40 - 62.50µm	3.5, 4.0 phi	3,75	74,33	9,17	47,98	34,40	2,82	-1,57
62.50 - 44.20µm	4.0, 4..5 phi	4,25	52,56	8,58	56,56	36,49	0,03	0,00
44.20 - 31.25µm	4.5, 5.0 phi	4,75	37,16	7,40	63,96	35,13	1,47	0,65
31.25 - 22.10µm	5.0, 5.5 phi	5,25	26,28	6,35	70,31	33,36	5,68	5,36
22.10 - 15.63µm	5.5, 6.0 phi	5,75	18,58	5,76	76,07	33,11	12,02	17,38
15.63 - 11.00µm	6.0, 6.5 phi	6,25	13,14	5,31	81,38	33,17	20,08	39,06
11.00 - 7.81µm	6.5, 7.0 phi	6,75	9,29	4,59	85,96	30,96	27,42	67,05
7.81 - 5.52µm	7.0, 7.5 phi	7,25	6,57	3,60	89,57	26,13	31,26	92,06
5.52 - 3.91µm	7.5, 8.0 phi	7,75	4,65	2,74	92,31	21,23	32,51	112,01
3.91 - 2.76µm	8.0, 8.5 phi	8,25	3,28	2,24	94,55	18,48	34,87	137,56
2.76 - 1.95µm	8.5, 9.0 phi	8,75	2,32	1,90	96,45	16,63	37,55	166,93
1.95 - 1.38µm	9.0, 9.5 phi	9,25	1,64	1,45	97,90	13,42	35,48	175,45
1.38 - 0.98µm	9.5, 10.0 phi	9,75	1,16	0,93	98,83	9,05	27,51	149,80
0.98 - 0.69µm	10.0, 10.5 phi	10,25	0,82	0,54	99,36	5,51	19,00	112,96
0.69 - 0.49µm	10.5, 11.0 phi	10,75	0,58	0,34	99,71	3,67	14,19	91,44
0.49 - 0.35µm	11.0 , 11.5 phi	11,25	0,41	0,24	99,95	2,71	11,61	80,62
0.35 - 0.24µm	11.5, 12.0 phi	11,75	0,29	0,05	100,00	0,63	2,98	22,20
0.24 - 0.17µm	12.0, 12.5 phi	12,25	0,21	0,00	100,00	0,00	0,00	0,00
0.17 - 0.12µm	12.5, 13.0 phi	12,75	0,15	0,00	100,00	0,00	0,00	0,00
0.12 - 0.09µm	13.0, 13.5 phi	13,25	0,10	0,00	100,00	0,00	0,00	0,00
0.09 - 0.06µm	13.5, 14.0phi	13,75	0,07	0,00	100,00	0,00	0,00	0,00
0.06 - 0.04µm	14.0, 14.5 phi	14,25	0,05	0,00	100,00	0,00	0,00	0,00
0.04 - 0.03µm	14.5, 15.0 phi	14,75	0,04	0,00	100,00	0,00	0,00	0,00
0.03 - 0.02µm	15.0, 15.5 phi	15,25	0,03	0,00	100,00	0,00	0,00	0,00
METHOD: MALVERN laser sedimentograph (particles <2mm)				100,00		430,49	576,15	405,04
Sieving (particles> 0.5mm)								

Main Classes individual percentages:

Pebble	0,00
Gravel	0,00
Sand	47,98
Silt	44,33
Clay	7,69

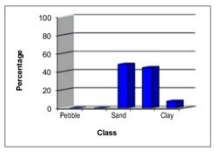

Statistical Parameters:

Mean	4,30
Standard Deviation	2,40
Asymmetry	0,29
P90	7,57
P50	4,12
P5	0,50
Mode	3,75

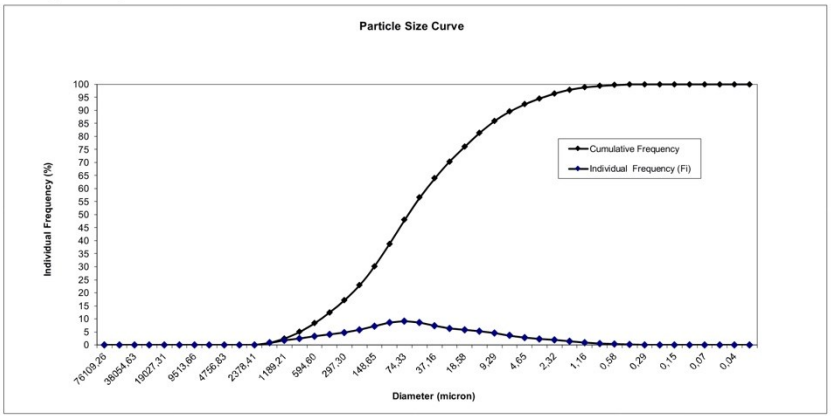

Technician: *Fernanda Dias*

Date:

INSTITUTO HIDROGRÁFICO
DIVISÃO DE GEOLOGIA MARINHA

Sation: **2107**

Diameter (class)	Diameter phi	Class midpoint (ci)	Class midpoint (mm)	Individual Frequency (Fi)	Cumulative Frequency	Fi x ci	Fi x (ci-X)^2	Fi x (ci-X)^3
>64.00mm	<6.0 phi	-6,25	76109,26	0,00	0,00	0,00	0,00	0,00
45.25-64.00mm	-5.5,6.0 phi	-5,75	53817,37	0,00	0,00	0,00	0,00	0,00
32.00-45.25mm	-5.0,-5.5 phi	-5,25	38054,63	0,00	0,00	0,00	0,00	0,00
22.63-32.00mm	-4.5,-5.0 phi	-4,75	26908,69	0,00	0,00	0,00	0,00	0,00
16.00-22.63mm	-4.0,-4.5 phi	-4,25	19027,31	0,00	0,00	0,00	0,00	0,00
11.31-16.00mm	-3.5,-4.0 phi	-3,75	13454,34	0,00	0,00	0,00	0,00	0,00
8.00-11.31mm	-3.0,-3.5 phi	-3,25	9513,66	0,00	0,00	0,00	0,00	0,00
5.66-8.00mm	-2.5,-3.0 phi	-2,75	6727,17	0,00	0,00	0,00	0,00	0,00
4.00-5.66mm	-2.5,-2.0 phi	-2,25	4756,83	0,00	0,00	0,00	0,00	0,00
4.00 - 2.83mm	-2.0, -1.5 phi	-1,75	3363,59	0,00	0,00	0,00	0,00	0,00
2.83 - 2.00mm	-1.5, -1.0 phi	-1,25	2378,41	0,00	0,00	0,00	0,00	0,00
2.00 - 1.41mm	-1.0, -0.5 phi	-0,75	1681,79	0,00	0,00	0,00	0,13	-0,89
1.41 - 1.00mm	-0.5, 0.0 phi	-0,25	1189,21	0,02	0,02	0,00	0,71	-4,33
1.00 - 0.71mm	0.0, 0.5 phi	0,25	840,90	0,02	0,04	0,01	0,73	-4,14
0.71 - 0.50mm	0.5, 1.0 phi	0,75	594,60	0,15	0,19	0,11	3,87	-19,89
500.00 - 354.00µm	1.0, 1.5 phi	1,25	420,45	0,35	0,54	0,43	7,45	-34,52
354.00 - 250.00µm	1.5, 2.0 phi	1,75	297,30	0,48	1,02	0,85	8,28	-34,25
250.00 - 177.00µm	2.0, 2.5 phi	2,25	210,22	1,07	2,09	2,40	14,09	-51,22
177.00 - 125.00µm	2.5, 3.0 phi	2,75	148,65	2,75	4,84	7,57	27,06	-84,83
125.00 - 88.40µm	3.0, 3.5 phi	3,25	105,11	5,39	10,23	17,51	37,41	-98,58
88.40 - 62.50µm	3.5, 4.0 phi	3,75	74,33	7,87	18,10	29,50	35,86	-76,56
62.50 - 44.20µm	4.0, 4..5 phi	4,25	52,56	9,19	27,28	39,04	24,55	-40,15
44.20 - 31.25µm	4.5, 5.0 phi	4,75	37,16	9,29	36,57	44,11	11,96	-13,58
31.25 - 22.10µm	5.0, 5.5 phi	5,25	26,28	9,03	45,60	47,41	3,64	-2,31
22.10 - 15.63µm	5.5, 6.0 phi	5,75	18,58	9,02	54,62	51,84	0,16	-0,02
15.63 - 11.00µm	6.0, 6.5 phi	6,25	13,14	8,96	63,57	55,99	1,19	0,44
11.00 - 7.81µm	6.5, 7.0 phi	6,75	9,29	8,25	71,83	55,72	6,18	5,34
7.81 - 5.52µm	7.0, 7.5 phi	7,25	6,57	6,91	78,74	50,12	12,88	17,58
5.52 - 3.91µm	7.5, 8.0 phi	7,75	4,65	5,57	84,31	43,18	19,38	36,14
3.91 - 2.76µm	8.0, 8.5 phi	8,25	3,28	4,68	89,00	38,65	26,20	61,97
2.76 - 1.95µm	8.5, 9.0 phi	8,75	2,32	3,93	92,93	34,42	32,28	92,50
1.95 - 1.38µm	9.0, 9.5 phi	9,25	1,64	2,92	95,85	27,04	33,11	111,40
1.38 - 0.98µm	9.5, 10.0 phi	9,75	1,16	1,82	97,68	17,77	27,22	105,21
0.98 - 0.69µm	10.0, 10.5 phi	10,25	0,82	1,04	98,72	10,68	19,86	86,68
0.69 - 0.49µm	10.5, 11.0 phi	10,75	0,58	0,66	99,38	7,10	15,63	76,03
0.49 - 0.35µm	11.0 , 11.5 phi	11,25	0,41	0,45	99,83	5,02	12,84	68,89
0.35 - 0.24µm	11.5, 12.0 phi	11,75	0,29	0,17	100,00	2,05	6,00	35,21
0.24 - 0.17µm	12.0, 12.5 phi	12,25	0,21	0,00	100,00	0,00	0,00	0,00
0.17 - 0.12µm	12.5, 13.0 phi	12,75	0,15	0,00	100,00	0,00	0,00	0,00
0.12 - 0.09µm	13.0, 13.5 phi	13,25	0,10	0,00	100,00	0,00	0,00	0,00
0.09 - 0.06µm	13.5, 14.0phi	13,75	0,07	0,00	100,00	0,00	0,00	0,00
0.06 - 0.04µm	14.0, 14.5 phi	14,25	0,05	0,00	100,00	0,00	0,00	0,00
0.04 - 0.03µm	14.5, 15.0 phi	14,75	0,04	0,00	100,00	0,00	0,00	0,00
0.03 - 0.02µm	15.0, 15.5 phi	15,25	0,03	0,00	100,00	0,00	0,00	0,00
METHOD: MALVERN laser sedimentograph (particles <2mm)				100,00		588,50	388,69	232,11
Sieving (particles> 0.5mm)								

Main Classes individual percentages:

Pebble	0,00
Gravel	0,00
Sand	18,10
Silt	66,22
Clay	15,69

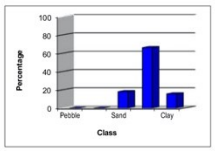

Statistical Parameters:

Mean	5,89
Standard Deviation	1,97
Asymmetry	0,30
P90	8,61
P50	5,74
P5	3,02
Mode	4,75

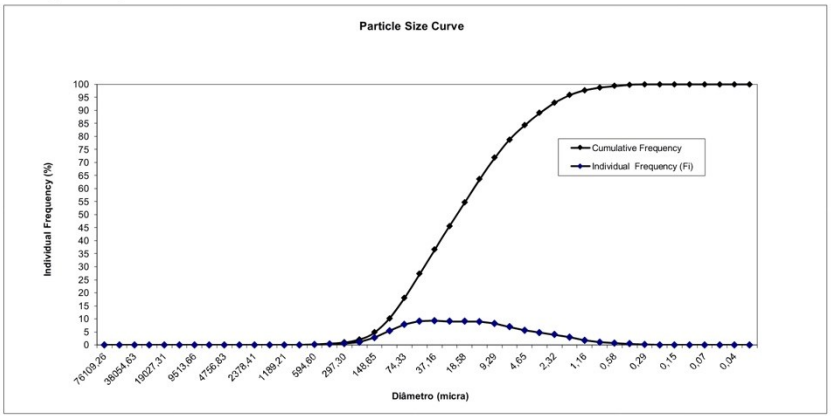

Technician: *Fernanda Dias*

Date:

INSTITUTO HIDROGRÁFICO
DIVISÃO DE GEOLOGIA MARINHA

Station: **2108**

Diameter (class)	Diameter phi	Class midpoint (ci)	Class midpoint (mm)	Individual Frequency (Fi)	Cumulative Frequency	Fi x ci	Fi x (ci-X)^2	Fi x (ci-X)^3
>64.00mm	<6.0 phi	-6,25	76109,26	0,00	0,00	0,00	0,00	0,00
45.25-64.00mm	-5.5,6.0 phi	-5,75	53817,37	0,00	0,00	0,00	0,00	0,00
32.00-45.25mm	-5.0,-5.5 phi	-5,25	38054,63	0,00	0,00	0,00	0,00	0,00
22.63-32.00mm	-4.5,-5.0 phi	-4,75	26908,69	0,00	0,00	0,00	0,00	0,00
16.00-22.63mm	-4.0,-4.5 phi	-4,25	19027,31	0,00	0,00	0,00	0,00	0,00
11.31-16.00mm	-3.5,-4.0 phi	-3,75	13454,34	0,00	0,00	0,00	0,00	0,00
8.00-11.31mm	-3.0,-3.5 phi	-3,25	9513,66	0,00	0,00	0,00	0,00	0,00
5.66-8.00mm	-2.5,-3.0 phi	-2,75	6727,17	0,00	0,00	0,00	0,00	0,00
4.00-5.66mm	-2.5,-2.0 phi	-2,25	4756,83	0,00	0,00	0,00	0,00	0,00
4.00 - 2.83mm	-2.0, -1.5 phi	-1,75	3363,59	0,00	0,00	0,00	0,00	0,00
2.83 - 2.00mm	-1.5, -1.0 phi	-1,25	2378,41	0,00	0,00	0,00	0,00	0,00
2.00 - 1.41mm	-1.0, -0.5 phi	-0,75	1681,79	0,03	0,03	-0,02	1,25	-8,21
1.41 - 1.00mm	-0.5, 0.0 phi	-0,25	1189,21	0,02	0,05	0,00	0,73	-4,43
1.00 - 0.71mm	0.0, 0.5 phi	0,25	840,90	0,06	0,11	0,02	1,89	-10,50
0.71 - 0.50mm	0.5, 1.0 phi	0,75	594,60	0,16	0,27	0,12	3,98	-20,13
500.00 - 354.00µm	1.0, 1.5 phi	1,25	420,45	0,31	0,57	0,38	6,37	-29,06
354.00 - 250.00µm	1.5, 2.0 phi	1,75	297,30	0,47	1,05	0,83	7,83	-31,82
250.00 - 177.00µm	2.0, 2.5 phi	2,25	210,22	1,12	2,16	2,51	14,15	-50,42
177.00 - 125.00µm	2.5, 3.0 phi	2,75	148,65	2,89	5,05	7,95	27,10	-83,00
125.00 - 88.40µm	3.0, 3.5 phi	3,25	105,11	5,61	10,66	18,23	36,83	-94,37
88.40 - 62.50µm	3.5, 4.0 phi	3,75	74,33	8,18	18,84	30,66	34,77	-71,71
62.50 - 44.20µm	4.0, 4..5 phi	4,25	52,56	9,58	28,42	40,73	23,39	-36,54
44.20 - 31.25µm	4.5, 5.0 phi	4,75	37,16	9,72	38,14	46,15	10,96	-11,65
31.25 - 22.10µm	5.0, 5.5 phi	5,25	26,28	9,36	47,50	49,16	2,96	-1,66
22.10 - 15.63µm	5.5, 6.0 phi	5,75	18,58	9,12	56,62	52,46	0,04	0,00
15.63 - 11.00µm	6.0, 6.5 phi	6,25	13,14	8,80	65,43	55,03	1,69	0,74
11.00 - 7.81µm	6.5, 7.0 phi	6,75	9,29	7,92	73,35	53,49	6,97	6,53
7.81 - 5.52µm	7.0, 7.5 phi	7,25	6,57	6,53	79,88	47,34	13,50	19,40
5.52 - 3.91µm	7.5, 8.0 phi	7,75	4,65	5,22	85,10	40,43	19,59	37,95
3.91 - 2.76µm	8.0, 8.5 phi	8,25	3,28	4,39	89,48	36,19	26,07	63,55
2.76 - 1.95µm	8.5, 9.0 phi	8,75	2,32	3,71	93,19	32,45	32,01	94,03
1.95 - 1.38µm	9.0, 9.5 phi	9,25	1,64	2,78	95,97	25,74	32,88	113,04
1.38 - 0.98µm	9.5, 10.0 phi	9,75	1,16	1,75	97,73	17,09	27,17	107,00
0.98 - 0.69µm	10.0, 10.5 phi	10,25	0,82	1,01	98,74	10,39	19,97	88,62
0.69 - 0.49µm	10.5, 11.0 phi	10,75	0,58	0,65	99,39	6,96	15,78	77,94
0.49 - 0.35µm	11.0 , 11.5 phi	11,25	0,41	0,44	99,83	4,93	12,96	70,50
0.35 - 0.24µm	11.5, 12.0 phi	11,75	0,29	0,17	100,00	2,03	6,10	36,23
0.24 - 0.17µm	12.0, 12.5 phi	12,25	0,21	0,00	100,00	0,00	0,00	0,00
0.17 - 0.12µm	12.5, 13.0 phi	12,75	0,15	0,00	100,00	0,00	0,00	0,00
0.12 - 0.09µm	13.0, 13.5 phi	13,25	0,10	0,00	100,00	0,00	0,00	0,00
0.09 - 0.06µm	13.5, 14.0phi	13,75	0,07	0,00	100,00	0,00	0,00	0,00
0.06 - 0.04µm	14.0, 14.5 phi	14,25	0,05	0,00	100,00	0,00	0,00	0,00
0.04 - 0.03µm	14.5, 15.0 phi	14,75	0,04	0,00	100,00	0,00	0,00	0,00
0.03 - 0.02µm	15.0, 15.5 phi	15,25	0,03	0,00	100,00	0,00	0,00	0,00
				100,00		581,23	386,95	262,03

METHOD: MALVERN laser sedimentograph (particles <2mm)
Sieving (particles> 0.5mm)

Main Classes individual percentages:

Pebble	0,00
Gravel	0,00
Sand	18,84
Silt	66,26
Clay	14,90

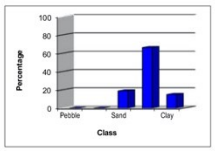

Statistical Parameters:

Mean	5,81
Standard Deviation	1,97
Asymmetry	0,34
P90	8,56
P50	5,64
P5	2,99
Mode	4,75

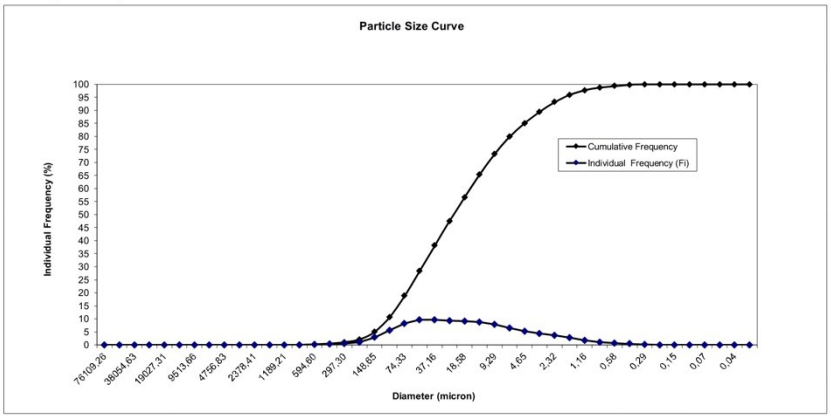

Technician: *Fernanda Dias*

Date:

INSTITUTO HIDROGRÁFICO
DIVISÃO DE GEOLOGIA MARINHA

Station: **2109**

Diameter (class)	Diameter phi	Class midpoint (ci)	Class midpoint (mm)	Individual Frequency (Fi)	Cumulative Frequency	Fi x ci	Fi x (ci-X)^2	Fi x (ci-X)^3
>64.00mm	<6.0 phi	-6,25	76109,26	0,00	0,00	0,00	0,00	0,00
45.25-64.00mm	-5.5,6.0 phi	-5,75	53817,37	0,00	0,00	0,00	0,00	0,00
32.00-45.25mm	-5.0,-5.5 phi	-5,25	38054,63	0,00	0,00	0,00	0,00	0,00
22.63-32.00mm	-4.5,-5.0 phi	-4,75	26908,69	0,00	0,00	0,00	0,00	0,00
16.00-22.63mm	-4.0,-4.5 phi	-4,25	19027,31	0,00	0,00	0,00	0,00	0,00
11.31-16.00mm	-3.5,-4.0 phi	-3,75	13454,34	0,00	0,00	0,00	0,00	0,00
8.00-11.31mm	-3.0,-3.5 phi	-3,25	9513,66	0,00	0,00	0,00	0,00	0,00
5.66-8.00mm	-2.5,-3.0 phi	-2,75	6727,17	0,00	0,00	0,00	0,00	0,00
4.00-5.66mm	-2.5,-2.0 phi	-2,25	4756,83	0,00	0,00	0,00	0,00	0,00
4.00 - 2.83mm	-2.0, -1.5 phi	-1,75	3363,59	0,00	0,00	0,00	0,00	0,00
2.83 - 2.00mm	-1.5, -1.0 phi	-1,25	2378,41	0,00	0,00	0,00	0,00	0,00
2.00 - 1.41mm	-1.0, -0.5 phi	-0,75	1681,79	0,00	0,00	0,00	0,00	0,00
1.41 - 1.00mm	-0.5, 0.0 phi	-0,25	1189,21	0,03	0,03	-0,01	1,35	-8,42
1.00 - 0.71mm	0.0, 0.5 phi	0,25	840,90	0,08	0,11	0,02	2,58	-14,74
0.71 - 0.50mm	0.5, 1.0 phi	0,75	594,60	0,26	0,37	0,19	7,07	-36,93
500.00 - 354.00µm	1.0, 1.5 phi	1,25	420,45	0,37	0,75	0,47	8,30	-39,20
354.00 - 250.00µm	1.5, 2.0 phi	1,75	297,30	0,56	1,30	0,97	9,93	-41,92
250.00 - 177.00µm	2.0, 2.5 phi	2,25	210,22	1,17	2,48	2,64	16,27	-60,54
177.00 - 125.00µm	2.5, 3.0 phi	2,75	148,65	2,74	5,21	7,53	28,42	-91,59
125.00 - 88.40µm	3.0, 3.5 phi	3,25	105,11	5,03	10,24	16,35	37,28	-101,48
88.40 - 62.50µm	3.5, 4.0 phi	3,75	74,33	7,18	17,43	26,93	35,47	-78,83
62.50 - 44.20µm	4.0, 4..5 phi	4,25	52,56	8,46	25,88	35,95	25,09	-43,22
44.20 - 31.25µm	4.5, 5.0 phi	4,75	37,16	8,77	34,66	41,66	13,10	-16,02
31.25 - 22.10µm	5.0, 5.5 phi	5,25	26,28	8,77	43,42	46,03	4,58	-3,30
22.10 - 15.63µm	5.5, 6.0 phi	5,75	18,58	8,95	52,37	51,46	0,44	-0,10
15.63 - 11.00µm	6.0, 6.5 phi	6,25	13,14	9,05	61,42	56,55	0,70	0,19
11.00 - 7.81µm	6.5, 7.0 phi	6,75	9,29	8,46	69,88	57,12	5,12	3,98
7.81 - 5.52µm	7.0, 7.5 phi	7,25	6,57	7,17	77,05	51,97	11,70	14,95
5.52 - 3.91µm	7.5, 8.0 phi	7,75	4,65	5,83	82,88	45,16	18,41	32,74
3.91 - 2.76µm	8.0, 8.5 phi	8,25	3,28	4,95	87,83	40,85	25,69	58,51
2.76 - 1.95µm	8.5, 9.0 phi	8,75	2,32	4,22	92,06	36,95	32,58	90,51
1.95 - 1.38µm	9.0, 9.5 phi	9,25	1,64	3,20	95,26	29,63	34,42	112,81
1.38 - 0.98µm	9.5, 10.0 phi	9,75	1,16	2,05	97,31	19,96	29,22	110,37
0.98 - 0.69µm	10.0, 10.5 phi	10,25	0,82	1,20	98,51	12,31	21,98	94,04
0.69 - 0.49µm	10.5, 11.0 phi	10,75	0,58	0,77	99,28	8,26	17,54	83,79
0.49 - 0.35µm	11.0 , 11.5 phi	11,25	0,41	0,52	99,79	5,81	14,40	75,98
0.35 - 0.24µm	11.5, 12.0 phi	11,75	0,29	0,21	100,00	2,43	6,91	39,93
0.24 - 0.17µm	12.0, 12.5 phi	12,25	0,21	0,00	100,00	0,00	0,00	0,00
0.17 - 0.12µm	12.5, 13.0 phi	12,75	0,15	0,00	100,00	0,00	0,00	0,00
0.12 - 0.09µm	13.0, 13.5 phi	13,25	0,10	0,00	100,00	0,00	0,00	0,00
0.09 - 0.06µm	13.5, 14.0phi	13,75	0,07	0,00	100,00	0,00	0,00	0,00
0.06 - 0.04µm	14.0, 14.5 phi	14,25	0,05	0,00	100,00	0,00	0,00	0,00
0.04 - 0.03µm	14.5, 15.0 phi	14,75	0,04	0,00	100,00	0,00	0,00	0,00
0.03 - 0.02µm	15.0, 15.5 phi	15,25	0,03	0,00	100,00	0,00	0,00	0,00
METHOD: MALVERN laser sedimentograph (particles <2mm)				100,00		597,23	408,55	181,51
Sieving (particles> 0.5mm)								

Main Classes individual percentages:

Pebble	0,00
Gravel	0,00
Sand	17,43
Silt	65,45
Clay	17,12

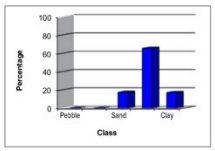

Statistical Parameters:

Mean	5,97
Standard Deviation	2,02
Asymmetry	0,22
P90	8,74
P50	5,87
P5	2,97
Mode	6,25

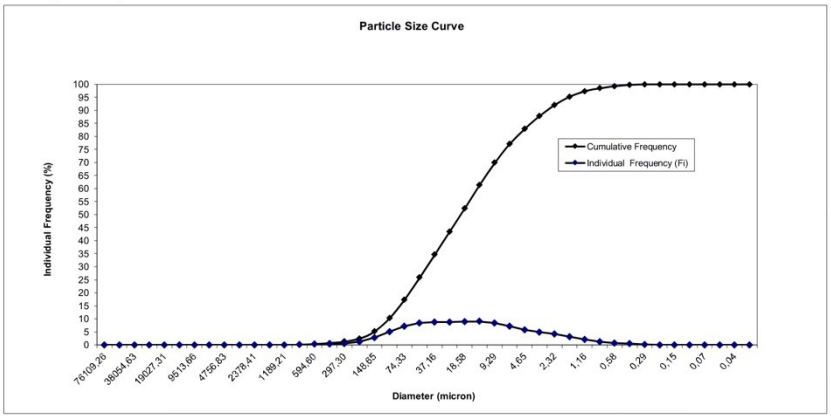

Technician: *Fernanda Dias*

Date:

INSTITUTO HIDROGRÁFICO
DIVISÃO DE GEOLOGIA MARINHA

Station: **2110**

Diameter (class)	Diameter phi	Class midpoint (ci)	Class midpoint (mm)	Individual Frequency (Fi)	Cumulative Frequency	Fi x ci	Fi x (ci-X)^2	Fi x (ci-X)^3
>64.00mm	<6.0 phi	-6,25	76109,26	0,00	0,00	0,00	0,00	0,00
45.25-64.00mm	-5.5,6.0 phi	-5,75	53817,37	0,00	0,00	0,00	0,00	0,00
32.00-45.25mm	-5.0,-5.5 phi	-5,25	38054,63	0,00	0,00	0,00	0,00	0,00
22.63-32.00mm	-4.5,-5.0 phi	-4,75	26908,69	0,00	0,00	0,00	0,00	0,00
16.00-22.63mm	-4.0,-4.5 phi	-4,25	19027,31	0,00	0,00	0,00	0,00	0,00
11.31-16.00mm	-3.5,-4.0 phi	-3,75	13454,34	0,00	0,00	0,00	0,00	0,00
8.00-11.31mm	-3.0,-3.5 phi	-3,25	9513,66	0,00	0,00	0,00	0,00	0,00
5.66-8.00mm	-2.5,-3.0 phi	-2,75	6727,17	0,00	0,00	0,00	0,00	0,00
4.00-5.66mm	-2.5,-2.0 phi	-2,25	4756,83	0,00	0,00	0,00	0,00	0,00
4.00 - 2.83mm	-2.0, -1.5 phi	-1,75	3363,59	0,00	0,00	0,00	0,00	0,00
2.83 - 2.00mm	-1.5, -1.0 phi	-1,25	2378,41	0,00	0,00	0,00	0,00	0,00
2.00 - 1.41mm	-1.0, -0.5 phi	-0,75	1681,79	0,00	0,00	0,00	0,00	0,00
1.41 - 1.00mm	-0.5, 0.0 phi	-0,25	1189,21	0,04	0,04	-0,01	1,71	-10,94
1.00 - 0.71mm	0.0, 0.5 phi	0,25	840,90	0,02	0,06	0,00	0,69	-4,09
0.71 - 0.50mm	0.5, 1.0 phi	0,75	594,60	0,08	0,14	0,06	2,36	-12,74
500.00 - 354.00µm	1.0, 1.5 phi	1,25	420,45	0,09	0,23	0,11	2,10	-10,30
354.00 - 250.00µm	1.5, 2.0 phi	1,75	297,30	0,31	0,55	0,55	6,07	-26,69
250.00 - 177.00µm	2.0, 2.5 phi	2,25	210,22	0,84	1,39	1,90	12,79	-49,84
177.00 - 125.00µm	2.5, 3.0 phi	2,75	148,65	2,20	3,59	6,04	25,33	-86,01
125.00 - 88.40µm	3.0, 3.5 phi	3,25	105,11	4,31	7,90	14,00	36,12	-104,56
88.40 - 62.50µm	3.5, 4.0 phi	3,75	74,33	6,50	14,39	24,36	37,26	-89,25
62.50 - 44.20µm	4.0, 4.,5 phi	4,25	52,56	8,00	22,39	34,01	28,74	-54,47
44.20 - 31.25µm	4.5, 5.0 phi	4,75	37,16	8,58	30,98	40,76	16,70	-23,30
31.25 - 22.10µm	5.0, 5.5 phi	5,25	26,28	8,81	39,79	46,27	7,06	-6,32
22.10 - 15.63µm	5.5, 6.0 phi	5,75	18,58	9,21	49,00	52,96	1,44	-0,57
15.63 - 11.00µm	6.0, 6.5 phi	6,25	13,14	9,47	58,47	59,18	0,10	0,01
11.00 - 7.81µm	6.5, 7.0 phi	6,75	9,29	8,96	67,42	60,45	3,28	1,98
7.81 - 5.52µm	7.0, 7.5 phi	7,25	6,57	7,67	75,10	55,63	9,37	10,35
5.52 - 3.91µm	7.5, 8.0 phi	7,75	4,65	6,33	81,43	49,05	16,30	26,16
3.91 - 2.76µm	8.0, 8.5 phi	8,25	3,28	5,44	86,86	44,87	24,10	50,72
2.76 - 1.95µm	8.5, 9.0 phi	8,75	2,32	4,65	91,51	40,65	31,53	82,12
1.95 - 1.38µm	9.0, 9.5 phi	9,25	1,64	3,50	95,01	32,36	33,72	104,71
1.38 - 0.98µm	9.5, 10.0 phi	9,75	1,16	2,20	97,21	21,46	28,60	103,10
0.98 - 0.69µm	10.0, 10.5 phi	10,25	0,82	1,26	98,47	12,95	21,29	87,41
0.69 - 0.49µm	10.5, 11.0 phi	10,75	0,58	0,79	99,27	8,54	16,85	77,62
0.49 - 0.35µm	11.0 , 11.5 phi	11,25	0,41	0,53	99,80	5,95	13,79	70,39
0.35 - 0.24µm	11.5, 12.0 phi	11,75	0,29	0,20	100,00	2,39	6,38	35,77
0.24 - 0.17µm	12.0, 12.5 phi	12,25	0,21	0,00	100,00	0,00	0,00	0,00
0.17 - 0.12µm	12.5, 13.0 phi	12,75	0,15	0,00	100,00	0,00	0,00	0,00
0.12 - 0.09µm	13.0, 13.5 phi	13,25	0,10	0,00	100,00	0,00	0,00	0,00
0.09 - 0.06µm	13.5, 14.0phi	13,75	0,07	0,00	100,00	0,00	0,00	0,00
0.06 - 0.04µm	14.0, 14.5 phi	14,25	0,05	0,00	100,00	0,00	0,00	0,00
0.04 - 0.03µm	14.5, 15.0 phi	14,75	0,04	0,00	100,00	0,00	0,00	0,00
0.03 - 0.02µm	15.0, 15.5 phi	15,25	0,03	0,00	100,00	0,00	0,00	0,00
METHOD: MALVERN laser sedimentograph (particles <2mm)				100,00		614,51	383,71	171,26
Sieving (particles> 0.5mm)								

Main Classes individual percentages:

Pebble	0,00
Gravel	0,00
Sand	14,39
Silt	67,03
Clay	18,57

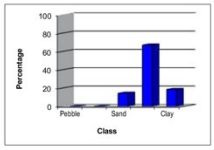

Statistical Parameters:

Mean	6,15
Standard Deviation	1,96
Asymmetry	0,23
P90	8,82
P50	6,05
P5	3,20
Mode	6,25

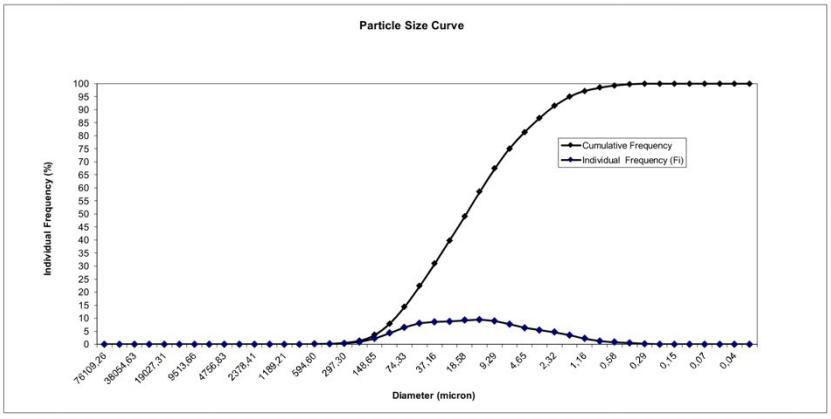

Technician: *Fernanda Dias*

Date:

INSTITUTO HIDROGRÁFICO
DIVISÃO DE GEOLOGIA MARINHA

Station: **2111**

Diameter (class)	Diameter phi	Class midpoint (ci)	Class midpoint (mm)	Individual Frequency (Fi)	Cumulative Frequency	Fi x ci	Fi x (ci-X)^2	Fi x (ci-X)^3
>64.00mm	<6.0 phi	-6,25	76109,26	0,00	0,00	0,00	0,00	0,00
45.25-64.00mm	-5.5,6.0 phi	-5,75	53817,37	0,00	0,00	0,00	0,00	0,00
32.00-45.25mm	-5.0,-5.5 phi	-5,25	38054,63	0,00	0,00	0,00	0,00	0,00
22.63-32.00mm	-4.5,-5.0 phi	-4,75	26908,69	0,00	0,00	0,00	0,00	0,00
16.00-22.63mm	-4.0,-4.5 phi	-4,25	19027,31	0,00	0,00	0,00	0,00	0,00
11.31-16.00mm	-3.5,-4.0 phi	-3,75	13454,34	0,00	0,00	0,00	0,00	0,00
8.00-11.31mm	-3.0,-3.5 phi	-3,25	9513,66	0,00	0,00	0,00	0,00	0,00
5.66-8.00mm	-2.5,-3.0 phi	-2,75	6727,17	0,00	0,00	0,00	0,00	0,00
4.00-5.66mm	-2.5,-2.0 phi	-2,25	4756,83	0,00	0,00	0,00	0,00	0,00
4.00 - 2.83mm	-2.0, -1.5 phi	-1,75	3363,59	0,00	0,00	0,00	0,00	0,00
2.83 - 2.00mm	-1.5, -1.0 phi	-1,25	2378,41	0,00	0,00	0,00	0,00	0,00
2.00 - 1.41mm	-1.0, -0.5 phi	-0,75	1681,79	0,06	0,06	-0,04	2,76	-18,75
1.41 - 1.00mm	-0.5, 0.0 phi	-0,25	1189,21	0,01	0,07	0,00	0,36	-2,24
1.00 - 0.71mm	0.0, 0.5 phi	0,25	840,90	0,02	0,09	0,01	0,76	-4,42
0.71 - 0.50mm	0.5, 1.0 phi	0,75	594,60	0,24	0,33	0,18	6,65	-35,19
500.00 - 354.00µm	1.0, 1.5 phi	1,25	420,45	0,41	0,74	0,51	9,44	-45,26
354.00 - 250.00µm	1.5, 2.0 phi	1,75	297,30	0,49	1,23	0,86	9,09	-39,04
250.00 - 177.00µm	2.0, 2.5 phi	2,25	210,22	0,83	2,07	1,88	12,00	-45,52
177.00 - 125.00µm	2.5, 3.0 phi	2,75	148,65	2,02	4,08	5,55	21,88	-72,07
125.00 - 88.40µm	3.0, 3.5 phi	3,25	105,11	4,07	8,16	13,24	31,80	-88,85
88.40 - 62.50µm	3.5, 4.0 phi	3,75	74,33	6,37	14,52	23,88	33,50	-76,86
62.50 - 44.20µm	4.0, 4.,5 phi	4,25	52,56	8,13	22,65	34,54	26,15	-46,92
44.20 - 31.25µm	4.5, 5.0 phi	4,75	37,16	9,02	31,67	42,83	15,10	-19,53
31.25 - 22.10µm	5.0, 5.5 phi	5,25	26,28	9,46	41,13	49,69	5,97	-4,74
22.10 - 15.63µm	5.5, 6.0 phi	5,75	18,58	9,85	50,98	56,65	0,85	-0,25
15.63 - 11.00µm	6.0, 6.5 phi	6,25	13,14	9,88	60,86	61,74	0,42	0,09
11.00 - 7.81µm	6.5, 7.0 phi	6,75	9,29	9,05	69,91	61,06	4,51	3,18
7.81 - 5.52µm	7.0, 7.5 phi	7,25	6,57	7,49	77,40	54,32	10,90	13,14
5.52 - 3.91µm	7.5, 8.0 phi	7,75	4,65	5,97	83,37	46,26	17,37	29,64
3.91 - 2.76µm	8.0, 8.5 phi	8,25	3,28	4,98	88,35	41,08	24,24	53,47
2.76 - 1.95µm	8.5, 9.0 phi	8,75	2,32	4,17	92,52	36,51	30,55	82,68
1.95 - 1.38µm	9.0, 9.5 phi	9,25	1,64	3,10	95,63	28,72	31,91	102,31
1.38 - 0.98µm	9.5, 10.0 phi	9,75	1,16	1,94	97,56	18,87	26,59	98,53
0.98 - 0.69µm	10.0, 10.5 phi	10,25	0,82	1,10	98,66	11,31	19,52	82,09
0.69 - 0.49µm	10.5, 11.0 phi	10,75	0,58	0,69	99,36	7,45	15,35	72,24
0.49 - 0.35µm	11.0 , 11.5 phi	11,25	0,41	0,46	99,82	5,22	12,58	65,50
0.35 - 0.24µm	11.5, 12.0 phi	11,75	0,29	0,18	100,00	2,10	5,82	33,21
0.24 - 0.17µm	12.0, 12.5 phi	12,25	0,21	0,00	100,00	0,00	0,00	0,00
0.17 - 0.12µm	12.5, 13.0 phi	12,75	0,15	0,00	100,00	0,00	0,00	0,00
0.12 - 0.09µm	13.0, 13.5 phi	13,25	0,10	0,00	100,00	0,00	0,00	0,00
0.09 - 0.06µm	13.5, 14.0phi	13,75	0,07	0,00	100,00	0,00	0,00	0,00
0.06 - 0.04µm	14.0, 14.5 phi	14,25	0,05	0,00	100,00	0,00	0,00	0,00
0.04 - 0.03µm	14.5, 15.0 phi	14,75	0,04	0,00	100,00	0,00	0,00	0,00
0.03 - 0.02µm	15.0, 15.5 phi	15,25	0,03	0,00	100,00	0,00	0,00	0,00
METHOD: MALVERN laser sedimentograph (particles <2mm)				100,00		604,39	376,06	136,47
Sieving (particles> 0.5mm)								

Main Classes individual percentages:

Pebble	0,00
Gravel	0,00
Sand	14,52
Silt	68,84
Clay	16,63

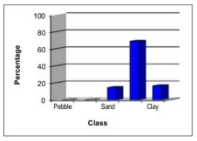

Statistical Parameters:

Mean	6,04
Standard Deviation	1,94
Asymmetry	0,19
P90	8,68
P50	5,95
P5	3,14
Mode	6,25

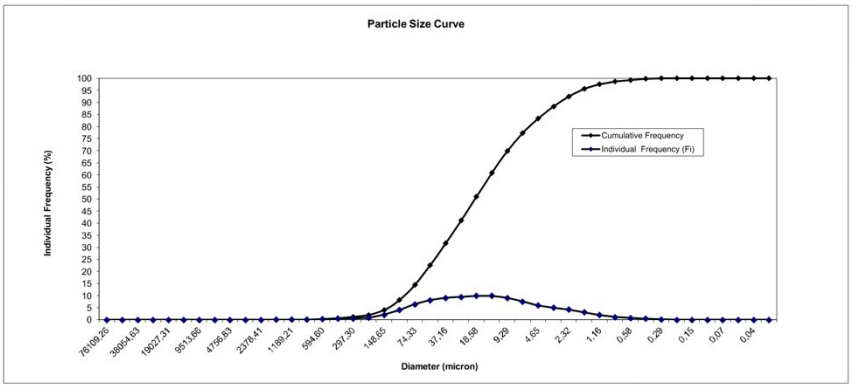

Technician: *Fernanda Dias*

Date:

INSTITUTO HIDROGRÁFICO
DIVISÃO DE GEOLOGIA MARINHA

Station: **2112**

Diameter (class)	Diameter phi	Class midpoint (ci)	Class midpoint (mm)	Individual Frequency (Fi)	Cumulative Frequency	Fi x ci	Fi x (ci-X)^2	Fi x (ci-X)^3
>64.00mm	<6.0 phi	-6,25	76109,26	0,00	0,00	0,00	0,00	0,00
45.25-64.00mm	-5.5,6.0 phi	-5,75	53817,37	0,00	0,00	0,00	0,00	0,00
32.00-45.25mm	-5.0,-5.5 phi	-5,25	38054,63	0,00	0,00	0,00	0,00	0,00
22.63-32.00mm	-4.5,-5.0 phi	-4,75	26908,69	0,00	0,00	0,00	0,00	0,00
16.00-22.63mm	-4.0,-4.5 phi	-4,25	19027,31	0,00	0,00	0,00	0,00	0,00
11.31-16.00mm	-3.5,-4.0 phi	-3,75	13454,34	0,00	0,00	0,00	0,00	0,00
8.00-11.31mm	-3.0,-3.5 phi	-3,25	9513,66	0,00	0,00	0,00	0,00	0,00
5.66-8.00mm	-2.5,-3.0 phi	-2,75	6727,17	0,00	0,00	0,00	0,00	0,00
4.00-5.66mm	-2.5,-2.0 phi	-2,25	4756,83	0,00	0,00	0,00	0,00	0,00
4.00 - 2.83mm	-2.0, -1.5 phi	-1,75	3363,59	0,00	0,00	0,00	0,00	0,00
2.83 - 2.00mm	-1.5, -1.0 phi	-1,25	2378,41	0,00	0,00	0,00	0,00	0,00
2.00 - 1.41mm	-1.0, -0.5 phi	-0,75	1681,79	0,04	0,04	-0,03	1,73	-11,63
1.41 - 1.00mm	-0.5, 0.0 phi	-0,25	1189,21	0,05	0,09	-0,01	1,90	-11,81
1.00 - 0.71mm	0.0, 0.5 phi	0,25	840,90	0,14	0,23	0,04	4,59	-26,23
0.71 - 0.50mm	0.5, 1.0 phi	0,75	594,60	0,38	0,61	0,29	10,41	-54,26
500.00 - 354.00µm	1.0, 1.5 phi	1,25	420,45	0,42	1,03	0,52	9,32	-43,92
354.00 - 250.00µm	1.5, 2.0 phi	1,75	297,30	0,50	1,53	0,88	8,88	-37,38
250.00 - 177.00µm	2.0, 2.5 phi	2,25	210,22	1,06	2,59	2,38	14,58	-54,12
177.00 - 125.00µm	2.5, 3.0 phi	2,75	148,65	2,61	5,20	7,18	26,93	-86,49
125.00 - 88.40µm	3.0, 3.5 phi	3,25	105,11	4,92	10,12	15,99	36,17	-98,06
88.40 - 62.50µm	3.5, 4.0 phi	3,75	74,33	7,09	17,21	26,58	34,66	-76,65
62.50 - 44.20µm	4.0, 4..5 phi	4,25	52,56	8,40	25,61	35,71	24,61	-42,11
44.20 - 31.25µm	4.5, 5.0 phi	4,75	37,16	8,80	34,41	41,80	12,91	-15,64
31.25 - 22.10µm	5.0, 5.5 phi	5,25	26,28	8,92	43,33	46,82	4,51	-3,21
22.10 - 15.63µm	5.5, 6.0 phi	5,75	18,58	9,18	52,51	52,80	0,41	-0,09
15.63 - 11.00µm	6.0, 6.5 phi	6,25	13,14	9,24	61,75	57,72	0,77	0,22
11.00 - 7.81µm	6.5, 7.0 phi	6,75	9,29	8,52	70,27	57,49	5,30	4,18
7.81 - 5.52µm	7.0, 7.5 phi	7,25	6,57	7,12	77,39	51,60	11,82	15,23
5.52 - 3.91µm	7.5, 8.0 phi	7,75	4,65	5,75	83,14	44,57	18,40	32,91
3.91 - 2.76µm	8.0, 8.5 phi	8,25	3,28	4,89	88,03	40,35	25,62	58,64
2.76 - 1.95µm	8.5, 9.0 phi	8,75	2,32	4,18	92,21	36,57	32,50	90,64
1.95 - 1.38µm	9.0, 9.5 phi	9,25	1,64	3,17	95,37	29,30	34,26	112,68
1.38 - 0.98µm	9.5, 10.0 phi	9,75	1,16	2,02	97,39	19,65	28,93	109,61
0.98 - 0.69µm	10.0, 10.5 phi	10,25	0,82	1,17	98,56	12,03	21,58	92,55
0.69 - 0.49µm	10.5, 11.0 phi	10,75	0,58	0,74	99,31	8,00	17,07	81,75
0.49 - 0.35µm	11.0 , 11.5 phi	11,25	0,41	0,50	99,80	5,60	13,92	73,61
0.35 - 0.24µm	11.5, 12.0 phi	11,75	0,29	0,20	100,00	2,29	6,54	37,89
0.24 - 0.17µm	12.0, 12.5 phi	12,25	0,21	0,00	100,00	0,00	0,00	0,00
0.17 - 0.12µm	12.5, 13.0 phi	12,75	0,15	0,00	100,00	0,00	0,00	0,00
0.12 - 0.09µm	13.0, 13.5 phi	13,25	0,10	0,00	100,00	0,00	0,00	0,00
0.09 - 0.06µm	13.5, 14.0phi	13,75	0,07	0,00	100,00	0,00	0,00	0,00
0.06 - 0.04µm	14.0, 14.5 phi	14,25	0,05	0,00	100,00	0,00	0,00	0,00
0.04 - 0.03µm	14.5, 15.0 phi	14,75	0,04	0,00	100,00	0,00	0,00	0,00
0.03 - 0.02µm	15.0, 15.5 phi	15,25	0,03	0,00	100,00	0,00	0,00	0,00
				100,00		596,13	408,34	148,34

METHOD: MALVERN laser sedimentograph (particles <2mm)
Sieving (particles> 0.5mm)

Main Classes individual percentages:

Pebble	0,00
Gravel	0,00
Sand	17,21
Silt	65,92
Clay	16,86

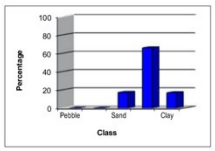

Statistical Parameters:

Mean	5,96
Standard Deviation	2,02
Asymmetry	0,18
P90	8,72
P50	5,86
P5	2,97
Mode	6,25

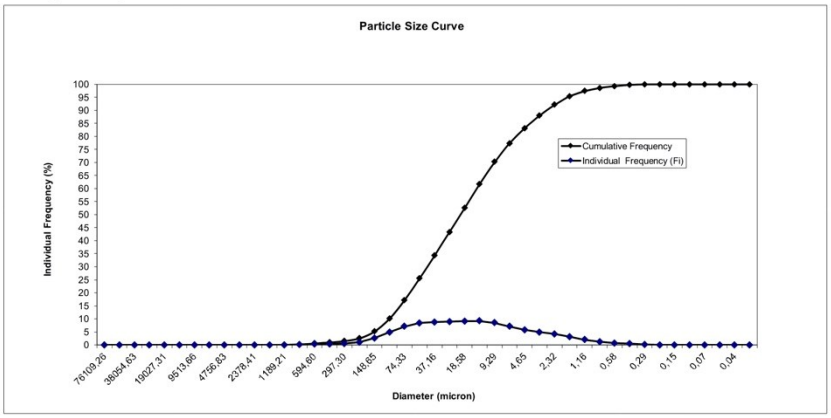

Technician: *Fernanda Dias*

Date:

INSTITUTO HIDROGRÁFICO
DIVISÃO DE GEOLOGIA MARINHA

Station: **2113**

Diameter (class)	Diameter phi	Class midpoint (ci)	Class midpoint (mm)	Individual Frequency (Fi)	Cumulative Frequency	Fi x ci	Fi x (ci-X)^2	Fi x (ci-X)^3
>64.00mm	<6.0 phi	-6,25	76109,26	0,00	0,00	0,00	0,00	0,00
45.25-64.00mm	-5.5,6.0 phi	-5,75	53817,37	0,00	0,00	0,00	0,00	0,00
32.00-45.25mm	-5.0,-5.5 phi	-5,25	38054,63	0,00	0,00	0,00	0,00	0,00
22.63-32.00mm	-4.5,-5.0 phi	-4,75	26908,69	0,00	0,00	0,00	0,00	0,00
16.00-22.63mm	-4.0,-4.5 phi	-4,25	19027,31	0,00	0,00	0,00	0,00	0,00
11.31-16.00mm	-3.5,-4.0 phi	-3,75	13454,34	0,00	0,00	0,00	0,00	0,00
8.00-11.31mm	-3.0,-3.5 phi	-3,25	9513,66	0,00	0,00	0,00	0,00	0,00
5.66-8.00mm	-2.5,-3.0 phi	-2,75	6727,17	0,00	0,00	0,00	0,00	0,00
4.00-5.66mm	-2.5,-2.0 phi	-2,25	4756,83	0,00	0,00	0,00	0,00	0,00
4.00 - 2.83mm	-2.0, -1.5 phi	-1,75	3363,59	0,00	0,00	0,00	0,00	0,00
2.83 - 2.00mm	-1.5, -1.0 phi	-1,25	2378,41	0,00	0,00	0,00	0,00	0,00
2.00 - 1.41mm	-1.0, -0.5 phi	-0,75	1681,79	0,06	0,06	-0,05	2,64	-17,09
1.41 - 1.00mm	-0.5, 0.0 phi	-0,25	1189,21	0,00	0,06	0,00	0,03	-0,19
1.00 - 0.71mm	0.0, 0.5 phi	0,25	840,90	0,09	0,15	0,02	2,73	-14,97
0.71 - 0.50mm	0.5, 1.0 phi	0,75	594,60	0,31	0,47	0,23	7,74	-38,60
500.00 - 354.00µm	1.0, 1.5 phi	1,25	420,45	0,56	1,03	0,70	11,31	-50,71
354.00 - 250.00µm	1.5, 2.0 phi	1,75	297,30	0,85	1,87	1,48	13,42	-53,49
250.00 - 177.00µm	2.0, 2.5 phi	2,25	210,22	1,61	3,49	3,63	19,59	-68,24
177.00 - 125.00µm	2.5, 3.0 phi	2,75	148,65	3,45	6,93	9,48	30,70	-91,61
125.00 - 88.40µm	3.0, 3.5 phi	3,25	105,11	5,97	12,91	19,42	36,87	-91,61
88.40 - 62.50µm	3.5, 4.0 phi	3,75	74,33	8,12	21,03	30,44	31,97	-63,44
62.50 - 44.20µm	4.0, 4..5 phi	4,25	52,56	9,17	30,19	38,96	20,20	-29,99
44.20 - 31.25µm	4.5, 5.0 phi	4,75	37,16	9,20	39,39	43,69	8,91	-8,77
31.25 - 22.10µm	5.0, 5.5 phi	5,25	26,28	8,94	48,33	46,92	2,10	-1,02
22.10 - 15.63µm	5.5, 6.0 phi	5,75	18,58	8,85	57,18	50,90	0,00	0,00
15.63 - 11.00µm	6.0, 6.5 phi	6,25	13,14	8,66	65,84	54,11	2,30	1,19
11.00 - 7.81µm	6.5, 7.0 phi	6,75	9,29	7,85	73,69	52,98	8,09	8,22
7.81 - 5.52µm	7.0, 7.5 phi	7,25	6,57	6,49	80,18	47,04	14,90	22,59
5.52 - 3.91µm	7.5, 8.0 phi	7,75	4,65	5,18	85,36	40,16	21,05	42,43
3.91 - 2.76µm	8.0, 8.5 phi	8,25	3,28	4,34	89,70	35,81	27,47	69,09
2.76 - 1.95µm	8.5, 9.0 phi	8,75	2,32	3,65	93,35	31,95	33,21	100,14
1.95 - 1.38µm	9.0, 9.5 phi	9,25	1,64	2,73	96,08	25,27	33,77	118,70
1.38 - 0.98µm	9.5, 10.0 phi	9,75	1,16	1,72	97,80	16,74	27,68	111,14
0.98 - 0.69µm	10.0, 10.5 phi	10,25	0,82	0,99	98,79	10,12	20,13	90,91
0.69 - 0.49µm	10.5, 11.0 phi	10,75	0,58	0,62	99,41	6,72	15,72	78,83
0.49 - 0.35µm	11.0 , 11.5 phi	11,25	0,41	0,42	99,83	4,75	12,83	70,79
0.35 - 0.24µm	11.5, 12.0 phi	11,75	0,29	0,17	100,00	1,97	6,08	36,57
0.24 - 0.17µm	12.0, 12.5 phi	12,25	0,21	0,00	100,00	0,00	0,00	0,00
0.17 - 0.12µm	12.5, 13.0 phi	12,75	0,15	0,00	100,00	0,00	0,00	0,00
0.12 - 0.09µm	13.0, 13.5 phi	13,25	0,10	0,00	100,00	0,00	0,00	0,00
0.09 - 0.06µm	13.5, 14.0phi	13,75	0,07	0,00	100,00	0,00	0,00	0,00
0.06 - 0.04µm	14.0, 14.5 phi	14,25	0,05	0,00	100,00	0,00	0,00	0,00
0.04 - 0.03µm	14.5, 15.0 phi	14,75	0,04	0,00	100,00	0,00	0,00	0,00
0.03 - 0.02µm	15.0, 15.5 phi	15,25	0,03	0,00	100,00	0,00	0,00	0,00
				100,00		573,44	411,44	220,86

METHOD: MALVERN laser sedimentograph (particles <2mm)
Sieving (particles> 0.5mm)

Main Classes individual percentages:

Pebble	0,00
Gravel	0,00
Sand	21,03
Silt	64,33
Clay	14,64

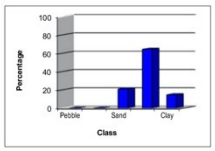

Statistical Parameters:

Mean	5,73
Standard Deviation	2,03
Asymmetry	0,26
P90	8,54
P50	5,59
P5	2,75
Mode	4,75

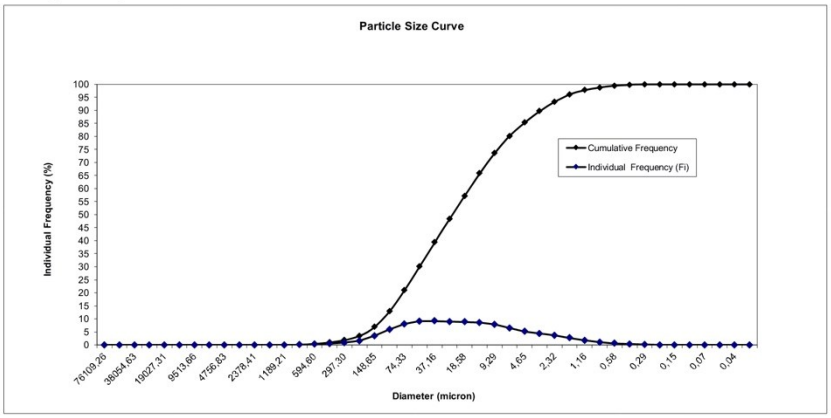

Technician: *Fernanda Dias*

Date:

INSTITUTO HIDROGRÁFICO
DIVISÃO DE GEOLOGIA MARINHA

Station: **2114**

Diameter (class)	Diameter phi	Class midpoint (ci)	Class midpoint (mm)	Individual Frequency (Fi)	Cumulative Frequency	Fi x ci	Fi x (ci-X)^2	Fi x (ci-X)^3
>64.00mm	<6.0 phi	-6,25	76109,26	0,00	0,00	0,00	0,00	0,00
45.25-64.00mm	-5.5,6.0 phi	-5,75	53817,37	0,00	0,00	0,00	0,00	0,00
32.00-45.25mm	-5.0,-5.5 phi	-5,25	38054,63	0,00	0,00	0,00	0,00	0,00
22.63-32.00mm	-4.5,-5.0 phi	-4,75	26908,69	0,00	0,00	0,00	0,00	0,00
16.00-22.63mm	-4.0,-4.5 phi	-4,25	19027,31	0,00	0,00	0,00	0,00	0,00
11.31-16.00mm	-3.5,-4.0 phi	-3,75	13454,34	0,00	0,00	0,00	0,00	0,00
8.00-11.31mm	-3.0,-3.5 phi	-3,25	9513,66	0,00	0,00	0,00	0,00	0,00
5.66-8.00mm	-2.5,-3.0 phi	-2,75	6727,17	0,00	0,00	0,00	0,00	0,00
4.00-5.66mm	-2.5,-2.0 phi	-2,25	4756,83	0,00	0,00	0,00	0,00	0,00
4.00 - 2.83mm	-2.0, -1.5 phi	-1,75	3363,59	0,00	0,00	0,00	0,00	0,00
2.83 - 2.00mm	-1.5, -1.0 phi	-1,25	2378,41	0,00	0,00	0,00	0,00	0,00
2.00 - 1.41mm	-1.0, -0.5 phi	-0,75	1681,79	0,04	0,04	-0,03	1,56	-10,35
1.41 - 1.00mm	-0.5, 0.0 phi	-0,25	1189,21	0,07	0,10	-0,02	2,52	-15,48
1.00 - 0.71mm	0.0, 0.5 phi	0,25	840,90	0,09	0,19	0,02	2,83	-15,94
0.71 - 0.50mm	0.5, 1.0 phi	0,75	594,60	0,23	0,42	0,17	5,97	-30,66
500.00 - 354.00µm	1.0, 1.5 phi	1,25	420,45	0,30	0,72	0,38	6,50	-30,13
354.00 - 250.00µm	1.5, 2.0 phi	1,75	297,30	0,45	1,17	0,79	7,67	-31,72
250.00 - 177.00µm	2.0, 2.5 phi	2,25	210,22	1,16	2,33	2,60	15,26	-55,46
177.00 - 125.00µm	2.5, 3.0 phi	2,75	148,65	3,01	5,34	8,29	29,61	-92,80
125.00 - 88.40µm	3.0, 3.5 phi	3,25	105,11	5,70	11,04	18,53	39,56	-104,22
88.40 - 62.50µm	3.5, 4.0 phi	3,75	74,33	8,05	19,10	30,20	36,67	-78,26
62.50 - 44.20µm	4.0, 4..5 phi	4,25	52,56	9,12	28,22	38,76	24,35	-39,79
44.20 - 31.25µm	4.5, 5.0 phi	4,75	37,16	8,94	37,15	42,45	11,49	-13,04
31.25 - 22.10µm	5.0, 5.5 phi	5,25	26,28	8,50	45,65	44,63	3,42	-2,17
22.10 - 15.63µm	5.5, 6.0 phi	5,75	18,58	8,52	54,18	49,01	0,15	-0,02
15.63 - 11.00µm	6.0, 6.5 phi	6,25	13,14	8,67	62,85	54,17	1,16	0,42
11.00 - 7.81µm	6.5, 7.0 phi	6,75	9,29	8,18	71,02	55,21	6,13	5,31
7.81 - 5.52µm	7.0, 7.5 phi	7,25	6,57	6,97	77,99	50,51	13,00	17,76
5.52 - 3.91µm	7.5, 8.0 phi	7,75	4,65	5,68	83,67	43,99	19,76	36,88
3.91 - 2.76µm	8.0, 8.5 phi	8,25	3,28	4,81	88,48	39,67	26,92	63,68
2.76 - 1.95µm	8.5, 9.0 phi	8,75	2,32	4,07	92,55	35,61	33,43	95,80
1.95 - 1.38µm	9.0, 9.5 phi	9,25	1,64	3,06	95,60	28,29	34,66	116,65
1.38 - 0.98µm	9.5, 10.0 phi	9,75	1,16	1,93	97,54	18,86	28,91	111,77
0.98 - 0.69µm	10.0, 10.5 phi	10,25	0,82	1,12	98,66	11,48	21,35	93,23
0.69 - 0.49µm	10.5, 11.0 phi	10,75	0,58	0,70	99,36	7,58	16,69	81,20
0.49 - 0.35µm	11.0 , 11.5 phi	11,25	0,41	0,46	99,83	5,21	13,32	71,50
0.35 - 0.24µm	11.5, 12.0 phi	11,75	0,29	0,17	100,00	2,03	5,96	34,95
0.24 - 0.17µm	12.0, 12.5 phi	12,25	0,21	0,00	100,00	0,00	0,00	0,00
0.17 - 0.12µm	12.5, 13.0 phi	12,75	0,15	0,00	100,00	0,00	0,00	0,00
0.12 - 0.09µm	13.0, 13.5 phi	13,25	0,10	0,00	100,00	0,00	0,00	0,00
0.09 - 0.06µm	13.5, 14.0phi	13,75	0,07	0,00	100,00	0,00	0,00	0,00
0.06 - 0.04µm	14.0, 14.5 phi	14,25	0,05	0,00	100,00	0,00	0,00	0,00
0.04 - 0.03µm	14.5, 15.0 phi	14,75	0,04	0,00	100,00	0,00	0,00	0,00
0.03 - 0.02µm	15.0, 15.5 phi	15,25	0,03	0,00	100,00	0,00	0,00	0,00
				100,00		588,41	408,88	209,09

METHOD: MALVERN laser sedimentograph (particles <2mm)
Sieving (particles> 0.5mm)

Main Classes individual percentages:

Pebble	0,00
Gravel	0,00
Sand	19,10
Silt	64,57
Clay	16,33

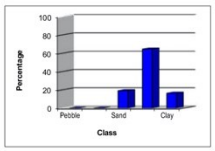

Statistical Parameters:

Mean	5,88
Standard Deviation	2,02
Asymmetry	0,25
P90	8,67
P50	5,75
P5	2,96
Mode	4,25

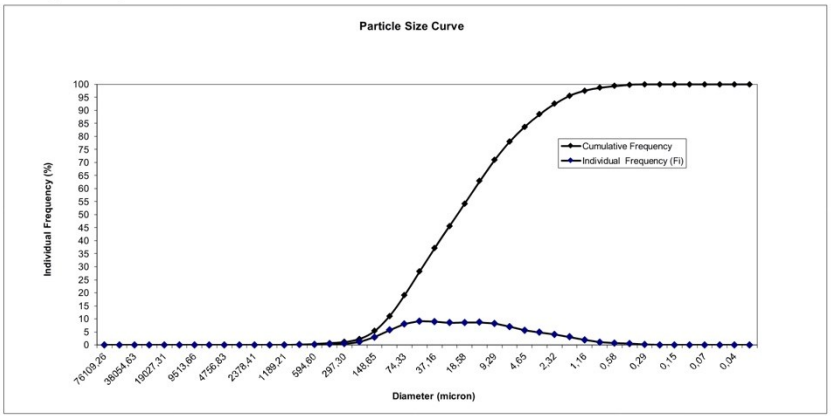

Técnico Responsável: *Fernanda Dias*

Data:

INSTITUTO HIDROGRÁFICO
DIVISÃO DE GEOLOGIA MARINHA

Station: **2115**

Diameter (class)	Diameter phi	Class midpoint (ci)	Class midpoint (mm)	Individual Frequency (Fi)	Cumulative Frequency	Fi x ci	Fi x (ci-X)^2	Fi x (ci-X)^3
>64.00mm	<6.0 phi	-6,25	76109,26	0,00	0,00	0,00	0,00	0,00
45.25-64.00mm	-5.5,6.0 phi	-5,75	53817,37	0,00	0,00	0,00	0,00	0,00
32.00-45.25mm	-5.0,-5.5 phi	-5,25	38054,63	0,00	0,00	0,00	0,00	0,00
22.63-32.00mm	-4.5,-5.0 phi	-4,75	26908,69	0,00	0,00	0,00	0,00	0,00
16.00-22.63mm	-4.0,-4.5 phi	-4,25	19027,31	0,00	0,00	0,00	0,00	0,00
11.31-16.00mm	-3.5,-4.0 phi	-3,75	13454,34	0,00	0,00	0,00	0,00	0,00
8.00-11.31mm	-3.0,-3.5 phi	-3,25	9513,66	0,00	0,00	0,00	0,00	0,00
5.66-8.00mm	-2.5,-3.0 phi	-2,75	6727,17	0,00	0,00	0,00	0,00	0,00
4.00-5.66mm	-2.5,-2.0 phi	-2,25	4756,83	0,00	0,00	0,00	0,00	0,00
4.00 - 2.83mm	-2.0, -1.5 phi	-1,75	3363,59	0,11	0,11	-0,20	6,68	-51,65
2.83 - 2.00mm	-1.5, -1.0 phi	-1,25	2378,41	0,00	0,11	0,00	0,00	0,00
2.00 - 1.41mm	-1.0, -0.5 phi	-0,75	1681,79	0,00	0,11	0,00	0,00	0,00
1.41 - 1.00mm	-0.5, 0.0 phi	-0,25	1189,21	0,07	0,18	-0,02	2,53	-15,77
1.00 - 0.71mm	0.0, 0.5 phi	0,25	840,90	0,09	0,27	0,02	3,00	-17,20
0.71 - 0.50mm	0.5, 1.0 phi	0,75	594,60	0,38	0,64	0,28	10,31	-53,96
500.00 - 354.00µm	1.0, 1.5 phi	1,25	420,45	0,37	1,02	0,47	8,40	-39,77
354.00 - 250.00µm	1.5, 2.0 phi	1,75	297,30	0,47	1,48	0,81	8,34	-35,33
250.00 - 177.00µm	2.0, 2.5 phi	2,25	210,22	1,07	2,56	2,41	14,93	-55,76
177.00 - 125.00µm	2.5, 3.0 phi	2,75	148,65	2,77	5,32	7,60	28,93	-93,56
125.00 - 88.40µm	3.0, 3.5 phi	3,25	105,11	5,24	10,56	17,02	39,16	-107,09
88.40 - 62.50µm	3.5, 4.0 phi	3,75	74,33	7,41	17,96	27,77	36,97	-82,61
62.50 - 44.20µm	4.0, 4.,5 phi	4,25	52,56	8,42	26,38	35,77	25,32	-43,91
44.20 - 31.25µm	4.5, 5.0 phi	4,75	37,16	8,35	34,73	39,65	12,72	-15,70
31.25 - 22.10µm	5.0, 5.5 phi	5,25	26,28	8,17	42,90	42,91	4,41	-3,24
22.10 - 15.63µm	5.5, 6.0 phi	5,75	18,58	8,51	51,42	48,95	0,47	-0,11
15.63 - 11.00µm	6.0, 6.5 phi	6,25	13,14	8,90	60,32	55,65	0,63	0,17
11.00 - 7.81µm	6.5, 7.0 phi	6,75	9,29	8,53	68,85	57,59	5,00	3,83
7.81 - 5.52µm	7.0, 7.5 phi	7,25	6,57	7,35	76,20	53,29	11,78	14,90
5.52 - 3.91µm	7.5, 8.0 phi	7,75	4,65	6,07	82,27	47,05	18,93	33,42
3.91 - 2.76µm	8.0, 8.5 phi	8,25	3,28	5,21	87,49	43,01	26,76	60,63
2.76 - 1.95µm	8.5, 9.0 phi	8,75	2,32	4,44	91,93	38,89	33,99	94,01
1.95 - 1.38µm	9.0, 9.5 phi	9,25	1,64	3,34	95,27	30,88	35,60	116,25
1.38 - 0.98µm	9.5, 10.0 phi	9,75	1,16	2,09	97,36	20,43	29,71	111,86
0.98 - 0.69µm	10.0, 10.5 phi	10,25	0,82	1,20	98,56	12,30	21,83	93,11
0.69 - 0.49µm	10.5, 11.0 phi	10,75	0,58	0,75	99,31	8,08	17,07	81,35
0.49 - 0.35µm	11.0 , 11.5 phi	11,25	0,41	0,50	99,81	5,60	13,79	72,64
0.35 - 0.24µm	11.5, 12.0 phi	11,75	0,29	0,19	100,00	2,21	6,26	36,12
0.24 - 0.17µm	12.0, 12.5 phi	12,25	0,21	0,00	100,00	0,00	0,00	0,00
0.17 - 0.12µm	12.5, 13.0 phi	12,75	0,15	0,00	100,00	0,00	0,00	0,00
0.12 - 0.09µm	13.0, 13.5 phi	13,25	0,10	0,00	100,00	0,00	0,00	0,00
0.09 - 0.06µm	13.5, 14.0phi	13,75	0,07	0,00	100,00	0,00	0,00	0,00
0.06 - 0.04µm	14.0, 14.5 phi	14,25	0,05	0,00	100,00	0,00	0,00	0,00
0.04 - 0.03µm	14.5, 15.0 phi	14,75	0,04	0,00	100,00	0,00	0,00	0,00
0.03 - 0.02µm	15.0, 15.5 phi	15,25	0,03	0,00	100,00	0,00	0,00	0,00
				100,00		598,43	423,51	102,64

METHOD: MALVERN laser sedimentograph (particles <2mm)
Sieving (particles> 0.5mm)

Main Classes individual percentages:

Pebble	0,00
Gravel	0,11
Sand	17,85
Silt	64,31
Clay	17,73

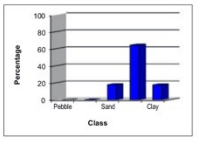

Statistical Parameters:

Mean	5,98
Standard Deviation	2,06
Asymmetry	0,12
P90	8,76
P50	5,92
P5	2,95
Mode	6,25

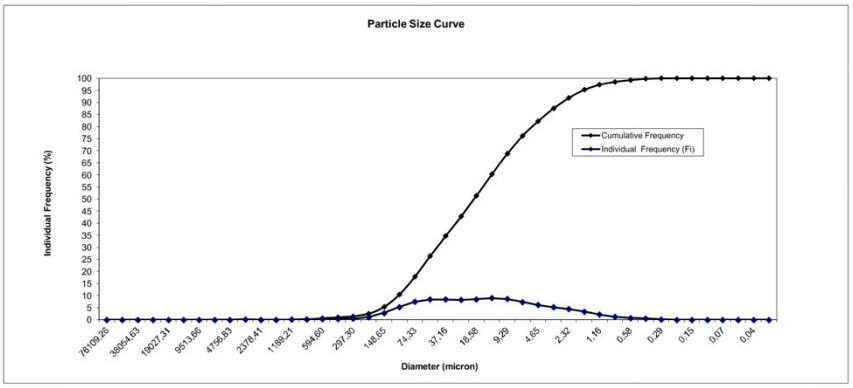

Technician: *Fernanda Dias*

Date:

INSTITUTO HIDROGRÁFICO
DIVISÃO DE GEOLOGIA MARINHA

Station: **2116**

Diameter (class)	Diameter phi	Class midpoint (ci)	Class midpoint (mm)	Individual Frequency (Fi)	Cumulative Frequency	Fi x ci	Fi x (ci-X)^2	Fi x (ci-X)^3
>64.00mm	<6.0 phi	-6,25	76109,26	0,00	0,00	0,00	0,00	0,00
45.25-64.00mm	-5.5,6.0 phi	-5,75	53817,37	0,00	0,00	0,00	0,00	0,00
32.00-45.25mm	-5.0,-5.5 phi	-5,25	38054,63	0,00	0,00	0,00	0,00	0,00
22.63-32.00mm	-4.5,-5.0 phi	-4,75	26908,69	0,00	0,00	0,00	0,00	0,00
16.00-22.63mm	-4.0,-4.5 phi	-4,25	19027,31	0,00	0,00	0,00	0,00	0,00
11.31-16.00mm	-3.5,-4.0 phi	-3,75	13454,34	0,00	0,00	0,00	0,00	0,00
8.00-11.31mm	-3.0,-3.5 phi	-3,25	9513,66	0,00	0,00	0,00	0,00	0,00
5.66-8.00mm	-2.5,-3.0 phi	-2,75	6727,17	0,00	0,00	0,00	0,00	0,00
4.00-5.66mm	-2.5,-2.0 phi	-2,25	4756,83	0,42	0,42	-0,95	29,07	-240,90
4.00 - 2.83mm	-2.0, -1.5 phi	-1,75	3363,59	0,00	0,42	0,00	0,00	0,00
2.83 - 2.00mm	-1.5, -1.0 phi	-1,25	2378,41	0,00	0,42	0,00	0,00	0,00
2.00 - 1.41mm	-1.0, -0.5 phi	-0,75	1681,79	0,00	0,42	0,00	0,00	0,00
1.41 - 1.00mm	-0.5, 0.0 phi	-0,25	1189,21	0,05	0,48	-0,01	2,12	-13,36
1.00 - 0.71mm	0.0, 0.5 phi	0,25	840,90	0,13	0,61	0,03	4,41	-25,54
0.71 - 0.50mm	0.5, 1.0 phi	0,75	594,60	0,31	0,92	0,23	8,61	-45,54
500.00 - 354.00µm	1.0, 1.5 phi	1,25	420,45	0,30	1,22	0,38	6,90	-33,04
354.00 - 250.00µm	1.5, 2.0 phi	1,75	297,30	0,35	1,57	0,62	6,48	-27,80
250.00 - 177.00µm	2.0, 2.5 phi	2,25	210,22	0,87	2,44	1,96	12,48	-47,26
177.00 - 125.00µm	2.5, 3.0 phi	2,75	148,65	2,41	4,85	6,64	26,06	-85,66
125.00 - 88.40µm	3.0, 3.5 phi	3,25	105,11	4,82	9,67	15,66	37,41	-104,25
88.40 - 62.50µm	3.5, 4.0 phi	3,75	74,33	7,12	16,79	26,70	37,22	-85,11
62.50 - 44.20µm	4.0, 4..5 phi	4,25	52,56	8,33	25,13	35,42	26,60	-47,52
44.20 - 31.25µm	4.5, 5.0 phi	4,75	37,16	8,35	33,47	39,65	13,82	-17,78
31.25 - 22.10µm	5.0, 5.5 phi	5,25	26,28	8,13	41,60	42,67	5,03	-3,96
22.10 - 15.63µm	5.5, 6.0 phi	5,75	18,58	8,45	50,05	48,59	0,69	-0,20
15.63 - 11.00µm	6.0, 6.5 phi	6,25	13,14	8,95	59,00	55,96	0,41	0,09
11.00 - 7.81µm	6.5, 7.0 phi	6,75	9,29	8,74	67,74	58,99	4,45	3,17
7.81 - 5.52µm	7.0, 7.5 phi	7,25	6,57	7,62	75,36	55,23	11,22	13,61
5.52 - 3.91µm	7.5, 8.0 phi	7,75	4,65	6,29	81,65	48,76	18,47	31,65
3.91 - 2.76µm	8.0, 8.5 phi	8,25	3,28	5,37	87,02	44,30	26,31	58,22
2.76 - 1.95µm	8.5, 9.0 phi	8,75	2,32	4,57	91,59	39,95	33,62	91,22
1.95 - 1.38µm	9.0, 9.5 phi	9,25	1,64	3,45	95,03	31,87	35,58	114,34
1.38 - 0.98µm	9.5, 10.0 phi	9,75	1,16	2,19	97,22	21,31	30,14	111,92
0.98 - 0.69µm	10.0, 10.5 phi	10,25	0,82	1,27	98,49	12,98	22,48	94,72
0.69 - 0.49µm	10.5, 11.0 phi	10,75	0,58	0,79	99,28	8,54	17,64	83,17
0.49 - 0.35µm	11.0 , 11.5 phi	11,25	0,41	0,52	99,80	5,87	14,18	73,91
0.35 - 0.24µm	11.5, 12.0 phi	11,75	0,29	0,20	100,00	2,33	6,49	37,05
0.24 - 0.17µm	12.0, 12.5 phi	12,25	0,21	0,00	100,00	0,00	0,00	0,00
0.17 - 0.12µm	12.5, 13.0 phi	12,75	0,15	0,00	100,00	0,00	0,00	0,00
0.12 - 0.09µm	13.0, 13.5 phi	13,25	0,10	0,00	100,00	0,00	0,00	0,00
0.09 - 0.06µm	13.5, 14.0phi	13,75	0,07	0,00	100,00	0,00	0,00	0,00
0.06 - 0.04µm	14.0, 14.5 phi	14,25	0,05	0,00	100,00	0,00	0,00	0,00
0.04 - 0.03µm	14.5, 15.0 phi	14,75	0,04	0,00	100,00	0,00	0,00	0,00
0.03 - 0.02µm	15.0, 15.5 phi	15,25	0,03	0,00	100,00	0,00	0,00	0,00
				100,00		603,66	437,90	-64,82

METHOD: MALVERN laser sedimentograph (particles <2mm)
Sieving (particles> 0.5mm)

Main Classes individual percentages:

Pebble	0,00
Gravel	0,42
Sand	16,37
Silt	64,86
Clay	18,35

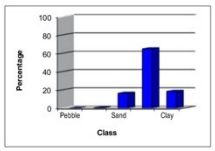

Statistical Parameters:

Mean	6,04
Standard Deviation	2,09
Asymmetry	-0,07
P90	8,81
P50	6,00
P5	3,02
Mode	6,25

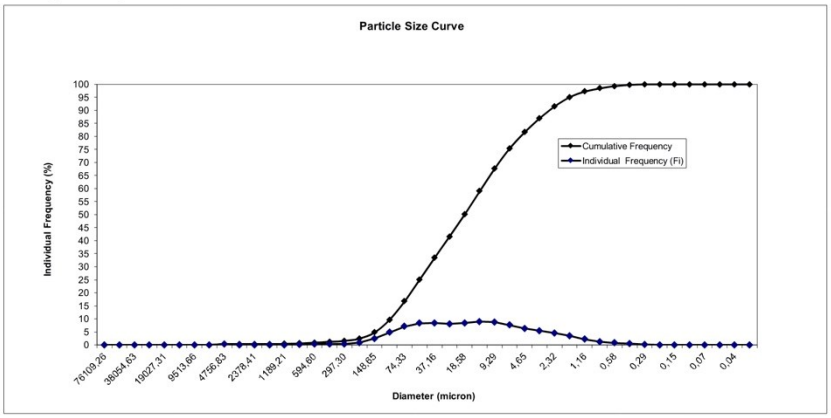

Technician: *Fernanda Dias*

Date:

INSTITUTO HIDROGRÁFICO
DIVISÃO DE GEOLOGIA MARINHA

Station: **2117**

Diameter (class)	Diameter phi	Class midpoint (ci)	Class midpoint (mm)	Individual Frequency (Fi)	Cumulative Frequency	Fi x ci	Fi x (ci-X)^2	Fi x (ci-X)^3
>64.00mm	<6.0 phi	-6,25	76109,26	0,00	0,00	0,00	0,00	0,00
45.25-64.00mm	-5.5,6.0 phi	-5,75	53817,37	0,00	0,00	0,00	0,00	0,00
32.00-45.25mm	-5.0,-5.5 phi	-5,25	38054,63	0,00	0,00	0,00	0,00	0,00
22.63-32.00mm	-4.5,-5.0 phi	-4,75	26908,69	0,00	0,00	0,00	0,00	0,00
16.00-22.63mm	-4.0,-4.5 phi	-4,25	19027,31	0,00	0,00	0,00	0,00	0,00
11.31-16.00mm	-3.5,-4.0 phi	-3,75	13454,34	0,00	0,00	0,00	0,00	0,00
8.00-11.31mm	-3.0,-3.5 phi	-3,25	9513,66	0,00	0,00	0,00	0,00	0,00
5.66-8.00mm	-2.5,-3.0 phi	-2,75	6727,17	0,00	0,00	0,00	0,00	0,00
4.00-5.66mm	-2.5,-2.0 phi	-2,25	4756,83	0,00	0,00	0,00	0,00	0,00
4.00 - 2.83mm	-2.0, -1.5 phi	-1,75	3363,59	0,00	0,00	0,00	0,00	0,00
2.83 - 2.00mm	-1.5, -1.0 phi	-1,25	2378,41	0,00	0,00	0,00	0,00	0,00
2.00 - 1.41mm	-1.0, -0.5 phi	-0,75	1681,79	0,03	0,03	-0,03	1,57	-10,57
1.41 - 1.00mm	-0.5, 0.0 phi	-0,25	1189,21	0,09	0,12	-0,02	3,41	-21,15
1.00 - 0.71mm	0.0, 0.5 phi	0,25	840,90	0,23	0,35	0,06	7,48	-42,73
0.71 - 0.50mm	0.5, 1.0 phi	0,75	594,60	0,42	0,77	0,31	11,39	-59,37
500.00 - 354.00µm	1.0, 1.5 phi	1,25	420,45	0,38	1,15	0,47	8,41	-39,60
354.00 - 250.00µm	1.5, 2.0 phi	1,75	297,30	0,46	1,61	0,81	8,22	-34,61
250.00 - 177.00µm	2.0, 2.5 phi	2,25	210,22	1,10	2,71	2,47	15,12	-56,13
177.00 - 125.00µm	2.5, 3.0 phi	2,75	148,65	2,73	5,45	7,52	28,18	-90,48
125.00 - 88.40µm	3.0, 3.5 phi	3,25	105,11	5,09	10,54	16,54	37,41	-101,42
88.40 - 62.50µm	3.5, 4.0 phi	3,75	74,33	7,25	17,79	27,19	35,45	-78,38
62.50 - 44.20µm	4.0, 4..5 phi	4,25	52,56	8,44	26,23	35,88	24,72	-42,29
44.20 - 31.25µm	4.5, 5.0 phi	4,75	37,16	8,63	34,86	40,99	12,65	-15,32
31.25 - 22.10µm	5.0, 5.5 phi	5,25	26,28	8,56	43,42	44,93	4,33	-3,08
22.10 - 15.63µm	5.5, 6.0 phi	5,75	18,58	8,76	52,18	50,39	0,39	-0,08
15.63 - 11.00µm	6.0, 6.5 phi	6,25	13,14	8,93	61,12	55,84	0,75	0,22
11.00 - 7.81µm	6.5, 7.0 phi	6,75	9,29	8,44	69,55	56,94	5,25	4,14
7.81 - 5.52µm	7.0, 7.5 phi	7,25	6,57	7,22	76,78	52,38	12,00	15,47
5.52 - 3.91µm	7.5, 8.0 phi	7,75	4,65	5,94	82,72	46,05	19,02	34,03
3.91 - 2.76µm	8.0, 8.5 phi	8,25	3,28	5,08	87,80	41,91	26,62	60,93
2.76 - 1.95µm	8.5, 9.0 phi	8,75	2,32	4,32	92,12	37,79	33,60	93,71
1.95 - 1.38µm	9.0, 9.5 phi	9,25	1,64	3,25	95,37	30,04	35,13	115,54
1.38 - 0.98µm	9.5, 10.0 phi	9,75	1,16	2,05	97,41	19,95	29,38	111,32
0.98 - 0.69µm	10.0, 10.5 phi	10,25	0,82	1,18	98,59	12,06	21,65	92,85
0.69 - 0.49µm	10.5, 11.0 phi	10,75	0,58	0,74	99,33	7,92	16,90	80,95
0.49 - 0.35µm	11.0 , 11.5 phi	11,25	0,41	0,49	99,81	5,48	13,64	72,12
0.35 - 0.24µm	11.5, 12.0 phi	11,75	0,29	0,19	100,00	2,20	6,28	36,33
0.24 - 0.17µm	12.0, 12.5 phi	12,25	0,21	0,00	100,00	0,00	0,00	0,00
0.17 - 0.12µm	12.5, 13.0 phi	12,75	0,15	0,00	100,00	0,00	0,00	0,00
0.12 - 0.09µm	13.0, 13.5 phi	13,25	0,10	0,00	100,00	0,00	0,00	0,00
0.09 - 0.06µm	13.5, 14.0phi	13,75	0,07	0,00	100,00	0,00	0,00	0,00
0.06 - 0.04µm	14.0, 14.5 phi	14,25	0,05	0,00	100,00	0,00	0,00	0,00
0.04 - 0.03µm	14.5, 15.0 phi	14,75	0,04	0,00	100,00	0,00	0,00	0,00
0.03 - 0.02µm	15.0, 15.5 phi	15,25	0,03	0,00	100,00	0,00	0,00	0,00
METHOD: MALVERN laser sedimentograph (particles <2mm)				100,00		596,10	418,94	122,39
Sieving (particles> 0.5mm)								

Main Classes individual percentages:

Pebble	0,00
Gravel	0,00
Sand	17,79
Silt	64,93
Clay	17,28

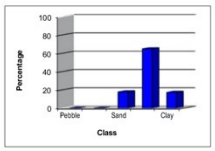

Statistical Parameters:

Mean	5,96
Standard Deviation	2,05
Asymmetry	0,14
P90	8,73
P50	5,88
P5	2,94
Mode	6,25

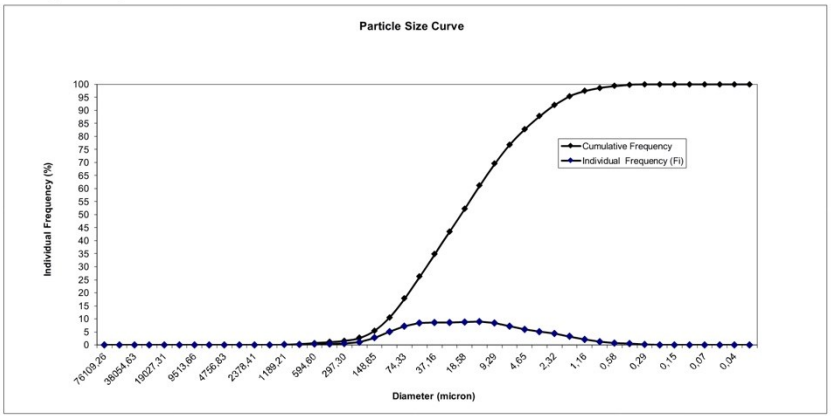

Technician: *Fernanda Dias*

Date:

INSTITUTO HIDROGRÁFICO
DIVISÃO DE GEOLOGIA MARINHA

Station: **2118**

Diameter (class)	Diameter phi	Class midpoint (ci)	Class midpoint (mm)	Individual Frequency (Fi)	Cumulative Frequency	Fi x ci	Fi x (ci-X)^2	Fi x (ci-X)^3
>64.00mm	<6.0 phi	-6,25	76109,26	0,00	0,00	0,00	0,00	0,00
45.25-64.00mm	-5.5,6.0 phi	-5,75	53817,37	0,00	0,00	0,00	0,00	0,00
32.00-45.25mm	-5.0,-5.5 phi	-5,25	38054,63	0,00	0,00	0,00	0,00	0,00
22.63-32.00mm	-4.5,-5.0 phi	-4,75	26908,69	0,00	0,00	0,00	0,00	0,00
16.00-22.63mm	-4.0,-4.5 phi	-4,25	19027,31	0,00	0,00	0,00	0,00	0,00
11.31-16.00mm	-3.5,-4.0 phi	-3,75	13454,34	0,00	0,00	0,00	0,00	0,00
8.00-11.31mm	-3.0,-3.5 phi	-3,25	9513,66	0,00	0,00	0,00	0,00	0,00
5.66-8.00mm	-2.5,-3.0 phi	-2,75	6727,17	0,00	0,00	0,00	0,00	0,00
4.00-5.66mm	-2.5,-2.0 phi	-2,25	4756,83	0,00	0,00	0,00	0,00	0,00
4.00 - 2.83mm	-2.0, -1.5 phi	-1,75	3363,59	0,00	0,00	0,00	0,00	0,00
2.83 - 2.00mm	-1.5, -1.0 phi	-1,25	2378,41	0,00	0,00	0,00	0,00	0,00
2.00 - 1.41mm	-1.0, -0.5 phi	-0,75	1681,79	0,00	0,00	0,00	0,00	0,00
1.41 - 1.00mm	-0.5, 0.0 phi	-0,25	1189,21	0,04	0,04	-0,01	1,68	-10,41
1.00 - 0.71mm	0.0, 0.5 phi	0,25	840,90	0,10	0,14	0,02	3,11	-17,72
0.71 - 0.50mm	0.5, 1.0 phi	0,75	594,60	0,35	0,49	0,26	9,40	-48,87
500.00 - 354.00µm	1.0, 1.5 phi	1,25	420,45	0,44	0,93	0,55	9,77	-45,90
354.00 - 250.00µm	1.5, 2.0 phi	1,75	297,30	0,60	1,53	1,05	10,60	-44,51
250.00 - 177.00µm	2.0, 2.5 phi	2,25	210,22	1,19	2,72	2,67	16,23	-60,03
177.00 - 125.00µm	2.5, 3.0 phi	2,75	148,65	2,75	5,47	7,57	28,17	-90,11
125.00 - 88.40µm	3.0, 3.5 phi	3,25	105,11	5,09	10,56	16,55	37,10	-100,15
88.40 - 62.50µm	3.5, 4.0 phi	3,75	74,33	7,22	17,78	27,08	34,94	-76,84
62.50 - 44.20µm	4.0, 4..5 phi	4,25	52,56	8,31	26,10	35,34	24,01	-40,80
44.20 - 31.25µm	4.5, 5.0 phi	4,75	37,16	8,45	34,54	40,12	12,15	-14,57
31.25 - 22.10µm	5.0, 5.5 phi	5,25	26,28	8,54	43,08	44,83	4,18	-2,92
22.10 - 15.63µm	5.5, 6.0 phi	5,75	18,58	9,04	52,12	51,99	0,36	-0,07
15.63 - 11.00µm	6.0, 6.5 phi	6,25	13,14	9,37	61,49	58,54	0,85	0,25
11.00 - 7.81µm	6.5, 7.0 phi	6,75	9,29	8,76	70,25	59,12	5,61	4,50
7.81 - 5.52µm	7.0, 7.5 phi	7,25	6,57	7,32	77,57	53,06	12,38	16,10
5.52 - 3.91µm	7.5, 8.0 phi	7,75	4,65	5,86	83,43	45,44	19,01	34,23
3.91 - 2.76µm	8.0, 8.5 phi	8,25	3,28	4,93	88,36	40,66	26,09	60,02
2.76 - 1.95µm	8.5, 9.0 phi	8,75	2,32	4,16	92,52	36,38	32,61	91,33
1.95 - 1.38µm	9.0, 9.5 phi	9,25	1,64	3,11	95,62	28,72	33,83	111,65
1.38 - 0.98µm	9.5, 10.0 phi	9,75	1,16	1,94	97,56	18,90	28,00	106,43
0.98 - 0.69µm	10.0, 10.5 phi	10,25	0,82	1,10	98,66	11,32	20,42	87,83
0.69 - 0.49µm	10.5, 11.0 phi	10,75	0,58	0,69	99,36	7,44	15,96	76,60
0.49 - 0.35µm	11.0 , 11.5 phi	11,25	0,41	0,46	99,82	5,22	13,03	69,08
0.35 - 0.24µm	11.5, 12.0 phi	11,75	0,29	0,18	100,00	2,12	6,07	35,20
0.24 - 0.17µm	12.0, 12.5 phi	12,25	0,21	0,00	100,00	0,00	0,00	0,00
0.17 - 0.12µm	12.5, 13.0 phi	12,75	0,15	0,00	100,00	0,00	0,00	0,00
0.12 - 0.09µm	13.0, 13.5 phi	13,25	0,10	0,00	100,00	0,00	0,00	0,00
0.09 - 0.06µm	13.5, 14.0phi	13,75	0,07	0,00	100,00	0,00	0,00	0,00
0.06 - 0.04µm	14.0, 14.5 phi	14,25	0,05	0,00	100,00	0,00	0,00	0,00
0.04 - 0.03µm	14.5, 15.0 phi	14,75	0,04	0,00	100,00	0,00	0,00	0,00
0.03 - 0.02µm	15.0, 15.5 phi	15,25	0,03	0,00	100,00	0,00	0,00	0,00
METHOD: MALVERN laser sedimentograph (particles <2mm)				100,00		594,93	405,54	140,30
Sieving (particles> 0.5mm)								

Main Classes individual percentages:

Pebble	0,00
Gravel	0,00
Sand	17,78
Silt	65,65
Clay	16,57

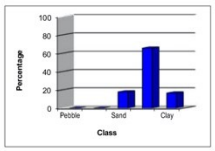

Statistical Parameters:

Mean	5,95
Standard Deviation	2,01
Asymmetry	0,17
P90	8,68
P50	5,88
P5	2,93
Mode	6,25

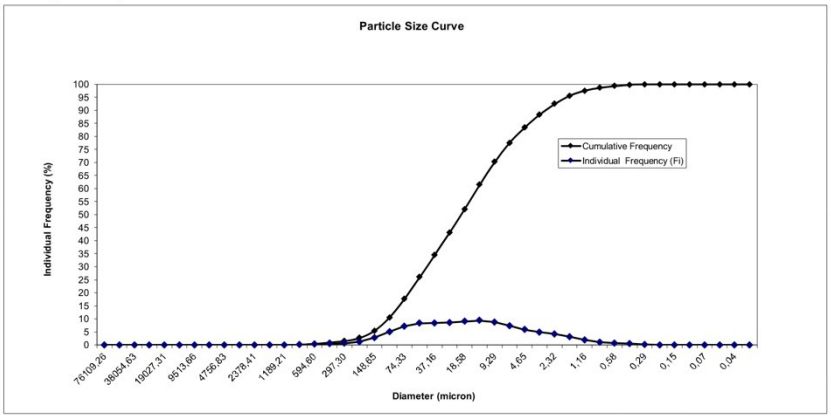

Technician: *Fernanda Dias*

Date:

INSTITUTO HIDROGRÁFICO
DIVISÃO DE GEOLOGIA MARINHA

Station: **2119**

Diameter (class)	Diameter phi	Class midpoint (ci)	Class midpoint (mm)	Individual Frequency (Fi)	Cumulative Frequency	Fi x ci	Fi x (ci-X)^2	Fi x (ci-X)^3
>64.00mm	<6.0 phi	-6,25	76109,26	0,00	0,00	0,00	0,00	0,00
45.25-64.00mm	-5.5,6.0 phi	-5,75	53817,37	0,00	0,00	0,00	0,00	0,00
32.00-45.25mm	-5.0,-5.5 phi	-5,25	38054,63	0,00	0,00	0,00	0,00	0,00
22.63-32.00mm	-4.5,-5.0 phi	-4,75	26908,69	0,00	0,00	0,00	0,00	0,00
16.00-22.63mm	-4.0,-4.5 phi	-4,25	19027,31	0,00	0,00	0,00	0,00	0,00
11.31-16.00mm	-3.5,-4.0 phi	-3,75	13454,34	0,00	0,00	0,00	0,00	0,00
8.00-11.31mm	-3.0,-3.5 phi	-3,25	9513,66	0,00	0,00	0,00	0,00	0,00
5.66-8.00mm	-2.5,-3.0 phi	-2,75	6727,17	0,00	0,00	0,00	0,00	0,00
4.00-5.66mm	-2.5,-2.0 phi	-2,25	4756,83	0,00	0,00	0,00	0,00	0,00
4.00 - 2.83mm	-2.0, -1.5 phi	-1,75	3363,59	0,00	0,00	0,00	0,00	0,00
2.83 - 2.00mm	-1.5, -1.0 phi	-1,25	2378,41	0,08	0,08	-0,10	4,21	-30,60
2.00 - 1.41mm	-1.0, -0.5 phi	-0,75	1681,79	0,00	0,08	0,00	0,00	0,00
1.41 - 1.00mm	-0.5, 0.0 phi	-0,25	1189,21	0,11	0,19	-0,03	4,34	-27,17
1.00 - 0.71mm	0.0, 0.5 phi	0,25	840,90	0,06	0,25	0,01	1,84	-10,59
0.71 - 0.50mm	0.5, 1.0 phi	0,75	594,60	0,29	0,54	0,22	8,17	-43,04
500.00 - 354.00µm	1.0, 1.5 phi	1,25	420,45	0,40	0,94	0,50	9,14	-43,56
354.00 - 250.00µm	1.5, 2.0 phi	1,75	297,30	0,54	1,48	0,95	9,87	-42,12
250.00 - 177.00µm	2.0, 2.5 phi	2,25	210,22	1,14	2,63	2,57	16,23	-61,14
177.00 - 125.00µm	2.5, 3.0 phi	2,75	148,65	2,78	5,41	7,65	29,70	-97,05
125.00 - 88.40µm	3.0, 3.5 phi	3,25	105,11	5,24	10,65	17,03	40,15	-111,13
88.40 - 62.50µm	3.5, 4.0 phi	3,75	74,33	7,46	18,10	27,96	38,35	-86,99
62.50 - 44.20µm	4.0, 4..5 phi	4,25	52,56	8,44	26,54	35,86	26,37	-46,63
44.20 - 31.25µm	4.5, 5.0 phi	4,75	37,16	8,17	34,71	38,83	13,14	-16,67
31.25 - 22.10µm	5.0, 5.5 phi	5,25	26,28	7,79	42,50	40,90	4,59	-3,53
22.10 - 15.63µm	5.5, 6.0 phi	5,75	18,58	8,12	50,62	46,70	0,58	-0,16
15.63 - 11.00µm	6.0, 6.5 phi	6,25	13,14	8,72	59,34	54,48	0,47	0,11
11.00 - 7.81µm	6.5, 7.0 phi	6,75	9,29	8,56	67,90	57,77	4,59	3,36
7.81 - 5.52µm	7.0, 7.5 phi	7,25	6,57	7,45	75,35	54,01	11,31	13,93
5.52 - 3.91µm	7.5, 8.0 phi	7,75	4,65	6,15	81,50	47,66	18,45	31,95
3.91 - 2.76µm	8.0, 8.5 phi	8,25	3,28	5,29	86,79	43,67	26,37	58,86
2.76 - 1.95µm	8.5, 9.0 phi	8,75	2,32	4,57	91,36	39,97	34,09	93,13
1.95 - 1.38µm	9.0, 9.5 phi	9,25	1,64	3,50	94,86	32,34	36,52	118,03
1.38 - 0.98µm	9.5, 10.0 phi	9,75	1,16	2,25	97,10	21,91	31,29	116,79
0.98 - 0.69µm	10.0, 10.5 phi	10,25	0,82	1,32	98,42	13,50	23,60	99,86
0.69 - 0.49µm	10.5, 11.0 phi	10,75	0,58	0,83	99,25	8,93	18,60	88,00
0.49 - 0.35µm	11.0 , 11.5 phi	11,25	0,41	0,54	99,79	6,11	14,87	77,78
0.35 - 0.24µm	11.5, 12.0 phi	11,75	0,29	0,21	100,00	2,42	6,76	38,73
0.24 - 0.17µm	12.0, 12.5 phi	12,25	0,21	0,00	100,00	0,00	0,00	0,00
0.17 - 0.12µm	12.5, 13.0 phi	12,75	0,15	0,00	100,00	0,00	0,00	0,00
0.12 - 0.09µm	13.0, 13.5 phi	13,25	0,10	0,00	100,00	0,00	0,00	0,00
0.09 - 0.06µm	13.5, 14.0phi	13,75	0,07	0,00	100,00	0,00	0,00	0,00
0.06 - 0.04µm	14.0, 14.5 phi	14,25	0,05	0,00	100,00	0,00	0,00	0,00
0.04 - 0.03µm	14.5, 15.0 phi	14,75	0,04	0,00	100,00	0,00	0,00	0,00
0.03 - 0.02µm	15.0, 15.5 phi	15,25	0,03	0,00	100,00	0,00	0,00	0,00
				100,00		601,80	433,57	120,14

METHOD: MALVERN laser sedimentograph (particles <2mm)
Sieving (particles> 0.5mm)

Main Classes individual percentages:

Pebble	0,00
Gravel	0,08
Sand	18,02
Silt	63,40
Clay	18,50

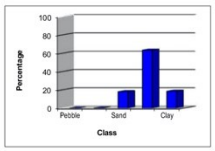

Statistical Parameters:

Mean	6,02
Standard Deviation	2,08
Asymmetry	0,13
P90	8,83
P50	5,96
P5	2,94
Mode	6,25

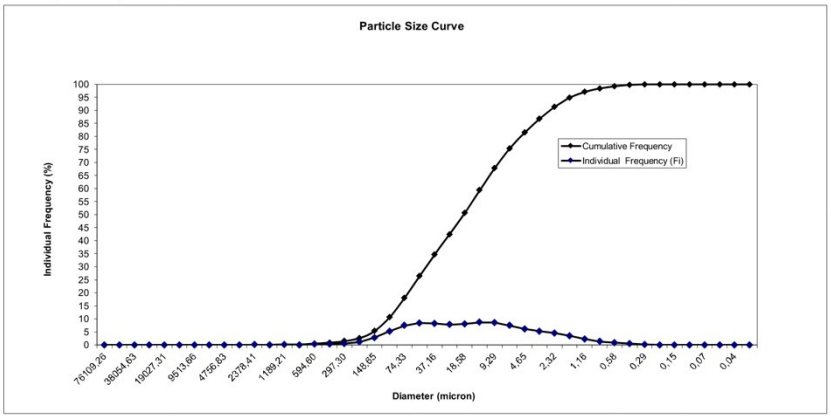

Technician: *Fernanda Dias*

Date:

INSTITUTO HIDROGRÁFICO
DIVISÃO DE GEOLOGIA MARINHA

Station: **2120**

Diameter (class)	Diameter phi	Class midpoint (ci)	Class midpoint (mm)	Individual Frequency (Fi)	Cumulative Frequency	Fi x ci	Fi x (ci-X)^2	Fi x (ci-X)^3
>64.00mm	<6.0 phi	-6,25	76109,26	0,00	0,00	0,00	0,00	0,00
45.25-64.00mm	-5.5,6.0 phi	-5,75	53817,37	0,00	0,00	0,00	0,00	0,00
32.00-45.25mm	-5.0,-5.5 phi	-5,25	38054,63	0,00	0,00	0,00	0,00	0,00
22.63-32.00mm	-4.5,-5.0 phi	-4,75	26908,69	0,00	0,00	0,00	0,00	0,00
16.00-22.63mm	-4.0,-4.5 phi	-4,25	19027,31	0,00	0,00	0,00	0,00	0,00
11.31-16.00mm	-3.5,-4.0 phi	-3,75	13454,34	0,00	0,00	0,00	0,00	0,00
8.00-11.31mm	-3.0,-3.5 phi	-3,25	9513,66	0,00	0,00	0,00	0,00	0,00
5.66-8.00mm	-2.5,-3.0 phi	-2,75	6727,17	0,00	0,00	0,00	0,00	0,00
4.00-5.66mm	-2.5,-2.0 phi	-2,25	4756,83	0,00	0,00	0,00	0,00	0,00
4.00 - 2.83mm	-2.0, -1.5 phi	-1,75	3363,59	0,00	0,00	0,00	0,00	0,00
2.83 - 2.00mm	-1.5, -1.0 phi	-1,25	2378,41	0,11	0,11	-0,14	6,04	-44,10
2.00 - 1.41mm	-1.0, -0.5 phi	-0,75	1681,79	0,06	0,18	-0,05	2,89	-19,67
1.41 - 1.00mm	-0.5, 0.0 phi	-0,25	1189,21	0,28	0,45	-0,07	10,94	-69,00
1.00 - 0.71mm	0.0, 0.5 phi	0,25	840,90	0,17	0,62	0,04	5,75	-33,36
0.71 - 0.50mm	0.5, 1.0 phi	0,75	594,60	0,19	0,82	0,15	5,49	-29,13
500.00 - 354.00µm	1.0, 1.5 phi	1,25	420,45	0,23	1,04	0,28	5,23	-25,16
354.00 - 250.00µm	1.5, 2.0 phi	1,75	297,30	0,39	1,43	0,68	7,26	-31,25
250.00 - 177.00µm	2.0, 2.5 phi	2,25	210,22	1,02	2,45	2,29	14,73	-56,08
177.00 - 125.00µm	2.5, 3.0 phi	2,75	148,65	2,66	5,11	7,32	29,08	-96,15
125.00 - 88.40µm	3.0, 3.5 phi	3,25	105,11	5,07	10,18	16,48	39,92	-112,04
88.40 - 62.50µm	3.5, 4.0 phi	3,75	74,33	7,16	17,34	26,85	38,09	-87,85
62.50 - 44.20µm	4.0, 4..5 phi	4,25	52,56	8,05	25,39	34,23	26,28	-47,46
44.20 - 31.25µm	4.5, 5.0 phi	4,75	37,16	7,90	33,30	37,53	13,48	-17,61
31.25 - 22.10µm	5.0, 5.5 phi	5,25	26,28	7,78	41,07	40,84	5,06	-4,08
22.10 - 15.63µm	5.5, 6.0 phi	5,75	18,58	8,32	49,40	47,85	0,78	-0,24
15.63 - 11.00µm	6.0, 6.5 phi	6,25	13,14	8,98	58,38	56,14	0,34	0,07
11.00 - 7.81µm	6.5, 7.0 phi	6,75	9,29	8,82	67,20	59,55	4,24	2,94
7.81 - 5.52µm	7.0, 7.5 phi	7,25	6,57	7,71	74,91	55,90	10,99	13,11
5.52 - 3.91µm	7.5, 8.0 phi	7,75	4,65	6,40	81,31	49,58	18,35	31,08
3.91 - 2.76µm	8.0, 8.5 phi	8,25	3,28	5,49	86,80	45,27	26,41	57,93
2.76 - 1.95µm	8.5, 9.0 phi	8,75	2,32	4,68	91,47	40,91	33,93	91,39
1.95 - 1.38µm	9.0, 9.5 phi	9,25	1,64	3,52	94,99	32,57	35,92	114,70
1.38 - 0.98µm	9.5, 10.0 phi	9,75	1,16	2,22	97,21	21,65	30,29	111,89
0.98 - 0.69µm	10.0, 10.5 phi	10,25	0,82	1,27	98,49	13,05	22,39	93,91
0.69 - 0.49µm	10.5, 11.0 phi	10,75	0,58	0,79	99,28	8,51	17,44	81,87
0.49 - 0.35µm	11.0 , 11.5 phi	11,25	0,41	0,52	99,80	5,86	14,05	72,96
0.35 - 0.24µm	11.5, 12.0 phi	11,75	0,29	0,20	100,00	2,36	6,51	37,07
0.24 - 0.17µm	12.0, 12.5 phi	12,25	0,21	0,00	100,00	0,00	0,00	0,00
0.17 - 0.12µm	12.5, 13.0 phi	12,75	0,15	0,00	100,00	0,00	0,00	0,00
0.12 - 0.09µm	13.0, 13.5 phi	13,25	0,10	0,00	100,00	0,00	0,00	0,00
0.09 - 0.06µm	13.5, 14.0phi	13,75	0,07	0,00	100,00	0,00	0,00	0,00
0.06 - 0.04µm	14.0, 14.5 phi	14,25	0,05	0,00	100,00	0,00	0,00	0,00
0.04 - 0.03µm	14.5, 15.0 phi	14,75	0,04	0,00	100,00	0,00	0,00	0,00
0.03 - 0.02µm	15.0, 15.5 phi	15,25	0,03	0,00	100,00	0,00	0,00	0,00
				100,00		605,63	431,87	35,73

METHOD: MALVERN laser sedimentograph (particles <2mm)
Sieving (particles> 0.5mm)

Main Classes individual percentages:

Pebble	0,00
Gravel	0,11
Sand	17,23
Silt	63,97
Clay	18,69

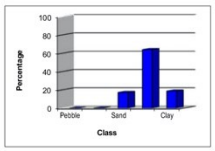

Statistical Parameters:

Mean	6,06
Standard Deviation	2,08
Asymmetry	0,04
P90	8,82
P50	6,03
P5	2,98
Mode	6,25

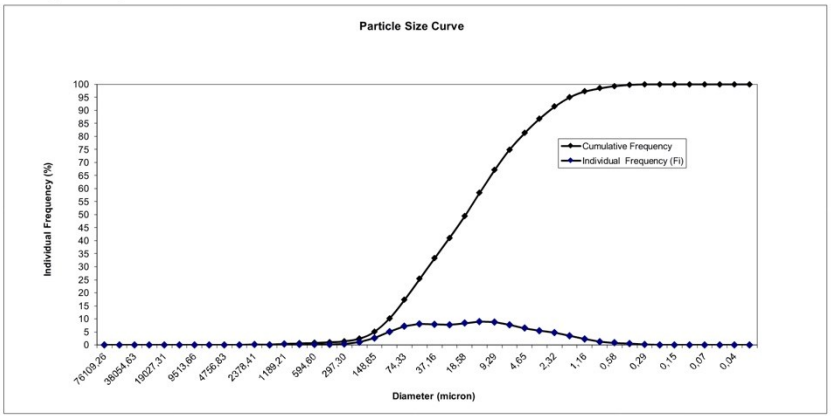

Technician: *Fernanda Dias*

Date:

INSTITUTO HIDROGRÁFICO
DIVISÃO DE GEOLOGIA MARINHA

Station: **2121**

Diameter (class)	Diameter phi	Class midpoint (ci)	Class midpoint (mm)	Individual Frequency (Fi)	Cumulative Frequency	Fi x ci	Fi x (ci-X)^2	Fi x (ci-X)^3
>64.00mm	<6.0 phi	-6,25	76109,26	0,00	0,00	0,00	0,00	0,00
45.25-64.00mm	-5.5,6.0 phi	-5,75	53817,37	0,00	0,00	0,00	0,00	0,00
32.00-45.25mm	-5.0,-5.5 phi	-5,25	38054,63	0,00	0,00	0,00	0,00	0,00
22.63-32.00mm	-4.5,-5.0 phi	-4,75	26908,69	0,00	0,00	0,00	0,00	0,00
16.00-22.63mm	-4.0,-4.5 phi	-4,25	19027,31	0,00	0,00	0,00	0,00	0,00
11.31-16.00mm	-3.5,-4.0 phi	-3,75	13454,34	0,00	0,00	0,00	0,00	0,00
8.00-11.31mm	-3.0,-3.5 phi	-3,25	9513,66	0,00	0,00	0,00	0,00	0,00
5.66-8.00mm	-2.5,-3.0 phi	-2,75	6727,17	0,00	0,00	0,00	0,00	0,00
4.00-5.66mm	-2.5,-2.0 phi	-2,25	4756,83	0,00	0,00	0,00	0,00	0,00
4.00 - 2.83mm	-2.0, -1.5 phi	-1,75	3363,59	0,00	0,00	0,00	0,00	0,00
2.83 - 2.00mm	-1.5, -1.0 phi	-1,25	2378,41	0,00	0,00	0,00	0,00	0,00
2.00 - 1.41mm	-1.0, -0.5 phi	-0,75	1681,79	0,00	0,00	0,00	0,00	0,00
1.41 - 1.00mm	-0.5, 0.0 phi	-0,25	1189,21	0,07	0,07	-0,02	3,02	-19,19
1.00 - 0.71mm	0.0, 0.5 phi	0,25	840,90	0,15	0,23	0,04	5,30	-31,02
0.71 - 0.50mm	0.5, 1.0 phi	0,75	594,60	0,31	0,54	0,23	8,83	-47,29
500.00 - 354.00µm	1.0, 1.5 phi	1,25	420,45	0,29	0,83	0,36	6,85	-33,26
354.00 - 250.00µm	1.5, 2.0 phi	1,75	297,30	0,40	1,23	0,70	7,65	-33,32
250.00 - 177.00µm	2.0, 2.5 phi	2,25	210,22	1,01	2,24	2,27	15,00	-57,85
177.00 - 125.00µm	2.5, 3.0 phi	2,75	148,65	2,60	4,84	7,15	29,32	-98,43
125.00 - 88.40µm	3.0, 3.5 phi	3,25	105,11	4,87	9,71	15,83	39,77	-113,63
88.40 - 62.50µm	3.5, 4.0 phi	3,75	74,33	6,79	16,50	25,45	37,71	-88,88
62.50 - 44.20µm	4.0, 4..5 phi	4,25	52,56	7,61	24,11	32,33	26,24	-48,73
44.20 - 31.25µm	4.5, 5.0 phi	4,75	37,16	7,59	31,69	36,04	13,97	-18,97
31.25 - 22.10µm	5.0, 5.5 phi	5,25	26,28	7,77	39,47	40,81	5,71	-4,90
22.10 - 15.63µm	5.5, 6.0 phi	5,75	18,58	8,65	48,11	49,72	1,10	-0,39
15.63 - 11.00µm	6.0, 6.5 phi	6,25	13,14	9,48	57,59	59,25	0,19	0,03
11.00 - 7.81µm	6.5, 7.0 phi	6,75	9,29	9,27	66,86	62,55	3,83	2,46
7.81 - 5.52µm	7.0, 7.5 phi	7,25	6,57	7,98	74,84	57,85	10,42	11,91
5.52 - 3.91µm	7.5, 8.0 phi	7,75	4,65	6,51	81,34	50,41	17,56	28,84
3.91 - 2.76µm	8.0, 8.5 phi	8,25	3,28	5,52	86,86	45,51	25,33	54,28
2.76 - 1.95µm	8.5, 9.0 phi	8,75	2,32	4,68	91,54	40,97	32,71	86,44
1.95 - 1.38µm	9.0, 9.5 phi	9,25	1,64	3,52	95,06	32,56	34,77	109,28
1.38 - 0.98µm	9.5, 10.0 phi	9,75	1,16	2,21	97,27	21,54	29,32	106,80
0.98 - 0.69µm	10.0, 10.5 phi	10,25	0,82	1,25	98,53	12,86	21,53	89,21
0.69 - 0.49µm	10.5, 11.0 phi	10,75	0,58	0,77	99,30	8,30	16,65	77,29
0.49 - 0.35µm	11.0 , 11.5 phi	11,25	0,41	0,51	99,81	5,70	13,39	68,88
0.35 - 0.24µm	11.5, 12.0 phi	11,75	0,29	0,19	100,00	2,28	6,19	34,91
0.24 - 0.17µm	12.0, 12.5 phi	12,25	0,21	0,00	100,00	0,00	0,00	0,00
0.17 - 0.12µm	12.5, 13.0 phi	12,75	0,15	0,00	100,00	0,00	0,00	0,00
0.12 - 0.09µm	13.0, 13.5 phi	13,25	0,10	0,00	100,00	0,00	0,00	0,00
0.09 - 0.06µm	13.5, 14.0phi	13,75	0,07	0,00	100,00	0,00	0,00	0,00
0.06 - 0.04µm	14.0, 14.5 phi	14,25	0,05	0,00	100,00	0,00	0,00	0,00
0.04 - 0.03µm	14.5, 15.0 phi	14,75	0,04	0,00	100,00	0,00	0,00	0,00
0.03 - 0.02µm	15.0, 15.5 phi	15,25	0,03	0,00	100,00	0,00	0,00	0,00
				100,00		610,71	412,35	74,47

METHOD: MALVERN laser sedimentograph (particles <2mm)
Sieving (particles> 0.5mm)

Main Classes individual percentages:

Pebble	0,00
Gravel	0,00
Sand	16,50
Silt	64,85
Clay	18,66

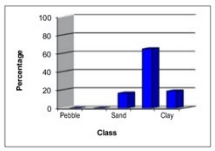

Statistical Parameters:

Mean	6,11
Standard Deviation	2,03
Asymmetry	0,09
P90	8,82
P50	6,10
P5	3,02
Mode	6,25

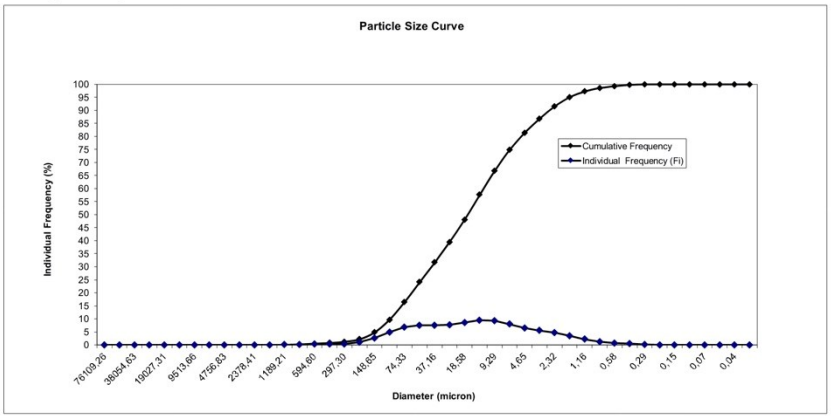

Technician: *Fernanda Dias*

Date:

INSTITUTO HIDROGRÁFICO
DIVISÃO DE GEOLOGIA MARINHA

Station: **2122**

Diameter (class)	Diameter phi	Class midpoint (ci)	Class midpoint (mm)	Individual Frequency (Fi)	Cumulative Frequency	Fi x ci	Fi x (ci-X)^2	Fi x (ci-X)^3
>64.00mm	<6.0 phi	-6,25	76109,26	0,00	0,00	0,00	0,00	0,00
45.25-64.00mm	-5.5,6.0 phi	-5,75	53817,37	0,00	0,00	0,00	0,00	0,00
32.00-45.25mm	-5.0,-5.5 phi	-5,25	38054,63	0,00	0,00	0,00	0,00	0,00
22.63-32.00mm	-4.5,-5.0 phi	-4,75	26908,69	0,00	0,00	0,00	0,00	0,00
16.00-22.63mm	-4.0,-4.5 phi	-4,25	19027,31	0,00	0,00	0,00	0,00	0,00
11.31-16.00mm	-3.5,-4.0 phi	-3,75	13454,34	0,00	0,00	0,00	0,00	0,00
8.00-11.31mm	-3.0,-3.5 phi	-3,25	9513,66	0,00	0,00	0,00	0,00	0,00
5.66-8.00mm	-2.5,-3.0 phi	-2,75	6727,17	0,00	0,00	0,00	0,00	0,00
4.00-5.66mm	-2.5,-2.0 phi	-2,25	4756,83	0,00	0,00	0,00	0,00	0,00
4.00 - 2.83mm	-2.0, -1.5 phi	-1,75	3363,59	0,00	0,00	0,00	0,00	0,00
2.83 - 2.00mm	-1.5, -1.0 phi	-1,25	2378,41	0,00	0,00	0,00	0,00	0,00
2.00 - 1.41mm	-1.0, -0.5 phi	-0,75	1681,79	0,17	0,17	-0,13	7,46	-49,35
1.41 - 1.00mm	-0.5, 0.0 phi	-0,25	1189,21	0,10	0,27	-0,02	3,56	-21,78
1.00 - 0.71mm	0.0, 0.5 phi	0,25	840,90	0,23	0,50	0,06	7,27	-40,80
0.71 - 0.50mm	0.5, 1.0 phi	0,75	594,60	0,50	1,00	0,38	13,09	-66,96
500.00 - 354.00µm	1.0, 1.5 phi	1,25	420,45	0,56	1,56	0,71	12,01	-55,43
354.00 - 250.00µm	1.5, 2.0 phi	1,75	297,30	0,67	2,23	1,17	11,32	-46,56
250.00 - 177.00µm	2.0, 2.5 phi	2,25	210,22	1,33	3,56	2,99	17,34	-62,68
177.00 - 125.00µm	2.5, 3.0 phi	2,75	148,65	3,24	6,80	8,90	31,40	-97,78
125.00 - 88.40µm	3.0, 3.5 phi	3,25	105,11	5,97	12,77	19,42	40,83	-106,72
88.40 - 62.50µm	3.5, 4.0 phi	3,75	74,33	8,07	20,84	30,26	36,08	-76,28
62.50 - 44.20µm	4.0, 4.,5 phi	4,25	52,56	8,56	29,41	36,40	22,31	-36,01
44.20 - 31.25µm	4.5, 5.0 phi	4,75	37,16	7,91	37,32	37,57	9,82	-10,93
31.25 - 22.10µm	5.0, 5.5 phi	5,25	26,28	7,50	44,82	39,37	2,83	-1,74
22.10 - 15.63µm	5.5, 6.0 phi	5,75	18,58	7,98	52,79	45,87	0,10	-0,01
15.63 - 11.00µm	6.0, 6.5 phi	6,25	13,14	8,64	61,43	54,00	1,29	0,50
11.00 - 7.81µm	6.5, 7.0 phi	6,75	9,29	8,46	69,89	57,11	6,64	5,88
7.81 - 5.52µm	7.0, 7.5 phi	7,25	6,57	7,31	77,20	52,99	14,04	19,46
5.52 - 3.91µm	7.5, 8.0 phi	7,75	4,65	5,95	83,15	46,12	21,17	39,92
3.91 - 2.76µm	8.0, 8.5 phi	8,25	3,28	5,01	88,16	41,33	28,52	68,04
2.76 - 1.95µm	8.5, 9.0 phi	8,75	2,32	4,22	92,39	36,96	35,18	101,52
1.95 - 1.38µm	9.0, 9.5 phi	9,25	1,64	3,17	95,55	29,28	36,29	122,87
1.38 - 0.98µm	9.5, 10.0 phi	9,75	1,16	1,99	97,54	19,36	29,99	116,54
0.98 - 0.69µm	10.0, 10.5 phi	10,25	0,82	1,13	98,67	11,58	21,73	95,31
0.69 - 0.49µm	10.5, 11.0 phi	10,75	0,58	0,70	99,36	7,50	16,65	81,35
0.49 - 0.35µm	11.0 , 11.5 phi	11,25	0,41	0,46	99,82	5,16	13,31	71,68
0.35 - 0.24µm	11.5, 12.0 phi	11,75	0,29	0,18	100,00	2,08	6,13	36,09
0.24 - 0.17µm	12.0, 12.5 phi	12,25	0,21	0,00	100,00	0,00	0,00	0,00
0.17 - 0.12µm	12.5, 13.0 phi	12,75	0,15	0,00	100,00	0,00	0,00	0,00
0.12 - 0.09µm	13.0, 13.5 phi	13,25	0,10	0,00	100,00	0,00	0,00	0,00
0.09 - 0.06µm	13.5, 14.0phi	13,75	0,07	0,00	100,00	0,00	0,00	0,00
0.06 - 0.04µm	14.0, 14.5 phi	14,25	0,05	0,00	100,00	0,00	0,00	0,00
0.04 - 0.03µm	14.5, 15.0 phi	14,75	0,04	0,00	100,00	0,00	0,00	0,00
0.03 - 0.02µm	15.0, 15.5 phi	15,25	0,03	0,00	100,00	0,00	0,00	0,00
METHOD: MALVERN laser sedimentograph (particles <2mm)				100,00		586,40	446,35	86,14

Sieving (particles> 0.5mm)

Main Classes individual percentages:

Pebble	0,00
Gravel	0,00
Sand	20,84
Silt	62,31
Clay	16,85

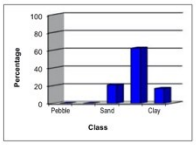

Statistical Parameters:

Mean	5,86
Standard Deviation	2,11
Asymmetry	0,09
P90	8,70
P50	5,83
P5	2,75
Mode	6,25

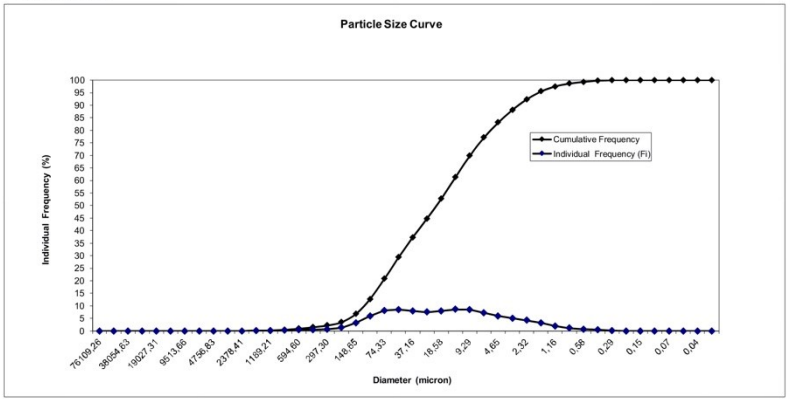

Technician: *Fernanda Dias*

Date:

INSTITUTO HIDROGRÁFICO
DIVISÃO DE GEOLOGIA MARINHA

Station: **2123**

Diameter (class)	Diameter phi	Class midpoint (ci)	Class midpoint (mm)	Individual Frequency (Fi)	Cumulative Frequency	Fi x ci	Fi x (ci-X)^2	Fi x (ci-X)^3
>64.00mm	<6.0 phi	-6,25	76109,26	0,00	0,00	0,00	0,00	0,00
45.25-64.00mm	-5.5,6.0 phi	-5,75	53817,37	0,00	0,00	0,00	0,00	0,00
32.00-45.25mm	-5.0,-5.5 phi	-5,25	38054,63	0,00	0,00	0,00	0,00	0,00
22.63-32.00mm	-4.5,-5.0 phi	-4,75	26908,69	0,00	0,00	0,00	0,00	0,00
16.00-22.63mm	-4.0,-4.5 phi	-4,25	19027,31	0,00	0,00	0,00	0,00	0,00
11.31-16.00mm	-3.5,-4.0 phi	-3,75	13454,34	0,00	0,00	0,00	0,00	0,00
8.00-11.31mm	-3.0,-3.5 phi	-3,25	9513,66	0,00	0,00	0,00	0,00	0,00
5.66-8.00mm	-2.5,-3.0 phi	-2,75	6727,17	0,00	0,00	0,00	0,00	0,00
4.00-5.66mm	-2.5,-2.0 phi	-2,25	4756,83	0,00	0,00	0,00	0,00	0,00
4.00 - 2.83mm	-2.0, -1.5 phi	-1,75	3363,59	0,00	0,00	0,00	0,00	0,00
2.83 - 2.00mm	-1.5, -1.0 phi	-1,25	2378,41	0,04	0,04	-0,05	1,74	-12,08
2.00 - 1.41mm	-1.0, -0.5 phi	-0,75	1681,79	0,08	0,11	-0,06	3,18	-20,49
1.41 - 1.00mm	-0.5, 0.0 phi	-0,25	1189,21	0,07	0,19	-0,02	2,61	-15,53
1.00 - 0.71mm	0.0, 0.5 phi	0,25	840,90	0,21	0,40	0,05	6,21	-33,80
0.71 - 0.50mm	0.5, 1.0 phi	0,75	594,60	0,43	0,82	0,32	10,45	-51,67
500.00 - 354.00µm	1.0, 1.5 phi	1,25	420,45	0,60	1,42	0,75	11,79	-52,44
354.00 - 250.00µm	1.5, 2.0 phi	1,75	297,30	0,96	2,38	1,68	15,00	-59,18
250.00 - 177.00µm	2.0, 2.5 phi	2,25	210,22	2,04	4,42	4,58	24,18	-83,35
177.00 - 125.00µm	2.5, 3.0 phi	2,75	148,65	4,34	8,76	11,94	37,71	-111,13
125.00 - 88.40µm	3.0, 3.5 phi	3,25	105,11	7,18	15,94	23,33	42,98	-105,17
88.40 - 62.50µm	3.5, 4.0 phi	3,75	74,33	8,99	24,93	33,73	34,09	-66,36
62.50 - 44.20µm	4.0, 4..5 phi	4,25	52,56	9,03	33,96	38,36	18,89	-27,33
44.20 - 31.25µm	4.5, 5.0 phi	4,75	37,16	7,94	41,90	37,73	7,12	-6,74
31.25 - 22.10µm	5.0, 5.5 phi	5,25	26,28	7,14	49,04	37,47	1,42	-0,64
22.10 - 15.63µm	5.5, 6.0 phi	5,75	18,58	7,24	56,28	41,64	0,02	0,00
15.63 - 11.00µm	6.0, 6.5 phi	6,25	13,14	7,70	63,98	48,11	2,36	1,30
11.00 - 7.81µm	6.5, 7.0 phi	6,75	9,29	7,58	71,56	51,18	8,41	8,86
7.81 - 5.52µm	7.0, 7.5 phi	7,25	6,57	6,68	78,24	48,43	16,12	25,03
5.52 - 3.91µm	7.5, 8.0 phi	7,75	4,65	5,57	83,81	43,16	23,48	48,20
3.91 - 2.76µm	8.0, 8.5 phi	8,25	3,28	4,77	88,58	39,36	31,10	79,41
2.76 - 1.95µm	8.5, 9.0 phi	8,75	2,32	4,05	92,64	35,48	37,80	115,42
1.95 - 1.38µm	9.0, 9.5 phi	9,25	1,64	3,05	95,69	28,23	38,53	136,92
1.38 - 0.98µm	9.5, 10.0 phi	9,75	1,16	1,92	97,61	18,76	31,62	128,16
0.98 - 0.69µm	10.0, 10.5 phi	10,25	0,82	1,10	98,71	11,29	22,84	104,01
0.69 - 0.49µm	10.5, 11.0 phi	10,75	0,58	0,68	99,39	7,31	17,37	87,79
0.49 - 0.35µm	11.0 , 11.5 phi	11,25	0,41	0,44	99,84	4,96	13,61	75,55
0.35 - 0.24µm	11.5, 12.0 phi	11,75	0,29	0,16	100,00	1,93	6,01	36,37
0.24 - 0.17µm	12.0, 12.5 phi	12,25	0,21	0,00	100,00	0,00	0,00	0,00
0.17 - 0.12µm	12.5, 13.0 phi	12,75	0,15	0,00	100,00	0,00	0,00	0,00
0.12 - 0.09µm	13.0, 13.5 phi	13,25	0,10	0,00	100,00	0,00	0,00	0,00
0.09 - 0.06µm	13.5, 14.0phi	13,75	0,07	0,00	100,00	0,00	0,00	0,00
0.06 - 0.04µm	14.0, 14.5 phi	14,25	0,05	0,00	100,00	0,00	0,00	0,00
0.04 - 0.03µm	14.5, 15.0 phi	14,75	0,04	0,00	100,00	0,00	0,00	0,00
0.03 - 0.02µm	15.0, 15.5 phi	15,25	0,03	0,00	100,00	0,00	0,00	0,00
METHOD: MALVERN laser sedimentograph (particles <2mm)				100,00		569,67	466,63	201,11
Sieving (particles> 0.5mm)								

Main Classes individual percentages:

Pebble	0,00
Gravel	0,04
Sand	24,90
Silt	58,88
Clay	16,19

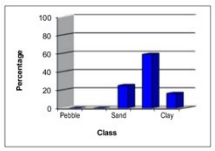

Statistical Parameters:

Mean	5,70
Standard Deviation	2,16
Asymmetry	0,20
P90	8,66
P50	5,57
P5	2,59
Mode	4,25

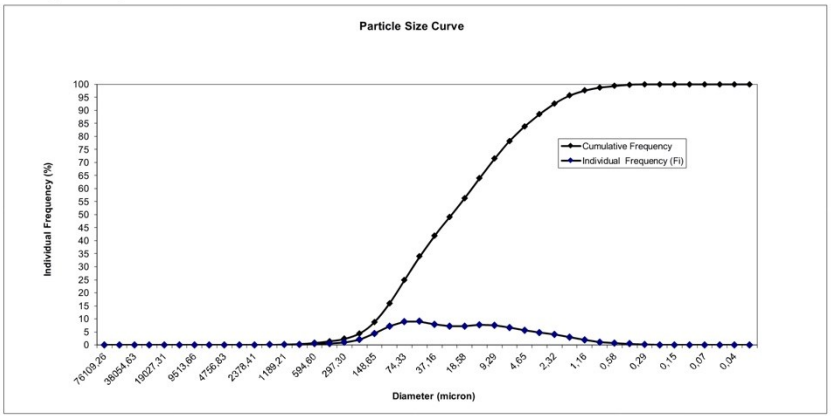

Technician: *Fernanda Dias*

Date:

INSTITUTO HIDROGRÁFICO
DIVISÃO DE GEOLOGIA MARINHA

Station: **2124**

Diameter (class)	Diameter phi	Class midpoint (ci)	Class midpoint (mm)	Individual Frequency (Fi)	Cumulative Frequency	Fi x ci	Fi x (ci-X)^2	Fi x (ci-X)^3
>64.00mm	<6.0 phi	-6,25	76109,26	0,00	0,00	0,00	0,00	0,00
45.25-64.00mm	-5.5,6.0 phi	-5,75	53817,37	0,00	0,00	0,00	0,00	0,00
32.00-45.25mm	-5.0,-5.5 phi	-5,25	38054,63	0,00	0,00	0,00	0,00	0,00
22.63-32.00mm	-4.5,-5.0 phi	-4,75	26908,69	0,00	0,00	0,00	0,00	0,00
16.00-22.63mm	-4.0,-4.5 phi	-4,25	19027,31	0,00	0,00	0,00	0,00	0,00
11.31-16.00mm	-3.5,-4.0 phi	-3,75	13454,34	0,00	0,00	0,00	0,00	0,00
8.00-11.31mm	-3.0,-3.5 phi	-3,25	9513,66	0,00	0,00	0,00	0,00	0,00
5.66-8.00mm	-2.5,-3.0 phi	-2,75	6727,17	0,00	0,00	0,00	0,00	0,00
4.00-5.66mm	-2.5,-2.0 phi	-2,25	4756,83	0,21	0,21	-0,48	12,80	-99,55
4.00 - 2.83mm	-2.0, -1.5 phi	-1,75	3363,59	0,06	0,27	-0,10	3,12	-22,68
2.83 - 2.00mm	-1.5, -1.0 phi	-1,25	2378,41	0,05	0,32	-0,06	2,21	-15,01
2.00 - 1.41mm	-1.0, -0.5 phi	-0,75	1681,79	0,14	0,46	-0,10	5,49	-34,46
1.41 - 1.00mm	-0.5, 0.0 phi	-0,25	1189,21	0,17	0,62	-0,04	5,57	-32,18
1.00 - 0.71mm	0.0, 0.5 phi	0,25	840,90	0,34	0,96	0,08	9,36	-49,39
0.71 - 0.50mm	0.5, 1.0 phi	0,75	594,60	0,66	1,62	0,49	15,07	-71,99
500.00 - 354.00µm	1.0, 1.5 phi	1,25	420,45	0,71	2,33	0,89	13,03	-55,75
354.00 - 250.00µm	1.5, 2.0 phi	1,75	297,30	0,99	3,33	1,74	14,20	-53,66
250.00 - 177.00µm	2.0, 2.5 phi	2,25	210,22	2,04	5,36	4,58	21,89	-71,75
177.00 - 125.00µm	2.5, 3.0 phi	2,75	148,65	4,42	9,78	12,15	34,12	-94,81
125.00 - 88.40µm	3.0, 3.5 phi	3,25	105,11	7,44	17,22	24,19	38,64	-88,04
88.40 - 62.50µm	3.5, 4.0 phi	3,75	74,33	9,45	26,67	35,42	29,88	-53,14
62.50 - 44.20µm	4.0, 4..5 phi	4,25	52,56	9,55	36,22	40,58	15,61	-19,96
44.20 - 31.25µm	4.5, 5.0 phi	4,75	37,16	8,40	44,62	39,92	5,09	-3,97
31.25 - 22.10µm	5.0, 5.5 phi	5,25	26,28	7,47	52,10	39,24	0,58	-0,16
22.10 - 15.63µm	5.5, 6.0 phi	5,75	18,58	7,41	59,51	42,63	0,36	0,08
15.63 - 11.00µm	6.0, 6.5 phi	6,25	13,14	7,64	67,15	47,73	3,97	2,87
11.00 - 7.81µm	6.5, 7.0 phi	6,75	9,29	7,26	74,41	49,03	10,84	13,24
7.81 - 5.52µm	7.0, 7.5 phi	7,25	6,57	6,17	80,58	44,74	18,29	31,48
5.52 - 3.91µm	7.5, 8.0 phi	7,75	4,65	4,98	85,56	38,60	24,58	54,60
3.91 - 2.76µm	8.0, 8.5 phi	8,25	3,28	4,20	89,76	34,64	31,09	84,62
2.76 - 1.95µm	8.5, 9.0 phi	8,75	2,32	3,58	93,34	31,28	37,10	119,53
1.95 - 1.38µm	9.0, 9.5 phi	9,25	1,64	2,72	96,05	25,13	37,63	140,02
1.38 - 0.98µm	9.5, 10.0 phi	9,75	1,16	1,73	97,79	16,89	30,88	130,34
0.98 - 0.69µm	10.0, 10.5 phi	10,25	0,82	1,00	98,79	10,30	22,40	105,76
0.69 - 0.49µm	10.5, 11.0 phi	10,75	0,58	0,63	99,42	6,77	17,18	89,70
0.49 - 0.35µm	11.0 , 11.5 phi	11,25	0,41	0,42	99,84	4,67	13,60	77,79
0.35 - 0.24µm	11.5, 12.0 phi	11,75	0,29	0,16	100,00	1,94	6,38	39,66
0.24 - 0.17µm	12.0, 12.5 phi	12,25	0,21	0,00	100,00	0,00	0,00	0,00
0.17 - 0.12µm	12.5, 13.0 phi	12,75	0,15	0,00	100,00	0,00	0,00	0,00
0.12 - 0.09µm	13.0, 13.5 phi	13,25	0,10	0,00	100,00	0,00	0,00	0,00
0.09 - 0.06µm	13.5, 14.0phi	13,75	0,07	0,00	100,00	0,00	0,00	0,00
0.06 - 0.04µm	14.0, 14.5 phi	14,25	0,05	0,00	100,00	0,00	0,00	0,00
0.04 - 0.03µm	14.5, 15.0 phi	14,75	0,04	0,00	100,00	0,00	0,00	0,00
0.03 - 0.02µm	15.0, 15.5 phi	15,25	0,03	0,00	100,00	0,00	0,00	0,00
				100,00		552,86	480,94	123,19

METHOD: MALVERN laser sedimentograph (particles <2mm)
Sieving (particles> 0.5mm)

Main Classes individual percentages:

Pebble	0,00
Gravel	0,32
Sand	26,35
Silt	58,89
Clay	14,44

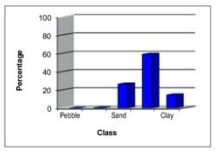

Statistical Parameters:

Mean	5,53
Standard Deviation	2,19
Asymmetry	0,12
P90	8,53
P50	5,36
P5	2,42
Mode	4,25

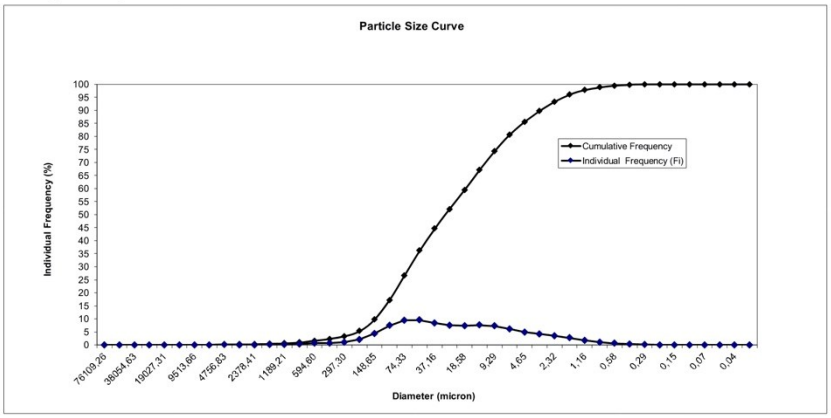

Technician: *Fernanda Dias*

Date:

INSTITUTO HIDROGRÁFICO
DIVISÃO DE GEOLOGIA MARINHA

Station: **2125**

Diameter (class)	Diameter phi	Class midpoint (ci)	Class midpoint (mm)	Individual Frequency (Fi)	Cumulative Frequency	Fi x ci	Fi x (ci-X)^2	Fi x (ci-X)^3
>64.00mm	<6.0 phi	-6,25	76109,26	0,00	0,00	0,00	0,00	0,00
45.25-64.00mm	-5.5,6.0 phi	-5,75	53817,37	0,00	0,00	0,00	0,00	0,00
32.00-45.25mm	-5.0,-5.5 phi	-5,25	38054,63	0,00	0,00	0,00	0,00	0,00
22.63-32.00mm	-4.5,-5.0 phi	-4,75	26908,69	0,00	0,00	0,00	0,00	0,00
16.00-22.63mm	-4.0,-4.5 phi	-4,25	19027,31	0,00	0,00	0,00	0,00	0,00
11.31-16.00mm	-3.5,-4.0 phi	-3,75	13454,34	0,00	0,00	0,00	0,00	0,00
8.00-11.31mm	-3.0,-3.5 phi	-3,25	9513,66	0,00	0,00	0,00	0,00	0,00
5.66-8.00mm	-2.5,-3.0 phi	-2,75	6727,17	0,00	0,00	0,00	0,00	0,00
4.00-5.66mm	-2.5,-2.0 phi	-2,25	4756,83	0,00	0,00	0,00	0,00	0,00
4.00 - 2.83mm	-2.0, -1.5 phi	-1,75	3363,59	0,00	0,00	0,00	0,00	0,00
2.83 - 2.00mm	-1.5, -1.0 phi	-1,25	2378,41	0,00	0,00	0,00	0,00	0,00
2.00 - 1.41mm	-1.0, -0.5 phi	-0,75	1681,79	0,04	0,04	-0,03	1,32	-7,68
1.41 - 1.00mm	-0.5, 0.0 phi	-0,25	1189,21	0,06	0,10	-0,02	1,72	-9,10
1.00 - 0.71mm	0.0, 0.5 phi	0,25	840,90	0,14	0,24	0,04	3,32	-15,96
0.71 - 0.50mm	0.5, 1.0 phi	0,75	594,60	0,52	0,77	0,39	9,68	-41,65
500.00 - 354.00µm	1.0, 1.5 phi	1,25	420,45	1,00	1,76	1,25	14,42	-54,84
354.00 - 250.00µm	1.5, 2.0 phi	1,75	297,30	1,95	3,72	3,42	21,33	-70,46
250.00 - 177.00µm	2.0, 2.5 phi	2,25	210,22	3,81	7,53	8,58	29,95	-83,96
177.00 - 125.00µm	2.5, 3.0 phi	2,75	148,65	6,99	14,52	19,22	37,07	-85,37
125.00 - 88.40µm	3.0, 3.5 phi	3,25	105,11	10,44	24,96	33,94	33,96	-61,23
88.40 - 62.50µm	3.5, 4.0 phi	3,75	74,33	12,14	37,10	45,51	20,61	-26,86
62.50 - 44.20µm	4.0, 4..5 phi	4,25	52,56	11,23	48,32	47,71	7,24	-5,82
44.20 - 31.25µm	4.5, 5.0 phi	4,75	37,16	8,81	57,14	41,85	0,81	-0,25
31.25 - 22.10µm	5.0, 5.5 phi	5,25	26,28	6,73	63,86	35,31	0,26	0,05
22.10 - 15.63µm	5.5, 6.0 phi	5,75	18,58	5,80	69,66	33,37	2,82	1,96
15.63 - 11.00µm	6.0, 6.5 phi	6,25	13,14	5,59	75,25	34,91	8,00	9,58
11.00 - 7.81µm	6.5, 7.0 phi	6,75	9,29	5,24	80,49	35,35	15,08	25,59
7.81 - 5.52µm	7.0, 7.5 phi	7,25	6,57	4,48	84,97	32,52	21,64	47,55
5.52 - 3.91µm	7.5, 8.0 phi	7,75	4,65	3,69	88,66	28,62	26,86	72,43
3.91 - 2.76µm	8.0, 8.5 phi	8,25	3,28	3,20	91,87	26,42	32,73	104,64
2.76 - 1.95µm	8.5, 9.0 phi	8,75	2,32	2,80	94,67	24,54	38,32	141,67
1.95 - 1.38µm	9.0, 9.5 phi	9,25	1,64	2,18	96,85	20,14	38,34	160,92
1.38 - 0.98µm	9.5, 10.0 phi	9,75	1,16	1,41	98,26	13,76	31,13	146,20
0.98 - 0.69µm	10.0, 10.5 phi	10,25	0,82	0,83	99,09	8,46	22,30	115,87
0.69 - 0.49µm	10.5, 11.0 phi	10,75	0,58	0,51	99,60	5,52	16,67	94,96
0.49 - 0.35µm	11.0 , 11.5 phi	11,25	0,41	0,33	99,93	3,73	12,73	78,88
0.35 - 0.24µm	11.5, 12.0 phi	11,75	0,29	0,07	100,00	0,82	3,12	20,91
0.24 - 0.17µm	12.0, 12.5 phi	12,25	0,21	0,00	100,00	0,00	0,00	0,00
0.17 - 0.12µm	12.5, 13.0 phi	12,75	0,15	0,00	100,00	0,00	0,00	0,00
0.12 - 0.09µm	13.0, 13.5 phi	13,25	0,10	0,00	100,00	0,00	0,00	0,00
0.09 - 0.06µm	13.5, 14.0phi	13,75	0,07	0,00	100,00	0,00	0,00	0,00
0.06 - 0.04µm	14.0, 14.5 phi	14,25	0,05	0,00	100,00	0,00	0,00	0,00
0.04 - 0.03µm	14.5, 15.0 phi	14,75	0,04	0,00	100,00	0,00	0,00	0,00
0.03 - 0.02µm	15.0, 15.5 phi	15,25	0,03	0,00	100,00	0,00	0,00	0,00
				100,00		505,32	451,43	558,03

METHOD: MALVERN laser sedimentograph (particles <2mm)
Sieving (particles> 0.5mm)

Main Classes individual percentages:

Pebble	0,00
Gravel	0,00
Sand	37,10
Silt	51,57
Clay	11,34

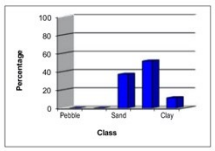

Statistical Parameters:

Mean	5,05
Standard Deviation	2,12
Asymmetry	0,58
P90	8,19
P50	4,59
P5	2,20
Mode	3,75

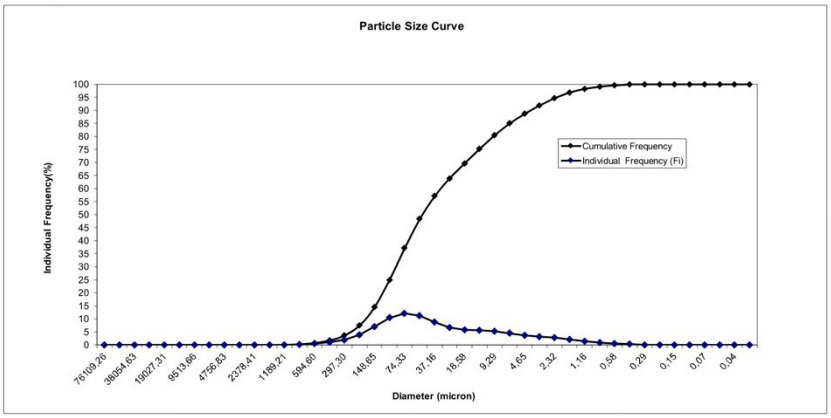

Technician: *Fernanda Dias*

Date:

INSTITUTO HIDROGRÁFICO
DIVISÃO DE GEOLOGIA MARINHA

Station: **2126**

Diameter (class)	Diameter phi	Class midpoint (ci)	Class midpoint (mm)	Individual Frequency (Fi)	Cumulative Frequency	Fi x ci	Fi x (ci-X)^2	Fi x (ci-X)^3
>64.00mm	<6.0 phi	-6,25	76109,26	0,00	0,00	0,00	0,00	0,00
45.25-64.00mm	-5.5,6.0 phi	-5,75	53817,37	0,00	0,00	0,00	0,00	0,00
32.00-45.25mm	-5.0,-5.5 phi	-5,25	38054,63	0,00	0,00	0,00	0,00	0,00
22.63-32.00mm	-4.5,-5.0 phi	-4,75	26908,69	0,00	0,00	0,00	0,00	0,00
16.00-22.63mm	-4.0,-4.5 phi	-4,25	19027,31	0,00	0,00	0,00	0,00	0,00
11.31-16.00mm	-3.5,-4.0 phi	-3,75	13454,34	0,00	0,00	0,00	0,00	0,00
8.00-11.31mm	-3.0,-3.5 phi	-3,25	9513,66	0,00	0,00	0,00	0,00	0,00
5.66-8.00mm	-2.5,-3.0 phi	-2,75	6727,17	0,00	0,00	0,00	0,00	0,00
4.00-5.66mm	-2.5,-2.0 phi	-2,25	4756,83	0,00	0,00	0,00	0,00	0,00
4.00 - 2.83mm	-2.0, -1.5 phi	-1,75	3363,59	0,00	0,00	0,00	0,00	0,00
2.83 - 2.00mm	-1.5, -1.0 phi	-1,25	2378,41	0,17	0,17	-0,21	6,42	-39,70
2.00 - 1.41mm	-1.0, -0.5 phi	-0,75	1681,79	0,07	0,24	-0,05	2,20	-12,52
1.41 - 1.00mm	-0.5, 0.0 phi	-0,25	1189,21	0,14	0,38	-0,04	3,88	-20,11
1.00 - 0.71mm	0.0, 0.5 phi	0,25	840,90	0,25	0,63	0,06	5,53	-25,91
0.71 - 0.50mm	0.5, 1.0 phi	0,75	594,60	0,62	1,25	0,47	10,86	-45,47
500.00 - 354.00µm	1.0, 1.5 phi	1,25	420,45	0,91	2,16	1,14	12,35	-45,52
354.00 - 250.00µm	1.5, 2.0 phi	1,75	297,30	1,76	3,92	3,08	17,84	-56,82
250.00 - 177.00µm	2.0, 2.5 phi	2,25	210,22	3,64	7,56	8,19	26,25	-70,48
177.00 - 125.00µm	2.5, 3.0 phi	2,75	148,65	7,11	14,67	19,55	33,94	-74,17
125.00 - 88.40µm	3.0, 3.5 phi	3,25	105,11	10,98	25,65	35,69	31,18	-52,54
88.40 - 62.50µm	3.5, 4.0 phi	3,75	74,33	12,93	38,59	48,50	18,16	-21,52
62.50 - 44.20µm	4.0, 4..5 phi	4,25	52,56	11,96	50,55	50,84	5,61	-3,84
44.20 - 31.25µm	4.5, 5.0 phi	4,75	37,16	9,22	59,77	43,81	0,32	-0,06
31.25 - 22.10µm	5.0, 5.5 phi	5,25	26,28	6,77	66,55	35,57	0,67	0,21
22.10 - 15.63µm	5.5, 6.0 phi	5,75	18,58	5,62	72,17	32,34	3,74	3,04
15.63 - 11.00µm	6.0, 6.5 phi	6,25	13,14	5,31	77,48	33,18	9,18	12,07
11.00 - 7.81µm	6.5, 7.0 phi	6,75	9,29	4,92	82,40	33,20	16,20	29,40
7.81 - 5.52µm	7.0, 7.5 phi	7,25	6,57	4,15	86,54	30,05	22,21	51,42
5.52 - 3.91µm	7.5, 8.0 phi	7,75	4,65	3,35	89,89	25,96	26,54	74,72
3.91 - 2.76µm	8.0, 8.5 phi	8,25	3,28	2,87	92,76	23,66	31,52	104,49
2.76 - 1.95µm	8.5, 9.0 phi	8,75	2,32	2,50	95,26	21,88	36,39	138,83
1.95 - 1.38µm	9.0, 9.5 phi	9,25	1,64	1,94	97,20	17,91	36,06	155,60
1.38 - 0.98µm	9.5, 10.0 phi	9,75	1,16	1,25	98,45	12,19	28,98	139,52
0.98 - 0.69µm	10.0, 10.5 phi	10,25	0,82	0,73	99,18	7,47	20,59	109,45
0.69 - 0.49µm	10.5, 11.0 phi	10,75	0,58	0,46	99,63	4,91	15,46	89,90
0.49 - 0.35µm	11.0 , 11.5 phi	11,25	0,41	0,30	99,94	3,39	12,01	75,82
0.35 - 0.24µm	11.5, 12.0 phi	11,75	0,29	0,06	100,00	0,76	2,99	20,35
0.24 - 0.17µm	12.0, 12.5 phi	12,25	0,21	0,00	100,00	0,00	0,00	0,00
0.17 - 0.12µm	12.5, 13.0 phi	12,75	0,15	0,00	100,00	0,00	0,00	0,00
0.12 - 0.09µm	13.0, 13.5 phi	13,25	0,10	0,00	100,00	0,00	0,00	0,00
0.09 - 0.06µm	13.5, 14.0phi	13,75	0,07	0,00	100,00	0,00	0,00	0,00
0.06 - 0.04µm	14.0, 14.5 phi	14,25	0,05	0,00	100,00	0,00	0,00	0,00
0.04 - 0.03µm	14.5, 15.0 phi	14,75	0,04	0,00	100,00	0,00	0,00	0,00
0.03 - 0.02µm	15.0, 15.5 phi	15,25	0,03	0,00	100,00	0,00	0,00	0,00
METHOD: MALVERN laser sedimentograph (particles <2mm)				100,00		493,50	437,09	536,20
Sieving (particles> 0.5mm)								

Main Classes individual percentages:

Pebble	0,00
Gravel	0,17
Sand	38,42
Silt	51,31
Clay	10,11

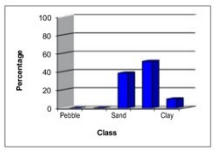

Statistical Parameters:

Mean	4,94
Standard Deviation	2,09
Asymmetry	0,59
P90	8,02
P50	4,48
P5	2,18
Mode	3,75

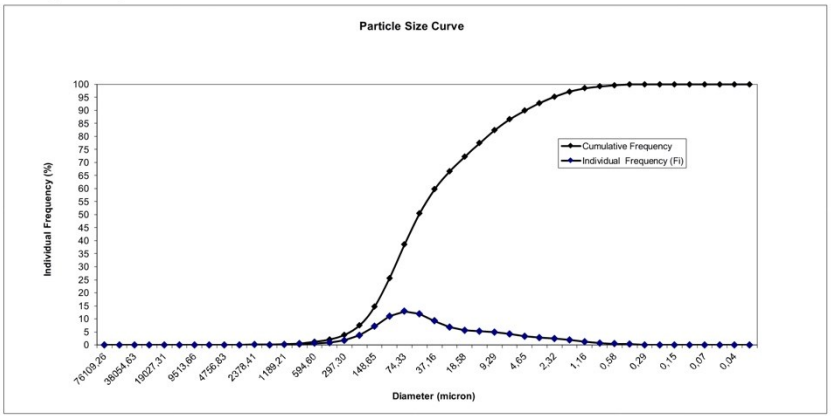

Technician: *Fernanda Dias*

Date:

INSTITUTO HIDROGRÁFICO
DIVISÃO DE GEOLOGIA MARINHA

Station: **2127**

Diameter (class)	Diameter phi	Class midpoint (ci)	Class midpoint (mm)	Individual Frequency (Fi)	Cumulative Frequency	Fi x ci	Fi x (ci-X)^2	Fi x (ci-X)^3
>64.00mm	<6.0 phi	-6,25	76109,26	0,00	0,00	0,00	0,00	0,00
45.25-64.00mm	-5.5,6.0 phi	-5,75	53817,37	0,00	0,00	0,00	0,00	0,00
32.00-45.25mm	-5.0,-5.5 phi	-5,25	38054,63	0,00	0,00	0,00	0,00	0,00
22.63-32.00mm	-4.5,-5.0 phi	-4,75	26908,69	0,00	0,00	0,00	0,00	0,00
16.00-22.63mm	-4.0,-4.5 phi	-4,25	19027,31	0,00	0,00	0,00	0,00	0,00
11.31-16.00mm	-3.5,-4.0 phi	-3,75	13454,34	0,00	0,00	0,00	0,00	0,00
8.00-11.31mm	-3.0,-3.5 phi	-3,25	9513,66	0,00	0,00	0,00	0,00	0,00
5.66-8.00mm	-2.5,-3.0 phi	-2,75	6727,17	0,00	0,00	0,00	0,00	0,00
4.00-5.66mm	-2.5,-2.0 phi	-2,25	4756,83	0,00	0,00	0,00	0,00	0,00
4.00 - 2.83mm	-2.0, -1.5 phi	-1,75	3363,59	1,40	1,40	-2,45	61,11	-403,79
2.83 - 2.00mm	-1.5, -1.0 phi	-1,25	2378,41	0,08	1,48	-0,10	3,00	-18,35
2.00 - 1.41mm	-1.0, -0.5 phi	-0,75	1681,79	0,14	1,62	-0,10	4,34	-24,35
1.41 - 1.00mm	-0.5, 0.0 phi	-0,25	1189,21	0,29	1,90	-0,07	7,47	-38,16
1.00 - 0.71mm	0.0, 0.5 phi	0,25	840,90	0,42	2,33	0,11	8,96	-41,29
0.71 - 0.50mm	0.5, 1.0 phi	0,75	594,60	0,89	3,21	0,67	14,99	-61,58
500.00 - 354.00µm	1.0, 1.5 phi	1,25	420,45	1,00	4,21	1,24	12,96	-46,77
354.00 - 250.00µm	1.5, 2.0 phi	1,75	297,30	1,73	5,94	3,03	16,71	-51,93
250.00 - 177.00µm	2.0, 2.5 phi	2,25	210,22	3,40	9,34	7,64	23,10	-60,26
177.00 - 125.00µm	2.5, 3.0 phi	2,75	148,65	6,66	16,00	18,33	29,62	-62,43
125.00 - 88.40µm	3.0, 3.5 phi	3,25	105,11	10,48	26,48	34,05	27,09	-43,57
88.40 - 62.50µm	3.5, 4.0 phi	3,75	74,33	12,50	38,98	46,87	15,35	-17,01
62.50 - 44.20µm	4.0, 4..5 phi	4,25	52,56	11,63	50,61	49,43	4,30	-2,62
44.20 - 31.25µm	4.5, 5.0 phi	4,75	37,16	9,00	59,61	42,77	0,11	-0,01
31.25 - 22.10µm	5.0, 5.5 phi	5,25	26,28	6,69	66,30	35,12	1,03	0,40
22.10 - 15.63µm	5.5, 6.0 phi	5,75	18,58	5,63	71,93	32,39	4,48	4,00
15.63 - 11.00µm	6.0, 6.5 phi	6,25	13,14	5,33	77,26	33,30	10,32	14,37
11.00 - 7.81µm	6.5, 7.0 phi	6,75	9,29	4,90	82,16	33,09	17,54	33,19
7.81 - 5.52µm	7.0, 7.5 phi	7,25	6,57	4,11	86,28	29,82	23,53	56,28
5.52 - 3.91µm	7.5, 8.0 phi	7,75	4,65	3,34	89,62	25,89	27,94	80,81
3.91 - 2.76µm	8.0, 8.5 phi	8,25	3,28	2,90	92,52	23,92	33,36	113,15
2.76 - 1.95µm	8.5, 9.0 phi	8,75	2,32	2,56	95,08	22,39	38,75	150,82
1.95 - 1.38µm	9.0, 9.5 phi	9,25	1,64	2,00	97,07	18,49	38,55	169,30
1.38 - 0.98µm	9.5, 10.0 phi	9,75	1,16	1,30	98,37	12,67	31,09	152,08
0.98 - 0.69µm	10.0, 10.5 phi	10,25	0,82	0,76	99,14	7,82	22,18	119,62
0.69 - 0.49µm	10.5, 11.0 phi	10,75	0,58	0,48	99,62	5,16	16,67	98,22
0.49 - 0.35µm	11.0 , 11.5 phi	11,25	0,41	0,32	99,93	3,55	12,91	82,51
0.35 - 0.24µm	11.5, 12.0 phi	11,75	0,29	0,07	100,00	0,79	3,21	22,13
0.24 - 0.17µm	12.0, 12.5 phi	12,25	0,21	0,00	100,00	0,00	0,00	0,00
0.17 - 0.12µm	12.5, 13.0 phi	12,75	0,15	0,00	100,00	0,00	0,00	0,00
0.12 - 0.09µm	13.0, 13.5 phi	13,25	0,10	0,00	100,00	0,00	0,00	0,00
0.09 - 0.06µm	13.5, 14.0phi	13,75	0,07	0,00	100,00	0,00	0,00	0,00
0.06 - 0.04µm	14.0, 14.5 phi	14,25	0,05	0,00	100,00	0,00	0,00	0,00
0.04 - 0.03µm	14.5, 15.0 phi	14,75	0,04	0,00	100,00	0,00	0,00	0,00
0.03 - 0.02µm	15.0, 15.5 phi	15,25	0,03	0,00	100,00	0,00	0,00	0,00
				100,00		485,81	510,68	224,75

METHOD: MALVERN laser sedimentograph (particles <2mm)
Sieving (particles> 0.5mm)

Main Classes individual percentages:

Pebble	0,00
Gravel	1,48
Sand	37,50
Silt	50,64
Clay	10,38

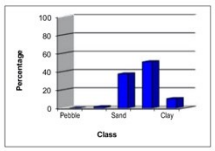

Statistical Parameters:

Mean	4,86
Standard Deviation	2,26
Asymmetry	0,19
P90	8,06
P50	4,47
P5	1,75
Mode	3,75

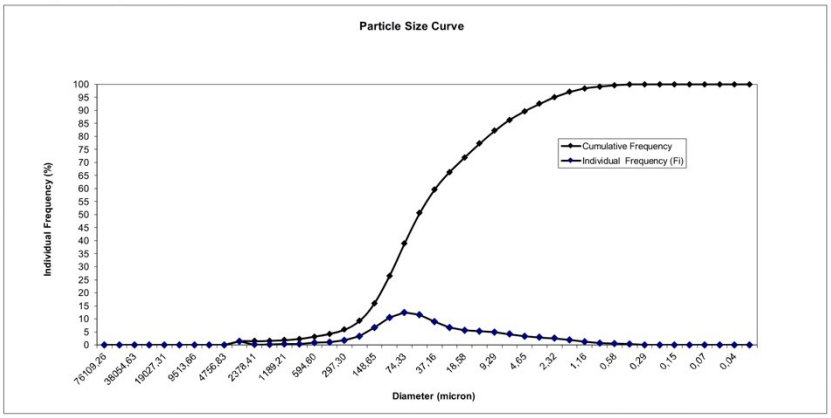

Technician: *Fernanda Dias*

Date:

INSTITUTO HIDROGRÁFICO
DIVISÃO DE GEOLOGIA MARINHA

Station: **2128**

Diameter (class)	Diameter phi	Class midpoint (ci)	Class midpoint (mm)	Individual Frequency (Fi)	Cumulative Frequency	Fi x ci	Fi x (ci-X)^2	Fi x (ci-X)^3
>64.00mm	<6.0 phi	-6,25	76109,26	0,00	0,00	0,00	0,00	0,00
45.25-64.00mm	-5.5,6.0 phi	-5,75	53817,37	0,00	0,00	0,00	0,00	0,00
32.00-45.25mm	-5.0,-5.5 phi	-5,25	38054,63	0,00	0,00	0,00	0,00	0,00
22.63-32.00mm	-4.5,-5.0 phi	-4,75	26908,69	0,00	0,00	0,00	0,00	0,00
16.00-22.63mm	-4.0,-4.5 phi	-4,25	19027,31	0,00	0,00	0,00	0,00	0,00
11.31-16.00mm	-3.5,-4.0 phi	-3,75	13454,34	0,00	0,00	0,00	0,00	0,00
8.00-11.31mm	-3.0,-3.5 phi	-3,25	9513,66	0,00	0,00	0,00	0,00	0,00
5.66-8.00mm	-2.5,-3.0 phi	-2,75	6727,17	0,00	0,00	0,00	0,00	0,00
4.00-5.66mm	-2.5,-2.0 phi	-2,25	4756,83	0,35	0,35	-0,78	16,52	-113,67
4.00 - 2.83mm	-2.0, -1.5 phi	-1,75	3363,59	0,04	0,39	-0,07	1,67	-10,66
2.83 - 2.00mm	-1.5, -1.0 phi	-1,25	2378,41	0,10	0,49	-0,13	3,56	-20,97
2.00 - 1.41mm	-1.0, -0.5 phi	-0,75	1681,79	0,22	0,71	-0,17	6,43	-34,62
1.41 - 1.00mm	-0.5, 0.0 phi	-0,25	1189,21	0,28	0,99	-0,07	6,56	-32,04
1.00 - 0.71mm	0.0, 0.5 phi	0,25	840,90	0,45	1,44	0,11	8,69	-38,09
0.71 - 0.50mm	0.5, 1.0 phi	0,75	594,60	0,83	2,27	0,62	12,49	-48,47
500.00 - 354.00µm	1.0, 1.5 phi	1,25	420,45	1,20	3,48	1,51	13,77	-46,57
354.00 - 250.00µm	1.5, 2.0 phi	1,75	297,30	2,67	6,14	4,67	22,15	-63,84
250.00 - 177.00µm	2.0, 2.5 phi	2,25	210,22	5,20	11,34	11,70	29,49	-70,23
177.00 - 125.00µm	2.5, 3.0 phi	2,75	148,65	8,83	20,18	24,29	31,28	-58,86
125.00 - 88.40µm	3.0, 3.5 phi	3,25	105,11	12,12	32,29	39,39	23,14	-31,97
88.40 - 62.50µm	3.5, 4.0 phi	3,75	74,33	13,08	45,37	49,05	10,17	-8,97
62.50 - 44.20µm	4.0, 4..5 phi	4,25	52,56	11,34	56,72	48,22	1,65	-0,63
44.20 - 31.25µm	4.5, 5.0 phi	4,75	37,16	8,36	65,08	39,73	0,12	0,01
31.25 - 22.10µm	5.0, 5.5 phi	5,25	26,28	5,98	71,06	31,38	2,28	1,41
22.10 - 15.63µm	5.5, 6.0 phi	5,75	18,58	4,89	75,95	28,15	6,12	6,84
15.63 - 11.00µm	6.0, 6.5 phi	6,25	13,14	4,58	80,54	28,63	12,00	19,42
11.00 - 7.81µm	6.5, 7.0 phi	6,75	9,29	4,22	84,76	28,49	18,94	40,12
7.81 - 5.52µm	7.0, 7.5 phi	7,25	6,57	3,55	88,31	25,77	24,37	63,81
5.52 - 3.91µm	7.5, 8.0 phi	7,75	4,65	2,88	91,20	22,35	28,05	87,45
3.91 - 2.76µm	8.0, 8.5 phi	8,25	3,28	2,48	93,68	20,48	32,50	117,59
2.76 - 1.95µm	8.5, 9.0 phi	8,75	2,32	2,17	95,85	18,99	36,82	151,62
1.95 - 1.38µm	9.0, 9.5 phi	9,25	1,64	1,69	97,54	15,60	35,98	166,15
1.38 - 0.98µm	9.5, 10.0 phi	9,75	1,16	1,09	98,63	10,67	28,67	146,74
0.98 - 0.69µm	10.0, 10.5 phi	10,25	0,82	0,64	99,27	6,59	20,29	114,01
0.69 - 0.49µm	10.5, 11.0 phi	10,75	0,58	0,40	99,68	4,35	15,15	92,70
0.49 - 0.35µm	11.0 , 11.5 phi	11,25	0,41	0,27	99,95	3,01	11,72	77,59
0.35 - 0.24µm	11.5, 12.0 phi	11,75	0,29	0,05	100,00	0,65	2,78	19,81
0.24 - 0.17µm	12.0, 12.5 phi	12,25	0,21	0,00	100,00	0,00	0,00	0,00
0.17 - 0.12µm	12.5, 13.0 phi	12,75	0,15	0,00	100,00	0,00	0,00	0,00
0.12 - 0.09µm	13.0, 13.5 phi	13,25	0,10	0,00	100,00	0,00	0,00	0,00
0.09 - 0.06µm	13.5, 14.0phi	13,75	0,07	0,00	100,00	0,00	0,00	0,00
0.06 - 0.04µm	14.0, 14.5 phi	14,25	0,05	0,00	100,00	0,00	0,00	0,00
0.04 - 0.03µm	14.5, 15.0 phi	14,75	0,04	0,00	100,00	0,00	0,00	0,00
0.03 - 0.02µm	15.0, 15.5 phi	15,25	0,03	0,00	100,00	0,00	0,00	0,00
METHOD: MALVERN laser sedimentograph (particles <2mm)				100,00		463,17	463,37	525,69
Sieving (particles> 0.5mm)								

Main Classes individual percentages:

Pebble	0,00
Gravel	0,49
Sand	44,88
Silt	45,82
Clay	8,80

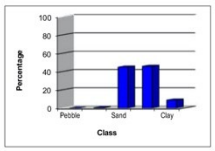

Statistical Parameters:

Mean	4,63
Standard Deviation	2,15
Asymmetry	0,53
P90	7,78
P50	4,20
P5	1,81
Mode	3,75

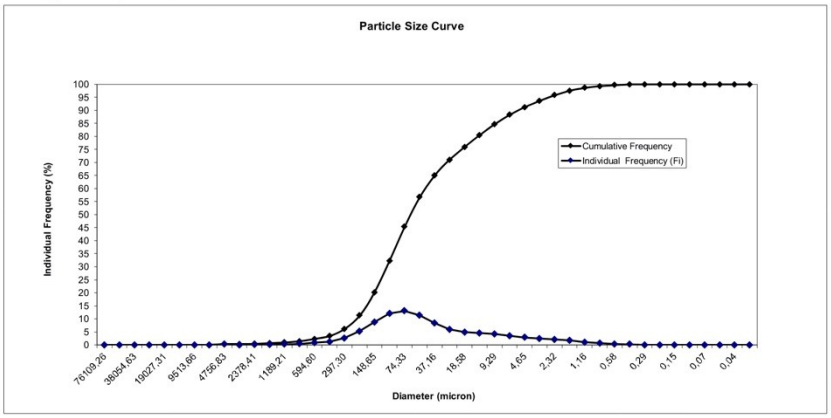

Technician: *Fernanda Dias*

Date:

INSTITUTO HIDROGRÁFICO
DIVISÃO DE GEOLOGIA MARINHA

Station: **2129**

Diameter (class)	Diameter phi	Class midpoint (ci)	Class midpoint (mm)	Individual Frequency (Fi)	Cumulative Frequency	Fi x ci	Fi x (ci-X)^2	Fi x (ci-X)^3
>64.00mm	<6.0 phi	-6,25	76109,26	0,00	0,00	0,00	0,00	0,00
45.25-64.00mm	-5.5,6.0 phi	-5,75	53817,37	0,00	0,00	0,00	0,00	0,00
32.00-45.25mm	-5.0,-5.5 phi	-5,25	38054,63	0,00	0,00	0,00	0,00	0,00
22.63-32.00mm	-4.5,-5.0 phi	-4,75	26908,69	0,00	0,00	0,00	0,00	0,00
16.00-22.63mm	-4.0,-4.5 phi	-4,25	19027,31	0,00	0,00	0,00	0,00	0,00
11.31-16.00mm	-3.5,-4.0 phi	-3,75	13454,34	0,00	0,00	0,00	0,00	0,00
8.00-11.31mm	-3.0,-3.5 phi	-3,25	9513,66	0,00	0,00	0,00	0,00	0,00
5.66-8.00mm	-2.5,-3.0 phi	-2,75	6727,17	0,00	0,00	0,00	0,00	0,00
4.00-5.66mm	-2.5,-2.0 phi	-2,25	4756,83	0,44	0,44	-1,00	27,80	-220,23
4.00 - 2.83mm	-2.0, -1.5 phi	-1,75	3363,59	0,25	0,70	-0,44	13,93	-103,40
2.83 - 2.00mm	-1.5, -1.0 phi	-1,25	2378,41	0,32	1,01	-0,40	15,22	-105,35
2.00 - 1.41mm	-1.0, -0.5 phi	-0,75	1681,79	0,41	1,42	-0,30	16,73	-107,45
1.41 - 1.00mm	-0.5, 0.0 phi	-0,25	1189,21	0,44	1,86	-0,11	15,55	-92,08
1.00 - 0.71mm	0.0, 0.5 phi	0,25	840,90	0,73	2,59	0,18	21,50	-116,57
0.71 - 0.50mm	0.5, 1.0 phi	0,75	594,60	0,99	3,58	0,74	23,95	-117,87
500.00 - 354.00µm	1.0, 1.5 phi	1,25	420,45	0,38	3,97	0,48	7,51	-33,23
354.00 - 250.00µm	1.5, 2.0 phi	1,75	297,30	0,59	4,55	1,03	9,07	-35,57
250.00 - 177.00µm	2.0, 2.5 phi	2,25	210,22	1,30	5,85	2,92	15,18	-51,96
177.00 - 125.00µm	2.5, 3.0 phi	2,75	148,65	3,10	8,95	8,53	26,48	-77,38
125.00 - 88.40µm	3.0, 3.5 phi	3,25	105,11	5,62	14,57	18,26	32,98	-79,88
88.40 - 62.50µm	3.5, 4.0 phi	3,75	74,33	7,62	22,19	28,56	28,15	-54,12
62.50 - 44.20µm	4.0, 4..5 phi	4,25	52,56	8,33	30,51	35,39	16,85	-23,97
44.20 - 31.25µm	4.5, 5.0 phi	4,75	37,16	8,12	38,64	38,59	6,91	-6,38
31.25 - 22.10µm	5.0, 5.5 phi	5,25	26,28	8,04	46,68	42,22	1,44	-0,61
22.10 - 15.63µm	5.5, 6.0 phi	5,75	18,58	8,46	55,14	48,66	0,05	0,00
15.63 - 11.00µm	6.0, 6.5 phi	6,25	13,14	8,76	63,90	54,75	2,92	1,69
11.00 - 7.81µm	6.5, 7.0 phi	6,75	9,29	8,19	72,09	55,26	9,50	10,24
7.81 - 5.52µm	7.0, 7.5 phi	7,25	6,57	6,84	78,93	49,57	17,01	26,84
5.52 - 3.91µm	7.5, 8.0 phi	7,75	4,65	5,48	84,41	42,45	23,64	49,11
3.91 - 2.76µm	8.0, 8.5 phi	8,25	3,28	4,61	89,02	38,06	30,65	79,00
2.76 - 1.95µm	8.5, 9.0 phi	8,75	2,32	3,91	92,93	34,20	37,02	113,93
1.95 - 1.38µm	9.0, 9.5 phi	9,25	1,64	2,93	95,86	27,14	37,56	134,36
1.38 - 0.98µm	9.5, 10.0 phi	9,75	1,16	1,84	97,70	17,94	30,60	124,76
0.98 - 0.69µm	10.0, 10.5 phi	10,25	0,82	1,05	98,75	10,75	21,98	100,60
0.69 - 0.49µm	10.5, 11.0 phi	10,75	0,58	0,65	99,40	7,01	16,81	85,37
0.49 - 0.35µm	11.0 , 11.5 phi	11,25	0,41	0,43	99,84	4,85	13,41	74,80
0.35 - 0.24µm	11.5, 12.0 phi	11,75	0,29	0,16	100,00	1,93	6,08	36,96
0.24 - 0.17µm	12.0, 12.5 phi	12,25	0,21	0,00	100,00	0,00	0,00	0,00
0.17 - 0.12µm	12.5, 13.0 phi	12,75	0,15	0,00	100,00	0,00	0,00	0,00
0.12 - 0.09µm	13.0, 13.5 phi	13,25	0,10	0,00	100,00	0,00	0,00	0,00
0.09 - 0.06µm	13.5, 14.0phi	13,75	0,07	0,00	100,00	0,00	0,00	0,00
0.06 - 0.04µm	14.0, 14.5 phi	14,25	0,05	0,00	100,00	0,00	0,00	0,00
0.04 - 0.03µm	14.5, 15.0 phi	14,75	0,04	0,00	100,00	0,00	0,00	0,00
0.03 - 0.02µm	15.0, 15.5 phi	15,25	0,03	0,00	100,00	0,00	0,00	0,00
METHOD: MALVERN laser sedimentograph (particles <2mm)				100,00		567,25	526,48	-388,39
Sieving (particles> 0.5mm)								

Main Classes individual percentages:

Pebble	0,00
Gravel	1,01
Sand	21,17
Silt	62,22
Clay	15,59

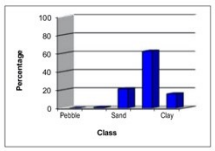

Statistical Parameters:

Mean	5,67
Standard Deviation	2,29
Asymmetry	-0,32
P90	8,61
P50	5,70
P5	2,18
Mode	6,25

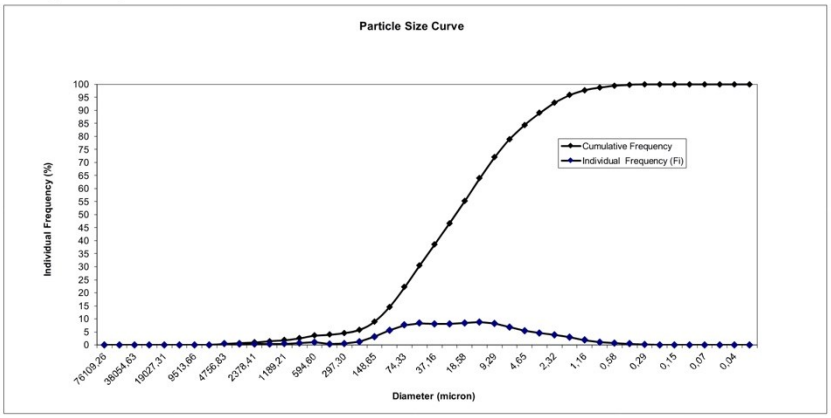

Technician: *Fernanda Dias*

Date:

INSTITUTO HIDROGRÁFICO
DIVISÃO DE GEOLOGIA MARINHA

Station: **2130**

Diameter (class)	Diameter phi	Class midpoint (ci)	Class midpoint (mm)	Individual Frequency (Fi)	Cumulative Frequency	Fi x ci	Fi x (ci-X)^2	Fi x (ci-X)^3
>64.00mm	<6.0 phi	-6,25	76109,26	0,00	0,00	0,00	0,00	0,00
45.25-64.00mm	-5.5,6.0 phi	-5,75	53817,37	0,00	0,00	0,00	0,00	0,00
32.00-45.25mm	-5.0,-5.5 phi	-5,25	38054,63	0,00	0,00	0,00	0,00	0,00
22.63-32.00mm	-4.5,-5.0 phi	-4,75	26908,69	0,00	0,00	0,00	0,00	0,00
16.00-22.63mm	-4.0,-4.5 phi	-4,25	19027,31	0,00	0,00	0,00	0,00	0,00
11.31-16.00mm	-3.5,-4.0 phi	-3,75	13454,34	0,00	0,00	0,00	0,00	0,00
8.00-11.31mm	-3.0,-3.5 phi	-3,25	9513,66	0,00	0,00	0,00	0,00	0,00
5.66-8.00mm	-2.5,-3.0 phi	-2,75	6727,17	0,00	0,00	0,00	0,00	0,00
4.00-5.66mm	-2.5,-2.0 phi	-2,25	4756,83	0,42	0,42	-0,94	25,68	-201,32
4.00 - 2.83mm	-2.0, -1.5 phi	-1,75	3363,59	0,17	0,59	-0,30	9,09	-66,70
2.83 - 2.00mm	-1.5, -1.0 phi	-1,25	2378,41	0,51	1,09	-0,63	23,74	-162,41
2.00 - 1.41mm	-1.0, -0.5 phi	-0,75	1681,79	0,85	1,94	-0,64	34,14	-216,46
1.41 - 1.00mm	-0.5, 0.0 phi	-0,25	1189,21	0,94	2,88	-0,23	32,03	-187,09
1.00 - 0.71mm	0.0, 0.5 phi	0,25	840,90	1,37	4,25	0,34	39,18	-209,26
0.71 - 0.50mm	0.5, 1.0 phi	0,75	594,60	1,54	5,80	1,16	36,10	-174,79
500.00 - 354.00µm	1.0, 1.5 phi	1,25	420,45	0,48	6,27	0,60	9,00	-39,08
354.00 - 250.00µm	1.5, 2.0 phi	1,75	297,30	0,59	6,87	1,04	8,75	-33,59
250.00 - 177.00µm	2.0, 2.5 phi	2,25	210,22	1,23	8,10	2,77	13,74	-45,91
177.00 - 125.00µm	2.5, 3.0 phi	2,75	148,65	2,95	11,04	8,10	23,79	-67,58
125.00 - 88.40µm	3.0, 3.5 phi	3,25	105,11	5,31	16,35	17,25	29,09	-68,11
88.40 - 62.50µm	3.5, 4.0 phi	3,75	74,33	7,16	23,51	26,84	24,26	-44,66
62.50 - 44.20µm	4.0, 4..5 phi	4,25	52,56	7,83	31,33	33,26	14,07	-18,88
44.20 - 31.25µm	4.5, 5.0 phi	4,75	37,16	7,69	39,02	36,51	5,44	-4,57
31.25 - 22.10µm	5.0, 5.5 phi	5,25	26,28	7,70	46,72	40,43	0,90	-0,31
22.10 - 15.63µm	5.5, 6.0 phi	5,75	18,58	8,20	54,93	47,17	0,21	0,03
15.63 - 11.00µm	6.0, 6.5 phi	6,25	13,14	8,59	63,52	53,70	3,73	2,46
11.00 - 7.81µm	6.5, 7.0 phi	6,75	9,29	8,13	71,65	54,90	10,92	12,66
7.81 - 5.52µm	7.0, 7.5 phi	7,25	6,57	6,88	78,53	49,87	18,93	31,40
5.52 - 3.91µm	7.5, 8.0 phi	7,75	4,65	5,56	84,09	43,08	25,91	55,93
3.91 - 2.76µm	8.0, 8.5 phi	8,25	3,28	4,70	88,78	38,74	33,20	88,27
2.76 - 1.95µm	8.5, 9.0 phi	8,75	2,32	3,98	92,76	34,84	39,73	125,50
1.95 - 1.38µm	9.0, 9.5 phi	9,25	1,64	2,99	95,76	27,70	40,09	146,68
1.38 - 0.98µm	9.5, 10.0 phi	9,75	1,16	1,88	97,64	18,37	32,59	135,52
0.98 - 0.69µm	10.0, 10.5 phi	10,25	0,82	1,08	98,72	11,03	23,35	108,78
0.69 - 0.49µm	10.5, 11.0 phi	10,75	0,58	0,67	99,39	7,18	17,77	91,66
0.49 - 0.35µm	11.0 , 11.5 phi	11,25	0,41	0,44	99,83	4,97	14,14	80,02
0.35 - 0.24µm	11.5, 12.0 phi	11,75	0,29	0,17	100,00	2,02	6,53	40,19
0.24 - 0.17µm	12.0, 12.5 phi	12,25	0,21	0,00	100,00	0,00	0,00	0,00
0.17 - 0.12µm	12.5, 13.0 phi	12,75	0,15	0,00	100,00	0,00	0,00	0,00
0.12 - 0.09µm	13.0, 13.5 phi	13,25	0,10	0,00	100,00	0,00	0,00	0,00
0.09 - 0.06µm	13.5, 14.0phi	13,75	0,07	0,00	100,00	0,00	0,00	0,00
0.06 - 0.04µm	14.0, 14.5 phi	14,25	0,05	0,00	100,00	0,00	0,00	0,00
0.04 - 0.03µm	14.5, 15.0 phi	14,75	0,04	0,00	100,00	0,00	0,00	0,00
0.03 - 0.02µm	15.0, 15.5 phi	15,25	0,03	0,00	100,00	0,00	0,00	0,00
				100,00		559,11	596,07	-621,62

METHOD: MALVERN laser sedimentograph (particles <2mm)
Sieving (particles> 0.5mm)

Main Classes individual percentages:

Pebble	0,00
Gravel	1,09
Sand	22,42
Silt	60,58
Clay	15,91

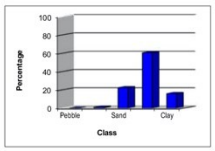

Statistical Parameters:

Mean	5,59
Standard Deviation	2,44
Asymmetry	-0,43
P90	8,64
P50	5,70
P5	0,76
Mode	6,25

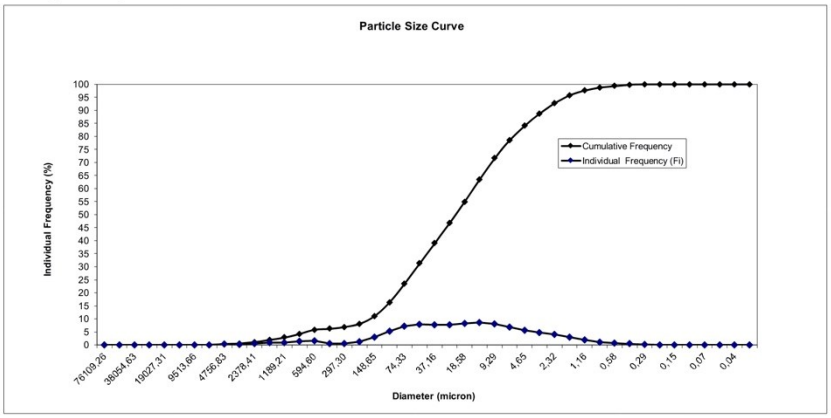

Technician: *Fernanda Dias*

Date:

INSTITUTO HIDROGRÁFICO
DIVISÃO DE GEOLOGIA MARINHA

Station: **2131**

Diameter (class)	Diameter phi	Class midpoint (ci)	Class midpoint (mm)	Individual Frequency (Fi)	Cumulative Frequency	Fi x ci	Fi x (ci-X)^2	Fi x (ci-X)^3
>64.00mm	<6.0 phi	-6,25	76109,26	0,00	0,00	0,00	0,00	0,00
45.25-64.00mm	-5.5,6.0 phi	-5,75	53817,37	0,00	0,00	0,00	0,00	0,00
32.00-45.25mm	-5.0,-5.5 phi	-5,25	38054,63	0,00	0,00	0,00	0,00	0,00
22.63-32.00mm	-4.5,-5.0 phi	-4,75	26908,69	0,00	0,00	0,00	0,00	0,00
16.00-22.63mm	-4.0,-4.5 phi	-4,25	19027,31	0,00	0,00	0,00	0,00	0,00
11.31-16.00mm	-3.5,-4.0 phi	-3,75	13454,34	0,00	0,00	0,00	0,00	0,00
8.00-11.31mm	-3.0,-3.5 phi	-3,25	9513,66	0,00	0,00	0,00	0,00	0,00
5.66-8.00mm	-2.5,-3.0 phi	-2,75	6727,17	0,00	0,00	0,00	0,00	0,00
4.00-5.66mm	-2.5,-2.0 phi	-2,25	4756,83	0,21	0,21	-0,47	9,28	-61,93
4.00 - 2.83mm	-2.0, -1.5 phi	-1,75	3363,59	0,12	0,33	-0,21	4,62	-28,49
2.83 - 2.00mm	-1.5, -1.0 phi	-1,25	2378,41	0,43	0,76	-0,54	13,79	-78,18
2.00 - 1.41mm	-1.0, -0.5 phi	-0,75	1681,79	0,74	1,50	-0,55	19,79	-102,31
1.41 - 1.00mm	-0.5, 0.0 phi	-0,25	1189,21	0,98	2,48	-0,25	21,43	-100,09
1.00 - 0.71mm	0.0, 0.5 phi	0,25	840,90	1,72	4,20	0,43	29,94	-124,90
0.71 - 0.50mm	0.5, 1.0 phi	0,75	594,60	2,48	6,68	1,86	33,40	-122,62
500.00 - 354.00µm	1.0, 1.5 phi	1,25	420,45	1,65	8,33	2,06	16,59	-52,60
354.00 - 250.00µm	1.5, 2.0 phi	1,75	297,30	2,57	10,90	4,50	18,34	-48,99
250.00 - 177.00µm	2.0, 2.5 phi	2,25	210,22	4,51	15,41	10,14	21,25	-46,13
177.00 - 125.00µm	2.5, 3.0 phi	2,75	148,65	8,10	23,51	22,28	22,62	-37,81
125.00 - 88.40µm	3.0, 3.5 phi	3,25	105,11	11,94	35,45	38,80	16,37	-19,17
88.40 - 62.50µm	3.5, 4.0 phi	3,75	74,33	13,35	48,80	50,06	6,01	-4,03
62.50 - 44.20µm	4.0, 4..5 phi	4,25	52,56	11,44	60,24	48,63	0,33	-0,06
44.20 - 31.25µm	4.5, 5.0 phi	4,75	37,16	7,92	68,16	37,63	0,86	0,28
31.25 - 22.10µm	5.0, 5.5 phi	5,25	26,28	5,15	73,31	27,01	3,54	2,93
22.10 - 15.63µm	5.5, 6.0 phi	5,75	18,58	4,00	77,30	22,98	7,06	9,38
15.63 - 11.00µm	6.0, 6.5 phi	6,25	13,14	3,83	81,14	23,95	12,82	23,44
11.00 - 7.81µm	6.5, 7.0 phi	6,75	9,29	3,70	84,83	24,97	20,06	46,73
7.81 - 5.52µm	7.0, 7.5 phi	7,25	6,57	3,25	88,09	23,59	26,04	73,66
5.52 - 3.91µm	7.5, 8.0 phi	7,75	4,65	2,75	90,84	21,30	30,46	101,39
3.91 - 2.76µm	8.0, 8.5 phi	8,25	3,28	2,46	93,29	20,27	36,01	137,90
2.76 - 1.95µm	8.5, 9.0 phi	8,75	2,32	2,22	95,51	19,42	41,59	180,05
1.95 - 1.38µm	9.0, 9.5 phi	9,25	1,64	1,77	97,29	16,41	41,37	199,76
1.38 - 0.98µm	9.5, 10.0 phi	9,75	1,16	1,18	98,47	11,54	33,61	179,13
0.98 - 0.69µm	10.0, 10.5 phi	10,25	0,82	0,71	99,19	7,32	24,28	141,50
0.69 - 0.49µm	10.5, 11.0 phi	10,75	0,58	0,45	99,64	4,89	18,22	115,31
0.49 - 0.35µm	11.0 , 11.5 phi	11,25	0,41	0,30	99,94	3,34	13,83	94,46
0.35 - 0.24µm	11.5, 12.0 phi	11,75	0,29	0,06	100,00	0,74	3,39	24,86
0.24 - 0.17µm	12.0, 12.5 phi	12,25	0,21	0,00	100,00	0,00	0,00	0,00
0.17 - 0.12µm	12.5, 13.0 phi	12,75	0,15	0,00	100,00	0,00	0,00	0,00
0.12 - 0.09µm	13.0, 13.5 phi	13,25	0,10	0,00	100,00	0,00	0,00	0,00
0.09 - 0.06µm	13.5, 14.0phi	13,75	0,07	0,00	100,00	0,00	0,00	0,00
0.06 - 0.04µm	14.0, 14.5 phi	14,25	0,05	0,00	100,00	0,00	0,00	0,00
0.04 - 0.03µm	14.5, 15.0 phi	14,75	0,04	0,00	100,00	0,00	0,00	0,00
0.03 - 0.02µm	15.0, 15.5 phi	15,25	0,03	0,00	100,00	0,00	0,00	0,00
				100,00		442,11	546,90	503,48

METHOD: MALVERN laser sedimentograph (particles <2mm)
Sieving (particles> 0.5mm)

Main Classes individual percentages:

Pebble	0,00
Gravel	0,76
Sand	48,04
Silt	42,04
Clay	9,16

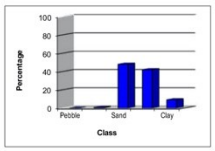

Statistical Parameters:

Mean	4,42
Standard Deviation	2,34
Asymmetry	0,39
P90	7,84
P50	4,05
P5	0,68
Mode	3,75

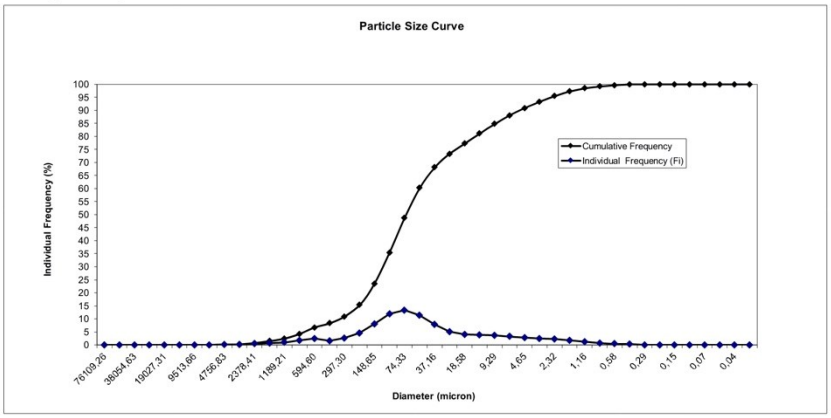

Technician: *Fernanda Dias*

Date:

INSTITUTO HIDROGRÁFICO
DIVISÃO DE GEOLOGIA MARINHA

Station: **2132**

Diameter (class)	Diameter phi	Class midpoint (ci)	Class midpoint (mm)	Individual Frequency (Fi)	Cumulative Frequency	Fi x ci	Fi x (ci-X)^2	Fi x (ci-X)^3
>64.00mm	<6.0 phi	-6,25	76109,26	0,00	0,00	0,00	0,00	0,00
45.25-64.00mm	-5.5,6.0 phi	-5,75	53817,37	0,00	0,00	0,00	0,00	0,00
32.00-45.25mm	-5.0,-5.5 phi	-5,25	38054,63	0,00	0,00	0,00	0,00	0,00
22.63-32.00mm	-4.5,-5.0 phi	-4,75	26908,69	0,00	0,00	0,00	0,00	0,00
16.00-22.63mm	-4.0,-4.5 phi	-4,25	19027,31	0,00	0,00	0,00	0,00	0,00
11.31-16.00mm	-3.5,-4.0 phi	-3,75	13454,34	0,00	0,00	0,00	0,00	0,00
8.00-11.31mm	-3.0,-3.5 phi	-3,25	9513,66	0,00	0,00	0,00	0,00	0,00
5.66-8.00mm	-2.5,-3.0 phi	-2,75	6727,17	0,00	0,00	0,00	0,00	0,00
4.00-5.66mm	-2.5,-2.0 phi	-2,25	4756,83	0,00	0,00	0,00	0,00	0,00
4.00 - 2.83mm	-2.0, -1.5 phi	-1,75	3363,59	0,65	0,65	-1,14	23,87	-144,41
2.83 - 2.00mm	-1.5, -1.0 phi	-1,25	2378,41	0,39	1,04	-0,48	11,86	-65,84
2.00 - 1.41mm	-1.0, -0.5 phi	-0,75	1681,79	0,74	1,78	-0,55	18,85	-95,21
1.41 - 1.00mm	-0.5, 0.0 phi	-0,25	1189,21	1,29	3,07	-0,32	26,76	-121,75
1.00 - 0.71mm	0.0, 0.5 phi	0,25	840,90	2,07	5,14	0,52	34,02	-137,77
0.71 - 0.50mm	0.5, 1.0 phi	0,75	594,60	3,02	8,17	2,27	38,07	-135,11
500.00 - 354.00µm	1.0, 1.5 phi	1,25	420,45	1,64	9,80	2,05	15,23	-46,46
354.00 - 250.00µm	1.5, 2.0 phi	1,75	297,30	2,69	12,49	4,70	17,46	-44,51
250.00 - 177.00µm	2.0, 2.5 phi	2,25	210,22	4,71	17,20	10,60	19,78	-40,55
177.00 - 125.00µm	2.5, 3.0 phi	2,75	148,65	8,29	25,49	22,80	19,91	-30,85
125.00 - 88.40µm	3.0, 3.5 phi	3,25	105,11	12,04	37,53	39,13	13,26	-13,92
88.40 - 62.50µm	3.5, 4.0 phi	3,75	74,33	13,38	50,91	50,18	4,04	-2,22
62.50 - 44.20µm	4.0, 4..5 phi	4,25	52,56	11,43	62,35	48,60	0,03	0,00
44.20 - 31.25µm	4.5, 5.0 phi	4,75	37,16	7,82	70,17	37,15	1,59	0,71
31.25 - 22.10µm	5.0, 5.5 phi	5,25	26,28	4,90	75,07	25,74	4,43	4,21
22.10 - 15.63µm	5.5, 6.0 phi	5,75	18,58	3,64	78,71	20,93	7,66	11,11
15.63 - 11.00µm	6.0, 6.5 phi	6,25	13,14	3,44	82,15	21,47	13,07	25,49
11.00 - 7.81µm	6.5, 7.0 phi	6,75	9,29	3,34	85,48	22,52	20,04	49,10
7.81 - 5.52µm	7.0, 7.5 phi	7,25	6,57	2,97	88,46	21,55	25,88	76,35
5.52 - 3.91µm	7.5, 8.0 phi	7,75	4,65	2,56	91,02	19,86	30,51	105,28
3.91 - 2.76µm	8.0, 8.5 phi	8,25	3,28	2,35	93,37	19,39	36,69	144,93
2.76 - 1.95µm	8.5, 9.0 phi	8,75	2,32	2,17	95,54	18,96	42,91	190,97
1.95 - 1.38µm	9.0, 9.5 phi	9,25	1,64	1,75	97,29	16,20	42,91	212,42
1.38 - 0.98µm	9.5, 10.0 phi	9,75	1,16	1,18	98,46	11,47	34,96	190,52
0.98 - 0.69µm	10.0, 10.5 phi	10,25	0,82	0,72	99,18	7,33	25,33	150,71
0.69 - 0.49µm	10.5, 11.0 phi	10,75	0,58	0,46	99,64	4,92	19,06	122,94
0.49 - 0.35µm	11.0 , 11.5 phi	11,25	0,41	0,30	99,94	3,36	14,45	100,40
0.35 - 0.24µm	11.5, 12.0 phi	11,75	0,29	0,06	100,00	0,75	3,53	26,32
0.24 - 0.17µm	12.0, 12.5 phi	12,25	0,21	0,00	100,00	0,00	0,00	0,00
0.17 - 0.12µm	12.5, 13.0 phi	12,75	0,15	0,00	100,00	0,00	0,00	0,00
0.12 - 0.09µm	13.0, 13.5 phi	13,25	0,10	0,00	100,00	0,00	0,00	0,00
0.09 - 0.06µm	13.5, 14.0phi	13,75	0,07	0,00	100,00	0,00	0,00	0,00
0.06 - 0.04µm	14.0, 14.5 phi	14,25	0,05	0,00	100,00	0,00	0,00	0,00
0.04 - 0.03µm	14.5, 15.0 phi	14,75	0,04	0,00	100,00	0,00	0,00	0,00
0.03 - 0.02µm	15.0, 15.5 phi	15,25	0,03	0,00	100,00	0,00	0,00	0,00
				100,00		429,95	566,15	532,88

METHOD: MALVERN laser sedimentograph (particles <2mm)
Sieving (particles> 0.5mm)

Main Classes individual percentages:

Pebble	0,00
Gravel	1,04
Sand	49,88
Silt	40,10
Clay	8,98

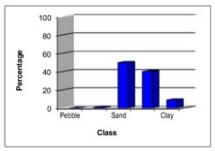

Statistical Parameters:

Mean	4,30
Standard Deviation	2,38
Asymmetry	0,40
P90	7,79
P50	3,97
P5	0,47
Mode	3,75

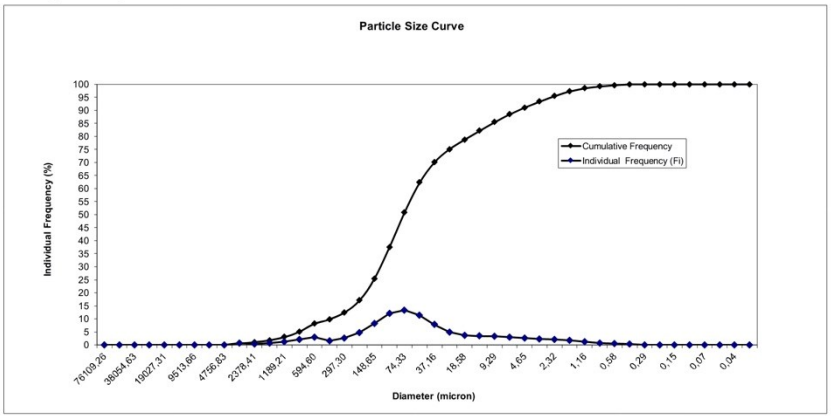

Technician: *Fernanda Dias*

Date:

INSTITUTO HIDROGRÁFICO
DIVISÃO DE GEOLOGIA MARINHA

Station: **2133**

Diameter (class)	Diameter phi	Class midpoint (ci)	Class midpoint (mm)	Individual Frequency (Fi)	Cumulative Frequency	Fi x ci	Fi x (ci-X)^2	Fi x (ci-X)^3
>64.00mm	<6.0 phi	-6,25	76109,26	0,00	0,00	0,00	0,00	0,00
45.25-64.00mm	-5.5,6.0 phi	-5,75	53817,37	0,00	0,00	0,00	0,00	0,00
32.00-45.25mm	-5.0,-5.5 phi	-5,25	38054,63	0,00	0,00	0,00	0,00	0,00
22.63-32.00mm	-4.5,-5.0 phi	-4,75	26908,69	0,00	0,00	0,00	0,00	0,00
16.00-22.63mm	-4.0,-4.5 phi	-4,25	19027,31	0,00	0,00	0,00	0,00	0,00
11.31-16.00mm	-3.5,-4.0 phi	-3,75	13454,34	0,00	0,00	0,00	0,00	0,00
8.00-11.31mm	-3.0,-3.5 phi	-3,25	9513,66	0,00	0,00	0,00	0,00	0,00
5.66-8.00mm	-2.5,-3.0 phi	-2,75	6727,17	0,00	0,00	0,00	0,00	0,00
4.00-5.66mm	-2.5,-2.0 phi	-2,25	4756,83	0,00	0,00	0,00	0,00	0,00
4.00 - 2.83mm	-2.0, -1.5 phi	-1,75	3363,59	0,31	0,31	-0,55	11,79	-72,20
2.83 - 2.00mm	-1.5, -1.0 phi	-1,25	2378,41	0,31	0,63	-0,39	9,83	-55,29
2.00 - 1.41mm	-1.0, -0.5 phi	-0,75	1681,79	0,54	1,17	-0,41	14,29	-73,18
1.41 - 1.00mm	-0.5, 0.0 phi	-0,25	1189,21	0,94	2,11	-0,23	20,08	-92,82
1.00 - 0.71mm	0.0, 0.5 phi	0,25	840,90	1,90	4,01	0,48	32,36	-133,41
0.71 - 0.50mm	0.5, 1.0 phi	0,75	594,60	2,94	6,96	2,21	38,60	-139,82
500.00 - 354.00µm	1.0, 1.5 phi	1,25	420,45	1,70	8,66	2,12	16,57	-51,73
354.00 - 250.00µm	1.5, 2.0 phi	1,75	297,30	2,70	11,35	4,72	18,54	-48,62
250.00 - 177.00µm	2.0, 2.5 phi	2,25	210,22	4,69	16,04	10,55	21,12	-44,83
177.00 - 125.00µm	2.5, 3.0 phi	2,75	148,65	8,30	24,34	22,81	21,83	-35,41
125.00 - 88.40µm	3.0, 3.5 phi	3,25	105,11	12,11	36,45	39,35	15,24	-17,11
88.40 - 62.50µm	3.5, 4.0 phi	3,75	74,33	13,48	49,92	50,54	5,22	-3,25
62.50 - 44.20µm	4.0, 4.,5 phi	4,25	52,56	11,51	61,43	48,90	0,17	-0,02
44.20 - 31.25µm	4.5, 5.0 phi	4,75	37,16	7,89	69,32	37,46	1,13	0,43
31.25 - 22.10µm	5.0, 5.5 phi	5,25	26,28	5,02	74,34	26,37	3,87	3,40
22.10 - 15.63µm	5.5, 6.0 phi	5,75	18,58	3,82	78,16	21,99	7,26	10,00
15.63 - 11.00µm	6.0, 6.5 phi	6,25	13,14	3,63	81,80	22,71	12,81	24,06
11.00 - 7.81µm	6.5, 7.0 phi	6,75	9,29	3,51	85,30	23,66	19,82	47,13
7.81 - 5.52µm	7.0, 7.5 phi	7,25	6,57	3,10	88,40	22,49	25,69	73,94
5.52 - 3.91µm	7.5, 8.0 phi	7,75	4,65	2,66	91,06	20,60	30,33	102,46
3.91 - 2.76µm	8.0, 8.5 phi	8,25	3,28	2,41	93,47	19,86	36,20	140,39
2.76 - 1.95µm	8.5, 9.0 phi	8,75	2,32	2,18	95,65	19,06	41,74	182,74
1.95 - 1.38µm	9.0, 9.5 phi	9,25	1,64	1,73	97,38	15,98	41,11	200,53
1.38 - 0.98µm	9.5, 10.0 phi	9,75	1,16	1,14	98,52	11,13	33,01	177,51
0.98 - 0.69µm	10.0, 10.5 phi	10,25	0,82	0,69	99,20	7,02	23,67	139,12
0.69 - 0.49µm	10.5, 11.0 phi	10,75	0,58	0,44	99,64	4,73	17,90	114,17
0.49 - 0.35µm	11.0 , 11.5 phi	11,25	0,41	0,29	99,94	3,30	13,88	95,48
0.35 - 0.24µm	11.5, 12.0 phi	11,75	0,29	0,06	100,00	0,75	3,47	25,60
0.24 - 0.17µm	12.0, 12.5 phi	12,25	0,21	0,00	100,00	0,00	0,00	0,00
0.17 - 0.12µm	12.5, 13.0 phi	12,75	0,15	0,00	100,00	0,00	0,00	0,00
0.12 - 0.09µm	13.0, 13.5 phi	13,25	0,10	0,00	100,00	0,00	0,00	0,00
0.09 - 0.06µm	13.5, 14.0phi	13,75	0,07	0,00	100,00	0,00	0,00	0,00
0.06 - 0.04µm	14.0, 14.5 phi	14,25	0,05	0,00	100,00	0,00	0,00	0,00
0.04 - 0.03µm	14.5, 15.0 phi	14,75	0,04	0,00	100,00	0,00	0,00	0,00
0.03 - 0.02µm	15.0, 15.5 phi	15,25	0,03	0,00	100,00	0,00	0,00	0,00
METHOD: MALVERN laser sedimentograph (particles <2mm)				100,00		437,21	537,56	569,29
Sieving (particles> 0.5mm)								

Main Classes individual percentages:

Pebble	0,00
Gravel	0,63
Sand	49,30
Silt	41,14
Clay	8,94

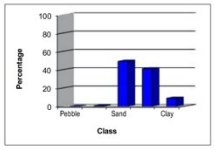

Statistical Parameters:

Mean	4,37
Standard Deviation	2,32
Asymmetry	0,46
P90	7,79
P50	4,00
P5	0,69
Mode	3,75

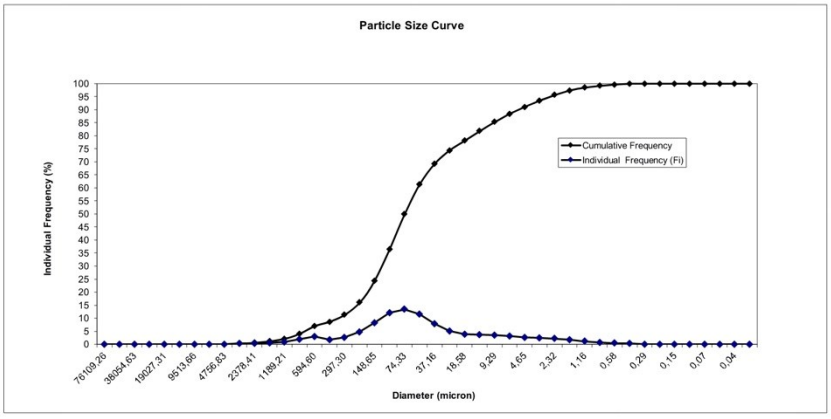

Technician: *Fernanda Dias*

Date:

INSTITUTO HIDROGRÁFICO
DIVISÃO DE GEOLOGIA MARINHA

Station: **2134**

Diameter (class)	Diameter phi	Class midpoint (ci)	Class midpoint (mm)	Individual Frequency (Fi)	Cumulative Frequency	Fi x ci	Fi x (ci-X)^2	Fi x (ci-X)^3
>64.00mm	<6.0 phi	-6,25	76109,26	0,00	0,00	0,00	0,00	0,00
45.25-64.00mm	-5.5,6.0 phi	-5,75	53817,37	0,00	0,00	0,00	0,00	0,00
32.00-45.25mm	-5.0,-5.5 phi	-5,25	38054,63	0,00	0,00	0,00	0,00	0,00
22.63-32.00mm	-4.5,-5.0 phi	-4,75	26908,69	0,00	0,00	0,00	0,00	0,00
16.00-22.63mm	-4.0,-4.5 phi	-4,25	19027,31	0,00	0,00	0,00	0,00	0,00
11.31-16.00mm	-3.5,-4.0 phi	-3,75	13454,34	0,00	0,00	0,00	0,00	0,00
8.00-11.31mm	-3.0,-3.5 phi	-3,25	9513,66	0,00	0,00	0,00	0,00	0,00
5.66-8.00mm	-2.5,-3.0 phi	-2,75	6727,17	0,00	0,00	0,00	0,00	0,00
4.00-5.66mm	-2.5,-2.0 phi	-2,25	4756,83	0,22	0,22	-0,49	9,19	-59,76
4.00 - 2.83mm	-2.0, -1.5 phi	-1,75	3363,59	0,14	0,35	-0,24	4,89	-29,36
2.83 - 2.00mm	-1.5, -1.0 phi	-1,25	2378,41	0,48	0,83	-0,60	14,60	-80,39
2.00 - 1.41mm	-1.0, -0.5 phi	-0,75	1681,79	0,71	1,54	-0,53	17,72	-88,70
1.41 - 1.00mm	-0.5, 0.0 phi	-0,25	1189,21	1,00	2,55	-0,25	20,38	-91,80
1.00 - 0.71mm	0.0, 0.5 phi	0,25	840,90	1,97	4,52	0,49	31,63	-126,68
0.71 - 0.50mm	0.5, 1.0 phi	0,75	594,60	2,80	7,32	2,10	34,41	-120,57
500.00 - 354.00µm	1.0, 1.5 phi	1,25	420,45	1,54	8,87	1,93	13,95	-41,90
354.00 - 250.00µm	1.5, 2.0 phi	1,75	297,30	2,59	11,46	4,53	16,24	-40,68
250.00 - 177.00µm	2.0, 2.5 phi	2,25	210,22	4,83	16,28	10,86	19,39	-38,87
177.00 - 125.00µm	2.5, 3.0 phi	2,75	148,65	8,80	25,08	24,20	19,92	-29,97
125.00 - 88.40µm	3.0, 3.5 phi	3,25	105,11	12,92	38,00	41,98	13,03	-13,09
88.40 - 62.50µm	3.5, 4.0 phi	3,75	74,33	14,31	52,31	53,66	3,64	-1,84
62.50 - 44.20µm	4.0, 4..5 phi	4,25	52,56	12,04	64,35	51,16	0,00	0,00
44.20 - 31.25µm	4.5, 5.0 phi	4,75	37,16	7,97	72,32	37,87	1,96	0,97
31.25 - 22.10µm	5.0, 5.5 phi	5,25	26,28	4,74	77,06	24,91	4,70	4,68
22.10 - 15.63µm	5.5, 6.0 phi	5,75	18,58	3,36	80,42	19,32	7,51	11,24
15.63 - 11.00µm	6.0, 6.5 phi	6,25	13,14	3,13	83,55	19,57	12,47	24,87
11.00 - 7.81µm	6.5, 7.0 phi	6,75	9,29	3,04	86,59	20,53	18,94	47,26
7.81 - 5.52µm	7.0, 7.5 phi	7,25	6,57	2,71	89,31	19,66	24,33	72,88
5.52 - 3.91µm	7.5, 8.0 phi	7,75	4,65	2,35	91,66	18,21	28,71	100,34
3.91 - 2.76µm	8.0, 8.5 phi	8,25	3,28	2,17	93,83	17,92	34,68	138,56
2.76 - 1.95µm	8.5, 9.0 phi	8,75	2,32	2,01	95,84	17,60	40,65	182,73
1.95 - 1.38µm	9.0, 9.5 phi	9,25	1,64	1,63	97,47	15,05	40,59	202,77
1.38 - 0.98µm	9.5, 10.0 phi	9,75	1,16	1,09	98,56	10,65	33,00	181,34
0.98 - 0.69µm	10.0, 10.5 phi	10,25	0,82	0,67	99,22	6,83	23,94	143,52
0.69 - 0.49µm	10.5, 11.0 phi	10,75	0,58	0,43	99,65	4,63	18,15	117,92
0.49 - 0.35µm	11.0 , 11.5 phi	11,25	0,41	0,28	99,94	3,20	13,91	97,32
0.35 - 0.24µm	11.5, 12.0 phi	11,75	0,29	0,06	100,00	0,72	3,43	25,70
0.24 - 0.17µm	12.0, 12.5 phi	12,25	0,21	0,00	100,00	0,00	0,00	0,00
0.17 - 0.12µm	12.5, 13.0 phi	12,75	0,15	0,00	100,00	0,00	0,00	0,00
0.12 - 0.09µm	13.0, 13.5 phi	13,25	0,10	0,00	100,00	0,00	0,00	0,00
0.09 - 0.06µm	13.5, 14.0phi	13,75	0,07	0,00	100,00	0,00	0,00	0,00
0.06 - 0.04µm	14.0, 14.5 phi	14,25	0,05	0,00	100,00	0,00	0,00	0,00
0.04 - 0.03µm	14.5, 15.0 phi	14,75	0,04	0,00	100,00	0,00	0,00	0,00
0.03 - 0.02µm	15.0, 15.5 phi	15,25	0,03	0,00	100,00	0,00	0,00	0,00
METHOD: MALVERN laser sedimentograph (particles <2mm)				100,00		425,45	525,96	588,47
Sieving (particles> 0.5mm)								

Main Classes individual percentages:

Pebble	0,00
Gravel	0,83
Sand	51,47
Silt	39,35
Clay	8,34

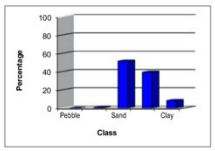

Statistical Parameters:

Mean	4,25
Standard Deviation	2,29
Asymmetry	0,49
P90	7,64
P50	3,92
P5	0,60
Mode	3,75

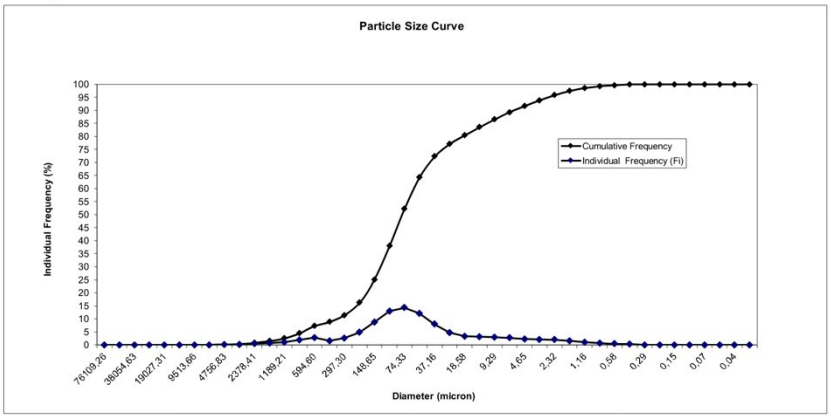

Technician: *Fernanda Dias*

Date:

INSTITUTO HIDROGRÁFICO
DIVISÃO DE GEOLOGIA MARINHA

Station: **2135**

Diameter (class)	Diameter phi	Class midpoint (ci)	Class midpoint (mm)	Individual Frequency (Fi)	Cumulative Frequency	Fi x ci	Fi x (ci-X)^2	Fi x (ci-X)^3
>64.00mm	<6.0 phi	-6,25	76109,26	0,00	0,00	0,00	0,00	0,00
45.25-64.00mm	-5.5,6.0 phi	-5,75	53817,37	0,00	0,00	0,00	0,00	0,00
32.00-45.25mm	-5.0,-5.5 phi	-5,25	38054,63	0,00	0,00	0,00	0,00	0,00
22.63-32.00mm	-4.5,-5.0 phi	-4,75	26908,69	0,00	0,00	0,00	0,00	0,00
16.00-22.63mm	-4.0,-4.5 phi	-4,25	19027,31	0,00	0,00	0,00	0,00	0,00
11.31-16.00mm	-3.5,-4.0 phi	-3,75	13454,34	0,00	0,00	0,00	0,00	0,00
8.00-11.31mm	-3.0,-3.5 phi	-3,25	9513,66	0,00	0,00	0,00	0,00	0,00
5.66-8.00mm	-2.5,-3.0 phi	-2,75	6727,17	0,00	0,00	0,00	0,00	0,00
4.00-5.66mm	-2.5,-2.0 phi	-2,25	4756,83	0,00	0,00	0,00	0,00	0,00
4.00 - 2.83mm	-2.0, -1.5 phi	-1,75	3363,59	0,29	0,29	-0,51	10,11	-59,71
2.83 - 2.00mm	-1.5, -1.0 phi	-1,25	2378,41	0,80	1,09	-1,00	23,29	-125,95
2.00 - 1.41mm	-1.0, -0.5 phi	-0,75	1681,79	0,89	1,97	-0,67	21,37	-104,88
1.41 - 1.00mm	-0.5, 0.0 phi	-0,25	1189,21	1,34	3,32	-0,34	26,11	-115,11
1.00 - 0.71mm	0.0, 0.5 phi	0,25	840,90	2,66	5,98	0,66	40,62	-158,76
0.71 - 0.50mm	0.5, 1.0 phi	0,75	594,60	3,59	9,57	2,69	41,70	-142,12
500.00 - 354.00µm	1.0, 1.5 phi	1,25	420,45	1,62	11,18	2,02	13,66	-39,73
354.00 - 250.00µm	1.5, 2.0 phi	1,75	297,30	2,80	13,98	4,89	16,21	-39,03
250.00 - 177.00µm	2.0, 2.5 phi	2,25	210,22	4,98	18,96	11,20	18,13	-34,59
177.00 - 125.00µm	2.5, 3.0 phi	2,75	148,65	8,66	27,62	23,83	17,18	-24,19
125.00 - 88.40µm	3.0, 3.5 phi	3,25	105,11	12,41	40,03	40,33	10,23	-9,29
88.40 - 62.50µm	3.5, 4.0 phi	3,75	74,33	13,61	53,64	51,04	2,27	-0,92
62.50 - 44.20µm	4.0, 4..5 phi	4,25	52,56	11,41	65,05	48,49	0,10	0,01
44.20 - 31.25µm	4.5, 5.0 phi	4,75	37,16	7,57	72,62	35,94	2,65	1,57
31.25 - 22.10µm	5.0, 5.5 phi	5,25	26,28	4,54	77,16	23,83	5,41	5,91
22.10 - 15.63µm	5.5, 6.0 phi	5,75	18,58	3,26	80,42	18,77	8,27	13,17
15.63 - 11.00µm	6.0, 6.5 phi	6,25	13,14	3,08	83,50	19,27	13,49	28,23
11.00 - 7.81µm	6.5, 7.0 phi	6,75	9,29	3,03	86,53	20,43	20,34	52,71
7.81 - 5.52µm	7.0, 7.5 phi	7,25	6,57	2,73	89,26	19,78	26,08	80,64
5.52 - 3.91µm	7.5, 8.0 phi	7,75	4,65	2,38	91,64	18,47	30,75	110,46
3.91 - 2.76µm	8.0, 8.5 phi	8,25	3,28	2,20	93,85	18,17	36,88	150,93
2.76 - 1.95µm	8.5, 9.0 phi	8,75	2,32	2,02	95,87	17,70	42,65	195,87
1.95 - 1.38µm	9.0, 9.5 phi	9,25	1,64	1,62	97,49	14,99	42,02	213,95
1.38 - 0.98µm	9.5, 10.0 phi	9,75	1,16	1,08	98,57	10,54	33,79	188,94
0.98 - 0.69µm	10.0, 10.5 phi	10,25	0,82	0,66	99,23	6,73	24,37	148,44
0.69 - 0.49µm	10.5, 11.0 phi	10,75	0,58	0,43	99,65	4,58	18,53	122,15
0.49 - 0.35µm	11.0 , 11.5 phi	11,25	0,41	0,29	99,94	3,21	14,36	101,87
0.35 - 0.24µm	11.5, 12.0 phi	11,75	0,29	0,06	100,00	0,73	3,58	27,21
0.24 - 0.17µm	12.0, 12.5 phi	12,25	0,21	0,00	100,00	0,00	0,00	0,00
0.17 - 0.12µm	12.5, 13.0 phi	12,75	0,15	0,00	100,00	0,00	0,00	0,00
0.12 - 0.09µm	13.0, 13.5 phi	13,25	0,10	0,00	100,00	0,00	0,00	0,00
0.09 - 0.06µm	13.5, 14.0phi	13,75	0,07	0,00	100,00	0,00	0,00	0,00
0.06 - 0.04µm	14.0, 14.5 phi	14,25	0,05	0,00	100,00	0,00	0,00	0,00
0.04 - 0.03µm	14.5, 15.0 phi	14,75	0,04	0,00	100,00	0,00	0,00	0,00
0.03 - 0.02µm	15.0, 15.5 phi	15,25	0,03	0,00	100,00	0,00	0,00	0,00
				100,00		415,81	564,17	587,76

METHOD: MALVERN laser sedimentograph (particles <2mm)
Sieving (particles> 0.5mm)

Main Classes individual percentages:

Pebble	0,00
Gravel	1,09
Sand	52,56
Silt	38,00
Clay	8,36

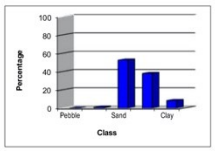

Statistical Parameters:

Mean	4,16
Standard Deviation	2,38
Asymmetry	0,44
P90	7,65
P50	3,87
P5	0,34
Mode	3,75

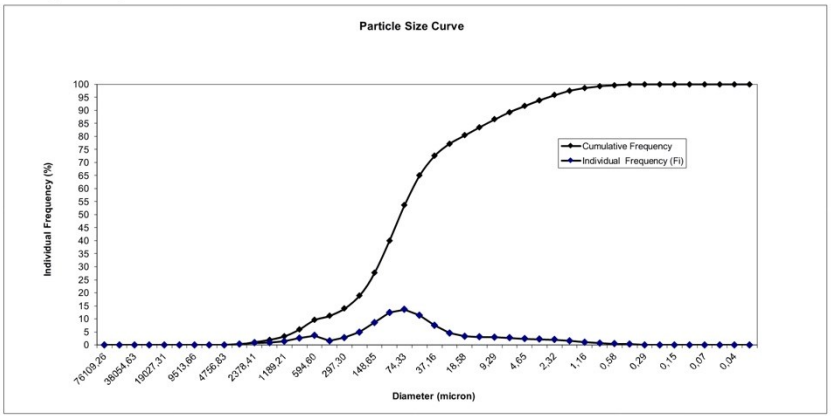

Technician: *Fernanda Dias*

Date:

INSTITUTO HIDROGRÁFICO
DIVISÃO DE GEOLOGIA MARINHA

Station: **2136**

Diameter (class)	Diameter phi	Class midpoint (ci)	Class midpoint (mm)	Individual Frequency (Fi)	Cumulative Frequency	Fi x ci	Fi x (ci-X)^2	Fi x (ci-X)^3
>64.00mm	<6.0 phi	-6,25	76109,26	0,00	0,00	0,00	0,00	0,00
45.25-64.00mm	-5.5,6.0 phi	-5,75	53817,37	0,00	0,00	0,00	0,00	0,00
32.00-45.25mm	-5.0,-5.5 phi	-5,25	38054,63	0,00	0,00	0,00	0,00	0,00
22.63-32.00mm	-4.5,-5.0 phi	-4,75	26908,69	0,00	0,00	0,00	0,00	0,00
16.00-22.63mm	-4.0,-4.5 phi	-4,25	19027,31	0,00	0,00	0,00	0,00	0,00
11.31-16.00mm	-3.5,-4.0 phi	-3,75	13454,34	0,00	0,00	0,00	0,00	0,00
8.00-11.31mm	-3.0,-3.5 phi	-3,25	9513,66	0,00	0,00	0,00	0,00	0,00
5.66-8.00mm	-2.5,-3.0 phi	-2,75	6727,17	0,00	0,00	0,00	0,00	0,00
4.00-5.66mm	-2.5,-2.0 phi	-2,25	4756,83	0,00	0,00	0,00	0,00	0,00
4.00 - 2.83mm	-2.0, -1.5 phi	-1,75	3363,59	0,35	0,35	-0,61	14,05	-89,03
2.83 - 2.00mm	-1.5, -1.0 phi	-1,25	2378,41	0,60	0,95	-0,75	20,38	-118,93
2.00 - 1.41mm	-1.0, -0.5 phi	-0,75	1681,79	1,13	2,08	-0,85	32,27	-172,17
1.41 - 1.00mm	-0.5, 0.0 phi	-0,25	1189,21	1,63	3,71	-0,41	38,16	-184,48
1.00 - 0.71mm	0.0, 0.5 phi	0,25	840,90	2,59	6,31	0,65	48,72	-211,22
0.71 - 0.50mm	0.5, 1.0 phi	0,75	594,60	3,10	9,40	2,32	45,52	-174,57
500.00 - 354.00µm	1.0, 1.5 phi	1,25	420,45	1,16	10,56	1,45	12,87	-42,91
354.00 - 250.00µm	1.5, 2.0 phi	1,75	297,30	1,99	12,54	3,47	15,95	-45,23
250.00 - 177.00µm	2.0, 2.5 phi	2,25	210,22	3,68	16,22	8,28	20,06	-46,84
177.00 - 125.00µm	2.5, 3.0 phi	2,75	148,65	6,64	22,86	18,26	22,35	-41,02
125.00 - 88.40µm	3.0, 3.5 phi	3,25	105,11	9,75	32,62	31,70	17,38	-23,20
88.40 - 62.50µm	3.5, 4.0 phi	3,75	74,33	11,06	43,68	41,49	7,71	-6,44
62.50 - 44.20µm	4.0, 4..5 phi	4,25	52,56	9,93	53,61	42,21	1,11	-0,37
44.20 - 31.25µm	4.5, 5.0 phi	4,75	37,16	7,60	61,21	36,12	0,21	0,03
31.25 - 22.10µm	5.0, 5.5 phi	5,25	26,28	5,83	67,04	30,59	2,58	1,71
22.10 - 15.63µm	5.5, 6.0 phi	5,75	18,58	5,20	72,24	29,90	7,06	8,22
15.63 - 11.00µm	6.0, 6.5 phi	6,25	13,14	5,12	77,36	32,02	14,20	23,65
11.00 - 7.81µm	6.5, 7.0 phi	6,75	9,29	4,82	82,19	32,56	22,61	48,95
7.81 - 5.52µm	7.0, 7.5 phi	7,25	6,57	4,13	86,31	29,92	29,31	78,12
5.52 - 3.91µm	7.5, 8.0 phi	7,75	4,65	3,40	89,72	26,37	34,09	107,89
3.91 - 2.76µm	8.0, 8.5 phi	8,25	3,28	2,95	92,66	24,31	39,58	145,06
2.76 - 1.95µm	8.5, 9.0 phi	8,75	2,32	2,55	95,22	22,34	44,30	184,50
1.95 - 1.38µm	9.0, 9.5 phi	9,25	1,64	1,95	97,17	18,03	42,41	197,86
1.38 - 0.98µm	9.5, 10.0 phi	9,75	1,16	1,24	98,40	12,06	33,01	170,51
0.98 - 0.69µm	10.0, 10.5 phi	10,25	0,82	0,71	99,12	7,33	22,94	129,96
0.69 - 0.49µm	10.5, 11.0 phi	10,75	0,58	0,45	99,57	4,87	17,22	106,17
0.49 - 0.35µm	11.0 , 11.5 phi	11,25	0,41	0,31	99,88	3,43	13,55	90,32
0.35 - 0.24µm	11.5, 12.0 phi	11,75	0,29	0,12	100,00	1,45	6,32	45,27
0.24 - 0.17µm	12.0, 12.5 phi	12,25	0,21	0,00	100,00	0,00	0,00	0,00
0.17 - 0.12µm	12.5, 13.0 phi	12,75	0,15	0,00	100,00	0,00	0,00	0,00
0.12 - 0.09µm	13.0, 13.5 phi	13,25	0,10	0,00	100,00	0,00	0,00	0,00
0.09 - 0.06µm	13.5, 14.0phi	13,75	0,07	0,00	100,00	0,00	0,00	0,00
0.06 - 0.04µm	14.0, 14.5 phi	14,25	0,05	0,00	100,00	0,00	0,00	0,00
0.04 - 0.03µm	14.5, 15.0 phi	14,75	0,04	0,00	100,00	0,00	0,00	0,00
0.03 - 0.02µm	15.0, 15.5 phi	15,25	0,03	0,00	100,00	0,00	0,00	0,00
METHOD: MALVERN laser sedimentograph (particles <2mm)				100,00		458,50	625,93	181,79
Sieving (particles> 0.5mm)								

Main Classes individual percentages:

Pebble	0,00
Gravel	0,95
Sand	42,73
Silt	46,04
Clay	10,28

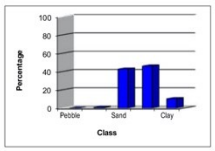

Statistical Parameters:

Mean	4,58
Standard Deviation	2,50
Asymmetry	0,12
P90	8,04
P50	4,32
P5	0,27
Mode	3,75

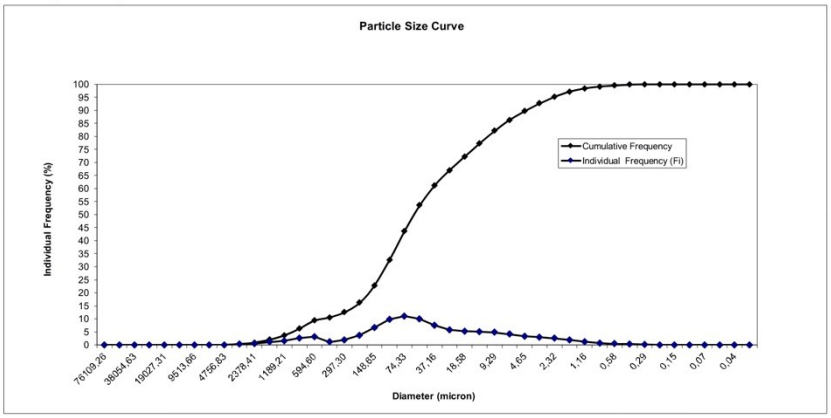

Technician: *Fernanda Dias*

Date:

INSTITUTO HIDROGRÁFICO
DIVISÃO DE GEOLOGIA MARINHA

Station: **2137**

Diameter (class)	Diameter phi	Class midpoint (ci)	Class midpoint (mm)	Individual Frequency (Fi)	Cumulative Frequency	Fi x ci	Fi x (ci-X)^2	Fi x (ci-X)^3
>64.00mm	<6.0 phi	-6,25	76109,26	0,00	0,00	0,00	0,00	0,00
45.25-64.00mm	-5.5,6.0 phi	-5,75	53817,37	0,00	0,00	0,00	0,00	0,00
32.00-45.25mm	-5.0,-5.5 phi	-5,25	38054,63	0,00	0,00	0,00	0,00	0,00
22.63-32.00mm	-4.5,-5.0 phi	-4,75	26908,69	0,00	0,00	0,00	0,00	0,00
16.00-22.63mm	-4.0,-4.5 phi	-4,25	19027,31	0,00	0,00	0,00	0,00	0,00
11.31-16.00mm	-3.5,-4.0 phi	-3,75	13454,34	0,00	0,00	0,00	0,00	0,00
8.00-11.31mm	-3.0,-3.5 phi	-3,25	9513,66	0,00	0,00	0,00	0,00	0,00
5.66-8.00mm	-2.5,-3.0 phi	-2,75	6727,17	0,26	0,26	-0,72	11,16	-72,85
4.00-5.66mm	-2.5,-2.0 phi	-2,25	4756,83	0,10	0,36	-0,23	3,67	-22,11
4.00 - 2.83mm	-2.0, -1.5 phi	-1,75	3363,59	0,74	1,10	-1,29	22,61	-125,02
2.83 - 2.00mm	-1.5, -1.0 phi	-1,25	2378,41	1,18	2,29	-1,48	29,91	-150,43
2.00 - 1.41mm	-1.0, -0.5 phi	-0,75	1681,79	1,77	4,06	-1,33	36,35	-164,61
1.41 - 1.00mm	-0.5, 0.0 phi	-0,25	1189,21	2,65	6,71	-0,66	43,06	-173,50
1.00 - 0.71mm	0.0, 0.5 phi	0,25	840,90	4,58	11,29	1,15	57,08	-201,42
0.71 - 0.50mm	0.5, 1.0 phi	0,75	594,60	5,72	17,02	4,29	52,52	-159,07
500.00 - 354.00µm	1.0, 1.5 phi	1,25	420,45	2,00	19,02	2,50	12,79	-32,35
354.00 - 250.00µm	1.5, 2.0 phi	1,75	297,30	2,89	21,91	5,06	11,91	-24,16
250.00 - 177.00µm	2.0, 2.5 phi	2,25	210,22	4,71	26,62	10,59	11,00	-16,82
177.00 - 125.00µm	2.5, 3.0 phi	2,75	148,65	7,98	34,60	21,96	8,45	-8,70
125.00 - 88.40µm	3.0, 3.5 phi	3,25	105,11	11,34	45,94	36,84	3,17	-1,68
88.40 - 62.50µm	3.5, 4.0 phi	3,75	74,33	12,35	58,29	46,32	0,01	0,00
62.50 - 44.20µm	4.0, 4..5 phi	4,25	52,56	10,30	68,59	43,79	2,29	1,08
44.20 - 31.25µm	4.5, 5.0 phi	4,75	37,16	6,79	75,39	32,27	6,41	6,22
31.25 - 22.10µm	5.0, 5.5 phi	5,25	26,28	4,02	79,40	21,10	8,70	12,79
22.10 - 15.63µm	5.5, 6.0 phi	5,75	18,58	2,82	82,23	16,24	10,97	21,63
15.63 - 11.00µm	6.0, 6.5 phi	6,25	13,14	2,65	84,88	16,55	16,17	39,95
11.00 - 7.81µm	6.5, 7.0 phi	6,75	9,29	2,63	87,50	17,74	23,20	68,91
7.81 - 5.52µm	7.0, 7.5 phi	7,25	6,57	2,41	89,91	17,45	29,00	100,67
5.52 - 3.91µm	7.5, 8.0 phi	7,75	4,65	2,14	92,05	16,59	33,76	134,07
3.91 - 2.76µm	8.0, 8.5 phi	8,25	3,28	2,02	94,07	16,64	40,31	180,24
2.76 - 1.95µm	8.5, 9.0 phi	8,75	2,32	1,89	95,96	16,52	46,65	231,92
1.95 - 1.38µm	9.0, 9.5 phi	9,25	1,64	1,54	97,50	14,26	46,15	252,51
1.38 - 0.98µm	9.5, 10.0 phi	9,75	1,16	1,05	98,55	10,24	37,43	223,52
0.98 - 0.69µm	10.0, 10.5 phi	10,25	0,82	0,65	99,20	6,68	27,27	176,47
0.69 - 0.49µm	10.5, 11.0 phi	10,75	0,58	0,43	99,63	4,57	20,68	144,16
0.49 - 0.35µm	11.0 , 11.5 phi	11,25	0,41	0,28	99,91	3,15	15,63	116,80
0.35 - 0.24µm	11.5, 12.0 phi	11,75	0,29	0,09	100,00	1,11	6,02	47,97
0.24 - 0.17µm	12.0, 12.5 phi	12,25	0,21	0,00	100,00	0,00	0,00	0,00
0.17 - 0.12µm	12.5, 13.0 phi	12,75	0,15	0,00	100,00	0,00	0,00	0,00
0.12 - 0.09µm	13.0, 13.5 phi	13,25	0,10	0,00	100,00	0,00	0,00	0,00
0.09 - 0.06µm	13.5, 14.0phi	13,75	0,07	0,00	100,00	0,00	0,00	0,00
0.06 - 0.04µm	14.0, 14.5 phi	14,25	0,05	0,00	100,00	0,00	0,00	0,00
0.04 - 0.03µm	14.5, 15.0 phi	14,75	0,04	0,00	100,00	0,00	0,00	0,00
0.03 - 0.02µm	15.0, 15.5 phi	15,25	0,03	0,00	100,00	0,00	0,00	0,00
METHOD: MALVERN laser sedimentograph (particles <2mm)				100,00		377,89	674,34	606,19
Sieving (particles> 0.5mm)								

Main Classes individual percentages:

Pebble	0,00
Gravel	2,29
Sand	56,00
Silt	33,76
Clay	7,95

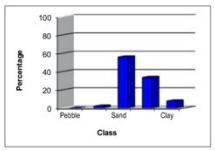

Statistical Parameters:

Mean	3,78
Standard Deviation	2,60
Asymmetry	0,35
P90	7,52
P50	3,66
P5	-0,30
Mode	3,75

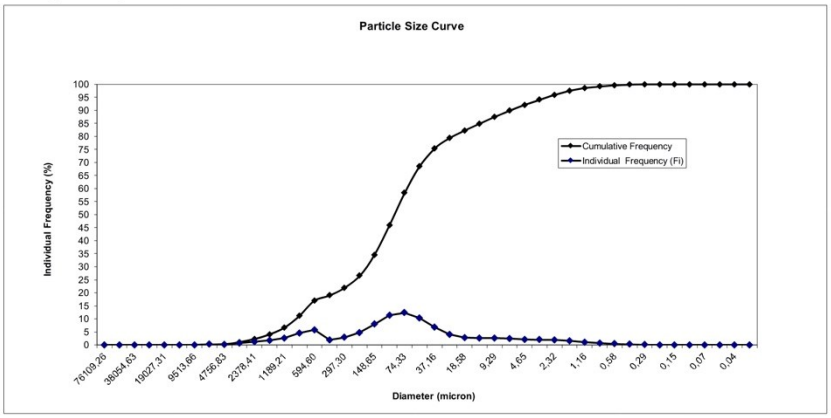

Technician: *Fernanda Dias*

Date:

INSTITUTO HIDROGRÁFICO
DIVISÃO DE GEOLOGIA MARINHA

Station: **2138**

Diameter (class)	Diameter phi	Class midpoint (ci)	Class midpoint (mm)	Individual Frequency (Fi)	Cumulative Frequency	Fi x ci	Fi x (ci-X)^2	Fi x (ci-X)^3
>64.00mm	<6.0 phi	-6,25	76109,26	0,00	0,00	0,00	0,00	0,00
45.25-64.00mm	-5.5,6.0 phi	-5,75	53817,37	0,00	0,00	0,00	0,00	0,00
32.00-45.25mm	-5.0,-5.5 phi	-5,25	38054,63	0,00	0,00	0,00	0,00	0,00
22.63-32.00mm	-4.5,-5.0 phi	-4,75	26908,69	0,00	0,00	0,00	0,00	0,00
16.00-22.63mm	-4.0,-4.5 phi	-4,25	19027,31	0,00	0,00	0,00	0,00	0,00
11.31-16.00mm	-3.5,-4.0 phi	-3,75	13454,34	0,00	0,00	0,00	0,00	0,00
8.00-11.31mm	-3.0,-3.5 phi	-3,25	9513,66	0,00	0,00	0,00	0,00	0,00
5.66-8.00mm	-2.5,-3.0 phi	-2,75	6727,17	0,00	0,00	0,00	0,00	0,00
4.00-5.66mm	-2.5,-2.0 phi	-2,25	4756,83	0,00	0,00	0,00	0,00	0,00
4.00 - 2.83mm	-2.0, -1.5 phi	-1,75	3363,59	1,53	1,53	-2,67	40,28	-206,86
2.83 - 2.00mm	-1.5, -1.0 phi	-1,25	2378,41	2,67	4,19	-3,33	57,32	-265,73
2.00 - 1.41mm	-1.0, -0.5 phi	-0,75	1681,79	2,31	6,50	-1,73	39,51	-163,44
1.41 - 1.00mm	-0.5, 0.0 phi	-0,25	1189,21	4,07	10,57	-1,02	53,76	-195,48
1.00 - 0.71mm	0.0, 0.5 phi	0,25	840,90	6,04	16,61	1,51	59,38	-186,23
0.71 - 0.50mm	0.5, 1.0 phi	0,75	594,60	6,69	23,30	5,02	46,49	-122,55
500.00 - 354.00µm	1.0, 1.5 phi	1,25	420,45	1,90	25,20	2,38	8,68	-18,54
354.00 - 250.00µm	1.5, 2.0 phi	1,75	297,30	2,77	27,96	4,84	7,40	-12,11
250.00 - 177.00µm	2.0, 2.5 phi	2,25	210,22	4,61	32,57	10,37	5,95	-6,76
177.00 - 125.00µm	2.5, 3.0 phi	2,75	148,65	7,80	40,37	21,46	3,16	-2,01
125.00 - 88.40µm	3.0, 3.5 phi	3,25	105,11	10,92	51,29	35,48	0,20	-0,03
88.40 - 62.50µm	3.5, 4.0 phi	3,75	74,33	11,73	63,02	43,98	1,55	0,56
62.50 - 44.20µm	4.0, 4..5 phi	4,25	52,56	9,67	72,69	41,10	7,22	6,23
44.20 - 31.25µm	4.5, 5.0 phi	4,75	37,16	6,31	78,99	29,95	11,73	15,99
31.25 - 22.10µm	5.0, 5.5 phi	5,25	26,28	3,66	82,65	19,19	12,70	23,67
22.10 - 15.63µm	5.5, 6.0 phi	5,75	18,58	2,49	85,14	14,30	13,90	32,86
15.63 - 11.00µm	6.0, 6.5 phi	6,25	13,14	2,28	87,42	14,26	18,71	53,59
11.00 - 7.81µm	6.5, 7.0 phi	6,75	9,29	2,25	89,67	15,18	25,44	85,59
7.81 - 5.52µm	7.0, 7.5 phi	7,25	6,57	2,05	91,72	14,88	30,64	118,40
5.52 - 3.91µm	7.5, 8.0 phi	7,75	4,65	1,81	93,53	14,01	34,42	150,19
3.91 - 2.76µm	8.0, 8.5 phi	8,25	3,28	1,67	95,20	13,82	39,62	192,71
2.76 - 1.95µm	8.5, 9.0 phi	8,75	2,32	1,55	96,75	13,53	44,50	238,67
1.95 - 1.38µm	9.0, 9.5 phi	9,25	1,64	1,25	98,00	11,59	43,07	252,53
1.38 - 0.98µm	9.5, 10.0 phi	9,75	1,16	0,85	98,85	8,27	34,33	218,49
0.98 - 0.69µm	10.0, 10.5 phi	10,25	0,82	0,52	99,37	5,37	24,70	169,56
0.69 - 0.49µm	10.5, 11.0 phi	10,75	0,58	0,34	99,72	3,70	18,69	137,62
0.49 - 0.35µm	11.0 , 11.5 phi	11,25	0,41	0,23	99,95	2,60	14,28	112,33
0.35 - 0.24µm	11.5, 12.0 phi	11,75	0,29	0,05	100,00	0,59	3,52	29,40
0.24 - 0.17µm	12.0, 12.5 phi	12,25	0,21	0,00	100,00	0,00	0,00	0,00
0.17 - 0.12µm	12.5, 13.0 phi	12,75	0,15	0,00	100,00	0,00	0,00	0,00
0.12 - 0.09µm	13.0, 13.5 phi	13,25	0,10	0,00	100,00	0,00	0,00	0,00
0.09 - 0.06µm	13.5, 14.0phi	13,75	0,07	0,00	100,00	0,00	0,00	0,00
0.06 - 0.04µm	14.0, 14.5 phi	14,25	0,05	0,00	100,00	0,00	0,00	0,00
0.04 - 0.03µm	14.5, 15.0 phi	14,75	0,04	0,00	100,00	0,00	0,00	0,00
0.03 - 0.02µm	15.0, 15.5 phi	15,25	0,03	0,00	100,00	0,00	0,00	0,00
				100,00		338,62	701,15	658,66

METHOD: MALVERN laser sedimentograph (particles <2mm)
Sieving (particles> 0.5mm)

Main Classes individual percentages:

Pebble	0,00
Gravel	4,19
Sand	58,82
Silt	30,51
Clay	6,47

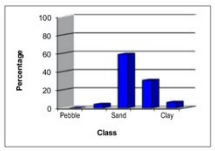

Statistical Parameters:

Mean	3,39
Standard Deviation	2,65
Asymmetry	0,35
P90	7,08
P50	3,44
P5	-0,80
Mode	3,75

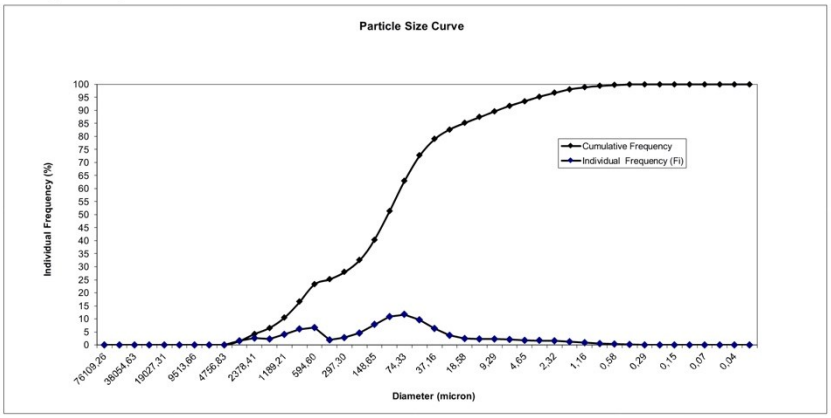

Technician: *Fernanda Dias*

Date:

INSTITUTO HIDROGRÁFICO
DIVISÃO DE GEOLOGIA MARINHA

Station: **2139**

Diameter (class)	Diameter phi	Class midpoint (ci)	Class midpoint (mm)	Individual Frequency (Fi)	Cumulative Frequency	Fi x ci	Fi x (ci-X)^2	Fi x (ci-X)^3
>64.00mm	<6.0 phi	-6,25	76109,26	0,00	0,00	0,00	0,00	0,00
45.25-64.00mm	-5.5,6.0 phi	-5,75	53817,37	0,00	0,00	0,00	0,00	0,00
32.00-45.25mm	-5.0,-5.5 phi	-5,25	38054,63	0,00	0,00	0,00	0,00	0,00
22.63-32.00mm	-4.5,-5.0 phi	-4,75	26908,69	0,00	0,00	0,00	0,00	0,00
16.00-22.63mm	-4.0,-4.5 phi	-4,25	19027,31	0,00	0,00	0,00	0,00	0,00
11.31-16.00mm	-3.5,-4.0 phi	-3,75	13454,34	0,00	0,00	0,00	0,00	0,00
8.00-11.31mm	-3.0,-3.5 phi	-3,25	9513,66	0,00	0,00	0,00	0,00	0,00
5.66-8.00mm	-2.5,-3.0 phi	-2,75	6727,17	0,45	0,45	-1,22	12,82	-68,80
4.00-5.66mm	-2.5,-2.0 phi	-2,25	4756,83	1,75	2,19	-3,93	41,36	-201,30
4.00 - 2.83mm	-2.0, -1.5 phi	-1,75	3363,59	2,70	4,89	-4,73	51,50	-224,90
2.83 - 2.00mm	-1.5, -1.0 phi	-1,25	2378,41	3,80	8,70	-4,75	56,88	-219,96
2.00 - 1.41mm	-1.0, -0.5 phi	-0,75	1681,79	4,52	13,21	-3,39	51,23	-172,49
1.41 - 1.00mm	-0.5, 0.0 phi	-0,25	1189,21	6,19	19,41	-1,55	50,90	-145,94
1.00 - 0.71mm	0.0, 0.5 phi	0,25	840,90	10,07	29,47	2,52	56,39	-133,49
0.71 - 0.50mm	0.5, 1.0 phi	0,75	594,60	10,16	39,63	7,62	35,40	-66,09
500.00 - 354.00µm	1.0, 1.5 phi	1,25	420,45	1,94	41,57	2,43	3,63	-4,96
354.00 - 250.00µm	1.5, 2.0 phi	1,75	297,30	2,55	44,11	4,46	1,91	-1,66
250.00 - 177.00µm	2.0, 2.5 phi	2,25	210,22	3,75	47,86	8,43	0,50	-0,19
177.00 - 125.00µm	2.5, 3.0 phi	2,75	148,65	5,92	53,78	16,29	0,10	0,01
125.00 - 88.40µm	3.0, 3.5 phi	3,25	105,11	8,09	61,88	26,30	3,24	2,05
88.40 - 62.50µm	3.5, 4.0 phi	3,75	74,33	8,67	70,54	32,50	11,13	12,61
62.50 - 44.20µm	4.0, 4..5 phi	4,25	52,56	7,22	77,76	30,68	19,25	31,43
44.20 - 31.25µm	4.5, 5.0 phi	4,75	37,16	4,80	82,56	22,80	21,83	46,57
31.25 - 22.10µm	5.0, 5.5 phi	5,25	26,28	2,85	85,41	14,95	19,74	51,98
22.10 - 15.63µm	5.5, 6.0 phi	5,75	18,58	1,96	87,37	11,29	19,27	60,38
15.63 - 11.00µm	6.0, 6.5 phi	6,25	13,14	1,81	89,19	11,34	23,94	86,98
11.00 - 7.81µm	6.5, 7.0 phi	6,75	9,29	1,82	91,01	12,27	31,05	128,34
7.81 - 5.52µm	7.0, 7.5 phi	7,25	6,57	1,70	92,70	12,32	36,47	168,97
5.52 - 3.91µm	7.5, 8.0 phi	7,75	4,65	1,53	94,24	11,87	40,35	207,13
3.91 - 2.76µm	8.0, 8.5 phi	8,25	3,28	1,44	95,68	11,89	45,74	257,65
2.76 - 1.95µm	8.5, 9.0 phi	8,75	2,32	1,34	97,02	11,75	50,50	309,72
1.95 - 1.38µm	9.0, 9.5 phi	9,25	1,64	1,10	98,12	10,16	48,35	320,68
1.38 - 0.98µm	9.5, 10.0 phi	9,75	1,16	0,76	98,88	7,41	38,64	275,64
0.98 - 0.69µm	10.0, 10.5 phi	10,25	0,82	0,49	99,36	4,98	28,29	215,92
0.69 - 0.49µm	10.5, 11.0 phi	10,75	0,58	0,33	99,69	3,52	21,68	176,33
0.49 - 0.35µm	11.0 , 11.5 phi	11,25	0,41	0,22	99,91	2,47	16,34	141,10
0.35 - 0.24µm	11.5, 12.0 phi	11,75	0,29	0,09	100,00	1,05	7,43	67,87
0.24 - 0.17µm	12.0, 12.5 phi	12,25	0,21	0,00	100,00	0,00	0,00	0,00
0.17 - 0.12µm	12.5, 13.0 phi	12,75	0,15	0,00	100,00	0,00	0,00	0,00
0.12 - 0.09µm	13.0, 13.5 phi	13,25	0,10	0,00	100,00	0,00	0,00	0,00
0.09 - 0.06µm	13.5, 14.0phi	13,75	0,07	0,00	100,00	0,00	0,00	0,00
0.06 - 0.04µm	14.0, 14.5 phi	14,25	0,05	0,00	100,00	0,00	0,00	0,00
0.04 - 0.03µm	14.5, 15.0 phi	14,75	0,04	0,00	100,00	0,00	0,00	0,00
0.03 - 0.02µm	15.0, 15.5 phi	15,25	0,03	0,00	100,00	0,00	0,00	0,00
METHOD: MALVERN laser sedimentograph (particles <2mm)				100,00		261,70	845,89	1321,58
Sieving (particles> 0.5mm)								

Main Classes individual percentages:

Pebble	0,00
Gravel	8,70
Sand	61,85
Silt	23,69
Clay	5,76

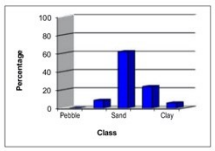

Statistical Parameters:

Mean	2,62
Standard Deviation	2,91
Asymmetry	0,54
P90	6,72
P50	2,68
P5	-1,48
Mode	0,75

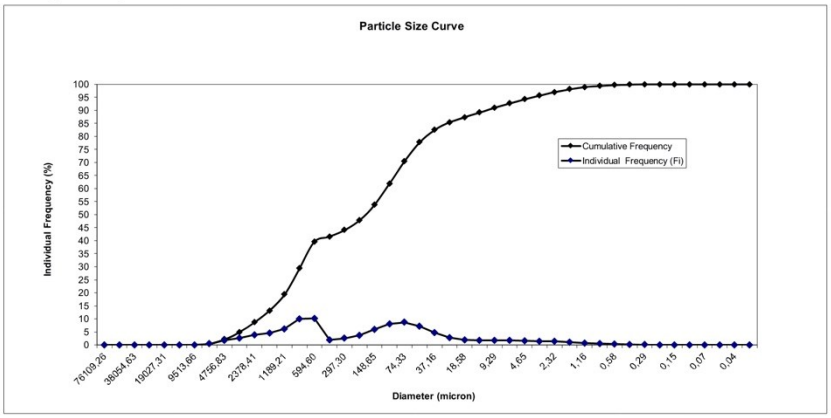

Technician: *Fernanda Dias*

Date:

INSTITUTO HIDROGRÁFICO
DIVISÃO DE GEOLOGIA MARINHA

Station: **2140**

Diameter (class)	Diameter phi	Class midpoint (ci)	Class midpoint (mm)	Individual Frequency (Fi)	Cumulative Frequency	Fi x ci	Fi x (ci-X)^2	Fi x (ci-X)^3
>64.00mm	<6.0 phi	-6,25	76109,26	0,00	0,00	0,00	0,00	0,00
45.25-64.00mm	-5.5,6.0 phi	-5,75	53817,37	0,00	0,00	0,00	0,00	0,00
32.00-45.25mm	-5.0,-5.5 phi	-5,25	38054,63	0,00	0,00	0,00	0,00	0,00
22.63-32.00mm	-4.5,-5.0 phi	-4,75	26908,69	0,00	0,00	0,00	0,00	0,00
16.00-22.63mm	-4.0,-4.5 phi	-4,25	19027,31	0,00	0,00	0,00	0,00	0,00
11.31-16.00mm	-3.5,-4.0 phi	-3,75	13454,34	0,00	0,00	0,00	0,00	0,00
8.00-11.31mm	-3.0,-3.5 phi	-3,25	9513,66	0,00	0,00	0,00	0,00	0,00
5.66-8.00mm	-2.5,-3.0 phi	-2,75	6727,17	1,94	1,94	-5,33	47,40	-234,35
4.00-5.66mm	-2.5,-2.0 phi	-2,25	4756,83	1,42	3,36	-3,20	28,12	-124,97
4.00 - 2.83mm	-2.0, -1.5 phi	-1,75	3363,59	3,31	6,67	-5,79	51,50	-203,12
2.83 - 2.00mm	-1.5, -1.0 phi	-1,25	2378,41	5,75	12,43	-7,19	68,25	-235,06
2.00 - 1.41mm	-1.0, -0.5 phi	-0,75	1681,79	5,65	18,08	-4,24	48,98	-144,19
1.41 - 1.00mm	-0.5, 0.0 phi	-0,25	1189,21	7,44	25,52	-1,86	44,47	-108,68
1.00 - 0.71mm	0.0, 0.5 phi	0,25	840,90	11,58	37,10	2,89	43,75	-85,05
0.71 - 0.50mm	0.5, 1.0 phi	0,75	594,60	12,30	49,40	9,22	25,64	-37,02
500.00 - 354.00µm	1.0, 1.5 phi	1,25	420,45	2,08	51,47	2,59	1,85	-1,75
354.00 - 250.00µm	1.5, 2.0 phi	1,75	297,30	2,58	54,06	4,52	0,51	-0,23
250.00 - 177.00µm	2.0, 2.5 phi	2,25	210,22	3,40	57,46	7,65	0,01	0,00
177.00 - 125.00µm	2.5, 3.0 phi	2,75	148,65	4,75	62,20	13,05	1,47	0,82
125.00 - 88.40µm	3.0, 3.5 phi	3,25	105,11	5,93	68,13	19,27	6,61	6,98
88.40 - 62.50µm	3.5, 4.0 phi	3,75	74,33	6,07	74,20	22,75	14,69	22,86
62.50 - 44.20µm	4.0, 4..5 phi	4,25	52,56	5,07	79,27	21,54	21,43	44,06
44.20 - 31.25µm	4.5, 5.0 phi	4,75	37,16	3,60	82,86	17,08	23,49	60,04
31.25 - 22.10µm	5.0, 5.5 phi	5,25	26,28	2,43	85,30	12,78	22,73	69,45
22.10 - 15.63µm	5.5, 6.0 phi	5,75	18,58	1,90	87,20	10,95	24,09	85,66
15.63 - 11.00µm	6.0, 6.5 phi	6,25	13,14	1,81	89,02	11,34	29,85	121,07
11.00 - 7.81µm	6.5, 7.0 phi	6,75	9,29	1,80	90,81	12,14	37,32	170,04
7.81 - 5.52µm	7.0, 7.5 phi	7,25	6,57	1,68	92,49	12,18	42,96	217,20
5.52 - 3.91µm	7.5, 8.0 phi	7,75	4,65	1,54	94,03	11,93	47,51	263,95
3.91 - 2.76µm	8.0, 8.5 phi	8,25	3,28	1,48	95,51	12,17	54,11	327,72
2.76 - 1.95µm	8.5, 9.0 phi	8,75	2,32	1,39	96,90	12,14	59,66	391,11
1.95 - 1.38µm	9.0, 9.5 phi	9,25	1,64	1,14	98,04	10,55	56,79	400,69
1.38 - 0.98µm	9.5, 10.0 phi	9,75	1,16	0,79	98,83	7,72	45,19	341,42
0.98 - 0.69µm	10.0, 10.5 phi	10,25	0,82	0,51	99,34	5,21	33,00	265,89
0.69 - 0.49µm	10.5, 11.0 phi	10,75	0,58	0,34	99,68	3,69	25,16	215,28
0.49 - 0.35µm	11.0 , 11.5 phi	11,25	0,41	0,23	99,91	2,58	18,78	170,08
0.35 - 0.24µm	11.5, 12.0 phi	11,75	0,29	0,09	100,00	1,06	8,24	78,77
0.24 - 0.17µm	12.0, 12.5 phi	12,25	0,21	0,00	100,00	0,00	0,00	0,00
0.17 - 0.12µm	12.5, 13.0 phi	12,75	0,15	0,00	100,00	0,00	0,00	0,00
0.12 - 0.09µm	13.0, 13.5 phi	13,25	0,10	0,00	100,00	0,00	0,00	0,00
0.09 - 0.06µm	13.5, 14.0phi	13,75	0,07	0,00	100,00	0,00	0,00	0,00
0.06 - 0.04µm	14.0, 14.5 phi	14,25	0,05	0,00	100,00	0,00	0,00	0,00
0.04 - 0.03µm	14.5, 15.0 phi	14,75	0,04	0,00	100,00	0,00	0,00	0,00
0.03 - 0.02µm	15.0, 15.5 phi	15,25	0,03	0,00	100,00	0,00	0,00	0,00
				100,00		219,40	933,55	2078,65

METHOD: MALVERN laser sedimentograph (particles <2mm)
Sieving (particles> 0.5mm)

Main Classes individual percentages:

Pebble	0,00
Gravel	12,43
Sand	61,77
Silt	19,84
Clay	5,97

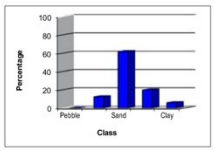

Statistical Parameters:

Mean	2,19
Standard Deviation	3,06
Asymmetry	0,73
P90	6,77
P50	1,15
P5	-1,72
Mode	0,75

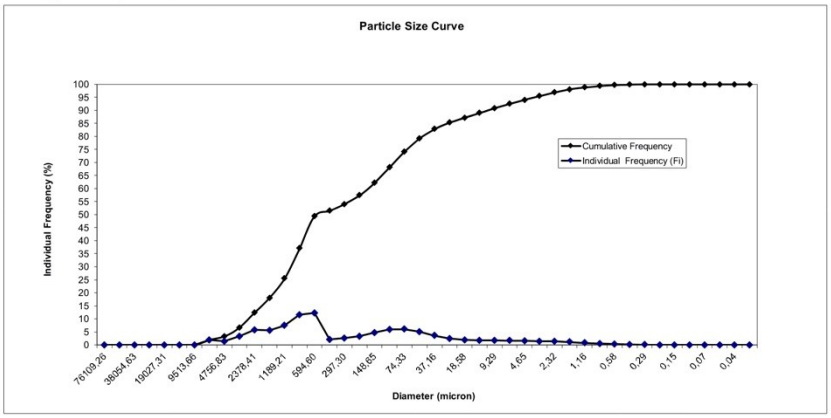

Technician: *Fernanda Dias*

Date:

INSTITUTO HIDROGRÁFICO
DIVISÃO DE GEOLOGIA MARINHA

Station: **2141**

Diameter (class)	Diameter phi	Class midpoint (ci)	Class midpoint (mm)	Individual Frequency (Fi)	Cumulative Frequency	Fi x ci	Fi x (ci-X)^2	Fi x (ci-X)^3
>64.00mm	<6.0 phi	-6,25	76109,26	0,00	0,00	0,00	0,00	0,00
45.25-64.00mm	-5.5,6.0 phi	-5,75	53817,37	0,00	0,00	0,00	0,00	0,00
32.00-45.25mm	-5.0,-5.5 phi	-5,25	38054,63	0,00	0,00	0,00	0,00	0,00
22.63-32.00mm	-4.5,-5.0 phi	-4,75	26908,69	0,00	0,00	0,00	0,00	0,00
16.00-22.63mm	-4.0,-4.5 phi	-4,25	19027,31	0,00	0,00	0,00	0,00	0,00
11.31-16.00mm	-3.5,-4.0 phi	-3,75	13454,34	0,00	0,00	0,00	0,00	0,00
8.00-11.31mm	-3.0,-3.5 phi	-3,25	9513,66	2,22	2,22	-7,21	51,68	-249,48
5.66-8.00mm	-2.5,-3.0 phi	-2,75	6727,17	1,59	3,81	-4,37	29,72	-128,62
4.00-5.66mm	-2.5,-2.0 phi	-2,25	4756,83	2,63	6,44	-5,92	38,53	-147,46
4.00 - 2.83mm	-2.0, -1.5 phi	-1,75	3363,59	3,17	9,60	-5,55	35,08	-116,73
2.83 - 2.00mm	-1.5, -1.0 phi	-1,25	2378,41	4,92	14,52	-6,14	39,29	-111,08
2.00 - 1.41mm	-1.0, -0.5 phi	-0,75	1681,79	5,20	19,72	-3,90	28,15	-65,50
1.41 - 1.00mm	-0.5, 0.0 phi	-0,25	1189,21	9,27	28,99	-2,32	30,95	-56,55
1.00 - 0.71mm	0.0, 0.5 phi	0,25	840,90	15,75	44,73	3,94	27,73	-36,81
0.71 - 0.50mm	0.5, 1.0 phi	0,75	594,60	16,14	60,88	12,11	11,05	-9,14
500.00 - 354.00µm	1.0, 1.5 phi	1,25	420,45	3,01	63,88	3,76	0,32	-0,11
354.00 - 250.00µm	1.5, 2.0 phi	1,75	297,30	3,07	66,96	5,38	0,09	0,02
250.00 - 177.00µm	2.0, 2.5 phi	2,25	210,22	3,05	70,01	6,86	1,38	0,93
177.00 - 125.00µm	2.5, 3.0 phi	2,75	148,65	3,37	73,38	9,27	4,64	5,44
125.00 - 88.40µm	3.0, 3.5 phi	3,25	105,11	3,72	77,10	12,08	10,41	17,41
88.40 - 62.50µm	3.5, 4.0 phi	3,75	74,33	3,63	80,73	13,61	17,13	37,23
62.50 - 44.20µm	4.0, 4..5 phi	4,25	52,56	3,07	83,80	13,06	21,96	58,69
44.20 - 31.25µm	4.5, 5.0 phi	4,75	37,16	2,35	86,15	11,15	23,63	74,96
31.25 - 22.10µm	5.0, 5.5 phi	5,25	26,28	1,80	87,94	9,43	24,24	89,03
22.10 - 15.63µm	5.5, 6.0 phi	5,75	18,58	1,57	89,52	9,05	27,42	114,41
15.63 - 11.00µm	6.0, 6.5 phi	6,25	13,14	1,57	91,09	9,81	34,26	160,11
11.00 - 7.81µm	6.5, 7.0 phi	6,75	9,29	1,56	92,65	10,51	41,68	215,60
7.81 - 5.52µm	7.0, 7.5 phi	7,25	6,57	1,44	94,08	10,41	46,22	262,17
5.52 - 3.91µm	7.5, 8.0 phi	7,75	4,65	1,28	95,36	9,94	48,87	301,68
3.91 - 2.76µm	8.0, 8.5 phi	8,25	3,28	1,19	96,55	9,82	52,98	353,54
2.76 - 1.95µm	8.5, 9.0 phi	8,75	2,32	1,09	97,64	9,52	55,98	401,52
1.95 - 1.38µm	9.0, 9.5 phi	9,25	1,64	0,88	98,52	8,11	51,61	395,99
1.38 - 0.98µm	9.5, 10.0 phi	9,75	1,16	0,60	99,12	5,84	40,04	327,25
0.98 - 0.69µm	10.0, 10.5 phi	10,25	0,82	0,38	99,50	3,91	28,70	248,89
0.69 - 0.49µm	10.5, 11.0 phi	10,75	0,58	0,26	99,76	2,77	21,71	199,12
0.49 - 0.35µm	11.0 , 11.5 phi	11,25	0,41	0,17	99,93	1,94	16,16	156,32
0.35 - 0.24µm	11.5, 12.0 phi	11,75	0,29	0,07	100,00	0,82	7,19	73,11
0.24 - 0.17µm	12.0, 12.5 phi	12,25	0,21	0,00	100,00	0,00	0,00	0,00
0.17 - 0.12µm	12.5, 13.0 phi	12,75	0,15	0,00	100,00	0,00	0,00	0,00
0.12 - 0.09µm	13.0, 13.5 phi	13,25	0,10	0,00	100,00	0,00	0,00	0,00
0.09 - 0.06µm	13.5, 14.0phi	13,75	0,07	0,00	100,00	0,00	0,00	0,00
0.06 - 0.04µm	14.0, 14.5 phi	14,25	0,05	0,00	100,00	0,00	0,00	0,00
0.04 - 0.03µm	14.5, 15.0 phi	14,75	0,04	0,00	100,00	0,00	0,00	0,00
0.03 - 0.02µm	15.0, 15.5 phi	15,25	0,03	0,00	100,00	0,00	0,00	0,00
				100,00		157,72	868,80	2571,94

METHOD: MALVERN laser sedimentograph (particles <2mm)
Sieving (particles> 0.5mm)

Main Classes individual percentages:

Pebble	0,00
Gravel	14,52
Sand	66,21
Silt	14,64
Clay	4,64

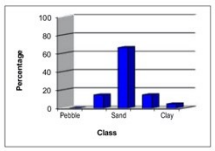

Statistical Parameters:

Mean	1,58
Standard Deviation	2,95
Asymmetry	1,00
P90	6,15
P50	0,66
P5	-2,25
Mode	0,75

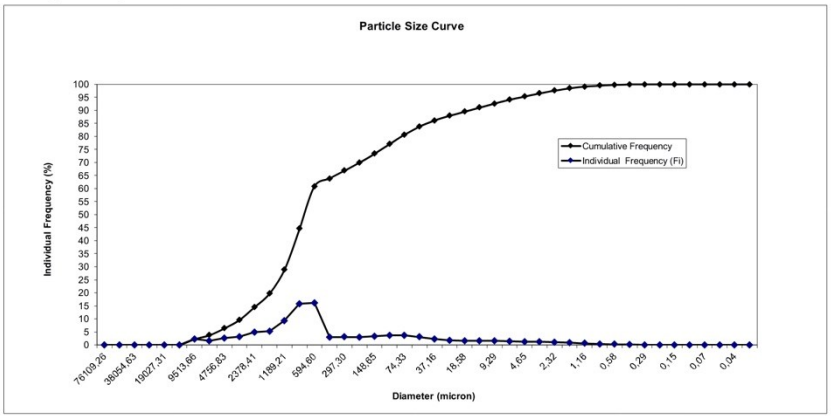

Technician: *Fernanda Dias*

Date:

INSTITUTO HIDROGRÁFICO
DIVISÃO DE GEOLOGIA MARINHA

Station: **2142**

Diameter (class)	Diameter phi	Class midpoint (ci)	Class midpoint (mm)	Individual Frequency (Fi)	Cumulative Frequency	Fi x ci	Fi x (ci-X)^2	Fi x (ci-X)^3
>64.00mm	<6.0 phi	-6,25	76109,26	0,00	0,00	0,00	0,00	0,00
45.25-64.00mm	-5.5,6.0 phi	-5,75	53817,37	0,00	0,00	0,00	0,00	0,00
32.00-45.25mm	-5.0,-5.5 phi	-5,25	38054,63	0,00	0,00	0,00	0,00	0,00
22.63-32.00mm	-4.5,-5.0 phi	-4,75	26908,69	0,00	0,00	0,00	0,00	0,00
16.00-22.63mm	-4.0,-4.5 phi	-4,25	19027,31	0,00	0,00	0,00	0,00	0,00
11.31-16.00mm	-3.5,-4.0 phi	-3,75	13454,34	0,00	0,00	0,00	0,00	0,00
8.00-11.31mm	-3.0,-3.5 phi	-3,25	9513,66	0,00	0,00	0,00	0,00	0,00
5.66-8.00mm	-2.5,-3.0 phi	-2,75	6727,17	0,27	0,27	-0,74	7,63	-40,49
4.00-5.66mm	-2.5,-2.0 phi	-2,25	4756,83	1,77	2,04	-3,99	40,98	-197,03
4.00 - 2.83mm	-2.0, -1.5 phi	-1,75	3363,59	2,65	4,70	-4,64	49,22	-212,06
2.83 - 2.00mm	-1.5, -1.0 phi	-1,25	2378,41	4,55	9,24	-5,69	65,98	-251,24
2.00 - 1.41mm	-1.0, -0.5 phi	-0,75	1681,79	4,95	14,20	-3,71	54,18	-179,24
1.41 - 1.00mm	-0.5, 0.0 phi	-0,25	1189,21	7,26	21,46	-1,82	57,26	-160,80
1.00 - 0.71mm	0.0, 0.5 phi	0,25	840,90	11,21	32,67	2,80	59,71	-137,82
0.71 - 0.50mm	0.5, 1.0 phi	0,75	594,60	12,54	45,21	9,41	41,00	-74,14
500.00 - 354.00µm	1.0, 1.5 phi	1,25	420,45	3,38	48,59	4,22	5,78	-7,56
354.00 - 250.00µm	1.5, 2.0 phi	1,75	297,30	3,56	52,14	6,22	2,32	-1,88
250.00 - 177.00µm	2.0, 2.5 phi	2,25	210,22	3,77	55,91	8,48	0,36	-0,11
177.00 - 125.00µm	2.5, 3.0 phi	2,75	148,65	4,41	60,32	12,12	0,16	0,03
125.00 - 88.40µm	3.0, 3.5 phi	3,25	105,11	5,02	65,34	16,31	2,40	1,66
88.40 - 62.50µm	3.5, 4.0 phi	3,75	74,33	5,01	70,35	18,79	7,12	8,48
62.50 - 44.20µm	4.0, 4..5 phi	4,25	52,56	4,33	74,67	18,38	12,38	20,95
44.20 - 31.25µm	4.5, 5.0 phi	4,75	37,16	3,34	78,01	15,85	16,03	35,14
31.25 - 22.10µm	5.0, 5.5 phi	5,25	26,28	2,56	80,57	13,43	18,54	49,91
22.10 - 15.63µm	5.5, 6.0 phi	5,75	18,58	2,29	82,85	13,14	23,28	74,32
15.63 - 11.00µm	6.0, 6.5 phi	6,25	13,14	2,38	85,23	14,86	32,42	119,67
11.00 - 7.81µm	6.5, 7.0 phi	6,75	9,29	2,46	87,69	16,62	43,26	181,35
7.81 - 5.52µm	7.0, 7.5 phi	7,25	6,57	2,34	90,03	16,96	51,50	241,62
5.52 - 3.91µm	7.5, 8.0 phi	7,75	4,65	2,13	92,16	16,51	57,41	298,09
3.91 - 2.76µm	8.0, 8.5 phi	8,25	3,28	2,00	94,16	16,47	64,69	368,22
2.76 - 1.95µm	8.5, 9.0 phi	8,75	2,32	1,84	95,99	16,06	70,37	435,72
1.95 - 1.38µm	9.0, 9.5 phi	9,25	1,64	1,48	97,48	13,73	66,47	444,84
1.38 - 0.98µm	9.5, 10.0 phi	9,75	1,16	1,02	98,50	9,94	52,71	379,06
0.98 - 0.69µm	10.0, 10.5 phi	10,25	0,82	0,65	99,15	6,67	38,47	295,94
0.69 - 0.49µm	10.5, 11.0 phi	10,75	0,58	0,44	99,59	4,72	29,49	241,55
0.49 - 0.35µm	11.0 , 11.5 phi	11,25	0,41	0,30	99,88	3,32	22,30	193,79
0.35 - 0.24µm	11.5, 12.0 phi	11,75	0,29	0,12	100,00	1,39	10,02	92,12
0.24 - 0.17µm	12.0, 12.5 phi	12,25	0,21	0,00	100,00	0,00	0,00	0,00
0.17 - 0.12µm	12.5, 13.0 phi	12,75	0,15	0,00	100,00	0,00	0,00	0,00
0.12 - 0.09µm	13.0, 13.5 phi	13,25	0,10	0,00	100,00	0,00	0,00	0,00
0.09 - 0.06µm	13.5, 14.0phi	13,75	0,07	0,00	100,00	0,00	0,00	0,00
0.06 - 0.04µm	14.0, 14.5 phi	14,25	0,05	0,00	100,00	0,00	0,00	0,00
0.04 - 0.03µm	14.5, 15.0 phi	14,75	0,04	0,00	100,00	0,00	0,00	0,00
0.03 - 0.02µm	15.0, 15.5 phi	15,25	0,03	0,00	100,00	0,00	0,00	0,00
				100,00		255,81	1003,45	2220,09

METHOD: MALVERN laser sedimentograph (particles <2mm)
Sieving (particles> 0.5mm)

Main Classes individual percentages:

Pebble	0,00
Gravel	9,24
Sand	61,10
Silt	21,82
Clay	7,84

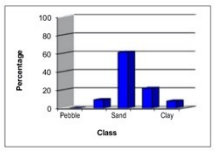

Statistical Parameters:

Mean	2,56
Standard Deviation	3,17
Asymmetry	0,70
P90	7,49
P50	1,70
P5	-1,46
Mode	0,75

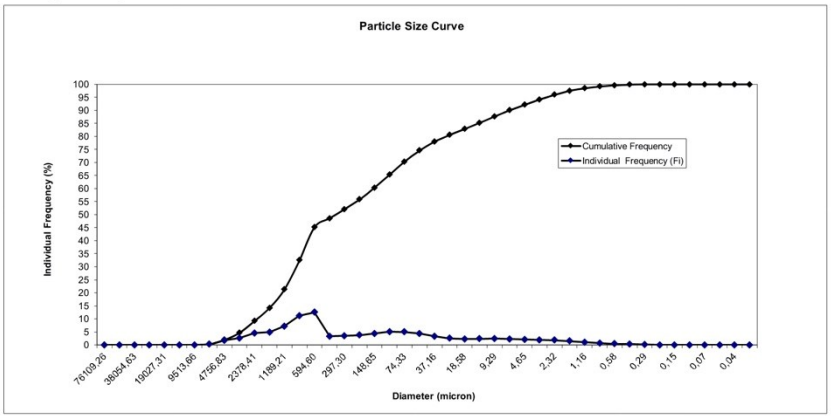

Technician: *Fernanda Dias*

Date:

INSTITUTO HIDROGRÁFICO
DIVISÃO DE GEOLOGIA MARINHA

Station: **2143**

Diameter (class)	Diameter phi	Class midpoint (ci)	Class midpoint (mm)	Individual Frequency (Fi)	Cumulative Frequency	Fi x ci	Fi x (ci-X)^2	Fi x (ci-X)^3
>64.00mm	<6.0 phi	-6,25	76109,26	0,00	0,00	0,00	0,00	0,00
45.25-64.00mm	-5.5,6.0 phi	-5,75	53817,37	0,00	0,00	0,00	0,00	0,00
32.00-45.25mm	-5.0,-5.5 phi	-5,25	38054,63	0,00	0,00	0,00	0,00	0,00
22.63-32.00mm	-4.5,-5.0 phi	-4,75	26908,69	0,00	0,00	0,00	0,00	0,00
16.00-22.63mm	-4.0,-4.5 phi	-4,25	19027,31	0,00	0,00	0,00	0,00	0,00
11.31-16.00mm	-3.5,-4.0 phi	-3,75	13454,34	0,00	0,00	0,00	0,00	0,00
8.00-11.31mm	-3.0,-3.5 phi	-3,25	9513,66	0,72	0,72	-2,34	18,53	-93,93
5.66-8.00mm	-2.5,-3.0 phi	-2,75	6727,17	0,90	1,62	-2,47	18,74	-85,66
4.00-5.66mm	-2.5,-2.0 phi	-2,25	4756,83	0,94	2,56	-2,11	15,56	-63,33
4.00 - 2.83mm	-2.0, -1.5 phi	-1,75	3363,59	1,86	4,42	-3,25	23,70	-84,60
2.83 - 2.00mm	-1.5, -1.0 phi	-1,25	2378,41	4,74	9,16	-5,93	44,71	-137,26
2.00 - 1.41mm	-1.0, -0.5 phi	-0,75	1681,79	8,14	17,30	-6,11	53,77	-138,18
1.41 - 1.00mm	-0.5, 0.0 phi	-0,25	1189,21	11,44	28,74	-2,86	49,02	-101,46
1.00 - 0.71mm	0.0, 0.5 phi	0,25	840,90	14,74	43,48	3,69	36,34	-57,06
0.71 - 0.50mm	0.5, 1.0 phi	0,75	594,60	14,08	57,57	10,56	16,12	-17,25
500.00 - 354.00µm	1.0, 1.5 phi	1,25	420,45	3,41	60,98	4,26	1,11	-0,63
354.00 - 250.00µm	1.5, 2.0 phi	1,75	297,30	3,63	64,60	6,35	0,02	0,00
250.00 - 177.00µm	2.0, 2.5 phi	2,25	210,22	3,71	68,31	8,35	0,69	0,30
177.00 - 125.00µm	2.5, 3.0 phi	2,75	148,65	3,94	72,25	10,83	3,41	3,17
125.00 - 88.40µm	3.0, 3.5 phi	3,25	105,11	3,99	76,25	12,98	8,17	11,68
88.40 - 62.50µm	3.5, 4.0 phi	3,75	74,33	3,62	79,87	13,59	13,50	26,06
62.50 - 44.20µm	4.0, 4..5 phi	4,25	52,56	2,96	82,83	12,56	17,46	42,42
44.20 - 31.25µm	4.5, 5.0 phi	4,75	37,16	2,23	85,06	10,61	19,18	56,21
31.25 - 22.10µm	5.0, 5.5 phi	5,25	26,28	1,69	86,76	8,90	19,94	68,39
22.10 - 15.63µm	5.5, 6.0 phi	5,75	18,58	1,47	88,23	8,46	22,72	89,29
15.63 - 11.00µm	6.0, 6.5 phi	6,25	13,14	1,48	89,71	9,27	29,11	128,94
11.00 - 7.81µm	6.5, 7.0 phi	6,75	9,29	1,52	91,23	10,24	36,87	181,76
7.81 - 5.52µm	7.0, 7.5 phi	7,25	6,57	1,46	92,69	10,58	43,01	233,57
5.52 - 3.91µm	7.5, 8.0 phi	7,75	4,65	1,38	94,07	10,70	48,55	287,88
3.91 - 2.76µm	8.0, 8.5 phi	8,25	3,28	1,37	95,44	11,29	56,58	363,79
2.76 - 1.95µm	8.5, 9.0 phi	8,75	2,32	1,33	96,76	11,60	63,69	441,35
1.95 - 1.38µm	9.0, 9.5 phi	9,25	1,64	1,12	97,89	10,41	62,10	461,42
1.38 - 0.98µm	9.5, 10.0 phi	9,75	1,16	0,81	98,70	7,94	51,20	406,02
0.98 - 0.69µm	10.0, 10.5 phi	10,25	0,82	0,55	99,25	5,64	39,13	329,88
0.69 - 0.49µm	10.5, 11.0 phi	10,75	0,58	0,39	99,64	4,14	30,74	274,47
0.49 - 0.35µm	11.0 , 11.5 phi	11,25	0,41	0,26	99,90	2,91	22,97	216,61
0.35 - 0.24µm	11.5, 12.0 phi	11,75	0,29	0,10	100,00	1,21	10,14	100,74
0.24 - 0.17µm	12.0, 12.5 phi	12,25	0,21	0,00	100,00	0,00	0,00	0,00
0.17 - 0.12µm	12.5, 13.0 phi	12,75	0,15	0,00	100,00	0,00	0,00	0,00
0.12 - 0.09µm	13.0, 13.5 phi	13,25	0,10	0,00	100,00	0,00	0,00	0,00
0.09 - 0.06µm	13.5, 14.0phi	13,75	0,07	0,00	100,00	0,00	0,00	0,00
0.06 - 0.04µm	14.0, 14.5 phi	14,25	0,05	0,00	100,00	0,00	0,00	0,00
0.04 - 0.03µm	14.5, 15.0 phi	14,75	0,04	0,00	100,00	0,00	0,00	0,00
0.03 - 0.02µm	15.0, 15.5 phi	15,25	0,03	0,00	100,00	0,00	0,00	0,00
				100,00		182,00	876,77	2944,58

METHOD: MALVERN laser sedimentograph (particles <2mm)
Sieving (particles> 0.5mm)

Main Classes individual percentages:

Pebble	0,00
Gravel	9,16
Sand	70,71
Silt	14,20
Clay	5,93

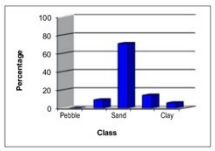

Statistical Parameters:

Mean	1,82
Standard Deviation	2,96
Asymmetry	1,13
P90	6,59
P50	0,73
P5	-1,42
Mode	0,25

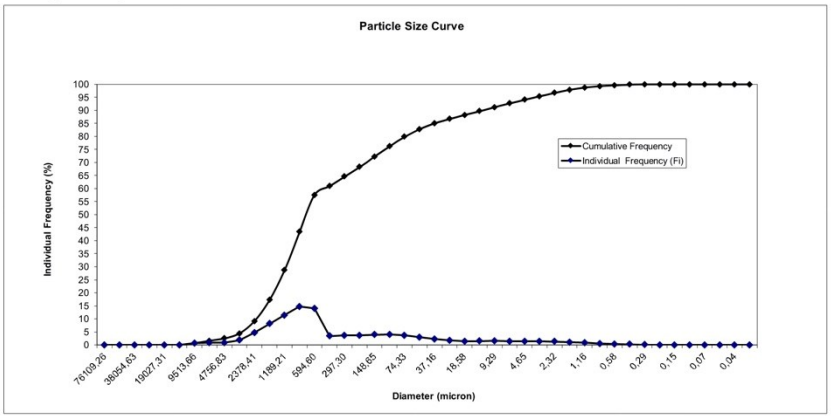

Technician: *Fernanda Dias*

Date:

INSTITUTO HIDROGRÁFICO
DIVISÃO DE GEOLOGIA MARINHA

Station: **2144**

Diameter (class)	Diameter phi	Class midpoint (ci)	Class midpoint (mm)	Individual Frequency (Fi)	Cumulative Frequency	Fi x ci	Fi x (ci-X)^2	Fi x (ci-X)^3
>64.00mm	<6.0 phi	-6,25	76109,26	0,00	0,00	0,00	0,00	0,00
45.25-64.00mm	-5.5,6.0 phi	-5,75	53817,37	0,00	0,00	0,00	0,00	0,00
32.00-45.25mm	-5.0,-5.5 phi	-5,25	38054,63	0,00	0,00	0,00	0,00	0,00
22.63-32.00mm	-4.5,-5.0 phi	-4,75	26908,69	0,00	0,00	0,00	0,00	0,00
16.00-22.63mm	-4.0,-4.5 phi	-4,25	19027,31	0,00	0,00	0,00	0,00	0,00
11.31-16.00mm	-3.5,-4.0 phi	-3,75	13454,34	0,00	0,00	0,00	0,00	0,00
8.00-11.31mm	-3.0,-3.5 phi	-3,25	9513,66	0,91	0,91	-2,97	22,11	-108,80
5.66-8.00mm	-2.5,-3.0 phi	-2,75	6727,17	0,68	1,59	-1,87	13,29	-58,74
4.00-5.66mm	-2.5,-2.0 phi	-2,25	4756,83	1,05	2,64	-2,35	16,08	-63,04
4.00 - 2.83mm	-2.0, -1.5 phi	-1,75	3363,59	1,66	4,30	-2,90	19,43	-66,46
2.83 - 2.00mm	-1.5, -1.0 phi	-1,25	2378,41	5,24	9,54	-6,55	44,75	-130,74
2.00 - 1.41mm	-1.0, -0.5 phi	-0,75	1681,79	9,24	18,79	-6,93	54,20	-131,23
1.41 - 1.00mm	-0.5, 0.0 phi	-0,25	1189,21	11,64	30,43	-2,91	42,98	-82,58
1.00 - 0.71mm	0.0, 0.5 phi	0,25	840,90	14,18	44,61	3,55	28,65	-40,72
0.71 - 0.50mm	0.5, 1.0 phi	0,75	594,60	13,50	58,11	10,12	11,46	-10,56
500.00 - 354.00µm	1.0, 1.5 phi	1,25	420,45	3,91	62,02	4,88	0,69	-0,29
354.00 - 250.00µm	1.5, 2.0 phi	1,75	297,30	4,18	66,20	7,32	0,03	0,00
250.00 - 177.00µm	2.0, 2.5 phi	2,25	210,22	4,17	70,36	9,38	1,40	0,81
177.00 - 125.00µm	2.5, 3.0 phi	2,75	148,65	4,20	74,57	11,56	4,89	5,27
125.00 - 88.40µm	3.0, 3.5 phi	3,25	105,11	4,05	78,61	13,15	10,08	15,91
88.40 - 62.50µm	3.5, 4.0 phi	3,75	74,33	3,50	82,11	13,13	15,13	31,45
62.50 - 44.20µm	4.0, 4..5 phi	4,25	52,56	2,75	84,86	11,69	18,28	47,15
44.20 - 31.25µm	4.5, 5.0 phi	4,75	37,16	2,04	86,91	9,71	19,37	59,64
31.25 - 22.10µm	5.0, 5.5 phi	5,25	26,28	1,55	88,46	8,15	19,88	71,14
22.10 - 15.63µm	5.5, 6.0 phi	5,75	18,58	1,33	89,79	7,65	22,14	90,32
15.63 - 11.00µm	6.0, 6.5 phi	6,25	13,14	1,30	91,09	8,12	27,23	124,67
11.00 - 7.81µm	6.5, 7.0 phi	6,75	9,29	1,30	92,38	8,74	33,41	169,66
7.81 - 5.52µm	7.0, 7.5 phi	7,25	6,57	1,24	93,62	8,97	38,51	214,82
5.52 - 3.91µm	7.5, 8.0 phi	7,75	4,65	1,18	94,80	9,14	43,59	264,94
3.91 - 2.76µm	8.0, 8.5 phi	8,25	3,28	1,18	95,98	9,76	51,22	336,99
2.76 - 1.95µm	8.5, 9.0 phi	8,75	2,32	1,16	97,14	10,13	58,01	410,60
1.95 - 1.38µm	9.0, 9.5 phi	9,25	1,64	0,99	98,13	9,14	56,74	430,04
1.38 - 0.98µm	9.5, 10.0 phi	9,75	1,16	0,72	98,85	7,01	46,93	379,11
0.98 - 0.69µm	10.0, 10.5 phi	10,25	0,82	0,49	99,34	5,01	35,97	308,61
0.69 - 0.49µm	10.5, 11.0 phi	10,75	0,58	0,34	99,68	3,68	28,24	256,40
0.49 - 0.35µm	11.0 , 11.5 phi	11,25	0,41	0,23	99,91	2,57	20,99	201,08
0.35 - 0.24µm	11.5, 12.0 phi	11,75	0,29	0,09	100,00	1,06	9,19	92,57
0.24 - 0.17µm	12.0, 12.5 phi	12,25	0,21	0,00	100,00	0,00	0,00	0,00
0.17 - 0.12µm	12.5, 13.0 phi	12,75	0,15	0,00	100,00	0,00	0,00	0,00
0.12 - 0.09µm	13.0, 13.5 phi	13,25	0,10	0,00	100,00	0,00	0,00	0,00
0.09 - 0.06µm	13.5, 14.0phi	13,75	0,07	0,00	100,00	0,00	0,00	0,00
0.06 - 0.04µm	14.0, 14.5 phi	14,25	0,05	0,00	100,00	0,00	0,00	0,00
0.04 - 0.03µm	14.5, 15.0 phi	14,75	0,04	0,00	100,00	0,00	0,00	0,00
0.03 - 0.02µm	15.0, 15.5 phi	15,25	0,03	0,00	100,00	0,00	0,00	0,00
METHOD: MALVERN laser sedimentograph (particles <2mm)				100,00		167,13	814,85	2818,01
Sieving (particles> 0.5mm)								

Main Classes individual percentages:

Pebble	0,00
Gravel	9,54
Sand	72,57
Silt	12,69
Clay	5,20

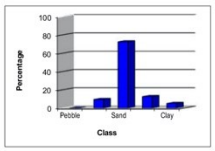

Statistical Parameters:

Mean	1,67
Standard Deviation	2,85
Asymmetry	1,21
P90	6,08
P50	0,70
P5	-1,41
Mode	0,25

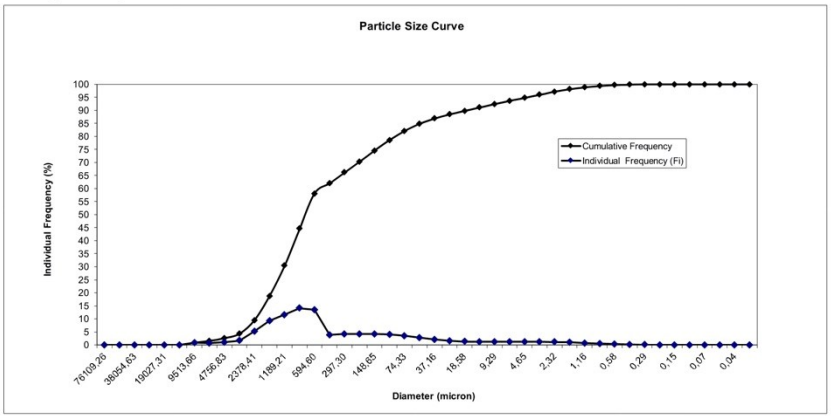

Technician: *Fernanda Dias*

Date:

INSTITUTO HIDROGRÁFICO
DIVISÃO DE GEOLOGIA MARINHA

Station: **2145**

Diameter (class)	Diameter phi	Class midpoint (ci)	Class midpoint (mm)	Individual Frequency (Fi)	Cumulative Frequency	Fi x ci	Fi x (ci-X)^2	Fi x (ci-X)^3
>64.00mm	<6.0 phi	-6,25	76109,26	0,00	0,00	0,00	0,00	0,00
45.25-64.00mm	-5.5,6.0 phi	-5,75	53817,37	0,00	0,00	0,00	0,00	0,00
32.00-45.25mm	-5.0,-5.5 phi	-5,25	38054,63	0,00	0,00	0,00	0,00	0,00
22.63-32.00mm	-4.5,-5.0 phi	-4,75	26908,69	0,00	0,00	0,00	0,00	0,00
16.00-22.63mm	-4.0,-4.5 phi	-4,25	19027,31	0,00	0,00	0,00	0,00	0,00
11.31-16.00mm	-3.5,-4.0 phi	-3,75	13454,34	0,00	0,00	0,00	0,00	0,00
8.00-11.31mm	-3.0,-3.5 phi	-3,25	9513,66	0,00	0,00	0,00	0,00	0,00
5.66-8.00mm	-2.5,-3.0 phi	-2,75	6727,17	0,00	0,00	0,00	0,00	0,00
4.00-5.66mm	-2.5,-2.0 phi	-2,25	4756,83	0,89	0,89	-2,01	13,19	-50,72
4.00 - 2.83mm	-2.0, -1.5 phi	-1,75	3363,59	2,25	3,14	-3,93	25,14	-84,08
2.83 - 2.00mm	-1.5, -1.0 phi	-1,25	2378,41	5,49	8,63	-6,86	44,40	-126,30
2.00 - 1.41mm	-1.0, -0.5 phi	-0,75	1681,79	10,05	18,67	-7,53	55,22	-129,45
1.41 - 1.00mm	-0.5, 0.0 phi	-0,25	1189,21	13,32	31,99	-3,33	45,32	-83,59
1.00 - 0.71mm	0.0, 0.5 phi	0,25	840,90	14,96	46,95	3,74	27,04	-36,35
0.71 - 0.50mm	0.5, 1.0 phi	0,75	594,60	13,43	60,38	10,07	9,58	-8,09
500.00 - 354.00µm	1.0, 1.5 phi	1,25	420,45	4,18	64,57	5,23	0,50	-0,17
354.00 - 250.00µm	1.5, 2.0 phi	1,75	297,30	4,26	68,83	7,46	0,10	0,02
250.00 - 177.00µm	2.0, 2.5 phi	2,25	210,22	4,05	72,87	9,10	1,74	1,14
177.00 - 125.00µm	2.5, 3.0 phi	2,75	148,65	3,91	76,79	10,75	5,22	6,03
125.00 - 88.40µm	3.0, 3.5 phi	3,25	105,11	3,62	80,41	11,78	9,93	16,45
88.40 - 62.50µm	3.5, 4.0 phi	3,75	74,33	3,05	83,46	11,43	14,16	30,52
62.50 - 44.20µm	4.0, 4..5 phi	4,25	52,56	2,38	85,84	10,11	16,78	44,55
44.20 - 31.25µm	4.5, 5.0 phi	4,75	37,16	1,81	87,65	8,60	18,03	56,88
31.25 - 22.10µm	5.0, 5.5 phi	5,25	26,28	1,42	89,07	7,46	18,99	69,40
22.10 - 15.63µm	5.5, 6.0 phi	5,75	18,58	1,23	90,30	7,08	21,27	88,40
15.63 - 11.00µm	6.0, 6.5 phi	6,25	13,14	1,18	91,48	7,39	25,62	119,29
11.00 - 7.81µm	6.5, 7.0 phi	6,75	9,29	1,15	92,63	7,76	30,57	157,58
7.81 - 5.52µm	7.0, 7.5 phi	7,25	6,57	1,08	93,71	7,83	34,56	195,43
5.52 - 3.91µm	7.5, 8.0 phi	7,75	4,65	1,04	94,75	8,03	39,27	241,73
3.91 - 2.76µm	8.0, 8.5 phi	8,25	3,28	1,08	95,82	8,87	47,65	317,11
2.76 - 1.95µm	8.5, 9.0 phi	8,75	2,32	1,10	96,93	9,64	56,41	403,61
1.95 - 1.38µm	9.0, 9.5 phi	9,25	1,64	0,99	97,91	9,14	57,93	443,51
1.38 - 0.98µm	9.5, 10.0 phi	9,75	1,16	0,76	98,68	7,43	50,68	413,36
0.98 - 0.69µm	10.0, 10.5 phi	10,25	0,82	0,55	99,23	5,64	41,21	356,68
0.69 - 0.49µm	10.5, 11.0 phi	10,75	0,58	0,40	99,63	4,30	33,52	306,90
0.49 - 0.35µm	11.0 , 11.5 phi	11,25	0,41	0,27	99,89	3,01	24,97	241,14
0.35 - 0.24µm	11.5, 12.0 phi	11,75	0,29	0,11	100,00	1,24	10,89	110,54
0.24 - 0.17µm	12.0, 12.5 phi	12,25	0,21	0,00	100,00	0,00	0,00	0,00
0.17 - 0.12µm	12.5, 13.0 phi	12,75	0,15	0,00	100,00	0,00	0,00	0,00
0.12 - 0.09µm	13.0, 13.5 phi	13,25	0,10	0,00	100,00	0,00	0,00	0,00
0.09 - 0.06µm	13.5, 14.0phi	13,75	0,07	0,00	100,00	0,00	0,00	0,00
0.06 - 0.04µm	14.0, 14.5 phi	14,25	0,05	0,00	100,00	0,00	0,00	0,00
0.04 - 0.03µm	14.5, 15.0 phi	14,75	0,04	0,00	100,00	0,00	0,00	0,00
0.03 - 0.02µm	15.0, 15.5 phi	15,25	0,03	0,00	100,00	0,00	0,00	0,00
METHOD: MALVERN laser sedimentograph (particles <2mm)				100,00		159,45	779,87	3101,50
Sieving (particles> 0.5mm)								

Main Classes individual percentages:

Pebble	0,00
Gravel	8,63
Sand	74,83
Silt	11,29
Clay	5,25

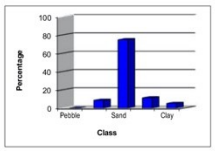

Statistical Parameters:

Mean	1,59
Standard Deviation	2,79
Asymmetry	1,42
P90	5,87
P50	0,61
P5	-1,28
Mode	0,25

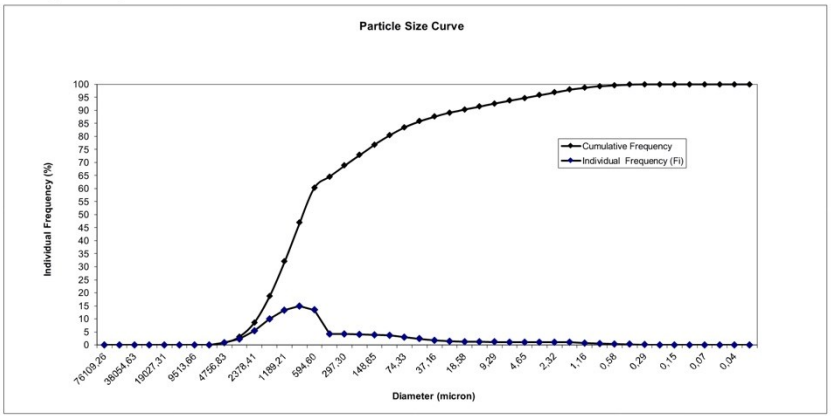

Technician: *Fernanda Dias*

Date:

INSTITUTO HIDROGRÁFICO
DIVISÃO DE GEOLOGIA MARINHA

Station: **2146**

Diameter (class)	Diameter phi	Class midpoint (ci)	Class midpoint (mm)	Individual Frequency (Fi)	Cumulative Frequency	Fi x ci	Fi x (ci-X)^2	Fi x (ci-X)^3
>64.00mm	<6.0 phi	-6,25	76109,26	0,00	0,00	0,00	0,00	0,00
45.25-64.00mm	-5.5,6.0 phi	-5,75	53817,37	0,00	0,00	0,00	0,00	0,00
32.00-45.25mm	-5.0,-5.5 phi	-5,25	38054,63	0,00	0,00	0,00	0,00	0,00
22.63-32.00mm	-4.5,-5.0 phi	-4,75	26908,69	0,00	0,00	0,00	0,00	0,00
16.00-22.63mm	-4.0,-4.5 phi	-4,25	19027,31	0,00	0,00	0,00	0,00	0,00
11.31-16.00mm	-3.5,-4.0 phi	-3,75	13454,34	3,75	3,75	-14,06	88,07	-426,83
8.00-11.31mm	-3.0,-3.5 phi	-3,25	9513,66	0,41	4,16	-1,33	7,72	-33,56
5.66-8.00mm	-2.5,-3.0 phi	-2,75	6727,17	1,74	5,90	-4,79	25,76	-99,06
4.00-5.66mm	-2.5,-2.0 phi	-2,25	4756,83	1,84	7,74	-4,14	20,61	-68,95
4.00 - 2.83mm	-2.0, -1.5 phi	-1,75	3363,59	4,32	12,06	-7,56	35,01	-99,64
2.83 - 2.00mm	-1.5, -1.0 phi	-1,25	2378,41	7,96	20,02	-9,95	43,80	-102,76
2.00 - 1.41mm	-1.0, -0.5 phi	-0,75	1681,79	10,36	30,38	-7,77	35,31	-65,19
1.41 - 1.00mm	-0.5, 0.0 phi	-0,25	1189,21	11,01	41,39	-2,75	19,95	-26,86
1.00 - 0.71mm	0.0, 0.5 phi	0,25	840,90	12,49	53,88	3,12	8,95	-7,57
0.71 - 0.50mm	0.5, 1.0 phi	0,75	594,60	11,46	65,34	8,60	1,37	-0,48
500.00 - 354.00µm	1.0, 1.5 phi	1,25	420,45	3,53	68,87	4,41	0,08	0,01
354.00 - 250.00µm	1.5, 2.0 phi	1,75	297,30	3,66	72,53	6,40	1,56	1,02
250.00 - 177.00µm	2.0, 2.5 phi	2,25	210,22	3,47	76,00	7,80	4,62	5,32
177.00 - 125.00µm	2.5, 3.0 phi	2,75	148,65	3,31	79,31	9,11	9,06	14,98
125.00 - 88.40µm	3.0, 3.5 phi	3,25	105,11	3,05	82,36	9,92	14,15	30,48
88.40 - 62.50µm	3.5, 4.0 phi	3,75	74,33	2,58	84,94	9,67	18,17	48,21
62.50 - 44.20µm	4.0, 4..5 phi	4,25	52,56	2,06	87,00	8,74	20,44	64,48
44.20 - 31.25µm	4.5, 5.0 phi	4,75	37,16	1,62	88,62	7,69	21,62	78,98
31.25 - 22.10µm	5.0, 5.5 phi	5,25	26,28	1,32	89,94	6,93	22,77	94,60
22.10 - 15.63µm	5.5, 6.0 phi	5,75	18,58	1,17	91,10	6,72	25,31	117,78
15.63 - 11.00µm	6.0, 6.5 phi	6,25	13,14	1,13	92,23	7,07	30,03	154,77
11.00 - 7.81µm	6.5, 7.0 phi	6,75	9,29	1,11	93,35	7,50	35,51	200,74
7.81 - 5.52µm	7.0, 7.5 phi	7,25	6,57	1,05	94,40	7,64	39,92	245,65
5.52 - 3.91µm	7.5, 8.0 phi	7,75	4,65	1,01	95,41	7,80	44,56	296,49
3.91 - 2.76µm	8.0, 8.5 phi	8,25	3,28	1,02	96,42	8,39	52,02	372,10
2.76 - 1.95µm	8.5, 9.0 phi	8,75	2,32	1,00	97,43	8,78	58,78	449,87
1.95 - 1.38µm	9.0, 9.5 phi	9,25	1,64	0,87	98,29	8,03	57,71	470,53
1.38 - 0.98µm	9.5, 10.0 phi	9,75	1,16	0,64	98,94	6,29	48,28	417,76
0.98 - 0.69µm	10.0, 10.5 phi	10,25	0,82	0,45	99,39	4,60	37,60	344,23
0.69 - 0.49µm	10.5, 11.0 phi	10,75	0,58	0,32	99,71	3,43	29,71	286,85
0.49 - 0.35µm	11.0 , 11.5 phi	11,25	0,41	0,21	99,92	2,38	21,83	221,70
0.35 - 0.24µm	11.5, 12.0 phi	11,75	0,29	0,08	100,00	0,96	9,31	99,19
0.24 - 0.17µm	12.0, 12.5 phi	12,25	0,21	0,00	100,00	0,00	0,00	0,00
0.17 - 0.12µm	12.5, 13.0 phi	12,75	0,15	0,00	100,00	0,00	0,00	0,00
0.12 - 0.09µm	13.0, 13.5 phi	13,25	0,10	0,00	100,00	0,00	0,00	0,00
0.09 - 0.06µm	13.5, 14.0phi	13,75	0,07	0,00	100,00	0,00	0,00	0,00
0.06 - 0.04µm	14.0, 14.5 phi	14,25	0,05	0,00	100,00	0,00	0,00	0,00
0.04 - 0.03µm	14.5, 15.0 phi	14,75	0,04	0,00	100,00	0,00	0,00	0,00
0.03 - 0.02µm	15.0, 15.5 phi	15,25	0,03	0,00	100,00	0,00	0,00	0,00
				100,00		109,63	889,58	3084,82

METHOD: MALVERN laser sedimentograph (particles <2mm)
Sieving (particles> 0.5mm)

Main Classes individual percentages:

Pebble	0,00
Gravel	20,02
Sand	64,92
Silt	10,47
Clay	4,59

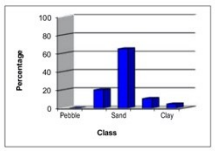

Statistical Parameters:

Mean	1,10
Standard Deviation	2,98
Asymmetry	1,16
P90	5,53
P50	0,35
P5	-2,74
Mode	0,25

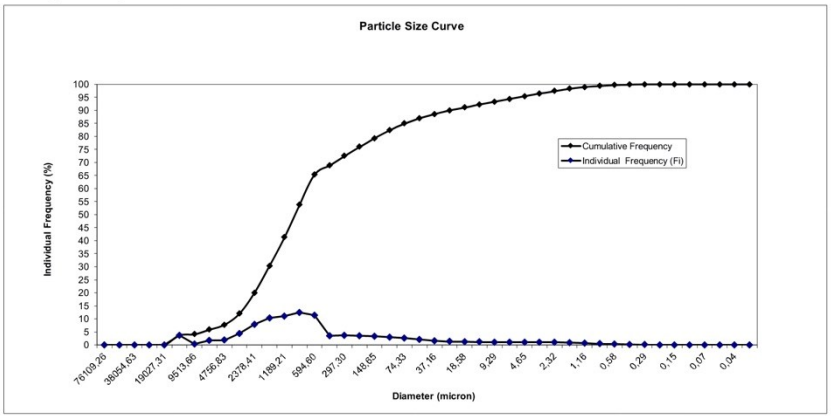

Technician: *Fernanda Dias*

Date:

INSTITUTO HIDROGRÁFICO
DIVISÃO DE GEOLOGIA MARINHA

Station: **2147**

Diameter (class)	Diameter phi	Class midpoint (ci)	Class midpoint (mm)	Individual Frequency (Fi)	Cumulative Frequency	Fi x ci	Fi x (ci-X)^2	Fi x (ci-X)^3
>64.00mm	<6.0 phi	-6,25	76109,26	0,00	0,00	0,00	0,00	0,00
45.25-64.00mm	-5.5,6.0 phi	-5,75	53817,37	0,00	0,00	0,00	0,00	0,00
32.00-45.25mm	-5.0,-5.5 phi	-5,25	38054,63	0,00	0,00	0,00	0,00	0,00
22.63-32.00mm	-4.5,-5.0 phi	-4,75	26908,69	0,00	0,00	0,00	0,00	0,00
16.00-22.63mm	-4.0,-4.5 phi	-4,25	19027,31	0,00	0,00	0,00	0,00	0,00
11.31-16.00mm	-3.5,-4.0 phi	-3,75	13454,34	1,98	1,98	-7,41	46,83	-227,94
8.00-11.31mm	-3.0,-3.5 phi	-3,25	9513,66	0,00	1,98	0,00	0,00	0,00
5.66-8.00mm	-2.5,-3.0 phi	-2,75	6727,17	1,97	3,95	-5,42	29,49	-114,07
4.00-5.66mm	-2.5,-2.0 phi	-2,25	4756,83	1,03	4,97	-2,31	11,64	-39,20
4.00 - 2.83mm	-2.0, -1.5 phi	-1,75	3363,59	4,26	9,24	-7,46	35,07	-100,57
2.83 - 2.00mm	-1.5, -1.0 phi	-1,25	2378,41	7,80	17,04	-9,75	43,72	-103,51
2.00 - 1.41mm	-1.0, -0.5 phi	-0,75	1681,79	9,50	26,53	-7,12	33,13	-61,87
1.41 - 1.00mm	-0.5, 0.0 phi	-0,25	1189,21	11,81	38,34	-2,95	22,09	-30,22
1.00 - 0.71mm	0.0, 0.5 phi	0,25	840,90	14,46	52,80	3,61	10,88	-9,44
0.71 - 0.50mm	0.5, 1.0 phi	0,75	594,60	13,76	66,56	10,32	1,86	-0,68
500.00 - 354.00µm	1.0, 1.5 phi	1,25	420,45	3,69	70,25	4,61	0,06	0,01
354.00 - 250.00µm	1.5, 2.0 phi	1,75	297,30	3,80	74,05	6,65	1,52	0,96
250.00 - 177.00µm	2.0, 2.5 phi	2,25	210,22	3,58	77,64	8,07	4,60	5,20
177.00 - 125.00µm	2.5, 3.0 phi	2,75	148,65	3,36	80,99	9,23	8,94	14,59
125.00 - 88.40µm	3.0, 3.5 phi	3,25	105,11	3,00	83,99	9,75	13,64	29,09
88.40 - 62.50µm	3.5, 4.0 phi	3,75	74,33	2,47	86,47	9,28	17,14	45,12
62.50 - 44.20µm	4.0, 4..5 phi	4,25	52,56	1,93	88,40	8,20	18,92	59,26
44.20 - 31.25µm	4.5, 5.0 phi	4,75	37,16	1,48	89,87	7,02	19,49	70,79
31.25 - 22.10µm	5.0, 5.5 phi	5,25	26,28	1,16	91,04	6,11	19,86	82,09
22.10 - 15.63µm	5.5, 6.0 phi	5,75	18,58	1,00	92,04	5,78	21,56	99,88
15.63 - 11.00µm	6.0, 6.5 phi	6,25	13,14	0,97	93,01	6,05	25,49	130,83
11.00 - 7.81µm	6.5, 7.0 phi	6,75	9,29	0,96	93,97	6,45	30,34	170,86
7.81 - 5.52µm	7.0, 7.5 phi	7,25	6,57	0,92	94,88	6,64	34,43	211,17
5.52 - 3.91µm	7.5, 8.0 phi	7,75	4,65	0,89	95,77	6,87	38,98	258,53
3.91 - 2.76µm	8.0, 8.5 phi	8,25	3,28	0,91	96,68	7,51	46,32	330,40
2.76 - 1.95µm	8.5, 9.0 phi	8,75	2,32	0,91	97,59	7,99	53,20	406,06
1.95 - 1.38µm	9.0, 9.5 phi	9,25	1,64	0,80	98,39	7,40	52,89	430,10
1.38 - 0.98µm	9.5, 10.0 phi	9,75	1,16	0,60	98,99	5,85	44,70	385,85
0.98 - 0.69µm	10.0, 10.5 phi	10,25	0,82	0,42	99,41	4,32	35,18	321,24
0.69 - 0.49µm	10.5, 11.0 phi	10,75	0,58	0,30	99,72	3,25	28,09	270,54
0.49 - 0.35µm	11.0 , 11.5 phi	11,25	0,41	0,20	99,92	2,29	20,89	211,70
0.35 - 0.24µm	11.5, 12.0 phi	11,75	0,29	0,08	100,00	0,95	9,16	97,40
0.24 - 0.17µm	12.0, 12.5 phi	12,25	0,21	0,00	100,00	0,00	0,00	0,00
0.17 - 0.12µm	12.5, 13.0 phi	12,75	0,15	0,00	100,00	0,00	0,00	0,00
0.12 - 0.09µm	13.0, 13.5 phi	13,25	0,10	0,00	100,00	0,00	0,00	0,00
0.09 - 0.06µm	13.5, 14.0phi	13,75	0,07	0,00	100,00	0,00	0,00	0,00
0.06 - 0.04µm	14.0, 14.5 phi	14,25	0,05	0,00	100,00	0,00	0,00	0,00
0.04 - 0.03µm	14.5, 15.0 phi	14,75	0,04	0,00	100,00	0,00	0,00	0,00
0.03 - 0.02µm	15.0, 15.5 phi	15,25	0,03	0,00	100,00	0,00	0,00	0,00
METHOD: MALVERN laser sedimentograph (particles <2mm)				100,00		111,77	780,12	2944,19
Sieving (particles> 0.5mm)								

Main Classes individual percentages:

Pebble	0,00
Gravel	17,04
Sand	69,43
Silt	9,30
Clay	4,23

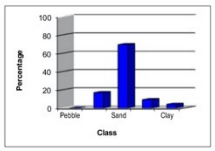

Statistical Parameters:

Mean	1,12
Standard Deviation	2,79
Asymmetry	1,35
P90	5,05
P50	0,40
P5	-2,00
Mode	0,25

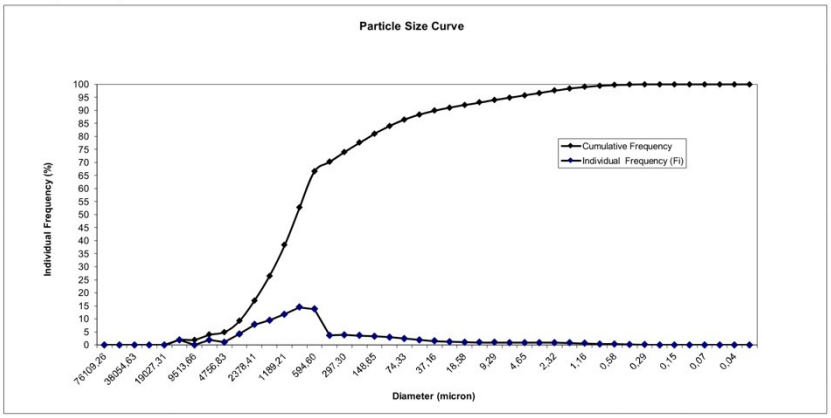

Technician: *Fernanda Dias*

Date:

INSTITUTO HIDROGRÁFICO
DIVISÃO DE GEOLOGIA MARINHA

Station: **2148**

Diameter (class)	Diameter phi	Class midpoint (ci)	Class midpoint (mm)	Individual Frequency (Fi)	Cumulative Frequency	Fi x ci	Fi x (ci-X)^2	Fi x (ci-X)^3
>64.00mm	<6.0 phi	-6,25	76109,26	0,00	0,00	0,00	0,00	0,00
45.25-64.00mm	-5.5,6.0 phi	-5,75	53817,37	0,00	0,00	0,00	0,00	0,00
32.00-45.25mm	-5.0,-5.5 phi	-5,25	38054,63	0,00	0,00	0,00	0,00	0,00
22.63-32.00mm	-4.5,-5.0 phi	-4,75	26908,69	0,00	0,00	0,00	0,00	0,00
16.00-22.63mm	-4.0,-4.5 phi	-4,25	19027,31	0,00	0,00	0,00	0,00	0,00
11.31-16.00mm	-3.5,-4.0 phi	-3,75	13454,34	3,92	3,92	-14,68	72,90	-314,59
8.00-11.31mm	-3.0,-3.5 phi	-3,25	9513,66	3,12	7,04	-10,14	45,42	-173,28
5.66-8.00mm	-2.5,-3.0 phi	-2,75	6727,17	1,43	8,47	-3,93	15,71	-52,09
4.00-5.66mm	-2.5,-2.0 phi	-2,25	4756,83	3,13	11,59	-7,04	24,79	-69,79
4.00 - 2.83mm	-2.0, -1.5 phi	-1,75	3363,59	5,59	17,19	-9,79	29,98	-69,40
2.83 - 2.00mm	-1.5, -1.0 phi	-1,25	2378,41	10,29	27,48	-12,86	33,91	-61,55
2.00 - 1.41mm	-1.0, -0.5 phi	-0,75	1681,79	11,78	39,26	-8,83	20,37	-26,79
1.41 - 1.00mm	-0.5, 0.0 phi	-0,25	1189,21	11,00	50,25	-2,75	7,31	-5,96
1.00 - 0.71mm	0.0, 0.5 phi	0,25	840,90	11,40	61,65	2,85	1,13	-0,36
0.71 - 0.50mm	0.5, 1.0 phi	0,75	594,60	10,33	71,98	7,74	0,35	0,07
500.00 - 354.00µm	1.0, 1.5 phi	1,25	420,45	3,15	75,13	3,94	1,48	1,01
354.00 - 250.00µm	1.5, 2.0 phi	1,75	297,30	3,31	78,45	5,80	4,65	5,51
250.00 - 177.00µm	2.0, 2.5 phi	2,25	210,22	3,12	81,57	7,03	8,87	14,94
177.00 - 125.00µm	2.5, 3.0 phi	2,75	148,65	2,89	84,46	7,94	13,78	30,10
125.00 - 88.40µm	3.0, 3.5 phi	3,25	105,11	2,53	86,98	8,21	18,21	48,90
88.40 - 62.50µm	3.5, 4.0 phi	3,75	74,33	2,02	89,00	7,56	20,46	65,16
62.50 - 44.20µm	4.0, 4..5 phi	4,25	52,56	1,52	90,52	6,47	20,66	76,15
44.20 - 31.25µm	4.5, 5.0 phi	4,75	37,16	1,16	91,68	5,51	20,30	84,95
31.25 - 22.10µm	5.0, 5.5 phi	5,25	26,28	0,94	92,62	4,94	20,66	96,78
22.10 - 15.63µm	5.5, 6.0 phi	5,75	18,58	0,84	93,47	4,85	22,65	117,46
15.63 - 11.00µm	6.0, 6.5 phi	6,25	13,14	0,82	94,29	5,12	26,50	150,65
11.00 - 7.81µm	6.5, 7.0 phi	6,75	9,29	0,80	95,09	5,42	30,71	189,95
7.81 - 5.52µm	7.0, 7.5 phi	7,25	6,57	0,76	95,85	5,50	33,88	226,50
5.52 - 3.91µm	7.5, 8.0 phi	7,75	4,65	0,72	96,57	5,62	37,42	268,86
3.91 - 2.76µm	8.0, 8.5 phi	8,25	3,28	0,74	97,31	6,10	43,67	335,63
2.76 - 1.95µm	8.5, 9.0 phi	8,75	2,32	0,74	98,05	6,47	49,55	405,58
1.95 - 1.38µm	9.0, 9.5 phi	9,25	1,64	0,65	98,70	5,99	48,85	424,25
1.38 - 0.98µm	9.5, 10.0 phi	9,75	1,16	0,49	99,18	4,74	41,04	376,98
0.98 - 0.69µm	10.0, 10.5 phi	10,25	0,82	0,34	99,53	3,51	32,13	311,15
0.69 - 0.49µm	10.5, 11.0 phi	10,75	0,58	0,25	99,77	2,64	25,45	259,18
0.49 - 0.35µm	11.0 , 11.5 phi	11,25	0,41	0,16	99,94	1,84	18,68	199,64
0.35 - 0.24µm	11.5, 12.0 phi	11,75	0,29	0,06	100,00	0,75	7,99	89,40
0.24 - 0.17µm	12.0, 12.5 phi	12,25	0,21	0,00	100,00	0,00	0,00	0,00
0.17 - 0.12µm	12.5, 13.0 phi	12,75	0,15	0,00	100,00	0,00	0,00	0,00
0.12 - 0.09µm	13.0, 13.5 phi	13,25	0,10	0,00	100,00	0,00	0,00	0,00
0.09 - 0.06µm	13.5, 14.0phi	13,75	0,07	0,00	100,00	0,00	0,00	0,00
0.06 - 0.04µm	14.0, 14.5 phi	14,25	0,05	0,00	100,00	0,00	0,00	0,00
0.04 - 0.03µm	14.5, 15.0 phi	14,75	0,04	0,00	100,00	0,00	0,00	0,00
0.03 - 0.02µm	15.0, 15.5 phi	15,25	0,03	0,00	100,00	0,00	0,00	0,00
				100,00		56,51	799,49	3004,98

METHOD: MALVERN laser sedimentograph (particles <2mm)
Sieving (particles> 0.5mm)

Main Classes individual percentages:

Pebble	0,00
Gravel	27,48
Sand	61,52
Silt	7,57
Clay	3,43

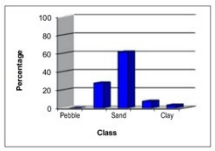

Statistical Parameters:

Mean	0,57
Standard Deviation	2,83
Asymmetry	1,33
P90	4,32
P50	-0,01
P5	-3,30
Mode	-0,75

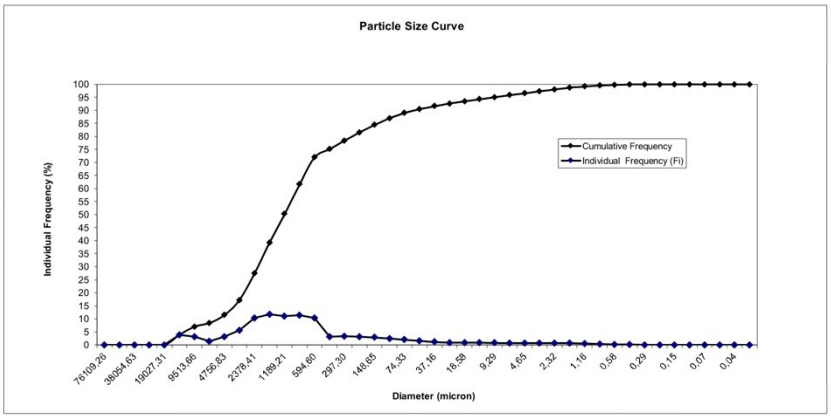

Technician: *Fernanda Dias*

Date:

INSTITUTO HIDROGRÁFICO
DIVISÃO DE GEOLOGIA MARINHA

Station: **2149**

Diameter (class)	Diameter phi	Class midpoint (ci)	Class midpoint (mm)	Individual Frequency (Fi)	Cumulative Frequency	Fi x ci	Fi x (ci-X)^2	Fi x (ci-X)^3
>64.00mm	<6.0 phi	-6,25	76109,26	0,00	0,00	0,00	0,00	0,00
45.25-64.00mm	-5.5,6.0 phi	-5,75	53817,37	0,00	0,00	0,00	0,00	0,00
32.00-45.25mm	-5.0,-5.5 phi	-5,25	38054,63	0,00	0,00	0,00	0,00	0,00
22.63-32.00mm	-4.5,-5.0 phi	-4,75	26908,69	0,00	0,00	0,00	0,00	0,00
16.00-22.63mm	-4.0,-4.5 phi	-4,25	19027,31	0,00	0,00	0,00	0,00	0,00
11.31-16.00mm	-3.5,-4.0 phi	-3,75	13454,34	0,00	0,00	0,00	0,00	0,00
8.00-11.31mm	-3.0,-3.5 phi	-3,25	9513,66	4,49	4,49	-14,60	49,87	-166,16
5.66-8.00mm	-2.5,-3.0 phi	-2,75	6727,17	5,87	10,36	-16,15	47,10	-133,39
4.00-5.66mm	-2.5,-2.0 phi	-2,25	4756,83	4,17	14,54	-9,39	22,69	-52,92
4.00 - 2.83mm	-2.0, -1.5 phi	-1,75	3363,59	6,90	21,43	-12,07	23,15	-42,42
2.83 - 2.00mm	-1.5, -1.0 phi	-1,25	2378,41	13,02	34,45	-16,28	23,11	-30,78
2.00 - 1.41mm	-1.0, -0.5 phi	-0,75	1681,79	13,27	47,72	-9,95	9,19	-7,64
1.41 - 1.00mm	-0.5, 0.0 phi	-0,25	1189,21	11,46	59,18	-2,87	1,26	-0,42
1.00 - 0.71mm	0.0, 0.5 phi	0,25	840,90	10,46	69,63	2,61	0,29	0,05
0.71 - 0.50mm	0.5, 1.0 phi	0,75	594,60	9,46	79,09	7,09	4,22	2,82
500.00 - 354.00µm	1.0, 1.5 phi	1,25	420,45	3,59	82,68	4,48	4,89	5,71
354.00 - 250.00µm	1.5, 2.0 phi	1,75	297,30	3,29	85,97	5,76	9,16	15,27
250.00 - 177.00µm	2.0, 2.5 phi	2,25	210,22	2,58	88,55	5,81	12,13	26,31
177.00 - 125.00µm	2.5, 3.0 phi	2,75	148,65	1,99	90,54	5,46	14,14	37,72
125.00 - 88.40µm	3.0, 3.5 phi	3,25	105,11	1,53	92,06	4,96	15,32	48,52
88.40 - 62.50µm	3.5, 4.0 phi	3,75	74,33	1,11	93,18	4,18	14,99	54,96
62.50 - 44.20µm	4.0, 4..5 phi	4,25	52,56	0,79	93,97	3,38	13,80	57,52
44.20 - 31.25µm	4.5, 5.0 phi	4,75	37,16	0,60	94,58	2,86	13,14	61,33
31.25 - 22.10µm	5.0, 5.5 phi	5,25	26,28	0,51	95,09	2,68	13,64	70,47
22.10 - 15.63µm	5.5, 6.0 phi	5,75	18,58	0,48	95,56	2,75	15,38	87,16
15.63 - 11.00µm	6.0, 6.5 phi	6,25	13,14	0,48	96,04	2,97	18,10	111,63
11.00 - 7.81µm	6.5, 7.0 phi	6,75	9,29	0,47	96,51	3,14	20,68	137,87
7.81 - 5.52µm	7.0, 7.5 phi	7,25	6,57	0,44	96,94	3,18	22,51	161,36
5.52 - 3.91µm	7.5, 8.0 phi	7,75	4,65	0,43	97,37	3,34	25,36	194,47
3.91 - 2.76µm	8.0, 8.5 phi	8,25	3,28	0,47	97,85	3,90	31,56	257,75
2.76 - 1.95µm	8.5, 9.0 phi	8,75	2,32	0,52	98,36	4,51	38,76	336,00
1.95 - 1.38µm	9.0, 9.5 phi	9,25	1,64	0,49	98,86	4,55	41,38	379,41
1.38 - 0.98µm	9.5, 10.0 phi	9,75	1,16	0,40	99,26	3,94	37,75	364,95
0.98 - 0.69µm	10.0, 10.5 phi	10,25	0,82	0,31	99,57	3,15	31,74	322,69
0.69 - 0.49µm	10.5, 11.0 phi	10,75	0,58	0,23	99,79	2,44	25,84	275,68
0.49 - 0.35µm	11.0 , 11.5 phi	11,25	0,41	0,15	99,94	1,68	18,61	207,81
0.35 - 0.24µm	11.5, 12.0 phi	11,75	0,29	0,06	100,00	0,66	7,70	89,81
0.24 - 0.17µm	12.0, 12.5 phi	12,25	0,21	0,00	100,00	0,00	0,00	0,00
0.17 - 0.12µm	12.5, 13.0 phi	12,75	0,15	0,00	100,00	0,00	0,00	0,00
0.12 - 0.09µm	13.0, 13.5 phi	13,25	0,10	0,00	100,00	0,00	0,00	0,00
0.09 - 0.06µm	13.5, 14.0phi	13,75	0,07	0,00	100,00	0,00	0,00	0,00
0.06 - 0.04µm	14.0, 14.5 phi	14,25	0,05	0,00	100,00	0,00	0,00	0,00
0.04 - 0.03µm	14.5, 15.0 phi	14,75	0,04	0,00	100,00	0,00	0,00	0,00
0.03 - 0.02µm	15.0, 15.5 phi	15,25	0,03	0,00	100,00	0,00	0,00	0,00
METHOD: MALVERN laser sedimentograph (particles <2mm)				100,00		8,22	627,44	2873,55
Sieving (particles> 0.5mm)								

Main Classes individual percentages:

Pebble	0,00
Gravel	34,45
Sand	58,72
Silt	4,20
Clay	2,63

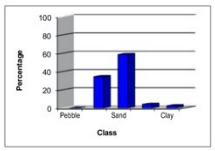

Statistical Parameters:

Mean	0,08
Standard Deviation	2,50
Asymmetry	1,83
P90	2,86
P50	-0,40
P5	-2,94
Mode	-0,75

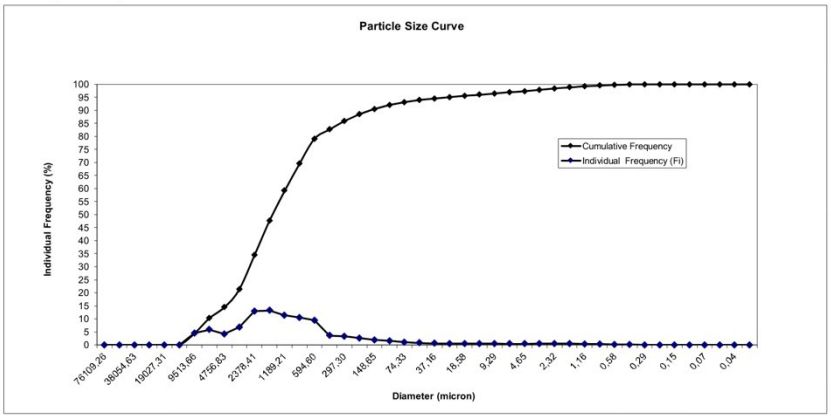

Technician: *Fernanda Dias*

Date:

Annex 11. Sortable silt

Sortable Silt								
Sample	Depth	Sample Weight Total (g)	Capsule	Capsule Weight	Decarbonated Capsule Weight	Final Weight	Carbonate Residue	% SS Carbonated
2104	1	2,372	40,000	31,484	33,201	1,717	0,655	8,127
2105	2	4,727	115,000	41,706	45,208	3,502	1,226	8,350
2106	3	2,158	13,000	39,041	40,633	1,592	0,566	6,680
2107	4	3,224	72,000	43,825	46,257	2,432	0,792	9,095
2108	5	3,263	66,000	41,333	43,850	2,516	0,747	9,318
2109	6	2,820	94,000	41,287	43,444	2,157	0,663	8,799
2110	7	3,126	64,000	44,143	46,536	2,393	0,732	8,815
2111	8	4,002	225,000	40,853	43,964	3,111	0,891	9,268
2112	9	3,086	153,000	42,456	44,832	2,376	0,710	8,908
2113	10	3,822	113,000	31,723	34,711	2,988	0,834	8,963
2114	11	4,558	146,000	50,200	53,780	3,580	0,978	8,750
2115	12	3,135	235,000	45,370	47,833	2,463	0,672	8,471
2116	13	3,279	108,000	42,842	45,410	2,569	0,710	8,443
2117	14	3,725	55,000	37,283	40,216	2,933	0,792	8,666
2118	15	2,692	70,000	44,268	46,360	2,092	0,600	8,742
2119	16	1,666	10,000	41,210	42,484	1,274	0,392	8,248
2120	17	3,067	62,000	39,433	41,832	2,399	0,669	8,207
2121	18	2,667	14,000	40,737	42,867	2,130	0,537	8,219
2122	19	2,563	29,000	41,029	43,058	2,029	0,534	8,118
2123	20	3,588	121,000	35,152	37,977	2,825	0,763	7,809
2124	25	3,796	81,000	32,808	34,823	2,016	1,780	8,095
2125	30	2,887	74,000	33,981	36,200	2,219	0,669	7,630
2126	35	3,332	140,000	41,450	43,943	2,493	0,839	7,779
2127	40	3,353	136,000	33,356	35,837	2,481	0,872	7,657
2128	45	3,814	123,000	45,165	47,941	2,776	1,038	7,032
2129	50	3,792	30,000	41,742	44,490	2,748	1,044	8,344
2130	55	4,807	8,000	42,437	45,898	3,461	1,346	8,002
2131	60	2,887	216,000	43,148	45,155	2,007	0,880	6,468
2132	65	4,516	111,000	40,182	43,270	3,089	1,427	6,247
2133	70	3,992	126,000	35,072	37,813	2,740	1,252	6,375
2134	75	4,794	141,000	41,866	45,069	3,203	1,590	6,249
2135	80	4,161	68,000	40,190	42,970	2,780	1,380	5,973
2136	85	4,112	232,000	45,865	48,720	2,855	1,256	6,737
2137	90	4,432	7,000	39,746	42,584	2,839	1,594	5,318
2138	95	3,368	52,000	41,291	43,427	2,136	1,232	4,880
2139	100	3,456	124,000	39,560	41,638	2,078	1,378	3,729
2140	105	3,787	75,000	32,549	34,620	2,071	1,716	2,964
2141	110	3,772	109,000	42,280	44,297	2,017	1,756	2,072
2142	115	3,830	173,000	44,833	46,847	2,014	1,816	2,977
2143	120	4,564	150,000	62,003	64,083	2,080	2,485	1,968
2144	125	3,849	60,000	44,272	46,043	1,772	2,078	1,795
2145	130	4,935	26,000	44,713	47,138	2,425	2,510	1,605
2146	135	5,748	54,000	32,249	34,815	2,566	3,182	1,459
2147	140	4,542	9,000	39,382	41,402	2,020	2,523	1,308
2148	160	6,325	131,000	43,975	46,854	2,879	3,446	1,057
2149	165	3,696	4,000	45,116	46,461	1,345	2,351	0,573
2105D		4,833	84,000	33,706	37,353	3,647	1,185	
2124D		4,398	96,000	37,269	40,719	3,450	0,948	
2144D		4,504	93,000	41,999	43,992	1,994	2,510	
2148D		5,251	149,000	61,052	63,013	1,961	3,291	

Annex 12. Sandy fraction morphoscopy

Morphoscopy - Fraction 1_0

Sample	Quartz	Philosilicates	Aggregates	Terrigenes	Mollusks	For_Plant	For_Bent	Biogenics	Glauconia	Sum	Quartz	Philosilicates	Aggregates	Terrigenes	Mollusks	For_Plant	For_Bent	Biogenics	Glauconia	Sum	1_0	Fraction Sum
2104										0	#DIV/0!	#DIV/0!	#DIV/0!	#DIV/0!	#DIV/0!	#DIV/0!	#DIV/0!	#DIV/0!	#DIV/0!	#DIV/0!	0,0075	1,1520
2105										0	#DIV/0!	#DIV/0!	#DIV/0!	#DIV/0!	#DIV/0!	#DIV/0!	#DIV/0!	#DIV/0!	#DIV/0!	#DIV/0!	0,0263	3,5301
2106										0	#DIV/0!	#DIV/0!	#DIV/0!	#DIV/0!	#DIV/0!	#DIV/0!	#DIV/0!	#DIV/0!	#DIV/0!	#DIV/0!	0,0044	2,0313
2107										0	#DIV/0!	#DIV/0!	#DIV/0!	#DIV/0!	#DIV/0!	#DIV/0!	#DIV/0!	#DIV/0!	#DIV/0!	#DIV/0!	0,0050	3,2857
2108										0	#DIV/0!	#DIV/0!	#DIV/0!	#DIV/0!	#DIV/0!	#DIV/0!	#DIV/0!	#DIV/0!	#DIV/0!	#DIV/0!	0,0101	2,9645
2109										0	#DIV/0!	#DIV/0!	#DIV/0!	#DIV/0!	#DIV/0!	#DIV/0!	#DIV/0!	#DIV/0!	#DIV/0!	#DIV/0!	0,0048	1,6929
2110										0	#DIV/0!	#DIV/0!	#DIV/0!	#DIV/0!	#DIV/0!	#DIV/0!	#DIV/0!	#DIV/0!	#DIV/0!	#DIV/0!	0,0067	1,7299
2111										0	#DIV/0!	#DIV/0!	#DIV/0!	#DIV/0!	#DIV/0!	#DIV/0!	#DIV/0!	#DIV/0!	#DIV/0!	#DIV/0!	0,0115	1,7703
2112										0	#DIV/0!	#DIV/0!	#DIV/0!	#DIV/0!	#DIV/0!	#DIV/0!	#DIV/0!	#DIV/0!	#DIV/0!	#DIV/0!	0,0146	2,1173
2113										0	#DIV/0!	#DIV/0!	#DIV/0!	#DIV/0!	#DIV/0!	#DIV/0!	#DIV/0!	#DIV/0!	#DIV/0!	#DIV/0!	0,0145	3,5454
2114										0	#DIV/0!	#DIV/0!	#DIV/0!	#DIV/0!	#DIV/0!	#DIV/0!	#DIV/0!	#DIV/0!	#DIV/0!	#DIV/0!	0,0214	3,3409
2115										0	#DIV/0!	#DIV/0!	#DIV/0!	#DIV/0!	#DIV/0!	#DIV/0!	#DIV/0!	#DIV/0!	#DIV/0!	#DIV/0!	0,0102	2,4553
2116										0	#DIV/0!	#DIV/0!	#DIV/0!	#DIV/0!	#DIV/0!	#DIV/0!	#DIV/0!	#DIV/0!	#DIV/0!	#DIV/0!	0,0104	2,7146
2117										0	#DIV/0!	#DIV/0!	#DIV/0!	#DIV/0!	#DIV/0!	#DIV/0!	#DIV/0!	#DIV/0!	#DIV/0!	#DIV/0!	0,0231	2,9680
2118										0	#DIV/0!	#DIV/0!	#DIV/0!	#DIV/0!	#DIV/0!	#DIV/0!	#DIV/0!	#DIV/0!	#DIV/0!	#DIV/0!	0,0063	2,2082
2119										0	#DIV/0!	#DIV/0!	#DIV/0!	#DIV/0!	#DIV/0!	#DIV/0!	#DIV/0!	#DIV/0!	#DIV/0!	#DIV/0!	0,0072	0,9958
2120										0	#DIV/0!	#DIV/0!	#DIV/0!	#DIV/0!	#DIV/0!	#DIV/0!	#DIV/0!	#DIV/0!	#DIV/0!	#DIV/0!	0,0806	3,7001
2121										0	#DIV/0!	#DIV/0!	#DIV/0!	#DIV/0!	#DIV/0!	#DIV/0!	#DIV/0!	#DIV/0!	#DIV/0!	#DIV/0!	0,0150	3,1451
2122										0	#DIV/0!	#DIV/0!	#DIV/0!	#DIV/0!	#DIV/0!	#DIV/0!	#DIV/0!	#DIV/0!	#DIV/0!	#DIV/0!	0,0452	2,7742
2123										0	#DIV/0!	#DIV/0!	#DIV/0!	#DIV/0!	#DIV/0!	#DIV/0!	#DIV/0!	#DIV/0!	#DIV/0!	#DIV/0!	0,0342	4,1132
2124										0	#DIV/0!	#DIV/0!	#DIV/0!	#DIV/0!	#DIV/0!	#DIV/0!	#DIV/0!	#DIV/0!	#DIV/0!	#DIV/0!	0,1354	10,7396
2125										0	#DIV/0!	#DIV/0!	#DIV/0!	#DIV/0!	#DIV/0!	#DIV/0!	#DIV/0!	#DIV/0!	#DIV/0!	#DIV/0!	0,0546	13,4681
2126										0	#DIV/0!	#DIV/0!	#DIV/0!	#DIV/0!	#DIV/0!	#DIV/0!	#DIV/0!	#DIV/0!	#DIV/0!	#DIV/0!	0,1138	14,3714
2127										0	#DIV/0!	#DIV/0!	#DIV/0!	#DIV/0!	#DIV/0!	#DIV/0!	#DIV/0!	#DIV/0!	#DIV/0!	#DIV/0!	0,2588	18,1572
2128										0	#DIV/0!	#DIV/0!	#DIV/0!	#DIV/0!	#DIV/0!	#DIV/0!	#DIV/0!	#DIV/0!	#DIV/0!	#DIV/0!	0,3385	22,9352
2129										0	#DIV/0!	#DIV/0!	#DIV/0!	#DIV/0!	#DIV/0!	#DIV/0!	#DIV/0!	#DIV/0!	#DIV/0!	#DIV/0!	0,4485	18,9258
2130										0	#DIV/0!	#DIV/0!	#DIV/0!	#DIV/0!	#DIV/0!	#DIV/0!	#DIV/0!	#DIV/0!	#DIV/0!	#DIV/0!	1,0805	23,6365
2131	28		38	78	112			44		300	9,3333	0,0000	12,6667	26,0000	37,3333	0,0000	0,0000	14,6667	0,0000	100,0000	1,1706	28,7788
2132	30		43	80	101		1	44		299	10,0334	0,0000	14,3813	26,7559	33,7793	0,0000	0,3344	14,7157	0,0000	100,0000	1,4240	30,3566
2133	35		44	82	125			9		295	11,8644	0,0000	14,9153	27,7966	42,3729	0,0000	0,0000	3,0508	0,0000	100,0000	1,0087	30,5988
2134	64		54	95	140			47		400	16,0000	0,0000	13,5000	23,7500	35,0000	0,0000	0,0000	11,7500	0,0000	100,0000	1,1424	29,8792
2135	40		39	77	110			34		300	13,3333	0,0000	13,0000	25,6667	36,6667	0,0000	0,0000	11,3333	0,0000	100,0000	1,6166	33,8080
2136	33		52	93	122					300	11,0000	0,0000	17,3333	31,0000	40,6667	0,0000	0,0000	0,0000	0,0000	100,0000	2,0765	30,3435
2137	38		44	88	101			29		300	12,6667	0,0000	14,6667	29,3333	33,6667	0,0000	0,0000	9,6667	0,0000	100,0000	2,8941	32,3847
2138	42		50	96	106			6		300	14,0000	0,0000	16,6667	32,0000	35,3333	0,0000	0,0000	2,0000	0,0000	100,0000	4,4001	36,4487
2139	58		63	69	90		2	23		305	19,0164	0,0000	20,6557	22,6230	29,5082	0,0000	0,6557	7,5410	0,0000	100,0000	7,5523	40,1963
2140	43		54	82	116			15		310	13,8710	0,0000	17,4194	26,4516	37,4194	0,0000	0,0000	4,8387	0,0000	100,0000	11,5192	51,9722
2141	36		56	97	98	1	2	9		299	12,0401	0,0000	18,7291	32,4415	32,7759	0,3344	0,6689	3,0100	0,0000	100,0000	10,6071	45,8082
2142	20		42	147	71			24		304	6,5789	0,0000	13,8158	48,3553	23,3553	0,0000	0,0000	7,8947	0,0000	100,0000	10,9818	44,7413
2143	34		56	108	91			11		300	11,3333	0,0000	18,6667	36,0000	30,3333	0,0000	0,0000	3,6667	0,0000	100,0000	20,4827	72,5698
2144	59		28	120	84			9		300	19,6667	0,0000	9,3333	40,0000	28,0000	0,0000	0,0000	3,0000	0,0000	100,0000	22,1988	71,8122
2145	64		56	85	90			5		300	21,3333	0,0000	18,6667	28,3333	30,0000	0,0000	0,0000	1,6667	0,0000	100,0000	25,6973	80,2481
2146	48		46	103	100			3		300	16,0000	0,0000	15,3333	34,3333	33,3333	0,0000	0,0000	1,0000	0,0000	100,0000	28,0663	83,0821
2147	49		54	107	75			15		300	16,3333	0,0000	18,0000	35,6667	25,0000	0,0000	0,0000	5,0000	0,0000	100,0000	28,8555	92,3212
2148	36		47	127	75			15		300	12,0000	0,0000	15,6667	42,3333	25,0000	0,0000	0,0000	5,0000	0,0000	100,0000	87,9936	230,0933
2149	56		32	142	64			6		300	18,6667	0,0000	10,6667	47,3333	21,3333	0,0000	0,0000	2,0000	0,0000	100,0000	29,2870	64,9531

Mosphoscopy - Fraction 0_1

Sample	Quartz	Philosilicates	Aggregates	Terrigenes	Mollusks	For_Plant	For_Bent	Biogenics	Glauconia	Sum	Quartz	Philosilicates	Aggregates	Terrigenes	Mollusks	For_Plant	For_Bent	Biogenics	Glauconia	Sum	0_1	Fraction Sum
2104										0	#DIV/0!	#DIV/0!	#DIV/0!	#DIV/0!	#DIV/0!	#DIV/0!	#DIV/0!	#DIV/0!	#DIV/0!	#DIV/0!	0,0141	1,1520
2105										0	#DIV/0!	#DIV/0!	#DIV/0!	#DIV/0!	#DIV/0!	#DIV/0!	#DIV/0!	#DIV/0!	#DIV/0!	#DIV/0!	0,0507	3,5301
2106										0	#DIV/0!	#DIV/0!	#DIV/0!	#DIV/0!	#DIV/0!	#DIV/0!	#DIV/0!	#DIV/0!	#DIV/0!	#DIV/0!	0,0236	2,0313
2107										0	#DIV/0!	#DIV/0!	#DIV/0!	#DIV/0!	#DIV/0!	#DIV/0!	#DIV/0!	#DIV/0!	#DIV/0!	#DIV/0!	0,0154	3,2857
2108										0	#DIV/0!	#DIV/0!	#DIV/0!	#DIV/0!	#DIV/0!	#DIV/0!	#DIV/0!	#DIV/0!	#DIV/0!	#DIV/0!	0,0316	2,9645
2109										0	#DIV/0!	#DIV/0!	#DIV/0!	#DIV/0!	#DIV/0!	#DIV/0!	#DIV/0!	#DIV/0!	#DIV/0!	#DIV/0!	0,0273	1,6929
2110										0	#DIV/0!	#DIV/0!	#DIV/0!	#DIV/0!	#DIV/0!	#DIV/0!	#DIV/0!	#DIV/0!	#DIV/0!	#DIV/0!	0,0162	1,7299
2111										0	#DIV/0!	#DIV/0!	#DIV/0!	#DIV/0!	#DIV/0!	#DIV/0!	#DIV/0!	#DIV/0!	#DIV/0!	#DIV/0!	0,0143	1,7703
2112										0	#DIV/0!	#DIV/0!	#DIV/0!	#DIV/0!	#DIV/0!	#DIV/0!	#DIV/0!	#DIV/0!	#DIV/0!	#DIV/0!	0,0214	2,1173
2113										0	#DIV/0!	#DIV/0!	#DIV/0!	#DIV/0!	#DIV/0!	#DIV/0!	#DIV/0!	#DIV/0!	#DIV/0!	#DIV/0!	0,0452	3,5454
2114										0	#DIV/0!	#DIV/0!	#DIV/0!	#DIV/0!	#DIV/0!	#DIV/0!	#DIV/0!	#DIV/0!	#DIV/0!	#DIV/0!	0,0504	3,3409
2115										0	#DIV/0!	#DIV/0!	#DIV/0!	#DIV/0!	#DIV/0!	#DIV/0!	#DIV/0!	#DIV/0!	#DIV/0!	#DIV/0!	0,0479	2,4553
2116										0	#DIV/0!	#DIV/0!	#DIV/0!	#DIV/0!	#DIV/0!	#DIV/0!	#DIV/0!	#DIV/0!	#DIV/0!	#DIV/0!	0,0525	2,7146
2117										0	#DIV/0!	#DIV/0!	#DIV/0!	#DIV/0!	#DIV/0!	#DIV/0!	#DIV/0!	#DIV/0!	#DIV/0!	#DIV/0!	0,0449	2,9680
2118										0	#DIV/0!	#DIV/0!	#DIV/0!	#DIV/0!	#DIV/0!	#DIV/0!	#DIV/0!	#DIV/0!	#DIV/0!	#DIV/0!	0,0346	2,2082
2119										0	#DIV/0!	#DIV/0!	#DIV/0!	#DIV/0!	#DIV/0!	#DIV/0!	#DIV/0!	#DIV/0!	#DIV/0!	#DIV/0!	0,0123	0,9958
2120										0	#DIV/0!	#DIV/0!	#DIV/0!	#DIV/0!	#DIV/0!	#DIV/0!	#DIV/0!	#DIV/0!	#DIV/0!	#DIV/0!	0,0731	3,7001
2121										0	#DIV/0!	#DIV/0!	#DIV/0!	#DIV/0!	#DIV/0!	#DIV/0!	#DIV/0!	#DIV/0!	#DIV/0!	#DIV/0!	0,0660	3,1451
2122										0	#DIV/0!	#DIV/0!	#DIV/0!	#DIV/0!	#DIV/0!	#DIV/0!	#DIV/0!	#DIV/0!	#DIV/0!	#DIV/0!	0,0619	2,7742
2123										0	#DIV/0!	#DIV/0!	#DIV/0!	#DIV/0!	#DIV/0!	#DIV/0!	#DIV/0!	#DIV/0!	#DIV/0!	#DIV/0!	0,0776	4,1132
2124										0	#DIV/0!	#DIV/0!	#DIV/0!	#DIV/0!	#DIV/0!	#DIV/0!	#DIV/0!	#DIV/0!	#DIV/0!	#DIV/0!	0,1785	10,7396
2125										0	#DIV/0!	#DIV/0!	#DIV/0!	#DIV/0!	#DIV/0!	#DIV/0!	#DIV/0!	#DIV/0!	#DIV/0!	#DIV/0!	0,1862	13,4681
2126	79		50	69	66	7	2	37	4	314	25,1592	0,0000	15,9236	21,9745	21,0191	2,2293	0,6369	11,7834	1,2739	100,0000	0,2939	14,3714
2127	49		22	65	113			51		300	16,3333	0,0000	7,3333	21,6667	37,6667	0,0000	0,0000	17,0000	0,0000	100,0000	0,5350	18,1572
2128	52		42	54	79	4	7	63		301	17,2757	0,0000	13,9535	17,9402	26,2458	1,3289	2,3256	20,9302	0,0000	100,0000	0,6619	22,9352
2129	49		39	66	79	67		34		334	14,6707	0,0000	11,6766	19,7605	23,6527	20,0599	0,0000	10,1796	0,0000	100,0000	0,8531	18,9258
2130	86		51	67	72			28		304	28,2895	0,0000	16,7763	22,0395	23,6842	0,0000	0,0000	9,2105	0,0000	100,0000	1,6033	23,6365
2131	67		30	96	70	2	2	32		299	22,4080	0,0000	10,0334	32,1070	23,4114	0,6689	0,6689	10,7023	0,0000	100,0000	2,1498	28,7788
2132	74		42	67	76	2		38		299	24,7492	0,0000	14,0468	22,4080	25,4181	0,6689	0,0000	12,7090	0,0000	100,0000	2,9887	30,3566
2133	111		25	81	45			39		301	36,8771	0,0000	8,3056	26,9103	14,9502	0,0000	0,0000	12,9568	0,0000	100,0000	2,6168	30,5988
2134	118		21	76	55	4	3	23		300	39,3333	0,0000	7,0000	25,3333	18,3333	1,3333	1,0000	7,6667	0,0000	100,0000	2,5906	29,8792
2135	79		50	96	37	3		35		300	26,3333	0,0000	16,6667	32,0000	12,3333	1,0000	0,0000	11,6667	0,0000	100,0000	3,9570	33,8080
2136	70		35	64	95	1	2	33		300	23,3333	0,0000	11,6667	21,3333	31,6667	0,3333	0,6667	11,0000	0,0000	100,0000	3,8820	30,3435
2137	45		33	95	102		2	23		300	15,0000	0,0000	11,0000	31,6667	34,0000	0,0000	0,6667	7,6667	0,0000	100,0000	5,8155	32,3847
2138	58		39	95	109	2	5	12		320	18,1250	0,0000	12,1875	29,6875	34,0625	0,6250	1,5625	3,7500	0,0000	100,0000	7,7326	36,4487
2139	64		28	116	56	3	13	20		300	21,3333	0,0000	9,3333	38,6667	18,6667	1,0000	4,3333	6,6667	0,0000	100,0000	13,1092	40,1963
2140	69		18	92	64	6	25	36		310	22,2581	0,0000	5,8065	29,6774	20,6452	1,9355	8,0645	11,6129	0,0000	100,0000	19,4435	51,9722
2141	78		9	88	69	5	38	14	3	304	25,6579	0,0000	2,9605	28,9474	22,6974	1,6447	12,5000	4,6053	0,9868	100,0000	21,2307	45,8082
2142	47		23	119	88		15	8		300	15,6667	0,0000	7,6667	39,6667	29,3333	0,0000	5,0000	2,6667	0,0000	100,0000	18,4664	44,7413
2143	73		51	99	63	2	2	16		306	23,8562	0,0000	16,6667	32,3529	20,5882	0,6536	0,6536	5,2288	0,0000	100,0000	26,5785	72,5698
2144	57		29	124	61		6	24		301	18,9369	0,0000	9,6346	41,1960	20,2658	0,0000	1,9934	7,9734	0,0000	100,0000	25,3085	71,8122
2145	49		33	95	98	4	5	16		300	16,3333	0,0000	11,0000	31,6667	32,6667	1,3333	1,6667	5,3333	0,0000	100,0000	26,4006	80,2481
2146	64		28	95	96	12	3	3		301	21,2625	0,0000	9,3023	31,5615	31,8937	3,9867	0,9967	0,9967	0,0000	100,0000	26,7501	83,0821
2147	70		28	85	81	4	12	20		300	23,3333	0,0000	9,3333	28,3333	27,0000	1,3333	4,0000	6,6667	0,0000	100,0000	33,1957	92,3212
2148	54		39	80	87	7	9	24		300	18,0000	0,0000	13,0000	26,6667	29,0000	2,3333	3,0000	8,0000	0,0000	100,0000	71,8090	230,0933
2149	52		36	102	91	4	3	12	3	303	17,1617	0,0000	11,8812	33,6634	30,0330	1,3201	0,9901	3,9604	0,9901	100,0000	18,7456	64,9531

Mosphoscopy - Fraction 1_2

Sample	Quartz	Philosilicates	Aggregates	Terrigenes	Mollusks	For_Plant	For_Bent	Biogenics	Glauconia	Sum	Quartz	Philosilicates	Aggregates	Terrigenes	Mollusks	For_Plant	For_Bent	Biogenics	Glauconia	Sum	1_2	Fraction Sum
2104		23			23	121	80	75		322	0,0000	7,1429	0,0000	0,0000	7,1429	37,5776	24,8447	23,2919	0,0000	100,0000	0,0351	1,1520
2105	6	15			22	122	86	50	15	316	1,8987	4,7468	0,0000	0,0000	6,9620	38,6076	27,2152	15,8228	4,7468	100,0000	0,0950	3,5301
2106		9			15	138	84	64		310	0,0000	2,9032	0,0000	0,0000	4,8387	44,5161	27,0968	20,6452	0,0000	100,0000	0,0505	2,0313
2107	3	16			9	117	109	46	11	311	0,9646	5,1447	0,0000	0,0000	2,8939	37,6206	35,0482	14,7910	3,5370	100,0000	0,0817	3,2857
2108	1	13			13	117	94	64	13	315	0,3175	4,1270	0,0000	0,0000	4,1270	37,1429	29,8413	20,3175	4,1270	100,0000	0,0807	2,9645
2109	3	25			12	114	87	63		304	0,9868	8,2237	0,0000	0,0000	3,9474	37,5000	28,6184	20,7237	0,0000	100,0000	0,0476	1,6929
2110	5	6			12	119	82	76	10	310	1,6129	1,9355	0,0000	0,0000	3,8710	38,3871	26,4516	24,5161	3,2258	100,0000	0,0414	1,7299
2111		35			6	114	85	60		300	0,0000	11,6667	0,0000	0,0000	2,0000	38,0000	28,3333	20,0000	0,0000	100,0000	0,0473	1,7703
2112		27			7	121	85	60	3	303	0,0000	8,9109	0,0000	0,0000	2,3102	39,9340	28,0528	19,8020	0,9901	100,0000	0,0587	2,1173
2113	2	21			7	116	85	69	4	304	0,6579	6,9079	0,0000	0,0000	2,3026	38,1579	27,9605	22,6974	1,3158	100,0000	0,1001	3,5454
2114		9			18	81	95	97	4	304	0,0000	2,9605	0,0000	0,0000	5,9211	26,6447	31,2500	31,9079	1,3158	100,0000	0,0971	3,3409
2115	2	19	3	5	20	89	106	56	3	303	0,6601	6,2706	0,9901	1,6502	6,6007	29,3729	34,9835	18,4818	0,9901	100,0000	0,0708	2,4553
2116	3	5			7	120	102	63		300	1,0000	1,6667	0,0000	0,0000	2,3333	40,0000	34,0000	21,0000	0,0000	100,0000	0,0600	2,7146
2117	2	8			10	125	103	52		300	0,6667	2,6667	0,0000	0,0000	3,3333	41,6667	34,3333	17,3333	0,0000	100,0000	0,0650	2,9680
2118		16			25	79	94	87		301	0,0000	5,3156	0,0000	0,0000	8,3056	26,2458	31,2292	28,9037	0,0000	100,0000	0,0667	2,2082
2119	2		2	1	18	119	106	53		301	0,6645	0,0000	0,6645	0,3322	5,9801	39,5349	35,2159	17,6080	0,0000	100,0000	0,0300	0,9958
2120		20			58	159	101	73		411	0,0000	4,8662	0,0000	0,0000	14,1119	38,6861	24,5742	17,7616	0,0000	100,0000	0,0858	3,7001
2121	2	9			27	117	79	66	5	305	0,6557	2,9508	0,0000	0,0000	8,8525	38,3607	25,9016	21,6393	1,6393	100,0000	0,0887	3,1451
2122	2				37	104	86	71	3	303	0,6601	0,0000	0,0000	0,0000	12,2112	34,3234	28,3828	23,4323	0,9901	100,0000	0,0752	2,7742
2123					33	125	96	47	4	305	0,0000	0,0000	0,0000	0,0000	10,8197	40,9836	31,4754	15,4098	1,3115	100,0000	0,1126	4,1132
2124	2	15			26	104	74	75	7	303	0,6601	4,9505	0,0000	0,0000	8,5809	34,3234	24,4224	24,7525	2,3102	100,0000	0,2733	10,7396
2125					34	129	72	65	6	306	0,0000	0,0000	0,0000	0,0000	11,1111	42,1569	23,5294	21,2418	1,9608	100,0000	0,4847	13,4681
2126	2				55	85	67	92	4	305	0,6557	0,0000	0,0000	0,0000	18,0328	27,8689	21,9672	30,1639	1,3115	100,0000	0,4801	14,3714
2127	2	5			34	124	79	56	8	308	0,6494	1,6234	0,0000	0,0000	11,0390	40,2597	25,6494	18,1818	2,5974	100,0000	0,7152	18,1572
2128			3	5	46	112	59	75	6	306	0,0000	0,0000	0,9804	1,6340	15,0327	36,6013	19,2810	24,5098	1,9608	100,0000	1,0177	22,9352
2129	1		7	10	70	117	104	90	10	409	0,2445	0,0000	1,7115	2,4450	17,1149	28,6064	25,4279	22,0049	2,4450	100,0000	0,8464	18,9258
2130				7	55	100	67	72	8	309	0,0000	0,0000	0,0000	2,2654	17,7994	32,3625	21,6828	23,3010	2,5890	100,0000	1,1196	23,6365
2131	2			5	33	95	70	94	7	306	0,6536	0,0000	0,0000	1,6340	10,7843	31,0458	22,8758	30,7190	2,2876	100,0000	1,5363	28,7788
2132	2		2	4	56	104	63	68	11	310	0,6452	0,0000	0,6452	1,2903	18,0645	33,5484	20,3226	21,9355	3,5484	100,0000	1,8835	30,3566
2133	4	8			25	115	65	82	9	308	1,2987	2,5974	0,0000	0,0000	8,1169	37,3377	21,1039	26,6234	2,9221	100,0000	1,8180	30,5988
2134	4		10		47	117	65	57	9	309	1,2945	0,0000	3,2362	0,0000	15,2104	37,8641	21,0356	18,4466	2,9126	100,0000	1,6631	29,8792
2135	3		3	8	42	106	82	56	3	303	0,9901	0,0000	0,9901	2,6403	13,8614	34,9835	27,0627	18,4818	0,9901	100,0000	2,1340	33,8080
2136	4		1	10	49	113	81	52	2	312	1,2821	0,0000	0,3205	3,2051	15,7051	36,2179	25,9615	16,6667	0,6410	100,0000	1,7542	30,3435
2137	7		6	7	52	95	76	57	3	303	2,3102	0,0000	1,9802	2,3102	17,1617	31,3531	25,0825	18,8119	0,9901	100,0000	2,0684	32,3847
2138	8			12	34	94	95	57	2	302	2,6490	0,0000	0,0000	3,9735	11,2583	31,1258	31,4570	18,8742	0,6623	100,0000	2,2231	36,4487
2139	19		14	27	42	63	86	49	6	306	6,2092	0,0000	4,5752	8,8235	13,7255	20,5882	28,1046	16,0131	1,9608	100,0000	2,8396	40,1963
2140	41			53	52	47	68	39	7	307	13,3550	0,0000	0,0000	17,2638	16,9381	15,3094	22,1498	12,7036	2,2801	100,0000	4,6145	51,9722
2141	53		5	68	69	17	54	34	16	316	16,7722	0,0000	1,5823	21,5190	21,8354	5,3797	17,0886	10,7595	5,0633	100,0000	4,3543	45,8082
2142	59		11	63	62	35	56	14	11	311	18,9711	0,0000	3,5370	20,2572	19,9357	11,2540	18,0064	4,5016	3,5370	100,0000	4,3790	44,7413
2143	50		16	74	78	14	40	28	17	317	15,7729	0,0000	5,0473	23,3438	24,6057	4,4164	12,6183	8,8328	5,3628	100,0000	7,6664	72,5698
2144	55		18	50	68	27	57	25	23	323	17,0279	0,0000	5,5728	15,4799	21,0526	8,3591	17,6471	7,7399	7,1207	100,0000	7,7608	71,8122
2145	80		16	77	62	8	29	26	15	313	25,5591	0,0000	5,1118	24,6006	19,8083	2,5559	9,2652	8,3067	4,7923	100,0000	8,9832	80,2481
2146	40		19	74	109	12	30	26	5	315	12,6984	0,0000	6,0317	23,4921	34,6032	3,8095	9,5238	8,2540	1,5873	100,0000	9,0299	83,0821
2147	77		25	47	74	12	25	40	6	306	25,1634	0,0000	8,1699	15,3595	24,1830	3,9216	8,1699	13,0719	1,9608	100,0000	10,2452	92,3212
2148	44		32	63	83	13	31	34	4	304	14,4737	0,0000	10,5263	20,7237	27,3026	4,2763	10,1974	11,1842	1,3158	100,0000	23,7023	230,0933
2149	59		19	65	134	1	11	11	2	302	19,5364	0,0000	6,2914	21,5232	44,3709	0,3311	3,6424	3,6424	0,6623	100,0000	6,9449	64,9531

Mosphoscopy - Fraction 2_3

Sample	Quartz	Philosilicates	Aggregates	Terrigenes	Mollusks	For_Plant	For_Bent	Biogenics	Glauconia	Sum	Quartz	Philosilicates	Aggregates	Terrigenes	Mollusks	For_Plant	For_Bent	Biogenics	Glauconia	Sum	2_3	Fraction Sum
2104	5	13			4	133	91	74	34	354	1,4124	3,6723	0,0000	0,0000	1,1299	37,5706	25,7062	20,9040	9,6045	100,0000	0,2415	1,1520
2105		51			2	109	76	64	15	317	0,0000	16,0883	0,0000	0,0000	0,6309	34,3849	23,9748	20,1893	4,7319	100,0000	0,7301	3,3301
2106		43			5	113	92	57	13	323	0,0000	13,3127	0,0000	0,0000	1,5480	34,9845	28,4830	17,6471	4,0248	100,0000	0,4270	2,0313
2107		73				102	64	61	19	319	0,0000	22,8840	0,0000	0,0000	0,0000	31,9749	20,0627	19,1223	5,9561	100,0000	0,6791	3,2857
2108		49			3	99	107	43	28	329	0,0000	14,8936	0,0000	0,0000	0,9119	30,0912	32,5228	13,0699	8,5106	100,0000	0,5994	2,9645
2109		35			4	97	124	40	25	325	0,0000	10,7692	0,0000	0,0000	1,2308	29,8462	38,1538	12,3077	7,6923	100,0000	0,3342	1,6929
2110		50				84	105	61	21	321	0,0000	15,5763	0,0000	0,0000	0,0000	26,1682	32,7103	19,0031	6,5421	100,0000	0,3236	1,7299
2111		58				97	70	76	29	330	0,0000	17,5758	0,0000	0,0000	0,0000	29,3939	21,2121	23,0303	8,7879	100,0000	0,3410	1,7703
2112		45				96	94	65	13	313	0,0000	14,3770	0,0000	0,0000	0,0000	30,6709	30,0319	20,7668	4,1534	100,0000	0,4277	2,1173
2113		61				84	97	68	11	321	0,0000	19,0031	0,0000	0,0000	0,0000	26,1682	30,2181	21,1838	3,4268	100,0000	0,7464	3,5454
2114		68			3	108	91	64	13	347	0,0000	19,5965	0,0000	0,0000	0,8646	31,1239	26,2248	18,4438	3,7464	100,0000	0,7140	3,3409
2115		39			10	119	86	46	8	308	0,0000	12,6623	0,0000	0,0000	3,2468	38,6364	27,9221	14,9351	2,5974	100,0000	0,5233	2,4553
2116		55			3	86	108	48	8	308	0,0000	17,8571	0,0000	0,0000	0,9740	27,9221	35,0649	15,5844	2,5974	100,0000	0,5301	2,7146
2117	2	37			5	125	110	35	21	335	0,5970	11,0448	0,0000	0,0000	1,4925	37,3134	32,8358	10,4478	6,2687	100,0000	0,5640	2,9680
2118		43			15	100	79	63	15	315	0,0000	13,6508	0,0000	0,0000	4,7619	31,7460	25,0794	20,0000	4,7619	100,0000	0,4570	2,2082
2119		20			28	120	82	50	18	318	0,0000	6,2893	0,0000	0,0000	8,8050	37,7358	25,7862	15,7233	5,6604	100,0000	0,2147	0,9958
2120		40			22	105	104	39	7	317	0,0000	12,6183	0,0000	0,0000	6,9401	33,1230	32,8076	12,3028	2,2082	100,0000	0,7308	3,7001
2121		56			25	102	81	35	9	308	0,0000	18,1818	0,0000	0,0000	8,1169	33,1169	26,2987	11,3636	2,9221	100,0000	0,6962	3,1451
2122	3	37			4	95	85	33	7	307	0,9772	12,0521	0,0000	0,0000	15,3094	30,9446	27,6873	10,7492	2,2801	100,0000	0,5619	2,7742
2123		42			30	116	74	38	8	308	0,0000	13,6364	0,0000	0,0000	9,7403	37,6623	24,0260	12,3377	2,5974	100,0000	0,8402	4,1132
2124	2	34			37	144	69	14	12	312	0,6410	10,8974	0,0000	0,0000	11,8590	46,1538	22,1154	4,4872	3,8462	100,0000	2,1356	10,7396
2125		38			42	106	81	34	10	311	0,0000	12,2186	0,0000	0,0000	13,5048	34,0836	26,0450	10,9325	3,2154	100,0000	3,1279	13,4681
2126	8	34			46	114	66	32	8	308	2,5974	11,0390	0,0000	0,0000	14,9351	37,0130	21,4286	10,3896	2,5974	100,0000	3,4259	14,3714
2127		25			38	122	83	37	12	317	0,0000	7,8864	0,0000	0,0000	11,9874	38,4858	26,1830	11,6719	3,7855	100,0000	4,3617	18,1572
2128		30			46	95	86	43	15	315	0,0000	9,5238	0,0000	0,0000	14,6032	30,1587	27,3016	13,6508	4,7619	100,0000	5,5258	22,9352
2129	5	34		3	28	133	57	41	10	311	1,6077	10,9325	0,0000	0,9646	9,0032	42,7653	18,3280	13,1833	3,2154	100,0000	4,4048	18,9258
2130		40		2	42	97	62	48	11	302	0,0000	13,2450	0,0000	0,6623	13,9073	32,1192	20,5298	15,8940	3,6424	100,0000	5,3108	23,6365
2131	9	31			12	128	76	64	8	328	2,7439	9,4512	0,0000	0,0000	3,6585	39,0244	23,1707	19,5122	2,4390	100,0000	6,5124	28,7788
2132	1	5		1	42	108	86	78	8	329	0,3040	1,5198	0,0000	0,3040	12,7660	32,8267	26,1398	23,7082	2,4316	100,0000	6,5936	30,3566
2133	2	20			53	101	88	54	7	325	0,6154	6,1538	0,0000	0,0000	16,3077	31,0769	27,0769	16,6154	2,1538	100,0000	6,8509	30,5988
2134	3	16			28	109	77	68	10	311	0,9646	5,1447	0,0000	0,0000	9,0032	35,0482	24,7588	21,8650	3,2154	100,0000	6,4681	29,8792
2135	3	16			43	84	85	69	8	308	0,9740	5,1948	0,0000	0,0000	13,9610	27,2727	27,5974	22,4026	2,5974	100,0000	7,3832	33,8080
2136	2	18		3	35	99	71	72	7	307	0,6515	5,8632	0,0000	0,9772	11,4007	32,2476	23,1270	23,4528	2,2801	100,0000	6,2916	30,3435
2137	3	23		5	45	89	77	58	6	306	0,9804	7,5163	0,0000	1,6340	14,7059	29,0850	25,1634	18,9542	1,9608	100,0000	6,1231	32,3847
2138	9	19		4	38	83	89	58	5	305	2,9508	6,2295	0,0000	1,3115	12,4590	27,2131	29,1803	19,0164	1,6393	100,0000	6,2095	36,4487
2139	22	13	1	14	47	86	89	28	2	302	7,2848	4,3046	0,3311	4,6358	15,5629	28,4768	29,4702	9,2715	0,6623	100,0000	5,0236	40,1963
2140	40	6		12	42	86	93	34	9	322	12,4224	1,8634	0,0000	3,7267	13,0435	26,7081	28,8820	10,5590	2,7950	100,0000	5,8232	51,9722
2141	45			30	31	54	99	41	5	305	14,7541	0,0000	0,0000	9,8361	10,1639	17,7049	32,4590	13,4426	1,6393	100,0000	4,0656	45,8082
2142	37			25	53	74	63	48	7	307	12,0521	0,0000	0,0000	8,1433	17,2638	24,1042	20,5212	15,6352	2,2801	100,0000	4,6553	44,7413
2143	101			17	56	47	51	28	7	307	32,8990	0,0000	0,0000	5,5375	18,2410	15,3094	16,6124	9,1205	2,2801	100,0000	8,2542	72,5698
2144	69	6	1	63	47	33	42	47	9	317	21,7666	1,8927	0,3155	19,8738	14,8265	10,4101	13,2492	14,8265	2,8391	100,0000	8,6639	71,8122
2145	109			32	63	18	42	42	7	313	34,8243	0,0000	0,0000	10,2236	20,1278	5,7508	13,4185	13,4185	2,2364	100,0000	9,4270	80,2481
2146	104		12	30	40	24	46	44	7	307	33,8762	0,0000	3,9088	9,7720	13,0293	7,8176	14,9837	14,3322	2,2801	100,0000	9,4290	83,0821
2147	85		7	53	43	35	50	40	11	324	26,2346	0,0000	2,1605	16,3580	13,2716	10,8025	15,4321	12,3457	3,3951	100,0000	10,0093	92,3212
2148	96		2	52	57	25	36	36	5	309	31,0680	0,0000	0,6472	16,8285	18,4466	8,0906	11,6505	11,6505	1,6181	100,0000	23,5110	230,0933
2149	94		4	63	93	7	24	15	7	307	30,6189	0,0000	1,3029	20,5212	30,2932	2,2801	7,8176	4,8860	2,2801	100,0000	5,5679	64,9531

Mosphoscopy - Fraction 3_4

Sample	Quartz	Philosilicates	Aggregates	Terrigenes	Mollusks	For_Plant	For_Bent	Biogenics	Glauconia	Sum	Quartz	Philosilicates	Aggregates	Terrigenes	Mollusks	For_Plant	For_Bent	Biogenics	Glauconia	Sum	3_4	Fraction Sum
2104	53	39				67	83	56	31	329	16,1094	11,8541	0,0000	0,0000	0,0000	20,3647	25,2280	17,0213	9,4225	100,0000	0,8538	1,1520
2105	27	63				66	94	50	21	321	8,4112	19,6262	0,0000	0,0000	0,0000	20,5607	29,2835	15,5763	6,5421	100,0000	2,6280	3,5301
2106	25	58				70	83	63	10	309	8,0906	18,7702	0,0000	0,0000	0,0000	22,6537	26,8608	20,3883	3,2362	100,0000	1,5258	2,0313
2107	25	83				58	88	46	26	326	7,6687	25,4601	0,0000	0,0000	0,0000	17,7914	26,9939	14,1104	7,9755	100,0000	2,5045	3,2857
2108	54	77				68	81	21	35	336	16,0714	22,9167	0,0000	0,0000	0,0000	20,2381	24,1071	6,2500	10,4167	100,0000	2,2427	2,9645
2109	36	64				70	72	58	36	336	10,7143	19,0476	0,0000	0,0000	0,0000	20,8333	21,4286	17,2619	10,7143	100,0000	1,2790	1,6929
2110	31	40				75	104	45	14	309	10,0324	12,9450	0,0000	0,0000	0,0000	24,2718	33,6570	14,5631	4,5307	100,0000	1,3430	1,7299
2111	26	65				76	86	38	31	322	8,0745	20,1863	0,0000	0,0000	0,0000	23,6025	26,7081	11,8012	9,6273	100,0000	1,3562	1,7703
2112	29	52				92	111	16	10	310	9,3548	16,7742	0,0000	0,0000	0,0000	29,6774	35,8065	5,1613	3,2258	100,0000	1,5949	2,1173
2113	21	56				80	105	48	15	325	6,4615	17,2308	0,0000	0,0000	0,0000	24,6154	32,3077	14,7692	4,6154	100,0000	2,6392	3,5454
2114	49	67				95	61	28	30	330	14,8485	20,3030	0,0000	0,0000	0,0000	28,7879	18,4848	8,4848	9,0909	100,0000	2,4580	3,3409
2115	28	50			3	111	82	26	13	313	8,9457	15,9744	0,0000	0,0000	0,9585	35,4633	26,1981	8,3067	4,1534	100,0000	1,8031	2,4553
2116	16	61				83	99	41	15	315	5,0794	19,3651	0,0000	0,0000	0,0000	26,3492	31,4286	13,0159	4,7619	100,0000	2,0636	2,7146
2117	31	51				97	82	39	10	310	10,0000	16,4516	0,0000	0,0000	0,0000	31,2903	26,4516	12,5806	3,2258	100,0000	2,2710	2,9680
2118	29	67			4	78	71	51	33	333	8,7087	20,1201	0,0000	0,0000	1,2012	23,4234	21,3213	15,3153	9,9099	100,0000	1,6436	2,2082
2119	45	48			19	70	84	34	11	311	14,4695	15,4341	0,0000	0,0000	6,1093	22,5080	27,0096	10,9325	3,5370	100,0000	0,7316	0,9958
2120	23	46			14	76	106	35	18	318	7,2327	14,4654	0,0000	0,0000	4,4025	23,8994	33,3333	11,0063	5,6604	100,0000	2,2798	3,7001
2121	34	60			12	76	66	52	15	315	10,7937	19,0476	0,0000	0,0000	3,8095	24,1270	20,9524	16,5079	4,7619	100,0000	2,2792	3,1451
2122	36	75			13	54	64	49	12	303	11,8812	24,7525	0,0000	0,0000	4,2904	17,8218	21,1221	16,1716	3,9604	100,0000	2,0300	2,7742
2123	68	61			7	66	52	38	14	306	22,2222	19,9346	0,0000	0,0000	2,2876	21,5686	16,9935	12,4183	4,5752	100,0000	3,0486	4,1132
2124	61	40			26	71	72	31	11	312	19,5513	12,8205	0,0000	0,0000	8,3333	22,7564	23,0769	9,9359	3,5256	100,0000	8,0168	10,7396
2125	90	47			8	64	57	34	11	311	28,9389	15,1125	0,0000	0,0000	2,5723	20,5788	18,3280	10,9325	3,5370	100,0000	9,6147	13,4681
2126	64	46			26	77	66	21	12	312	20,5128	14,7436	0,0000	0,0000	8,3333	24,6795	21,1538	6,7308	3,8462	100,0000	10,0577	14,3714
2127	70	44			28	60	63	35	14	314	22,2930	14,0127	0,0000	0,0000	8,9172	19,1083	20,0637	11,1465	4,4586	100,0000	12,2865	18,1572
2128	55	51			17	72	68	37	20	320	17,1875	15,9375	0,0000	0,0000	5,3125	22,5000	21,2500	11,5625	6,2500	100,0000	15,3913	22,9352
2129	51	49			44	78	42	35	15	315	16,1905	15,5556	0,0000	0,0000	13,9683	25,0794	13,3333	11,1111	4,7619	100,0000	12,3730	18,9258
2130	54	36		7	24	71	73	31	9	305	17,7049	11,8033	0,0000	2,2951	7,8689	23,2787	23,9344	10,1639	2,9508	100,0000	14,5223	23,6365
2131	23	41			22	87	96	30	8	307	7,4919	13,3550	0,0000	0,0000	7,1661	28,3388	31,2704	9,7720	2,6059	100,0000	17,4097	28,7788
2132	52	18			52	102	53	23	9	309	16,8285	5,8252	0,0000	0,0000	16,8285	33,0097	17,1521	7,4434	2,9126	100,0000	17,4668	30,3566
2133	60	30			27	45	90	48	11	311	19,2926	9,6463	0,0000	0,0000	8,6817	14,4695	28,9389	15,4341	3,5370	100,0000	18,3044	30,5988
2134	71	29			26	56	83	35	12	312	22,7564	9,2949	0,0000	0,0000	8,3333	17,9487	26,6026	11,2179	3,8462	100,0000	18,0150	29,8792
2135	29	30			35	74	88	44	5	305	9,5082	9,8361	0,0000	0,0000	11,4754	24,2623	28,8525	14,4262	1,6393	100,0000	18,7172	33,8080
2136	40	21		11	33	58	81	56	6	306	13,0719	6,8627	0,0000	3,5948	10,7843	18,9542	26,4706	18,3007	1,9608	100,0000	16,3392	30,3435
2137	65		1	13	37	52	79	53	4	304	21,3816	0,0000	0,3289	4,2763	12,1711	17,1053	25,9868	17,4342	1,3158	100,0000	15,4836	32,3847
2138	77	19		11	31	55	71	36	2	302	25,4967	6,2914	0,0000	3,6424	10,2649	18,2119	23,5099	11,9205	0,6623	100,0000	15,8834	36,4487
2139	44	8		10	52	48	95	43	3	303	14,5215	2,6403	0,0000	3,3003	17,1617	15,8416	31,3531	14,1914	0,9901	100,0000	11,6716	40,1963
2140	47	20		9	26	48	88	62	5	305	15,4098	6,5574	0,0000	2,9508	8,5246	15,7377	28,8525	20,3279	1,6393	100,0000	10,5738	51,9722
2141	31			28	29	71	105	36	2	302	10,2649	0,0000	0,0000	9,2715	9,6026	23,5099	34,7682	11,9205	0,6623	100,0000	5,5505	45,8082
2142	49			10	47	72	83	39	5	305	16,0656	0,0000	0,0000	3,2787	15,4098	23,6066	27,2131	12,7869	1,6393	100,0000	6,2588	44,7413
2143	80			45	53	35	54	33	6	306	26,1438	0,0000	0,0000	14,7059	17,3203	11,4379	17,6471	10,7843	1,9608	100,0000	9,5880	72,5698
2144	99			17	61	33	52	38	4	304	32,5658	0,0000	0,0000	5,5921	20,0658	10,8553	17,1053	12,5000	1,3158	100,0000	7,8802	71,8122
2145	152			40	40	8	22	38	3	303	50,1650	0,0000	0,0000	13,2013	13,2013	2,6403	7,2607	12,5413	0,9901	100,0000	9,7400	80,2481
2146	117			53	49	18	32	33	5	307	38,1107	0,0000	0,0000	17,2638	15,9609	5,8632	10,4235	10,7492	1,6287	100,0000	9,8068	83,0821
2147	118			40	52	16	39	35	2	302	39,0728	0,0000	0,0000	13,2450	17,2185	5,2980	12,9139	11,5894	0,6623	100,0000	10,0155	92,3212
2148	137		2	48	60	9	26	18	3	303	45,2145	0,0000	0,6601	15,8416	19,8020	2,9703	8,5809	5,9406	0,9901	100,0000	23,0774	230,0933
2149	161			46	59	4	15	15	2	302	53,3113	0,0000	0,0000	15,2318	19,5364	1,3245	4,9669	4,9669	0,6623	100,0000	4,4077	64,9531

Morphoscopy - Fraction Weight

Sample	1_0	0_1	1_2	2_3	3_4	Fraction Sum	Tot Weight
2104	0,0075	0,0141	0,0351	0,2415	0,8538	1,1520	0,0770
2105	0,0263	0,0507	0,0950	0,7301	2,6280	3,5301	0,1147
2106	0,0044	0,0236	0,0505	0,4270	1,5258	2,0313	0,0374
2107	0,0050	0,0154	0,0817	0,6791	2,5045	3,2857	0,0385
2108	0,0101	0,0316	0,0807	0,5994	2,2427	2,9645	0,0631
2109	0,0048	0,0273	0,0476	0,3342	1,2790	1,6929	0,0408
2110	0,0067	0,0162	0,0414	0,3236	1,3420	1,7299	0,0330
2111	0,0115	0,0143	0,0473	0,3410	1,3562	1,7703	0,0317
2112	0,0146	0,0214	0,0587	0,4277	1,5949	2,1173	0,0655
2113	0,0145	0,0452	0,1001	0,7464	2,6392	3,5454	0,0693
2114	0,0214	0,0504	0,0971	0,7140	2,4580	3,3409	0,1296
2115	0,0102	0,0479	0,0708	0,5233	1,8031	2,4553	0,1339
2116	0,0104	0,0525	0,0600	0,5301	2,0616	2,7146	0,1711
2117	0,0231	0,0449	0,0650	0,5640	2,2710	2,9680	0,0955
2118	0,0063	0,0346	0,0667	0,4570	1,6436	2,2082	0,0676
2119	0,0072	0,0123	0,0300	0,2147	0,7316	0,9958	0,0399
2120	0,0806	0,0731	0,0858	0,7308	2,7298	3,7001	0,1953
2121	0,0150	0,0660	0,0887	0,6962	2,2792	3,1451	0,1263
2122	0,0452	0,0619	0,0752	0,5619	2,0300	2,7742	0,1141
2123	0,0342	0,0776	0,1126	0,8402	3,0486	4,1132	0,1399
2124	0,1354	0,1785	0,2733	2,1356	8,0168	10,7396	0,5149
2125	0,0546	0,1862	0,4847	3,1279	9,6147	13,4681	0,2782
2126	0,1138	0,2939	0,4801	3,4259	10,0577	14,3714	0,5701
2127	0,2588	0,5350	0,7152	4,3617	12,2865	18,1572	1,7563
2128	0,3385	0,6619	1,0177	5,5258	15,3913	22,9352	1,4797
2129	0,4485	0,8531	0,8464	4,4048	12,3730	18,9258	1,9762
2130	1,0805	1,6033	1,1196	5,3108	14,5223	23,6365	3,5938
2131	1,1706	2,1498	1,5363	6,5124	17,4097	28,7788	4,2604
2132	1,4240	2,9887	1,8835	6,5936	17,4668	30,3566	5,6255
2133	1,0087	2,6168	1,8180	6,8509	18,3044	30,5988	4,4979
2134	1,1424	2,5906	1,6631	6,4681	18,0150	29,8792	4,6098
2135	1,6166	3,9570	2,1340	7,3832	18,7172	33,8080	6,8311
2136	2,0765	3,8820	1,7542	6,2916	16,3392	30,3435	7,0890
2137	2,8941	5,8155	2,0684	6,1231	15,4836	32,3847	11,0782
2138	4,4001	7,7326	2,2231	6,2095	15,8834	36,4487	16,3782
2139	7,5523	13,1092	2,8396	5,0236	11,6716	40,1963	28,2343
2140	11,5192	19,4435	4,6145	5,8232	10,5718	51,9722	42,4874
2141	10,6071	21,2307	4,3543	4,0656	5,5505	45,8082	43,0992
2142	10,9818	18,4664	4,3790	4,6553	6,2588	44,7413	39,6241
2143	20,4827	26,5785	7,6664	8,2542	9,5880	72,5698	57,6560
2144	22,1988	25,3085	7,7608	8,6639	7,8802	71,8122	58,3148
2145	25,6973	26,4006	8,9832	9,4270	9,7400	80,2481	61,9284
2146	28,0663	26,7501	9,0299	9,4290	9,8068	83,0821	81,3943
2147	28,8555	33,1957	10,2452	10,0093	10,0155	92,3212	86,3513
2148	87,9936	71,8090	23,7023	23,5110	23,0774	230,0933	266,6073
2149	29,2870	18,7456	6,9449	5,5679	4,4077	64,9531	90,6058

Annex 13. Fine fraction mineralogy

Mineralogy - Fine Fraction															
Depth (cm)	Clorite (%)	Ilite (%)	Caulinite (%)	Quartzo (%)	Opala (%)	Anidrite (%)	Aragonite (%)	Felds_Potassico (%)	Plagioclase (%)	Calcite (%)	Calcite Mg (%)	Dolomite (%)	Siderite (%)	Pirite (%)	Fluorite (%)
2	2.35	24.29	4.32	10.10	3.47	1.31	0.00	5.29	12.47	30.46	0.00	1.00	0.81	2.20	1.79
4	0.00	12.78	2.77	15.03	4.39	1.68	0.00	5.00	8.93	44.17	0.00	0.00	1.15	2.07	2.65
6	0.00	12.35	2.29	12.24	2.93	1.53	0.00	18.36	5.63	34.95	0.00	6.02	1.29	1.41	1.68
8	1.91	19.88	2.93	12.02	5.67	1.69	0.00	4.87	7.77	38.80	0.00	0.00	1.20	1.97	1.51
10	0.00	17.27	0.00	13.39	5.31	1.79	2.77	6.19	8.10	39.80	0.00	0.00	1.22	2.14	2.52
12	1.23	11.01	2.90	11.39	6.52	1.52	0.00	17.09	7.40	35.70	0.00	0.00	1.47	1.76	2.18
14	2.00	13.19	2.78	12.68	5.22	1.32	0.00	5.50	10.14	37.50	0.00	2.85	2.02	3.21	2.25
16	1.67	17.09	2.84	13.00	4.17	1.04	2.92	11.35	7.75	34.60	0.00	0.00	0.81	1.69	1.27
18	1.99	9.15	2.97	13.64	3.55	1.09	0.00	20.46	8.16	32.60	0.00	2.19	0.92	1.90	1.93
20	1.34	12.11	2.21	13.58	3.96	0.00	2.82	4.75	12.23	40.40	0.00	2.26	1.23	2.07	1.87
25	0.00	14.24	2.69	14.09	4.46	1.74	2.09	6.37	7.67	38.20	0.00	3.81	1.46	2.19	1.85
30	0.00	15.12	2.73	11.31	4.42	1.69	0.00	4.89	7.13	44.67	0.00	2.49	1.88	3.65	0.00
40	0.00	6.07	1.91	10.60	1.68	1.57	3.90	15.90	5.26	46.30	0.00	1.65	1.52	2.68	1.74
50	1.27	6.11	1.88	14.43	7.09	1.40	2.90	3.45	6.72	44.60	0.00	3.09	1.43	3.44	2.23
60	0.00	10.59	2.25	12.38	6.10	0.94	3.13	4.32	4.81	43.60	0.00	6.35	0.76	2.98	2.40
70	0.00	10.19	1.59	11.09	3.04	2.22	5.01	4.70	5.56	47.70	0.00	2.95	0.67	3.26	2.76
80	0.00	9.65	3.38	10.89	2.72	1.32	3.58	3.38	7.62	49.80	0.00	0.00	0.58	3.73	3.07
90	1.74	6.20	1.37	11.36	3.07	0.86	3.40	17.03	6.20	29.80	10.35	0.31	3.42	3.42	2.11
100	0.00	8.97	1.08	13.78	2.85	0.76	3.60	20.67	6.19	23.90	9.85	0.00	3.64	3.64	1.85
110	0.00	4.13	1.05	8.99	0.00	0.39	6.55	13.49	5.25	33.90	11.96	0.00	6.16	6.16	2.09
120	0.00	5.49	1.11	5.72	1.06	0.00	8.63	8.57	2.16	37.90	14.21	0.00	6.66	6.66	2.57
130	0.00	4.02	0.94	5.67	0.00	0.00	10.27	8.50	1.95	33.90	18.12	0.00	7.57	7.57	2.14

Annex 14. Heavy mineral data

Heavy minerals percentage (%)

Depth (cm)	0.250 mm	0.125 mm	0.063 mm	Sum	Tour	And	Stau	Gar	Phylo	Zir
1	0,000	0,000	0,001	0,001	0,008	0,000	0,012	0,004	0,146	0,000
2	0,000	0,000	0,002	0,002	0,000	0,000	0,014	0,000	0,284	0,000
7	0,000	0,000	0,001	0,001	0,002	0,000	0,004	0,002	0,232	0,000
13	0,000	0,000	0,003	0,003	0,016	0,000	0,022	0,000	0,532	0,000
16	0,000	0,000	0,001	0,001	0,007	0,000	0,007	0,000	0,163	0,000
25	0,000	0,000	0,009	0,009	0,067	0,007	0,020	0,061	1,341	0,000
45	0,000	0,002	0,005	0,007	0,059	0,010	0,035	0,020	0,996	0,005
50	0,001	0,003	0,004	0,008	0,042	0,000	0,042	0,000	1,032	0,014
55	0,004	0,005	0,004	0,013	0,087	0,000	0,078	0,026	1,742	0,035
60	0,001	0,005	0,011	0,017	0,321	0,000	0,111	0,136	1,630	0,000
75	0,001	0,010	0,009	0,020	0,494	0,055	0,082	0,041	1,097	0,000
95	0,006	0,022	0,008	0,036	0,372	0,138	0,041	0,110	2,786	0,097
115	0,006	0,034	0,005	0,044	0,893	0,073	0,182	0,273	0,109	0,109
130	0,021	0,024	0,030	0,074	0,462	0,062	0,000	0,092	0,000	0,123
162	0,015	0,031	0,013	0,060	1,339	0,089	0,201	0,737	0,089	0,201

Annex 15. Foraminifera data

Foraminifera - Splitting

samples	splitted times			total sample (g)	counted weight	nº benthonic individuals	counted individuals	benthonic weight	g/cm3_benthonic	planktonic individuals	g/cm3_planktonic
0-2	11	1/2048	2048	4,87110	0,44283	183	286	0,283347521	24985,600000	103	14062,933333
2- 4	11	1/2048	2048	3,19920	0,29084	212	235	0,262371528	28945,066667	23	3140,266667
4-6	11	1/2048	2048	2,87920	0,26175	178	300	0,155302303	24302,933333	122	16657,066667
6-8	11	1/2048	2048	2,79360	0,25396	202	327	0,156882736	27579,733333	125	17066,666667
8-10	11	1/2048	2048	2,53130	0,23012	221	324	0,156963328	30173,866667	103	14062,933333
10-12	11	1/2048	2048	2,85840	0,25985	228	355	0,166892497	31129,600000	127	17339,733333
12-14	11	1/2048	2048	3,03370	0,27579	194	304	0,175998146	26487,466667	110	15018,666667
14-16	11	1/2048	2048	3,60700	0,32791	151	304	0,162875897	20616,533333	153	20889,600000
16-18	10	1/1024	1024	2,79290	0,27929	196	348	0,157301264	13380,266667	152	10376,533333
18-20	10	1/1024	1024	2,91700	0,29170	181	331	0,159509668	12356,266667	150	10240,000000
30	12	1/4096	4096	5,51120	0,45927	237	386	0,281984974	64716,800000	149	40686,933333
40	12	1/4096	4096	6,18190	0,51516	217	348	0,321233788	59255,466667	131	35771,733333
50	11	1/2048	2048	7,70880	0,70080	184	309	0,417304854	25122,133333	125	17066,666667
60	12	1/4096	4096	9,14370	0,76198	188	307	0,466616612	51336,533333	119	32494,933333
70	12	1/4096	4096	10,03490	0,83624	180	311	0,483998392	49152,000000	131	35771,733333
80	12	1/4096	4096	12,08910	1,00743	226	372	0,612037769	61713,066667	146	39867,733333
90	12	1/4096	4096	10,94620	0,91218	195	320	0,555861719	53248,000000	125	34133,333333
100	11	1/2048	2048	14,00370	1,27306	207	304	0,866855831	28262,400000	97	13243,733333
110	12	1/4096	4096	16,78460	1,39872	195	332	0,821535392	53248,000000	137	37410,133333
120	7	1/128	128	23,98120	3,42589	247	308	2,747382375	2107,733333	61	520,533333
130	7	1/128	128	24,36190	3,48027	234	301	2,705593071	1996,800000	67	571,733333
140	6	1/64	64	22,10620	3,68437	266	422	2,322373302	1134,933333	156	665,600000
150	6	1/64	64	19,80480	3,30080	234	308	2,507750649	998,400000	74	315,733333

Foraminifera - 0-2 cm

sample	split	
0-2 cm	11	1/2048

		Screening 2048					%	Volume	Density/cm3
Ammonia beccarii	7		0,038251	-3,26358	-0,12484	14336	3,8251	#DIV/0!	#DIV/0!
Asterigerinata cf. mamilla	2		0,010929	-4,51634	-0,04936	4096	1,0929	#DIV/0!	#DIV/0!
Bolivina difformis	15		0,081967	-2,50144	-0,20504	30720	8,1967	#DIV/0!	#DIV/0!
Bolivina ordinaria	12		0,065574	-2,72458	-0,17866	24576	6,5574	#DIV/0!	#DIV/0!
Bolivina pseudoplicata	6		0,032787	-3,41773	-0,11206	12288	3,2787	#DIV/0!	#DIV/0!
Brizalina alata	1		0,005464	-5,20969	-0,02847	2048	0,5464	#DIV/0!	#DIV/0!
Brizalina spathulata	21		0,114754	-2,16496	-0,24844	43008	11,4754	#DIV/0!	#DIV/0!
Bulimina aculeata	2		0,010929	-4,51634	-0,04936	4096	1,0929	#DIV/0!	#DIV/0!
Bulimina elongata	3		0,016393	-4,11087	-0,06739	6144	1,6393	#DIV/0!	#DIV/0!
Bulimina marginata	3		0,016393	-4,11087	-0,06739	6144	1,6393	#DIV/0!	#DIV/0!
Cassidulina laevigata	17		0,092896	-2,37627	-0,22075	34816	9,2896	#DIV/0!	#DIV/0!
Cassidulina obtusa	12		0,065574	-2,72458	-0,17866	24576	6,5574	#DIV/0!	#DIV/0!
Cibicides cf. pseudoungerianus	8		0,043716	-3,13004	-0,13683	16384	4,3716	#DIV/0!	#DIV/0!
Epistominella vitrea	18		0,098361	-2,31911	-0,22811	36864	9,8361	#DIV/0!	#DIV/0!
Fissurina globosocaudata	1		0,005464	-5,20969	-0,02847	2048	0,5464	#DIV/0!	#DIV/0!
Fissurina laevigata	1		0,005464	-5,20969	-0,02847	2048	0,5464	#DIV/0!	#DIV/0!
Fissurina orbignyana	1		0,005464	-5,20969	-0,02847	2048	0,5464	#DIV/0!	#DIV/0!
Gyroidina umbonata	2		0,010929	-4,51634	-0,04936	4096	1,0929	#DIV/0!	#DIV/0!
Lagena gracilima	1		0,005464	-5,20969	-0,02847	2048	0,5464	#DIV/0!	#DIV/0!
Lobatula lobatula	2		0,010929	-4,51634	-0,04936	4096	1,0929	#DIV/0!	#DIV/0!
Neoleniculina peregrina	2		0,010929	-4,51634	-0,04936	4096	1,0929	#DIV/0!	#DIV/0!
Nonion fabum	1		0,005464	-5,20969	-0,02847	2048	0,5464	#DIV/0!	#DIV/0!
Nonionella turgida	17		0,092896	-2,37627	-0,22075	34816	9,2896	#DIV/0!	#DIV/0!
Quinqueloculina skourisana	3		0,016393	-4,11087	-0,06739	6144	1,6393	#DIV/0!	#DIV/0!
Quinqueloculina stalkeri	16		0,087432	-2,4369	-0,21306	32768	8,7432	#DIV/0!	#DIV/0!
Rectuvigerina phlegeri	1		0,005464	-5,20969	-0,02847	2048	0,5464	#DIV/0!	#DIV/0!
Stainforthia complanata	3		0,016393	-4,11087	-0,06739	6144	1,6393	#DIV/0!	#DIV/0!
Stainforthia feylingi	3		0,016393	-4,11087	-0,06739	6144	1,6393	#DIV/0!	#DIV/0!
Trifarina angulosa	1		0,005464	-5,20969	-0,02847	2048	0,5464	#DIV/0!	#DIV/0!
Valvulineria bradyana	1		0,005464	-5,20969	-0,02847	2048	0,5464	#DIV/0!	#DIV/0!
Total	183	Total			-2,90714	370784	100	#DIV/0!	#DIV/0!

Bolivina difformis	8,1967
Bolivina ordinaria	6,5574
Brizalina spathulata	11,4754
Cassidulina laevigata	9,2896
Cassidulina obtusa	6,5574
Epistominella vitrea	9,8361
Nonionella turgida	9,2896
Quinqueloculina stalkeri	8,7432
A	26,2295

Asterigerinata cf. mamilla+Bolivina

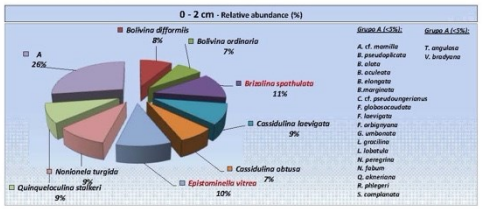

Planktonic	172352	31,46087416
Benthonic	374784	68,53912584
Total	548816	100,0

Foraminifera - 2-4 cm

sample	split	
2-4 cm	11	1/2048

		screening					%	Volume	Density/cm3
		2048							
Ammonia beccarii	2		0,006434	-4,66344	-0,04399	4086	0,9434	#DIV/0!	#DIV/0!
Astrorotinata cf. momilla	4		0,018868	-3,97029	-0,07491	8192	1,8868	#DIV/0!	#DIV/0!
Bolivina difformis	16		0,075472	-2,584	-0,19502	32768	7,5472	#DIV/0!	#DIV/0!
Bolivina ordinaria	17		0,080189	-2,52337	-0,20235	34816	8,0189	#DIV/0!	#DIV/0!
Bolivina pseudoplicata	2		0,006434	-4,66344	-0,04399	4086	0,9434	#DIV/0!	#DIV/0!
Bolivina sp.	2		0,006434	-4,66344	-0,04399	4086	0,9434	#DIV/0!	#DIV/0!
Bolivina striatula	4		0,018868	-3,97029	-0,07491	8192	1,8868	#DIV/0!	#DIV/0!
Brizalina alata	1		0,004717	-5,35659	-0,02527	2048	0,4717	#DIV/0!	#DIV/0!
Brizalina spathulata	20		0,09434	-2,36085	-0,22272	40960	9,4340	#DIV/0!	#DIV/0!
Bulimina alazanensis	3		0,014151	-4,25797	-0,06025	6144	1,4151	#DIV/0!	#DIV/0!
Bulimina elongata	2		0,006434	-4,66344	-0,04399	4086	0,9434	#DIV/0!	#DIV/0!
Bulimina marginata	4		0,018868	-3,97029	-0,07491	8192	1,8868	#DIV/0!	#DIV/0!
Cassidulina laevigata	32		0,150943	-1,89085	-0,28541	65536	15,0943	#DIV/0!	#DIV/0!
Cassidulina teretis	4		0,018868	-3,97029	-0,07491	8192	1,8868	#DIV/0!	#DIV/0!
Cibicides cf. pseudoungerianus	10		0,04717	-3,054	-0,14406	20480	4,7170	#DIV/0!	#DIV/0!
Chilostomella oolina	1		0,004717	-5,35659	-0,02527	2048	0,4717	#DIV/0!	#DIV/0!
Epistominella vitrea	12		0,056604	-2,87158	-0,16255	24576	5,6604	#DIV/0!	#DIV/0!
Gavelinopsis praegeri	2		0,006434	-4,66344	-0,04399	4086	0,9434	#DIV/0!	#DIV/0!
Globocassidulina rossensis	6		0,028302	-3,56483	-0,10089	12288	2,8302	#DIV/0!	#DIV/0!
Globocassidulina subglobosa	21		0,099057	-2,31296	-0,22903	43008	9,9057	#DIV/0!	#DIV/0!
Gyroidina umbonata	1		0,004717	-5,35659	-0,02527	2048	0,4717	#DIV/0!	#DIV/0!
Hyalinea baltica	2		0,006434	-4,66344	-0,04399	4086	0,9434	#DIV/0!	#DIV/0!
Nonionellina parapigrina	1		0,004717	-5,35659	-0,02527	2048	0,4717	#DIV/0!	#DIV/0!
Nonion fabum	8		0,037736	-3,27714	-0,12367	16384	3,7736	#DIV/0!	#DIV/0!
Nonionella turgida	5		0,023585	-3,74715	-0,08838	10240	2,3585	#DIV/0!	#DIV/0!
Quinqueloculina stalkeri	7		0,033019	-3,41068	-0,11262	14336	3,3019	#DIV/0!	#DIV/0!
Rectuvigerina phlegeri	8		0,037736	-3,27714	-0,12367	16384	3,7736	#DIV/0!	#DIV/0!
Steinforthia feylingai	2		0,006434	-4,66344	-0,04399	4086	0,9434	#DIV/0!	#DIV/0!
Triforina angulosa	1		0,004717	-5,35659	-0,02527	2048	0,4717	#DIV/0!	#DIV/0!
Uvigerina peregrina	4		0,018868	-3,97029	-0,07491	8192	1,8868	#DIV/0!	#DIV/0!
Valvulineria bradyana	1		0,004717	-5,35659	-0,02527	2048	0,4717	#DIV/0!	#DIV/0!
Ind.	7		0,033019	-3,41068	-0,11262	14336	3,3019	#DIV/0!	#DIV/0!
	212	Total			-1,686472	434176	100	#DIV/0!	#DIV/0!

Bolivina difformis	7,5472
Bolivina ordinaria	8,0189
Brizalina spathulata	9,4340
Cassidulina laevigata	15,0943
Epistominella vitrea	5,6604
Globocassidulina subglobosa	9,9057
A	44,3396

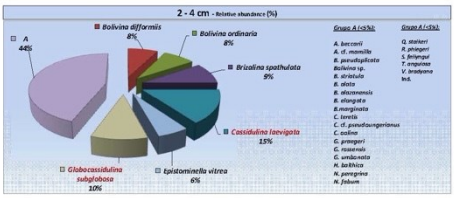

Planktonic	153920	26,13340418
Benthonic	434176	73,65759582
Total	587776	100,0

Foraminifera - 4-6 cm

sample	split	
4-6 cm	11	1/2048

		screening					%	Volume	Density/cm3
		2048							
Astrorotinata cf. momilla	1		0,006618	-5,11178	-0,02911	2048	0,5618	#DIV/0!	#DIV/0!
Bolivina difformis	22		0,123596	-2,09074	-0,25841	45056	12,3596	#DIV/0!	#DIV/0!
Bolivina ordinaria	20		0,11236	-2,18695	-0,24562	40960	11,2360	#DIV/0!	#DIV/0!
Bolivina pseudoplicata	3		0,016854	-4,08317	-0,06882	6144	1,6854	#DIV/0!	#DIV/0!
Brizalina alata	1		0,006618	-5,11178	-0,02911	2048	0,5618	#DIV/0!	#DIV/0!
Brizalina subaenariensis	4		0,022472	-3,79549	-0,08529	8192	2,2472	#DIV/0!	#DIV/0!
Brizalina spathulata	22		0,123596	-2,09074	-0,25841	45056	12,3596	#DIV/0!	#DIV/0!
Bulimina elongata	2		0,011236	-4,48864	-0,05043	4096	1,1236	#DIV/0!	#DIV/0!
Bulimina marginata	4		0,022472	-3,79549	-0,08529	8192	2,2472	#DIV/0!	#DIV/0!
Cassidulina laevigata	20		0,11236	-2,18695	-0,24562	40960	11,2360	#DIV/0!	#DIV/0!
Cassidulina teretis	3		0,016854	-4,08317	-0,06882	6144	1,6854	#DIV/0!	#DIV/0!
Cibicides cf. pseudoungerianus	2		0,011236	-4,48864	-0,05043	4096	1,1236	#DIV/0!	#DIV/0!
Epistominella vitrea	9		0,050562	-2,98456	-0,1509	18432	5,0562	#DIV/0!	#DIV/0!
Globocassidulina rossensis	30		0,168539	-1,78059	-0,3001	61440	16,8539	#DIV/0!	#DIV/0!
Gyroidina umbonata	4		0,022472	-3,79549	-0,08529	8192	2,2472	#DIV/0!	#DIV/0!
Heterolepa pseudoungerianus ?	7		0,039326	-3,23587	-0,12725	14336	3,9326	#DIV/0!	#DIV/0!
Nonionella turgida	2		0,011236	-4,48864	-0,05043	4096	1,1236	#DIV/0!	#DIV/0!
Planorbulina mediterranensis	1		0,006618	-5,11178	-0,02911	2048	0,5618	#DIV/0!	#DIV/0!
Quinqueloculina stalkeri	7		0,039326	-3,23587	-0,12725	14336	3,9326	#DIV/0!	#DIV/0!
Steinforthia complanata	3		0,016854	-4,08317	-0,06882	6144	1,6854	#DIV/0!	#DIV/0!
Triforina carinata	3		0,016854	-4,08317	-0,06882	6144	1,6854	#DIV/0!	#DIV/0!
Valvulineria bradyana	8		0,044944	-3,10234	-0,13943	16384	4,4944	#DIV/0!	#DIV/0!
	178	Total				364564	100		

Bolivina difformis	12,3596
Bolivina ordinaria	11,2360
Brizalina spathulata	12,3596
Cassidulina laevigata	11,2360
Epistominella vitrea	5,0562
Globocassidulina rossensis	16,8539
A	30,8989

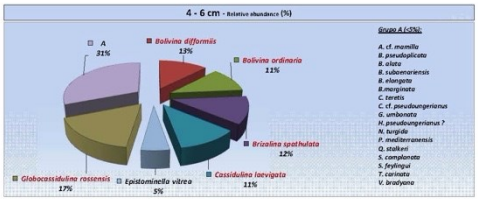

Planktonic	135168	37,04918003
Benthonic	364544	72,95081997
Total	499712	100,0

Foraminifera - 6-8 cm

sample	split	
6-8 cm	11	1/2048

		Screening 2048					%	Volume	Density/cm3
Bolivina difformis	24		0,118812	-2,13021	-0,25396	49152	11,8812	#DIV/0!	#DIV/0!
Bolivina ordinaria	22		0,108911	-2,21723	-0,24148	45056	10,8911	#DIV/0!	#DIV/0!
Bolivina pseudoplicata	4		0,019802	-3,92197	-0,07766	8192	1,9802	#DIV/0!	#DIV/0!
Bolivina striatula	2		0,009901	-4,61512	-0,04569	4096	0,9901	#DIV/0!	#DIV/0!
Brizalina spathulata	28		0,138614	-1,97696	-0,27391	57344	13,8614	#DIV/0!	#DIV/0!
Brizalina subaenariensis	2		0,009901	-4,61512	-0,04569	4096	0,9901	#DIV/0!	#DIV/0!
Bulimina marginata	5		0,024752	-3,69883	-0,09156	10240	2,4752	#DIV/0!	#DIV/0!
Cassidulina laevigata	18		0,089109	-2,4179	-0,21546	36864	8,9109	#DIV/0!	#DIV/0!
Cibicides cf. pseudoungerianus	11		0,054455	-2,91037	-0,15849	22528	5,4455	#DIV/0!	#DIV/0!
Epistominella vitrea	12		0,059406	-2,82336	-0,16772	24576	5,9406	#DIV/0!	#DIV/0!
Globocassidulina rossensis	45		0,222772	-1,50161	-0,33452	92160	22,2772	#DIV/0!	#DIV/0!
Gyroidina umbonata	5		0,024752	-3,69883	-0,09156	10240	2,4752	#DIV/0!	#DIV/0!
Heterolepa pseudoungerianus	6		0,029703	-3,51651	-0,10445	12288	2,9703	#DIV/0!	#DIV/0!
Nonion faburn	3		0,014851	-4,29966	-0,06252	6144	1,4851	#DIV/0!	#DIV/0!
Nonionella turgida	1		0,00495	-5,30827	-0,02628	2048	0,4950	#DIV/0!	#DIV/0!
Nonionoides clavatus	2		0,009901	-4,61512	-0,04569	4096	0,9901	#DIV/0!	#DIV/0!
Quinqueloculina stelkeri	2		0,009901	-4,61512	-0,04569	4096	0,9901	#DIV/0!	#DIV/0!
Reophaxgriesa phlegeri	3		0,014851	-4,29966	-0,06252	6144	1,4851	#DIV/0!	#DIV/0!
Stainforthia complanata	2		0,009901	-4,61512	-0,04569	4096	0,9901	#DIV/0!	#DIV/0!
Stainforthia fimbriata	1		0,00495	-5,30827	-0,02628	2048	0,4950	#DIV/0!	#DIV/0!
Triferina angulosa	2		0,009901	-4,61512	-0,04569	4096	0,9901	#DIV/0!	#DIV/0!
Uvigerina peregrina	2		0,009901	-4,61512	-0,04569	4096	0,9901	#DIV/0!	#DIV/0!
	202	Total			-2,50735	413696	100		

Bolivina difformis	11,8812
Bolivina ordinaria	10,8911
Brizalina spathulata	13,8614
Cassidulina laevigata	8,9109
Cibicides cf. pseudoungerianus	5,4455
Epistominella vitrea	5,9406
Globocassidulina rossensis	22,2772
A	20,7921

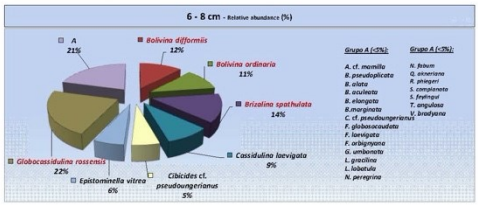

Planktonic	182272	30,58419244
Benthonic	413596	69,41580756
Total	595868	100,0

Foraminifera - 8-10 cm

sample	split	
8-10 cm	11	1/2048

		Screening 2048					%	Volume	Density/cm3
Ammonia beccarii	1		0,004525	-5,3816	-0,0244261	2048	0,4525	#DIV/0!	#DIV/0!
Amphicoryna scalaris	1		0,004525	-5,3816	-0,0244261	2048	0,4525	#DIV/0!	#DIV/0!
Astrorotalia cf. mamilla	9		0,040724	-3,20696	-0,1303349	18432	4,0724	#DIV/0!	#DIV/0!
Bolivina difformis	24		0,108597	-2,22011	-0,2410978	49152	10,8597	#DIV/0!	#DIV/0!
Bolivina ordinaria	43		0,19457	-1,63696	-0,318504	88064	19,4570	#DIV/0!	#DIV/0!
Bolivina pseudoplicata	3		0,013575	-4,29955	-0,0583349	6144	1,3575	#DIV/0!	#DIV/0!
Brizalina spathulata	13		0,058824	-2,83121	-0,1666396	26624	5,8824	#DIV/0!	#DIV/0!
Brizalina subaenariensis	3		0,013575	-4,29955	-0,0583349	6144	1,3575	#DIV/0!	#DIV/0!
Bulimina marginata	6		0,027149	-3,6064	-0,0979114	12288	2,7149	#DIV/0!	#DIV/0!
Cancris auricula	1		0,004525	-5,3816	-0,0244261	2048	0,4525	#DIV/0!	#DIV/0!
Cassidulina laevigata	18		0,081448	-2,5077	-0,2042345	36864	8,1448	#DIV/0!	#DIV/0!
Cibicides cf. pseudoungerianus	17		0,076923	-2,56476	-0,1973858	34816	7,6923	#DIV/0!	#DIV/0!
Epistominella vitrea	22		0,099548	-2,30712	-0,2296081	45056	9,9548	#DIV/0!	#DIV/0!
Fissurina orbignyana	1		0,004525	-5,3816	-0,0244261	2048	0,4525	#DIV/0!	#DIV/0!
Globocassidulina rossensis	20		0,090498	-2,4024	-0,2174545	40960	9,0498	#DIV/0!	#DIV/0!
Gyroidina umbonata	1		0,004525	-5,3816	-0,0244261	2048	0,4525	#DIV/0!	#DIV/0!
Heterolepa pseudoungerianus	2		0,00905	-4,70561	-0,0425793	4096	0,9050	#DIV/0!	#DIV/0!
Hyalinea balthica	2		0,00905	-4,70561	-0,0425793	4096	0,9050	#DIV/0!	#DIV/0!
Lagena sellegra	2		0,00905	-4,70561	-0,0425793	4096	0,9050	#DIV/0!	#DIV/0!
Nonion faburn	1		0,004525	-5,3816	-0,0244261	2048	0,4525	#DIV/0!	#DIV/0!
Nonionella bradi	4		0,0181	-4,01187	-0,072613	8192	1,8100	#DIV/0!	#DIV/0!
Melonis barleeanum	1		0,004525	-5,3816	-0,0244261	2048	0,4525	#DIV/0!	#DIV/0!
Quinqueloculina stelkeri	7		0,031674	-3,45425	-0,1093474	14336	3,1674	#DIV/0!	#DIV/0!
Reophaxgriesa phlegeri	2		0,00905	-4,70561	-0,0425793	4096	0,9050	#DIV/0!	#DIV/0!
Stainforthia complanata	3		0,013575	-4,29955	-0,0583349	6144	1,3575	#DIV/0!	#DIV/0!
Stainforthia fimbriata	5		0,022624	-3,78873	-0,0857178	10240	2,2624	#DIV/0!	#DIV/0!
Triferina angulosa	1		0,004525	-5,3816	-0,0244261	2048	0,4525	#DIV/0!	#DIV/0!
Triferina sarinata	1		0,004525	-5,3816	-0,0244261	2048	0,4525	#DIV/0!	#DIV/0!
Uvigerina peregrina	5		0,022624	-3,78873	-0,0857178	10240	2,2624	#DIV/0!	#DIV/0!
Valvulineria bradyana	2		0,00905	-4,70561	-0,0425793	4096	0,9050	#DIV/0!	#DIV/0!
Ind	221	Total			-2,7443965	452058	100		

Brizalina alata	1					2048	0,4586	#DIV/0!	#DIV/0!
Bulimina aculeata	2					4096	0,8771	#DIV/0!	#DIV/0!
Bulimina elongata	1					6144	1,3158	#DIV/0!	#DIV/0!
Cassidulina obtusa	12					24576	5,2632	#DIV/0!	#DIV/0!
Fissurina globonacuelata	1					2048	0,4386	#DIV/0!	#DIV/0!
Fissurina laevigata	1					2048	0,4386	#DIV/0!	#DIV/0!
Lagena gracilina	1					2048	0,4386	#DIV/0!	#DIV/0!
Labatula labatula	2					4096	0,8771	#DIV/0!	#DIV/0!
Neoeponidiuna peregrina	2					4096	0,8771	#DIV/0!	#DIV/0!
Nonionella turgida	17					34816	7,4561	#DIV/0!	#DIV/0!
Quinqueloculina elemeriana	3					6144	1,3158	#DIV/0!	#DIV/0!

Bolivina difformis	10,8597
Bolivina ordinaria	19,4570
Brizalina spathulata	5,8824
Cassidulina laevigata	8,1448
Cibicides cf. pseudoungerianus	7,6923
Epistominella vitrea	9,9548
Globocassidulina rossensis	9,0498
A	28,9593

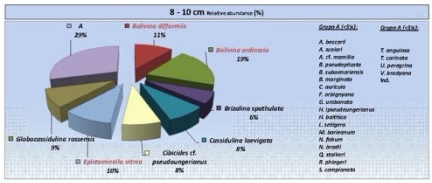

Planktonic	135168	22,99011588
Benthonic	452908	77,00988132
Total	587773	100,0

Foraminifera - 10-12 cm

sample	split	
10-12 cm	11	1/2048

		Screening						Volume	Density/cm3
		2048					%		
Ammonia beccarii	1	0,004386	-5,42935	-0,02381		2048	0,2193	#DIV/0!	#DIV/0!
Asterigerinata cf. mamilla	10	0,04386	-3,12676	-0,13714		20480	2,1930	#DIV/0!	#DIV/0!
Bolivina difformiis	22	0,096491	-2,3383	-0,22563		45056	4,8246	#DIV/0!	#DIV/0!
Bolivina ordinaria	23	0,100877	-2,29385	-0,2314		47104	5,0439	#DIV/0!	#DIV/0!
Bolivina pseudoplicata	9	0,039474	-3,23212	-0,12758		18432	1,9737	#DIV/0!	#DIV/0!
Brizalina spathulata	17	0,074561	-2,59613	-0,19357		34816	3,7281	#DIV/0!	#DIV/0!
Brizalina subaenariensis	5	0,02193	-3,81991	-0,08377		10240	1,0965	#DIV/0!	#DIV/0!
Bulimina elongata	6	0,026316	-3,63759	-0,09573		12288	1,3158	#DIV/0!	#DIV/0!
Bulimina marginata	5	0,02193	-3,81991	-0,08377		10240	1,0965	#DIV/0!	#DIV/0!
Cassidulina laevigata	9	0,039474	-3,23212	-0,12758		18432	1,9737	#DIV/0!	#DIV/0!
Cassidulina minuta	11	0,048246	-3,03145	-0,14625		22528	2,4123	#DIV/0!	#DIV/0!
Cassidulina teretis	11	0,048246	-3,03145	-0,14625		22528	2,4123	#DIV/0!	#DIV/0!
Chilostomella oolina	1	0,004386	-5,42935	-0,02381		2048	0,2193	#DIV/0!	#DIV/0!
Cibicides cf. pseudoungerianus	11	0,048246	-3,03145	-0,14625		22528	2,4123	#DIV/0!	#DIV/0!
Epistominella vitrea	9	0,039474	-3,23212	-0,12758		18432	1,9737	#DIV/0!	#DIV/0!
Fissurina fasciata	1	0,004386	-5,42935	-0,02381		2048	0,2193	#DIV/0!	#DIV/0!
Fissurina laevigata	1	0,004386	-5,42935	-0,02381		2048	0,2193	#DIV/0!	#DIV/0!
Fissurina orbignyana	1	0,004386	-5,42935	-0,02381		2048	0,2193	#DIV/0!	#DIV/0!
Globocassidulina rossensis	14	0,061404	-2,79029	-0,17133		28672	3,0702	#DIV/0!	#DIV/0!
Globocassidulina subglobosa	7	0,030702	-3,48344	-0,10695		14336	1,5351	#DIV/0!	#DIV/0!
Gyroidina umbonata	7	0,030702	-3,48344	-0,10695		14336	1,5351	#DIV/0!	#DIV/0!
Heterolepa pseudoungerianus	2	0,008772	-4,7362	-0,04155		4096	0,4386	#DIV/0!	#DIV/0!
Lagena laevis	1	0,004386	-5,42935	-0,02381		2048	0,2193	#DIV/0!	#DIV/0!
Melonis barleanum	1	0,004386	-5,42935	-0,02381		2048	0,2193	#DIV/0!	#DIV/0!
Nonion fabum	2	0,008772	-4,7362	-0,04155		4096	0,4386	#DIV/0!	#DIV/0!
Nonionela turgida	12	0,052632	-2,94444	-0,15497		24576	2,6316	#DIV/0!	#DIV/0!
Quinqueloculina stalkeri	4	0,017544	-4,04305	-0,07093		8192	0,8772	#DIV/0!	#DIV/0!
Rectuvigerina phlegeri	2	0,008772	-4,7362	-0,04155		4096	0,4386	#DIV/0!	#DIV/0!
Stainforthia complanata	4	0,017544	-4,04305	-0,07093		8192	0,8772	#DIV/0!	#DIV/0!
Stainforthia feylingi	2	0,008772	-4,7362	-0,04155		4096	0,4386	#DIV/0!	#DIV/0!
Trifarina carinata	3	0,013158	-4,33073	-0,05698		6144	0,6579	#DIV/0!	#DIV/0!
Uvigerina peregrina	3	0,013158	-4,33073	-0,05698		6144	0,6579	#DIV/0!	#DIV/0!
Valvulineria bradyana	11	0,048246	-3,03145	-0,14625		22528	2,4123	#DIV/0!	#DIV/0!
Ind	228	1	0	0		466944	50,0000	#DIV/0!	#DIV/0!
		Total	#VALUE!	-3,14767		933888	100		

Bolivina difformiis	4,8246
Bolivina ordinaria	5,0439
Brizalina spathulata	3,7281
Globocassidulina rossensis	3,0702
Nonionela turgida	2,6316
A	80,7018

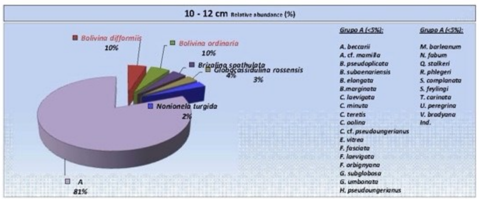

Planktonic	182272	16,33027523
Benthonic	933888	83,66972477
Total	1116160	100,0

Foraminifera - 12-14 cm

sample	split	
12-14 cm	11	1/2048

		Screening						Volume	Density/cm3
		2048					%		
Asterigerinata sp.	1	0,005155	-5,26786	-0,02715		2048	0,2577	#DIV/0!	#DIV/0!
Bolivina difformiis	16	0,082474	-2,49527	-0,2058		32768	4,1237	#DIV/0!	#DIV/0!
Bolivina ordinaria	21	0,108247	-2,22334	-0,24067		43008	5,4124	#DIV/0!	#DIV/0!
Bolivina pseudoplicata	7	0,036082	-3,32195	-0,11986		14336	1,8041	#DIV/0!	#DIV/0!
Brizalina spathulata	15	0,07732	-2,55981	-0,19792		30720	3,8660	#DIV/0!	#DIV/0!
Brizalina subaenariensis	6	0,030928	-3,4761	-0,10751		12288	1,5464	#DIV/0!	#DIV/0!
Bulimina alazanensis	2	0,010309	-4,57471	-0,04716		4096	0,5155	#DIV/0!	#DIV/0!
Bulimina elongata	2	0,010309	-4,57471	-0,04716		4096	0,5155	#DIV/0!	#DIV/0!
Bulimina marginata	1	0,005155	-5,26786	-0,02715		2048	0,2577	#DIV/0!	#DIV/0!
Cassidulina laevigata	26	0,134021	-2,00976	-0,26935		53248	6,7010	#DIV/0!	#DIV/0!
Cassidulina teretis	6	0,030928	-3,4761	-0,10751		12288	1,5464	#DIV/0!	#DIV/0!
Cibicides cf. pseudoungerianus	13	0,06701	-2,70291	-0,18112		26624	3,3505	#DIV/0!	#DIV/0!
Epistominella vitrea	10	0,051546	-2,96527	-0,15285		20480	2,5773	#DIV/0!	#DIV/0!
Fissurina marginata	1	0,005155	-5,26786	-0,02715		2048	0,2577	#DIV/0!	#DIV/0!
Fissurina orbignyana	1	0,005155	-5,26786	-0,02715		2048	0,2577	#DIV/0!	#DIV/0!
Globocassidulina rossensis	19	0,097938	-2,32342	-0,22755		38912	4,8969	#DIV/0!	#DIV/0!
Globocassidulina subglobosa	4	0,020619	-3,88156	-0,08003		8192	1,0309	#DIV/0!	#DIV/0!
Gyroidina umbonata	5	0,025773	-3,65842	-0,09429		10240	1,2887	#DIV/0!	#DIV/0!
Heterolepa pseudoungerianus	2	0,010309	-4,57471	-0,04716		4096	0,5155	#DIV/0!	#DIV/0!
Hyalinea balthica	3	0,015464	-4,16925	-0,06447		6144	0,7732	#DIV/0!	#DIV/0!
Lobatula lobatula	1	0,005155	-5,26786	-0,02715		2048	0,2577	#DIV/0!	#DIV/0!
Nonion fabum	2	0,010309	-4,57471	-0,04716		4096	0,5155	#DIV/0!	#DIV/0!
Nonionela turgida	11	0,056701	-2,86996	-0,16273		22528	2,8351	#DIV/0!	#DIV/0!
Quinqueloculina stalkeri	4	0,020619	-3,88156	-0,08003		8192	1,0309	#DIV/0!	#DIV/0!
Stainforthia complanata	4	0,020619	-3,88156	-0,08003		8192	1,0309	#DIV/0!	#DIV/0!
Stainforthia feylingui	2	0,010309	-4,57471	-0,04716		4096	0,5155	#DIV/0!	#DIV/0!
Trifarina bradyana	1	0,005155	-5,26786	-0,02715		2048	0,2577	#DIV/0!	#DIV/0!
Trifarina carinata	1	0,005155	-5,26786	-0,02715		2048	0,2577	#DIV/0!	#DIV/0!
Uvigerina peregrina	6	0,030928	-3,4761	-0,10751		12288	1,5464	#DIV/0!	#DIV/0!
Valvulineria bradyana	1	0,005155	-5,26786	-0,02715		2048	0,2577	#DIV/0!	#DIV/0!
ind	194			-2,93228		397312	50,0000	#DIV/0!	#DIV/0!
		Total				794624	100		

Ammonia beccarii	7					14336	3,5000	#DIV/0!	#DIV/0!
Asterigerinata cf. mamilla	2					4096	1,0000	#DIV/0!	#DIV/0!
Brizalina alata	1					2048	0,5000	#DIV/0!	#DIV/0!
Bulimina aculeata	2					4096	1,0000	#DIV/0!	#DIV/0!
Cassidulina obtusa	12					24576	6,0000	#DIV/0!	#DIV/0!
Fissurina globosocaudata	1					2048	0,5000	#DIV/0!	#DIV/0!
Fissurina laevigata	1					2048	0,5000	#DIV/0!	#DIV/0!
Lagena gracilina	1					2048	0,5000	#DIV/0!	#DIV/0!
Neolenticulina peregrina	2					4096	1,0000	#DIV/0!	#DIV/0!
Quinqueloculina akneriana	3					6144	1,5000	#DIV/0!	#DIV/0!
Rectuvigerina phlegeri	1					2048	0,5000	#DIV/0!	#DIV/0!
Trifarina angulosa	1					2048	0,5000	#DIV/0!	#DIV/0!

Bolivina difformiis	4,1237
Bolivina ordinaria	5,4124
Brizalina spathulata	3,8660
Cassidulina laevigata	6,7010
Cibicides cf. pseudoungerianus	3,3505
Epistominella vitrea	2,5773
Globocassidulina rossensis	4,8969
Nonionela turgida	2,8351
A	66,2371

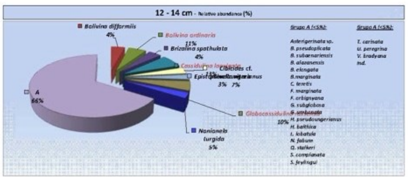

Planktonic	145408	15,46640959
Benthonic	794624	84,53359041
Total	940032	100,0

Foraminifera - 14-16 cm

sample	split	
14-16 cm	11	1/2048

		Screening						Volume	Density/cm3
		2048					%		
Ammonia beccarii	2		0,033245	-4,32413	-0,05727	4096	0,6623	#DIV/0!	#DIV/0!
Asterigerinata cf. mamilla	2		0,033245	-4,32413	-0,05727	4096	0,6623	#DIV/0!	#DIV/0!
Bolivina difformis	23		0,152318	-1,88179	-0,28663	47104	7,6159	#DIV/0!	#DIV/0!
Bolivina ordinaria	9		0,059603	-2,82006	-0,16808	18432	2,9801	#DIV/0!	#DIV/0!
Bolivina pseudoplicata	5		0,033113	-3,40784	-0,11284	10240	1,6556	#DIV/0!	#DIV/0!
Bolivina variabilis	1		0,006623	-5,01728	-0,03323	2048	0,3311	#DIV/0!	#DIV/0!
Brizalina spathulata	20		0,13245	-2,02155	-0,26775	40960	6,6225	#DIV/0!	#DIV/0!
Brizalina subaenariensis	4		0,02649	-3,63099	-0,09619	8192	1,3245	#DIV/0!	#DIV/0!
Bulimina alazanensis	2		0,033245	-4,32413	-0,05727	4096	0,6623	#DIV/0!	#DIV/0!
Bulimina elongata	2		0,033245	-4,32413	-0,05727	4096	0,6623	#DIV/0!	#DIV/0!
Bulimina marginata	1		0,006623	-5,01728	-0,03323	2048	0,3311	#DIV/0!	#DIV/0!
Chilostomella oolina	2		0,033245	-4,32413	-0,05727	4096	0,6623	#DIV/0!	#DIV/0!
Cibicides cf. pseudoungerianus	7		0,046358	-3,07137	-0,14238	14336	2,3179	#DIV/0!	#DIV/0!
Epistominella vitrea	5		0,033113	-3,40784	-0,11284	10240	1,6556	#DIV/0!	#DIV/0!
Fissurina fasciata	1		0,006623	-5,01728	-0,03323	2048	0,3311	#DIV/0!	#DIV/0!
Fissurina laevigata	1		0,006623	-5,01728	-0,03323	2048	0,3311	#DIV/0!	#DIV/0!
Fissurina orbignyana	1		0,006623	-5,01728	-0,03323	2048	0,3311	#DIV/0!	#DIV/0!
Globocassidulina rossensis	23		0,152318	-1,88179	-0,28663	47104	7,6159	#DIV/0!	#DIV/0!
Globocassidulina subglobosa	6		0,039735	-3,22552	-0,12817	12288	1,9868	#DIV/0!	#DIV/0!
Gavelinopsis praegeri	1		0,006623	-5,01728	-0,03323	2048	0,3311	#DIV/0!	#DIV/0!
Gyroidina umbonata	5		0,033113	-3,40784	-0,11284	10240	1,6556	#DIV/0!	#DIV/0!
Hyalinea balthica	3		0,019868	-3,91867	-0,07785	6144	0,9934	#DIV/0!	#DIV/0!
Melonis barleanum	1		0,006623	-5,01728	-0,03323	2048	0,3311	#DIV/0!	#DIV/0!
Neolenticulina peregrina	1		0,006623	-5,01728	-0,03323	2048	0,3311	#DIV/0!	#DIV/0!
Nonion fabum	1		0,006623	-5,01728	-0,03323	2048	0,3311	#DIV/0!	#DIV/0!
Nonionela turgida	1		0,006623	-5,01728	-0,03323	2048	0,3311	#DIV/0!	#DIV/0!
Oolina alcocki	1		0,006623	-5,01728	-0,03323	2048	0,3311	#DIV/0!	#DIV/0!
Oolina hexagona	1		0,006623	-5,01728	-0,03323	2048	0,3311	#DIV/0!	#DIV/0!
Planorbulina mediterranensis	1		0,006623	-5,01728	-0,03323	2048	0,3311	#DIV/0!	#DIV/0!
Quinqueloculina akneriana	1		0,006623	-5,01728	-0,03323	2048	0,3311	#DIV/0!	#DIV/0!
Quinqueloculina stalkeri	1		0,006623	-5,01728	-0,03323	2048	0,3311	#DIV/0!	#DIV/0!
Rectuvigerina phlegeri	5		0,033113	-3,40784	-0,11284	10240	1,6556	#DIV/0!	#DIV/0!
Trifarina carinata	1		0,006623	-5,01728	-0,03323	2048	0,3311	#DIV/0!	#DIV/0!
Uvigerina peregrina	7		0,046358	-3,07137	-0,14238	14336	2,3179	#DIV/0!	#DIV/0!
Valvulineria bradyana	3		0,019868	-3,91867	-0,07785	6144	0,9934	#DIV/0!	#DIV/0!
Ind.	151					309248	50,0000	#DIV/0!	#DIV/0!
		Total			-2,98325	618496	100		

Brizalina alata	1					2048	0,7194	#DIV/0!	#DIV/0!
Bulimina aculeata	2					4096	1,4388	#DIV/0!	#DIV/0!
Cassidulina laevigata	17					34816	12,2302	#DIV/0!	#DIV/0!
Cassidulina obtusa	12					24576	8,6331	#DIV/0!	#DIV/0!
Fissurina globosocaudata	1					2048	0,7194	#DIV/0!	#DIV/0!
Lagena gracilina	1					2048	0,7194	#DIV/0!	#DIV/0!
Lobatula lobatula	2					4096	1,4388	#DIV/0!	#DIV/0!
Stainforthia complanata	3					6144	2,1583	#DIV/0!	#DIV/0!
Stainforthia feylingui	3					6144	2,1583	#DIV/0!	#DIV/0!
Trifarina angulosa	1					2048	0,7194	#DIV/0!	#DIV/0!

Bolivina difformis	7,6159
Bolivina ordinaria	2,9801
Brizalina spathulata	6,6225
Globocassidulina rossensis	7,6159
A	75,1656

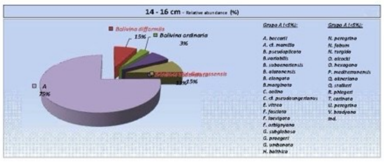

Planktonic	163840	20,94240838
Benthonic	618496	79,05759162
Total	782336	100,0

Foraminifera - 16-18 cm

sample	split	
16-18 cm	10	1/1024

		Screening						Volume	Density/cm3
		1024					%		
Ammonia beccarii	2		0,010204	-4,58497	-0,04679	2048	0,5102	#DIV/0!	#DIV/0!
Asterigerinata cf. mamilla	15		0,076531	-2,57006	-0,19669	15360	3,8265	#DIV/0!	#DIV/0!
Bolivina difformis	33		0,168367	-1,78161	-0,29996	33792	8,4184	#DIV/0!	#DIV/0!
Bolivina ordinaria	9		0,045918	-3,08089	-0,14147	9216	2,2959	#DIV/0!	#DIV/0!
Bolivina pseudoplicata	6		0,030612	-3,48636	-0,10673	6144	1,5306	#DIV/0!	#DIV/0!
Brizalina subaenariensis	4		0,020408	-3,89182	-0,07942	4096	1,0204	#DIV/0!	#DIV/0!
Brizalina spathulata	22		0,112245	-2,18707	-0,24549	22528	5,6122	#DIV/0!	#DIV/0!
Brizalina variabilis	2		0,010204	-4,58497	-0,04679	2048	0,5102	#DIV/0!	#DIV/0!
Bulimina gibba	4		0,020408	-3,89182	-0,07942	4096	1,0204	#DIV/0!	#DIV/0!
Cassidulina laevigata	24		0,122449	-2,10006	-0,25715	24576	6,1224	#DIV/0!	#DIV/0!
Chilostomella oolina	1		0,005102	-5,27811	-0,02693	1024	0,2551	#DIV/0!	#DIV/0!
Cibicides cf. pseudoungerianus	18		0,091837	-2,38774	-0,21928	18432	4,5918	#DIV/0!	#DIV/0!
Cibicides sp.	2		0,010204	-4,58497	-0,04679	2048	0,5102	#DIV/0!	#DIV/0!
Epistominella vitrea	3		0,015306	-4,1795	-0,06397	3072	0,7653	#DIV/0!	#DIV/0!
Globocassidulina rossensis	28		0,142857	-1,94591	-0,27799	28672	7,1429	#DIV/0!	#DIV/0!
Globocassidulina subglobosa	3		0,015306	-4,1795	-0,06397	3072	0,7653	#DIV/0!	#DIV/0!
Lagena cf. interrupta	1		0,005102	-5,27811	-0,02693	1024	0,2551	#DIV/0!	#DIV/0!
Melonis barleanum	1		0,005102	-5,27811	-0,02693	1024	0,2551	#DIV/0!	#DIV/0!
Nonion fabum	1		0,005102	-5,27811	-0,02693	1024	0,2551	#DIV/0!	#DIV/0!
Nonionela turgida	2		0,010204	-4,58497	-0,04679	2048	0,5102	#DIV/0!	#DIV/0!
Oolina alcocki	1		0,005102	-5,27811	-0,02693	1024	0,2551	#DIV/0!	#DIV/0!
Quinqueloculina stalkeri	3		0,015306	-4,1795	-0,06397	3072	0,7653	#DIV/0!	#DIV/0!
Rectuvigerina phlegeri	2		0,010204	-4,58497	-0,04679	2048	0,5102	#DIV/0!	#DIV/0!
Trifarina carinata	4		0,020408	-3,89182	-0,07942	4096	1,0204	#DIV/0!	#DIV/0!
Uvigerina peregrina	3		0,015306	-4,1795	-0,06397	3072	0,7653	#DIV/0!	#DIV/0!
Valvulineria bradyana	2		0,010204	-4,58497	-0,04679	2048	0,5102	#DIV/0!	#DIV/0!
Ind	196					200704	50,0000	#DIV/0!	#DIV/0!
		Total			-2,65428	401408	100	#DIV/0!	#DIV/0!

Asterigerinata cf. mamilla	3,8265
Bolivina difformis	8,4184
Brizalina spathulata	5,6122
Cassidulina laevigata	6,1224
Cibicides cf. pseudoungerianus	4,5918
Globocassidulina rossensis	7,1429
A	64,2857

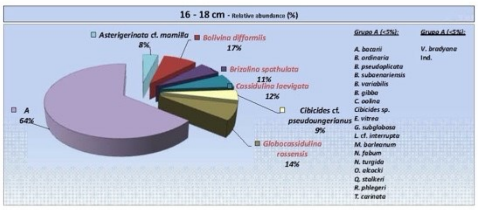

Planktonic	74752	15,69892473
Benthonic	401408	84,30107527
Total	476160	100,0

Foraminifera - 18-20 cm

sample	split	
18-20 cm	12	1/4096

		Screening 1024					%	Volume	Density/cm3
Amphicoryna scalaris	2		0,01196724	-4,595349851	-0,049782871	2048	0,5525	#DIV/0!	#DIV/0!
Astrorotinoides cf. mamilla	8		0,04419885	-3,119095549	-0,137858806	8192	2,2099	#DIV/0!	#DIV/0!
Bolivina difformis	25		0,138121547	-1,979621206	-0,273428343	25600	6,9061	#DIV/0!	#DIV/0!
Bolivina ordinaria	13		0,071823204	-2,633547674	-0,189149833	13312	3,5912	#DIV/0!	#DIV/0!
Bolivina pseudoplicata	6		0,033148171	-3,406737562	-0,112939527	6144	1,6575	#DIV/0!	#DIV/0!
Brizalina subaenariensis	5		0,027624309	-3,588959119	-0,09914528	5120	1,3812	#DIV/0!	#DIV/0!
Brizalina spathulata	13		0,071823204	-2,633547674	-0,189149833	13312	3,5912	#DIV/0!	#DIV/0!
Bulimina marginata	2		0,01196724	-4,595349851	-0,049782871	2048	0,5525	#DIV/0!	#DIV/0!
Cassidulina laevigata	18		0,099447514	-2,308125273	-0,22953732	18432	4,9724	#DIV/0!	#DIV/0!
Cibicides cf. pseudoungerianus	21		0,116022099	-2,153974594	-0,249998654	21504	5,8011	#DIV/0!	#DIV/0!
Epistominella vitrea	5		0,027624309	-3,588959119	-0,09914528	5120	1,3812	#DIV/0!	#DIV/0!
Fissurina orbignyana	2		0,01196724	-4,595349851	-0,049782871	2048	0,5525	#DIV/0!	#DIV/0!
Globocassidulina rossensis	27		0,149171271	-1,902660165	-0,283822235	27648	7,4586	#DIV/0!	#DIV/0!
Globocassidulina subglobosa	9		0,049723757	-3,001272454	-0,149234542	9216	2,4862	#DIV/0!	#DIV/0!
Hyalinea balthica	1		0,005524862	-5,198497081	-0,028729678	1024	0,2762	#DIV/0!	#DIV/0!
Lagena laevis	1		0,005524862	-5,198497081	-0,028729678	1024	0,2762	#DIV/0!	#DIV/0!
Melonis barleeanum	1		0,005524862	-5,198497081	-0,028729678	1024	0,2762	#DIV/0!	#DIV/0!
Nonion fabum	1		0,005524862	-5,198497081	-0,028729678	1024	0,2762	#DIV/0!	#DIV/0!
Nonionella turgida	1		0,005524862	-5,198497081	-0,028729678	1024	0,2762	#DIV/0!	#DIV/0!
Quinqueloculina stalkeri	4		0,022099448	-3,81220267	-0,084247573	4096	1,1050	#DIV/0!	#DIV/0!
Rectuvigerina phlegeri	1		0,005524862	-5,198497081	-0,028729678	1024	0,2762	#DIV/0!	#DIV/0!
Stainforthia complanata	3		0,016574586	-4,099884743	-0,067953891	3072	0,8287	#DIV/0!	#DIV/0!
Stainforthia fusiformis	3		0,016574586	-4,099884743	-0,067953891	3072	0,8287	#DIV/0!	#DIV/0!
Textularia deltoidea	4		0,022099448	-3,81220267	-0,084247573	4096	1,1050	#DIV/0!	#DIV/0!
Uvigerina peregrina	4		0,022099448	-3,81220267	-0,084247573	4096	1,1050	#DIV/0!	#DIV/0!
Valvulineria bradyana	1		0,005524862	-5,198497081	-0,028729678	1024	0,2762	#DIV/0!	#DIV/0!
Nid	181		1			185344	50,0000	#DIV/0!	#DIV/0!
		Total			-3,352356613	370688	100	#DIV/0!	#DIV/0!

Bolivina difformis	6,9061
Bolivina ordinaria	3,5912
Brizalina spathulata	3,5912
Cassidulina laevigata	4,9724
Cibicides cf. pseudoungerianus	5,8011
Globocassidulina rossensis	7,4586
Globocassidulina subglobosa	2,4862
A	65,1934

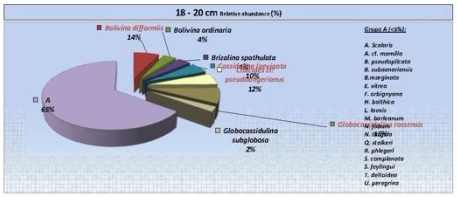

Planktonic	110592	29,8378334
Benthonic	370688	72,0317916
Total	481280	100,0

Foraminifera - 30 cm

sample	split	
30 cm	11	1/4096

		Screening 4096					%	Volume	Density/cm3
Amphicoryna scalaris	1		0,004219	-5,46896	-0,02307198	4096	0,4219	#DIV/0!	#DIV/0!
Ammonia beccarii	6		0,025316	-3,6763	-0,0930706	24576	2,5316	#DIV/0!	#DIV/0!
Astrorotinoides cf. mamilla	4		0,016878	-4,08177	-0,06889056	16384	1,6878	#DIV/0!	#DIV/0!
Astrorotinoides sp.	8		0,033755	-3,38842	-0,11438375	32768	3,3755	#DIV/0!	#DIV/0!
Bolivina albatrossi	1		0,004219	-5,46896	-0,02307198	4096	0,4219	#DIV/0!	#DIV/0!
Bolivina difformis	41		0,172996	-1,75449	-0,30351909	167936	17,2996	#DIV/0!	#DIV/0!
Bolivina ordinaria	21		0,086698	-2,42354	-0,21474385	86016	8,6698	#DIV/0!	#DIV/0!
Bolivina pseudoplicata	5		0,021097	-3,85842	-0,08140553	20480	2,1097	#DIV/0!	#DIV/0!
Brizalina spathulata	26		0,109705	-2,20936	-0,24244326	106496	10,9705	#DIV/0!	#DIV/0!
Brizalina subaenariensis	2		0,008439	-4,77431	-0,04029642	8192	0,8439	#DIV/0!	#DIV/0!
Brizalina variabilis	1		0,004219	-5,46896	-0,02307198	4096	0,4219	#DIV/0!	#DIV/0!
Bulimina elongata	5		0,021097	-3,85842	-0,08140553	20480	2,1097	#DIV/0!	#DIV/0!
Bulimina marginata	3		0,012658	-4,36945	-0,05530647	12288	1,2658	#DIV/0!	#DIV/0!
Cassidulina laevigata	26		0,109705	-2,20936	-0,24244326	106496	10,9705	#DIV/0!	#DIV/0!
Chilostomella oolina	1		0,004219	-5,46896	-0,02307198	4096	0,4219	#DIV/0!	#DIV/0!
Cibicides cf. pseudoungerianus	17		0,07173	-2,63485	-0,18899745	69632	7,1730	#DIV/0!	#DIV/0!
Cribroancora gerthi	1		0,004219	-5,46896	-0,02307198	4096	0,4219	#DIV/0!	#DIV/0!
Epistominella vitrea	8		0,033755	-3,38842	-0,11438375	32768	3,3755	#DIV/0!	#DIV/0!
Fissurina marginata	1		0,004219	-5,46896	-0,02307198	4096	0,4219	#DIV/0!	#DIV/0!
Fissurina orbignyana	1		0,004219	-5,46896	-0,02307198	4096	0,4219	#DIV/0!	#DIV/0!
Globocassidulina rossensis	30		0,126582	-2,06686	-0,2616282	122880	12,6582	#DIV/0!	#DIV/0!
Globocassidulina subglobosa	4		0,016878	-4,08177	-0,06889056	16384	1,6878	#DIV/0!	#DIV/0!
Gyroidina umbonata	2		0,008439	-4,77431	-0,04029642	8192	0,8439	#DIV/0!	#DIV/0!
Hyalinea balthica	1		0,004219	-5,46896	-0,02307198	4096	0,4219	#DIV/0!	#DIV/0!
Melonis barleeanum	1		0,004219	-5,46896	-0,02307198	4096	0,4219	#DIV/0!	#DIV/0!
Nonionella turgida	2		0,008439	-4,77431	-0,04029642	8192	0,8439	#DIV/0!	#DIV/0!
Oolina hirsla	1		0,004219	-5,46896	-0,02307198	4096	0,4219	#DIV/0!	#DIV/0!
Quinqueloculina stalkeri	3		0,012658	-4,36945	-0,05530647	12288	1,2658	#DIV/0!	#DIV/0!
Rectuvigerina phlegeri	2		0,008439	-4,77431	-0,04029642	8192	0,8439	#DIV/0!	#DIV/0!
Stainforthia complanata	4		0,016878	-4,08177	-0,06889056	16384	1,6878	#DIV/0!	#DIV/0!
Textularia deltoidea	2		0,008439	-4,77431	-0,04029642	8192	0,8439	#DIV/0!	#DIV/0!
Trifarina bradyana	1		0,004219	-5,46896	-0,02307198	4096	0,4219	#DIV/0!	#DIV/0!
Trifarina angulosa	1		0,004219	-5,46896	-0,02307198	4096	0,4219	#DIV/0!	#DIV/0!
Valvulineria bradyana	4		0,016878	-4,08177	-0,06889056	16384	1,6878	#DIV/0!	#DIV/0!
	237	Total			-2,80294283	970752	100	#DIV/0!	#DIV/0!

Bolivina difformis	17,2996
Bolivina ordinaria	8,8608
Brizalina spathulata	10,9705
Cassidulina laevigata	10,9705
Cibicides cf. pseudoungerianus	7,1730
Globocassidulina rossensis	12,6582
A	32,9675

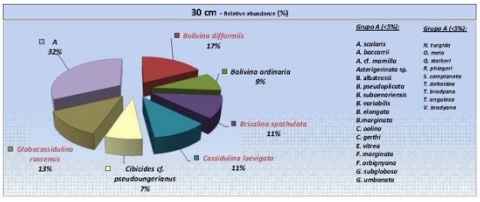

Planktonic	340864	35,1582383
Benthonic	970752	73,8317757
Total	1311616	100,0

Foraminifera - 40 cm

sample	split	
40 cm	12	1/4096

		Screening 4096				%	Volume	Density/cm3
Amphycorina scalaris	2		0,009217	-4,68675	-0,04319585	8192	0,9217	#DIV/0!	#DIV/0!
Ammonia beccarii	7		0,032258	-3,43399	-0,11077378	28672	3,2258	#DIV/0!	#DIV/0!
Asterigerinata cf. mamilla	18		0,082949	-2,48953	-0,20650443	73728	8,2949	#DIV/0!	#DIV/0!
Asterigerinata sp.	1		0,004608	-5,3789	-0,02479215	4096	0,4608	#DIV/0!	#DIV/0!
Bolivina difformis	34		0,156682	-1,85354	-0,29041591	139264	15,6682	#DIV/0!	#DIV/0!
Bolivina ordinaria	11		0,050691	-2,982	-0,1511614	45056	5,0691	#DIV/0!	#DIV/0!
Bolivina pseudoplicata	5		0,023041	-3,77046	-0,08687695	20480	2,3041	#DIV/0!	#DIV/0!
Bolivina striatula	1		0,004608	-5,3789	-0,02479215	4096	0,4608	#DIV/0!	#DIV/0!
Brizalina subcanariensis	5		0,023041	-3,77046	-0,08687695	20480	2,3041	#DIV/0!	#DIV/0!
Brizalina spathulata	17		0,078341	-2,54668	-0,19959681	69632	7,8341	#DIV/0!	#DIV/0!
Bulimina elongata	3		0,013825	-4,28129	-0,05918827	12288	1,3825	#DIV/0!	#DIV/0!
Bulimina marginata	3		0,013825	-4,28129	-0,05918827	12288	1,3825	#DIV/0!	#DIV/0!
Cassidulina laevigata	17		0,078341	-2,54668	-0,19959681	69632	7,8341	#DIV/0!	#DIV/0!
Chilostomella oolina	1		0,004608	-5,3789	-0,02479215	4096	0,4608	#DIV/0!	#DIV/0!
Cibicides cf. pseudoungerianus	19		0,087558	-2,43546	-0,2132429	77824	8,7558	#DIV/0!	#DIV/0!
Cibicides ungerianus	5		0,023041	-3,77046	-0,08687695	20480	2,3041	#DIV/0!	#DIV/0!
Fissurina fasciata	2		0,009217	-4,68675	-0,04319585	8192	0,9217	#DIV/0!	#DIV/0!
Fissurina laevigata	1		0,004608	-5,3789	-0,02479215	4096	0,4608	#DIV/0!	#DIV/0!
Fissurina orbignyana	2		0,009217	-4,68675	-0,04319585	8192	0,9217	#DIV/0!	#DIV/0!
Globocassidulina rossensis	26		0,119816	-2,1218	-0,25422438	106496	11,9816	#DIV/0!	#DIV/0!
Globocassidulina subglobosa	7		0,032258	-3,43399	-0,11077378	28672	3,2258	#DIV/0!	#DIV/0!
Gyroidina umbonata	1		0,004608	-5,3789	-0,02479215	4096	0,4608	#DIV/0!	#DIV/0!
Melonis barleeanum	1		0,004608	-5,3789	-0,02479215	4096	0,4608	#DIV/0!	#DIV/0!
Nonion fabum	1		0,004608	-5,3789	-0,02479215	4096	0,4608	#DIV/0!	#DIV/0!
Nonionella turgida	2		0,009217	-4,68675	-0,04319585	8192	0,9217	#DIV/0!	#DIV/0!
Oolina alcocki	1		0,004608	-5,3789	-0,02479215	4096	0,4608	#DIV/0!	#DIV/0!
Planorbulina mediterranensis	1		0,004608	-5,3789	-0,02479215	4096	0,4608	#DIV/0!	#DIV/0!
Quinqueloculina stalkeri	2		0,009217	-4,68675	-0,04319585	8192	0,9217	#DIV/0!	#DIV/0!
Rectuvigerina phlegeri	3		0,013825	-4,28129	-0,05918827	12288	1,3825	#DIV/0!	#DIV/0!
Stainforthia complanata	2		0,009217	-4,68675	-0,04319585	8192	0,9217	#DIV/0!	#DIV/0!
Textularia deltoidea	6		0,02765	-3,58814	-0,09921118	24576	2,7650	#DIV/0!	#DIV/0!
Trifarina angulosa	2		0,009217	-4,68675	-0,04319585	8192	0,9217	#DIV/0!	#DIV/0!
Uvigerina peregrina	4		0,018433	-3,9936	-0,0736148	16384	1,8433	#DIV/0!	#DIV/0!
Valvulineria bradyana	4		0,018433	-3,9936	-0,0736148	16384	1,8433	#DIV/0!	#DIV/0!
	217	Total			-3,9452536	888832	100	#DIV/0!	#DIV/0!

Asterigerinata cf. mamilla	8,2949
Bolivina difformis	15,6682
Bolivina ordinaria	5,0691
Brizalina spathulata	7,8341
Cassidulina laevigata	7,8341
Cibicides cf. pseudoungerianus	8,7558
Globocassidulina rossensis	11,9816
A	34,5622

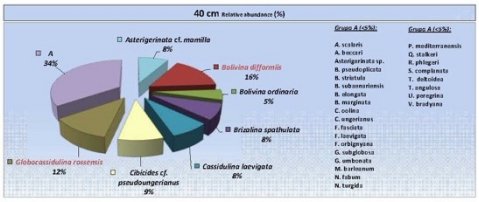

Planktonic	294912	24,91949481
Benthonic	888832	75,08050519
Total	1183744	100,0

Foraminifera - 50 cm

sample	split	
50 cm	11	1/2048

		Screening 2048				%	Volume	Density/cm3
Asterigerinata cf. mamilla	4		0,021739	-5,82864	-0,98323135	8192	2,1739	#DIV/0!	#DIV/0!
Asterigerinata sp.	7		0,038043	-5,26033	-0,12436106	14336	3,8043	#DIV/0!	#DIV/0!
Bolivina difformis	21		0,11413	-2,17941	-0,24771926	43008	11,4130	#DIV/0!	#DIV/0!
Bolivina ordinaria	13		0,070652	-2,64999	-0,1872273	26624	7,0652	#DIV/0!	#DIV/0!
Bolivina pseudoplicata	6		0,032609	-3,42318	-0,11162514	12288	3,2609	#DIV/0!	#DIV/0!
Bolivina sp.	2		0,01087	-4,52178	-0,04914876	4096	1,0870	#DIV/0!	#DIV/0!
Brizalina subcanariensis	4		0,021739	-5,82864	-0,98323135	8192	2,1739	#DIV/0!	#DIV/0!
Brizalina spathulata	10		0,054348	-2,91235	-0,15827927	20480	5,4348	#DIV/0!	#DIV/0!
Bulimina gibba	3		0,016304	-4,11632	-0,9671.1767	6144	1,6304	#DIV/0!	#DIV/0!
Bulimina marginata	4		0,021739	-5,82864	-0,98323135	8192	2,1739	#DIV/0!	#DIV/0!
Bulimina mexicana	1		0,005435	-5,21494	-0,02834042	2048	0,5435	#DIV/0!	#DIV/0!
Brizalina variabilis	1		0,005435	-5,21494	-0,02834042	2048	0,5435	#DIV/0!	#DIV/0!
Cassidulina laevigata	13		0,070652	-2,64999	-0,1872273	26624	7,0652	#DIV/0!	#DIV/0!
Cibicides cf. pseudoungerianus	10		0,054348	-2,91235	-0,15827927	20480	5,4348	#DIV/0!	#DIV/0!
Cibicides sp.1	1		0,005435	-5,21494	-0,02834042	2048	0,5435	#DIV/0!	#DIV/0!
Cibicides sp.2	1		0,005435	-5,21494	-0,02834042	2048	0,5435	#DIV/0!	#DIV/0!
Fissurina globosocaudata	1		0,005435	-5,21494	-0,02834042	2048	0,5435	#DIV/0!	#DIV/0!
Fissurina lucida	3		0,016304	-4,11632	-0,9671.1767	6144	1,6304	#DIV/0!	#DIV/0!
Globocassidulina rossensis	47		0,255435	-1,36478	-0,34861436	96256	25,5435	#DIV/0!	#DIV/0!
Globocassidulina subglobosa	4		0,021739	-5,82864	-0,98323135	8192	2,1739	#DIV/0!	#DIV/0!
Gyroidina umbonata	3		0,016304	-4,11632	-0,9671.1767	6144	1,6304	#DIV/0!	#DIV/0!
Lagoma sp.1	1		0,005435	-5,21494	-0,02834042	2048	0,5435	#DIV/0!	#DIV/0!
Lagoma sp.2	1		0,005435	-5,21494	-0,02834042	2048	0,5435	#DIV/0!	#DIV/0!
Nonion fabum	3		0,016304	-4,11632	-0,9671.1767	6144	1,6304	#DIV/0!	#DIV/0!
Nonionella turgida	3		0,016304	-4,11632	-0,9671.1767	6144	1,6304	#DIV/0!	#DIV/0!
Oolina sp.	1		0,005435	-5,21494	-0,02834042	2048	0,5435	#DIV/0!	#DIV/0!
Quinqueloculina stalkeri	1		0,005435	-5,21494	-0,02834042	2048	0,5435	#DIV/0!	#DIV/0!
Rectuvigerina phlegeri	2		0,01087	-4,52178	-0,04914876	4096	1,0870	#DIV/0!	#DIV/0!
Stainforthia complanata	2		0,01087	-4,52178	-0,04914876	4096	1,0870	#DIV/0!	#DIV/0!
Stainforthia feylingai	1		0,005435	-5,21494	-0,02834042	2048	0,5435	#DIV/0!	#DIV/0!
Textularia deltoidea	1		0,005435	-5,21494	-0,02834042	2048	0,5435	#DIV/0!	#DIV/0!
Trifarina angulosa	1		0,005435	-5,21494	-0,02834042	2048	0,5435	#DIV/0!	#DIV/0!
Uvigerina peregrina	3		0,016304	-4,11632	-0,9671.1767	6144	1,6304	#DIV/0!	#DIV/0!
Valvulineria bradyana	3		0,016304	-4,11632	-0,9671.1767	6144	1,6304	#DIV/0!	#DIV/0!
ind	2					4096	1,0870	#DIV/0!	#DIV/0!
	184	Total			-3,8139282715	376832	100	#DIV/0!	#DIV/0!

Bolivina difformis	11,4130
Bolivina ordinaria	7,0652
Brizalina spathulata	5,4348
Cassidulina laevigata	7,0652
Cibicides cf. pseudoungerianus	5,4348
Globocassidulina rossensis	25,5435
A	38,0435

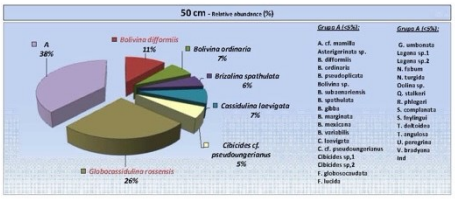

Planktonic	151792	30,03802281
Benthonic	376832	69,96197719
Total	528624	100,0

Foraminifera - 60 cm

sample	split	
60 cm	12	1/4096

		Screening					%	Volume	Density/cm3
		4096							
Asterigerinata cf. mamilla	4		0,012277	-3,85015	-0,08192	16384	2,1277	#DIV/0!	#DIV/0!
Asterigerinata sp.	17		0,090426	-2,40323	-0,21731	69632	9,0426	#DIV/0!	#DIV/0!
Bolivina difformis	26		0,138298	-1,97835	-0,2736	106496	13,8298	#DIV/0!	#DIV/0!
Bolivina ordinaria	9		0,047872	-3,03922	-0,14549	36864	4,7872	#DIV/0!	#DIV/0!
Bolivina pseudoplicata	3		0,015957	-4,13783	-0,06603	12288	1,5957	#DIV/0!	#DIV/0!
Bolivina sp.	1		0,005319	-5,23644	-0,02785	4096	0,5319	#DIV/0!	#DIV/0!
Brizalina subaenariensis	5		0,026596	-3,627	-0,09646	20480	2,6596	#DIV/0!	#DIV/0!
Brizalina spathulata	25		0,132979	-2,01757	-0,26829	102400	13,2979	#DIV/0!	#DIV/0!
Bulimina elongata	3		0,015957	-4,13783	-0,06603	12288	1,5957	#DIV/0!	#DIV/0!
Cassidulina laevigata	11		0,058511	-2,83855	-0,16609	45056	5,8511	#DIV/0!	#DIV/0!
Cassidulinoides bradyi	2		0,010638	-4,54329	-0,04833	8192	1,0638	#DIV/0!	#DIV/0!
Cibicides cf. pseudoungerianus	15		0,079787	-2,52839	-0,20173	61440	7,9787	#DIV/0!	#DIV/0!
Cribononion gerthi	3		0,015957	-4,13783	-0,06603	12288	1,5957	#DIV/0!	#DIV/0!
Fissurina laevigata	1		0,005319	-5,23644	-0,02785	4096	0,5319	#DIV/0!	#DIV/0!
Globocassidulina rossensis	32		0,170213	-1,77071	-0,3014	131072	17,0213	#DIV/0!	#DIV/0!
Globocassidulina subglobosa	5		0,026596	-3,627	-0,09646	20480	2,6596	#DIV/0!	#DIV/0!
Gyroidina umbonata	6		0,031915	-3,44408	-0,10994	24576	3,1915	#DIV/0!	#DIV/0!
Hyalinea balthica	1		0,005319	-5,23644	-0,02785	4096	0,5319	#DIV/0!	#DIV/0!
Melonis barleanum	1		0,005319	-5,23644	-0,02785	4096	0,5319	#DIV/0!	#DIV/0!
Nonion fabum	3		0,015957	-4,13783	-0,06603	12288	1,5957	#DIV/0!	#DIV/0!
Quinqueloculina stalkeri	3		0,015957	-4,13783	-0,06603	12288	1,5957	#DIV/0!	#DIV/0!
Quinqueloculina akneriana	1		0,005319	-5,23644	-0,02785	4096	0,5319	#DIV/0!	#DIV/0!
Rectuvigerina phlegeri	3		0,015957	-4,13783	-0,06603	12288	1,5957	#DIV/0!	#DIV/0!
Stainforthia complanata	1		0,005319	-5,23644	-0,02785	4096	0,5319	#DIV/0!	#DIV/0!
Trifarina angulosa	2		0,010638	-4,54329	-0,04833	8192	1,0638	#DIV/0!	#DIV/0!
Uvigerina peregrina	1		0,005319	-5,23644	-0,02785	4096	0,5319	#DIV/0!	#DIV/0!
Valvulineria bradyana	2		0,010638	-4,54329	-0,04833	8192	1,0638	#DIV/0!	#DIV/0!
Ind	2					8192	1,0638	#DIV/0!	#DIV/0!
	188	Total			-3,69485	770048	100	#DIV/0!	#DIV/0!

Asterigerinata sp.	9,0426
Bolivina difformis	13,8298
Brizalina spathulata	13,2979
Cibicides cf. pseudoungerianus	7,9787
Globocassidulina rossensis	17,0213
A	36,8298

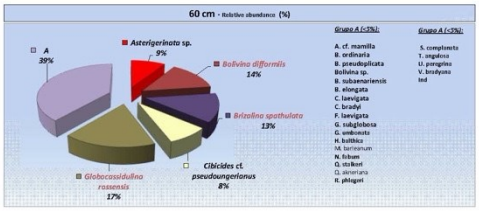

Planktonic	372736	32,61648746
Benthonic	770048	67,38351254
Total	1142784	100,0

Foraminifera - 70 cm

sample	split	
70 cm	12	1/4096

		Screening					%	Volume	Density/cm3
		4096							
Asterigerinata sp.	10		0,055556	-2,83037	-0,1805 7621	40960	5,5556	#DIV/0!	#DIV/0!
Bolivina difformis	37		0,205556	-1,54204	-0,32519683	151552	20,5556	#DIV/0!	#DIV/0!
Bolivina ordinaria	2		0,011111	-4,49981	-0,04999789	8192	1,1111	#DIV/0!	#DIV/0!
Bolivina pseudoplicata	14		0,077778	-2,5539	-0,19863663	57344	7,7778	#DIV/0!	#DIV/0!
Brizalina subaenariensis	7		0,038889	-3,24705	-0,12627404	28672	3,8889	#DIV/0!	#DIV/0!
Brizalina spathulata	12		0,066667	-2,70805	-0,1805 3668	49152	6,6667	#DIV/0!	#DIV/0!
Bulimina alazanensis	3		0,016667	-4,09434	-0,06823908	12288	1,6667	#DIV/0!	#DIV/0!
Bulimina gibba	8		0,044444	-3,11352	-0,13837846	32768	4,4444	#DIV/0!	#DIV/0!
Bulimina marginata	1		0,005556	-5,19296	-0,02884976	4096	0,5556	#DIV/0!	#DIV/0!
Cassidulina laevigata	12		0,066667	-2,70805	-0,1805 3668	49152	6,6667	#DIV/0!	#DIV/0!
Cassidulina teretis	2		0,011111	-4,49981	-0,04999789	8192	1,1111	#DIV/0!	#DIV/0!
Cibicides cf. pseudoungerianus	20		0,111111	-2,19722	-0,2441 3606	81920	11,1111	#DIV/0!	#DIV/0!
Cibicides sp.1	3		0,016667	-4,09434	-0,06823908	12288	1,6667	#DIV/0!	#DIV/0!
Epistominella vitrea	2		0,011111	-4,49981	-0,04999789	8192	1,1111	#DIV/0!	#DIV/0!
Fissurina lucida	2		0,011111	-4,49981	-0,04999789	8192	1,1111	#DIV/0!	#DIV/0!
Globocassidulina rossensis	19		0,105556	-2,24852	-0,23743455	77824	10,5556	#DIV/0!	#DIV/0!
Gyroidina umbonata	4		0,022222	-3,80666	-0,0845925	16384	2,2222	#DIV/0!	#DIV/0!
Hyalinea balthica	3		0,016667	-4,09434	-0,06823908	12288	1,6667	#DIV/0!	#DIV/0!
Neoiteticulina peregrina	2		0,011111	-4,49981	-0,04999789	8192	1,1111	#DIV/0!	#DIV/0!
Nonion fabum	4		0,022222	-3,80666	-0,0845925	16384	2,2222	#DIV/0!	#DIV/0!
Planorbulina mediterranensis	1		0,005556	-5,19296	-0,02884976	4096	0,5556	#DIV/0!	#DIV/0!
Quinqueloculina stalkeri	3		0,016667	-4,09434	-0,06823908	12288	1,6667	#DIV/0!	#DIV/0!
Rectuvigerina phlegeri	1		0,005556	-5,19296	-0,02884976	4096	0,5556	#DIV/0!	#DIV/0!
Trifarina angulosa	1		0,005556	-5,19296	-0,02884976	4096	0,5556	#DIV/0!	#DIV/0!
Uvigerina peregrina	2		0,011111	-4,49981	-0,04999789	8192	1,1111	#DIV/0!	#DIV/0!
Valvulineria bradyana	3		0,016667	-4,09434	-0,06823908	12288	1,6667	#DIV/0!	#DIV/0!
Ind	2					8192	1,1111	#DIV/0!	#DIV/0!
	180	Total			-3,71738194	737280	100	#DIV/0!	#DIV/0!

Asterigerinata sp.	5,5556
Bolivina difformis	20,5556
Bolivina pseudoplicata	7,7778
Brizalina spathulata	6,6667
Cassidulina laevigata	6,6667
Globocassidulina rossensis	10,5556
Cibicides cf. pseudoungerianus	11,1111
A	42,2222

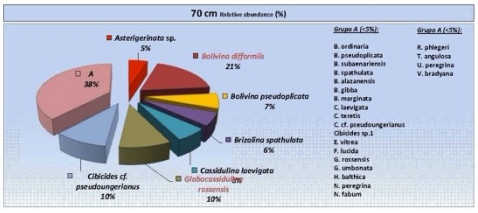

Planktonic	405504	35,48587057
Benthonic	737280	64,51412943
Total	1142784	100,0

Foraminifera - 80 cm

sample	split	
80 cm	12	1/4096

	Screening 4096				Volume %		Density/cm3
Astrigerinata sp.	11		0,048673	-1,62264	-0,14732	45056	4,8673	#DIV/0!	#DIV/0!
Bolivina difformis	30		0,132743	-1,69348	-0,22495	122880	13,2743	#DIV/0!	#DIV/0!
Bolivina ordinaria	9		0,039838	-1,94308	-0,11827	32768	3,9838	#DIV/0!	#DIV/0!
Bolivina pseudoplicata	10		0,044248	-1,91795	-0,13786	40960	4,4248	#DIV/0!	#DIV/0!
Bolivina variabilis	2		0,00885	-4,72738	-0,04184	8192	0,8850	#DIV/0!	#DIV/0!
Brizalina subaenariensis	1		0,004425	-5,42053	-0,02398	4096	0,4425	#DIV/0!	#DIV/0!
Brizalina spathulata	25		0,110619	-2,20166	-0,24355	102400	11,0619	#DIV/0!	#DIV/0!
Bulimina alazanensis	1		0,004425	-5,42053	-0,02398	4096	0,4425	#DIV/0!	#DIV/0!
Bulimina gibba	2		0,00885	-4,72738	-0,04184	8192	0,8850	#DIV/0!	#DIV/0!
Cassidulina laevigata	17		0,075221	-2,58762	-0,19462	69632	7,5221	#DIV/0!	#DIV/0!
Cibicides cf. pseudoungerianus	17		0,075221	-2,58762	-0,19462	69632	7,5221	#DIV/0!	#DIV/0!
Epistominella vitrea	1		0,004425	-5,42053	-0,02398	4096	0,4425	#DIV/0!	#DIV/0!
Fissurina fasciata	1		0,004425	-5,42053	-0,02398	4096	0,4425	#DIV/0!	#DIV/0!
Fissurina globoscrustata	1		0,004425	-5,42053	-0,02398	4096	0,4425	#DIV/0!	#DIV/0!
Fissurina laevigata	1		0,004425	-5,42053	-0,02398	4096	0,4425	#DIV/0!	#DIV/0!
Fissurina orbignyana	1		0,004425	-5,42053	-0,02398	4096	0,4425	#DIV/0!	#DIV/0!
Fissurina sp.	1		0,004425	-5,42053	-0,02398	4096	0,4425	#DIV/0!	#DIV/0!
Globocassidulina rossensis	31		0,137168	-1,98655	-0,27249	126976	13,7168	#DIV/0!	#DIV/0!
Globocassidulina subglobosa	3		0,013274	-4,32192	-0,05737	12288	1,3274	#DIV/0!	#DIV/0!
Gyroidina umbonata	16		0,070796	-2,64785	-0,18747	65536	7,0796	#DIV/0!	#DIV/0!
Lagena laevis	1		0,004425	-5,42053	-0,02398	4096	0,4425	#DIV/0!	#DIV/0!
Lagena sp.	2		0,00885	-4,72738	-0,04184	8192	0,8850	#DIV/0!	#DIV/0!
Nonion fabum	1		0,004425	-5,42053	-0,02398	4096	0,4425	#DIV/0!	#DIV/0!
Nonionella turgida	9		0,039823	-3,22331	-0,12835	36864	3,9823	#DIV/0!	#DIV/0!
Oolina hexagona	1		0,004425	-5,42053	-0,02398	4096	0,4425	#DIV/0!	#DIV/0!
Oolina silvicki	1		0,004425	-5,42053	-0,02398	4096	0,4425	#DIV/0!	#DIV/0!
Patellina corrugata	1		0,004425	-5,42053	-0,02398	4096	0,4425	#DIV/0!	#DIV/0!
Planorbulina mediterranensis	3		0,013274	-4,32192	-0,05737	12288	1,3274	#DIV/0!	#DIV/0!
Quinqueloculina venusta	5		0,022124	-3,8111	-0,08432	20480	2,2124	#DIV/0!	#DIV/0!
Quinqueloculina akneriana	4		0,017699	-4,03454	-0,0714	16384	1,7699	#DIV/0!	#DIV/0!
Stainforthia fusiformis	2		0,00885	-4,72738	-0,04184	8192	0,8850	#DIV/0!	#DIV/0!
Stainforthia elongata	1		0,004425	-5,42053	-0,02398	4096	0,4425	#DIV/0!	#DIV/0!
Textularia deltoidea	4		0,017699	-4,03454	-0,0714	16384	1,7699	#DIV/0!	#DIV/0!
Trifarina bradyana	4		0,017699	-4,03454	-0,0714	16384	1,7699	#DIV/0!	#DIV/0!
Uvigerina peregrina	3		0,013274	-4,32192	-0,05737	12288	1,3274	#DIV/0!	#DIV/0!
Valvulineria bradyana	1		0,004425	-5,42053	-0,02398	4096	0,4425	#DIV/0!	#DIV/0!
Ind	3					12288	1,3274	#DIV/0!	#DIV/0!
	226	Total			-1,69486	925696	100	#DIV/0!	#DIV/0!

Bolivina difformis	13,2743
Brizalina spathulata	11,0619
Cassidulina laevigata	7,5221
Cibicides cf. pseudoungerianus	7,5221
Globocassidulina rossensis	13,7168
Gyroidina umbonata	7,0796
A	39,8230

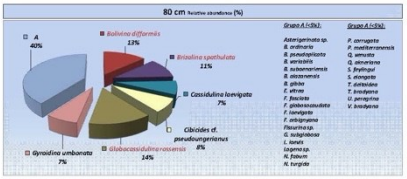

Planktonic	402304	34,59559914
Benthonic	925696	67,66670965
Total	1366464	100,0

Foraminifera - 90 cm

sample	split	
90 cm	12	1/4096

	Screening 4096				Volume %		Density/cm3
Astrigerinata sp.	20		0,101563	-2,27727	-0,23357	81920	10,2564	#DIV/0!	#DIV/0!
Amphycorina scalaris	1		0,005128	-5,273	-0,02704	4096	0,5128	#DIV/0!	#DIV/0!
Bolivina difformis	36		0,184615	-1,68948	-0,3119	147456	18,4615	#DIV/0!	#DIV/0!
Bolivina ordinaria	2		0,010256	-4,57985	-0,04697	8192	1,0256	#DIV/0!	#DIV/0!
Bolivina pseudoplicata	12		0,061538	-2,78809	-0,17157	49152	6,1538	#DIV/0!	#DIV/0!
Bolivina translucens	1		0,005128	-5,273	-0,02704	4096	0,5128	#DIV/0!	#DIV/0!
Brizalina subaenariensis	2		0,010256	-4,57985	-0,04697	8192	1,0256	#DIV/0!	#DIV/0!
Brizalina spathulata	6		0,030769	-3,48124	-0,10712	24576	3,0769	#DIV/0!	#DIV/0!
Bulimina alazanensis	1		0,005128	-5,273	-0,02704	4096	0,5128	#DIV/0!	#DIV/0!
Cassidulina laevigata	9		0,046154	-3,07577	-0,14196	36864	4,6154	#DIV/0!	#DIV/0!
Cibicides cf. pseudoungerianus	14		0,071795	-2,63394	-0,1891	57344	7,1795	#DIV/0!	#DIV/0!
Fissurina fasciata	1		0,005128	-5,273	-0,02704	4096	0,5128	#DIV/0!	#DIV/0!
Fissurina incomposita	1		0,005128	-5,273	-0,02704	4096	0,5128	#DIV/0!	#DIV/0!
Fissurina laevigata	1		0,005128	-5,273	-0,02704	4096	0,5128	#DIV/0!	#DIV/0!
Fissurina orbignyana	2		0,010256	-4,57985	-0,04697	8192	1,0256	#DIV/0!	#DIV/0!
Fissurina semimarginata	1		0,005128	-5,273	-0,02704	4096	0,5128	#DIV/0!	#DIV/0!
cassidulina crassa	19		0,097436	-2,32856	-0,22689	77824	9,7436	#DIV/0!	#DIV/0!
Globocassidulina minuta	10		0,051282	-2,97041	-0,15233	40960	5,1282	#DIV/0!	#DIV/0!
Globocassidulina rossensis	19		0,097436	-2,32856	-0,22689	77824	9,7436	#DIV/0!	#DIV/0!
Gyroidina umbonata	5		0,025641	-3,66356	-0,09394	20480	2,5641	#DIV/0!	#DIV/0!
Hyalinea balthica	1		0,005128	-5,273	-0,02704	4096	0,5128	#DIV/0!	#DIV/0!
Neolenticulina variabilis	1		0,005128	-5,273	-0,02704	4096	0,5128	#DIV/0!	#DIV/0!
Planorbulina mediterranensis	1		0,005128	-5,273	-0,02704	4096	0,5128	#DIV/0!	#DIV/0!
Quinqueloculina akneriana	2		0,010256	-4,57985	-0,04697	8192	1,0256	#DIV/0!	#DIV/0!
Quinqueloculina lamarckiana	1		0,005128	-5,273	-0,02704	4096	0,5128	#DIV/0!	#DIV/0!
Quinqueloculina stalkeri	2		0,010256	-4,57985	-0,04697	8192	1,0256	#DIV/0!	#DIV/0!
Textularia deltoidea	8		0,041026	-3,19356	-0,13102	32768	4,1026	#DIV/0!	#DIV/0!
Trifarina carinata	2		0,010256	-4,57985	-0,04697	8192	1,0256	#DIV/0!	#DIV/0!
Uvigerina peregrina	7		0,035897	-3,32709	-0,11943	28672	3,5897	#DIV/0!	#DIV/0!
Valvulineria bradyana	1		0,005128	-5,273	-0,02704	4096	0,5128	#DIV/0!	#DIV/0!
Valvulineria minuta	3		0,015385	-4,17439	-0,06422	12288	1,5385	#DIV/0!	#DIV/0!
Ind	3					12288	1,5385	#DIV/0!	#DIV/0!
	195	Total			-2,77626	798720	100	#DIV/0!	#DIV/0!

Asterigerinata sp.	10,2564
Bolivina difformis	18,4615
Bolivina pseudoplicata	6,1538
Cibicides cf. pseudoungerianus	7,1795
Cassidulina crassa	9,7436
Globocassidulina rossensis	9,7436
A	38,4615

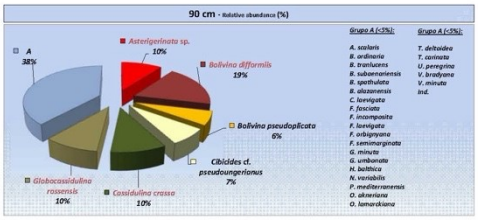

Planktonic	425984	34,78260870
Benthonic	798720	65,21739130
Total	1224704	100,0

Foraminifera - 100 cm

sample	split	
100 cm	11	1/2048

		Screening 2048					%	Volume	Density/cm3
Bolivina difformis	32		0,154589	-1,86698	-0,28862	65536	15,4589	#DIV/0!	#DIV/0!
Bolivina ordinaria	3		0,014493	-4,23411	-0,06136	6144	1,4493	#DIV/0!	#DIV/0!
Bolivina pseudoplicata	5		0,024155	-3,72328	-0,08993	10240	2,4155	#DIV/0!	#DIV/0!
Bolivina translucens	1		0,004831	-5,33272	-0,02576	2048	0,4831	#DIV/0!	#DIV/0!
Brizalina subaenariensis	3		0,014493	-4,23411	-0,06136	6144	1,4493	#DIV/0!	#DIV/0!
Brizalina spathulata	18		0,086957	-2,44235	-0,21238	36864	8,6957	#DIV/0!	#DIV/0!
Bulimina elongata	1		0,004831	-5,33272	-0,02576	2048	0,4831	#DIV/0!	#DIV/0!
Bulimina gibba	3		0,014493	-4,23411	-0,06136	6144	1,4493	#DIV/0!	#DIV/0!
Bulimina marginata	2		0,009662	-4,63957	-0,04483	4096	0,9662	#DIV/0!	#DIV/0!
Cassidulina laevigata	11		9,95314	-2,93482	-0,15586	22528	5,3140	#DIV/0!	#DIV/0!
Cassidulina minuta	10		0,048706	-3,03013	-0,14638	20480	4,8309	#DIV/0!	#DIV/0!
Cassidulina teretis	7		0,033816	-3,38681	-0,11453	14336	3,3816	#DIV/0!	#DIV/0!
Cibicides cf. pseudoungerianus	27		0,130435	-2,03688	-0,26568	55296	13,0435	#DIV/0!	#DIV/0!
Cibicides sp.	2		0,009662	-4,63957	-0,04483	4096	0,9662	#DIV/0!	#DIV/0!
Cribononion gerthi	3		0,014493	-4,23411	-0,06136	6144	1,4493	#DIV/0!	#DIV/0!
Epistominella vitrea	5		0,024155	-3,72328	-0,08993	10240	2,4155	#DIV/0!	#DIV/0!
Elphidium complanatum	1		0,004831	-5,33272	-0,02576	2048	0,4831	#DIV/0!	#DIV/0!
Fissurina orbignyana	3		0,014493	-4,23411	-0,06136	6144	1,4493	#DIV/0!	#DIV/0!
Fissurina submarginata	1		0,004831	-5,33272	-0,02576	2048	0,4831	#DIV/0!	#DIV/0!
Gyroidina umbonata	1		0,004831	-5,33272	-0,02576	2048	0,4831	#DIV/0!	#DIV/0!
Hyalinea balthica	2		0,009662	-4,63957	-0,04483	4096	0,9662	#DIV/0!	#DIV/0!
Nonion fabum	3		0,014493	-4,23411	-0,06136	6144	1,4493	#DIV/0!	#DIV/0!
Oridorsalis umbonatus	28		0,135266	-2,00951	-0,2706	57344	13,5266	#DIV/0!	#DIV/0!
Planorbulina mediterranensis	1		0,004831	-5,33272	-0,02576	2048	0,4831	#DIV/0!	#DIV/0!
Planigirella miqua	4		0,019324	-3,94642	-0,07626	8192	1,9324	#DIV/0!	#DIV/0!
Pyrgo depressa	3		0,014493	-4,23411	-0,06136	6144	1,4493	#DIV/0!	#DIV/0!
Quinqueloculina skourisna	3		0,014493	-4,23411	-0,06136	6144	1,4493	#DIV/0!	#DIV/0!
Quinqueloculina sp.	2		0,009662	-4,63957	-0,04483	4096	0,9662	#DIV/0!	#DIV/0!
Stainforthia feylingi	2		0,009662	-4,63957	-0,04483	4096	0,9662	#DIV/0!	#DIV/0!
Textularia deltoidea	10		0,048706	-3,03013	-0,14638	20480	4,8309	#DIV/0!	#DIV/0!
Triforina carinata	1		0,004831	-5,33272	-0,02576	2048	0,4831	#DIV/0!	#DIV/0!
Uvigerina peregrina	2		0,009662	-4,63957	-0,04483	4096	0,9662	#DIV/0!	#DIV/0!
Valvulineria bradyana	1		0,004831	-5,33272	-0,02576	2048	0,4831	#DIV/0!	#DIV/0!
ind	6					12288	2,8986	#DIV/0!	#DIV/0!
	207	Total			-2,82352	423936	100	#DIV/0!	#DIV/0!

Bolivina difformis	15,4589
Brizalina spathulata	8,6957
Cassidulina laevigata	5,3140
Cibicides cf. pseudoungerianus	13,0435
Oridorsalis umbonatus	13,5266
A	43,3624

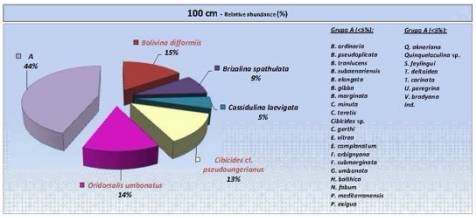

Planktonic	185368	30,59891375
Benthonic	420936	69,48306725
Total	610304	100,0

Foraminifera - 110 cm

sample	split	
110 cm	12	1/4096

		Screening 4096					%	Volume	Density/cm3
Amphycorina scalaris	1		0,005128	-5,273	-0,02704	4096	0,4444	#DIV/0!	#DIV/0!
Asterigerinata sp.1	28		0,14359	-1,9438	-0,27868	114688	12,4444	#DIV/0!	#DIV/0!
Asterigerinata sp.2	1		0,005128	-5,273	-0,02704	4096	0,4444	#DIV/0!	#DIV/0!
Bolivina difformis	33		0,169231	-1,77649	-0,30068	135168	14,6667	#DIV/0!	#DIV/0!
Bolivina ordinaria	5		0,025641	-3,66356	-0,09394	20480	2,2222	#DIV/0!	#DIV/0!
Bolivina pseudoplicata	5		0,025641	-3,66356	-0,09394	20480	2,2222	#DIV/0!	#DIV/0!
Bolivina striatula	2		0,010256	-4,57985	-0,04697	8192	0,8889	#DIV/0!	#DIV/0!
Bolivina sp.	1		0,005128	-5,273	-0,02704	4096	0,4444	#DIV/0!	#DIV/0!
Brizalina spathulata	13		0,066667	-2,70805	-0,18054	53248	5,7778	#DIV/0!	#DIV/0!
Bulimina alazanensis	1		0,005128	-5,273	-0,02704	4096	0,4444	#DIV/0!	#DIV/0!
Cancris auriculs	2		0,010256	-4,57985	-0,04697	8192	0,8889	#DIV/0!	#DIV/0!
Cassidulina laevigata	7		0,035897	-3,32706	-0,11943	28672	3,1111	#DIV/0!	#DIV/0!
Cassidulina minuta	11		0,09641	-2,8751	-0,16259	45056	4,8889	#DIV/0!	#DIV/0!
Cassidulina teretis	1		0,005128	-5,273	-0,02704	4096	0,4444	#DIV/0!	#DIV/0!
Cibicides cf. pseudoungerianus	18		0,092308	-2,38263	-0,21993	73728	8,0000	#DIV/0!	#DIV/0!
Cribononion gerthi	1		0,005128	-5,273	-0,02704	4096	0,4444	#DIV/0!	#DIV/0!
Epistominella vitrea	1		0,005128	-5,273	-0,02704	4096	0,4444	#DIV/0!	#DIV/0!
Fissurina orbignyana	3		0,015385	-4,17436	-0,06422	12288	1,3333	#DIV/0!	#DIV/0!
Fissurina fasciata var. carinata	3		0,015385	-4,17436	-0,06422	12288	1,3333	#DIV/0!	#DIV/0!
Globocassidulina rossensis	25		0,128205	-2,05412	-0,26335	102400	11,1111	#DIV/0!	#DIV/0!
Globocassidulina subglobosa	20		0,102564	-2,27727	-0,23357	81920	8,8889	#DIV/0!	#DIV/0!
Gyroidina umbonata	4		0,020513	-3,88671	-0,07973	16384	1,7778	#DIV/0!	#DIV/0!
Melonis barleanum	2		0,010256	-4,57985	-0,04697	8192	0,8889	#DIV/0!	#DIV/0!
Neoelentiadina peregrina	1		0,005128	-5,273	-0,02704	4096	0,4444	#DIV/0!	#DIV/0!
Neoelentiadina variabilis	2		0,010256	-4,57985	-0,04697	8192	0,8889	#DIV/0!	#DIV/0!
Nonion fabum	4		0,020513	-3,88671	-0,07973	16384	1,7778	#DIV/0!	#DIV/0!
Nonionella turgida	5		0,025641	-3,66356	-0,09394	20480	2,2222	#DIV/0!	#DIV/0!
Pyrgo murrhina	1		0,005128	-5,273	-0,02704	4096	0,4444	#DIV/0!	#DIV/0!
Quinqueloculina skneriana	1		0,005128	-5,273	-0,02704	4096	0,4444	#DIV/0!	#DIV/0!
Quinqueloculina stalkeri	3		0,015385	-4,17436	-0,06422	12288	1,3333	#DIV/0!	#DIV/0!
Quinqueloculina sp.	1		0,005128	-5,273	-0,02704	4096	0,4444	#DIV/0!	#DIV/0!
Textularia deltoidea	9		0,025641	-3,66356	-0,09394	20480	2,2222	#DIV/0!	#DIV/0!
Triforina carinata	2		0,010256	-4,57985	-0,04697	8192	0,8889	#DIV/0!	#DIV/0!
Uvigerina peregrina	1		0,005128	-5,273	-0,02704	4096	0,4444	#DIV/0!	#DIV/0!
Valvulineria bradyana	1		0,005128	-5,273	-0,02704	4096	0,4444	#DIV/0!	#DIV/0!
ind	19		0,051282	-2,97041	-0,15233	40960	4,4444	#DIV/0!	#DIV/0!
	195	Total			-3,07259	921600	100	#DIV/0!	#DIV/0!

Asterigerinata sp.1	12,4444
Bolivina difformis	14,6667
Brizalina spathulata	5,7778
Cibicides cf. pseudoungerianus	8,0000
Globocassidulina rossensis	11,1111
Globocassidulina subglobosa	8,8889
A	39,1111

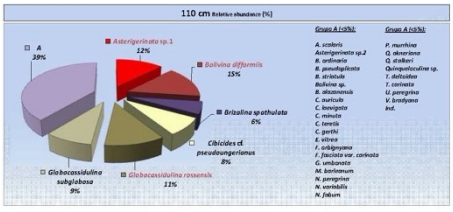

Planktonic	389120	39,6875
Benthonic	921600	70,3125
Total	1310720	100,0

Foraminifera - 120 cm

sample	split	
120	12	1/4096

		Screening					%	Volume	Density/cm3
		4096							
Amphycorina scalaris	1		0,000488	-5,59639	-0,02231	4096	0,4048	#DIV/0!	#DIV/0!
Ammonia beccarii	31		0,125596	-2,0754	-0,26048	126976	12,5596	#DIV/0!	#DIV/0!
Asterigerinata sp.1	25		0,102215	-2,29051	-0,23383	102400	10,1215	#DIV/0!	#DIV/0!
Asterigerinata sp.2	2		0,008197	-4,81624	-0,039	8192	0,8097	#DIV/0!	#DIV/0!
Bolivina difformis	44		0,178138	-1,7252	-0,30732	180224	17,8138	#DIV/0!	#DIV/0!
Bolivina pseudoplicata	3		0,012146	-4,41078	-0,05357	12288	1,2146	#DIV/0!	#DIV/0!
Bolivina striatula	1		0,000488	-5,59639	-0,02231	4096	0,4048	#DIV/0!	#DIV/0!
Bolivina sp.2	1		0,000488	-5,59639	-0,02231	4096	0,4048	#DIV/0!	#DIV/0!
Brizalina spathulata	3		0,012146	-4,41078	-0,05357	12288	1,2146	#DIV/0!	#DIV/0!
Bulimina alazanensis	1		0,000488	-5,59639	-0,02231	4096	0,4048	#DIV/0!	#DIV/0!
Bulimina elongata	2		0,008197	-4,81624	-0,039	8192	0,8097	#DIV/0!	#DIV/0!
Cassidulina laevigata	4		0,016394	-4,12399	-0,06677	16384	1,6194	#DIV/0!	#DIV/0!
Cassidulina minuta	11		0,044534	-3,11149	-0,13857	45056	4,4534	#DIV/0!	#DIV/0!
Cassidulinoides bradyi	1		0,000488	-5,59639	-0,02231	4096	0,4048	#DIV/0!	#DIV/0!
Cibicides cf. pseudoungerianus	52		0,210526	-1,55814	-0,32803	212992	21,0526	#DIV/0!	#DIV/0!
Elphidium articulatum	2		0,008197	-4,81624	-0,039	8192	0,8097	#DIV/0!	#DIV/0!
Elphidium complanatum	1		0,000488	-5,59639	-0,02231	4096	0,4048	#DIV/0!	#DIV/0!
Epistominella vitrea	1		0,000488	-5,59639	-0,02231	4096	0,4048	#DIV/0!	#DIV/0!
Fissurina orbignyana	1		0,000488	-5,59639	-0,02231	4096	0,4048	#DIV/0!	#DIV/0!
Globocassidulina rossensis	19		0,049486	-3,2968	-0,12983	45960	4,0486	#DIV/0!	#DIV/0!
Globocassidulina subglobosa	12		0,048583	-3,02448	-0,14684	49152	4,8583	#DIV/0!	#DIV/0!
Nonion fabum	1		0,000488	-5,59639	-0,02231	4096	0,4048	#DIV/0!	#DIV/0!
Nonionella iridea	1		0,000488	-5,59639	-0,02231	4096	0,4048	#DIV/0!	#DIV/0!
Nonionella turgida	1		0,000488	-5,59639	-0,02231	4096	0,4048	#DIV/0!	#DIV/0!
Oolina alcocki	1		0,000488	-5,59639	-0,02231	4096	0,4048	#DIV/0!	#DIV/0!
Planorbulina mediterranensis	1		0,000488	-5,59639	-0,02231	4096	0,4048	#DIV/0!	#DIV/0!
Quinqueloculina akneriana	2		0,008197	-4,81624	-0,039	8192	0,8097	#DIV/0!	#DIV/0!
Quinqueloculina stalkeri	2		0,008197	-4,81624	-0,039	8192	0,8097	#DIV/0!	#DIV/0!
Quinqueloculina sp.	2		0,008197	-4,81624	-0,039	8192	0,8097	#DIV/0!	#DIV/0!
Textularia deltoidea	15		0,060729	-2,80134	-0,17012	61440	6,0729	#DIV/0!	#DIV/0!
Trifarina carinata	2		0,008197	-4,81624	-0,039	8192	0,8097	#DIV/0!	#DIV/0!
Valvulineria bradyana	1		0,000488	-5,59639	-0,02231	4096	0,4048	#DIV/0!	#DIV/0!
Ind	9					36864	3,6437	#DIV/0!	#DIV/0!
	247	Total			-3,47229	1011712	100	#DIV/0!	#DIV/0!

Ammonia beccarii	12,5596
Asterigerinata sp.1	10,1215
Bolivina difformilis	17,8138
Cibicides cf. pseudoungerianus	21,0526
Textularia deltoidea	6,0729
A	32,3887

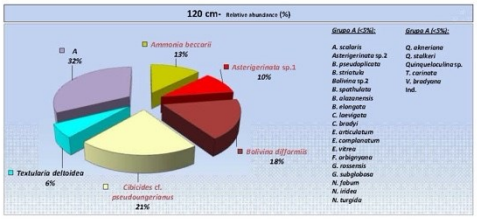

Planktonic	5376	0,5285178233
Benthonic	1011712	99,47148217
Total	1017088	100,0

Foraminifera - 130 cm

sample	split	
130 cm	7	1/128

		Screening					%	Volume	Density/cm3
		128							
Ammonia beccarii	7		0,029315	-3,5041	-0,10468	896	2,9315	#DIV/0!	#DIV/0!
Asterigerinata sp.1	37		0,15812	-1,8444	-0,29164	4736	15,8129	#DIV/0!	#DIV/0!
Bolivina difformis	48		0,205128	-1,58412	-0,32495	6144	20,5128	#DIV/0!	#DIV/0!
Bolivina ordinaria	2		0,008547	-4,76217	-0,0407	256	0,8547	#DIV/0!	#DIV/0!
Bolivina pseudoplicata	1		0,004274	-5,45532	-0,02331	128	0,4274	#DIV/0!	#DIV/0!
Bolivina subaenariensis	2		0,008547	-4,76217	-0,0407	256	0,8547	#DIV/0!	#DIV/0!
Bolivina variabilis	2		0,008547	-4,76217	-0,0407	256	0,8547	#DIV/0!	#DIV/0!
Brizalina spathulata	4		0,017094	-4,06935	-0,06956	512	1,7094	#DIV/0!	#DIV/0!
Bulimina elongata	3		0,012821	-4,35671	-0,05586	384	1,2821	#DIV/0!	#DIV/0!
Cassidulina laevigata	2		0,008547	-4,76217	-0,0407	256	0,8547	#DIV/0!	#DIV/0!
Cassidulina sp.	4		0,017094	-4,06935	-0,06956	512	1,7094	#DIV/0!	#DIV/0!
Cassidulinoides bradyi	1		0,004274	-5,45532	-0,02331	128	0,4274	#DIV/0!	#DIV/0!
Cibicides cf. pseudoungerianus	43		0,183761	-1,69412	-0,31131	5504	18,3761	#DIV/0!	#DIV/0!
Cribobobion gerthi	2		0,008547	-4,76217	-0,0407	256	0,8547	#DIV/0!	#DIV/0!
Elphidium discoidale	1		0,004274	-5,45532	-0,02331	128	0,4274	#DIV/0!	#DIV/0!
Elphidium complanatum	1		0,004274	-5,45532	-0,02331	128	0,4274	#DIV/0!	#DIV/0!
Fissurina fasciata	1		0,004274	-5,45532	-0,02331	128	0,4274	#DIV/0!	#DIV/0!
Fissurina orbignyana	4		0,017094	-4,06935	-0,06956	512	1,7094	#DIV/0!	#DIV/0!
Globocassidulina rossensis	7		0,029315	-3,5041	-0,10468	896	2,9315	#DIV/0!	#DIV/0!
Globocassidulina minuta	19		0,042735	-3,15274	-0,13473	1280	4,2735	#DIV/0!	#DIV/0!
Globocassidulina subglobosa	7		0,029315	-3,5041	-0,10468	896	2,9315	#DIV/0!	#DIV/0!
Gyroidina umbonata	4		0,017094	-4,06935	-0,06956	512	1,7094	#DIV/0!	#DIV/0!
Heterolepa pseudoungerianus	1		0,004274	-5,45532	-0,02331	128	0,4274	#DIV/0!	#DIV/0!
Lobatula lobatula	3		0,012821	-4,35671	-0,05586	384	1,2821	#DIV/0!	#DIV/0!
Nonion fabum	1		0,004274	-5,45532	-0,02331	128	0,4274	#DIV/0!	#DIV/0!
Nonionella turgida	1		0,004274	-5,45532	-0,02331	128	0,4274	#DIV/0!	#DIV/0!
Quinqueloculina akneriana	2		0,008547	-4,76217	-0,0407	256	0,8547	#DIV/0!	#DIV/0!
Quinqueloculina venusta	1		0,004274	-5,45532	-0,02331	128	0,4274	#DIV/0!	#DIV/0!
Rosalina globularis var anglica	6		0,025641	-3,66356	-0,09394	768	2,5641	#DIV/0!	#DIV/0!
Textularia deltoidea	19		0,042735	-3,15274	-0,13473	1280	4,2735	#DIV/0!	#DIV/0!
Trifarina carinata	3		0,012821	-4,35671	-0,05586	384	1,2821	#DIV/0!	#DIV/0!
Uvigerina peregrina	2		0,008547	-4,76217	-0,0407	256	0,8547	#DIV/0!	#DIV/0!
Ind	11					1408	4,7009	#DIV/0!	#DIV/0!
	234	Total			-2,54677	29952	100	#DIV/0!	#DIV/0!

Asterigerinata sp.1	15,8129
Bolivina difformis	20,5128
Cibicides cf. pseudoungerianus	18,3761
A	45,2991

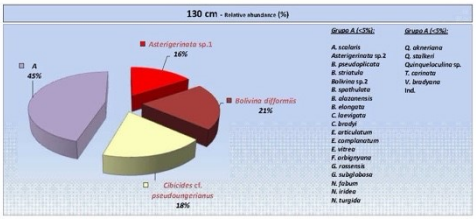

Planktonic	8192	21,47651007
Benthonic	29952	78,52348993
Total	38144	100,0

Foraminifera - 140 cm

sample	split	
140 cm	6	1/64

		Screening					Volume	Density/cm3
		64				%		
Amphicoryne scalaris	2		0,007519	-4,84935	-0,03676954	128	0,7519	#DIV/0!	#DIV/0!
Ammonia beccarii	1		0,003759	-5,5845	-0,02099059	64	0,3759	#DIV/0!	#DIV/0!
Asterigerinata sp.1	7		0,026316	-3,63959	-0,09575595	448	2,6316	#DIV/0!	#DIV/0!
Bolivina albatrosi	1		0,003759	-5,5845	-0,02099059	64	0,3759	#DIV/0!	#DIV/0!
Bolivina difformis	37		0,139098	-1,97158	-0,27438121	2368	13,9098	#DIV/0!	#DIV/0!
Bolivina pseudoplicata	5		0,018797	-3,97406	-0,07470035	320	1,8797	#DIV/0!	#DIV/0!
Bolivina variabilis	1		0,003759	-5,5845	-0,02099059	64	0,3759	#DIV/0!	#DIV/0!
Brizalina spathulata	4		0,015038	-4,1972	-0,06311582	256	1,5038	#DIV/0!	#DIV/0!
Bulimina alazanensis	1		0,003759	-5,5845	-0,02099059	64	0,3759	#DIV/0!	#DIV/0!
Bulimina elongata	6		0,022556	-3,78174	-0,0853179	384	2,2556	#DIV/0!	#DIV/0!
Bulimina marginata	1		0,003759	-5,5845	-0,02099059	64	0,3759	#DIV/0!	#DIV/0!
Cancris auricula	1		0,003759	-5,5845	-0,02099059	64	0,3759	#DIV/0!	#DIV/0!
Cassidulina laevigata	7		0,026316	-3,63959	-0,09575595	448	2,6316	#DIV/0!	#DIV/0!
Cassidulina minuta	6		0,022556	-3,78174	-0,0853179	384	2,2556	#DIV/0!	#DIV/0!
Cassidulina reniforme	2		0,007519	-4,84935	-0,03676954	128	0,7519	#DIV/0!	#DIV/0!
Cassidulina teretis	1		0,003759	-5,5845	-0,02099059	64	0,3759	#DIV/0!	#DIV/0!
Cassidulinoides bradyi	2		0,007519	-4,84935	-0,03676954	128	0,7519	#DIV/0!	#DIV/0!
Chilostomella oolina	2		0,007519	-4,84935	-0,03676954	128	0,7519	#DIV/0!	#DIV/0!
Cibicides cf. pseudoungerianus	82		0,308271	-1,17678	-0,36270586	5248	30,8271	#DIV/0!	#DIV/0!
Elphidium complanatum	2		0,007519	-4,84935	-0,03676954	128	0,7519	#DIV/0!	#DIV/0!
Elphidium crispum	1		0,003759	-5,5845	-0,02099059	64	0,3759	#DIV/0!	#DIV/0!
Fissurina laevigata	1		0,003759	-5,5845	-0,02099059	64	0,3759	#DIV/0!	#DIV/0!
Fissurina marginata	2		0,007519	-4,84935	-0,03676954	128	0,7519	#DIV/0!	#DIV/0!
Fissurina orbignyana	8		0,030075	-3,50405	-0,10538613	512	3,0075	#DIV/0!	#DIV/0!
Fissurina submarginata	1		0,003759	-5,5845	-0,02099059	64	0,3759	#DIV/0!	#DIV/0!
Globocassidulina subglobosa	5		0,018797	-3,97406	-0,07470035	320	1,8797	#DIV/0!	#DIV/0!
Gyroidina umbonata	1		0,003759	-5,5845	-0,02099059	64	0,3759	#DIV/0!	#DIV/0!
Heterolepa pseudoungerianus	1		0,003759	-5,5845	-0,02099059	64	0,3759	#DIV/0!	#DIV/0!
Lobatula lobatula	7		0,026316	-3,63959	-0,09575595	448	2,6316	#DIV/0!	#DIV/0!
Nonion fabum	1		0,003759	-5,5845	-0,02099059	64	0,3759	#DIV/0!	#DIV/0!
Oolina alcocki	1		0,003759	-5,5845	-0,02099059	64	0,3759	#DIV/0!	#DIV/0!
Oolina hexagona	1		0,003759	-5,5845	-0,02099059	64	0,3759	#DIV/0!	#DIV/0!
Quinqueloculina sp.1	1		0,003759	-5,5845	-0,02099059	64	0,3759	#DIV/0!	#DIV/0!
Quinqueloculina sp.2	1		0,003759	-5,5845	-0,02099059	64	0,3759	#DIV/0!	#DIV/0!
Quinqueloculina seminula	7		0,026316	-3,63959	-0,09575595	448	2,6316	#DIV/0!	#DIV/0!
Quinqueloculina seminulum	1		0,003759	-5,5845	-0,02099059	64	0,3759	#DIV/0!	#DIV/0!
Spiroloculina canaliculata	1		0,003759	-5,5845	-0,02099059	64	0,3759	#DIV/0!	#DIV/0!
Textularia deltoidea	39		0,146617	-1,91993	-0,28149418	2496	14,6617	#DIV/0!	#DIV/0!
Trifarina carinata	3		0,011278	-4,48486	-0,0505814	192	1,1278	#DIV/0!	#DIV/0!
Valvulineria bradyana	9		0,033835	-3,38627	-0,1145731	576	3,3835	#DIV/0!	#DIV/0!
Ind	2					128	0,7519	#DIV/0!	#DIV/0!
	266	Total			Planktonic	1924	100	#DIV/0!	#DIV/0!

Bolivina difformis	13,9098
Cibicides cf. pseudoungerianus	30,8271
Textularia deltoidea	14,6617
A	40,6015

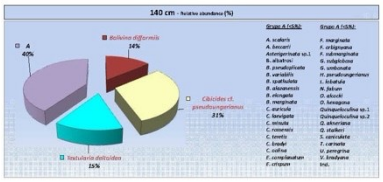

Planktonic	6730	36,30166679
Benthonic	17824	71,89813321
Total	24554	100,0

Foraminifera - 150 cm

sample	split	
150	6	1/64

		Screening					Volume	Density/cm3
		64				%		
Ammonia beccarii	38		0,162393	-1,81773	-0,29519	2432	16,2393	#DIV/0!	#DIV/0!
Asterigerinata cf. mamilla	9		0,038462	-4,35671	-0,05586	192	1,2821	#DIV/0!	#DIV/0!
Asterigerinata sp.1	14		0,059829	-2,81626	-0,16849	896	5,9829	#DIV/0!	#DIV/0!
Bolivina difformis	35		0,149573	-1,89997	-0,28418	2240	14,9573	#DIV/0!	#DIV/0!
Bolivina ordinaria	5		0,021368	-3,84588	-0,08218	320	2,1368	#DIV/0!	#DIV/0!
Bolivina pseudoplicata	1		0,004274	-5,45532	-0,02331	64	0,4274	#DIV/0!	#DIV/0!
Brizalina spathulata	5		0,021368	-3,84588	-0,08218	320	2,1368	#DIV/0!	#DIV/0!
Brizalina subaenariensis	1		0,004274	-5,45532	-0,02331	64	0,4274	#DIV/0!	#DIV/0!
Cassidulina laevigata	1		0,004274	-5,45532	-0,02331	64	0,4274	#DIV/0!	#DIV/0!
Cassidulina crassa	8		0,034188	-3,37588	-0,11541	512	3,4188	#DIV/0!	#DIV/0!
Cassidulina minuta	13		0,055556	-2,89037	-0,16058	832	5,5556	#DIV/0!	#DIV/0!
Chilostomella oolina	1		0,004274	-5,45532	-0,02331	64	0,4274	#DIV/0!	#DIV/0!
Cibicides cf. pseudoungerianus	43		0,183761	-1,69412	-0,31131	2752	18,3761	#DIV/0!	#DIV/0!
Cibicides ungerianus	17		0,07265	-2,62211	-0,1905	1088	7,2650	#DIV/0!	#DIV/0!
Cibicidoides paquilderma	2		0,008547	-4,76217	-0,0407	128	0,8547	#DIV/0!	#DIV/0!
Cibononion gerthi	0		0	0	0	0	0,0000	#DIV/0!	#DIV/0!
Elphidium complanatum	3		0,012821	-4,35671	-0,05586	192	1,2821	#DIV/0!	#DIV/0!
Elphidium articulatum	2		0,008547	-4,76217	-0,0407	128	0,8547	#DIV/0!	#DIV/0!
Globocassidulina subglobosa	5		0,021368	-3,84588	-0,08218	320	2,1368	#DIV/0!	#DIV/0!
Gyroidina umbonata	1		0,004274	-5,45532	-0,02331	64	0,4274	#DIV/0!	#DIV/0!
Hanzawaia nitidula	1		0,004274	-5,45532	-0,02331	64	0,4274	#DIV/0!	#DIV/0!
Heterolepa pseudoungerianus	1		0,004274	-5,45532	-0,02331	64	0,4274	#DIV/0!	#DIV/0!
Lobatula lobatula	6		0,025641	-3,68356	-0,09394	384	2,5641	#DIV/0!	#DIV/0!
Quinqueloculina seminula	2		0,008547	-4,76217	-0,0407	128	0,8547	#DIV/0!	#DIV/0!
Textularia deltoidea	15		0,064103	-2,74727	-0,17611	960	6,4103	#DIV/0!	#DIV/0!
Trifarina carinata	1		0,004274	-5,45532	-0,02331	64	0,4274	#DIV/0!	#DIV/0!
Ind	10					640	4,2735	#DIV/0!	#DIV/0!
	234	Total			-2,46256	14976	100	#DIV/0!	#DIV/0!

Ammonia beccarii	16,2393
Asterigerinata sp.1	5,9829
Bolivina difformis	14,9573
Cassidulina minuta	5,5556
Cibicides cf. pseudoungerianus	18,3761
Cibicides ungerianus	7,2650
Textularia deltoidea	6,4103
A	25,2137

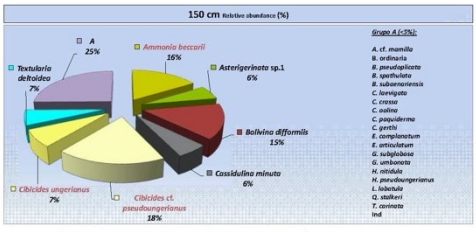

Planktonic	2880	18,12903226
Benthonic	14976	83,87096774
Total	17856	100,0

		Nº of species	Dominants Species (>10%)	Common Species (5 - 10%)	Bolivina difformis	Bolivina ordinaria	Brizalina spathulata	Cassidulina laevigata	Cassidulina obtusa	Cibicides cf. pseudoungeria nus	Cibicides ungerianus	Epistominella vitrea	Globocassidulina rossensis	Globocassidulina subglobosa	Nonionela turgida
0-2cm	1	30,000	2,000	6,000	8,197	6,557	11,475	9,290	6,557	4,372	0,000	9,836	0,000	0,000	9,290
2-4 cm	3	32,000	2,000	4,000	7,547	8,019	9,434	15,094	0,000	4,717	0,000	5,660	2,830	9,906	2,358
4-6 cm	5	22,000	5,000	1,000	12,360	11,236	12,360	11,236	0,000	1,124	0,000	5,056	16,854	0,000	1,124
6-8 cm	7	22,000	4,000	3,000	11,881	10,891	13,861	8,911	0,000	5,446	0,000	5,941	22,277	0,000	0,495
8-10 cm	9	30,000	3,000	4,000	10,860	19,457	5,882	8,145	0,000	7,692	0,000	9,955	9,050	0,000	0,000
10-12 cm	11	34,000	2,000	3,000	9,442	9,871	7,296	3,863	0,000	4,721	0,000	3,863	6,009	3,004	5,150
12-14 cm	13	31,000	3,000	5,000	8,163	10,714	7,653	13,265	0,000	6,633	0,000	5,102	9,694	2,041	5,612
14-16 cm	15	36,000	3,000	1,000	15,132	5,921	13,158	0,000	0,000	4,605	0,000	3,289	15,132	3,947	0,658
16-18 cm	17	27,000	4,000	2,000	16,667	4,545	11,111	12,121	0,000	9,091	0,000	1,515	14,141	1,515	1,010
18-20 cm	19	27,000	4,000	3,000	13,812	7,182	7,182	9,945	0,000	11,602	0,000	2,762	14,917	4,972	0,552
30 cm	35	34,000	4,000	2,000	17,300	8,861	10,970	10,970	0,000	7,173	0,000	3,376	12,658	1,688	0,844
40 cm	45	34,000	2,000	5,000	15,668	5,069	7,834	7,834	0,000	8,756	0,000	0,000	11,982	3,226	0,922
50 cm	55	34,000	2,000	4,000	11,413	7,065	5,435	7,065	0,000	5,435	0,000	0,000	25,543	2,174	1,630
60 cm	65	28,000	3,000	2,000	13,830	4,787	13,298	5,851	0,000	7,979	0,000	0,000	17,021	2,660	0,000
70 cm	75	27,000	2,000	4,000	20,556	1,111	6,667	6,667	0,000	11,111	0,000	1,111	10,556	0,000	0,000
80 cm	85	37,000	3,000	3,000	13,274	3,540	11,062	7,522	0,000	7,522	0,000	0,442	13,717	1,327	3,982
90 cm	95	32,000	4,000	2,000	18,462	1,026	3,077	4,615	0,000	7,179	0,000	0,000	9,744	0,000	0,000
100 cm	105	34,000	3,000	2,000	15,459	1,449	8,696	5,314	0,000	13,043	0,000	2,415	0,000	0,000	0,000
110 cm	115	36,000	3,000	3,000	14,667	2,222	5,778	3,111	0,000	8,000	0,000	0,444	11,111	8,889	2,222
120 cm	125	33,000	4,000	1,000	17,814	0,000	1,215	1,619	0,000	21,053	0,000	0,405	4,049	4,858	0,405
130 cm	135	33,000	3,000	0,000	20,513	0,855	1,709	0,855	0,000	18,376	0,000	0,000	2,991	2,991	0,427
140 cm	145	42,000	3,000	0,000	13,910	0,000	1,504	2,632	0,000	30,827	0,000	0,000	0,000	1,880	0,000
150 cm	155	27,000	3,000	7,000	14,957	2,137	2,137	0,427	0,000	18,376	7,265	0,000	0,000	2,137	0,000

		Quinqueloculina stalkeri	Asterigerinata cf. mamilla	Asterigerinata sp.	Bolivina pseudoplicata	Gyroidina umbonata	Globocassidulina crassa	Oridorsalis umbonatus	Ammonia beccarii	Textularia deltoidea	Cassidulina minuta	% de Planktonic	% de Benthonic
0-2cm	1	8,743	1,093	0,000	3,279	1,093	0,000	0,000	3,825	0,000	0,000	31,461	68,539
2-4 cm	3	3,302	1,887	0,000	0,943	0,472	0,000	0,000	0,943	0,000	0,000	26,132	73,868
4-6 cm	5	3,933	0,562	0,000	1,685	2,247	0,000	0,000	0,000	0,000	0,000	27,049	72,951
6-8 cm	7	0,990	0,000	0,000	1,980	2,475	0,000	0,000	0,000	0,000	0,000	30,584	69,416
8-10 cm	9	3,167	4,072	0,000	1,357	0,452	0,000	0,000	0,452	0,000	0,000	22,997	77,003
10-12 cm	11	1,717	4,292	0,000	3,863	3,004	0,000	0,000	0,429	0,000	0,000	27,640	72,360
12-14 cm	13	2,041	0,000	0,510	3,571	2,551	0,000	0,000	0,000	0,000	0,000	26,592	73,408
14-16 cm	15	0,658	1,316	0,000	3,289	3,289	0,000	0,000	1,316	0,000	0,000	34,483	65,517
16-18 cm	17	1,515	7,576	0,000	3,030	0,000	0,000	0,000	1,010	0,000	0,000	26,937	73,063
18-20 cm	19	2,210	4,420	0,000	3,315	0,000	0,000	0,000	0,000	0,000	0,000	37,370	62,630
30 cm	35	1,266	1,688	3,376	2,110	0,844	0,000	0,000	2,532	0,000	0,000	26,168	73,832
40 cm	45	0,922	8,295	0,461	2,304	0,461	0,000	0,000	3,226	0,000	0,000	24,913	75,087
50 cm	55	0,543	2,174	3,804	3,261	1,630	0,000	0,000	0,000	0,000	0,000	30,038	69,962
60 cm	65	1,596	2,128	9,043	1,596	3,191	0,000	0,000	0,000	0,000	0,000	32,616	67,384
70 cm	75	1,667	0,000	5,556	7,778	2,222	0,000	0,000	0,000	0,000	0,000	35,484	64,516
80 cm	85	0,000	0,000	4,867	4,425	7,080	0,000	0,000	0,000	0,000	0,000	32,335	67,665
90 cm	95	1,026	0,000	10,256	6,154	2,564	9,744	0,000	0,000	0,000	0,000	34,783	65,217
100 cm	105	0,000	0,000	0,000	2,415	0,483	0,000	13,527	0,000	0,000	0,000	30,537	69,463
110 cm	115	1,333	0,000	12,444	2,222	1,778	0,000	0,000	0,000	0,000	0,000	29,688	70,313
120 cm	125	0,810	0,000	10,121	1,215	0,000	0,000	0,000	12,551	6,073	0,000	0,529	99,471
130 cm	135	0,000	0,000	15,812	0,427	1,709	0,000	0,000	2,991	0,000	0,000	21,477	78,523
140 cm	145	0,376	0,000	2,632	1,880	0,376	0,000	0,000	0,376	14,662	0,000	28,302	71,698
150 cm	155	0,855	1,282	5,983	0,427	0,427	3,419	0,000	16,239	6,410	5,556	16,129	83,871

	Bolivina difformis	Bolivina ordinaria	Bifarina spathulata	Cassidulina laevigata	Cassidulina obtusa	Cibicides cf. pseudoungerianus	Cibicides ungerianus	Epistominella vitrea	Globocassidulina rosenvis	Globocassidulina subglobosa	Nonionella turgida	Quinqueloculina stalkeri	Asterigerinata cf. mamilla	Asterigerinata sp.	Bolivina pseudoplicata
0-2cm	8,1967	6,5574	11,4754	9,2896	6,5574	4,3716	0,0000	9,8361	0,0000	0,0000	9,2896	8,7432	1,0929	0,0000	3,2787
2-4 cm	7,5472	8,0189	9,4340	15,0943	0,0000	4,7170	0,0000	5,6604	2,8302	9,9057	2,3585	3,3019	1,8868	0,0000	0,9434
4-6 cm	12,3596	11,2360	12,3596	11,2360	0,0000	1,1236	0,0000	5,0562	16,8539	0,0000	1,1236	3,9326	0,5618	0,0000	1,6854
6-8 cm	11,8812	10,8911	13,8614	8,9109	0,0000	5,4455	0,0000	5,9406	22,2772	0,0000	0,4950	0,9901	0,0000	0,0000	1,9802
8-10 cm	10,8597	19,4570	5,8824	8,1448	0,0000	7,6923	0,0000	9,9548	9,0498	0,0000	0,0000	3,1674	4,0724	0,0000	1,3575
10-12 cm	9,4421	9,8712	7,2961	3,8627	0,0000	4,7210	0,0000	3,8627	6,0086	3,0043	5,1502	1,7167	4,2918	0,0000	3,8627
12-14 cm	8,1633	10,7143	7,6531	13,2653	0,0000	6,6327	0,0000	5,1020	9,6939	2,0408	5,6122	2,0408	0,0000	0,5102	3,5714
14-16 cm	15,1316	5,9211	13,1579	0,0000	0,0000	4,6053	0,0000	3,2895	15,1316	3,9474	0,6579	0,6579	1,3158	0,0000	3,2895
16-18 cm	16,6667	4,5455	11,1111	12,1212	0,0000	9,0909	0,0000	1,5152	14,1414	1,5152	1,0101	1,5152	7,5758	0,0000	3,0303
18-20 cm	13,8122	7,1823	7,1823	9,9448	0,0000	11,6022	0,0000	2,7624	14,9171	4,9724	0,5525	2,2099	4,4199	0,0000	3,3149
30 cm	17,2996	8,8608	10,9705	10,9705	0,0000	7,1730	0,0000	3,3755	12,6582	1,6878	0,8439	1,2658	1,6878	3,3755	2,1097
40 cm	15,6682	5,2691	7,8341	7,8341	0,0000	8,7558	0,0000	0,0000	11,9816	3,2258	0,9217	0,9217	8,2949	0,4608	2,3041
50 cm	11,4130	7,0652	5,4348	7,0652	0,0000	5,4348	0,0000	0,0000	25,5435	2,1739	1,6304	0,5435	2,1739	3,8043	3,2609
60 cm	13,8298	4,7872	13,2979	5,8511	0,0000	7,9787	0,0000	0,0000	17,0213	2,6596	0,0000	1,5957	2,1277	9,0426	1,5957
70 cm	20,5556	1,1111	6,6667	6,6667	0,0000	11,1111	0,0000	1,1111	10,5556	0,0000	0,0000	1,6667	0,0000	5,5556	7,7778
80 cm	13,2743	3,5398	11,0619	7,5221	0,0000	7,5221	0,0000	0,4425	13,7168	1,3274	3,9823	0,0000	0,0000	4,8673	4,4248
90 cm	18,4615	1,0256	3,0769	4,6154	0,0000	7,1795	0,0000	0,0000	9,7436	0,0000	0,0000	1,0256	0,0000	10,2564	6,1538
100 cm	15,4589	1,4493	8,6957	5,3140	0,0000	13,0435	0,0000	2,4155	0,0000	0,0000	0,0000	0,0000	0,0000	0,0000	2,4155
110 cm	14,6667	2,2222	5,7778	3,1111	0,0000	8,0000	0,0000	0,4444	11,1111	8,8889	2,2222	1,3333	0,0000	17,4444	2,2222
120 cm	17,8138	0,0000	1,2146	1,6194	0,0000	21,0526	0,0000	0,4049	4,0486	4,9393	0,4049	0,8097	0,0000	10,1215	1,2146
130 cm	20,5128	0,8547	1,7094	0,8547	0,0000	18,3761	0,0000	0,0000	2,9915	2,9915	0,4274	0,0000	0,0000	15,8120	0,4274
140 cm	13,9098	0,0000	1,5038	2,6316	0,0000	30,8271	0,0000	0,0000	0,0000	1,8797	0,0000	0,3759	0,0000	2,6316	1,8797
150 cm	14,9573	2,1368	2,1368	0,4274	0,0000	18,3761	7,2650	0,0000	0,0000	2,1368	0,0000	0,8547	1,2821	5,9829	0,4274

	Gyroidina umbonata	Globocassidulina crassa	Oridorsalis umbonatus	Ammonia beccarii	Textularia deltoidea	Cassidulina minuta	% de Planctónicos	% de Bentónicos
0-2cm	1,0929	0,0000	0,0000	3,8251	0,0000	0,0000	31,4607	68,5393
2-4 cm	0,4717	0,0000	0,0000	0,9434	0,0000	0,0000	26,1324	73,8676
4-6 cm	2,2472	0,0000	0,0000	0,0000	0,0000	0,0000	27,0492	72,9508
6-8 cm	2,4752	0,0000	0,0000	0,0000	0,0000	0,0000	30,5842	69,4158
8-10 cm	0,4525	0,0000	0,0000	0,4525	0,0000	0,0000	22,9965	77,0035
10-12 cm	3,0043	0,0000	0,0000	0,4292	0,0000	0,0000	27,6398	72,3602
12-14 cm	2,5510	0,0000	0,0000	0,0000	0,0000	0,0000	26,5918	73,4082
14-16 cm	3,2895	0,0000	0,0000	1,3158	0,0000	0,0000	34,4828	65,5172
16-18 cm	0,0000	0,0000	0,0000	1,0101	0,0000	0,0000	26,9373	73,0627
18-20 cm	0,0000	0,0000	0,0000	0,0000	0,0000	0,0000	37,3702	62,6298
30 cm	0,8439	0,0000	0,0000	2,5316	0,0000	0,0000	26,1682	73,8318
40 cm	0,4608	0,0000	0,0000	3,2258	0,0000	0,0000	24,9135	75,0865
50 cm	1,6304	0,0000	0,0000	0,0000	0,0000	0,0000	30,0380	69,9620
60 cm	3,1915	0,0000	0,0000	0,0000	0,0000	0,0000	32,6165	67,3835
70 cm	2,2222	0,0000	0,0000	0,0000	0,0000	0,0000	35,4839	64,5161
80 cm	7,0796	0,0000	0,0000	0,0000	0,0000	0,0000	32,3353	67,6647
90 cm	2,5641	9,7436	0,0000	0,0000	0,0000	0,0000	34,7826	65,2174
100 cm	0,4831	0,0000	13,5266	0,0000	0,0000	0,0000	30,5369	69,4631
110 cm	1,7778	0,0000	0,0000	0,0000	0,0000	0,0000	29,6875	70,3125
120 cm	0,0000	0,0000	0,0000	12,5506	6,0729	0,0000	0,5286	99,4714
130 cm	1,7094	0,0000	0,0000	2,9915	0,0000	0,0000	21,4765	78,5235
140 cm	0,3759	0,0000	0,0000	0,3759	14,6617	0,0000	28,3019	71,6981
150 cm	0,4274	3,4188	0,0000	16,2393	6,4103	5,5556	16,1290	83,8710

Annex 16. Calcareous Nannoplankton

Species Count

Depth (cm)	0-2	10-12	20-22	32-34	52-54	75-77	109-111	125-127	137-139	157-159
campos	30,000	18,000	28,000	29,000	12,000	58,000	46,000	109,000	110,000	130,000
EH	48,000	140,000	147,000	132,000	239,000	134,000	297,000	46,000	46,000	39,000
GE	32,000	107,000	123,000	94,000	182,000	114,000	113,000	24,000	26,000	9,000
GO	149,000	106,000	144,000	135,000	139,000	58,000	88,000	88,000	110,000	110,000
GM	21,000	36,000	7,000	12,000	14,000	12,000	10,000	11,000	9,000	19,000
CP	25,000	43,000	58,000	29,000	37,000	39,000	49,000	56,000	54,000	27,000
Calcidiscus	13,000	7,000	12,000	20,000	12,000	36,000	29,000	18,000	23,000	4,000
Pulchra	47,000	60,000	69,000	76,000	35,000	40,000	21,000	24,000	10,000	1,000
Bigelowii	2,000	2,000	6,000	3,000	1,000	3,000	3,000	4,000	3,000	5,000
Umbilicosfera	0,000	7,000	15,000	13,000	11,000	12,000	14,000	3,000	3,000	
HC	64,000	58,000	37,000	62,000	67,000	105,000	100,000	103,000	83,000	51,000
Calcioselenia	1,000	0,000	1,000	2,000	6,000	4,000	2,000	0,000	0,000	
Radosphaera	0,000	3,000	1,000	0,000	2,000	0,000	0,000	0,000	0,000	
Pontosphaera discopora				2,000	0,000	2,000	2,000	0,000	2,000	1,000
Reticulofenestra haqii								9,000	7,000	
Reticulofenestra antarticus								3,000	4,000	
Reticulofenestra minutula										2,000
Tubodiscus									2,000	
Spicules	9,000	14,000	0,000	0,000	2,000	3,000	3,000	3,000	0,000	
Total	411,000	583,000	620,000	580,000	747,000	562,000	731,000	392,000	382,000	268,000
Total Weight	0,198	0,200	0,198	0,192	0,205	0,201	0,198	0,199	0,200	0,205
V	10000,00	10000,00	10000,00	10000,00	10000,00	10000,00	10000,00	10000,00	10000,00	10000,00
Vp	1000,00	1000,00	1000,00	1000,00	1000,00	1000,00	1000,00	1000,00	1000,00	1000,00
Pa	160,000	160,000	160,000	160,000	160,000	160,000	160,000	160,000	160,000	160,000
Ao	0,600	0,360	0,560	0,580	0,240	1,160	0,920	2,180	2,200	2,600

Species Percentage

Depth (cm)	0-2	10-12	20-22	32-34	52-54	75-77	109-111	125-127	137-139	157-159
EH	11,679	84,813	23,710	22,759	31,995	23,843	40,629	11,735	12,042	14,552
GE	7,786	3,668	19,839	16,207	24,364	20,285	15,458	6,122	6,806	3,358
GO	36,253	3,634	23,226	23,276	18,608	10,320	12,038	22,449	28,796	41,045
GM	5,109	1,234	1,129	2,069	1,874	2,135	1,368	2,806	2,356	7,090
CP	6,083	1,474	9,355	5,000	4,953	6,940	6,703	14,286	14,136	10,075
Calcidiscus	3,163	0,240	1,935	3,448	1,606	6,406	3,967	4,592	6,021	1,493
Pulchra	11,436	2,057	11,129	13,103	4,685	7,117	2,873	6,122	2,618	0,373
Bigelowii	0,487	0,069	0,968	0,517	0,134	0,534	0,410	1,020	0,785	1,866
Umbilicosfera	0,000	0,240	2,419	2,241	1,473	2,135	1,915	0,765	0,785	0,000
HC	15,572	1,988	5,968	10,690	8,969	18,683	13,680	26,276	21,728	19,030
Calcioselenia	0,243	0,000	0,161	0,345	0,803	0,712	0,274	0,000	0,000	0,000
Radosphaera	0,000	0,103	0,161	0,000	0,268	0,000	0,000	0,000	0,000	0,000
Pontosphaera discopora	0,000	0,000	0,000	0,345	0,000	0,356	0,274	0,000	0,524	0,373
Reticulofenestra haqii	0,000	0,000	0,000	0,000	0,000	0,000	0,000	2,296	1,832	0,000
Reticulofenestra antarticus	0,000	0,000	0,000	0,000	0,000	0,000	0,000	0,765	1,047	0,000
Reticulofenestra minutula	0,000	0,000	0,000	0,000	0,000	0,000	0,000	0,000	0,000	0,746
Tubodiscus	0,000	0,000	0,000	0,000	0,000	0,000	0,000	0,000	0,524	0,000
Spicules	2,190	0,480	0,000	0,000	0,268	0,534	0,410	0,765	0,000	0,000
Total	100,000	100,000	100,000	100,000	100,000	100,000	100,000	100,000	100,000	100,000

Annex 17. Heavy metal data

Depth (cm)	Hg (mg/kg)	Cu (mg/kg)	Zn (mg/kg)	Mn (mg/kg)	Fe (%)	Pb (mg/kg)	Ni (mg/kg)	Cd (mg/kg)	Cr (mg/kg)	Al (%)	Li (mg/kg)	As (mg/kg)	TIC	CaCO3	dilution factor
1	0,055	13,000	68,000	240,000	2,500	12,300	13,400	0,200	46,000	6,200	68,000	14,900	2,800	23,324	1,304
2	0,044	12,000	64,000	250,000	2,500	11,300	13,000	0,200	45,000	6,000	66,000	14,000	3,400	28,322	1,395
3	0,024	12,000	62,000	250,000	2,700	7,770	13,200	0,200	49,000	6,500	74,000	14,000	2,800	23,324	1,304
4	0,027	13,000	63,000	250,000	2,700	9,330	13,800	0,200	45,000	5,800	71,000	15,700	2,800	23,324	1,304
5	0,049	12,000	66,000	240,000	2,400	12,500	13,000	0,200	42,000	5,700	65,000	12,900	3,100	25,823	1,348
6	0,036	12,000	64,000	250,000	2,300	10,300	14,300	0,200	44,000	6,200	68,000	13,100	2,900	24,157	1,319
7	0,019	13,000	61,000	260,000	2,600	6,720	13,800	0,200	48,000	6,200	70,000	13,500	2,800	23,324	1,304
8	0,017	12,000	59,000	260,000	2,500	4,120	13,400	0,200	46,000	6,000	67,000	10,700	2,900	24,157	1,319
9	0,015	11,000	56,000	250,000	2,300	3,630	12,600	0,200	45,000	5,800	64,000	14,800	3,000	24,990	1,333
10	0,012	11,000	62,000	230,000	2,300	8,520	17,300	0,200	47,000	5,700	61,000	16,200	3,100	25,823	1,348
11	0,066	11,000	67,000	230,000	2,200	13,700	11,100	0,200	44,000	6,100	53,000	10,200	3,200	26,656	1,363
12	0,072	12,000	70,000	240,000	2,200	14,500	11,500	0,200	44,000	5,300	58,000	9,630	3,300	27,489	1,379
13	0,080	13,000	74,000	240,000	2,400	16,400	12,100	0,200	45,000	5,500	60,000	10,800	3,100	25,823	1,348
14	0,090	13,000	77,000	250,000	2,500	17,800	13,200	0,200	46,000	5,600	63,000	13,800	2,900	24,157	1,319
15	0,080	14,000	77,000	250,000	2,500	17,700	13,500	0,200	46,000	5,800	63,000	11,100	3,000	24,990	1,333
16	0,090	14,000	77,000	250,000	2,500	17,700	13,000	0,200	48,000	5,800	64,000	10,900	3,100	25,823	1,348
17	0,090	14,000	78,000	250,000	2,500	19,200	14,200	0,200	47,000	5,800	64,000	12,300	2,900	24,157	1,319
18	0,090	14,000	82,000	260,000	2,600	21,000	14,000	0,200	51,000	6,200	72,000	12,600	2,700	22,491	1,290
19	0,076	13,000	76,000	250,000	2,500	17,900	12,000	0,300	46,000	5,700	63,000	12,000	2,800	23,324	1,304
20	0,069	13,000	75,000	250,000	2,500	17,100	12,800	0,200	47,000	5,900	64,000	12,200	3,200	26,656	1,363
25	0,012	10,600	55,000	250,000	2,500	4,660	11,600	0,313	42,000	5,400	67,000	12,800	3,500	29,155	1,412
30	0,013	9,300	48,000	220,000	2,200	3,900	9,940	0,200	37,000	4,900	56,000	14,700	3,800	31,654	1,463
35	0,031	9,500	53,000	220,000	2,100	8,210	9,260	0,200	37,000	4,500	52,000	10,200	3,900	32,487	1,481
40	0,021	10,400	51,000	230,000	2,300	2,590	9,360	0,200	39,000	5,300	59,000	10,200	3,500	29,155	1,412
45	0,007	6,600	33,000	190,000	1,800	1,000	3,560	0,200	29,000	3,600	38,000	9,610	4,300	35,819	1,558
50	0,007	6,300	33,000	180,000	1,800	1,000	3,580	0,200	28,000	3,400	38,000	10,100	4,600	38,318	1,621
55	0,009	6,300	31,000	180,000	1,700	1,000	3,460	0,200	26,000	3,200	36,000	9,080	4,600	38,318	1,621
60	0,006	5,800	28,000	170,000	1,500	1,000	3,210	0,200	24,000	3,000	33,000	7,660	4,900	40,817	1,690
65	0,006	5,700	27,000	160,000	1,400	1,000	2,460	0,200	24,000	2,700	29,000	7,980	4,900	40,817	1,690
70	0,006	5,100	26,000	160,000	1,400	1,000	2,110	0,200	23,000	2,700	28,000	7,160	4,500	37,485	1,600
75	0,006	4,000	25,000	170,000	1,300	1,000	2,220	0,200	22,000	2,600	27,000	7,410	5,000	41,650	1,714
80	0,006	4,000	24,000	160,000	1,300	1,000	0,100	0,200	22,000	2,600	26,000	5,600	5,000	41,650	1,714
85	0,006	6,100	29,000	180,000	1,500	1,000	4,210	0,300	27,000	3,100	34,000	8,190	5,000	41,650	1,714
90	0,004	4,000	21,000	150,000	1,200	1,000	0,100	0,200	19,900	2,300	22,000	6,100	5,000	41,650	1,714
95	0,004	4,000	20,000	140,000	1,200	1,000	0,100	0,200	19,700	2,100	22,000	8,320	5,000	41,650	1,714
100	0,003	4,000	20,000	150,000	1,200	1,000	0,100	0,200	19,900	2,100	22,000	8,000	6,000	49,980	1,999
105	0,003	4,000	16,000	120,000	1,000	1,000	2,690	0,200	23,000	1,450	18,000	10,400	6,000	49,980	1,999
110	0,003	4,000	14,000	110,000	0,900	1,000	5,110	0,200	29,000	1,360	17,200	11,800	6,000	49,980	1,999
115	0,003	4,000	17,000	110,000	1,200	1,000	3,680	0,200	24,000	1,540	22,000	15,500	7,000	58,310	2,399
120	0,003	4,000	14,000	120,000	0,820	1,000	5,280	0,200	29,000	1,350	17,400	11,200	6,000	49,980	1,999
125	0,002	4,000	10,900	110,000	0,740	1,000	2,550	0,200	22,000	1,120	15,100	10,700	6,000	49,980	1,999
130	0,002	4,000	12,000	110,000	0,740	1,000	5,540	0,200	29,000	1,190	15,600	13,600	7,000	58,310	2,399
135	0,002	4,000	12,000	110,000	0,750	1,000	4,800	0,200	28,000	1,270	14,800	10,500	7,000	58,310	2,399
140	0,002	4,000	11,500	110,000	0,730	1,000	5,940	0,200	30,000	1,080	14,700	9,350	7,000	58,310	2,399
160	0,002	4,000	9,700	110,000	0,670	1,000	3,430	0,200	24,000	1,050	12,200	12,400	7,000	58,310	2,399
162	0,002	4,000	12,000	100,000	0,630	1,000	10,500	0,200	40,000	1,080	13,400	7,980	7,000	58,310	2,399

Dilution

Depth (cm)	Hg (mg/kg)	Cu (mg/kg)	Zn (mg/kg)	Mn (mg/kg)	Fe (%)	Pb (mg/kg)	Ni (mg/kg)	Cd (mg/kg)	Cr (mg/kg)	Al (%)	Li (mg/kg)	As (mg/kg)
1	0,072	16,954	88,685	313,005	3,260	16,042	17,476	0,261	59,993	8,086	88,685	19,432
2	0,061	16,742	89,288	348,782	3,488	15,765	18,137	0,279	62,781	8,371	92,078	19,532
3	0,031	15,650	80,860	326,047	3,521	10,134	17,215	0,261	63,905	8,477	96,510	18,259
4	0,035	16,954	82,164	326,047	3,521	12,168	17,998	0,261	58,689	7,564	92,597	20,476
5	0,066	16,178	88,976	323,550	3,236	16,852	17,526	0,270	56,621	7,684	87,628	17,391
6	0,047	15,822	84,385	329,628	3,033	13,581	18,855	0,264	58,015	8,175	89,659	17,273
7	0,025	16,954	79,556	339,089	3,391	8,764	17,998	0,261	62,601	8,086	91,293	17,607
8	0,022	15,822	77,792	342,813	3,296	5,432	17,668	0,264	60,652	7,911	88,340	14,108
9	0,020	14,665	74,657	333,289	3,066	4,839	16,798	0,267	59,992	7,732	85,322	19,731
10	0,016	14,829	83,584	310,069	3,101	11,486	23,323	0,270	63,362	7,684	82,236	21,840
11	0,090	14,998	91,350	313,591	3,000	18,679	15,134	0,273	59,991	8,317	72,262	13,907
12	0,099	16,549	96,537	330,984	3,034	19,997	15,860	0,276	60,680	7,309	79,988	13,281
13	0,108	17,526	99,761	323,550	3,236	22,109	16,312	0,270	60,666	7,415	80,888	14,560
14	0,119	17,141	101,526	329,628	3,296	23,470	17,404	0,264	60,652	7,384	83,066	18,195
15	0,107	18,664	102,653	333,289	3,333	23,597	17,998	0,267	61,325	7,732	83,989	14,798
16	0,121	18,874	103,806	337,032	3,370	23,862	17,526	0,270	64,710	7,819	86,280	14,695
17	0,119	18,459	102,844	329,628	3,296	25,315	18,723	0,264	61,970	7,647	84,385	16,218
18	0,116	18,062	105,794	335,445	3,354	27,094	18,062	0,258	65,799	7,999	92,892	16,256
19	0,099	16,954	99,118	326,047	3,260	23,345	15,650	0,391	59,993	7,434	82,164	15,650
20	0,094	17,725	102,258	340,860	3,409	23,315	17,452	0,273	64,082	8,044	87,260	16,634
25	0,017	14,962	77,634	352,883	3,529	6,578	16,374	0,442	59,284	7,622	94,573	18,068
30	0,019	13,607	70,231	321,892	3,219	5,706	14,544	0,293	54,136	7,169	81,936	21,508
35	0,046	14,071	78,503	325,863	3,111	12,161	13,716	0,296	54,804	6,665	77,022	15,108
40	0,030	14,680	71,988	324,652	3,247	3,656	13,212	0,282	55,050	7,481	83,280	14,398
45	0,011	10,283	51,417	296,038	2,805	1,558	5,547	0,312	45,185	5,609	59,208	14,973
50	0,011	10,214	53,500	291,819	2,918	1,621	5,804	0,324	45,394	5,512	61,606	16,374
55	0,015	10,214	50,258	291,819	2,756	1,621	5,609	0,324	42,152	5,188	58,364	14,721
60	0,010	9,800	47,311	287,245	2,535	1,690	5,424	0,338	40,552	5,069	55,759	12,943
65	0,010	9,631	45,621	270,348	2,366	1,690	4,157	0,338	40,552	4,562	49,001	13,484
70	0,010	8,158	41,590	255,939	2,239	1,600	3,375	0,320	36,791	4,319	44,789	11,453
75	0,010	6,855	42,845	291,345	2,228	1,714	3,805	0,343	37,704	4,456	46,272	12,699
80	0,010	6,855	41,131	274,207	2,228	1,714	0,171	0,343	37,704	4,456	44,559	9,597
85	0,010	10,454	49,700	308,483	2,571	1,714	7,215	0,514	46,272	5,313	58,269	14,036
90	0,007	6,855	35,990	257,069	2,057	1,714	0,171	0,343	34,105	3,942	37,704	10,454
95	0,006	6,855	34,276	239,931	2,057	1,714	0,171	0,343	33,762	3,599	37,704	14,259
100	0,007	7,997	39,984	299,880	2,399	1,999	0,200	0,400	39,784	4,198	43,982	15,994
105	0,005	7,997	31,987	239,904	1,999	1,999	5,378	0,400	45,982	2,899	35,986	20,792
110	0,005	7,997	27,989	219,912	1,799	1,999	10,216	0,400	57,977	2,719	34,386	23,591
115	0,006	9,595	40,777	263,852	2,878	2,399	8,827	0,480	57,568	3,694	52,770	37,179
120	0,005	7,997	27,989	239,904	1,639	1,999	10,556	0,400	57,977	2,699	34,786	22,391
125	0,004	7,997	21,791	219,912	1,479	1,999	5,098	0,400	43,982	2,239	30,188	21,391
130	0,006	9,595	28,784	263,852	1,775	2,399	13,289	0,480	69,561	2,854	37,419	32,622
135	0,005	9,595	28,784	263,852	1,799	2,399	11,514	0,480	67,162	3,046	35,500	25,186
140	0,005	9,595	27,585	263,852	1,751	2,399	14,248	0,480	71,960	2,591	35,260	22,427
160	0,005	9,595	23,267	263,852	1,607	2,399	8,227	0,480	57,568	2,519	29,264	29,743
162	0,006	9,595	28,784	239,866	1,511	2,399	25,186	0,480	95,946	2,591	32,142	19,141

Normalization

Depth (cm)	Hg (mg/kg)	Cu (mg/kg)	Zn (mg/kg)	Mn (mg/kg)	Fe (%)	Pb (mg/kg)	Ni (mg/kg)	Cd (mg/kg)	Cr (mg/kg)	Li (mg/kg)	As (mg/kg)
1	8,87E-07	0,00021	0,001097	0,003871	0,403226	0,000198	0,000216	3,23E-06	0,000742	0,001097	0,00024
2	7,33E-07	0,0002	0,001067	0,004167	0,416667	0,000188	0,000217	3,33E-06	0,00075	0,0011	0,000233
3	3,69E-07	0,000185	0,000954	0,003846	0,415385	0,00012	0,000203	3,08E-06	0,000754	0,001138	0,000215
4	4,66E-07	0,000224	0,001086	0,00431	0,465517	0,000161	0,000238	3,45E-06	0,000776	0,001224	0,000271
5	8,6E-07	0,000211	0,001158	0,004211	0,421053	0,000219	0,000228	3,51E-06	0,000737	0,00114	0,000226
6	5,81E-07	0,000194	0,001032	0,004032	0,370968	0,000166	0,000231	3,23E-06	0,00071	0,001097	0,000211
7	3,06E-07	0,00021	0,000984	0,004194	0,419355	0,000108	0,000223	3,23E-06	0,000774	0,001129	0,000218
8	2,83E-07	0,0002	0,000983	0,004333	0,416667	6,87E-05	0,000223	3,33E-06	0,000767	0,001117	0,000178
9	2,59E-07	0,00019	0,000966	0,00431	0,396552	6,26E-05	0,000217	3,45E-06	0,000776	0,001103	0,000255
10	2,11E-07	0,000193	0,001088	0,004035	0,403509	0,000149	0,000304	3,51E-06	0,000825	0,00107	0,000284
11	1,08E-06	0,00018	0,001098	0,00377	0,360656	0,000225	0,000182	3,28E-06	0,000721	0,000869	0,000167
12	1,36E-06	0,000226	0,001321	0,004528	0,415094	0,000274	0,000217	3,77E-06	0,00083	0,001094	0,000182
13	1,45E-06	0,000236	0,001345	0,004364	0,436364	0,000298	0,00022	3,64E-06	0,000818	0,001091	0,000196
14	1,61E-06	0,000232	0,001375	0,004464	0,446429	0,000318	0,000236	3,57E-06	0,000821	0,001125	0,000246
15	1,38E-06	0,000241	0,001328	0,00431	0,431034	0,000305	0,000233	3,45E-06	0,000793	0,001086	0,000191
16	1,55E-06	0,000241	0,001328	0,00431	0,431034	0,000305	0,000224	3,45E-06	0,000828	0,001103	0,000188
17	1,55E-06	0,000241	0,001345	0,00431	0,431034	0,000331	0,000245	3,45E-06	0,00081	0,001103	0,000212
18	1,45E-06	0,000226	0,001323	0,004194	0,419355	0,000339	0,000226	3,23E-06	0,000823	0,001161	0,000203
19	1,33E-06	0,000228	0,001333	0,004386	0,438596	0,000314	0,000211	5,26E-06	0,000807	0,001105	0,000211
20	1,17E-06	0,00022	0,001271	0,004237	0,423729	0,00029	0,000217	3,39E-06	0,000797	0,001085	0,000207
25	2,22E-07	0,000196	0,001019	0,00463	0,462963	8,63E-05	0,000215	5,8E-06	0,000778	0,001241	0,000237
30	2,65E-07	0,00019	0,00098	0,00449	0,44898	7,96E-05	0,000203	4,08E-06	0,000755	0,001143	0,0003
35	6,89E-07	0,000211	0,001178	0,004889	0,466667	0,000182	0,000206	4,44E-06	0,000822	0,001156	0,000227
40	3,96E-07	0,000196	0,000962	0,00434	0,433962	4,89E-05	0,000177	3,77E-06	0,000736	0,001113	0,000192
45	1,94E-07	0,000183	0,000917	0,005278	0,5	2,78E-05	9,89E-05	5,56E-06	0,000806	0,001056	0,000267
50	2,06E-07	0,000185	0,000971	0,005294	0,529412	2,94E-05	0,000105	5,88E-06	0,000824	0,001118	0,000297
55	2,81E-07	0,000197	0,000969	0,005625	0,53125	3,13E-05	0,000108	6,25E-06	0,000813	0,001125	0,000284
60	2E-07	0,000193	0,000933	0,005667	0,5	3,33E-05	0,000107	6,67E-06	0,0008	0,0011	0,000255
65	2,22E-07	0,000211	0,001	0,005926	0,518519	3,7E-05	9,11E-05	7,41E-06	0,000889	0,001074	0,000296
70	2,22E-07	0,000189	0,000963	0,005926	0,518519	3,7E-05	7,81E-05	7,41E-06	0,000852	0,001037	0,000265
75	2,31E-07	0,000154	0,000962	0,006538	0,5	3,85E-05	8,54E-05	7,69E-06	0,000846	0,001038	0,000285
80	2,31E-07	0,000154	0,000923	0,006154	0,5	3,85E-05	3,85E-06	7,69E-06	0,000846	0,001	0,000215
85	1,94E-07	0,000197	0,000935	0,005806	0,483871	3,23E-05	0,000136	9,68E-06	0,000871	0,001097	0,000264
90	1,74E-07	0,000174	0,000913	0,006522	0,521739	4,35E-05	4,35E-06	8,7E-06	0,000865	0,000957	0,000265
95	1,67E-07	0,00019	0,000952	0,006667	0,571429	4,76E-05	4,76E-06	9,52E-06	0,000938	0,001048	0,000396
100	1,57E-07	0,00019	0,000952	0,007143	0,571429	4,76E-05	4,76E-06	9,52E-06	0,000948	0,001048	0,000381
105	1,79E-07	0,000276	0,001103	0,008276	0,689655	6,9E-05	0,000186	1,38E-05	0,001586	0,001241	0,000717
110	1,84E-07	0,000294	0,001029	0,008088	0,661765	7,35E-05	0,000376	1,47E-05	0,002132	0,001265	0,000868
115	1,62E-07	0,00026	0,001104	0,007143	0,779221	6,49E-05	0,000239	1,3E-05	0,001558	0,001429	0,001006
120	1,85E-07	0,000296	0,001037	0,008889	0,607407	7,41E-05	0,000391	1,48E-05	0,002148	0,001289	0,00083
125	1,96E-07	0,000357	0,000973	0,009821	0,660714	8,93E-05	0,000228	1,79E-05	0,001964	0,001348	0,000955
130	1,93E-07	0,000336	0,001008	0,009244	0,621849	8,4E-05	0,000466	1,68E-05	0,002437	0,001311	0,001143
135	1,65E-07	0,000315	0,000945	0,008661	0,590551	7,87E-05	0,000378	1,57E-05	0,002205	0,001165	0,000827
140	1,94E-07	0,00037	0,001065	0,010185	0,675926	9,26E-05	0,00055	1,85E-05	0,002778	0,001361	0,000866
160	1,9E-07	0,000381	0,000924	0,010476	0,638095	9,52E-05	0,000327	1,9E-05	0,002286	0,001162	0,001181
162	2,22E-07	0,00037	0,001111	0,009259	0,583333	9,26E-05	0,000972	1,85E-05	0,003704	0,001241	0,000739
Nose-100	1,85E-07	0,000313	0,001023	0,008835	0,643631	7,83E-05	0,000374	1,57E-05	0,002159	0,00126	0,000865
100-40	2,26E-07	0,000185	0,00095	0,005812	0,509058	3,71E-05	8,33E-05	7,19E-06	0,00084	0,001063	0,000274

Enrichment Factor

Depth (cm)	Hg (mg/kg)	Cu (mg/kg)	Zn (mg/kg)	Mn (mg/kg)	Fe (%)	Pb (mg/kg)	Ni (mg/kg)	Cd (mg/kg)	Cr (mg/kg)	Li (mg/kg)	As (mg/kg)
1	3,917	1,131	1,154	0,666	0,792	5,350	2,595	0,449	0,883	1,031	0,879
2	3,238	1,079	1,123	0,717	0,819	5,079	2,602	0,464	0,892	1,034	0,853
3	1,630	0,996	1,004	0,662	0,816	3,224	2,439	0,428	0,897	1,070	0,787
4	2,055	1,209	1,143	0,742	0,914	4,338	2,857	0,480	0,923	1,151	0,990
5	3,795	1,136	1,219	0,724	0,827	5,914	2,739	0,488	0,877	1,072	0,827
6	2,564	1,044	1,087	0,694	0,729	4,480	2,770	0,449	0,844	1,031	0,772
7	1,353	1,131	1,036	0,722	0,824	2,923	2,673	0,449	0,921	1,062	0,796
8	1,251	1,079	1,035	0,746	0,819	1,852	2,682	0,464	0,912	1,050	0,652
9	1,142	1,023	1,016	0,742	0,779	1,688	2,609	0,480	0,923	1,038	0,933
10	0,930	1,041	1,145	0,694	0,793	4,031	3,645	0,488	0,981	1,006	1,039
11	4,777	0,973	1,156	0,649	0,708	6,056	2,185	0,456	0,858	0,817	0,611
12	5,998	1,222	1,390	0,779	0,815	7,378	2,606	0,525	0,988	1,029	0,664
13	6,422	1,275	1,416	0,751	0,857	8,041	2,642	0,506	0,974	1,026	0,718
14	7,096	1,253	1,447	0,768	0,877	8,572	2,831	0,497	0,977	1,058	0,901
15	6,090	1,302	1,397	0,742	0,847	8,229	2,795	0,480	0,944	1,021	0,700
16	6,851	1,302	1,397	0,742	0,847	8,229	2,691	0,480	0,985	1,038	0,687
17	6,851	1,302	1,416	0,742	0,847	8,927	2,940	0,480	0,964	1,038	0,775
18	6,409	1,218	1,392	0,722	0,824	9,134	2,712	0,449	0,979	1,092	0,743
19	5,887	1,231	1,403	0,755	0,862	8,468	2,528	0,732	0,960	1,039	0,770
20	5,163	1,189	1,338	0,729	0,832	7,816	2,605	0,472	0,948	1,020	0,756
25	0,981	1,059	1,072	0,797	0,909	2,327	2,580	0,807	0,925	1,167	0,867
30	1,171	1,024	1,031	0,773	0,882	2,146	2,436	0,568	0,899	1,075	1,097
35	3,042	1,139	1,240	0,841	0,917	4,920	2,471	0,619	0,978	1,087	0,829
40	1,749	1,059	1,013	0,747	0,852	1,318	2,121	0,525	0,876	1,047	0,704
45	1,054	0,585	0,896	0,597	0,777	0,355	0,264	0,355	0,373	0,838	0,309
50	1,116	0,591	0,949	0,599	0,823	0,375	0,281	0,375	0,381	0,887	0,344
55	1,524	0,628	0,947	0,637	0,825	0,399	0,289	0,399	0,376	0,893	0,328
60	1,084	0,617	0,912	0,641	0,777	0,426	0,286	0,426	0,371	0,873	0,295
65	1,204	0,674	0,978	0,671	0,806	0,473	0,243	0,473	0,412	0,852	0,342
70	1,204	0,603	0,941	0,671	0,806	0,473	0,209	0,473	0,395	0,823	0,307
75	1,250	0,491	0,940	0,740	0,777	0,491	0,228	0,491	0,392	0,824	0,330
80	1,250	0,491	0,902	0,697	0,777	0,491	0,010	0,491	0,392	0,794	0,249
85	1,049	0,628	0,914	0,657	0,752	0,412	0,363	0,618	0,403	0,870	0,306
90	0,942	0,555	0,893	0,738	0,811	0,555	0,012	0,555	0,401	0,759	0,307
95	0,903	0,608	0,931	0,755	0,888	0,608	0,013	0,608	0,435	0,831	0,458
100	0,852	0,608	0,931	0,808	0,888	0,608	0,013	0,608	0,439	0,831	0,441
105	0,972	0,880	1,079	0,937	1,072	0,880	0,496	0,880	0,735	0,985	0,829
110	0,996	0,939	1,006	0,915	1,028	0,939	1,004	0,939	0,988	1,004	1,003
115	0,880	0,829	1,079	0,808	1,211	0,829	0,639	0,829	0,722	1,134	1,164
120	1,003	0,946	1,014	1,006	0,944	0,946	1,045	0,946	0,995	1,023	0,959
125	1,064	1,140	0,951	1,112	1,027	1,140	0,608	1,140	0,910	1,070	1,105
130	1,047	1,073	0,986	1,046	0,966	1,073	1,244	1,073	1,129	1,040	1,322
135	0,896	1,005	0,924	0,980	0,918	1,005	1,010	1,005	1,021	0,925	0,956
140	1,054	1,182	1,041	1,153	1,050	1,182	1,470	1,182	1,287	1,080	1,001
160	1,032	1,216	0,903	1,186	0,991	1,216	0,873	1,216	1,059	0,922	1,366
162	1,204	1,182	1,086	1,048	0,906	1,182	2,598	1,182	1,716	0,985	0,854

Annex 18. Radiocarbon analysis

Beta Analytic Inc.
4985 SW 74 Court
Miami, Florida 33155 USA
Tel: 305 667 5167
Fax: 305 663 0964
Beta@radiocarbon.com
www.radiocarbon.com

Consistent Accuracy . . .
. . . Delivered On-time

May 16, 2012

Ms. Maria Balsinha
Instituto Hidrografico
Rua das Trinas, 49
Lisboa, 1249-093
Portugal

RE: Radiocarbon Dating Results For Samples CORE 110cm, CORE 120cm

Dear Ms. Balsinha:

Enclosed are the radiocarbon dating results for two samples recently sent to us. They each provided plenty of carbon for accurate measurements and all the analyses proceeded normally. The report sheet contains the dating result, method used, material type, applied pretreatment and two-sigma calendar calibration result (where applicable) for each sample.

This report has been both mailed and sent electronically, along with a separate publication quality calendar calibration page. This is useful for incorporating directly into your reports. It is also digitally available in Windows metafile (.wmf) format upon request. Calibrations are calculated using the newest (2004) calibration database. References are quoted on the bottom of each calibration page. Multiple probability ranges may appear in some cases, due to short-term variations in the atmospheric 14C contents at certain time periods. Examining the calibration graphs will help you understand this phenomenon. Calibrations may not be included with all analyses. The upper limit is about 20,000 years, the lower limit is about 250 years and some material types are not suitable for calibration (e.g. water).

We analyzed these samples on a sole priority basis. No students or intern researchers who would necessarily be distracted with other obligations and priorities were used in the analyses. We analyzed them with the combined attention of our entire professional staff.

Information pages are enclosed with the mailed copy of this report. They should answer most of questions you may have. If they do not, or if you have specific questions about the analyses, please do not hesitate to contact us. Someone is always available to answer your questions.

Our invoice has been sent separately. Thank you for your prior efforts in arranging payment. As always, if you have any questions or would like to discuss the results, don't hesitate to contact me.

Sincerely,

Darden Hood
Digital signature on file

BETA ANALYTIC INC.
DR. M.A. TAMERS and MR. D.G. HOOD
4985 S.W. 74 COURT
MIAMI, FLORIDA, USA 33155
PH: 305-667-5167 FAX:305-663-0964
beta@radiocarbon.com

REPORT OF RADIOCARBON DATING ANALYSES

Ms. Maria Balsinha — Report Date: 5/16/2012

Instituto Hidrografico — Material Received: 4/18/2012

Sample Data	Measured Radiocarbon Age	13C/12C Ratio	Conventional Radiocarbon Age(*)
Beta - 320533	6710 +/- 40 BP	0.0 o/oo	7120 +/- 40 BP
SAMPLE : CORE 110cm			
ANALYSIS : AMS-Standard delivery			
MATERIAL/PRETREATMENT : (foraminifera): none			
2 SIGMA CALIBRATION : Cal BC 5590 to 5330 (Cal BP 7540 to 7280)			
Beta - 320534	7750 +/- 50 BP	+0.5 o/oo	8170 +/- 50 BP
SAMPLE : CORE 120cm			
ANALYSIS : AMS-Standard delivery			
MATERIAL/PRETREATMENT : (foraminifera): none			
2 SIGMA CALIBRATION : Cal BC 6620 to 6330 (Cal BP 8570 to 8280)			

Dates are reported as RCYBP (radiocarbon years before present, "present" = AD 1950). By international convention, the modern reference standard was 95% the 14C activity of the National Institute of Standards and Technology (NIST) Oxalic Acid (SRM 4990C) and calculated using the Libby 14C half-life (5568 years). Quoted errors represent 1 relative standard deviation statistics (68% probability) counting errors based on the combined measurements of the sample, background, and modern reference standards. Measured 13C/12C ratios (delta 13C) were calculated relative to the PDB-1 standard.

The Conventional Radiocarbon Age represents the Measured Radiocarbon Age corrected for isotopic fractionation, calculated using the delta 13C. On rare occasion where the Conventional Radiocarbon Age was calculated using an assumed delta 13C, the ratio and the Conventional Radiocarbon Age will be followed by "*". The Conventional Radiocarbon Age is not calendar calibrated. When available, the Calendar Calibrated result is calculated from the Conventional Radiocarbon Age and is listed as the "Two Sigma Calibrated Result" for each sample.

CALIBRATION OF RADIOCARBON AGE TO CALENDAR YEARS

(Variables: C13/C12=0:Delta-R=222±60:Glob res=-200 to 500:lab. mult=1)

Laboratory number: **Beta-320533**

Conventional radiocarbon age: **7120±40 BP**

(6900±70 adjusted for local reservoir correction)

2 Sigma calibrated result: (95% probability) **Cal BC 5590 to 5330 (Cal BP 7540 to 7280)**

Intercept data

Intercept of radiocarbon age with calibration curve: Cal BC 5460 (Cal BP 7410)

1 Sigma calibrated result: (68% probability) Cal BC 5510 to 5410 (Cal BP 7460 to 7360)

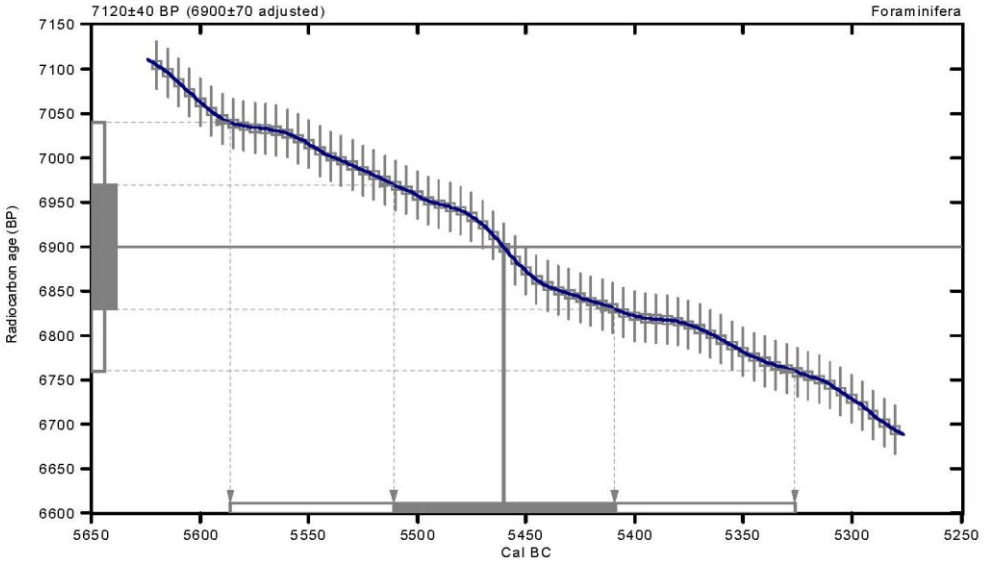

References:

Database used

MARINE09

References to INTCAL09 database

Heaton,et.al.,2009, Radiocarbon 51(4):1151-1164, Reimer,et.al, 2009, Radiocarbon 51(4):1111-1150, Stuiver,et.al,1993, Radiocarbon 35(1):137-189, Oeschger,et.al.,1975,Tellus 27:168-192

Mathematics used for calibration scenario

A Simplified Approach to Calibrating C14 Dates
Talma, A. S., Vogel, J. C., 1993, Radiocarbon 35(2):317-322

Beta Analytic Radiocarbon Dating Laboratory

4985 S.W. 74th Court, Miami, Florida 33155 • Tel: (305)667-5167 • Fax: (305)663-0964 • E-Mail: beta@radiocarbon.com

CALIBRATION OF RADIOCARBON AGE TO CALENDAR YEARS

(Variables: C13/C12=0.5:Delta-R=222±60:Glob res=-200 to 500:lab. mult=1)

Laboratory number: **Beta-320534**

Conventional radiocarbon age: **8170±50 BP**

(7950±80 adjusted for local reservoir correction)

2 Sigma calibrated result: **Cal BC 6620 to 6330 (Cal BP 8570 to 8280)**
(95% probability)

Intercept data

Intercept of radiocarbon age with calibration curve: Cal BC 6440 (Cal BP 8390)

1 Sigma calibrated result: Cal BC 6540 to 6390 (Cal BP 8490 to 8340)
(68% probability)

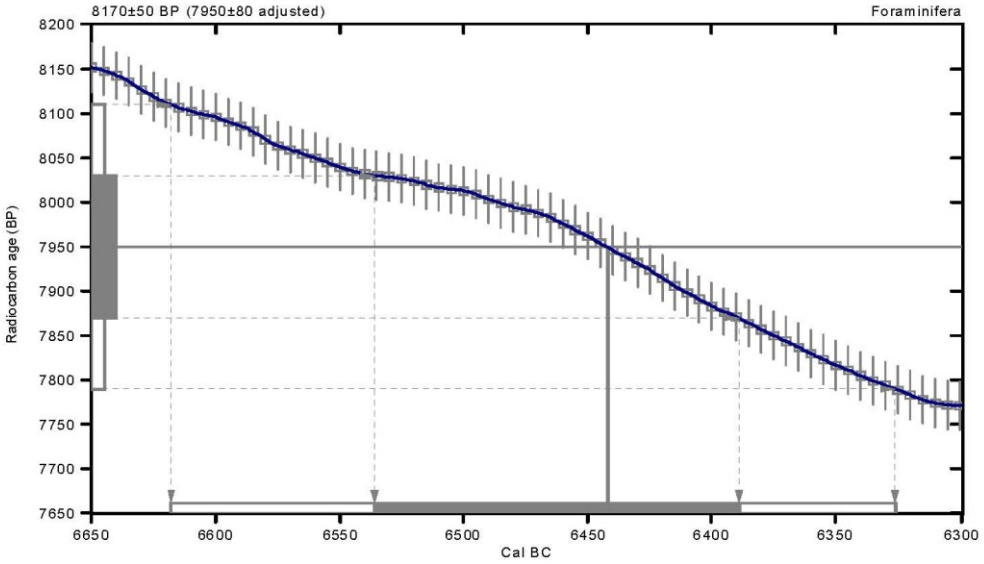

References:

Database used

MARINE09

References to INTCAL09 database

Heaton,et.al.,2009, Radiocarbon 51(4):1151-1164, Reimer,et.al, 2009, Radiocarbon 51(4):1111-1150, Stuiver,et.al,1993, Radiocarbon 35(1):137-189, Oeschger,et.al.,1975,Tellus 27:168-192

Mathematics used for calibration scenario

A Simplified Approach to Calibrating C14 Dates
Talma, A. S., Vogel, J. C., 1993, Radiocarbon 35(2):317-322

Beta Analytic Radiocarbon Dating Laboratory

4985 S.W. 74th Court, Miami, Florida 33155 • Tel: (305)667-5167 • Fax: (305)663-0964 • E-Mail: beta@radiocarbon.com

Beta Analytic Inc.
4985 SW 74 Court
Miami, Florida 33155 USA
Tel: 305 667 5167
Fax: 305 663 0964
Beta@radiocarbon.com
www.radiocarbon.com

Consistent Accuracy . . .
. . . Delivered On-time

July 12, 2011

Ms. Maria Balsinha
Instituto Hidrografico
Rua das Trinas, 49
Lisboa, 1249-093
Portugal

RE: Radiocarbon Dating Result For Sample ERICEIRA BASE

Dear Ms. Balsinha:

Enclosed is the radiocarbon dating result for one sample recently sent to us. It provided plenty of carbon for an accurate measurement and the analysis proceeded normally. The report sheet contains the method used, material type, and applied pretreatments and, where applicable, the two-sigma calendar calibration range.

This report has been both mailed and sent electronically. All results (excluding some inappropriate material types) which are less than about 20,000 years BP and more than about ~250 BP include a calendar calibration page (also digitally available in Windows metafile (.wmf) format upon request). Calibration is calculated using the newest (2004) calibration database with references quoted on the bottom of the page. Multiple probability ranges may appear in some cases, due to short-term variations in the atmospheric 14C contents at certain time periods. Examining the calibration graph will help you understand this phenomenon. Don't hesitate to contact us if you have questions about calibration.

We analyzed this sample on a sole priority basis. No students or intern researchers who would necessarily be distracted with other obligations and priorities were used in the analysis. We analyzed it with the combined attention of our entire professional staff.

Information pages are also enclosed with the mailed copy of this report. If you have any specific questions about the analysis, please do not hesitate to contact us. Someone is always available to answer your questions.

Thank you for prepaying the analyses. A receipt is enclosed. As always, if you have any questions or would like to discuss the results, don't hesitate to contact me.

Sincerely,

Darden Hood
Digital signature on file

BETA ANALYTIC INC.
DR. M.A. TAMERS and MR. D.G. HOOD
4985 S.W. 74 COURT
MIAMI, FLORIDA, USA 33155
PH: 305-667-5167 FAX:305-663-0964
beta@radiocarbon.com

REPORT OF RADIOCARBON DATING ANALYSES

Ms. Maria Balsinha — Report Date: 7/12/2011

Instituto Hidrografico — Material Received: 7/1/2011

Sample Data	Measured Radiocarbon Age	13C/12C Ratio	Conventional Radiocarbon Age(*)
Beta - 301809	8840 +/- 40 BP	+2.7 o/oo	9290 +/- 40 BP
SAMPLE : ERICEIRA BASE			
ANALYSIS : AMS-Standard delivery			
MATERIAL/PRETREATMENT : (shell): acid etch			
2 SIGMA CALIBRATION : Cal BC 8140 to 7600 (Cal BP 10090 to 9540)			

Dates are reported as RCYBP (radiocarbon years before present, "present" = AD 1950). By international convention, the modern reference standard was 95% the 14C activity of the National Institute of Standards and Technology (NIST) Oxalic Acid (SRM 4990C) and calculated using the Libby 14C half-life (5568 years). Quoted errors represent 1 relative standard deviation statistics (68% probability) counting errors based on the combined measurements of the sample, background, and modern reference standards. Measured 13C/12C ratios (delta 13C) were calculated relative to the PDB-1 standard.

The Conventional Radiocarbon Age represents the Measured Radiocarbon Age corrected for isotopic fractionation, calculated using the delta 13C. On rare occasion where the Conventional Radiocarbon Age was calculated using an assumed delta 13C, the ratio and the Conventional Radiocarbon Age will be followed by "*". The Conventional Radiocarbon Age is not calendar calibrated. When available, the Calendar Calibrated result is calculated from the Conventional Radiocarbon Age and is listed as the "Two Sigma Calibrated Result" for each sample.

CALIBRATION OF RADIOCARBON AGE TO CALENDAR YEARS

(Variables: C13/C12=2.7:Delta-R=222±60:Glob res=-200 to 500:lab. mult=1)

Laboratory number: **Beta-301809**

Conventional radiocarbon age: **9290±40 BP**

(9070±70 adjusted for local reservoir correction)

2 Sigma calibrated result: (95% probability) **Cal BC 8140 to 7600 (Cal BP 10090 to 9540)**

Intercept data

Intercept of radiocarbon age with calibration curve: Cal BC 7830 (Cal BP 9780)

1 Sigma calibrated result: (68% probability) Cal BC 7950 to 7710 (Cal BP 9900 to 9660)

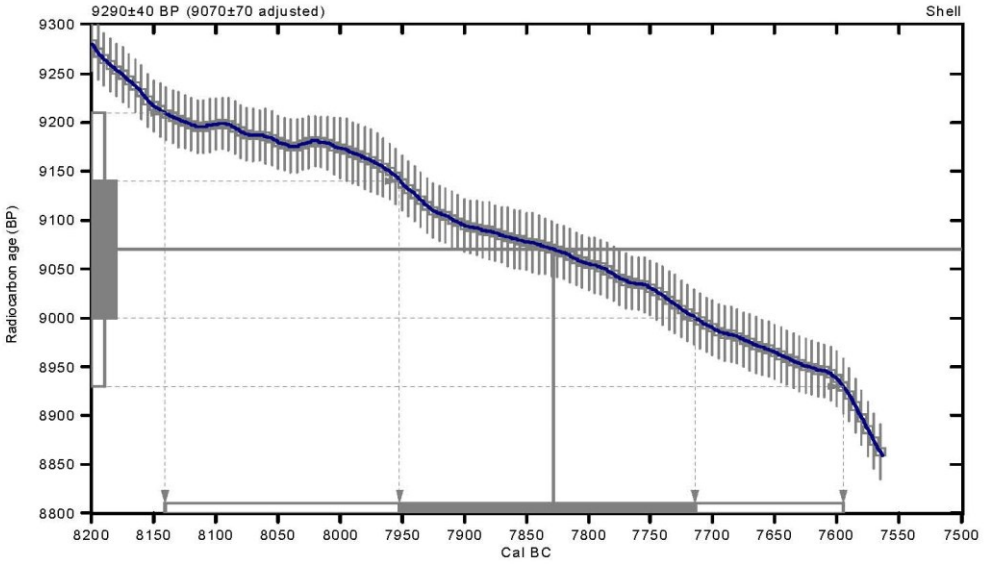

References:

Database used

MARINE04

Calibration Database

INTCAL04 Radiocarbon Age Calibration

IntCal04: Calibration Issue of Radiocarbon (Volume 46, nr 3, 2004).

Mathematics

A Simplified Approach to Calibrating C14 Dates

Talma, A. S., Vogel, J. C., 1993, Radiocarbon 35(2), p317-322

Beta Analytic Radiocarbon Dating Laboratory

4985 S.W. 74th Court, Miami, Florida 33155 • Tel: (305)667-5167 • Fax: (305)663-0964 • E-Mail: beta@radiocarbon.com

Annex 19. GSTA (grain size trend analysis)

GSTA Entry File

	Long	Lat	Mean	Standard Deviation	Skewness
156	0,7756	0,0629	1000	1,645	
1	-9,52868	39,37586	5,2333	1,4612	0,2898
2	-9,28822	39,40903	3,3285	0,1822	1,9007
3	-9,25988	39,42651	3,5009	0,5714	3,1461
4	-9,29734	39,42626	5,8811	1,2315	-0,4084
5	-9,34027	39,42556	4,9910	1,4840	0,3675
6	-9,22231	39,45987	3,5043	0,6192	2,8848
7	-9,36019	39,45865	4,5005	1,4812	0,8860
8	-9,26542	39,51095	4,5588	1,5269	0,9163
9	-9,22170	39,50990	5,6094	1,2954	-0,1485
10	-9,56002	39,35451	4,2296	1,7522	1,2553
11	-9,58820	39,35505	3,9102	1,5146	1,8889
12	-9,63428	39,35497	6,9714	0,5375	0,0603
13	-9,83562	39,36786	5,3018	1,5706	0,1389
14	-9,79524	39,36839	4,5319	1,4852	0,9718
15	-9,76266	39,36877	5,5011	1,5442	-0,0114
16	-9,71616	39,36895	5,5190	1,5110	0,0030
17	-9,61105	39,37280	4,8475	1,7144	0,4403
18	-9,56850	39,37557	5,2962	1,5913	0,1452
19	-9,78505	39,40053	6,0441	1,3217	-0,5324
20	-9,67595	39,39353	6,0878	1,2499	-0,5332
21	-9,58362	39,40356	5,0656	1,5162	0,3892
22	-9,56709	39,42431	5,0819	1,5089	0,3952
23	-9,45841	39,47349	4,2787	1,3675	1,2641
24	-9,41930	39,45825	5,1500	1,5752	0,2885
25	-9,94350	39,31600	4,4250	1,4544	1,0641
26	-9,96433	39,31600	4,5784	1,5289	0,8754
27	-10,05683	39,31800	4,3253	1,4176	1,1944
28	-9,99283	39,31567	4,4495	1,4756	1,0142
29	-9,88717	39,31600	4,6474	1,5088	0,7981
30	-9,84683	39,31500	4,5971	1,5311	0,8635
31	-9,80467	39,31767	4,4542	1,4454	1,0434
32	-9,76167	39,31700	4,1610	0,5707	-0,4123
33	-9,67250	39,31750	5,2860	2,0266	0,0266
34	-9,56817	39,31750	3,8882	0,3698	0,0982
35	-9,50333	39,31783	4,0378	0,3762	0,1735
36	-9,46100	39,31683	4,0898	0,3834	0,1158
37	-9,41950	39,31733	4,8126	1,5872	0,6249
38	-10,15267	39,30100	4,9990	1,3670	0,4293
39	-9,48683	39,26683	3,9545	0,3457	0,1534
40	-9,56833	39,26667	5,2820	1,1726	0,4832
41	-9,61683	39,26750	4,2011	0,6220	-0,5058
42	-9,68150	39,26600	4,8519	1,4614	0,7396
43	-9,70400	39,26833	5,6915	1,3903	-0,2512
44	-9,72767	39,26517	4,5430	1,5086	0,9233
45	-9,76833	39,26517	5,0894	1,5984	0,3049
46	-9,80650	39,26717	4,7749	1,5211	0,6671
47	-9,85067	39,26850	4,7156	1,5655	0,6780
48	-9,89667	39,26583	4,4437	1,4912	0,9864
49	-9,94267	39,26933	4,2436	1,4432	1,3074
50	-9,98433	39,26900	4,4029	1,4710	1,1074
51	-10,02833	39,26700	4,5399	1,5891	0,8809
52	-10,07417	39,26767	4,7542	1,5710	0,6934
53	-10,11383	39,26900	5,4383	1,5853	-0,0279
54	-10,15733	39,26867	4,4636	1,5310	1,0378
55	-10,09350	39,23500	4,2486	1,4252	1,3342
56	-10,07417	39,21767	4,1069	1,2684	1,6667
57	-10,02967	39,21633	4,3199	1,4700	1,1910
58	-9,98950	39,21800	4,3449	1,4769	1,0923
59	-9,95000	39,21600	4,7214	1,5265	0,7215
60	-9,90533	39,21800	4,8840	1,5089	0,5661
61	-9,85967	39,21733	4,7784	1,5304	0,6523
62	-9,81817	39,21767	4,5394	1,5168	0,9031
63	-9,75433	39,21700	5,7133	1,3873	-0,2708
64	-9,70850	39,21750	3,2500	0,0000	1,0000
65	-9,62300	39,21717	5,4347	1,3439	0,1642
66	-9,53617	39,21600	5,2250	1,6213	0,1559
67	-10,15067	39,20217	5,0303	1,5059	0,3892
68	-9,70800	39,16950	4,8979	1,5446	0,4842
69	-9,81133	39,16617	4,7110	1,4847	0,7721
70	-9,85567	39,16750	4,4828	1,4374	1,0293
71	-9,89917	39,16867	4,8562	1,5942	0,5731
72	-9,94200	39,16200	4,8919	1,6338	0,5052
73	-9,98117	39,16517	4,8496	1,5834	0,5744
74	-10,02850	39,16567	4,5326	1,5397	0,9236
75	-10,07283	39,16500	4,6801	1,5039	0,7426
76	-10,11717	39,16600	5,0161	1,5954	0,4133
77	-10,15167	39,10967	4,3391	1,4395	1,1874
78	-10,11067	39,10717	4,7756	1,6149	0,6101

	Long	Lat	Mean	Standard Deviation	Skewness
78	-10,11067	39,10717	4,7756	1,6149	0,6101
79	-10,06150	39,11667	4,9595	1,6012	0,4507
80	-10,01900	39,11667	4,6098	1,5415	0,8332
81	-9,97500	39,11650	4,7548	1,5306	0,6753
82	-9,97483	39,06233	4,3996	1,4144	1,1280
83	-10,01767	39,06633	4,4324	1,4872	1,0653
84	-10,08300	39,06583	5,5710	1,2914	0,1660
85	-10,12667	39,06583	5,4296	1,4389	0,1710
86	-9,49577	39,21613	6,6343	0,6978	0,0572
87	-9,45198	39,21707	5,1667	1,4183	0,4871
88	-9,49062	39,16678	5,4519	1,4495	0,0389
89	-9,53468	39,16655	4,6216	1,5436	0,8150
90	-9,57828	39,16713	4,5374	1,4427	0,9928
91	-9,62163	39,16580	4,8578	1,5134	0,6051
92	-9,93282	39,11495	4,8138	1,5696	0,5985
93	-9,89087	39,11485	5,5694	1,4410	-0,1053
94	-9,84738	39,11672	5,9532	1,1908	-0,3565
95	-9,78107	39,11702	5,4141	1,5115	0,0179
96	-9,76038	39,11612	5,1254	1,4796	0,2793
97	-9,69710	39,11423	4,8089	1,4110	0,6553
98	-9,65090	39,11622	5,6389	1,4297	-0,2135
99	-9,56478	39,11673	5,3721	1,6294	0,0192
100	-9,52063	39,11668	5,3405	1,5489	0,0708
101	-9,65450	39,06567	5,4714	1,4897	-0,0108
102	-9,71950	39,06565	4,5713	1,5013	0,9076
103	-9,76135	39,06455	5,2856	1,6217	0,1256
104	-9,80555	39,06393	4,8654	1,5905	0,5602
105	-9,84752	39,06460	5,1924	1,6298	0,2033
106	-9,92998	39,06578	5,0931	1,6238	0,3210
107	-10,22342	39,06378	4,0430	1,2543	1,7309
108	-10,17595	39,01643	3,8659	1,0741	2,1524
109	-10,13278	39,01473	4,2354	1,3594	1,3754
110	-10,09188	39,01398	5,2483	1,4548	0,4293
111	-10,00247	39,01387	5,4207	1,4437	-0,0249
112	-9,95895	39,01458	5,0740	1,4475	0,3721
113	-9,91260	39,01445	5,3084	1,3558	0,1583
114	-9,85353	39,01300	5,3422	1,2886	0,2137
115	-9,78723	39,01463	4,6886	1,3664	0,7818
116	-9,70132	39,01475	5,3678	1,4205	0,0796
117	-9,65882	39,01480	4,2052	1,3154	1,4254
118	-9,61448	39,01533	4,2705	1,3421	1,1805
119	-9,57665	39,01497	5,1623	1,3981	0,2781
120	-9,53128	39,01438	5,6272	1,2442	-0,0574
121	-9,51380	39,00023	5,5987	1,2244	0,0253
122	-9,52935	38,96687	4,6347	1,4908	0,8114
123	-9,57207	38,96605	5,7969	1,4032	-0,3429
124	-9,61480	38,96568	5,1551	1,6039	0,2261
125	-9,65817	38,96620	4,3227	1,4149	1,2237
126	-9,72092	38,96623	4,9615	1,5759	0,4529
127	-9,80540	38,96573	4,3714	1,4434	1,1408
128	-9,85003	38,96598	4,6208	1,5645	0,7691
129	-9,89218	38,96663	3,8495	1,0595	2,2480
130	-9,93443	38,96613	3,9063	1,0917	2,1173
131	-9,97913	38,96515	4,8633	1,5231	0,5552
132	-10,06578	38,96750	5,2703	1,5741	0,1424
133	-10,12817	38,96820	5,0248	1,6060	0,3324
134	-10,17358	38,96592	5,4925	1,4135	0,0423
135	-10,20058	38,92455	4,7754	1,5371	0,6674
136	-10,15142	38,91663	4,4544	1,4525	0,9883
137	-10,09430	38,91455	5,1145	1,4167	0,3636
138	-10,05540	38,91393	5,0661	1,4515	0,3163
139	-10,01033	38,91453	5,4240	1,4475	0,0204
140	-9,96573	38,91220	5,1279	1,4491	0,2539
141	-9,91862	38,91453	4,9442	1,4291	0,5005
142	-9,87960	38,91428	5,1100	1,3207	0,3359
143	-9,78853	38,91545	5,1624	1,3321	0,2781
144	-9,73115	38,91608	4,6294	1,6121	0,6276
145	-9,66622	38,91513	3,2644	0,0837	5,6324
146	-9,62222	38,91553	3,4706	0,2999	1,0138
147	-9,58002	38,91590	4,2619	1,2051	1,4220
148	-9,53865	38,91675	5,8005	1,2568	-0,2267
149	-9,49547	38,91373	3,2500	0,0000	-1,0000
150	-9,38042	39,26701	3,3777	0,2277	1,3933
151	-9,42251	39,26696	3,3160	0,1695	2,1848
152	-9,40933	39,21662	3,3250	0,1793	1,9985
153	-9,36702	39,21664	3,3756	0,2260	1,4088
154	-9,48056	39,11639	3,4309	0,2733	1,1861
155	-9,46444	38,96585	3,2719	0,1024	4,4540
156	-9,45293	38,91682	3,5047	0,5115	3,3831

Annex 20. Current meter data

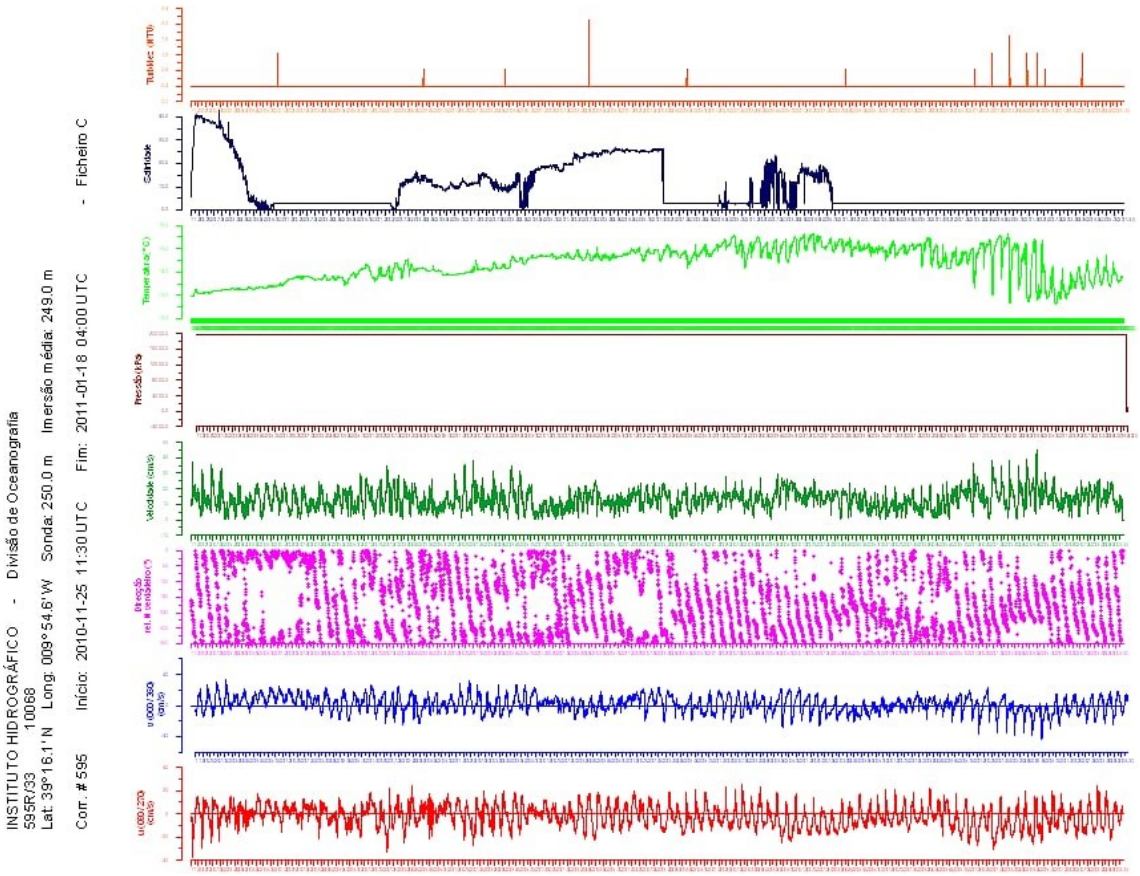
INSTITUTO HIDROGRÁFICO - Divisão de Oceanografia
595R/33
Lat: 39°16.1'N Long: 009°54.6'W Sonda: 250.0 m Imersão média: 249.0 m
Cor. # 595 Início: 2010-11-25 11:30 UTC Fim: 2011-01-18 04:00 UTC - Ficheiro C
Turbidez (NTU)
Condução
Temperatura (°C)
Pressão (kPa)
Velocidade (cm/s)
Direcção rel. a verdadeiro (°)
u (000/ 300 cm/s)
v (000/ 300 cm/s)